HIGH-GRADE METAMORPHISM AND MIGMATIZATION OF THE NAMAQUA METAMORPHIC COMPLEX AROUND AUS IN THE SOUTHERN NAMIB DESERT, SOUTH WEST AFRICA

by

M.P.A. JACKSON

Thesis submitted in fulfilment of the requirements for the degree of Doctor of Philosophy in the Department of Geology, University of Cape Town

March 1976

HIGH-GRADE METAMORPHISM AND MIGMATIZATION OF THE NAMAQUA METAMORPHIC COMPLEX AROUND AUS IN THE SOUTHERN NAMIB DESERT, SOUTH WEST AFRICA

ABSTRACT

Rocks of the Namaqua Metamorphic Complex are exposed in an area of 10 000 km^2 in the northwestern part of the Namaqua Mobile Belt east of Lüderitz.

The Garub sequence represents the oldest rocks in the Aus area and comprises a diverse group of layered rocks of mainly semi-pelitic, pelitic, mafic, calcareous and quartzose composition. These rocks have been metamorphosed to form marbles, calcitic gneisses, metaquartzites, biotite schists, sillimanite-cordierite-garnet gneisses, amphibolites and granolites with minor amounts of iron formation and magnesian rocks. The principal metasediments are concentrated in west-trending zones. A central zone of calcareous rocks broadens westwards and contains the largest known bodies of carbonate rocks in the Namaqua Metamorphic Complex. The calcareous zone is bounded in the north by a narrow belt of quartzose rocks and in the south, by a broad zone of aluminous rocks. Gradational rock types between these zones are compatible with original sedimentary lithofacies changes. Layered biotite gneiss of psammitic composition has been interfolded with units of the Garub sequence. Both these rock units are present as inclusions within a tonalitic augen gneiss.

These rocks underwent three episodes of deformation under conditions of high-grade metamorphism during a period of high heat flow. Ultramafic rocks were intruded on a small scale between D_1 and D_2. Widespread intrusion of granitoids into the older rocks took place between D_2 and D_3, beginning with the emplacement of the granodioritic Jakkalskop charnockites. Granite gneisses, represented by schlieric or megacrystic potash granites and biotite granites, were then emplaced.

Two zones of granulite metamorphism, some 1350 km^2 in extent are present east of Aus. The Jakkalskop charnockites are widespread within, but entirely restricted to the granulite zones, and appear to have been intruded under conditions of granulite facies metamorphism. Pressure estimates for this metamorphism are P_t = 5-7 kb, P_{H_2O} = 2 kb. The presence of carbonic fluid inclusions within the charnockite suggests that juvenile CO_2 may have been introduced during their intrusion. Dilution of the hydrous fluid phase in the country rocks by CO_2 may have been partly responsible for the development of granulite facies metamorphism.

Granulite metamorphism was restricted in time to the period just after D_2, and in place, to the east-centre of the area. In contrast, amphibolite metamorphism took place during all the early episodes of deformation (D_1-D_3) and has affected the entire area, resulting in a metamorphic zonation; metamorphic grade increases towards the centre of the area. On the fringes of the area, zone I is medium grade with 'muscovite + quartz + plagioclase' and 'epi-

dote + quartz' stable. Zone II is high grade with 'muscovite + quartz' stable in the absence of plagioclase and 'epidote + quartz' unstable. Within zone III, in the centre of the area, muscovite is not stable in any combination. Diopside and forsterite are present in calcareous metamorphites, throughout the area but coexist only in zone III, where grossularite, wollastonite and anthophyllite are stable; sillimanite is the only Al_2SiO_5 polymorph. In metabasites epidote is present only in zone I and diopside, only in zone III. Hornblendes in the metabasites change in *Z* absorption colour from blue green in zone I through green brown to brown in zone III; these colour changes are correlated with an increase in mean titanium content of the hornblendes from 0,06 to 0,13 cations. The mean content of *A*-site alkalis in hornblendes also increases from 0,43 in the zone of lowest metamorphic grade to 0,62 in the highest metamorphic zone.

Amphibolite-facies metamorphism took place under high geothermal gradients of 30-50°C/km. The metamorphic facies series is of the low-pressure type and appears to have been essentially isobaric between pressure limits of 4-6 kb. Low-pressure metamorphism is indicated by 'cordierite + almandine' or 'cordierite alone' in metapelites and the absence of kyanite from these rocks, the absence of almandine and the presence of cummingtonite in the metabasites and the low Si and Al^{VI} content of hornblendes in them. A thermal dome was centred around the locality of Aus during amphibolite metamorphism; temperature estimates range from 620-650°C in zone I to 780-800°C in the centre of zone III. High temperatures in zone III are indicated by the formation of periclase from the breakdown of dolomite and the formation of 'wollastonite + anorthite' by reaction of 'grossularite + quartz' in calcareous rocks, the presence of 'hercynite + sillimanite + quartz' in metapelites, and the high (up to An_{95}) anorthite values of plagioclase in metabasites, together with advanced edenitic and titanium substitution in the hornblendes.

Under these high-temperature conditions, melting of semi-pelitic and pelitic rock types has taken place to produce migmatites. In zone I layered migmatites contain only quartz-feldspar neosomes. In zone III biotite has been melted in addition to the quartzofeldspathic fraction and migmatite neosomes are granitic and biotite-bearing; migmatites become increasingly more homogeneous as the migmatization process has advanced. Thus in the core of zone III large masses of homogeneous granitoids have been produced by melting of the Garub sequence, and possibly its basement, during the culmination of regional migmatization accompanying amphibolite facies metamorphism.

Waning of tectonic activity, attributable either to uplift of the crust or cessation of high heat flow, is indicated by widespread but sparsely developed retrogressive metamorphism accompanied by deformation producing kink-bands, chevron and flex-slip folds. Two major northwest-trending mylonite belts formed: the Excelsior mylonite belt in the north and the Kuckaus belt in the south; the latter probably represents the extension of the Pofadder Lineament to the southeast. In the north high-level intrusive and extrusive igneous activity resulted in the formation of the Naisib River Complex, comprising rocks of intermediate composition. These rocks are overlain or intruded by rocks of the Sinclair Group and may represent an early phase of the same period of igneous activity.

TABLE OF CONTENTS

PREFACE

A number of words have been used in a restricted sense in the following study:

Specimen refers to rock specimens that have been examined in thin section

Sample is used in a statistical sense to refer to a set of observations obtained from a larger set (population) for the purposes of making inferences about the population

Colour of minerals, unless otherwise specified, refers to the absorption colour parallel to *Z*

Granulite refers to a metamorphic facies or metamorphic zone

Granolite refers to rocks diagnostic of the granulite facies (Winkler and Sen, 1973)

The facies concept has been adhered to but the concept of sub-facies has not been used (following Turner, 1968). Winkler's (1970) classification of metamorphic grade has been used to distinguish between medium- and high-grade metamorphism.

In addition to standard mathematical chemical and physical (metric) symbols, the following have been used:

P_t - total pressure
P_f - fluid pressure
P_{H_2O} - partial pressure of H_2O
P_{CO_2} - partial pressure of CO_2
X_{CO_2} - mole fraction of CO_2
T - temperature

$\bar{x}$ - sample mean
s - sample standard deviation
n - no. of observations in sample
Ma - 10^6 years
Ga - 10^9 years

Mineral Abbreviations Used

Aa	Allanite	*Di*	Diopside
Ab	Albite	*Do*	Dolomite
Am	Amphibole	*En*	Enstatite
Ad	Andalusite	*Ep*	Epidote
Al	Almandine	*Fo*	Forsterite
An	Anorthite	*Ga*	Garnet
Ap	Apatite	*Gr*	Grandite
At	Anthophyllite	*Gu*	Grunerite
Bi	Biotite	*Hb*	Hornblende
Cc	Calcite	*He*	Hercynite
Cd	Cordierite	*Hy*	Hypersthene
Ch	Chlorite	*Il*	Ilmenite
Cm	Cummingtonite	*Kf*	K-feldspar
Co	Corundum	*Ky*	Kyanite
Cp	Clinopyroxene	*Ma*	Magnetite
Cz	Clinozoisite	*M*	Melt

Mc Microcline
Mu Muscovite
Ol Olivine
Op Orthopyroxene
Or Orthoclase
Pa Pargasite
Pe Periclase
Pg Plagioclase
Ph Phlogopite
Px Pyroxene
Py Pyrope
Qz Quartz
Sa Sapphirine
Sc Scapolite
Se Sericite
Si Sillimanite
Sn Sphene
Sp Spinel
Tc Talc
Tr Tremolite
V Vapour (CO_2, H_2O)
Vs Vesuvianite
Wo Wollastonite
Zc Zircon
Zo Zoisite

Chapter 1

INTRODUCTION

1.1. REGIONAL SETTING

The area on which the present study is based is situated in the Namib Desert east of Lüderitz and is bounded by meridians 15°56'E and 16°42'E and parallels 26°03'S and 27°17'S. The area is some 10 100 km^2 in extent but only a small proportion of this total area contains outcrop. It constitutes the eastern half of an area of basement rocks in the central Lüderitz District and is overlain by the end-Precambrian Nama Group (Germs, 1972) in the south and east, by the Namib Sand Sea in the northwest, and by the late-Precambrian Nagatis and Sinclair sequences (von Brunn, 1967; Watters, 1974) and associated intrusive rocks in the north (Fig. 1b).

The structural framework of southern Africa is illustrated in Figure 1a. The Namaqua-Natal Mobile Belt (Anhaeusser et al., 1968, p.3) is thought to span the entire width of the subcontinent; it lies between the Kaapvaal Craton (Pretorius, 1964) in the north and the Cape Fold Belt in the south. The western section of the mobile belt is known as the Namaqualand Mobile Belt (Truswell, 1970) and this name can be abbreviated (*after* Blignault, 1972) to Namaqua Mobile Belt. The extent of the Namaqua Mobile Belt is shown in Figure 1b. Within this area west of the Kaapvaal Craton all rocks underlying the Nama, Gariep (Martin, 1965; Kröner, 1974), Sinclair, Koras (du Toit, 1965) and younger sequences fall within the domain of the Namaqua belt.

Within the Namaqua Mobile Belt three major lithostratigraphic units can be differentiated. In the east the metasediments and metavolcanics of the *Kheis Group* (as redefined by Vajner, 1974, 1975) constitute a discrete lithostratigraphic unit. In the Richtersveld area the rocks comprise the plutonic Vioolsdrif suite, volcanics and sediments of the Orange River Group (Blignault, 1974b; Reid 1974) and recognizable metamorphic derivatives of these rocks together with older biotite gneisses (Bertrand, 1976); because they form a distinct and largely coeval lithologic group (Reid, pers. comm., 1976) these

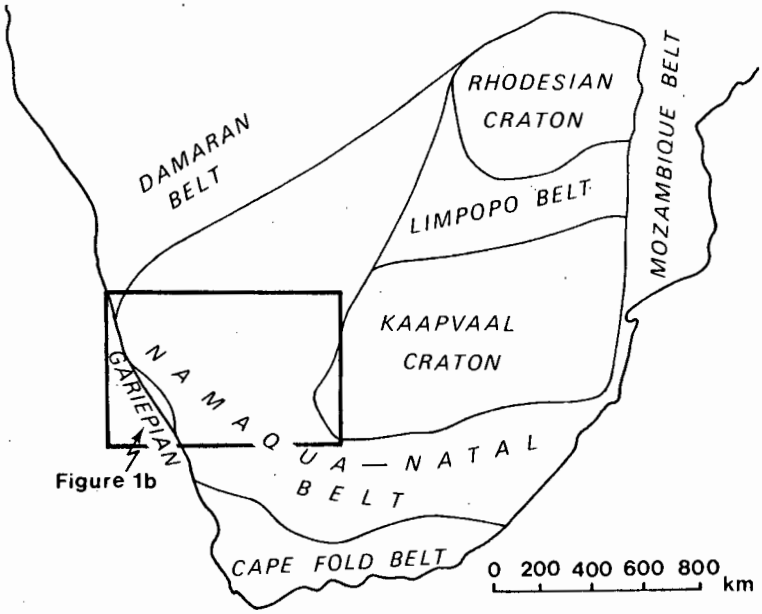

Figure 1a.
Sketch showing the regional setting of the Namaqua-Natal belt in the structural framework of southern Africa (*after* Anhaeusser et al., 1968; Clifford, 1970)

Figure 1b. The Namaqua Mobile Belt, showing its principal lithostratigraphic divisions and the regional setting of the Aus area.

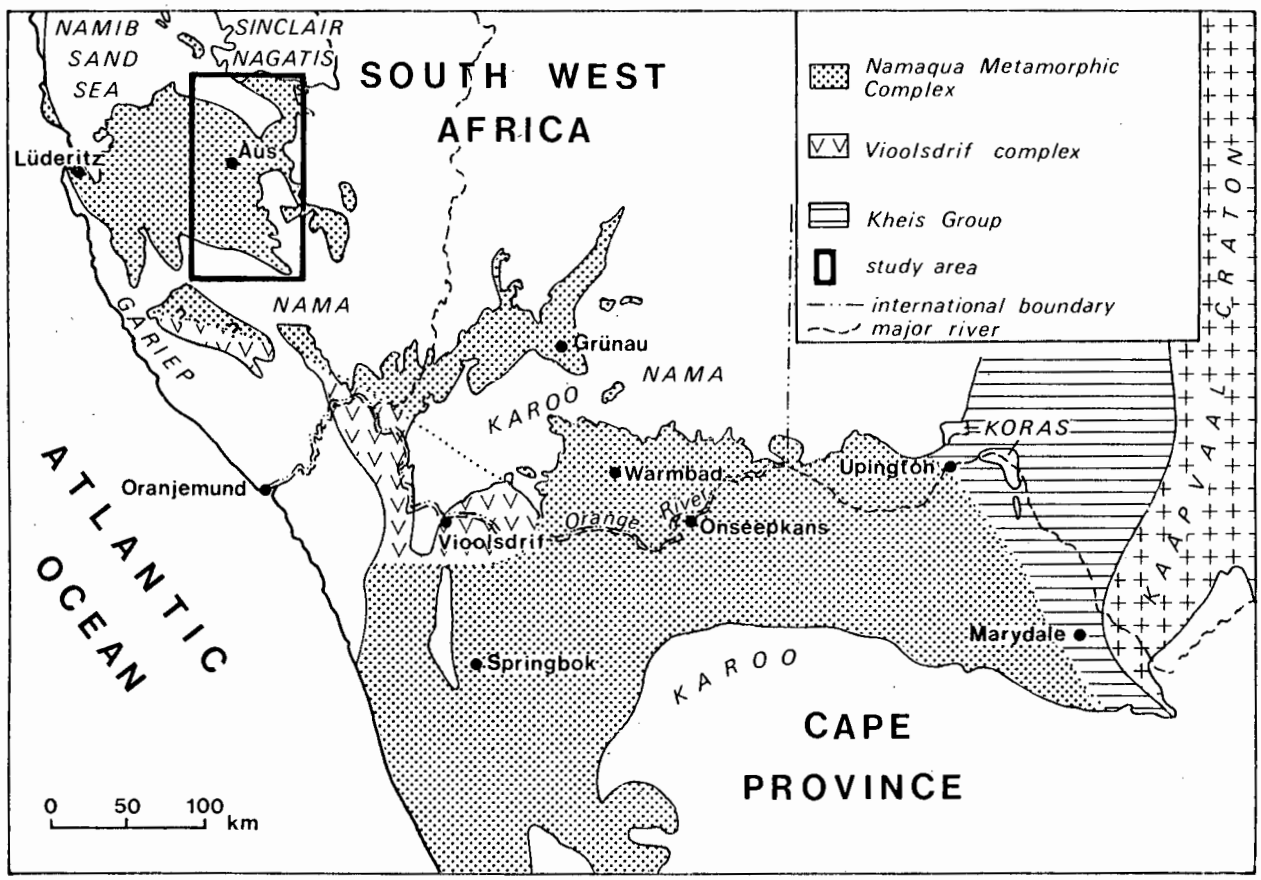

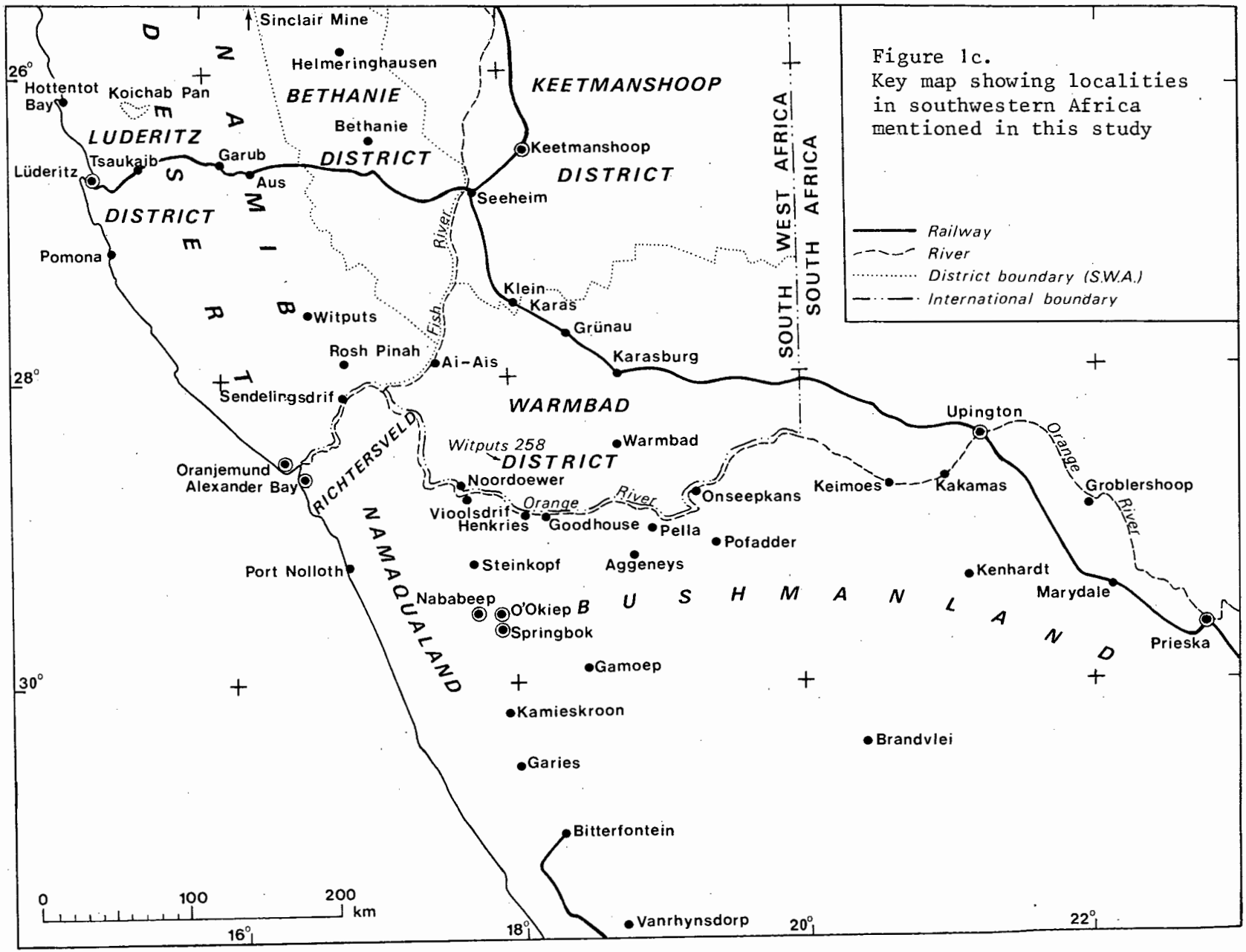

Figure 1c.
Key map showing localities in southwestern Africa mentioned in this study

rocks are grouped in the present study into an informal lithostratigraphic unit, the *Vioolsdrif complex*. The remainder of the rocks in the mobile belt constitute the *Namaqua Metamorphic Complex*; high-grade metamorphites and associated granite gneisses are characteristic of the Namaqua Metamorphic Complex and typically yield the 1,0-1,1 Ga radiometric ages first reported by Holmes (1951) and Nicolaysen and Burger (1965).

An alternative terminology has been proposed by Blignault (1974a); Blignault et al. (1974) and Kröner and Blignault (1976); this involves the separation of an infracrustal Namaqua Province from a supracrustal Richtersveld Province on a structural and geochronological basis. However, since this distinction involves detailed structural mapping to define the boundary and work done so far is controversial (see conflicting interpretations of Blignault et al., 1974; Toogood, 1975; Bertrand, 1976), this terminology is not used in the present study in which the boundaries of the Richtersveld domain are defined by lithostratigraphic criteria.

As a result of advances during the past decade, the domain of the Namaqua Mobile Belt has been steadily extended northwards to the presently recognized boundaries (Fig. 1b). On the Official Geological Map of South West Africa (1963) de Villiers and Martin proposed that the 'Namaqualand gneisses' extended into South West Africa as far north as the Aus area. Subsequently, however, Martin (1965, Plate I) placed the northern boundary of the 'Namaqualand Granite-Gneiss' along a line, subparallel with the Orange River, passing through a point 30 km south of Vioolsdrif (Fig. 1c); basement rocks north of here were designated as 'Kheis metarocks intruded by and metamorphosed to Grey Gneiss' (ibid.). The preliminary findings of Blignault (1972, p.20) showed that rocks in the latter category were confined to the Richtersveld area (designated the Vioolsdrif complex in the present report) and that east of here rocks north of the Orange River formed part of the Namaqua Metamorphic Complex. Joubert (1972, p.6) reported that the gneisses of Namaqualand extended through Bushmanland to the Aggeneys area (Fig. 1c).

Mapping by Geringer (1973) and Beukes (1973) west of Upington and south of Warmbad confirmed that the Namaqua Metamorphic Complex extended north of the Orange River. The preliminary findings of Toogood (1974), Jackson (1974) and Blignault (1974) were combined with the findings of Beukes (1973) and the Namaqua Metamorphic Complex was extended northwards from the Orange River to the Aus area on the basis of lithologic, structural and metamorphic similarities of the constituent rock units (Blignault et al., 1974).

1.2. PREVIOUS WORK AROUND AUS

Before the start of the present survey the Aus area was completely unmapped except in the north and its geology was virtually unknown. The rocks in this area have been referred to briefly by a number of workers during their exploration of the southern Namib during the early part of this century.

Range (1910) briefly mentioned large masses of intrusive granite, which he correlated with the basement, forming the mountainland around Aus, Kubub and, farther west, the Tsirub and Tschaukaib mountains.

Kaiser (1926) described the Magnettafelberg ultramafic intrusion and tentatively correlated 'limestone' of the Dicker Willem carbonatite with the Nama sequence; basement marbles at Koichab Pan and Hottentot Bay to the west of Aus were also correlated with the Nama by Klinghardt (*in* Kaiser, 1926).

Beetz (1924, p.3) referred to a metasedimentary sequence near Aus comprising mica schist, marble, conglomerate and amphibolites which represented the 'oldest undoubted sediments' found by him in the Namib Desert. Beetz (1924, p.21) described three main types of granite in the Aus area: augen gneisses and pegmatoid neosomes; garnetiferous 'gneiss-granite' which injected and assimilated the metasediments and was characterized by abundant schlieren and xenoliths; and coarse-grained porphyritic granite with megacrysts of feldspar.

On the Official Geological Map of South West Africa (1963) metasediments just north of Aus are erroneously correlated with the Gariep sequence. Martin (1965, p.59) referred to the presence of garnetiferous gneiss, granulite, amphibolite, metaquartzite and marble in the Aus area and suggested a correlation of these rocks with the Kheis sequence (ibid., Plate I).

1.3. PREVIOUS WORK IN ADJACENT AREAS

Three mapping projects had been carried out in neighbouring areas to the east, south and north of Aus before the start of the present study..

Rocks of the basement complex in a small area around Lüderitz were mapped by Greenman (1966). He described a suite of tonalitic migmatized biotite gneisses (with augen developed in places), amphibolites and minor metaquartzites which were overlain by sillimanite-garnet-mica schist of amphibolite facies grade of metamorphism. Small lenses of hypersthene-bearing 'granulite' within amphibolite southeast of Lüderitz (ibid., p.31) were considered by Kröner and Jackson (1974) to represent retrogressively metamorphosed gabbroids rather than granulite facies metabasites. Greenman (1966, p.15) stated that the basement rocks around Lüderitz showed affinities with both the Gariep sequence and the Kheis sequence.

The geological continuation of the Richtersveld in an area north of the Orange River between Witputs and Sendelingsdrif was mapped by McMillan (1968). The northern margin of the Vioolsdrif granite and associated metavolcanics and metasediments was reported to be a sheared contact with the Gaidab massif; the massif comprises pegmatoidal garnetiferous gneiss, augen gneiss, granites and pegmatites together with 'Kheis' mica schists and amphibolite. McMillan proposed that rocks of the Gaidab massif were formed at a 'higher crustal level of metamorphism than is visualized for the Vioolsdrif granite' by anatexis of underlying rocks (ibid., p.49), despite the fact that amphibolites are present within the massif. The low (greenschist facies) metamorphic grade of the metabasites within the Vioolsdrif complex was ascribed to end-

Precambrian retrogression accompanying the deformation of the Numees Formation (ibid.). The Gaidab massif was correlated by McMillan (1968, p.164) with the 'Namaqualand Granite-Gneiss Massif', an interpretation supported by the present writer.

During his investigation of the Nagatis and Sinclair sequences Von Brunn (1967, p.6) reported the presence of a group of rocks around the Tiras Mountains which he correlated with the Kheis sequence. This group comprised amphibolite, serpentinite, metasediments, schists and migmatites together with intrusive granites and gneiss. The 'Kheis' rocks are intruded by the 'Grey Granodiorite' which underlies the supracrustal Nagatis sequence farther north (ibid., p.7).

1.4. PRESENT INVESTIGATION

Since the area around Aus was geologically unknown at the start of the present survey, the aims of this research project were, of necessity, fairly broad:

(i) to map the basement rocks distributed over an area of 10 000 km^2 and, if possible, to correlate them with other areas of basement rocks in southwestern Africa

(ii) to remap the basement in the north of the area and determine the status of the paragneisses tentatively correlated with the Kheis sequence by von Brunn (1967)

(iii) to determine if the metasediments reported from the neighbourhood of Aus form part of the basement complex or represent younger formations

(iv) to unravel the metamorphic and structural history of the study area

(v) to study in greater detail significant aspects of the above history or any particular lithologic units

The Aus area was mapped over a period of 12 months during the winters of 1972 and 1973. The mapping project was preceded by a photogeological interpretation of the central part of the area and a rapid reconnaissance of the entire area. The study area was then systematically mapped in greater detail.

Reconnaissance trips were also made in the Diamond Area between Aus and Lüderitz and along the coast north and south of Lüderitz. Short visits to the Aus area during the following two years with various field parties enabled the writer to revist critical exposures for the purpose of intensive sampling and examination of important age relations. These field trips also provided the writer with opportunities to compare the basement rocks around Aus with rocks of the Namaqua Metamorphic Complex elsewhere in southern South West Africa and the northern Cape Province.

Field work was aided by the fact that almost all outcrop areas are easily reached by four-wheel-drive vehicle. The extensive sand sea north of the Koichab River, in which individual star dunes attain heights of 200 m, cannot be crossed by vehicle, but none of the other dune fields provide serious obstacles. Exposures of the basement along the Nama Escarpment are not readily accessible by vehicle because of the blanket of talus debris and network of drainage channels at their base (Annexure 8).

Inselbergs are virtually devoid of soil or vegetation cover, except in the east, and the excellent exposures within them serve to elucidate many complex field relations. However, the wide scattering of outcrop areas (Annexure 1, Fig. 73) proved to be a serious obstacle in structural correlation across the study area. Furthermore the short time available to cover such a large area required mapping to be done at great speed and provided little opportunity to revisit localities. Although in general little difficulty was experienced in the differentiation and recognition of the various map units, the distinction between the various biotite gneisses and the Garub biotite schist was difficult in places because of gradational varieties.

After the first field season an 'outcrop input document', closely modelled on that of Wynne-Edwards et al. (1970), was designed in order to replace the traditional field notebook (Appendix 1). This document sheet was reproduced and bound into notebooks and thereafter all structural and lithologic data were collected in the field according to this format. The data sheets enable a large amount of data to be systematically and speedily recorded at each outcrop. Subsequently the data are easily extracted because each attribute, whether structural or lithologic, is recorded in a consistent place on each page; furthermore the data are readily accessible for computer processing (Wynne-Edwards et al., 1970) should this be required.

Mapping was carried out with the aid of monochrome aerial photographs at a scale of approximately 1:36 000. Geological data were then transferred by means of optical projection from the photographs to unpublished 1:100 000 topographic maps supplied by the Trigonometrical Survey of South West Africa. In order to counteract distorsion caused by uneven shrinkage of the map sheets, the coordinate grid was redrawn on stable-base film and the geological data transferred onto this film. After updating the geology on the basis of laboratory work and further visits to the field, the final copy of the map was retraced. Annexure 1 is an outcrop map of the geology of the area. A conjectural geological sketch map, which includes non-exposed areas, is also presented (Fig. 76). p252

Laboratory work involved successive stages of specialization. Firstly the general petrology of all rock units was established by microscope work. Then a computer-assisted statistical study of the paragneiss units of the Garub sequence was carried out to determine the relative abundance and degree of relation of the constituent units. A detailed petrologic study of the Garub sequence enabled the metamorphic zonation and history to be determined. Finally electron microprobe analyses of hornblende and plagioclase in Garub metabasites of various grades were carried out to determine what compositional changes in these minerals accompanied prograde metamorphism and, if possible, to use these geochemical trends to

clarify certain aspects of the metamorphic study (full analyses in Appendix 5).

Because the geology of the Aus area was virtually unknown the present study, of necessity, entails considerable lithostratigraphic description of the various units in order to provide a foundation for the study of their metamorphism, migmatization and structural history.

The climate and geomorphology of the Aus area are described in Appendix 8.

1.5. ACKNOWLEDGEMENTS

I would like to express my gratitude to the late Prof. John de Villiers, Director of the Precambrian Research Unit, for arranging the project and for his initial supervision. Dr. A. Kröner obtained financial support and took over supervision of the work in 1974; thanks are due for his critical comments on the manuscript. I thank Profs. L.H. Ahrens, E.S.W. Simpson, A.O. Fuller and A.M. Reid for providing research facilities.

The project was funded by Moly-Copper Mining & Exploration Co. (S.W.A.) Ltd.; I thank Mr. G. Kahan for his personal interest in the project and for hospitality received in his home in Lüderitz. The Diamond Board for South West Africa granted unrestricted access to Diamond Area 1 and the security staff of the Consolidated Diamond Mines of S.W.A. gave their full cooperation during fieldwork. Mr. O. Weiss gave permission to enter the concession area held by Opdam Company S.W.A. (Pty).) Ltd. It is a pleasure to acknowledge the kind hospitality shown by Fritz and Dora Bolz of Klein Aus to my family and I during fieldwork.

I am indebted to the following people for their help during the course of research. My colleagues in the Precambrian Research Unit, especially D.J. Toogood, C.J. Hartnady and R. Schultz, provided stimulating and helpful discussions that significantly improved this study. Dr. A.R. Duncan of the Geochemistry Department assisted greatly in the presentation of geochemical data. R.S. Rickard of the Geochemistry technical staff instructed me on the use of the electron microprobe and on computer processing of the raw data. The following were imposed on to read parts of the manuscript: Dr. A.R. Duncan, Dr. P.D. Fleming, J.H.W. Ward, Dr. R. Schultz, D.J. Toogood, C.J. Hartnady and Prof. P. Joubert. I thank them all for carrying out this task and for their constructive and helpful criticism.

I would like to express my sincere appreciation of the 'production team' for their conscientious and skilful efforts: Mrs. J. Macdonald typed the final manuscript and much preliminary material; Miss P. Eloff drafted the figures in the text as well as the legend, screens and colour separation of the geological map. Special thanks are due to Mrs. H. Toogood for her photographic printing.

Finally, I will record my appreciation of the indispensible support from my wife Jo throughout the course of study.

Chapter 2

LITHOSTRATIGRAPHY AND TECTONIC CATEGORY

2.1. THE GEOLOGICAL ENVIRONMENT

The crystalline basement rocks that constitute the Namaqua mobile belt can be divided into (1) metamorphosed rocks of supracrustal origin and (2) other rocks, chiefly of granitoid composition. In the Namaqua belt around Aus the granitoid group is dominant; the metasediments and metavolcanics, which are named the Garub sequence, are represented only by lensoid bodies scattered through the granitoid terrain. Although they are widely dispersed, metasediments are found throughout the Aus area, suggesting that they once formed a more extensive cover (Fig. 2) p16 Uplift and erosion have exposed the crust sufficiently to remove all but the most deeply buried parts of the volcano-sedimentary pile.

This supracrustal succession was deposited on some sort of basement. This basement must have been largely remobilized at a later date because the Garub sequence is surrounded by younger granitoids. The metamorphic grade of the supracrustal rocks is upper amphibolite or granulite facies and many of them

show evidence of melting. Under these conditions of high-grade metamorphism, anatexis and deformation normal stratigraphic criteria would have been destroyed or invalidated. Primary way-up structures were obliterated. Because of the effects of several generations of isoclinal folding, the law of superposition cannot be applied. Extensive flattening on the limbs of large folds and movement between bodies of contrasting competency would have largely removed angular discordancies between formations. Boudinage and attenuation of individual layers has lead to their pinching out; horizons became interlayered and duplicated in multiple fashion to produce a new sequence. Anatexis of certain rock types in the metasedimentary sequence has formed granitoids that are not mapped as part of the sequence because of their resulting intrusive contacts, thus producing 'gaps' in the stratigraphic succession; anatexis of the basement has resulted in remobilized granitoids intruding the supracrustal cover, thereby reversing the original age relation.

These tectonic processes produced the complex group of meta-supracrustal rocks, gneisses, migmatites and plutonic rocks that characterize the katazone (*after* Grubenmann, 1904). The stratigraphic classification of these rocks is discussed below.

2.2. LITHOSTRATIGRAPHIC CLASSIFICATION

As pointed out by the International Subcommission on Stratigraphic Classification (Hedberg, 1970, p.5) and the South African Committee for Stratigraphy (1971, p.112) stratigraphic classification can only be applied to rocks *in normal sequence*. The rock units that form by the processes of deformation, metamorphism and anatexis described above are clearly not in normal stratigraphic sequence. If the traditional criteria for determining stratigraphic succession are absent or invalid, then the rocks of the katazone cannot be classified by normal stratigraphic methods. The ISSC (Hedberg, 1970, p.10) has recommended that metamorphic and other rocks that are not classifiable by normal stratigraphic methods should be discriminated mainly on their petrologic and structural features.

Because they control the formation of stratified sequences, it follows that criteria based on sedimentary processes (superposition, primary sedimentary structures, etc.) should form the basis for the stratigraphic classification of sediments; similar reasoning can be applied to the use of intrusive processes as age criteria for higher level igneous rocks. There is likewise a strong case for the use of structural-metamorphic criteria in the classification of high-grade metamorphic and plutonic rocks of the katazone. However, at present there is no widely accepted or proven method for the stratigraphic classification of rocks from the katazone.

2.3. TECTONIC CATEGORY

One method of classifying mesozonal rocks was introduced by Wynne-Edwards (1969) in the Grenville Tectonic Province. Rock units were divided into various tectonic categories which were broadly grouped as 'pretectonic', 'syntectonic' and 'post-tectonic' according to their role during the deformation and metamorphism that accompanied the Grenville orogeny. Some of these groups were subdivided; the pretectonic group comprised the following categories:

III Pretectonic intrusive rocks
II Pretectonic supracrustal rocks
I Pretectonic basement

All the pretectonic rocks existed prior to the Grenville orogeny and were affected by it; the syntectonic rocks were intruded during the orogeny and were distinguished from the pretectonic rocks by their 'absence of metamorphic characters' and by their K-Ar ages corresponding to the Grenville orogeny (ibid., p.165). The present writer considers these to be invalid criteria because many of the syntectonic rocks are described as gneissic (and are therefore metamorphic) and because radiometric ages can be reset. Furthermore, criteria used for the distinction of pretectonic igneous rocks, such as coarse grain and anhydrous mineralogy (ibid.), could be applied to igneous rocks of any tectonic category; the prevailing cataclastic texture, cited as a third criterion of pretectonic nature, would not necessarily have been produced early in the tectonic evolution because cataclasis can affect syntectonic intrusive rocks as well.

Thus although Wynne-Edwards (1969) introduced a valuable concept, the criteria used by him were, at least in part, poorly defined and subjective. However, these remarks do not necessarily invalidate the table of formations described by Wynne-Edwards; they are intended merely to cast doubt on the criteria used.

2.4. PROPOSED CLASSIFICATION

In the present study the lithostratigraphic principles recommended by the ISSC (Hedberg, 1970) for the naming of the various rock units are adopted together with a modified and more rigorously defined concept of tectonic category than that of Wynne-Edwards (1969) in order to classify the rock units according to structural criteria.

2. Lithologic Units

In this report almost all the map units have the rank of formation but because these rocks are not classifiable by normal stratigraphic methods, the

term 'formation' has been omitted as recommended by the ICCS (Hedberg, 1970, p.17); all names proposed are informal. For this reason the various formations of supracrustal origin have been classified together under the informal term 'sequence' rather than 'Group'. Type areas are given in the descriptions of rock units in the following chapter, but no formal stratotype description is given. However, other important features such as distinguishing characteristics, definition of boundaries and contact relations, dimensions and shape, relative age and correlation, are described.

Lithostratographic units are 'recognized and defined by observable physical features rather than by inferred geological history or mode of genesis' (ibid., p.5). For this reason rock types such as metaquartzite or amphibolite, which may occur at different parts of a structural sequence have been mapped as a single unit on the basis of their lithologic character rather than their position in a sequence of folded metamorphic rocks.

2. *Tectonic Category*

Wynne-Edwards (1969) based his tectonic categories on the Grenville orogeny; pre-Grenvillean rocks were thus termed pretectonic. This orogeny was predated, however, by three other orogenies (viz. the Elsonian, Hudsonian and Kenoran), which have been well established by systematic mapping of the belt since 1863 (see Wynne-Edwards, 1972).

By comparison the evolution of the Namaqua belt - most of which has only recently been investigated by reconnaissance mapping - is still controversial although the broad pattern of tectonic history is known. Attempts have been made to correlate deformational imprints over large areas (e.g. Joubert, 1971, 1974b) and to divide the tectonic history into different events (e.g. Joubert, 1971; Blignault et al., 1974; Cornell, 1975); but at present there is no well-established radiometric time-scale for these different events. For this reason the entire tectonic history of the Namaqua belt is classified as one orogenic event for the purposes of the present study. The beginning of orogeny can be defined as the first formation of a structural fabric. On this basis a tectonic classification was proposed (Jackson, 1974) for the rocks of the Aus area, based on their relation to deformation:

(i) *Pretectonic*: Rock units containing the structural and metamorphic imprint of the earliest recognizable period of deformation; hence assumed to predate the onset of orogeny.

(ii) *Syntectonic*: Rock units unaffected by the earliest period of deformation but showing the effects of later deformation.

(iii) *Post-tectonic*: Rock units that are unfoliated and undeformed; hence assumed to postdate all tectonic activity.

It should be emphasized that pretectonic rocks may be so thoroughly reconstituted by later deformation that no trace of the older structures remains; such rocks would therefore be classified as syntectonic even though they predated

TABLE 1

The tectonic category and lithostratigraphic grouping of rock units in the eastern Lüderitz District

TECTONIC CATEGORY	LITHOSTRATIGRAPHIC GROUPING		LITHOLOGIC UNIT
Post-tectonic intrusive rocks			Dicker Willem carbonatite
Post-tectonic platform-type sediments	Nama Group		Schwarzrand Formation Kuibis Formation
Mainly post-tectonic intrusive rocks	Sinclair Group		minor intrusions Tumuab granite
Late-syntectonic intrusive rocks	NAMAQUA METAMORPHIC COMPLEX	Naisib River Complex	Klein Tiras granite Houmoed granodiorite Tierkloof diorite
Syntectonic intrusive rocks			Tiras gneiss Pyramide granite gneiss Anib granite gneiss Biotite granite gneiss Aus granite gneiss Kubub granite gneiss Jakkalskop charnockite Magnettafelberg serpentinite
Pretectonic intrusive rocks			Tsirub gneiss
Pretectonic rocks of largely supracrustal origin			Layered biotite gneiss
		Garub sequence	Gb1 to Gb14

the start of orogeny in their original state. The syntectonic group is conveniently divided into early-syntectonic and late-syntectonic rock units; the latter show only the effects of the late-stage cataclasis (mylonitization).

The tectonic categories of lithologic units in the Aus area are shown in Table 1. Pretectonic rocks include the Garub sequence, comprising layered rocks of largely supracrustal origin and containing both metasediments and metamorphites of possible igneous origin. Biotite gneisses, many of which are layered, form a large part of the pretectonic group. Although it is possible that these biotite gneisses formed part of a hypothetical basement to the Garub sequence, there is at present no evidence for this hypothesis. The Tsirub gneiss unit, comprising augen gneisses of apparently intrusive origin, is also pretectonic.

All the syntectonic rocks are of intrusive or anatectic origin; they cut the earlier foliation developed in pretectonic rocks but were foliated during younger deformation. None of these rocks are layered. Syntectonic intrusive rocks of granitoid composition are termed 'granite gneisses' (Gary et al., 1972) in order to distinguish them from the pretectonic 'gneisses'. Late-tectonic rock units are largely unfoliated but a cataclastic foliation is present in places.

Post-tectonic units crosscut or overlie all other rocks. They are unfoliated, non-metamorphic rocks characteristic of the epizone and are of igneous (e.g. Dicker Willem carbonatite) or sedimentary (e.g. Nama Group) origin.

Chapter 3

LITHOLOGIC UNITS

3.1. GARUB SEQUENCE

The distribution of the Garub sequence is shown in Figure 2. The sequence comprises layered metamorphites of varying origin: some are apparently metasedimentary (metaquartzites, marbles, calc-silicate rocks, aluminous gneiss and iron formation); others are possibly igneous (mafic and magnesian rocks); while others are of uncertain origin (biotite schists).

Fourteen different rock types were differentiated in the field. Following Turner (1968, p.4) these rock types are grouped on a chemical or mineralogical basis as follows:

(i) Calcareous
(ii) Pelitic
(iii) Semi-pelitic
(iv) Quartzofeldspathic
(v) Quartzose
(vi) Ferruginous
(vii) Mafic
(viii) Magnesian

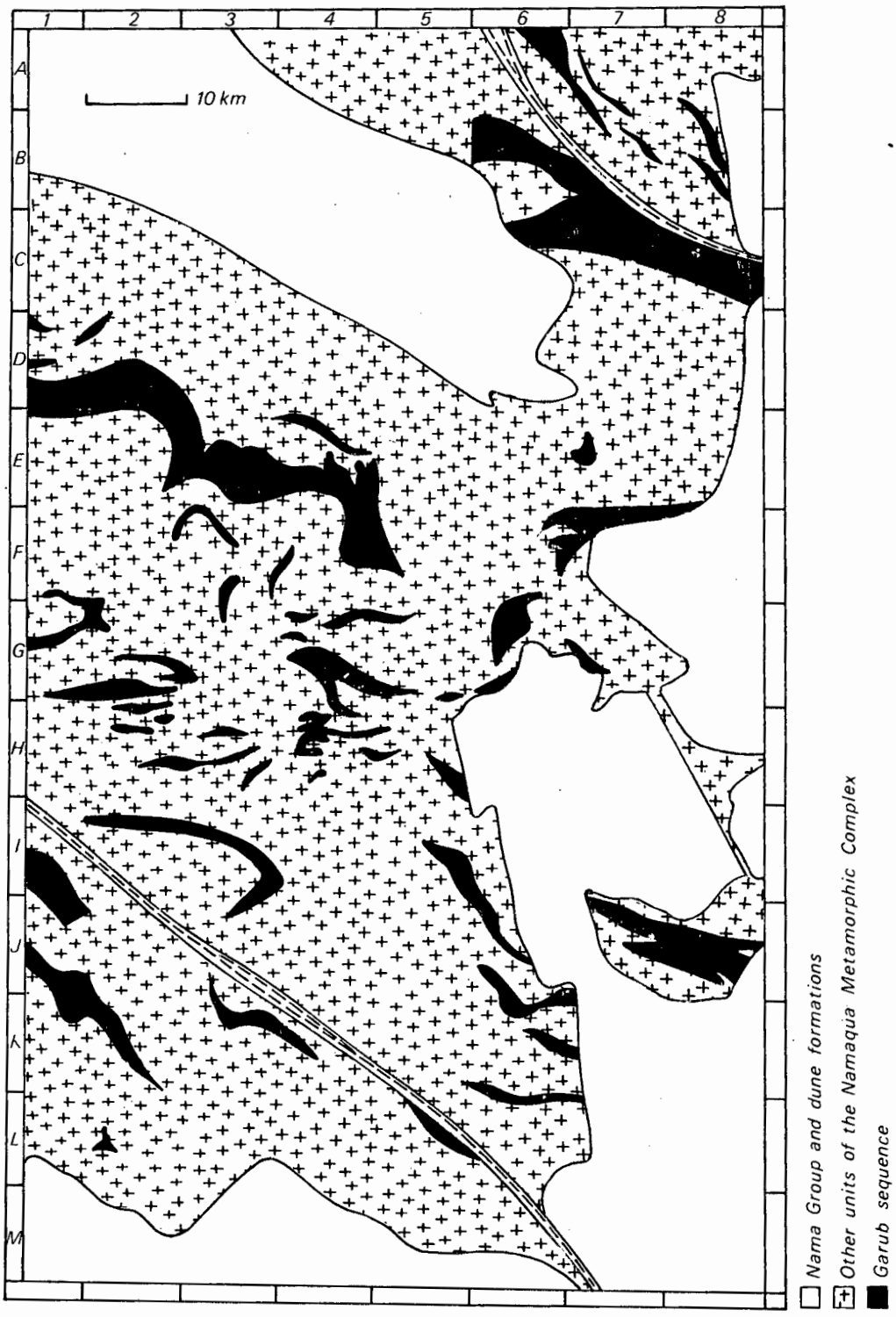

Figure 2. Sketch map of the Aus area showing extrapolated distribution of the Garub sequence

3. *Calcareous Metamorphites*

Map units: *Gb1 Marble and calc-granofels*
Gb2 Granofels

The map unit *Gb1* comprises all carbonate-bearing rocks of the Garub sequence. The map unit *Gb2* represents calc-silicate rocks that are carbonate-free.

Carbonate-bearing Rocks

Carbonate-bearing rocks have been subdivided into three groups on the basis of their modal percentages of carbonate (calcite or dolomite): *pure marbles* contain >90%, *impure marbles* contain 50-90% and *calc-granofelses* contain 1-49%. The most common group is that of the impure marbles and the least common group is that of the calc-granofelses. Because the three rock types are always found together, they are represented by a single map unit on the accompanying geological map (Annexure 1).

The carbonate-bearing rocks are restricted to a broad west-trending zone in the north-central part of the study area and are concentrated in the west of this zone.

The largest single outcrop of marbles is on Am Einschnitt Mountain (map reference E3) where these rocks cover an area of about 6 km^2 and have an estimated maximum thickness of 400 m. Repetition of units due to intense deformation has thickened the marble mass considerably and its original thickness cannot be estimated.

In the Diamond Area, between Am Einschnitt (E3) and Dicker Willem (E2) mountains, multiple bands of resistant marble crop out through the sand cover, whereas intervening areas of biotite schist are poorly exposed (Annexure 1). The strike of the sequence swings from a north-trending direction in the east to a west-trending direction south of Magnettafelberg (D3).

The hills just south of Garub Station (G1, G2) provide readily accessible exposures of carbonate rocks. The outcrop consists of two 'arms' which join at Zwischen den Dünen. From this hill the southern arm of marble can be traced in the form of inselbergs westwards for approximately 15 km.

Another major outcrop of carbonate rocks is present on Löwenberg Farm (E4, E5). This body occupies the same part of the structural succession as that of Am Einschnitt (E3).

Other rock types, chiefly amphibolite and metaquartzite, are present as thin layers within the various marble units. The reason for these intercalations is clearly displayed near Garub Station. Superposed isoclinal folding of two generations has produced an intricate intercalation and repetition of individual strata so that an intimate mixing of rock types has taken place. The second-generation folds have tightened and attenuated the earlier isoclinal folds and have themselves been subjected to the same process; this deformation has produced a pile of apparently concordant metasedimentary units with uniform dip and the appearance of a single highly variable sequence of rock types Fig. 3).

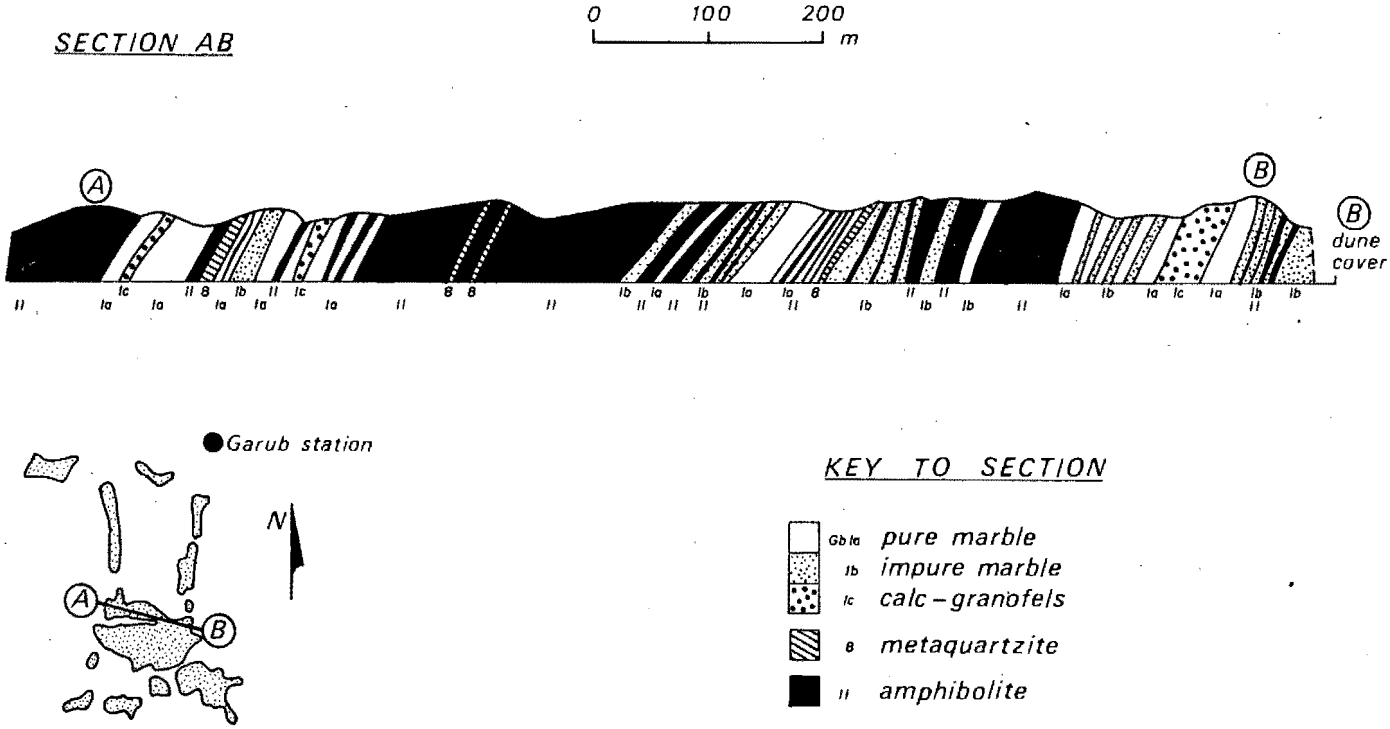

Figure 3. Cross-section of the main outcrop south of Garub Station showing intercalation and repetition of various rock units of the Garub sequence

The appearance of the carbonate-bearing rocks is distinctive and they are easily recognized in the field. The pure marbles are coarse-grained crystalline rocks composed almost entirely of dolomite. Wind-eroded or fresh surfaces are perfectly white but the rocks weather pale brown where not sandblasted. The pure marbles are granoblastic and rarely show any sort of linear or planar fabric.

The impure marbles are medium-grained or coarse-grained well-banded rocks. The calcite/dolomite ratio increases with the proportion of calc-silicate minerals (mainly diopside and forsterite). The calc-silicate minerals are either evenly distributed or concentrated in the form of distinct layers. These marbles usually contain a weak fabric defined by the preferred orientation of diopside. Where concentrated into layers forsterite and diopside-rich layers act more competently than the surrounding ductile marble and are often boudinaged (Plate 1). Thin layers of metaquartzite and calc-silicate rocks have been deformed by buckling in an incompetent matrix of marble.

Many calcareous rocks contain insufficient carbonate minerals to be termed marbles and consist largely of diopside, forsterite, grandite, scapolite, vesuvianite and wollastonite. All contain carbonate (usually calcite) except for the very high-grade varieties in which calcite and dolomite have reacted completely to form calc-silicate minerals.

Plate 1. Boudins of forsterite-rich calc-granofels in lower-viscosity Garub marble. Diamond Area (F2)

Plate 2. Porphyroblasts of garnet (dark) in anorthite-wollastonite matrix (light). MJ500 Garub calc-granofels. S end of Bienenstich Hills (E7)

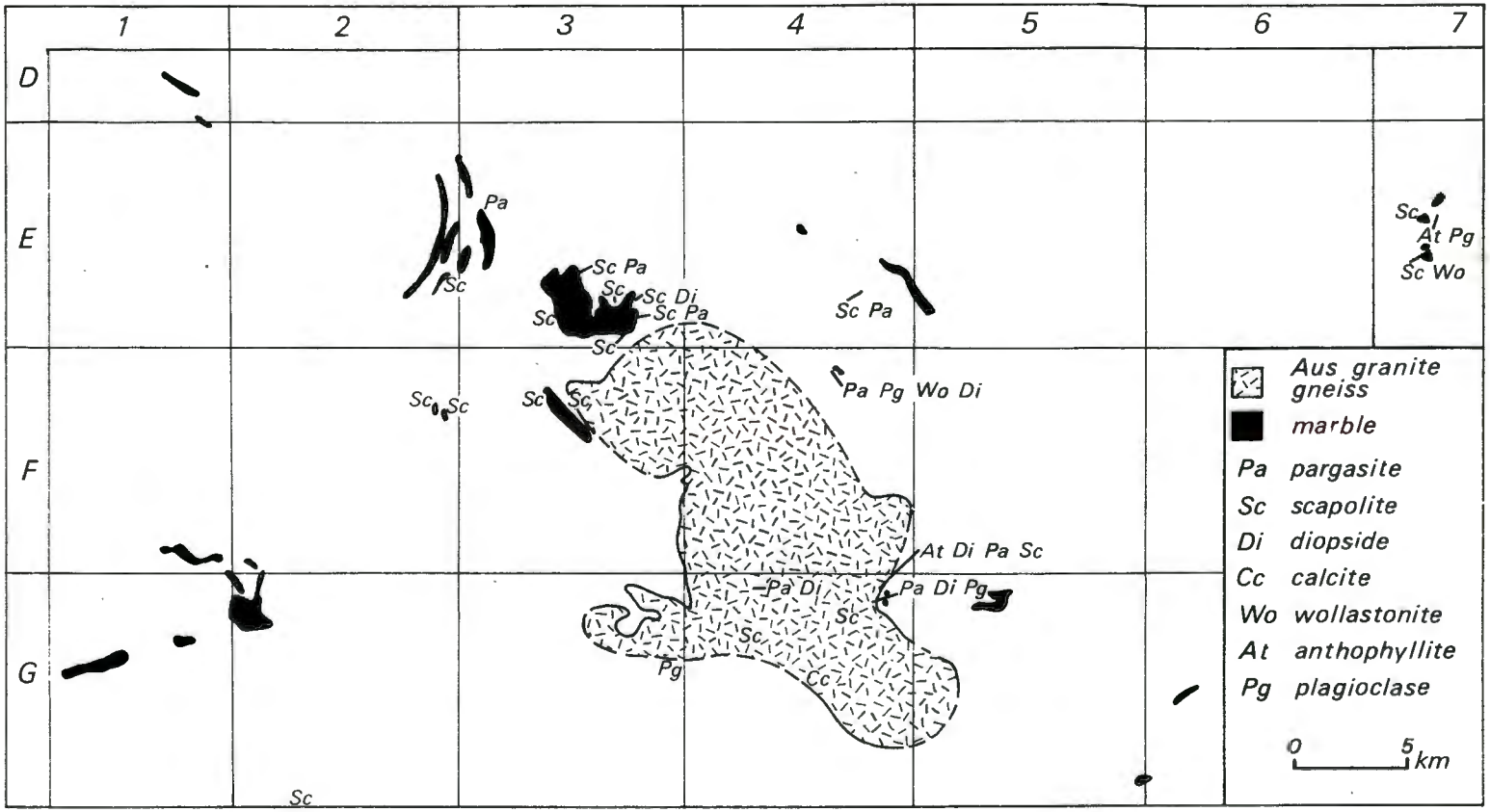

Figure 4. Sketch map showing distribution of calc-silicate segregations and their relation to the Aus granite gneiss

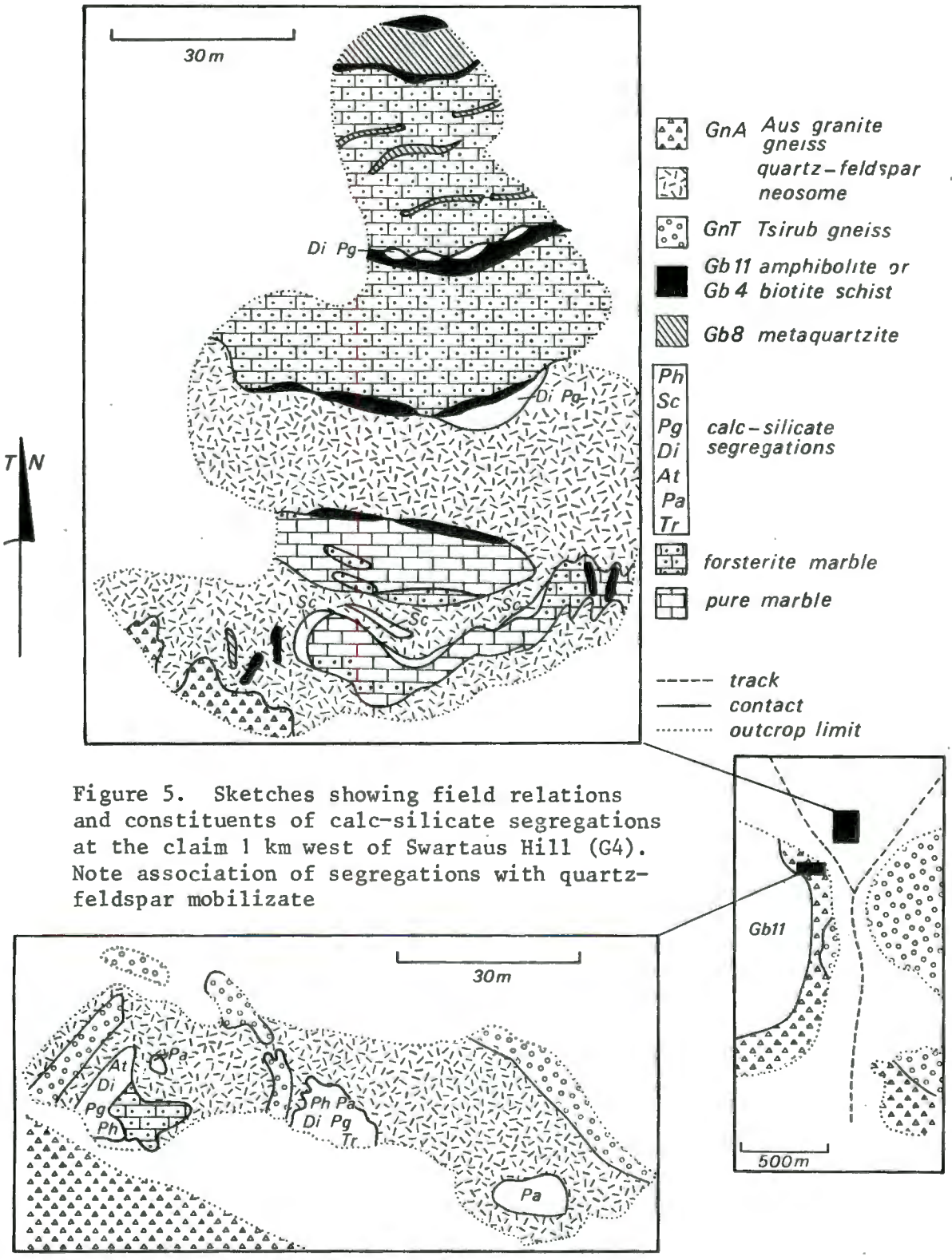

Figure 5. Sketches showing field relations and constituents of calc-silicate segregations at the claim 1 km west of Swartaus Hill (G4). Note association of segregations with quartz-feldspar mobilizate

In other areas of the Namaqua mobile belt such rocks are mapped under the sack-name 'calc-silicate' rock or gneiss (e.g. Beukes, 1973; Geringer, 1973; Joubert, 1972, 1974b; Blignault et al., 1974; Toogood, 1974, 1976; Moore, 1975; Schultz, 1975). Owing to the abundance and diversity of rocks containing calc-silicate minerals in the Aus area, it was felt that a rigorous threefold classification into marble (carbonate >50%), calc-granofels (carbonate 1-50%) and granofels (carbonate-free) should be adhered to and the vague and ill-defined term 'calc-silicate rock' dispensed with altogether.

The terms 'granofels' and 'calc-granofels' require some explanation. Granofels was defined by Goldsmith (1959) as a metamorphic rock displaying no apparent foliation and composed of an equigranular or granoblastic mosaic of minerals. Zeck (1972) suggested that the term should be applied to granoblastic rocks of regional metamorphic origin. Goldsmith (1959) applied the term to medium-grained or coarse-grained rocks and Mehnert et al. (1972) restricted it to rocks with a grain size of more than 3 mm. However, both Katz (1972) and Zeck (1972) put no restriction on grain size. There are no restrictions on mineral content or metamorphic facies.

Thus the term 'granofels' is most suitable for describing metamorphic rocks with a granoblastic medium-grained texture. The prefix 'calc-' serves to differentiate those rocks containing carbonate minerals.

The calc-granofelses are compact green-grey rocks largely composed of calcite, dolomite, diopside and plagioclase together with accessory amounts of wollastonite, garnet, forsterite, scapolite, vesuvianite, anthophyllite, pargasite, sphene, epidote, talc, tremolite, hornblende, chlorite, phlogopite, microcline and quartz. They are granoblastic and unfoliated, but a vague layering is present in some specimens.

Monomineralic segregations of calc-silicate minerals have been termed *calc-silicate segregations*. These segregations are commonly coarse-grained and the average grain size can exceed 10 mm. The calc-silicate segregations are widespread within the area occupied by the marbles and have the form of small discontinuous or lensoid bodies in contact with, or in the vicinity of, granite gneisses or quartzofeldspathic neosomes occurring either at the edge of large marble bodies or as isolated small pods. This setting indicates that the granite gneisses were responsible for their formation - possibly by contributing water and other volatiles during regional metamorphism. The very large (1-30 cm) crystals found in these segregations suggest that a vapour-rich phase existed during their growth.

The calc-silicate segregations consist of one or more of the following minerals: scapolite, diopside, pargasite, wollastonite, anthophyllite, tremolite, phlogopite and calcite. A representative selection of these mineral segregations is shown in Table 3. A sketch map (Fig. 4) indicates the principal localities and their relative abundance. The most accessible of these bodies is an abandoned claim just west of Swartaus Hill (G4); the field relations of these two bodies are shown in Figure 5.

Petrography of the marbles: The mineral assemblages of the marbles are shown in Table 2. Although only a few pure marbles are listed, they are almost as common in the field as the impure varieties. The dominant silicate mineral in

TABLE 2

Estimated modes (in volume %) of marbles from the Garub sequence. (15) = *retrograde mineral, percentage not included with host mineral.* (x) = *retrograde mineral, percentage included with host mineral.* m = <1%

Specimen No.	Dolomite	Calcite	Total Carbonate	Forsterite	Diopside	Garnet	Tremolite	Serpentine	*pe* Periclase *ph* Phlogopite *sn* Sphene *ep* Epidote *tc* Talc *ch* Chlorite *om* Opaque minerals	Locality
MJ705	100		100							E5
MJ853	100		100						m *ph*	G2
MJ1315	(25)	(45)	(70)				(30)			G1
MJ23	35	40	75	20			5		1 *om*	G2
MJ697		75	75				(25)			E3
MJ390	60	35	95					(x)	7 *ph*	D1
MJ699	15	45	60		40			(x)		E3
MJ844	80		80					(15)	5 *om*	F1
MJ846	40	(25)	65					(35)		G1
MJ2	45	35	80	20				(x)		G2
MJ3	45	30	75	25				(x)		G2
MJ4	45	35	80	20				(x)	1 *om*	G2
MJ7	20	50	70	30				(x)		G2
MJ12	40	25	65	35				(x)	x *om*	G2
MJ609	20	45	65	35				(x)		E2
MJ954	10	50	60	40				(x)		G6
MJ956	35	40	75	25				(x)		G6
MJ46	15	60	75	25					1 *pe*	G4
MJ114	25	40	65	30					5 *ph*	E3
MJ116	92		92	7					1 *ph*, (x *om*)	E3
MJ117	50	30	80	15					3 *tc*	E3
MJ389	55	30	85	12				(x)	m *ph*, 3 *tc*	D1
MJ644	35	35	70	25				(x)	(2 *om*), (2 *ep*) (1 *ch*)	E5
MJ833	15	45	60	35				(x)		E2
MJ600		60	60	35				(x)	2 *pe*, 1 *tc*	E2
MJ26	25	45	70	30	1					G4
MJ33	50	35	85	3	12			(x)	1 *sn*	G5
MJ115	15	45	60	25	15			(x)	(2 *om*)	E3
MJ147	50	10	60	20	15				(3 *tc*)	G4
MJ443	30	40	70	30	1			(x)		G6
MJ269	25	50	75	20		5		(x)	(x *om*)	G6

the marbles is forsterite, which is present in three quarters of the impure marble specimens. Diopside is present in approximately 20% of the impure marble specimens and is subordinate to forsterite. The accessory minerals tremolite, grandite, periclase, phlogopite, sphene and talc do not have a wide distribution and are present mainly in single specimens. Secondary minerals - particularly serpentine, carbonates and opaque minerals - are present in virtually all the specimens but their percentages have not been included in Table 2 if the primary mineral is still recognizable.

The pure and impure marbles differ texturally. The impure marbles are equally represented by fine-grained and medium-grained varieties, but in the pure marbles the texture is medium grained or coarse grained (grain size up to 10 mm). In the pure marbles boundaries of the carbonate grains have not been pinned by accessory minerals and their growth has been unrestricted. Most specimens have a seriate texture but some are equigranular. Local recrystallization has taken place in some of the finer-grained marbles and has produced scattered porphyroblasts of calcite or dolomite.

In almost all specimens the texture is granoblastic (i.e. composed of a mosaic of equigranular xenoblastic grains). The carbonate, forsterite and diopside aggregates commonly have smooth, curved or embayed crystal margins, but in a minority of specimens crystals have straight margins (granoblastic-polygonal texture). A criss-cross arrangement of subidioblastic amphibole fibres in the tremolite marbles has resulted in a decussate texture but these rocks are rare exceptions to the general granoblastic character of the marbles.

Both calcite and dolomite have a wide range of habits and were differentiated by staining of thin sections or polished slabs by means of the technique described in Appendix 3. The calcite/dolomite ratio varies with the proportion of silicate minerals: pure marbles are almost totally dolomitic, whereas in the impure marbles calcite predominates. Because of the lack of silica in the pure marbles, magnesium is in carbonate form and the rocks are therefore dolomitic. The calcite/dolomite ratio also increases with metamorphic grade.

The carbonate crystals are usually equant and xenoblastic with no preferred dimensional orientation. They are generally clear, but in one third of the specimens the carbonate is dark and cloudy. Calcite in one specimen contains irregular worm-like fluid inclusions.

Fine-grained granular or fibrous secondary calcite and dolomite are present in a third of the specimens. Calcite is a common alteration product of forsterite and, together with serpentine, forms pseudomorphs after olivine, which are surrounded by primary calcite.

Forsterite is the most common silicate mineral in the marbles and its form is characteristic and invariable: equant xenoblastic grains of forsterite have curved margins against the carbonates and straight boundaries between adjacent olivine crystals. The grains are commonly in the form of loose aggregates with a scalloped convex form resembling botryoidal clusters. Although commonly smaller in grain size than the carbonate crystals, forsterite is only rarely enclosed.

Forsterite is colourless or pale yellow with irregular fractures and almost invariably shows partial or total alteration to serpentine. Serpentiniza-

tion proceeded inwards from the rim via irregular anastomosing fractures, which isolated cores of fresh olivine. In many cases complete alteration led to the formation of feathery secondary calcite in the core rimmed by serpentine. Forsterite also shows alteration to a mixture of talc and carbonate.

Diopside is less common than forsterite and is present only in those marbles that contain low amounts of carbonate minerals. In the banded varieties diopside-rich layers alternate with forsterite-rich or carbonate-rich layers. Diopside is in the form of aggregates of equant xenoblastic colourless grains with straight or slightly curved mutual boundaries. If present in smaller quantities, diopside is in the form of rounded granules enclosed by calcite. In a few cases the diopside has been altered to serpentine, talc or dolomite.

Grandite (grossularite- and andradite-rich garnet) is rare and occurs as pale green granules with convex scalloped margins.

Tremolite occurs as well-developed colourless laths associated with forsterite or as ragged crystals associated with granular calcite and dolomite at Garub Station (G1). Tremolite is also present in the Am Einschnitt marble body (E3) as decussate subidioblastic fibres of colourless tremolite in a matrix of calcite.

Phlogopite is present in a number of specimens as scattered laths with no preferred orientation.

Periclase was only found in one specimen and has the form of well-developed isotropic, colourless octahedra. Sphene is relatively rare in the marbles. Talc is present in some marbles in the west of the area; cleavage lamellae are bent and twisted apart and the interstices are filled with calcite. Shreds of graphite are present in places, commonly confined to layers and oriented parallel to the banding.

Serpentine is by far the most common retrograde mineral. In almost every case the host mineral is identifiable as forsterite or diopside, but in two specimens the serpentine has the form of fibrous stellate sheafs, suggestive of tremolite, which is stable in this particular area. Chlorite is rare and has the form of pale-green twisted flecks. Retrograde epidote is present in one specimen as small pale-yellow laths arranged in a decussate texture and associated with chlorite.

Petrography of the calc-granofelses: This group of rocks is the most complex and varied in the Garub sequence. The mineral assemblages of specimens are shown in Table 3. Wollastonite has the form of colourless subidioblastic laths. In some specimens it has partly broken down to a fine-grained mixture of quartz and calcite.

Scapolite is more common as a calc-silicate segregation but it is also present in the calc-granofelses as large colourless equant grains with straight asymmetrical boundaries (Spry, 1969, p.21) that give rise to a granoblastic polygonal texture. It forms monomineralic veins with a decussate texture of scapolite-rich bands alternating with plagioclase-rich bands.

Vesuvianite is present as large well-formed crystals in a number of localities in the centre of the study area. Colourless or pale-yellow grains of vesuvianite up to 6 mm in length have irregular but fairly smooth boundar-

Specimen No.	Dolomite	Calcite	Σ Carbonate	Plagioclase	Quartz	Wollastonite	Garnet	Forsterite	Diopside	Scapolite	Vesuvianite	Anthophyllite	Pargasite	Sphene	Epidote/Zoisite	*tc* talc *tr* tremolite *hb* hornblende *ch* chlorite *ph* phlogopite *bi* biotite *mc* microcline *aa* allanite *om* opaque minerals	Locality
MJ118	5	10	15						10					3	(35)	(35*ch*)	F3
MJ258		3	3						22							(75*tc*)	H5
MJ8	20	25	45		5				25					2		15*mc*, (10*hb*)	G2
MJ21		5	5	45	5				40					2	(1)	(3*hb*)	G1
MJ854	10	20	30	30					40					2			G2
MJ1355		5	5	50	35				10					m			E3
MJ80									45	50				2	(1)		F4
MJ64				40					10	45				5	(1)	1*om*	F5
MJ149		5	5	5					30		60						G4
MJ134		3	3	50	7				25							3*mc*, 10*bi*	F3
MJ1903 AA		2	2						30		3	65					G4
MJ106													75			25*bi*	E3
MJ78	10	30	40					20	40							1*ph*	F4
MJ596		25	25					35	10		3		25				G5
MJ684	10	25	35					10	50							5*om*	F4
MJ11	5		5				10									(5*ch*) (80*ph*) 2*om*	G2
MJ259		3	3	10			40		40		7						H5
MJ16	25	15	40				15	15					25			5*om*	G2
MJ657		(5)	(5)		(5)	40			50								E4
MJ530		(2)	(2)	10	7		25		35	20							E7
MJ500a[1]				15		5	65		10					1	5		E7
b[2]				70		25			5								
c[3]				65		25	7		2						m		

MJ130						97			3			F3
MJ110	3	3				90			m	m	2*ph*,2*tc*	E3
MJ25	1	1		2		95				(1)	(2*om*)	G4
MJ941							100					E7
MJ137								98			2*om*	G3
MJ78B								100				F4
MJ41B								100				G4
MJ40						65		30			3*ph*	G4
MJ41A						80					10*tr*,10*ph*	G4
MJ45						100						G4
MJ43			80	3		15			5			G4
MJ146			70			30					1*aa*	G4
MJ47			15			50					20*ph*,15*bi*	G4
MJ27	(2)	(2)	75	20							1*aa*	G4

TABLE 3. *Estimated modes (in volume percentages) of calc-granofelses (top) and calc-silicate segregations (bottom) from the Garub sequence; retrograde minerals in parentheses*

m = <1%
[1] porphyroblast
[2] matrix
[3] whole rock

ies and enclose diopside and calcite.

Diopside is a common and widespread mineral in this rock group, occurring as equant xenoblastic crystals commonly of highly irregular shape. The diopside is usually pale green but may be neutral, pinkish or brownish in colour; the mineral is generally resistant to alteration, but in two specimens crystals of blue-green hornblende surround cores of altered diopside. Diopside has also altered to serpentine or clinozoisite and carbonate.

Forsterite is much less common in the calc-granofelses than in the closely related marbles. It is present as rounded partially serpentinized granules which are often concentrated in the calcite-rich layers.

Garnet, probably grandite, is present in a few specimens. The garnet is colourless, pale brown or pale green. Porphyroblastic crystals of garnet up to 5 cm in size enclose very small inclusions of diopside, plagioclase, wollastonite and epidote in a sieve structure at Bienenstich Hill (E7) (Plate 2). In specimen MJ 111 garnet is clearly a relict phase: crystals are in the form of shattered armoured relics which have altered to chlorite along their margins and are set in a matrix of phlogopite.

Plagioclase is present in half of the specimens. The crystals are xenoblastic with smooth margins and are commonly strained and show deformation twinning; saussuritization is common. In view of its importance as an indicator of metamorphic grade (Wenk, 1962), the anorthite content of plagioclase in contact with calcite was measured. After rejecting those specimens that were weathered or had plagioclase not in contact with calcite, only two specimens yielded results: values obtained were An_{74} and An_{78} (Carlsbad-albite twin method).

Calcite is present in almost all the carbonate-bearing calc-granofelses and in rocks with a considerable percentage of carbonate dolomite is also present. Secondary fine-grained calcite of fibrous appearance has formed from the breakdown of wollastonite in two specimens.

Pargasite, identified by means of its optical properties, is present as well-formed colourless subidioblastic laths up to 5 mm in length.

Talc is an uncommon mineral in this group and has the form of colourless subidioblastic laths with a decussate texture. Phlogopite is also rare but where present it constitutes the bulk of the rock in the form of pale yellow-brown laths with a weak preferred orientation. Biotite has the form of narrow laths arranged in decussate clumps which have altered to chlorite and ilmenite in places. Chlorite in the form of small irregular flakes has formed from the breakdown of diopside and garnet.

Sphene is a fairly common accessory mineral, present in over one third of the specimens. Small grains of epidote are present in a number of specimens, usually as granules of retrogressive origin; zoisite has formed by the breakdown of diopside. Opaque minerals are sometimes concentrated in garnet-rich or forsterite-rich layers.

Carbonate-free Calcareous Rocks

The granofelses are composed of diopside, plagioclase and, usually, quartz.

TABLE 4

Estimated modes (in volume %) of granofelses from the Garub sequence
m = 1%; *retrograde minerals in parentheses*

Specimen No.	Garnet	Diopside	Plagioclase/ Antiperthite	Quartz	Hornblende	Biotite	Sphene	Epidote group	Opaque minerals	*pa* Pargasite *mc* Microcline	Location
MJ398			30			(7)	2	13		50 *mc*	D1
MJ825			65	15			5	7	8		D2
MJ768		5	35	50		(7)		3	(1)		D2
MJ855			15	35	(5)				(1)	45 *mc*	G2
MJ1011			45	35	(2)	(10)		(10)			B6
MJ516			35	50		(15)					E7
MJ465			60	20		(15)	1	(6)			F6
MJ62			40	25		5		(30)			F5
MJ305			10	20					7	60 *pa*	L6
MJ469		2	75	10		10			1		F6
MJ15		35	40	10	(3)	10			2		G2
MJ94		35	40	20			1		5		E4
MJ97		30	25	35	(10)						E3
MJ107		20	45	30			3				E3
MJ145		75	5	15			3				G4
MJ169		20	20	60			1				H2
MJ260		50	35	10	(3)		3				H5
MJ267		35	35	25	(2)		2				G6
MJ442		40	50	7			3				G6
MJ523		20	25	50			3	(m)	1		E7
MJ799		15	25	55			1		2		H3
MJ907		30	30	35			2	(m)			F2
MJ1058		70	15	10			5				B7
MJ1064		20	20	60					2		A7
MJ647		20	75		(1)		2				E4
MJ806		40	50		5		3	(m)	1		H3
MJ927		45	50				4				F3
MJ730B	5	10	30	50			3	(2)	3		I3
MJ310	7	20	30	40			2	(1)			L6
MJ181	20	7	10	60					2		I3
MJ176	15	3	50	30			2				I3

Like the carbonate-bearing rocks, the granofelses are largely restricted to areas north of the railway. These rocks are present in two main areas: along the southern margin of the marble zone (around Magnettafelberg, D2; east of Hasenberg, F13; near Glatter Rucken, G4; Kahlerberg, G5 and on the southern part of Augustfelde Farm, G6); and in the extreme north of the area(on the farms Excelsior, B6, and Tiras, A7).

The granofelses are equigranular rocks which are commonly pale grey or green grey in colour when fresh. Like calc-granofelses, they have a dark-weathered surface. Banding is very common but although some of the minerals show a preferred orientation that is parallel to the banding, the rocks fracture irregularly.

Petrography of the granofelses: The mineral assemblages found in these rocks are listed in Table 4. The diopside-free granofelses (top of table) are all severely altered but are of identical appearance in the field. The former presence of diopside can be deduced either from relict unaltered patches or from pseudomorphs.

The petrographic descriptions below apply only to the unweathered rocks. Diopside and plagioclase are invariably present; quartz is present in 80% of the specimens. In the garnet-bearing varieties the quartz content is appreciably higher and the diopside content is lower than in non-garnetiferous varieties. In the quartz-free granofelses the proportion of diopside is the same as in the quartz-bearing varieties, but the proportion of plagioclase is much higher.

Sphene is present in three quarters of the specimens. The abundance of sphene is inversely proportional to that of the opaque minerals, which suggests that sphene is only present when there is insufficient iron to form ilmenite. Similarly specimens containing biotite do not contain sphene, which suggests that there is competition for the available titanium.

The majority of the granofelses are fine-grained rocks; the coarser-grained rocks are seriate, whereas the finer-grained specimens are almost all equigranular. The majority of the granofelses are granoblastic-polygonal.

Banding is produced by the alternation of diopside-rich and diopside-poor layers or by monomineralic layers of quartz. None of the major minerals of the granofelses shows a preferred orientation.

Diopside is commonly in the form of colourless or pale-green equant xenoblasts with smooth asymmetrical grain boundaries; these grains may form irregular aggregates. A second habit is represented by amoeboid xenoblasts with embayed margins, which may be poikiloblastic. The mineral is often altered to hornblende or, less commonly, to chlorite or calcite or to a mixture of biotite, epidote and zoisite.

Plagioclase is commonly in the form of equant subidioblastic grains usually associated with diopside. Antiperthitic flame structures are present in one specimen and a number of plagioclase crystals in other specimens show deformation twinning. Half the thin sections examined showed saussuritization of plagioclase.

Quartz commonly has the form of equant xenoblasts, but in many cases,

however, the quartz has segregated into large irregular crystals with sutured margins forming a coarse banding or rounded aggregates. The quartz is in textural equilibrium with pyroxene and plagioclase, but in one specimen quartz of a later generation with abundant inclusions is present. Cataclasis in the mylonite belts has shattered and strained the quartz grains and fragments are cemented by sericite. The quartz has also been reduced to a very fine-grained mortar aggregate in which much larger rounded clasts of other minerals are set.

Garnet is confined to the south of the study area, where it is present interstitially as small xenoblasts or, more usually, as large pale-brown amoeboid grains. Brown hornblende in apparent equilibrium with diopside was observed only in one specimen. Elsewhere blue-green hornblende is present as a retrograde mineral in the cleavage planes and grain boundaries of pyroxene. Biotite is usually retrograde and derived from the breakdown of pyroxene or, more rarely, from hornblende. Biotite is chloritized in places. Microcline is a rare mineral

Sphene is common as small scattered grains, which are irregular or ovoid in shape, or, rarely, as large poikiloblastic crystals.

Epidote is common in the altered specimens as large irregular aggregates. Clinozoisite and zoisite are also present.

Opaque minerals are present as small grains which, in some cases, appear to have formed retrogressively.

2. *Pelitic Metamorphites*

Map unit: *Gb3 Aluminous gneiss*

Included in this group are rocks containing large proportions of aluminous minerals such as sillimanite, biotite, cordierite and almandine-rich garnet. These rocks are layered gneisses variously known elsewhere as aluminous gneiss, metapelite, khondalite and kinzigite.

These rocks are largely confined to a WNW-trending zone situated south of the railway. Aluminous gneisses are especially common in the Kubub Mountains (H4), the northern part of Tsirub farm (G2), at Ganaam water-hole (J3) and on the farm Keerbank (J7).

The aluminous gneisses are instantly recognizable in the field because of their dark red-brown weathering colour and well-banded appearance. When the rock is fresh, however, it has a distinctive dark green-grey colour.

The aluminous gneisses are medium grained with alternating leucocratic and melanocratic layers of variable thickness. The dark layers are composed of biotite, cordierite and garnet. Biotite sheafs define a strong foliation. Cordierite is responsible for the greenish cast of the rock. Large pink porphyroblasts of garnet up to 2 cm in diameter are almost always present and are concentrated along the borders of the quartzofeldspathic lenses or in the dark layers. Sillimanite needles are usually visible in hand specimen and are often clumped together in large ovoid discs within the foliation surface; their common orientation defines a lineation.

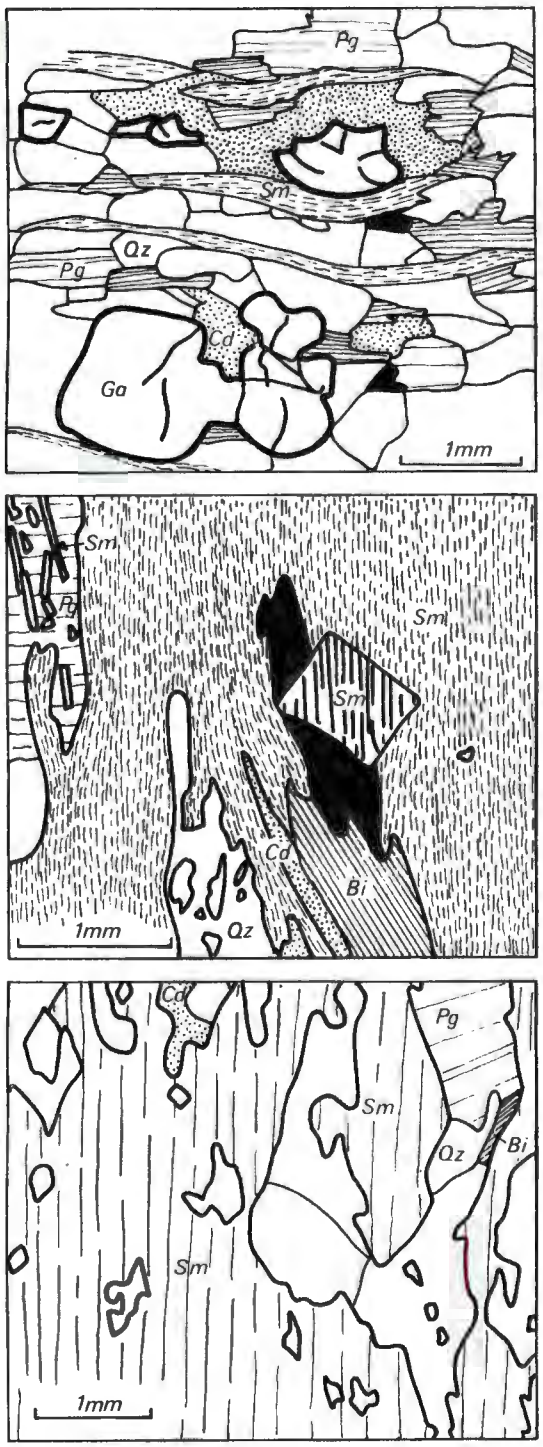

(a) Sheafs of fibrolite. MJ153. 1 km W of Zipfel, Kubub 15 (G4)

(b) Idioblastic crystal of sillimanite truncating mat of fibrolite with no evidence of reaction. Smaller idioblastic needles of sillimanite poikiloblastically enclosed in plagioclase. MJ154. 1 km W of Zipfel, Kubub 15 (G4)

(c) Coarsely-crystalline sillimanite in plates up to 6 mm in size. Adjacent grains are in optical continuity. MJ154

Figure 6. Habits of sillimanite in aluminous gneisses of the Garub sequence. Sm sillimanite, Bi biotite, Cd cordierite, Ga garnet, Qz quartz, Pg plagioclase

Three bodies of sillimanite rock, a few metres in width, are present 4 km north of Rundekuppe (H4) on the northern contact of a thin west-trending strip of aluminous gneiss with the surrounding granite gneiss. The rock is pale grey and consists entirely of sillimanite needles. More usually, the sillimanite is arranged in trains which are often enclosed in poikiloblastic grains of cordierite. A less common habit of sillimanite is shown in Figure 6a where sheafs of fibrolite form irregular aggregates. As shown in Figure 6b idioblastic crystals of sillimanite are surrounded by fibrolite with no evidence of reaction. Rarely, porphyroblastic coarsely-crystalline sillimanite has formed crystals with a width of 6 mm (Fig. 6c). Sillimanite is generally very well preserved but has altered to pseudomorphs of fine-grained sericite in a few specimens.

Cordierite is extremely widespread in the aluminous gneisses. The cordierite has the form of relatively large (2-3 mm) irregular crystals which are often segregated in layers and elongated parallel to the gneissic banding. The mineral is usually partly or wholly altered to amorphous yellowish sericite; alteration invariably proceeds from the margins inwards along irregular fractures towards the centre of the grain. Green-brown pleochroic halos are present around minute inclusions of zircon.

Garnet is present in widely varying amounts as porphyroblastic spheroidal crystals up to 3 cm in diameter; these crystals are usually cracked and the gneissic foliation bends around them. In contrast, garnet in textural equilibrium is present in two specimens as irregular poikiloblastic crystals with smooth embayed margins concentrated into layers. Garnet is almost invariably unaltered but in two specimens it is partially sericitized.

Biotite is almost invariably present and is usually in the form of narrow laths with a preferred orientation and are commonly concentrated as sheafs of crystals. Rarely, biotite mantles armoured relicts of cordierite. Pleochroism of the biotite is strong, with Z absorption being dark red-brown; abundant dark red-brown pleochroic haloes have formed around a zircon inclusion.

Quartz is invariably present as strained irregular grains with lobate margins that are commonly elongated parallel to the foliation of the rock. In cataclastic rocks quartz crystals are broken and equigranular with the fragments separated by a matrix of sericite.

Plagioclase is present in small but consistent amounts as fine-grained aggregates of polygonal crystals usually on the border of felsic/mafic bands; the grains do not show any morphological preferred orientation; they are commonly saussuritized and small myrmekitic intergrowths with perthite are rarely present. Antiperthite is rare and the K-feldspar component is in the form of an irregular stellate inclusion (possibly the result of three or more interpenetrant varieties) in the middle of the grain. Perthite is more common and forms a major part of the quartzofeldspathic bands in a quarter of the specimens. It contains very fine uniformly spaced lamellae concentrated in the centre of the grains. Both perthite and microcline coexist with plagioclase in these rocks but they seldom occur together. Microcline is restricted to the quartzofeldspathic layers of the gneiss and takes the form of large xenoblastic crystals with embayed margins.

TABLE 5

Estimated modes (in volume %) of aluminous gneisses from the Garub sequence. m = <1%

Specimen	Cordierite	Garnet	Sillimanite	Biotite	Quartz	Plagioclase	K-feldspar	Opaque minerals	Other zircon *zc* hercynite *he* muscovite *mu*	Locality
MJ154	25	5	40	10		5	12	3		G4
MJ461	5	20	20	30	20			1	m *he*	G6
MJ578	60	3	10	10	15			2	m *zc*	C8
MJ730	7	15	10	25	30	2	10		1 *zc*	I3
MJ153	20	7	7	5	25	25	10	2	1 *he*	G4
MJ447	25	25	5	10	15		20	2	m *zc*	G6
MJ512	25	3	5	12	15	7	30	3		E7
MJ789	30	20	5	7	15	7	12	2		H2
MJ783	15	25	3	10	35	1	10	3		G3
MJ182	5	20	3	7	30	7	25	2		J3
MJ2001	50	15	3	7	15	10		1	1 *he*	G4
MJ180	7	10	2	7	45	5	20	2		I4
MJ639	50	2	1	7	10	15	15	1	m *zc*	E4
MJ190	20	15		25	25		15			J3
MJ254	25	7		10	15		40	1		G4
MJ1329	15	7		5	55	20				J1
MJ82	20	3		10	30	35			m *zc*	F4
MJ385	30		7	25	35			2		J7
MJ1034	3		7	25	50		15			B7
MJ522	25		5	25	10	5	30	1	m *zc*	E7
MJ410	35		1	1	50	10		5		J8
MJ1321	15		3	10	60	10			2*zc*, 1*mu*	K1
MJ159			100							H4
MJ2024		3	90	7						H4
MJ466	25			15	30	5	25	m		F6

spacing of fracture planes	<10% Biotite mode	>10%
< 1cm		*biotite schist Gb4*
> 1cm	*biotite gneiss GnB, GnB1*	*mafic layered gneiss Gb4*

TABLE 6

The distinction between various biotite-bearing schists and gneisses in the Aus area

Opaque minerals, which include pyrite, magnetite and graphite, are almost always present in the form of small scattered crystals which are often intergrown with one particular silicate such as cordierite, spinel or garnet. Elongated opaque minerals are preferentially oriented parallel to the sillimanite needles.

Appreciable amounts of dark-green spinel (probably hercynite) were found in three specimens (Table 5) in the form of subidioblastic grains or irregular crystals enclosing needles of sillimanite. Zircon is present in the form of minute (less than 0,01 mm) ovoid granules.

3. *Semi-pelitic metamorphites*

Map units: *Gb4 Biotite schist*
Gb5 Hornblende-biotite schist

Biotite schist is the most common rock type in the Garub sequence. In contrast, hornblende-bearing schists and gneisses are more rare and are confined to two zones trending west-northwest. The southern zone is exposed in the Kuckaus Mountains (K3) and on the escarpment on the farm Kokerboomkloof (K6). The other zone is north of the farm Eureka (E3).

Biotite Schists

The biotite schists are fine grained and consist mainly of quartz, feldspar and biotite with traces of hornblende, garnet, diopside or muscovite. The term 'biotite schist' is convenient and useful to describe a mafic metamorphic rock in which biotite is the dominant ferromagnesian mineral (de Waard, 1973). According to one system of nomenclature of metamorphic rocks quoted by Winkler (1974, p.316), biotite schist should contain at least 50% biotite; the biotite schists of the Aus area contain 5-35% biotite and should be referred to as 'feldspar-quartz-biotite schists'. The rocks are referred to as schists because they are schistose in habit according to the definition of Wenk (1963) and to distinguish them from the biotite gneisses, which are not included in the Garub sequence. The biotite schists fracture into thin (less than 1 cm) plates parallel to the foliation, whereas gneisses fracture in thicker slabs. Furthermore the schists are darker and contain more biotite than do the biotite gneisses. These differences are summarized in Table 6.

The biotite schists are generally grey although chloritization of the biotite may give the rock a greenish tinge. The finer-grained varieties are commonly compact and homogeneous but an increase in the grain size is often accompanied by the development of millimetre-scale banding. With decrease of biotite content and consequent development of more widely spaced and more regular foliation planes, the rocks grade into biotite gneisses. In many cases it was difficult to classify these gradational varieties (Table 6).

With an increase of the scale of the banding (>1 cm) biotite-rich (>10%) rocks were mapped as *mafic layered gneiss* (Table 6); the term 'mafic' serves to distinguish them from the more leucocratic biotite gneisses described in

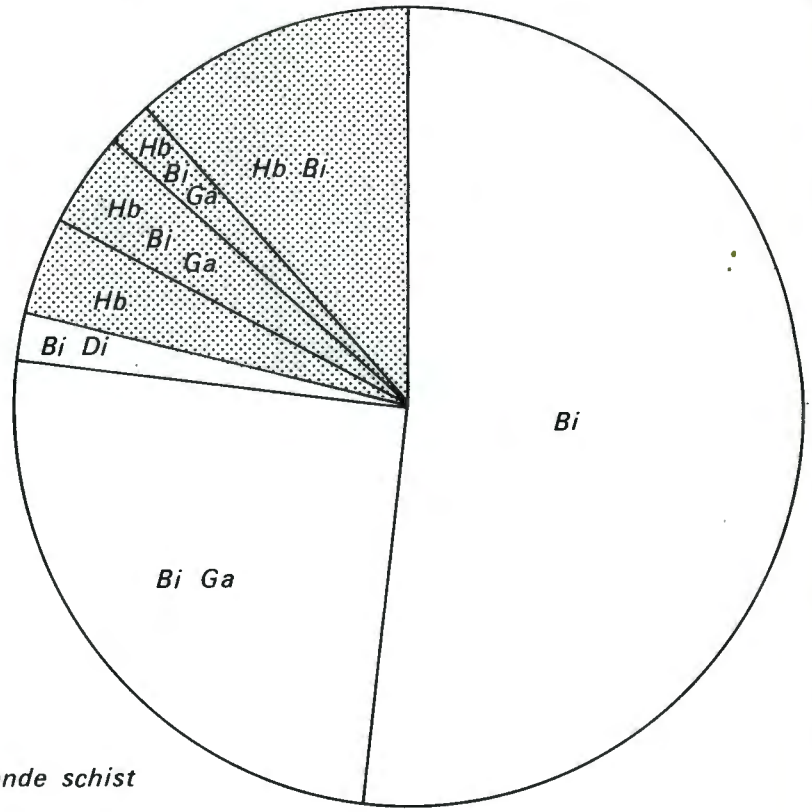

Figure 7. Relative abundance of lithologic varieties of the biotite schist group.

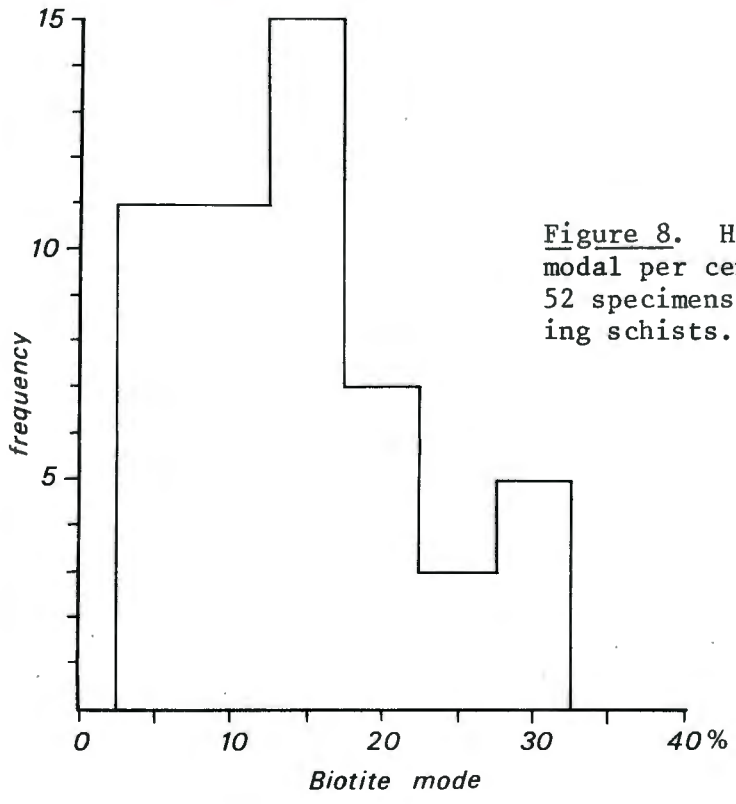

Figure 8. Histogram showing modal per cent of biotite in 52 specimens of biotite-bearing schists.

Plate 3. Mafic layered gneiss showing discontinuous quartzofeldspathic neosomes suggestive of in situ melting. Garub biotite schist. Compass case provides scale. 1 km N of Kububer Horn (H4)

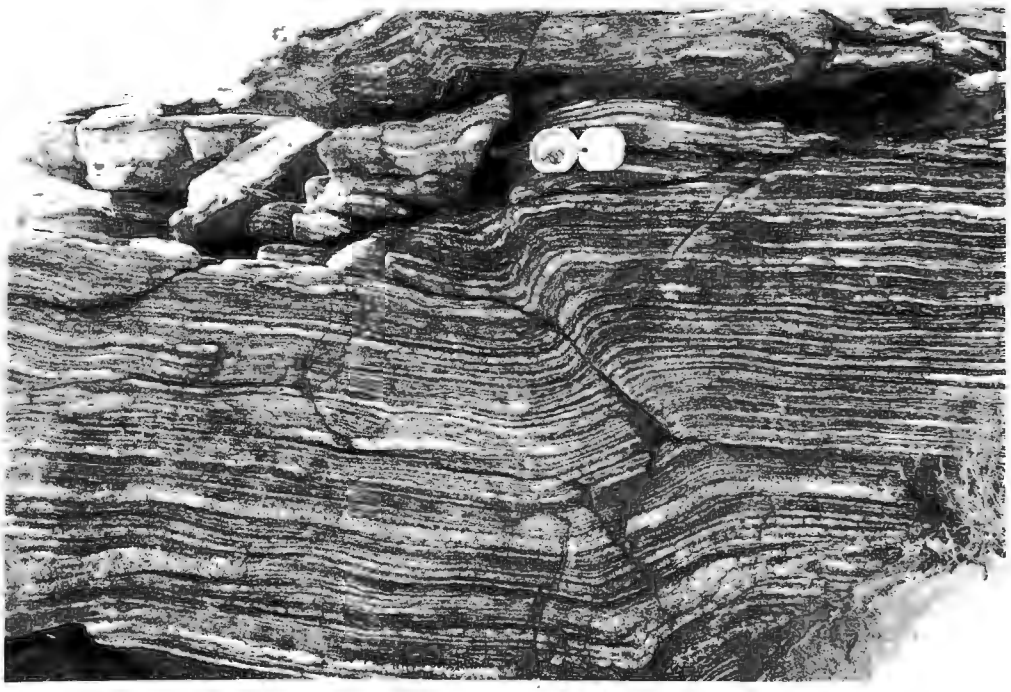

Plate 4. Mafic layered gneiss showing fine-scale, laterally-persistent layering defined by variations in biotite content. Structure interpreted as being derived from stratification in parent rock. Garub biotite schist. '10 km West' Hill, Tsirub 13 (H2)

a later section. The mafic layered gneisses have an identical mineralogy to the biotite schists and are included with them on the geological map (Annexure 1).

This coarse layering is generally of two types: most commonly as discontinuous lensoid segregations of quartz and feldspar (Plate 3) which are interpreted as neosomes produced *in situ* by partial melting (Section 5). Less commonly this layering consists of a regular alternation of layers containing varying amounts of biotite (Plate 4); these layers are only a few millimetres thick but are very persistent and are probably produced by primary lithologic variations (i.e. bedding) in the parent rock (Katz, 1970; Harris, 1974).

Biotite-hornblende schists

These rocks have lithologies intermediate between the biotite schists and the amphibolites. They are melanocratic dark-grey medium-grained schistose or gneissic rocks. They do not show persistent layering but often contain irregular neosome veining.

Petrography of the biotite schists and biotite-hornblende schists

The relative abundance of hornblende-free and hornblende-bearing varieties, based on the specimens collected, is shown in Figure 7. In most of the varieties shown in the figure the major part of the rock consists of quartz and plagioclase; minor amounts of K-feldspar are present in the hornblende-free varieties

The biotite content of all biotite-bearing schists examined is shown in Figure 8. The biotite content is independent of the hornblende content and averages ∿15% (in comparison the biotite content of the biotite gneisses varies between 2 and 10%); where present, hornblende averages ∿4%.

Eighty per cent of the biotite schists examined are fine grained and the remaining rocks are medium grained; the hornblende gneisses are fine grained. There is no apparent correlation between biotite content and grain size. Except for the garnetiferous varieties, most rocks examined are equigranular.

Quartz is the most abundant mineral and is always present. It is generally in the form of equant grains but it can show morphological and lattice-preferred orientation.

Plagioclase is the dominant feldspar and is ubiquitous. In places it is present in the form of antiperthite or mesoperthite and is commonly saussuritized. Microcline and perthite are present in small quantities in most specimens.

Biotite is the most abundant mafic mineral in this group, occurring as laths which are often segregated into layers. Chloritization and alteration to muscovite and ilmenite are common. Muscovite is extremely rare in the biotite schists and is stable only in the extreme southwest and northwest of the area, where the metamorphic grade is sufficiently low to allow stable coexistence with quartz and plagioclase. The mica is in the form of irregular subidioblastic flakes.

Garnet is widespread in the hornblende-free biotite schists and averages about 5% by volume. It is in the form of irregular lobate xenoblasts or

rounded crystals, generally less than 3 mm in diameter, which are often porphyroblastic and cracked. The garnet (probably almandine-rich) is colourless or pale pink in thin section.

Hornblende is commonly intergrown with biotite and often appears to have reacted with it. In the hornblende gneisses the mineral is in the form of tiny xenoblastic granules.

Diopside is rare, especially in the hornblende-free varieties, occurring as pale green or colourless xenoblasts sometimes with embayed margins and irregular form. It is prone to alteration to hornblende. Coexisting diopside and garnet were not found in these rocks.

Apatite, zircon and opaque minerals are common accessory minerals. Epidote, zoisite and sphene are less common and are found mainly in the north, usually as secondary minerals; they are absent from the diopside-bearing varieties.

4. *Quartzofeldspathic metamorphites*

Map units: *Gb6 White quartz-feldspar rock*
Gb7 Pink quartz-feldspar rock

All quartz-feldspar rocks of the Garub sequence with less than 5% mafic minerals are included in this rare group. The two main types are pink quartz-feldspar rocks and white quartz-feldspar rocks. The former group is more common and there are numerous outcrops just north of Aus Village (G4).

Pink Quartz-feldspar Rocks

The pink quartz-feldspar rocks are medium grained; their characteristic pale-pink colour is produced by an abundance of pink microcline and, commonly pink zoisite. The term 'leptynite', as used for rocks of similar composition in the Madras area of India (Bhattacharyya, 1972; Ramaswamy & Murty, 1973) could be applied to the Garub quartzofeldspathic metamorphites. But the term is not satisfactory in view of the different meaning it has acquired in other parts of the world. The term 'granofels' could also be applied to these rocks, but in the present report the term is restricted to the diopside-plagioclase metasediments (map unit 'Gb2').

The pink quartz-feldspar rocks are interlayered with amphibolites and marbles and have therefore been included in the Garub sequence. However, in some cases pegmatoid fractions of these rocks have intruded the surrounding rocks; this remobilization is either part of the syntectonic migmatization or part of the largely post-tectonic phase of intrusion of the K-feldspar-rich pink pegmatites and pink aplites (see legend in Annexure 1). It is possible that some of these pink quartz-feldspar rocks were intruded in their present position in the Garub sequence.

These rocks are commonly associated with epidote schists and cut by epidote veins. The pink quartz-feldspar rocks are composed of low-grade or

heavily altered minerals; they are therefore anomalous with respect to the high metamorphic grade of the surrounding rocks. Their present parageneses reflect one of the weakly developed periods of retrograde metamorphism.

The quartz content of these rocks ranges between 50% and 70% and averages about 60%. The quartz crystals show wide variations in size and enclose epidote granules and submicroscopic inclusions.

Microcline, in places perthitic, varies between 5-40% of the rock. It is cloudy and shows alteration to muscovite in places. Plagioclase is cloudy and saussuritized.

The main mafic mineral in the pink quartz-feldspar rocks is epidote. North of Aus Village (G4) minute (0,015 mm) yellow granules of epidote are enclosed in large quartz grains. In the southern foothills of Groot Löwenberg (F4) pink zoisite is present as stellate clusters (up to 0,2 mm) or as subidioblastic grains. Minor biotite (retrogressed to chlorite and ilmenite) and opaque minerals are rarely present.

White Quartz-feldspar Rocks

The white quartz-feldspar rocks are rare and restricted to the farm Tsirub (H2) where they are associated with metaquartzites. They are fine grained and contain abundant small pink garnets. They are granoblastic, but surfaces produced by cataclastic deformation are covered by a sheen of pale-green sericite and define a foliation although the rock has not been sufficiently sheared to be called mylonite. Larger crystals are strained or shattered and surrounded by a fine-grained aggregate of quartz crystals forming a mortar structure. The dominant feldspar is microcline and this has been perthitized (possibly by deformation) forming a string or bead texture. Quartz constitutes 30-85% of the rock and plagioclase is subordinate to microcline. Garnet is usually the sole mafic mineral and is present as very small (<0,6 mm) colourless round xenoblasts commonly altered to chlorite. Sphene takes the place of garnet in a specimen from Kleinspitz Hill (E3).

Included in this group is an unusual rock which was found in only one locality. A lenticular body consisting of interlayered and interfolded quartz-feldspar rock, marble and amphibolite is present at the lower contact of a band of biotite schist some ten metres thick which is enclosed within marble 8 km southwest of Garub Station (G1). The quartz-feldspar rock is very fine grained and contains rounded clasts or phenocrysts of feldspar up to 2 cm but generally 1-3 mm in length. The laminated structure of the rock resembles that of a mylonite in hand specimen but this was not the case in thin section. The lamination has been folded by two sets of isoclinal folds and is an early s-surface that may correspond to bedding. In thin section the rock shows alternating layers of fine-grained (average grain size 0,05 mm) and very fine-grained (0,005 mm) aggregates of quartz and feldspar crystals; the individual layers are extremely well defined and the grains are well sorted. This matrix contains clasts ranging in size from 0,1 to 30 mm. The foliation may curve around the clasts or it may abut against them; no pressure shadows were observed. The clasts are mainly microcline (in the form of patch perthite) but plagioclase (with bent deformation-lamellae and albite rims) is also common. Garnet, altering to chlorite, is present.

Thus although the rock shows sign of strain, its texture does not resemble that of a mylonite. The presence of extremely well-defined and well-sorted layers is compatible with a sorting process characteristic of sedimentary or volcanic origin and these pre-D_1 surfaces may be parallel to bedding. The ill-sorted nature of the clasts, combined with the finely-banded nature of the matrix, suggest that the rock represents a water-lain crystal tuff. It is also possible that some of the clasts may be later-formed porphyroblasts. Whatever the origin of this rock, however, it is curious that an extremely fine-grained rock could have escaped recrystallization during the high-grade regional metamorphism that accompanied the early periods of isoclinal folding.

5. *Quartzose metamorphites*

Map unit: *Gb8 Metaquartzite*

This group comprises all metamorphic rocks containing more than 80% quartz. They were completely recrystallized during metamorphism and are thus metaquartzites (Gary et al., 1972). Those containing more than 95% quartz are designated 'pure metaquartzites'; those containing 80-95% are designated 'impure metaquartzites' and prefixed by the name of the principal accessory mineral. The impure varieties are far more abundant than the pure metaquartzites.

Large (>500 m thick) bodies of metaquartzite are not common; they are present only on Excelsior Farm (B7) and to the east of Magnettafelberg (D2). Metaquartzites can be traced eastward from the Magnettafelberg area to the Nama escarpment as a minor constituent of the metasediments in numerous localities. Westwards from the Aus area, metaquartzite becomes more common and large outcrops are present south of the Koichab Pan and at Hottentot Bay.

The colour of the metaquartzites is generally grey, yellow-grey or green-grey when fresh. The accessory minerals are commonly feldspar (producing blocky-weathering rocks) or micas (producing flaggy or fissile rocks). Dark-brown magnetite metaquartzites are rare. In the extreme northwest of the area amphibole-biotite metaquartzite contains stellate clusters of green amphibole on the foliation surfaces. In places foliation surfaces a few millimetres or centimetres apart are defined by sillimanite or biotite. No sedimentary structures were recognized.

The metaquartzites have a wide variety of grain sizes ranging from fine grained, characteristic of the impure varieties, to coarse grained (8 mm), characteristic of the pure varieties. The metaquartzites are generally inequigranular. The grains are of irregular shape but are commonly elongated parallel to the foliation of the rocks. Grain boundary variations appear to be connected with composition: the purer varieties have the more irregular grain boundaries.

The accessory minerals are extremely varied and, except for microcline and garnet, are present in amounts less than 5%. The accessory minerals are discussed in order of decreasing frequency of occurrence.

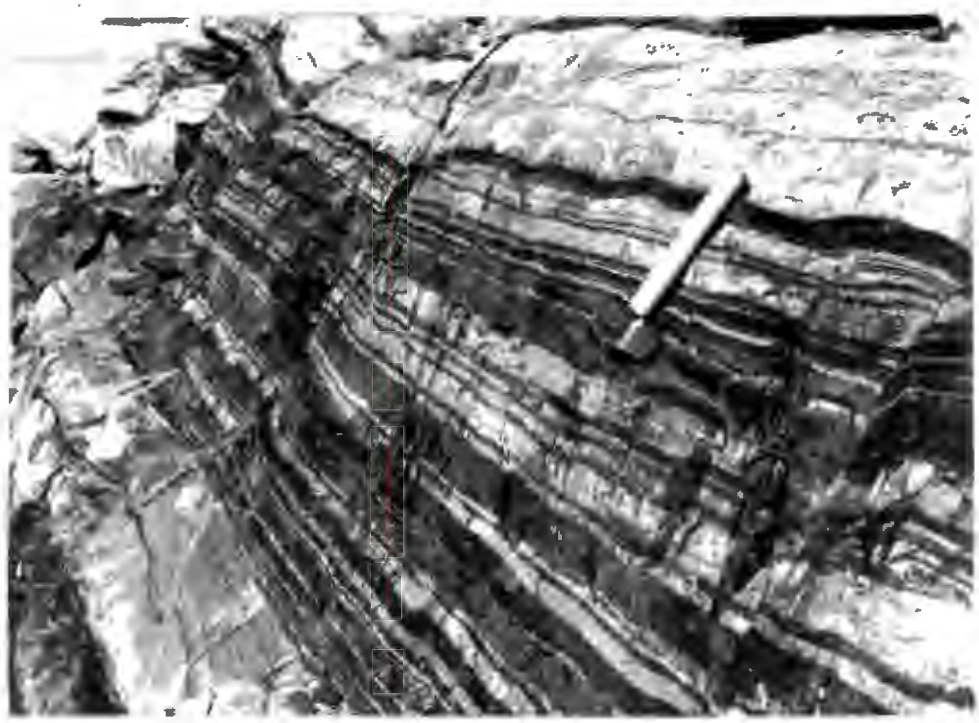

Plate 5. Garnetiferous metaquartzite interfolded with diopside amphibolite. Note isoclinally folded neosome (arrowed) in amphibolite. Garub sequence. Just below marble body, Löwenberg Farm (E5)

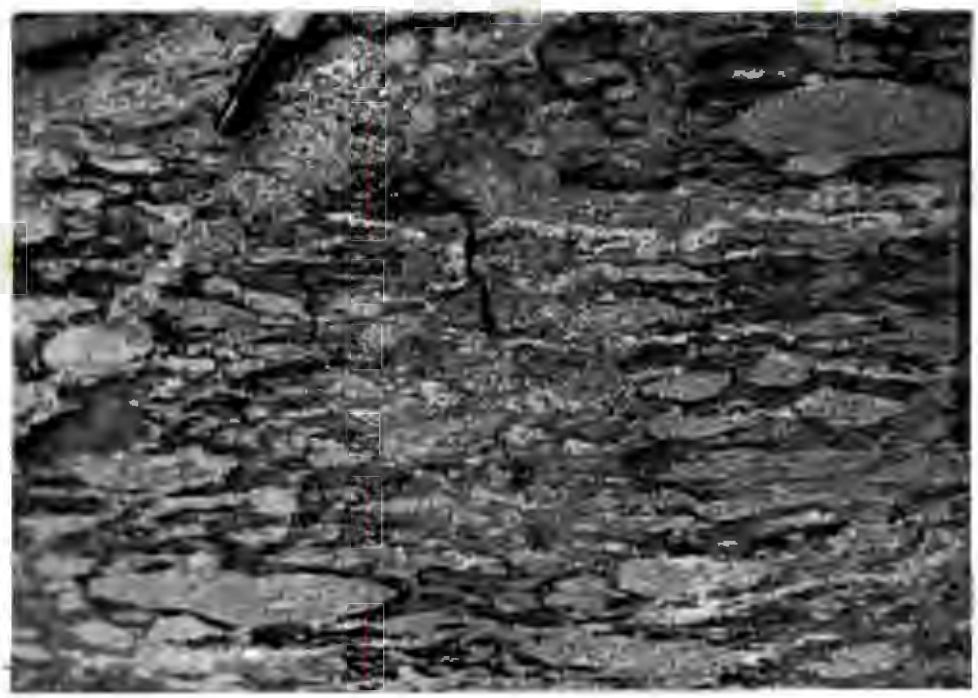

Plate 6. Fragmental texture in hypersthene granolite resembling flattened agglomerate. Horab River body, Garub sequence. 1 km NE of railway, Augustfelde 42 (G6)

Opaque minerals are present in small quantities in most of the specimens. A specimen from Kwessiepoort Farm (F6) contains haematite, and banded magnetite metaquartzites are present at Agub Mountain (K1), Aarkopf Hill (H5) and Ganaam water-hole (J3).

Biotite is common as small flakes, showing a strong preferred orientation and in places concentrated in layers parallel to the sillimanite bands. Biotite commonly shows alteration to muscovite and ilmenite or to chlorite.

Sillimanite is present in the large metaquartzite body east of Magnettafelberg (D2) and in biotite metaquartzites from Garub Station (G2) which also contain traces of hornblende. The sillimanite is in the form of small needles or fibrolite confined to layers spaced 1-2 cm apart. Because of the immobility of aluminium during metamorphism (Carmichael, 1969), it is probable that these layers reflect primary lithologic differences.

Microcline is present in the metaquartzites from both the above localities and is perthitic near Magnettafelberg (D2). Plagioclase is present in small amounts at both the above localities and also at Kwessiepoort Farm (F6).

Garnet is present in quantities of up to 12% in metaquartzites at Urus Mountain (K2) in association with traces of diopside and carbonate. Garnetiferous metaquartzite is also present in smaller quantities at the base of the marble sequence on the farm Löwenberg (Plate 5) and east of Magnettafelberg.

Muscovite is present in metaquartzite near Magnettafelberg and in the southwest of the area, north of Agub Mountain (J1). Epidote and chlorite are present in a few specimens as alteration products whereas trace amounts of zircon, apatite and sphene are common.

6. *Ferruginous Metamorphites*

Map unit: *Gb9 Iron formation*

All rocks containing more than 50% magnetite or haematite are included in this group. Bodies of iron formation are small (<20 m in width) but they have a wide distribution in the central and southern parts of the study area. The iron formations are of two types:

(i) Interlayered with other metasediments such as aluminous gneiss or magnetite metaquartzites.

(ii) Isolated bodies surrounded by syntectonic granite gneisses.

The former type is present on Kwessiepoort Farm (F6), Agub Mountain (K1), north of Festung Mountain (H2) and the Kuckaus Mountains (J3). These rocks consist primarily of magnetite and quartz and are commonly associated with magnetite metaquartzite. They are dark-brown fine- or medium-grained rocks. Irregular layers of coarse-grained quartz result in crude banding and a platy granoblastic texture. The largest outcrop of these metasediments, which is at Agub mountain, consists of magnetite, garnet and pinitized cordierite together

with small amounts of plagioclase and biotite. Elsewhere garnet is a common accessory mineral in the iron formations and may form up to 20% of the rock. Iron formation associated with granofels on Kwessiepoort Farm (F6) contains veins of calcite. Grunerite was found in minor quantities north of Festung Mountain (H2).

The second type of iron formation was found only on the farm Klein Aus at Glatter Rücken (G3) and near Zipfel Hill (G4). This formation is a virtually monomineralic rock consisting of cryptocrystalline grey haematite. The haematite bodies are surrounded by pegmatoid mobilizate or granite gneiss; they may be restite bodies formed by concentration of certain elements during the melting of their host rocks. In contrast the iron formations of the first type are likely to be metamorphosed chemical sediments because of their association with rocks of sedimentary origin such as magnetite metaquartzite.

7. *Mafic Metamorphites*

Map units: *Gb10 Granolite*
Gb11 Amphibolite
GB12 Epidote schist

This group of rocks is collectively referred to by the general term 'metabasites' which is used here to describe metamorphosed mafic rocks of igneous or sedimentary origin. These rocks contain ferromagnesian minerals in excess of 30%, together with plagioclase and quartz.

Granolites

The granolites contain hypersthene, plagioclase and, usually, hornblende, biotite or quartz; half the specimens contain diopside in addition. These rocks belong to a group of granulite facies metamorphites, the nomenclature of which is still the subject of debate. The generally accepted definition of 'granulite' (Mehnert et al., 1972) does not include mafic rocks; these high-grade metabasites cannot therefore be termed 'mafic granulites'. De Waard (1973) suggested the term 'pyriclasite' for rocks containing clinopyroxene or orthopyroxene and plagioclase and this term is also recommended by the consensus of Mehnert et al., (1972). However, this definition would include other diopside-bearing and plagioclase-bearing rocks of the Aus area (granofelses and diopside amphibolites) which are not confined to the granulite zone and should not be included with granulite facies metabasites. Berthelsen's (1960) original definition of pyriclasite restricted the term to rocks that contain *both* orthopyroxene and clinopyroxene; but this conflicts with the presently accepted usage of term (Mehnert et al., 1972).

In view of the confusion inherent in the terms 'granulite' and 'pyriclasite' the proposed terminology of Winkler and Sen (1973) is used in this report. The orthopyroxene-bearing metabasites of the Aus area will therefore be termed hypersthene-plagioclase granolites (diopside-free) and hypersthene-pyroclase granolites (diopside-bearing).

The granolites are restricted to the east-centre of the area and are interlayered with other rocks of the Garub sequence such as aluminous gneiss and biotite schist.

The largest concentration of granolites is on the farm Augustfelde (G6, F6). Scattered outcrops outline an ovoid body, at least 9 km in length, which is named the 'Horab River body' (after the drainage channel which cuts through its centre). The subcircular shape and apparent homogeneity of the body are compatible with an igneous origin, but no transgressive contacts with other Garub rocks are exposed and this granolite body is lithologically and structurally identical to the other granolites.

The granolites are dark-grey or black compact rocks; they are granoblastic or nematoblastic. Platy-quartz segregations and banding, defined by variations in mafic mineral content, are present in places. In the Horab River body the granolites display in one locality a fragmental texture: lenticular fragments (up to 5 cm wide and 20 cm long) of fine-grained granolite are set in a matrix of similar material (Plate 6). This texture resembles that of a flattened and deformed agglomerate.

The estimated modes of the granolites are given in Table 7. Table 8 shows the average mode of the diopside-free and diopside-bearing granolites and enables the following conclusions to be made:

(i) Both types of granolite are equally abundant

(ii) All granolite specimens contain either biotite or hornblende; half of the specimens contain both minerals

(iii) The diopside-bearing types contain slightly more mafic minerals

(iv) The proportion of hypersthene in each rock type is virtually identical

(v) Diopside appears to develop largely at the expense of hornblende and, to a lesser extent, plagioclase

(vi) Biotite shows a nearly four-fold increase in the hypersthene-pyroclase granolites, but the proportion of quartz and opaque minerals is virtually the same in both groups.

The two varieties of granolite are identical in their geological setting: both are present in the Horab River body and in the adjoining metasedimentary sequences and their distribution cannot be correlated with changes in metamorphic grade. Both types of granolite show similar textural relations and will therefore be discussed together.

The granolites are all fine grained or medium grained and most specimens have a seriate grain size distribution. The granolites are granoblastic with crystal margins being straight or slightly curved (plagioclase and hornblende) or embayed (pyroxenes). Small pyroxene crystals are often present at the triple point junctions of polygonal plagioclase grains. Preferred orientation is commonly shown by laths of biotite and, occasionally pyroxene.

Hypersthene is the diagnostic mineral of the granolites and its texture dominates these rocks. Figure 9a shows a common habit which is typically

TABLE 7

Estimated modes (in volume percentages) of hypersthene-plagioclase granolites (top) and hypersthene-pyroclase granolites (bottom) from the Garub sequence. x = *Horab River body;* m = <1%

Specimen	Hypersthene	Diopside	Plagioclase	Quartz	Hornblende	Biotite	Opaque minerals	Locality
MJ248	25	-	70	-	3	3	1	G5
MJ250	40	-	50	5	-	2	2	G5
MJ377	40	-	55	-	5	-	2	J7
MJ378	25	-	30	15	25	2	3	J7
MJ379	25	-	45	-	30	1	-	J7
MJ425	50	m	40	15	-	3	2	G7
MJ448	30	-	25	20	15	3	5	G6
MJ740	15	-	40	-	40	3	2	H4
MJ801	25	-	40	25	1	10	1	H3
MJ1079	45	-	45	-	1	3	5	D6
MJ326[x]	25	m	60	5	m	1	6	G6
MJ268[x]	30	10	40	5	15	-	3	G6
MJ327[x]	40	10	30	-	-	20	1	G6
MJ437[x]	20	10	15	-	55	-	-	G6
MJ1312A[x]	20	10	65	-	-	2	3	G6
MJ266	35	5	20	-	20	20	-	G6
MJ345	20	20	55	-	2	4	-	G6
MJ362	10	20	55	5	m	7	5	I8
MJ412	30	10	25	15	-	15	6	J8
MJ427	25	20	50	-	-	3	1	G7
MJ455	45	10	35	-	5	2	3	G6
MJ505	25	15	30	10	10	5	4	E7
MJ541	40	5	40	10	-	6	1	E8
MJ1309	25	15	55	-	-	6	1	G7
MJ804	30	7	40	15	-	1	5	H3

present in granolites with a large proportion of pyroxene: highly irregular grains of hypersthene are in optical continuity and are in places elongated parallel to their 'Z' axes resulting in a nematoblastic texture; rounded inclusions of plagioclase are common. Figure 9b shows a texture typical of pyroxene-poor rocks: minute xenoblastic granules of hypersthene are evenly distributed and enclosed in large grains of plagioclase. Figure 9c illustrates hypersthene in the form of aggregates of xenoblastic crystals bounded by

TABLE 8

Average estimated modal compositions of hypersthene-plagioclase granolites and hypersthene-pyroclase granolites in the Aus area

	Hy	Di	Pg	Qz	Hb	Bi	Oq
Hypersthene-plagioclase granolites (n=11)	31	0	45	8	11	2	3
Hypersthene-pyroclase granolites (n=14)	28	12	39	4	8	7	2

straight asymmetrical crystal margins producing a polygonal texture.

The orthopyroxene was confirmed to be hypersthene by electron microprobe analysis (Appendix 5). The mineral is invariably pale coloured and shows pleochroism characteristic of hypersthene. No twinning or zoning or exsolution - features characteristic of orthopyroxene crystallized from a magma - was found in any of the specimens. Hypersthene is occasionally rimmed by hornblende; but apart from this, the pyroxene is remarkably well preserved and only 10% of specimens showed alteration to biotite, epidote and chlorite.

Diopside is of identical form and habit to the hypersthene. Electron microprobe analyses (Appendix 5) show that this mineral is salite (i.e. iron-bearing diopside) but it is referred to here by the more familiar and general term 'diopside'. Its colour is pale green and pleochroism is absent or very weak. Rare twinning was observed, but no exsolution was found. Like the hypersthene, diopside is extremely well preserved. In a few thin sections rimming by hornblende was observed and in one specimen the pyroxene has altered along fractures to opaque minerals and to dark-green and red spinel.

Plagioclase is the most abundant mineral in the granolites and is usually in the form of xenoblastic equant grains. Boundaries between adjacent plagioclase grains are straight or curved and usually asymmetric. Microprobe analyses showed that the anorthite content of the plagioclase in the granolites varies between An_{70} and An_{96} with a mean of An_{82}. In half the specimens plagioclase is saussuritized. No zoning was visible in thin section (microprobe analyses showed slight reversed zoning).

Hornblende is present in two thirds of the granolites examined, occurring in two different habits:

(i) *Polygonal:* equant grains with straight asymmetric boundaries against adjacent hornblende crystals and embayed margins against adjacent grains of pyroxene. Rounded blebs of hornblende are rarely enclosed within the hypersthene but the contact of the two minerals is smooth with no evidence of reaction.

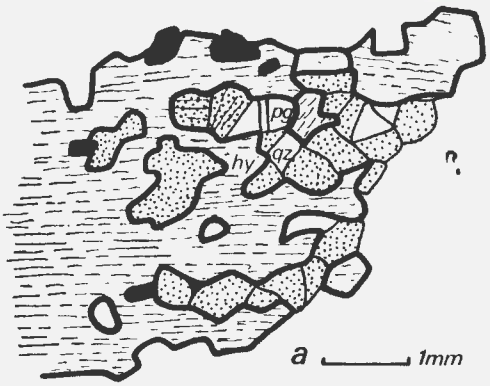

Figure 9.
Sketches of hypersthene in Garub granolites:

(a) large amoeboid xenoblasts of hypersthene in optical continuity. MJ455. 6 km WSW of Augustfelde farmhouse, 1 km NW of railway (G6)

(b) small scattered granules of hypersthene. MJ425. 7 km W of Jakkalskop farmstead (G7)

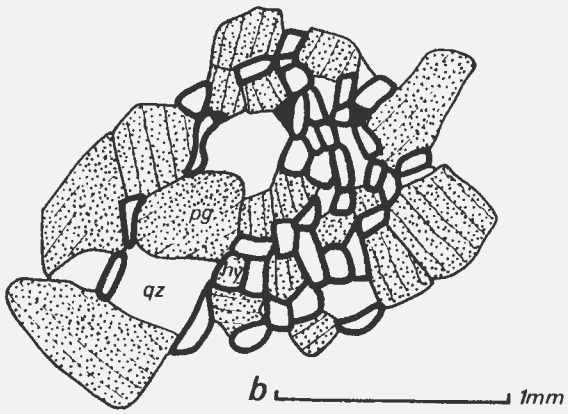

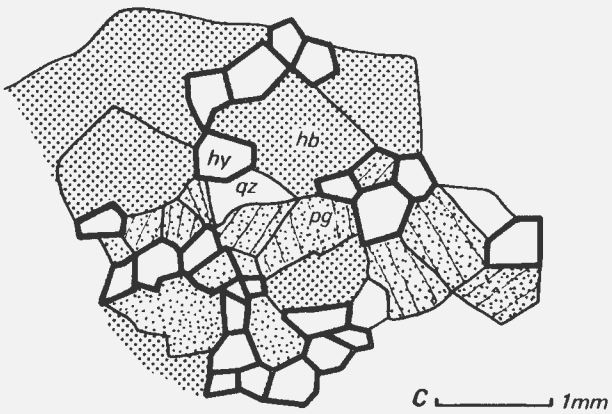

(c) xenoblastic hypersthene in granoblastic-polygonal texture with straight assymmetrical boundaries and triple-point junctions. MJ437. 3 km NW of Augustfelde farmhouse (G6)

(ii) *Closely associated with pyroxene and with irregular boundaries:* hornblende commonly surrounds the pyroxene as a thin rim; these rims may join with optically continuous amoeboid crystals of hornblende. The boundary between hornblende and pyroxene is smooth or, more usually, highly ragged with thin stringers of hornblende penetrating the cleavage planes of the pyroxene.

The hornblende is usually fresh but is rarely altered to chlorite.

Biotite is a common accessory mineral and is present in about 85% of the specimens, usually in the form of subidioblastic laths with preferred orientation. Where enclosed in pyroxene crystals the laths are in optical continuity

with each other. Biotite appears to be in equilibrium with pyroxene.

Quartz is a rare accessory mineral and is commonly in the form of segregations which are several millimetres in length and composed of medium-grained aggregates of clear quartz crystals. Quartz is also in the form of small scattered grains. The quartz grains are generally free of submicroscopic inclusions but often enclose blebs of pyroxene, plagioclase or biotite, together with minute inclusions of fluid rich in carbon dioxide.

Opaque minerals are consistently present in small amounts. Ilmenite and magnetite are present as scattered subidioblastic grains or, in rare cases, as idioblastic prisms.

Amphibolites

Amphibolite is one of the most common rock types of the Garub sequence; it is present throughout the study area and is especially abundant in the north.

The amphibolites are melanocratic rocks consisting mainly of hornblende, plagioclase and quartz. Their appearance varies with metamorphic grade. The high-grade amphibolites in the centre of the area are indistinguishable from the granolites in hand specimen: diopside-bearing varieties have a weak foliation, whereas diopside-free varieties are well foliated. The medium-grade amphibolites, which are found mainly in the north and north-west of the area, are greenish because of the difference in mineralogy of the hornblende and the presence of epidote (see Section 4.1.).

Most commonly the amphibolites are interlayered with metasediments and this intercalation may be on a very intricate scale with units being from 5 mm to 100 m thick (Plate 5 and Figure 3).

The repeated intercalation of amphibolite and marble illustrated in Figure 3 (accentuated by isoclinal folding) suggests that in this case the amphibolite is likely to have been derived from marls and is thus of metasedimentary origin (as suggested on chemical grounds for some Nosib Group metabasites by Nash, 1971). Amphibolite may occur as discrete units of much larger size such as on Excelsior Farm (B7) and Kwessiepoort Farm (F7).

Rarely, amphibolite is in the form of subcircular plugs as in the outcrops east of Magnettafelberg (D2). They may represent intrusive bodies formed early in the geological history of the area. They appear to crosscut the banding in the surrounding metasediments in places but they are largely concordant because of later deformation. Since they are very uncommon, they have not been differentiated from the other amphibolites on the geological map (Annex. 1). Slightly transgressive sill-like bodies (not shown on the map) are present on Löwenberg Farm (E5) and 4 km southwest of Kleinspitz Hill (E3). These metabasite bodies are of the same metamorphic grade as the country rocks.

The amphibolites are conveniently divided into diopside-bearing and diopside-free varieties. The former group is more common in the area adjoining the granolites and is described separately in the following section.

Petrography of the diopside amphibolites: The mineralogy of the diopside amphibolites is shown in Table 9. Diopside is abundant (average content 20%)

and so is hornblende but less so than in the diopside-free amphibolites (28% average content vs. approximately 50%); sphene is rare and epidote-group minerals are absent.

TABLE 9

Estimated modes (in volume percentages) of diopside amphibolites from the Garub sequence. Retrograde minerals in parentheses
m = <1%

Specimen	Hornblende	Diopside	Plagioclase	Quartz	Biotite	Opaque minerals	Other sphene *sn* zoisite *zo*	Locality
MJ272	50	10	20	20				H5
MJ546	40	15	30	10			3 *sn*	D8
MJ185	30	15	35	20				J3
MJ32	20	15	45	15	7			G5
MJ20	10	15	20	40	15			G2
MJ936	10	20	50	20		3		G4
MJ139	40	15	35	7		2		G4
MJ2025	35	15	30	20				H4
MJ1087	20	15	65					G4
MJ105	50	20	15	10	5			E3
MJ85	30	20	15	15	20			E4
MJ92	30	20	25	25		m		E5
MJ95	20	25	30	20			5 *sn*(m *zo*)	E4
MJ784	20	30	35	15				G2
MJ155	25	35	40	5				G4
MJ641	35	35	20	5				E5
MJ1319	15	40	40	5			2 *sn*	J1

These rocks are fine grained and inequigranular, usually seriate. Two thirds of the specimens are granoblastic and one third are granoblastic-polygonal; the majority of the latter were collected from the vicinity of the granolites. The diopside amphibolites are generally unfoliated but hornblende crystals show a weak alignment in places; if present, biotite defines a foliation but is only present in small quantities. Banding produced by variations in mafic content is present in some specimens. Poikiloblastic textures are rare but hornblende and diopside are commonly intergrown.

Basal sections of hornblende are equidimensional and xenoblastic; longitudinal sections have rational boundaries. Rounded inclusions of quartz and plagioclase are rarely present. The hornblende is almost invariably green-

brown or brown.

Diopside has the form of colourless irregular crystals with embayed margins. Electron microprobe analyses indicate that the composition of this mineral is that of salite (Appendix 5); it is slightly more calcic than the diopside in the granolites (as reported by Binns, 1965, for metabasites of the Broken Hill area). The mineral is usually fresh but in a few specimens it is altered to pale-green biotite along its cleavages.

Plagioclase is the most abundant mineral and has the form of equant xenoblasts evenly distributed through the rock. Grain boundaries between adjacent plagioclase grains are straight or curved, whereas those against other crystals are scalloped. In most specimens the plagioclase is partially or wholly saussuritized. Quartz is also abundant and has the form of xenoblastic equant grains.

Biotite is a common accessory mineral and is present in appreciable amounts (7-20%) in two thirds of the specimens. Prograde biotite is almost always red or red-brown.

Sphene is rare and occurs as small ovoid crystals or as granoblastic-polygonal aggregates of large crystals. Zoisite is present as a rare alteration product of plagioclase.

Petrography of the diopside-free amphibolites: Most of these rocks are fine-grained. There is a correlation between mineral content and texture: granoblastic and granoblastic-polygonal textures characterize the sphene-free and epidote-free amphibolites; hornblende crystals with ragged borders or many inclusions are more common in the epidote-bearing varieties. The frequency of these textures in the different varieties of diopside-free amphibolites is shown in Table 11.

TABLE 11

Percentages of diopside-free amphibolite specimens containing hornblende with ragged borders or abundant inclusions

Epidote-bearing amphibolite	60
Sphene-bearing amphibolite	33
Biotite-bearing amphibolite	31
Other amphibolite	20

The ragged or poikiloblastic textures indicate a lower metamorphic grade than that of amphibolites in which granoblastic-polygonal textures predominate (Spry, 1969, p.278). Binns (1964) described change from ragged boundaries to smooth straight boundaries and a decrease in the number of inclusions with increasing metamorphic grade in the Broken Hill area. In the Aus area there

TABLE 10

Estimated modes (in volume percentages) of diopside-free amphibolites from the Garub sequence. Retrograde minerals in parentheses
m = <1%

Specimen	Hornblende	Plagioclase	Quartz	Biotite	Sphene	Epidote group	Opaque minerals	Other apatite *ap* spinel *sp* muscovite *mu*	Location
MJ256	20	70	2	2	2	3	2		H5
MJ491	40	30	30			m	3		F7
MJ969	65	12	12			10			B6
MJ977	40	50	10			1		m *ap*	B7
MJ996	65		25			10	1		B6
MJ990	65	15	15			5			B6
MJ960	50	40	5	2			2		B6
MJ1054	45	30	10	10	5	m			B7
MJ1061	40	50	5	2	4				A7
MJ397	30	30	20	10	5	3			D1
MJ1350	40	25	25	5	m				B8
MJ835	25	50	20		2	2			D2
MJ958	60	30	5		2	2			B6
MJ980	70	10	15		5				C7
MJ559	80	10	5		5				B8
MJ1044	80	10	5		3	2			C7
MJ1053	25	55	15		5	2			B7
MJ974	45	25	25				1		B7
MJ1012	50	25	25						B6
MJ1020	55	30	15						B7
MJ1348	30	65	3		1		m		B8
MJ1027	90	10				m		(m *mu*)	B7
MJ1349	40	60					m		B8
MJ1021	80	10	10						B7
MJ1031	20		75	(5)			1		B7
MJ400	20	70		7					D1
MJ470	40	40	10	7			2		F6

TABLE 10 (continued)

Specimen	Hornblende	Plagioclase	Quartz	Biotite	Sphene	Epidote group	Opaque minerals	Other apatite *ap* spinel *sp* muscovite *mu*	Location
MJ764	80	10			5			2 *sp*	D2
MJ56	50	45	5			(m)	2		F4
MJ102	30	30	30				5		E3
MJ249	50	40	10						G5
MJ287	40	45	15				1		J6
MJ314	55	35	15						N7
MJ424	45	40	10				2		J8
MJ492	25	40	25				10		F7
MJ831	50	45	5				m		D1
MJ864	45	40	10				3		G2
MJ5	35	40	20	3					G2
MJ296	70	12	12	m			3		K6
MJ302	70	15	5	7			2		L6
MJ487	60	30	7	2			m		E7
MJ747	60	20	15	5		(m)			D2
MJ901	30	30	35	7			2		F2
MJ1314	65	15	15	5					G1
MJ83	50	25	20				6		F4
MJ183	60	30	10						J3
MJ515	65	25	5				5		E7
MJ510	55	45							E7
MJ798	65	20	15				2		H3
MJ13	60	20	15	5					G2
MJ28	25	65	10	m			2		F5
MJ49	40	40	15	2			3		G4
MJ84	40	40	15				5		F4
MJ392	80	15	5	2					D1
MJ545	70	12	8	7			3		D8
MJ712	40	45	10	m			5		E3
MJ196	25	30	40		7				K3

is no obvious difference in grain size between any of the four groups shown in Table 11 but there is a tendency towards equivalence in grain size with increase in metamorphic grade. The amphibolites are generally weakly foliated; biotite produces a strong lepidoblastic fabric and hornblende produces a weaker nematoblastic fabric. The lower-grade varieties contain decussate aggregates of amphibole laths.

The modes of the diopside-free amphibolites are shown in Table 10. The average content of hornblende in the biotite-bearing, epidote-bearing and sphene-bearing varieties is the same. The appearance of hornblende varies greatly with its metamorphic grade: in the high-grade amphibolites the crystal boundaries of hornblende are straight or gently curved; in the lower-grade amphibolites the mineral is in the form of subidioblastic laths with crystal boundaries being irregular and sutured. Hornblende is almost always fresh but rarely has altered to chlorite and to biotite.

Plagioclase is similar in appearance to that in the diopside amphibolites. The composition of specimens analysed by electron microprobe varies between An_{35} and An_{95}. Quartz is an essential constituent of virtually all the amphibolites and forms scattered equant xenoblasts.

Biotite is present in about 40% of the specimens, varying between 1% and 10% volume. It is the sole potassic mineral in the amphibolites. In medium-grade amphibolites biotite is present as small brown evenly-distributed xenoblasts with ragged crystal boundaries. In the high-grade amphibolites biotite displays two habits: more commonly that of well-oriented subidioblastic flakes concentrated into bands; more rarely that of polygonal grains. Biotite is seldom fresh and has altered to muscovite and ilmenite or chlorite; rarely biotite rims grains of hornblende.

Sphene is common. Where present in quantities of less than 3% it has the form of scattered ovoid grains but in larger amounts it occurs as aggregates of irregular crystals with lobate margins.

Epidote-group minerals are rare but where present comprise up to 10% by volume of the rock. Epidote occurs as very pale yellow-green prisms or as small colourless granules, apparently retrograde, on the margins of other grains. Zoisite is less common and has the form of small granules.

Scattered grains of opaque minerals are almost invariably present in the sphene-free amphibolites. Because the abundance of sphene is inversely proportional to that of the opaque minerals, this suggests that the opaque minerals are predominantly ilmenite rather than magnetite (as suggested by Leake, 1965).

Zircon is rare and is present as minute rounded inclusions in hornblende. Apatite is equally rare and is present in leucocratic parts of the rock. Dark green spinel is present in one specimen as intergranular xenoblastic crystals.

Epidote schists

These are quartz-epidote-chlorite schists, which are predominantly green or yellow-green in colour.

Just north of Aus Village, where high-grade metamorphic assemblages predominate, a mappable formation of epidote schist is interlayered with a partially remobilized epidote-bearing pink quartz-feldspar rock (described on p. 37). Other patches of retrograde epidote-bearing rocks are dispersed through the centre of the area but have not been mapped separately because of their small size. In the same area greenish biotite gneisses have been chloritized; metasediments show epidotization along veins, fractures and shear zones. This is attributed to a later phase of retrograde metamorphism. Northwest of Magnet-

tafelberg (D2) epidote schists are common, some of which are apparently associated with and caused by late-stage kink-folding and are therefore retrograde; but the presence of epidote in these rocks is compatible with a drop in regional metamorphic grade (indicated by mineral changes in metapelites and calcareous rocks) of the widespread earlier regional metamorphic event accompanying migmatization. South of the Excelsior mylonite belt (B7) epidote schists and talc schists (see following section) are present together with medium-grade amphibolites and cummingtonite schists. This association suggests that the low-grade schists here have been produced by retrogression of medium-grade mafic and magnesian rocks.

The quartz-epidote-chlorite schists are medium-grained or fine-grained equigranular rocks. A strong foliation is produced by the alignment of chloritized biotite and opaque minerals. The epidote minerals show a decussate texture where present in large quantities. The rocks can be finely banded due to variations in the quartz/epidote ratio but they are usually massive. The schists are commonly cut by veins of quartz and epidote.

Quartz has the form of large xenoblasts with smooth grain boundaries enclosing epidote grains. Epidote is present in the form of yellow-green idioblastic laths or irregular aggregates of xenoblastic granules. Brilliant pink-mauve crystals of piedmontite with ragged boundaries take the place of epidote in places. Clinozoisite and zoisite are also present. In one specimen remnants of brown biotite are preserved but in most cases abundant green chlorite has replaced it. Plagioclase, microcline and opaque minerals are also present.

8. Magnesian metamorphites

Map units: *Gb13 Cummingtonite schist*
Gb14 Chlorite schist

These rocks consist predominantly of magnesium-rich minerals such as cummingtonite, tremolite, chlorite and talc.

Cummingtonite Schist

The cummingtonite schists are rare and outcrops are less than 100 m thick. The schists are present at Glockenberg Mountain (C1) and in the hills in the southeast part of Excelsior Farm (B7, C7). Other occurrences, too small to show on the map (Annexure 1), are southwest of Magnettafelberg (D1) and in the southern foothills of the Kuckaus Mountains (K3).

The cummingtonite schists are dark-green medium-to-coarse-grained rocks which commonly show a foliation defined by alignment of amphibole laths. Amphibole constitutes 70-100% of the rock. The amphibole is in the form of colourless or very pale-green laths up to 4 mm in length. It has the optical properties of tremolite-actinolite (including the negative sign) but electron microprobe analysis of one specimen indicated a composition equivalent to cummingtonite:

$$(Mg_{4,4}Fe_{2,5})(Si_{7,9}O_{23})$$

It is probable therefore that these schists contain a mixture of amphiboles, mainly tremolite and cummingtonite. Small amounts of plagioclase and quartz are present in some specimens and traces of chlorite, muscovite, epidote and opaque minerals were also found.

Chlorite Schist

Like the other magnesian rocks of the Garub sequence, the chlorite schists are rare: mappable formations are confined to the hills in the southeast part of Excelsior Farm (B7, C7). The schists are associated with a large mass of amphibolite. The maximum thickness of this chlorite-schist horizon is about 150 m. Chlorite schist on the northern margin of the Excelsior Hills is cataclastic because of its proximity to the mylonite belt. On the southern margin of the hills the chlorite schist has been deformed by late-stage chevron folding.

The chlorite schists are pale green-grey and fine grained with a strong foliation. They consist mainly of small flakes of chlorite with a strong preferred orientation. Subidioblastic laths of colourless amphibole with the optical properties of tremolite, in amounts varying from 10% to 30% by volume, constitute the remainder of the rock; the amphibole is partially altered to talc. Small amounts of plagioclase and quartz are present in places.

The restriction of chlorite schist to occurrences of cummingtonite schist and its association with late-stage deformation suggest that the chlorite schists represent retrograded cummingtonite schist which altered more readily than did the amphibolites.

9. *Garub Sequence: Relative Abundance, Degree of Association and Type of Association of Component Units*

Considerations in Map Compilation

The distribution of the Garub sequence is shown on the geological map (Annexure 1). In many outcrops more than one Garub rock type is present; for example, west of Magnettafelberg (D1), hornblende schist contains thin intercalations of marble, amphibolite and metaquartzite. These intercalations are symbolized on the map as *Gb5:1:11:8*. The colon preceding the units 1,11 and 8 signifies that the rock types represented by these numbers are present in small amounts which are not sufficient to affect the naming of the unit as a whole.

In other outcrops, however, two or three rock types may be present in equal abundance. This situation produces difficulty in the naming of the formation; the proportion of components commonly varies over short distances so that the formation may have a completely different character nearby.

In view of these difficulties parts of the map were compiled selectively and it is therefore necessary to state the bias involved. Compilation was intentially biased against rock types that were extremely abundant or were not

restricted to a particular area (e.g. biotite schist and amphibolite); it was unavoidably biased against rocks that usually occur in association with other rock types (e.g. metaquartzite). Conversely compilation was intentionally biased towards rare rock types (e.g. magnesian and ferruginous types) or towards those that are restricted to certain zones (e.g. marbles, granofels and granolite). At outcrops containing only one rock type no bias in representation was necessary.

Because of the bias involved in its compilation and because much data were excluded, for reasons of clarity, the geological map cannot be reliably used for quantitative estimates of the abundance and degree of association of the components of the Garub sequence. Accordingly, the original field data have been processed to provide such estimates and the results are given below. These quantatitive results are intended to replace vague generalizations such as 'Rock A is fairly common' or 'Rock B frequently contains intercalations of Rock C'.

Data Collection

Units of the Garub sequence are present throughout the 10 000 km^2 study area. These units constitute only a small part of the basement complex which, in turn, is largely obscured by younger formations or overburden. For this reason the areal extent of exposed Garub rocks is only about 230 km^2. A total of 603 localities of Garub rocks were visited during mapping; each locality represents a single sampling station for structural and lithologic data and varies in area from approximately 15-5000 m^2. Sampling density is thus approximately 2,5 stations/km^2. A total of 961 separate rock types of the Garub sequence were recorded at the 603 sample stations; sample stations therefore contain an average of 1,6 different rock types. Sampling was not random because it was controlled by the outcrop pattern. Sample stations were evenly distributed within this outcrop pattern.

At each station the following points were recorded (See Appendix 1):

(i) What units were present

(ii) The relative abundance of each unit in terms of major (>20%) and minor (<20%) quantities

The rock types were therefore graded according to quantity as *major components* or *minor components*. The distinction between major and minor components is necessary because some rocks are almost always present as major components (e.g. aluminous gneiss and biotite schist), whereas others such as metaquartzite are usually present as minor components. This distinction is important in the estimation of the relative abundance of each rock type in the area as a whole.

Input

The data from each station were punched on computer cards and then entered into a data bank. A representative part of the data listing is shown in Figure

Sample Station		Garub Rock Types 1 3 5 7 9 11 13 / 2 4 6 8 10 12 14	Map Symbol
000398	000	00020000000000	
000399	000	00020000000000	*Gb4*
000400	000	00020002002000	
000401	000	00000002002000	*Gb8.11*
000402	000	00020000002000	
000403	000	00010002000000	*Gb8:4*
000404	000	00000000002000	
000405	000	00000000002000	
000406	000	00002000001000	*Gb5:11*
000407	000	00010000002000	
000408	000	00020002002000	*Gb4.11.8*
000409	000	00020000000000	

Figure 10. Representative example of data listing

10. Each row represents a single station; each column represents one of the 14 rock types making up the Garub sequence; the numbers *2* and *1* signify the presence of a particular rock type as a major or minor component respectively; zeros signify absence.

Results

All data were processed by means of a computer programme (Appendix 2) written for this purpose by C.J.H. Hartnady. The results are described below in three parts:

(i) relative abundance

(ii) degree of association

(iii) type of association

All the results are reproduced in the form of matrices; selected results are illustrated by means of tables and bar graphs. The accompanying text explains or emphasizes noteworthy conclusions.

Relative Abundance

The simplest task of the programme was to determine the total number of times that each rock type is present at the sample stations as a major and minor component and thus provide a measure of its relative abundance.

The results are shown in Table 12 and graphically displayed in part in Figure 11. The graph shows that biotite schist and amphibolite are the most common rock types, but that metaquartzite, marble and aluminous gneiss are also common. Seven of the fourteen rock types are so rare that they constitute less than 10% of all occurrences; these rock types are therefore largely ignored in the following sections because the amount of data on them is not statistically reliable and attention is focussed on the seven *principal rock types;* nevertheless results for all fourteen rock types are given in the matrices.

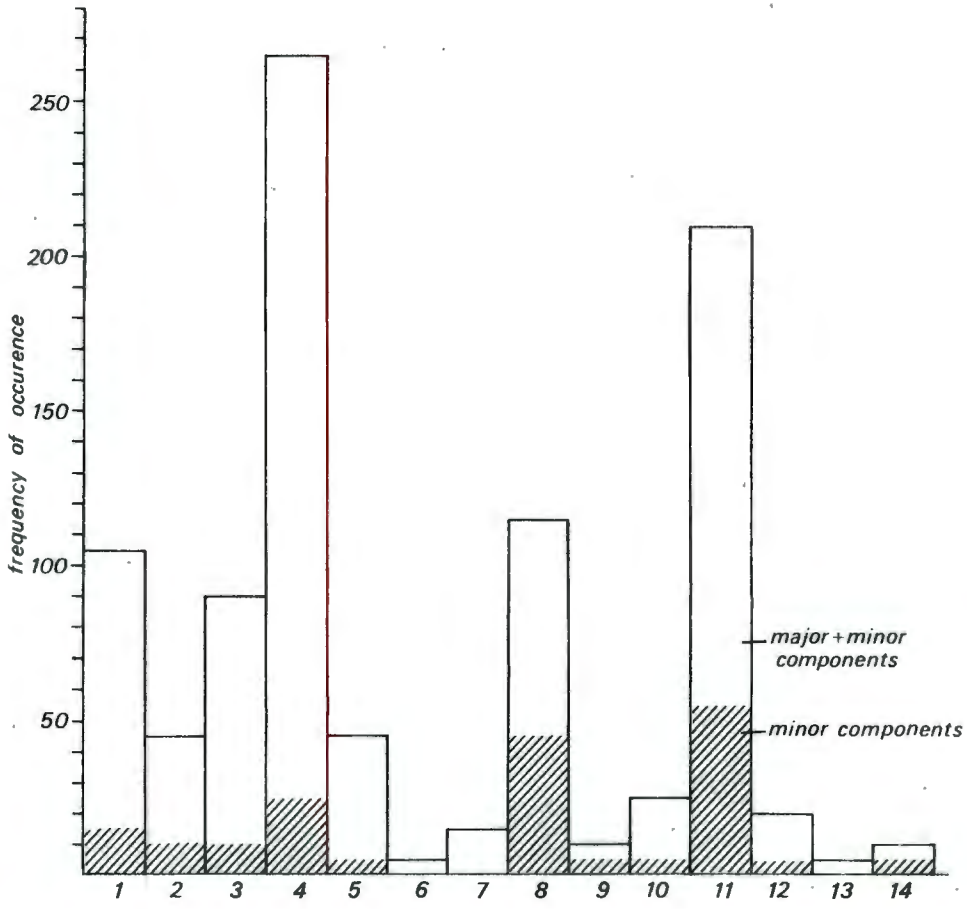

Figure 11. Bar graph showing frequency of occurrence of Garub rock types

Key:
1 marble and calc-granofels
2 granofels
3 metapelite
4 biotite schist
5 hornblende schist
6 pink qz-fp rock
7 white qz-fp rock
8 metaquartzite
9 iron formation
10 granolite
11 amphibolite
12 epidote schist
13 cummingtonite schist
14 chlorite schist

TABLE 12

Frequency of occurrence of Garub rock units

Rock unit	Major component	Minor component	Total	% Total
Gb 1	91	13	104	10,8
2	34	10	44	4,6
3	78	10	88	9,2
4	239	24	263	27,4
5	42	3	45	4,7
6	4	2	6	0,6
7	15	1	16	1,7
8	70	44	114	11,9
9	4	3	7	0,7
10	21	5	26	2,7
11	154	57	211	22,0
12	13	7	20	2,1
13	5	1	6	0,6
14	6	5	11	1,1
Σ	776	185	961	100,1

It is noteworthy that some rock types are present mainly as major components; for instance biotite schist is present as a minor component in only 9% of its occurrences. In contrast metaquartzite is present as a minor component in nearly 40% of its occurrences.

The frequency of occurrence of the major components of the rock types represents the relative abundance of the various compositional groups that constitute the Garub sequence. Table 13 shows that the Garub sequence consists mainly of semi-pelitic rocks and lesser amounts of basic, calcareous, pelitic and quartzose rocks; quartzofeldspathic, magnesian and ferruginous compositional groups are poorly represented.

Degree of General Association

The extent to which the 14 rock types are associated with other rock types of the Garub sequence is shown in the matrices of *association frequency* in Figures 12 and 13. Figure 12 consists of two symmetrical 14x14 matrices showing the frequency association of major components with major components and minor with minor components, symbolized thus: major/major and minor/minor. Figure 13 is a 14x14 asymmetrical matrix showing the association frequency of the major/minor components.

Results based on the above matrices for the seven principal rock types are shown in Figure 14. Because a rock type may be associated with more than one rock type at any one station, it follows that the number of times a rock is associated with other rocks can exceed the number of times a rock was recorded; e.g. unit *Gb7* was present as a major and minor component at 16

MINOR COMPONENTS

	1	2	3	4	5	6	7	8	9	10	11	12	13	14	Gb
	0	0	0	1	0	0	0	3	0	0	2	0	0	0	1
		0	0	0	0	0	0	2	0	1	2	0	0	1	2
			0	0	1	0	0	2	0	0	2	0	0	0	3
				0	0	0	0	3	1	0	5	0	0	0	4
1	0				0	0	0	1	0	0	0	0	0	0	5
2	3	0				0	0	0	0	0	0	0	0	0	6
3	0	1	0				0	0	0	0	0	0	0	0	7
4	15	1	5	0				0	1	0	11	1	0	0	8
5	1	1	0	1	0				0	0	0	0	0	0	9
6	0	0	0	0	1	0				0	0	0	0	0	10
7	0	1	0	2	0	0	0				0	1	0	1	11
8	7	1	4	31	6	2	0	0				0	0	0	12
9	1	0	0	2	0	0	0	1	0				0	0	13
10	0	6	5	0	0	0	1	0	0	0				0	14
11	14	10	3	55	3	0	5	17	0	0	0				
12	0	0	0	4	0	0	5	0	0	0	1	0			
13	0	1	0	0	0	0	0	0	0	0	1	0	0		
14	0	0	0	3	0	0	0	0	0	0	2	0	0	0	
Gb	1	2	3	4	5	6	7	8	9	10	11	12	13	14	

MAJOR COMPONENTS

MINOR COMPONENTS

MAJOR COMPONENTS

Figure 12. Two symmetrical matrices showing association frequency of major/major components and minor/minor components of the 14 rock types in the Garub sequence

Key:
1 marble and calc-granofels
2 granofels
3 metapelite
4 biotite schist
5 hornblende schist
6 pink qz-fp rock
7 white qz-fp rock
8 metaquartzite
9 iron formation
10 granolite
11 amphibolite
12 epidote schist
13 cummingtonite schist
14 chlorite schist

MINOR COMPONENTS

MAJOR COMPONENTS / Gb	1	2	3	4	5	6	7	8	9	10	11	12	13	14
1	0	2	1	3	0	1	0	8	0	1	12	1	0	1
2	2	0	0	2	0	0	0	2	1	0	1	0	0	0
3	1	3	0	2	0	0	0	6	0	1	6	1	0	0
4	4	3	6	0	1	0	0	17	1	0	27	2	0	2
5	1	1	0	1	0	0	0	3	0	1	2	1	0	0
6	0	0	0	0	0	0	0	0	0	0	1	0	0	0
7	0	0	0	1	1	0	0	1	0	0	1	1	0	0
8	3	2	0	2	0	0	0	0	0	1	2	0	1	1
9	0	0	0	1	0	0	0	0	0	0	0	0	0	1
10	0	0	0	3	1	0	0	0	0	0	0	0	0	0
11	5	3	3	5	0	1	1	11	1	0	0	2	0	1
12	1	0	0	1	0	0	0	0	0	0	0	0	0	0
13	0	0	0	0	0	0	0	0	0	0	1	0	0	2
14	0	0	0	0	0	0	0	1	0	0	0	0	0	0

Figure 13. Asymmetrical matrix showing association frequency between major/major components of the 14 rock types in the Garub sequence.

Key:
1 marble and calc-granofels
2 granofels
3 metapelite
4 biotite schist
5 hornblende schist
6 pink qz-fp rock
7 white qz-fp rock
8 metaquartzite
9 iron formation
10 granolite
11 amphibolite
12 epidote schist
13 cummingtonite schist
14 chlorite schist

TABLE 13

Relative abundance of main compositional groups of the Garub sequence

Rock unit	Compositional groups	Percentage Abundance as major component of outcrop
Gb 1.2	calcareous	16,1
Gb 3	pelitic	10,0
Gb 4.5	semi-pelitic	36,2
Gb 6.7	quartzofeldspathic	2,4
Gb 8	quartzose	9,0
Gb 9	ferruginous	0,5
Gb 11.12	mafic	24,2
Gb 13.14	magnesian	1,4
		Σ = 99,8

stations but was associated with different rocks 19 times.

Figure 14a demonstrates that the major components of the principal rock types show a widely varying degree of association with other major components: thus metaquartzite is commonly found associated with major components of other rock types, but aluminous gneiss and hornblende schist are seldom associated. In contrast Figure 14b illustrates that each of the seven principal rock types contains similar proportions of minor components.

The degree of association provides a measure of the degree of heterogeneity of each unit. Thus on the mesoscopic scale the units are equally heterogeneous (as demonstrated by their equal proportion of intercalations), but on a larger scale there are wide variations in the degree of homogeneity.

Type of Association

The purpose of this section is to examine which particular rock types are closely associated in the field. Therefore the data for all 14 rock types are summarized in a 28x28 matrix of *association probability* (Figure 15) in which each value represents the probability that a major or minor component of any rock type will be associated with major and minor components of any other rock type. The matrix is read 'from rows to columns'; each row sums up to one.

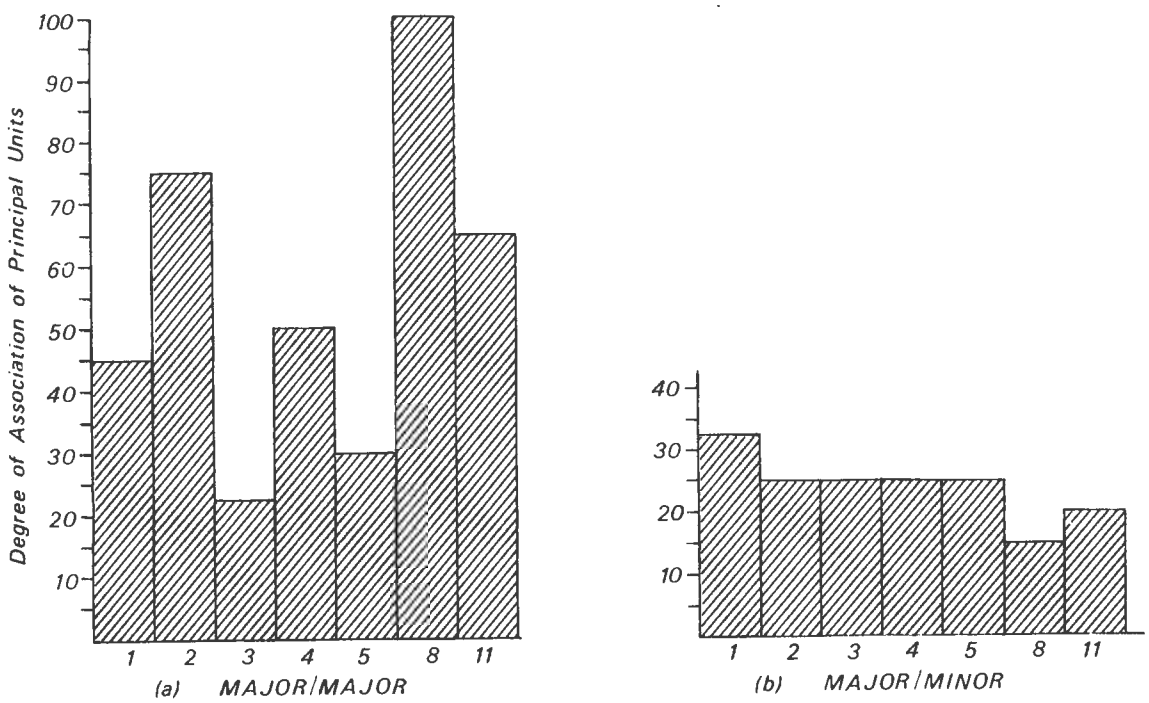

Figure 14. Bar graphs showing degree of association of the 7 principal rock types with all other (14) rock types of the Garub sequence

(a) major component with major component
(b) major component with minor component

Numbers 1-100 represent arbitrary units calculated by dividing the frequency of association of a unit by the number of its occurrences

Key:
1. marble and calc-granofels
2. granofels
3. metapelite
4. biotite schist
5. hornblende schist
8. metaquartzite
11. amphibolite

Figure 15 summarizes the associations of the seven principal rock types of the Garub sequence. Because of their abundance biotite schist and amphibolite are very frequently associated with other rocks and will therefore be discussed only at the end of this section.

Marble (Figure 16a) is commonly associated with metaquartzite and rather less so with granofels (the carbonate-quartzite association is typical of shelf-facies sediments). Conversely marble is rarely associated with aluminous gneiss or hornblende schist(which is compatible with the infrequent association of non-calcareous mud and limestones in present-day sedimentary environments).

Granofels (Figure 16b) is fairly closely associated with marble and less

	MAJOR														MINOR													
Gb	1	2	3	4	5	6	7	8	9	10	11	12	13	14	1	2	3	4	5	6	7	8	9	10	11	12	13	14
1	00	04	00	21	01	00	00	10	01	00	20	00	00	00	00	03	01	04	00	01	00	11	00	01	17	01	00	01
2	09	00	03	03	03	00	03	03	00	18	30	00	03	00	06	00	00	06	00	00	00	06	03	00	03	00	00	00
3	00	03	00	13	00	00	00	11	00	13	08	00	00	00	03	08	00	05	00	00	00	16	00	03	16	03	00	00
4	08	01	03	00	01	00	01	17	01	00	30	02	00	02	02	02	03	00	01	00	00	09	01	00	15	01	00	01
5	04	04	00	04	00	04	00	26	00	00	13	00	00	00	04	04	00	04	00	00	00	13	00	04	09	04	00	00
6	00	00	00	00	25	00	00	50	00	00	00	00	00	00	00	00	00	00	00	00	00	00	00	00	25	00	00	00
7	00	05	00	11	00	00	00	00	00	05	26	26	00	00	00	00	00	05	05	00	00	05	00	00	05	05	00	00
8	09	01	05	38	07	02	00	00	01	00	21	00	00	00	04	02	00	02	00	00	00	00	00	01	02	00	01	01
9	17	00	00	33	00	00	00	17	00	00	00	00	00	00	00	00	00	17	00	00	00	00	00	00	00	00	00	17
10	00	38	31	00	00	00	06	00	00	00	00	00	00	00	00	00	00	19	06	00	00	00	00	00	00	00	00	00
11	10	07	02	38	02	00	03	12	00	00	00	01	01	01	03	02	02	03	00	01	01	08	01	00	00	01	00	01
12	00	00	00	33	00	00	42	00	00	00	08	00	00	00	08	00	00	08	00	00	00	00	00	00	00	00	00	00
13	00	20	00	00	00	00	00	00	00	00	20	00	00	00	00	00	00	00	00	00	00	00	00	00	20	00	00	40
14	00	00	00	50	00	00	00	00	00	00	33	00	00	00	00	00	00	00	00	00	00	17	00	00	00	00	00	00
1	00	09	04	17	04	00	00	13	00	00	22	04	00	00	00	00	00	04	00	00	00	13	00	00	09	00	00	00
2	10	00	15	15	05	00	00	10	00	00	15	00	00	00	00	00	00	00	00	00	00	10	00	05	10	00	00	05
3	07	00	00	40	00	00	00	00	00	00	20	00	00	00	00	00	00	00	07	00	00	13	00	00	13	00	00	00
4	10	06	06	00	03	00	03	06	03	10	16	03	00	00	03	00	00	00	00	00	00	10	03	00	16	00	00	00
5	00	00	00	20	00	00	20	00	00	20	00	00	00	00	00	00	20	00	00	00	00	20	00	00	00	00	00	00
6	50	00	00	00	00	00	00	00	00	00	50	00	00	00	00	00	00	00	00	00	00	00	00	00	00	00	00	00
7	00	00	00	00	00	00	00	00	00	00	100	00	00	00	00	00	00	00	00	00	00	00	00	00	00	00	00	00
8	11	03	08	23	04	00	01	00	00	00	15	00	00	01	04	03	03	04	01	00	00	00	01	00	15	01	00	00
9	00	20	00	20	00	00	00	00	00	00	20	00	00	00	00	00	00	20	00	00	00	20	00	00	00	00	00	00
10	20	00	20	00	20	00	00	20	00	00	00	00	00	00	00	20	00	00	00	00	00	00	00	00	00	00	00	00
11	16	01	08	35	03	01	01	03	00	00	00	00	01	00	03	03	03	06	00	00	00	14	00	00	00	01	00	01
12	10	00	10	20	10	00	10	00	00	00	20	00	00	00	00	00	00	00	00	00	00	10	00	00	10	00	00	00
13	00	00	00	00	00	00	00	100	00	00	00	00	00	00	00	00	00	00	00	00	00	00	00	00	00	00	00	00
14	10	00	00	20	00	00	00	10	10	00	10	00	20	00	00	10	00	00	00	00	00	00	00	00	10	00	00	00

MAJOR

MINOR

Figure 15

Asymmetrical 28x28 matrix of association probability. Each value represents the probability that any rock type (represented by rows) will be associated with major and minor components of other rock types (represented by columns).

Key

Gb1 marble, calc-granofels
2 granofels
3 metapelite
4 biotite schist
5 hornblende schist
6 pink qz-fp rock
7 white qz-fp rock
8 metaquartzite
9 iron formation
10 granolite
11 amphibolite
12 epidote schist
13 cummingtonite schist
14 chlorite schist

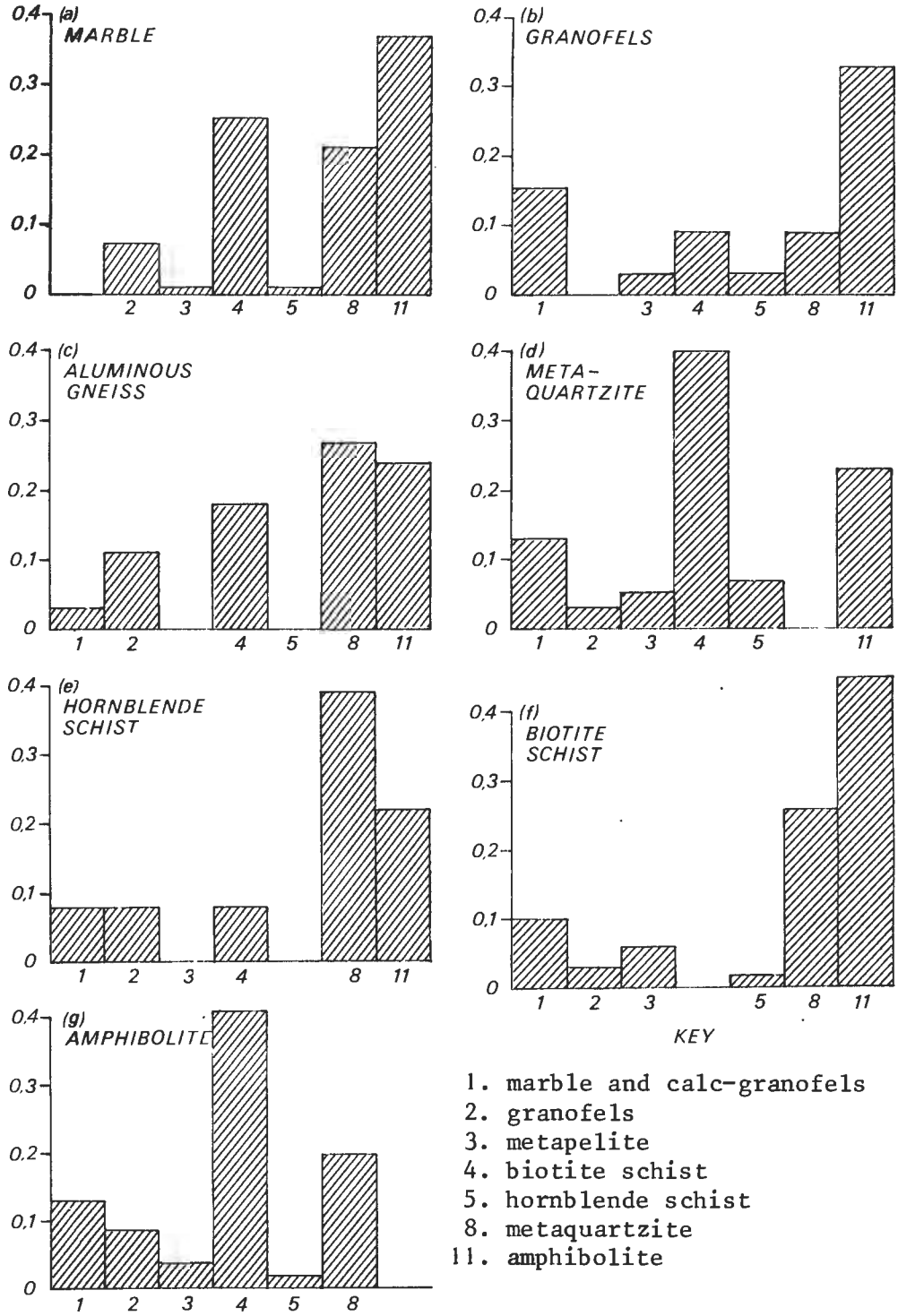

Figure 16. Bar graphs illustrating the probability of association of the 7 principal rock types with each other
Only associates of major components are considered and the probabilities of both major and minor associates are combined

so with metaquartzite (granofels is intermediate in composition between the calcareous and siliceous end-members of shelf facies sediments with additional amounts of clay). The rock type can be referred to as subcalcareous.

Aluminous gneiss (Figure 16c) is closely associated with metaquartzite and a little less so with granofels. As previously pointed out it is not commonly associated with marble.

Metaquartzite (Figure 16d) association reflects the mutually close connection with marble.

Hornblende schist (Figure 16e) is closely associated with metaquartzite. Although hornblende schist is very similar in composition to biotite schist (merely containing small amounts of hornblende in addition to the minerals in biotite schist), the two rock types are rarely associated.

It can be shown, therefore, that the above associations are compatible with the concept of variations in sedimentary facies: incompatible sedimentary facies like limestones and non-calcareous muds are rarely related in their metamorphic derivatives, whereas classic sedimentary associations such as the limestone-sandstone shelf-facies are reflected in the common association of marble with metaquartzite and granofels of intermediate composition.

Similar analogies can be used to throw light on the origins of the biotite schist and amphibolite units, the compositions of which could equally well reflect a sedimentary or igneous origin. Although amphibolite is less abundant than biotite schist, it is much more commonly associated with metasediments than is biotite schist. Amphibolite is the most common associate of the calcareous and subcalcareous group. (viz. marble, calc-granofels and granofels); this is compatible with a derivation of amphibolite from marls. In the case of hornblende schist and aluminous gneiss, amphibolite is also commonly associated but less so than metaquartzite. However, the generally high degree of association of amphibolite with such a wide variety of compositional groups could alternatively be explained by the hypothesis that much of the amphibolite is of igneous origin and is derived from basic magma that intruded the sedimentary pile in the form of a dyke-sill complex.

With regard to the origin of the biotite schist the mutually high association between this rock and metaquartzite (Figures 16f and g) is compatible with a derivation from a sedimentary succession that consisted largely of semi-pelitic sediments (i.e. largely psammitic but with a moderate proportion of clay) with intercalations of cleaner sand.

In summary, therefore, the association of biotite schist and amphibolite with the other rock types suggest a sedimentary origin for the former and a dual igneous-sedimentary origin for the latter. The statistical association of marbles, granofels, aluminous gneiss and metaquartzite suggests that all these rock types are of sedimentary origin and that they were formed in different sedimentary facies. The following section examines the distribution their gradations between these metasediments with a view to determining and palaeo-environment of deposition.

10. *Garub Sequence: Lithofacies Variations and Speculations on the Palaeo-environment of Metasediments*

During mapping it became evident that certain metasedimentary rock types predominated in certain areas; this fact was noted in a preliminary report (Jackson, 1974). It is believed that this distribution pattern may partly reflect original sedimentary facies, a possibility that is examined in this section.

The determination of palaeo-environments for highly deformed and metamorphosed sediments is extremely difficult. Many factors may have influenced the present distribution and character of the metasediments:

(i) Lithofacies variations may reflect rocks of different ages; the facies changes are therefore through time rather than through space.

(ii) Deformation has altered the original distribution of the metasediments and may have brought certain facies closer together.

(iii) Recrystallization during high-grade metamorphism has destroyed original textures so that the differentiation of sediments must be on the basis of composition alone and not on grain size.

(iv) Metamorphism may not in all cases have been isochemical, particularly in the case of migmatites in which anatexis has taken place and from which considerable quantities of melt have been removed. The estimation of original composition of some rocks is therefore subject to error.

(v) The wide scattering of the metasedimentary remnants may have resulted in key rock types being obscured by sand cover.

Nevertheless the large scale of the lithologic variations is compatible with sedimentary facies changes despite the influence of some of the above factors. The area shown in Figure 17 is more than 10 000 km^2 in extent and the width of individual lithofacies varies between 40 and 70 km.

The speculations that follow are of a controversial nature and are not definitive; they are intended to stimulate interest in other metasedimentary sequences in the Namaqua belt that are loosely grouped under the term 'Bushmanland sequence'. Studies of the type attempted here have important economic implications and may enable the prediction of rock types and their syngenetic mineralization in unmapped areas by extrapolation.

Regional Variations in Metasedimentary Lithofacies

The Garub sequence includes rock types of undoubted sedimentary parentage such as metaquartzite, marble and iron formation. The origin of the aluminous gneiss is, however, open to question; Joubert (1974b) suggested that the aluminous rocks in Namaqualand and Bushmanland were derived from leached volcanic rocks but there is no evidence of a volcanic origin for the aluminous rocks of the Aus area; the presence of graphite schist horizons and the close

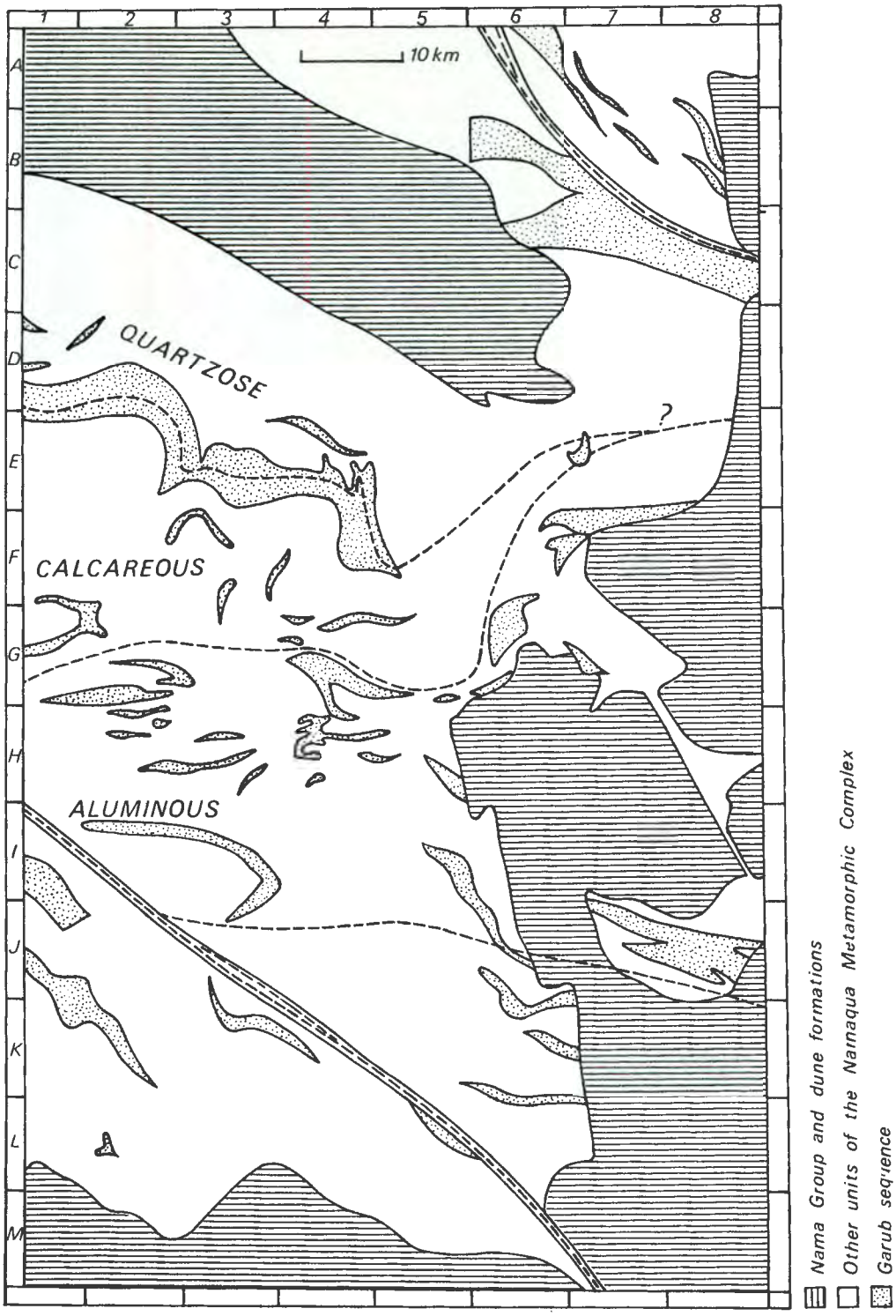

Figure 17. Lithofacies sketch map of the Garub sequence showing the concentration of calcareous, aluminous and quartzose metasediments within west-trending zones

association with metaquartzites (see previous section) suggest a sedimentary origin for the Garub aluminous gneiss. Similarly, because of its close association with marble (see previous section), granofels, which is subcalcareous, is likely to be of sedimentary origin. Disregarding iron formation because of its extreme rarity (see previous section), the four principal rock types classed as metasediments on compositional grounds are therefore the calcareous, subcalcareous, aluminous and quartzose groups.

Figure 17 indicates the concentration of these compositional groups in broad west-trending zones. The northern and southern limits of the calcareous group define a zone that increases in width westwards and, as far as can be gauged by the outcrop, lenses out eastwards. The southern boundary of the calcareous zone coincides with the northern limit of the aluminous zone. Quartzose rocks are also present in the south of the area but are especially common on the northern fringe of the calcareous zone.

Chemical Relations between Metasediments

The average compositions of the metasedimentary types referred to above have been estimated by means of their modes and the inferred composition of their constituent minerals. The chemical relations between these estimated compositions are shown in Figure 18a. The composition of the calcareous rocks varies widely because this group (*Gb1*) comprises pure marble, impure marble and calc-granofels, which contain carbonate in amounts ranging between 1 and 100%. Granofels (*Gb2*) has a subcalcareous composition intermediate between *Gb1* and both *Gb3* and *Gb8* units.

The estimated compositions of the calcareous group, aluminous group and subcalcareous group are compared in Figure 18b with those of modern sediments. The average mode of the aluminous group suggests a composition intermediate between Nockold's (*in* Winkler, 1974, p.45) aluminium-rich clays and greywackes. The mode of the subcalcareous group suggests a composition similar to that of marls (ibid.) but containing less FeO and MgO. Assuming isochemical metamorphism on a regional scale therefore, the *Gb1* and *Gb3* groups probably formed from carbonate-rich and clay-rich sediments respectively, but the *Gb2* unit is likely to have been derived from a clay-carbonate sediment mixture. The quartzose group *Gb8* (not shown in Figure 18b) would have formed from a quartz-rich sand.

Lithofacies Variations on the Margins of the Calcareous Zone

The area where calcareous rocks are exposed is enlarged in Figure 19, which shows the occurrence of the four rock types *Gb1*, *Gb2*, *Gb3* and *Gb8* (symbolized in the sketch map by numbers) including outcrops where the rock is present as a minor component and is not shown on the geological map (Annexure 1). On the northern margin of the calcareous zone, where rocks derived from carbonate-rich sediments (*Gb1*) are in contact with those from quartz-rich sediments (*Gb8*), clay-carbonate-quartz metasediments (*Gb2*) are preserved. Similarly on the southern margin of the calcareous zone, where carbonate-rich metasediments are associated with clay-rich metasediments (*Gb3*), as in the east, clay-carbonate-quartz metasediments are also preserved; but where the *Gb1* and *Gb3* units are not in contact, as in the west, the intermediate *Gb2* rock type

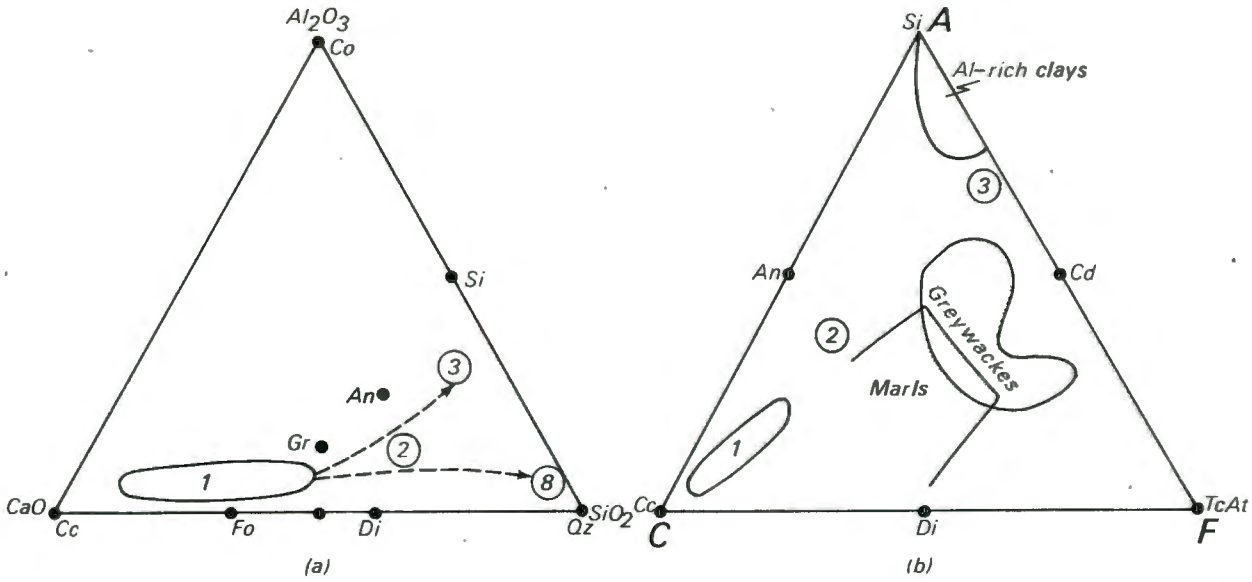

Figure 18. Ternary diagrams illustrating chemical relations between rock units *Gb1* (marble and calc-granofels), *Gb2* (granofels), *Gb3* (metapelite) and *Gb8* (metaquartzite) symbolized as 1, 2, 3 and 8 respectively. Chemical compositions estimated from modal compositions

(a) Al_2O_3 - CaO - SiO_2

(b) ACF

is not developed (or not exposed). Such gradations are compatible with facies changes in the original sedimentary environment. The maximum width of the calcareous zone, which broadens westwards, is about 40 km and the width of the aluminous zone varies between 40 and 70 km. Lithofacies changes of similar magnitude and type are produced by present-day sedimentation on the continental margin of South West Africa (Rogers, 1976).

Speculations on the Original Sedimentary Environment

Conditions for the accumulation of carbonate sediments are likely to have been present in a shallow, warm, quiet marine environment either in open sea (such as the Bahamas area) or esturinal-lagoonal (such as Florida Bay) (Bathurst, 1971). The substantial contamination with ferromagnesian material (resulting in impure marbles after metamorphism) indicates an esturine-lagoonal environment of deposition where terrigenous muds are expected to be present as well. Because calcareous rocks are rare or absent in the east but are common in the west of the study area and farther westwards (Koichab Pan area), it is likely that the basin of carbonate sedimentation broadened westwards and lensed out eastwards.

The gradation from calcareous rocks into a relatively narrow zone of granofels and metaquartzite on the northern rim of the calcareous zone is compatible with a lateral variation from the mainly carbonate sedimentation in the

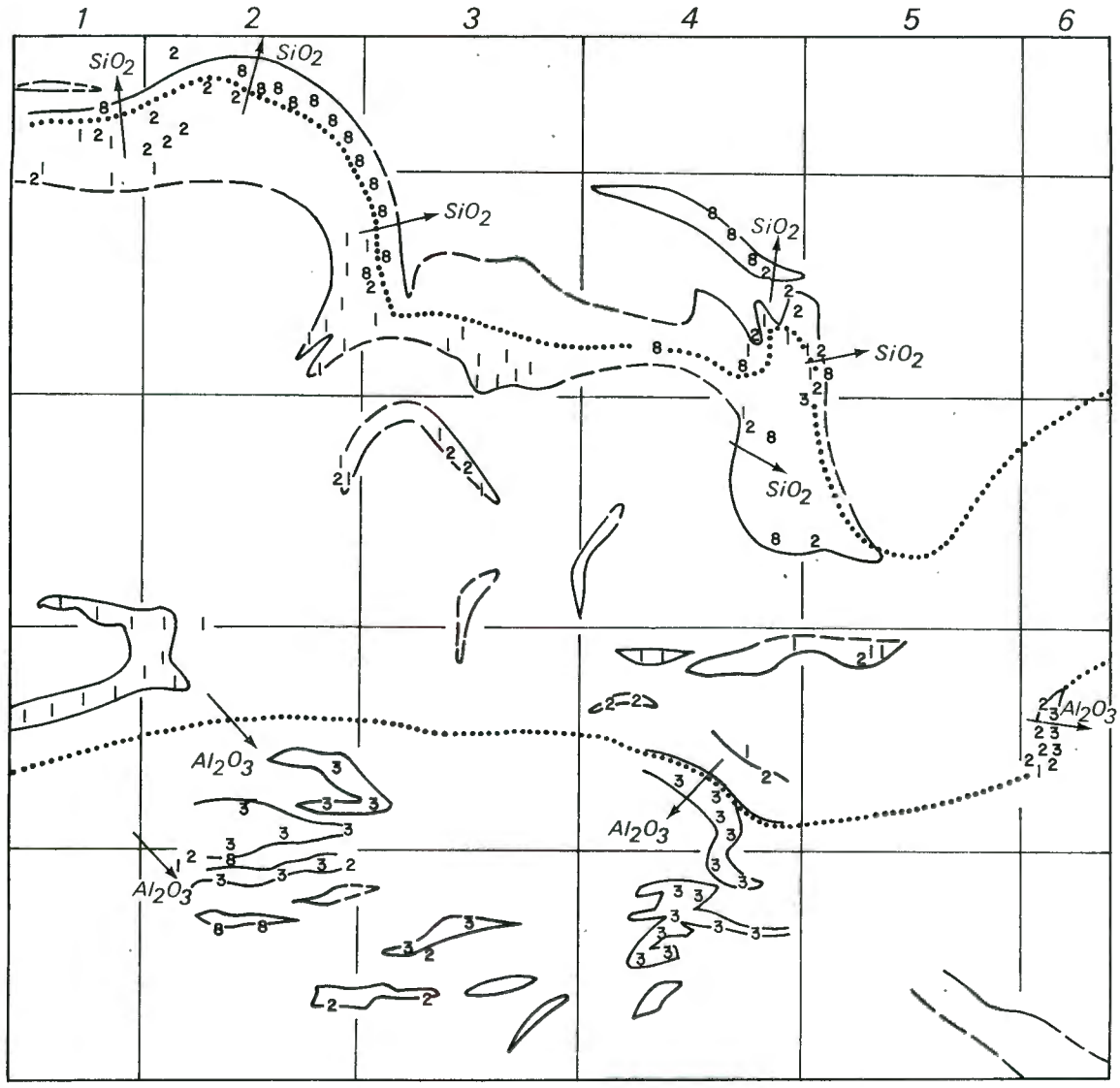

Figure 19. Lithofacies sketch map of the calcareous zone of the Garub sequence. Arrows show direction of increase in proportion of SiO_2 and Al_2O_3 in the rock types: marble and calc-granofels (1), granofels (2), metapelite (3) and metaquartzite (8)

postulated lagoon into firstly a clay-carbonate sediment and secondly quartz sand on the landward margins of the basin.

The much broader belt of pelitic rocks south of the calcareous zone may have been derived from a landmass to the south of the lagoonal system or may have been transported some distance along the coast by means of a littoral drift system. Such a system is analogous to the present-day transportation of clays southwards from the Orange River mouth for a distance of more than 300 km along the coast (Rogers, 1976). In Figure 20 two models of palaeoenvironments are suggested to explain the deposition of part of the Garub sequence. The symmetry of the lithofacies zonation, together with the extension of the carbonate rocks westwards for a distance of more than 100 km and the common association of metaquartzites and carbonate rocks in the study area and farther west, suggest that model (b) in Figure 20 may be more applicable.

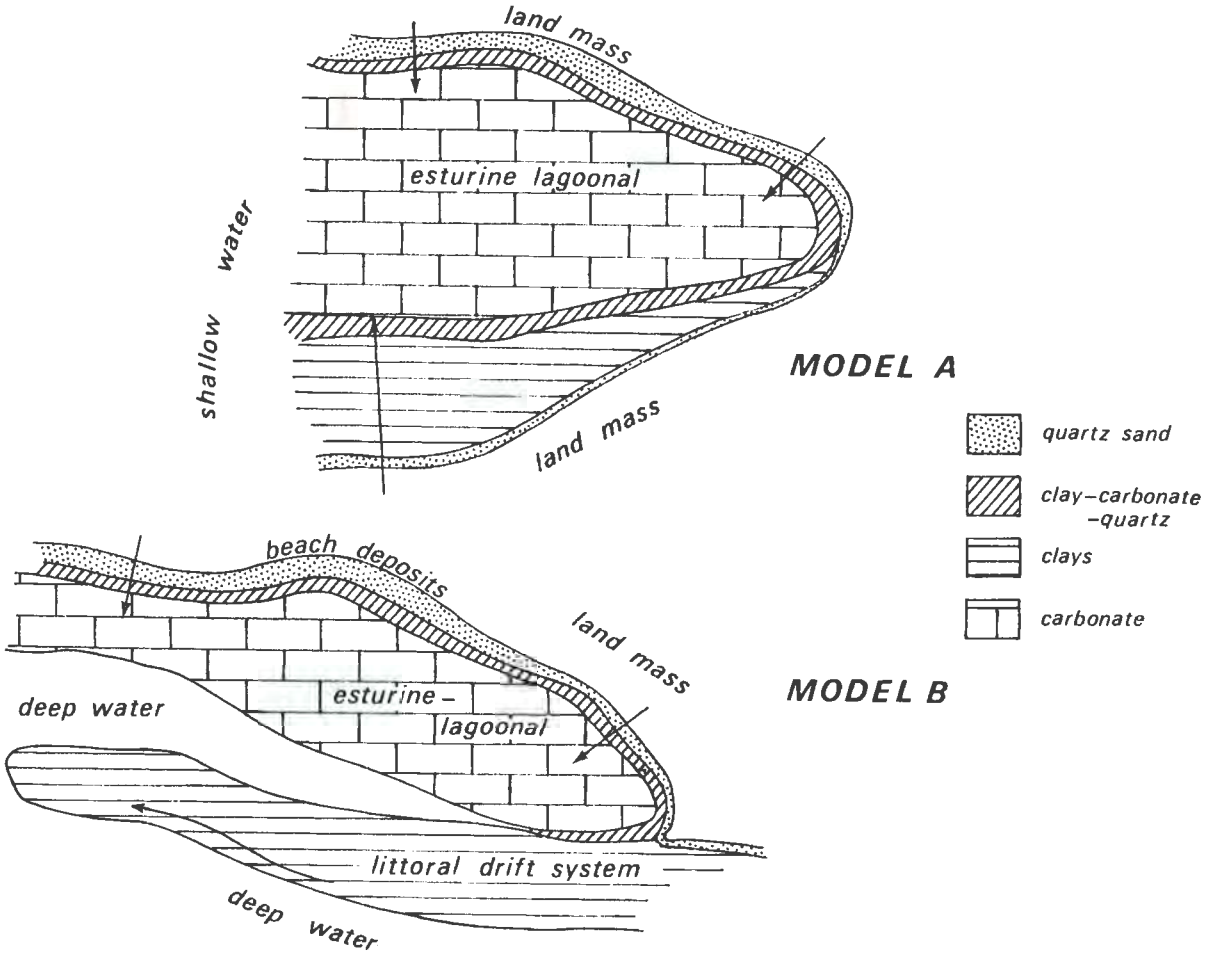

Figure 20. Speculative palaeoenvironmental models for the deposition of calcareous sediments and adjoining rocks of the Garub sequence (no allowance is made for later deformation)

3.2. LAYERED BIOTITE GNEISS

Map units: *GnB1* *Layered biotite gneiss*
GnB *Undifferentiated biotite gneiss*

1. Nomenclature

These rocks are pretectonic grey biotite-bearing gneisses. Layered biotite gneiss is a layered sequence of rocks of psammitic composition. Undifferentiated biotite gneiss is non-layered but of similar composition. The two varieties are closely associated and contacts are gradational. They have a similar mineralogy.

All biotite gneisses are shown as one colour on the geological map (Annexure 1) but are distinguished by their respective symbols. Because the biotite gneisses are essentially a 'sack-group', they have not been assigned a geographic name.

2. Distribution

Biotite gneiss is extremely widespread south of the Aus area where it is the dominant rock type over some 2000 km^2. Layering in these gneisses is well developed at the mountain south of Tsirub Letterkuppe (I1), the Chorasib Hill (I1), at Ganaam Waterhole (J3) and on the farm Nieu Tsaus (K5) but is not common in the north-centre of the study area.

3. Lithology

The biotite gneisses are leucocratic pale-grey medium-grained rocks with a strong foliation defined by biotite flakes. The gneisses are granitic and contain 1-10% biotite and, in many places, 1-3% garnet; hornblende is extremely rare. Layering, if present, is on a centimeter scale and produced by varying proportions of biotite in adjoining layers. Plate 7 illustrates the regularity and persistence of this fine-scale layering. Melting of the quartzofeldspathic fraction of the rock during migmatization has produced the irregular and discontinuous segregations of quartz-feldspar pegmatoid; such neosomes are easily differentiated from the layering because they are (1) rarely strictly concordant, (2) of highly variable thickness, (3) do not contain biotite, except as thin schlieren. Further migmatization has resulted in the predominance of a schlieric texture (Plate 8) which superficially resembles the layering referred to above but is much coarser and more irregular with the biotite concentrated into schlieren.

Thin layers of Garub rocks are intercalated with the biotite gneisses;

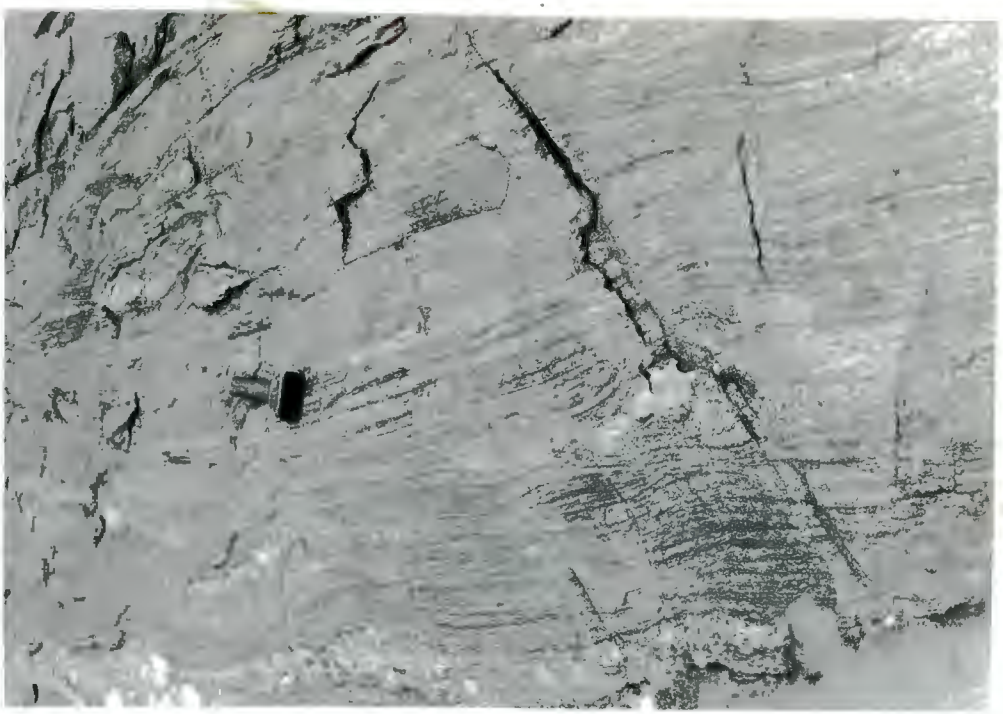

Plate 7. Layered biotite gneiss showing fine-scale, laterally persistent layering defined by variations in biotite content. Pegmatoidal mobilizate present in places. Layering interpreted to be derived from stratification in parent rock. Ganaam waterhole (J3)

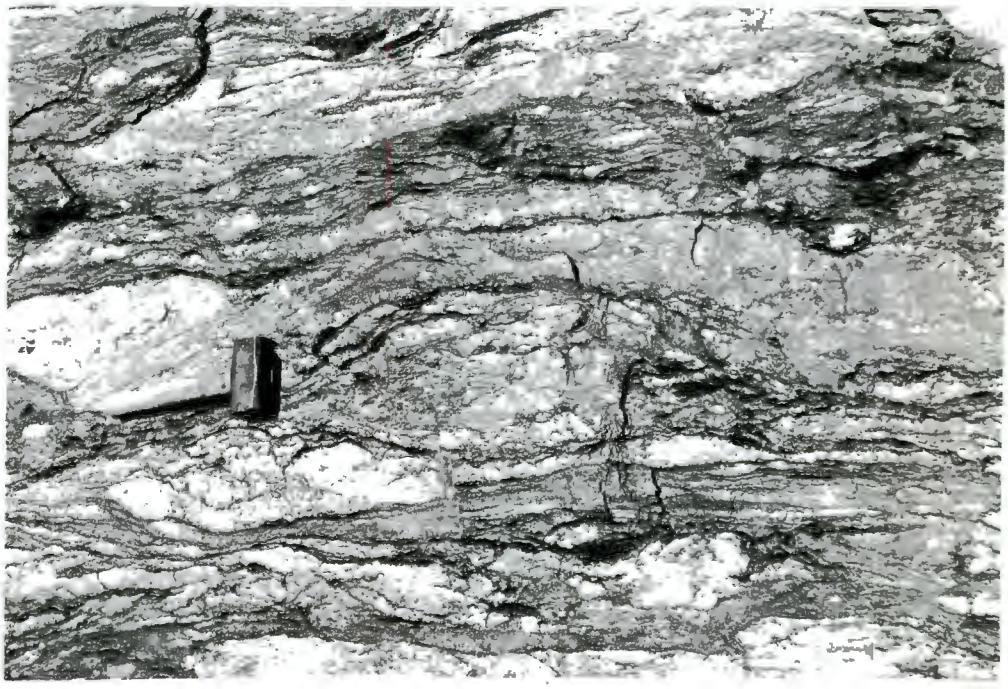

Plate 8. Strongly migmatized biotite gneiss with biotite schlieren (melanosomes) and irregular quartzofeldspathic neosomes. 5 km W of Kuckaus waterhole (J3)

amphibolite and biotite schist are the most common intercalations, but metasediments such as metaquartzite, iron formation and aluminous gneiss are also widespread.

4. *Internal Structure*

The foliation in the biotite gneisses is parallel to the layering. Intercalations of other rock types are concordant with this layering and the foliation in adjoining units is parallel.

In the Kuckaus mylonite belt the appearance of these rocks changes greatly over short distances. The style of weathering changes from spheroidal or slabby to a style giving rise to pinnacles; in thin section such rocks show straining of crystal lattices, granulation of the margins and development of shreds of muscovite. Anastomosing bands of sheared gneiss alternate with unsheared rock to form a flaser structure. Nearer the centre of the shear zone refoliation has formed a cataclastic fabric, the rocks are fine grained and broken fragments of larger crystals are visible in hand specimen; chloritization of biotite and the formation of muscovite are extensive. In the mylonitic core of the shear zone the gneisses are completely refoliated to form banded mylonites.

5. *External Structural Relations*

In contact with Garub rocks or Tsirub gneiss, the foliation of the biotite gneiss is parallel to that of the adjoining rocks. On Urus Mountain (K2) layered gneiss grades into irregular patches of homogenous biotite granite gneiss which cuts across the layering and foliation of the layered gneiss. This layering is also crosscut by the pegmatoid variety of Kubub granite gneiss. (GnK_2). Inclusions of layered biotite gneiss are present in the Jakkalskop charnockite.

6. *Mode of Origin*

The origin of layered gneisses in high-grade metamorphic terrains has been the subject of much speculation. Dietrich (1960, p.101) reviewed the most notable examples of layered gneisses and summarized evidence for the following processes leading to the formation of these rocks: relict igneous banding and sedimentary stratification, partial melting and lit-par-lit injection during migmatization, permeation during metasomatism, metamorphic segregation, and combinations of these processes. He concluded (ibid., p.116) that the layering in most gneisses probably directly reflects or is controlled by supracrustal stratification. Chemical-metamorphic differentiation was considered to be a subsidiary process that merely accentuated the original layering (ibid., p.117).

More recent work supports the above conclusions. As a result of the comparison of bed thickness in sedimentary rocks with layer thickness in layered gneisses in Quebec, Ceylon and Norway, Katz (1970) concluded that layering in gneisses was due to original sedimentary stratification; metamorphic differentiation could only modify pre-existing relict layering and did not greatly affect the overall size, shape and extent of layers. Harris (1974, p.326) concluded that the majority of finely banded migmatites in the Central Pyrenees were formed as a result of original sedimentary differences in the rocks; lenticular neosome segregations were concluded to have formed by anatexis.

With regard to the origin of the layered biotite gneiss in the Aus area, the extremely fine scale and continuity of individual layers suggest that they were derived from original stratification in these rocks. The layering in these gneisses is of similar appearance to that designated by Dietrich (1960, Fig. 3) as 'relict supracrustal type modified by migmatization'. Deformation, however, is capable of producing layered rocks on a small scale: Plate 9 illustrates the formation of finely banded gneiss by transposition of augen gneiss.

The presence of metasediments such as metaquartzite, iron formation and aluminous gneiss in the biotite gneisses suggest, but are not conclusive evidence for, a sedimentary origin for the layered gneiss. The parent rock could have been psammatic in composition, containing horizons of pelitic, ferruginous or siliceous material. It is possible that this predominantly psammitic succession is the same age as the Garub sequence, which contains metasediments of more extreme composition.

7. Relative Age

There is no evidence of a tectonic event separating the deposition of the layered biotite gneiss and the Garub sequence. Layered gneiss structurally underlies and overlies the rocks of the Garub sequence. The layered biotite gneiss predates the syntectonic Jakkalskop charnockite, Kubub granite gneiss and biotite granite gneiss.

8. Correlation

The biotite gneisses form part of the large hetereogeous group of rocks common throughout the Namaqua belt that are mapped under the sack-name of 'grey gneiss' or 'mixed gneiss' (Blignault et al., 1974). The writer is hesitant in correlating the layered biotite gneiss at Aus with other grey gneisses which may be of entirely different origin, but layered gneiss of similar appearance (Orangefall biotite gneiss) forms part of the pretectonic Onseepkans sequence in the Warmbad area (Toogood, 1976).

3.3. TSIRUB GNEISS

1. *Origin of Name and Distribution*

The Tsirub gneiss is named after the farm (H1, H2) on which extensive exposures of this rock unit are present. This formation comprises augen gneisses which are extremely abundant in the central part of the study area but are not found in the extreme south or north. Tsirub gneiss is preserved in four elongated zones; the zones trend westwards in the south, but in the north large-scale folding has produced irregular outcrops.

2. *Lithology*

The Tsirub gneiss has an extremely uniform appearance: it is a dark-grey medium-grained gneiss of tonalitic or, more rarely, granodioritic composition. The typifying feature of the Tsirub gneiss is the presence of ovoid quartzo-feldspathic segregations (Plate 10). There are four types of segregation, of which the first two listed are by far the most common:

(i) Plagioclase porphyroblasts, commonly tabular but with pressure shadows or quartz aggregates forming tails

(ii) Aggregates of small quartz crystals

(iii) Quartz porphyroblasts

(iv) Orthoclase porphyroblasts, fairly tabular

The first three segregations listed have the classic shape of augen. The shape of augen is controlled by the degree of deformation, which results in a progressive flattening and elongation of the augen, or by the degree of in situ partial melting, which results in the coalescence of augen tails.

The augen gneisses have a strong planar fabric defined by biotite; the long axes of the augen and of the opaque minerals also show a preferred orientation. The augen are commonly greatly elongated to give a banded appearence (Plate 11). Although the mineralogy of the augen gneisses is relatively simple, the textures of these rocks are extremely complex and appear to have been derived from the interaction of deformation, granulation and blastesis/recrystallization.

Because of their heterogenous textures, it is difficult to determine the mode of the augen gneisses in thin section. The plagioclase/(total feldspar) ratio varies between 0,82 and 1,00. Plagioclase is most common in the augen of the rock as crudely lath-shaped but xenoblastic crystals aligned parallel to the banding of the rock. Twin lamellae are commonly bent and deformation twinning is common. In the matrix plagioclase forms equant polygonal grains closely associated with biotite.

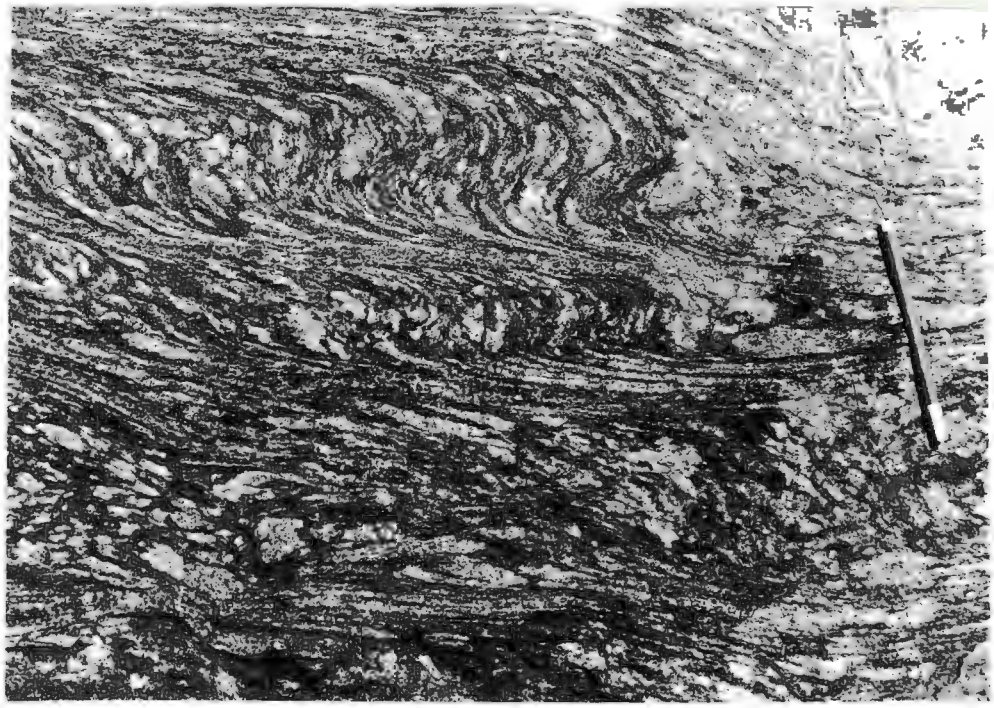

Plate 9. Transformation of augen gneiss to layered gneiss in mesoscopic shear zones with sinistral displacement. Tsirub gneiss. NE of Aarkopf Hill (H5)

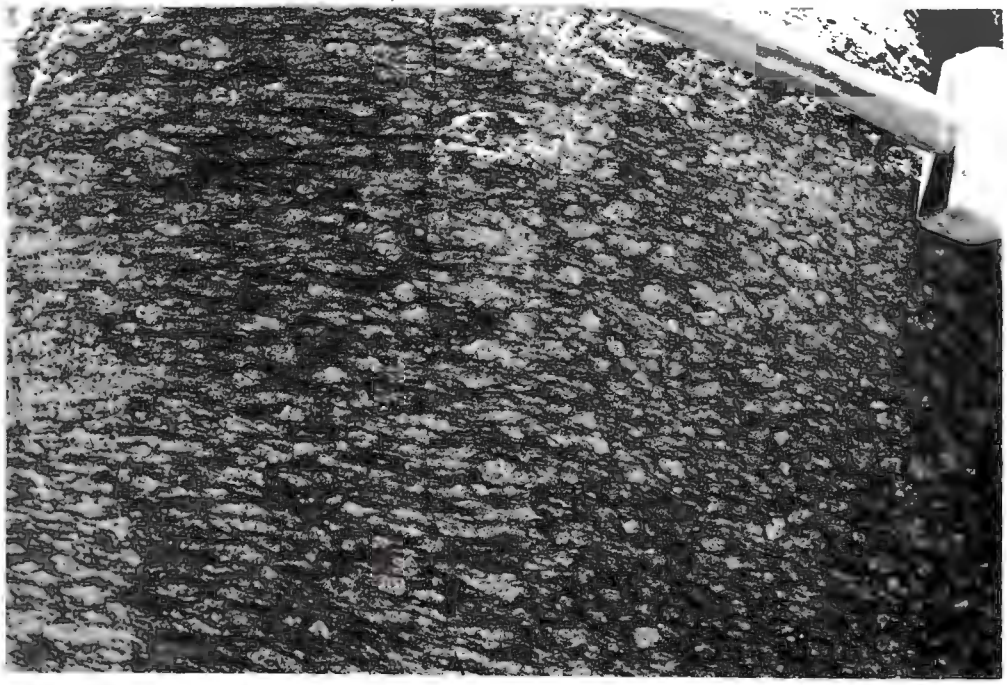

Plate 10. Tsirub gneiss showing typical form of augen. 1 km N of railway, Jakkalskop 130 (G7)

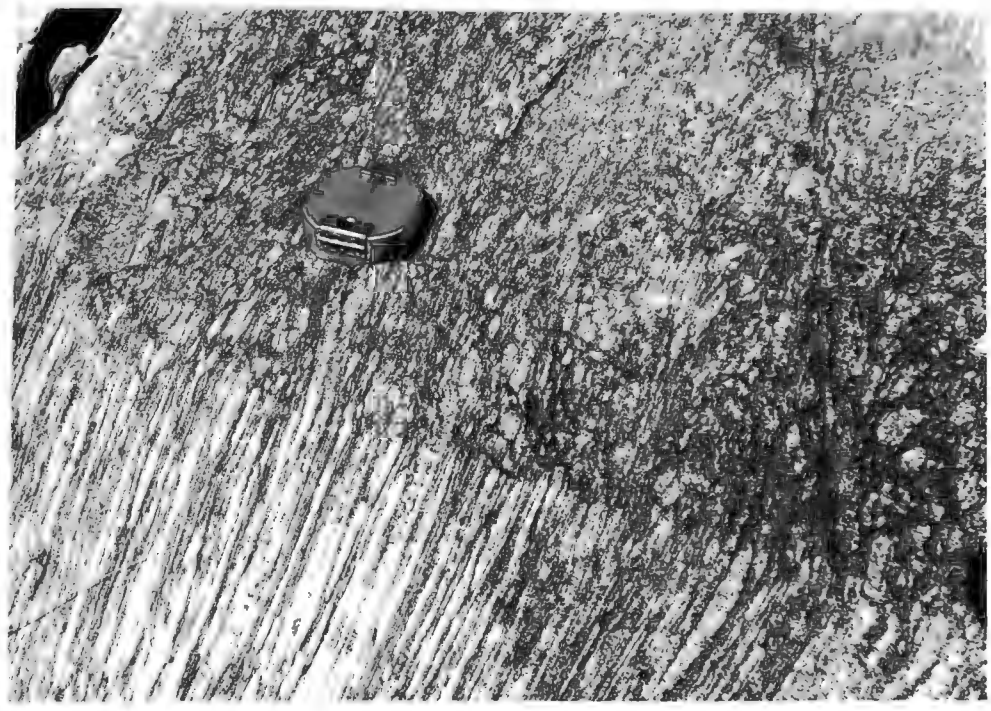

Plate 11. Sections parallel (below) and normal (above) to *b* showing rod-like nature of augen in Tsirub gneiss. NE of Aarkopf Hill (H5)

Plate 12. Angular inclusion of Garub biotite schist, interpreted as a deformed xenolith, in Tsirub gneiss. Kahler Berg (G5)

The rare porphyroblasts of orthoclase are cloudy and perthitic. The metacrysts, which are up to 15 mm long, are surrounded by a very fine-grained mortar structure of quartz and plagioclase. Microcline is present in small quantities in the matrix.

Biotite is present in amounts of 10-15%. It may be evenly distributed or, more commonly, segregated into mafic layers which often include garnet, plagioclase or opaque minerals.

Small quantities of pink garnet are found in the augen gneisses south of the railway. The garnet may be present as xenoblastic porphyroblasts with inclusions and embayed margins around which the foliation curves or, less commonly, as smaller (0,5 mm) idioblastic crystals which are free of inclusions and have unbroken, smooth margins. These textures suggest that garnet of different generations is present (Spry, 1968, 1969). Opaque minerals constitute 1-2% of the augen gneiss; zircon is an uncommon accessory mineral.

Generally the Tsirub gneiss is of uniform appearance and easy to differentiate from other rock units. However, in the vicinity of the Jakkalskop charnockite the normally-leucocratic Aus granite gneiss has reacted with charnockite to form a dark-coloured hybrid rock in the contact zone which might be confused with the Tsirub gneiss; but the tabular shape of the megacrysts in the hybrid rock distinguish it from the augen gneisses.

3. *Internal Structure*

The Tsirub gneiss has been refoliated a number of times on a regional scale. Augen gneisses containing fabrics which predate and postdate the intrusion of the Aus granite gneiss are of very similar appearance.

Cataclastic deformation in the cores of late shear zones, has profoundly affected the Tsirub gneiss. In the Kuckaus mylonite belt the first indication of deformation is that of a rotation of porphyroblasts and a streaky appearance of the rock. Porphyroblasts are then broken up to small angular clasts scattered through the rock; the matrix is granulated and crushed to form a weakly-banded fine-grained greenish mylonite.

4. *External Structural Relations*

The Tsirub gneiss commonly underlies the rocks of the Garub sequence - as in the northern part of Eureka Farm (F3); but in many other places the Tsirub gneiss overlies the sequence. This relation does not have stratigraphic significance but is merely the result of early folding. The presence of inclusions of Garub rock types in the augen gneisses suggests that the Tsirub gneiss was originally an intrusive rock that postdated the deposition of the Garub sequence. These inclusions, which are interpreted as flattened xenoliths, were only rarely found during the present survey and it is worthwhile describing the principal localities at which they are present. At Rooibank (G5) augen gneiss contains fragments of biotite schist within a few metres of the contact with

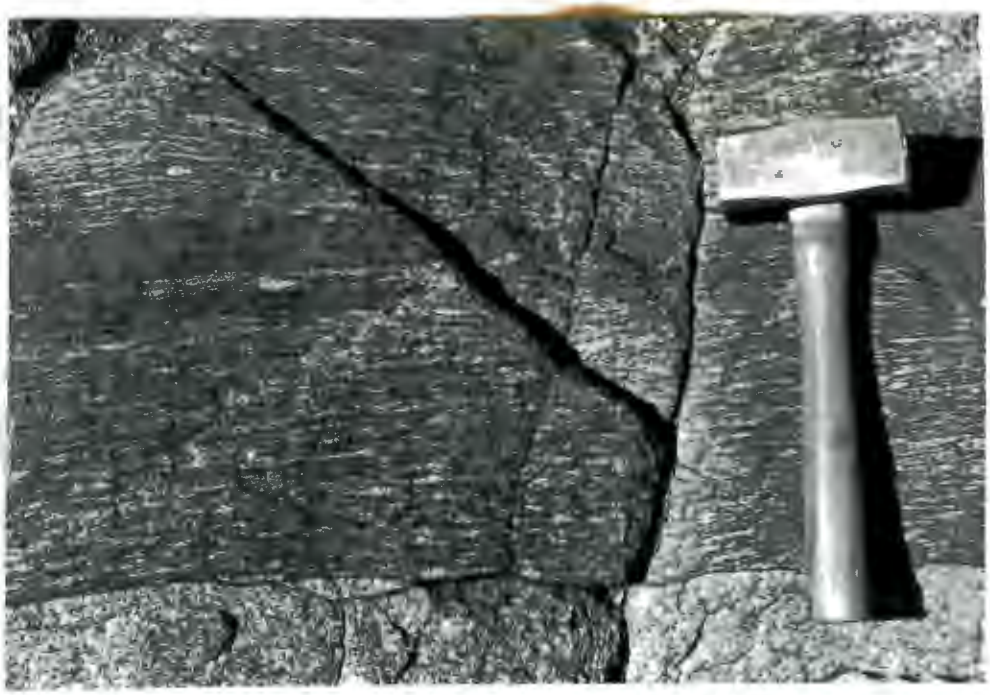

Plate 13. Contact between Tsirub gneiss (above) and Garub biotite schist (below) showing lenticular inclusions (interpreted as flattened xenoliths) of Garub hypersthene granolite. Note flattening of augen. By railway on SW part of Augustfelde 42 (G6)

Plate 14. Knife-sharp contact between younger Tsirub gneiss (below) and older Garub biotite schist (above) showing complete lack of augen development in schist. Augen are therefore interpreted as being deformed phenocrysts rather than porphyroblasts of secondary origin. Rooibank (G5)

biotite schist of the Garub sequence; Plate 12 illustrates a similar relation at Swartaus, a few kilometres to the west. Tsirub gneiss contains an inclusion of hypersthene granolite in the contact zone between these two units on Augustfelde Farm (G6); intense flattening has almost destroyed the augen (Plate 13). On the escarpment east of Narreis (H5) scattered inclusions of Garub metapelites are present within the augen gneiss.

Although the Tsirub gneiss appears to postdate the Garub sequence, no evidence was found for a tectonic event between their formation. At every contact examined the foliation in both rocks was parallel to the surface separating them; nowhere was a foliation found within the Garub rocks that was cut by structures in the augen gneisses. The Tsirub gneiss is therefore classed as pretectonic together with the Garub sequence.

5. *Mode of origin*

The uniformity of the augen gneisses on a regional scale is compatible with an igneous origin. The presence of inclusions further supports this conclusion but because transgressive relations that may have existed between the rocks of this unit and the Garub sequence appear to have been completely removed by intense deformation, the origin of the Tsirub gneiss remains a matter of speculation. However, analogy with similar rocks elsewhere in the Namaqua belt (see below) further supports an igneous origin. If the Tsirub gneiss was originally intrusive, it is probable that many of the augen represent deformed phenocrysts; they are not considered likely to be of blastic origin because adjoining formations of similar composition are completely devoid of augen and are separated by knife-sharp contacts from the augen gneiss (Plate 14).

6. *Relative Age*

The Tsirub gneiss postdates the Garub sequence and biotite gneiss and predates the syntectonic granite gneisses. The relation of the Tsirub gneiss to the Jakkalskop charnockite is not known (through lack of contacts).

7. *Correlation*

Augen gneisses closely resembling the Tsirub gneiss extend westwards beyond the project area to the coast. They are present in the Tschaukaib Mountains and at Splitterkuppe in Diamond Area I. Similar augen gneisses are also present on the coast at Lüderitz (Greenman, 1966), Pomona and Prince of Wales Bay (Beetz, 1924). However, porphyroblastic gneisses of intrusive origin at Hottentot Bay (Kröner and Jackson, 1974) are demonstrably younger than other intrusive rocks and are not correlates of the augen gneisses mentioned above.

The Tsirub gneiss is strikingly similar in appearance to deformed varieties of the Beenbreek (Toogood, 1976) and Eendoorn (Beukes, 1973) granites in the

Warmbad District, some 300 km to the southeast of the Aus area. Plagioclase phenocrysts and angular xenoliths of older rocks within the Beenbreek granite are converted by strong deformation to augen and lenticular inclusions of identical appearance to those that characterize the Tsirub gneiss. Undeformed contacts show that in the Warmbad District the Beenbreek granite intrudes the charnockites, a relation which is not evident in the Aus area. The Tsirub gneiss is also very similar in appearance to deformed varieties of the Nababeep gneiss in Namaqualand.

3.4. JAKKALSKOP CHARNOCKITE

Map unit: *GnJ Jakkalskop charnockite*

1. *Origin of Name*

Charnockite is used here as a general term to cover a broad range of rocks whose character was summarized by Turner (1968, p.33): 333

> The term *charnockite* is generally applied in India to rocks whose chemical compositions fall within the range of plutonic rocks (acid, basic and ultrabasic), whose textures recall those of corresponding plutonic rocks, but in which the characteristic mafic phase is hypersthene (with or without some combination of clinopyroxene, hornblende or almandine).

Charnockites in the Aus area were referred to in a preliminary report (Jackson, 1974, p.47) as 'meta-intrusives'. The two largest and best-preserved bodies are situated on the farm Jakkalskop; for this reason the name 'Jakkalskop charnockite' is used to represent the complete suite of charnockite rocks. The individual bodies have been named according to the farms on which their main outcrops are present, with the exception of the Schakalskuppe body, which is named after the railway station just north of it.

2. *Distribution*

All charnockites in the study area are situated close to the Nama escarpment east of Aus Village and large parts of these bodies are therefore covered by colluvium or Nama sediments; in the northeast a mantle of aeolian sand has obscured much of the charnockites.

From the existing outcrop pattern there appears to be six separate bodies, which range in size from outcrop areas less than 200 m in length to a possible maximum width of nearly 20 km, of which about 10 km is nearly continuously exposed. The positions and names of these bodies, together with their tentative boundaries are shown in Figure 21.

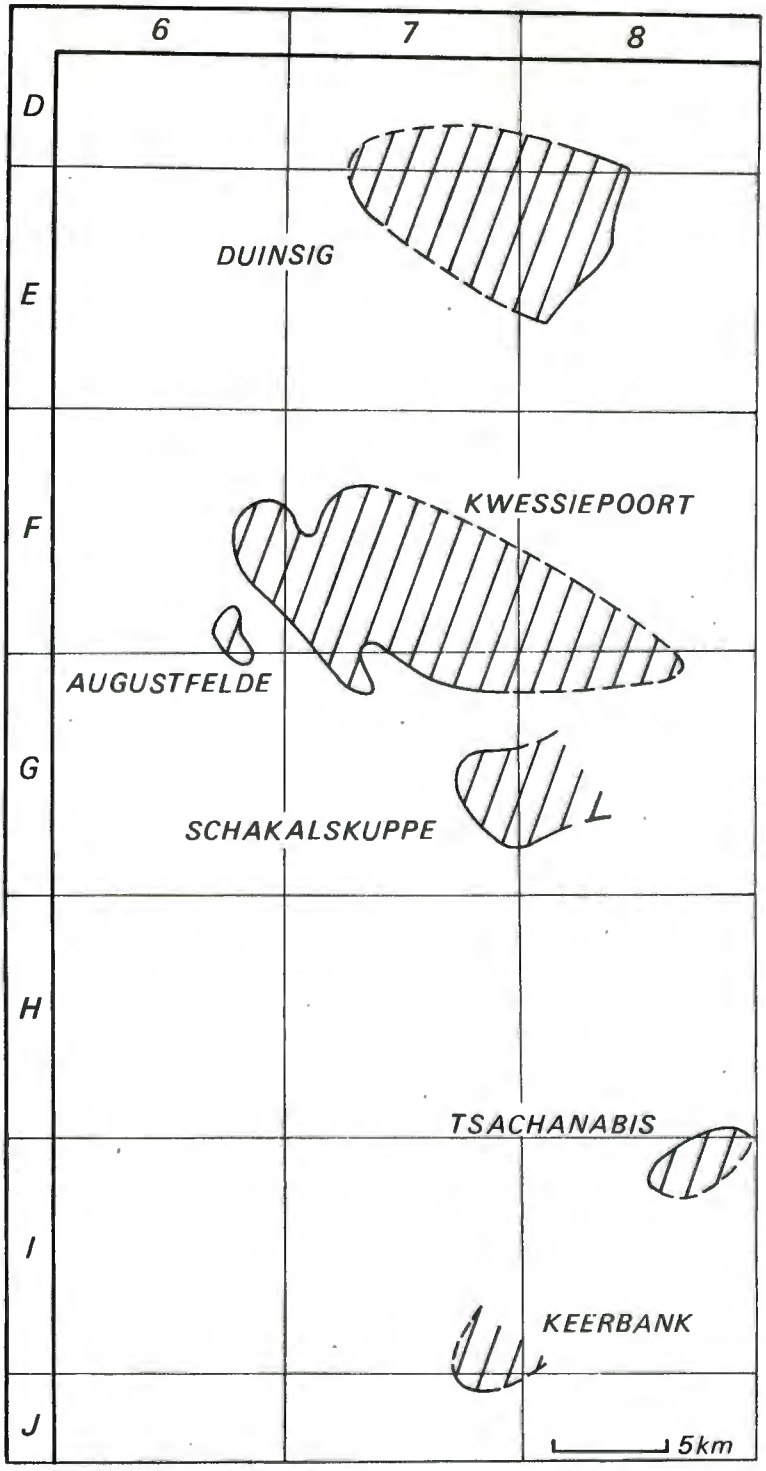

Figure 21. The Jakkalskop charnockite bodies east of Aus Village and their estimated extension (speculative) beneath younger cover

3. *Lithology*

The charnockites characteristically weather to form dark-brown boulders of igneous appearance. Where fresh the rocks ring when struck with a hammer and are extremely tough. The charnockites are medium grained or coarse grained and dark green-grey in colour. Quartz and feldspar constituents are strikingly dark in colour and in rare cases blue opalescent quartz is found. A weak but pervasive foliation is visible in some outcrops but this is not apparent in hand specimen. In the coarser-grained varieties large rounded megacrysts of plagioclase up to 7 cm in diameter are rarely present.

The nomenclature used for describing the charnockites needs some explanation. As yet no widely accepted or recommended classification of the charnockitic rock suite has been published. Tobi (1971) proposed a classification closely linked to the now widely used scheme of Streckeisen (1967) for plutonic rocks in general. Tobi revised his nomenclature (Tobi, 1972) after criticism by Torske (1972) and this revised nomenclature is followed in the present report. However, this nomenclature has not yet been formally accepted and all names cited will therefore be followed by the field number of Streckeisen's (1967) quartz-alkali feldspar-plagioclase triangle which is likely to form the basis for the final charnockite nomenclature.

The composition of specimens from the Jakkalskop charnockites bodies are plotted on Tobi's (1971, 1972) ternary diagram (Fig. 22). Part of the Keerbank body has an ultramafic composition and therefore cannot be represented in this scheme, but the noritic part is shown. In the intermediate charnockites very fine-scale perthite or mesoperthite textures are visible in the K-feldspar and this has been included with alkali feldspar in the modal estimates.

With reference to Figure 22, the following points may be made:

(i) All these specimens represented on the diagram are concentrated in or close to field 4. They are therefore properly termed charno-enderbites (or meso-charno-enderbites where mesoperthite is present).

(ii) There is a wide compositional variation within small areas of the same rock body: four out of five of the Schakalskuppe specimens (symbol D) were collected within 20 m of each other, and yet they plot in four different compositional fields.

(iii) The compositional variations between the five northern bodies are no larger than the internal variations described above. There is no marked compositional trend from north to south although the southernmost (Keerbank) body is much more mafic than the others.

The two ultramafic charnockitic bodies not represented in this classification can be described using Streckeisen's (1967) nomenclature. The Keerbank body consists partly of olivine websterite and the Letterkuppe body is a cummingtonite pyroxenite. Because of their very different compositions, the petrography of these two ultramafic bodies will be described separately from the more felsic charnockites.

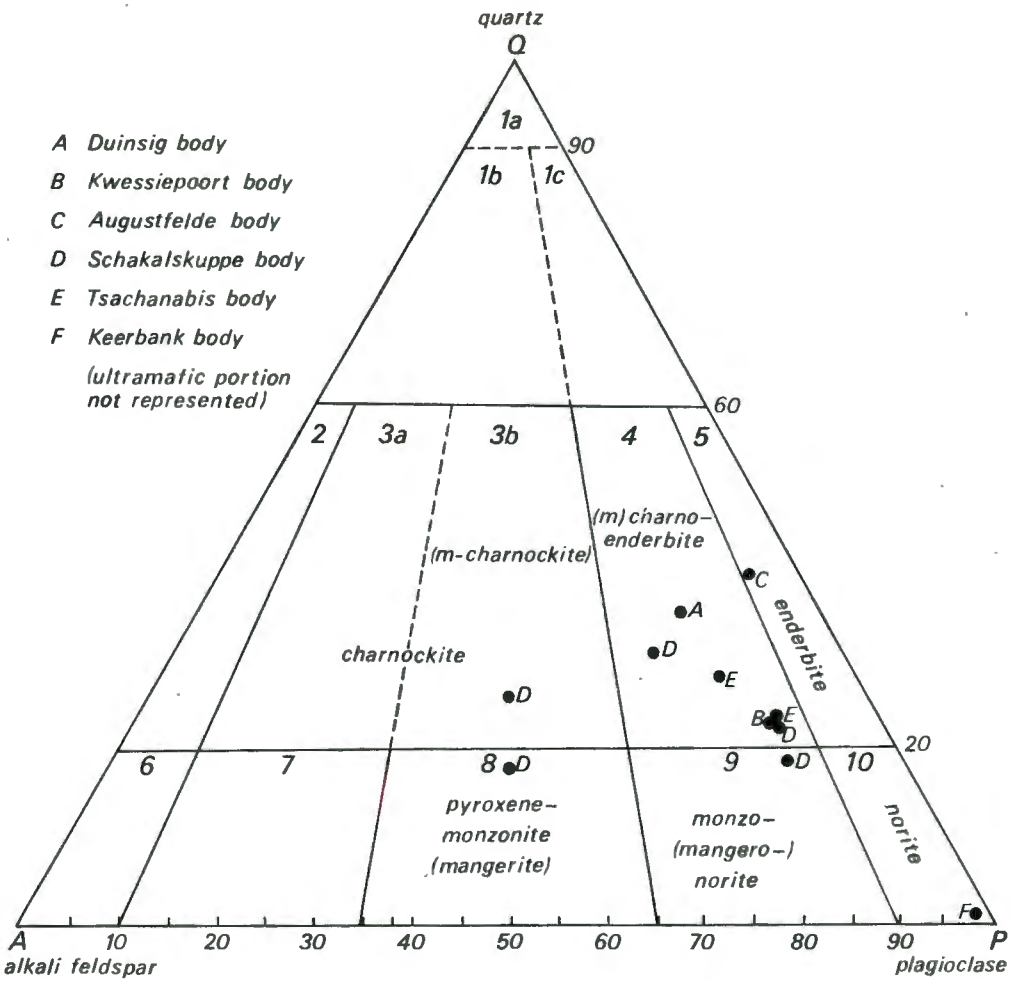

Figure 22. Estimated modal compositions of specimens from six bodies of Jakkalskop charnockite east of Aus Village plotted on the Q-A-P triangle showing Tobi's (1971, 1972) nomenclature for the appropriate fields (alkali feldspar includes perthite and mesoperthite)

The charnockites of the Aus area therefore form two different compositional groups: intermediate charnockites characteristic of the five northern bodies; and mafic and ultramafic charnockites constituting the Keerbank and Letterkuppe bodies. The estimated modes of specimens of Jakkalskop charnockite are shown in Table 14.

4. *Petrography of the Intermediate Charnockites*

These intermediate charnockites are generally medium grained and seriate; their general texture can be described as hypidimorphic granular. A foliation is usually lacking but in places it is weakly defined by alignment of pyroxene, biotite or opaque grains.

TABLE 14. *Estimated modes (in volume percentages) of specimens of Jakkalskop charnockite. Retrograde minerals in parentheses.* m = <1%

Specimen	Olivine	Cummingtonite	Clinopyroxene	Orthopyroxene	Biotite	Plagioclase/Myrmekite	Perthite/Mesoperthite	Quartz	Opaque minerals	Other hornblende *hb* hercynite *he* apatite *ap* zircon *zc*	Locality
MJ1409	35			55	7	3					J7
MJ1408			25	35	2	40				m	J7
MJ374	27		35	7	(5)	7					J7
MJ1036		33		60					m	7 *he*	H1
MJ331				15	5	55	10	15	2	m *ap*,m *zc*	G7
MJ332				12	2	35	35	15	2	m *ap*,m *zc*	G7
MJ363				2	15	50	8	17	m	m *ap*,m *zc*,(2)*hb*	I8
MJ364			3	10	15	40	10	20	2	m *ap*,m *zc*	I8
MJ429				8	3	55	10	20	2	m *ap*,m *zc*	G7
MJ339				3	5	60	10	20	m	m *ap*	G7
MJ331A				15	1	40	15	25	2	m *ap*	G7
MJ531				20	(5)	35	10	25	5	m *ap*	E7
MJ1311				5		35	35	25	m	m *ap*,m *zc*	G7
MJ462				5	5	45	5	40	m	(1) *hb*	

The dark colour and uniform appearance of all hand specimens is striking when the wide range in colour indices is considered (Table 15).

Orthopyroxene is diagnostic of the charnockitic suite; in the intermediate charnockites hypersthene is the chief mafic mineral and averages about 10% by volume. The hypersthene has a very different habit to that in the granolites, typically occurring as subhedral laths with rounded terminations and embayed margins (in contrast to the granoblastic hypersthene in the granolites). Smaller crystals can have the form of xenoblastic granules.

The hypersthene rarely shows alteration to rims of biotite, hornblende or chlorite by incipient hydration. The greatest degree of alteration is present in those specimens with very low (2-5%) contents of hypersthene.

Clinopyroxene is extremely rare and occurs as small quantities of pale green diopside. No reaction with hypersthene is apparent.

Biotite is common and is usually the sole hydrous mineral in the charnockites. It has the form of well-developed red subidioblastic laths. Rarely retrograde brown biotite with ragged boundaries rims hypersthene, but the two minerals generally are in textural equilibrium.

TABLE 15. *Colour index and percentage of hydrous minerals in specimens Jakkakskop charnockite*

Specimen	Colour index	Σ hydrous minerals %	Charnockite body
MJ531	30	5	Duinsig
MJ429	13	3	Kwessiepoort
MJ462	5	6	Augustfelde
MJ1311	5	0	Schakalskuppe
MJ331A	18	1	
MJ339	8	5	
MJ332	16	2	
MJ331	22	5	
MJ364	28	15	Tsachanabis
MJ363	18	15	
MJ1408	62	2	Keerbank
MJ1409	97	7	
MJ374	93	5	
MJ1036	100	33	Letterkuppe

Plagioclase is the most abundant mineral in the intermediate charnockites. The mineral is present both as discrete plagioclase (An∿50) and as a component of perthite and mesoperthite. Plagioclase has the form of clear subhedral crystals without visible zoning and is extremely rare. Myrmekitic reaction zones with K-feldspar are abundant.

Perthite: K-feldspar is present in the form of untwinned grains of orthoclase with a very fine perthitic structure. The proportion of included plagioclase could not be accurately determined but it appears to be sufficiently high in many cases to constitute mesoperthite. The larger crystals of perthite enclose pyroxene, plagioclase and opaque minerals.

The modal quantities of quartz are relatively constant, varying between 15% and 25%, rarely 40%. Abundant fluid inclusions are preserved in these grains and their significance is discussed in Section 4.6. No other inclusions are visible in the quartz, which may explain why the blue opalescent quartz that is so common in other charnockites (Pichamuthu, 1953) is not widespread in the Jakkalskop charnockites.

Zircon is consistently present in small quantities in the form of needles with rounded terminations and a length/breadth ratio of approximately 13/1. Acicular apatite is also consistently present in trace amounts; the max-

imum length/breadth ratio recorded is 40/1. Opaque minerals are present in all specimens in modal quantities of up to 5%.

5. *Petrography of the Mafic and Ultramafic Charnockites*

The Keerbank body greatly resembles the intermediate charnockite bodies in the field and may form part of the same suite. The Letterkuppe body, situated a few kilometres beyond the western boundary of the study area in unmapped terrain, is of uncertain affinity. Because of its remoteness no attempt is made here to correlate this body with any of the other charnockites. Both the Keerbank and Letterkuppe bodies are medium grained and unfoliated.

The Keerbank body, which is represented by a single small outcrop, has a colour index of 60%-100%. It is composed of orthopyroxene, clinopyroxene and olivine together with small quantities of plagioclase and biotite. Olivine (colourless forsterite) is present as large partially serpentinized anhedral grains.

Clinopyroxene has the form of large subhedral laths of augite with abundant exsolution lamallae, which are absent from all other pyroxene specimens from the Aus area. The orthopyroxene is colourless enstatite in the form of large anhedral crystals of irregular shape ophitically enclosing euhedral laths of plagioclase, which have well-developed Carlsbad twinning. Biotite is retrograde and has formed by alteration of pyroxene.

The Letterkuppe body is also ultramafic and orthopyroxene-bearing, but olivine is absent. The rock consists of orthopyroxene and amphibole. The orthopyroxene is enstatite and the amphibole has the optical properties of cummingtonite. Small amounts of dark-green spinel - probably hercynite - are present as small irregular grains associated with trace amounts of opaque minerals.

6. *External Structural Relations*

Relations between the charnockite and older rocks are clear. Angular xenoliths of biotite schist and granofels of the Garub sequence are abundant within the charnockites, especially in the Schakalskuppe and Kwessiepoort bodies. The charnockite contacts crosscut layering, foliation, lineation and minor folds within the xenoliths, whose size ranges up to 5 m; contacts are generally sharp. Plate 15 shows the charnockite crosscutting the layering/foliation of a large xenolith of biotite schist; Figure 23 illustrates a breccia within the charnockite contact zone; such structures suggest intrusion of a melt into shattered country rocks.

Plate 15. Jakkalskop charnockite (left) crosscutting foliation-layering of xenolith of Garub biotite schist (right) 3 m in length. 4 km NW of Schakalskuppe Station (G7)

Plate 16. Xenoliths of Jakkalskop charnockite (dark) in pegmatoid mobilizate (light) produced during regional migmatization. 3 km SW of Schakalskuppe Station (G7)

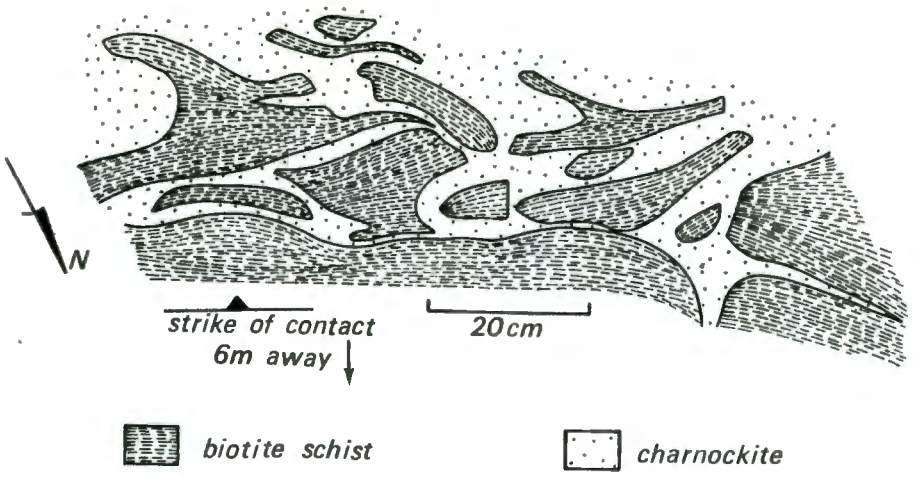

Figure 23. Field sketch of breccia structure in the contact zone of Jakkalskop charnockite. Southern contact of Kwessiepoort body, Jakkalskop Farm (G7).

Abundant inclusions of hypersthene granolite are also present within the charnockite. They do not show evidence of a pre-charnockitic fabric and may have recrystallized during the intrusion of the charnockites. These inclusions are lithologically similar to Garub granolites adjoining the charnockites, some of which have a fabric.

The relation of the Jakkalskop charnockite to the biotite granite gneiss is clear. On the central part of Kwessiepoort Farm (F6) and on Duinsig Farm (E8) veins of biotite granite gneiss have intruded the charnockite. The Jakkalskop charnockite is therefore older than the biotite granite gneiss.

The Jakkalskop charnockite is closely associated with the Aus granite gneiss, a syntectonic granitoid of intrusive origin. However, contacts between these two rock units are ambiguous. Gradational contacts are common: the normally-leucocratic Aus granite gneiss is dark and biotite-rich at the contact and K-feldspar megacrysts, which typify the Aus granite gneiss, are present for a few centimetres within the charnockite. Where contacts are sharp, (less than 5 mm wide) they are either straight or undulating: rounded inclusions, which may be apophyses or xenoliths of granite gneiss or charnockite, are present within each unit. However, the charnockites are commonly cut by sheets and irregular masses of pegmatoid mobilizate (Plate 16) which, elsewhere in the area, are genetically related to the Aus granite gneiss. This relation suggests that the charnockite is older than the granite gneiss and its associated mobilizate.

Similar relations are displayed in an area some 180 km to the southeast of Aus. North of Klein Karas, rocks of similar appearance are present. Leucocratic megacrystic Grabwasser granite gneiss (*after* Genis *in* Blignault, 1975) clearly intrudes the intermediate Signalberg charnockite (ibid.). The granite gneiss is darker than normal near the contact and, in places, a rock type intermediate between charnockite and granite gneiss is present. This hybrid rock consists of a dark biotite-rich matrix containing euhedral megacrysts of K-feldspar similar to those in the adjoining granite gneiss. This field relation is interpreted as follows: hydrous leucocratic melt reacted with the already crystal-

lized charnockite and hydrated the mafic minerals in it (mainly orthopyroxene) to form the dark biotite-rich hybrid phase; blastic growth of K-feldspar then took place within this rock. On cooling, the leucocratic granite gneiss would have expelled chemically uncombined water during crystallization (Mehnert, 1968, p.242).

The similarity of field relations between these rock types in the Klein Karas and Aus areas is striking. The presence of a very similar biotite-rich hybrid phase between the Aus granite gneiss and the Jakkalskop charnockite, and the growth of megacrysts in the border zone of the charnockite indicate a similar age relation to that described in the previous paragraph.

7. Mode of Origin

The presence of abundant xenoliths and the absence of chilled contacts suggests that the Jakkalskop charnockites were intruded into heated country rocks. The environment of intrusion and the broader aspects of their origin are discussed in Section 4.6.

Petrographic evidence for the origin of the Jakkalskop charnockites is ambiguous because their textures show features of both magmatic crystallization and solid-state recrystallization. Crystallization from a melt is suggested by the following features in the Jakkalskop charnockites:

(i) The interpenetrative relations of the various minerals and their development of crystal faces are broadly compatible with a sequence of crystallization following Bowen's (1922) reaction series for igneous rocks; the observed sequence is orthopyroxene → clinopyroxene → perthite → quartz → biotite

(ii) The presence of lath-shaped euhedral hypersthene

(iii) In the Keerbank body abundant exsolution textures in the clinopyroxene, well-developed Carlsbad twinning in the plagioclase and ophitic texture between plagioclase and pyroxene

(iv) Lack of foliation (although not diagnostic) despite the presence of prismatic crystals

(v) Extreme elongation of apatite and zircon crystals, indicative of high temperatures of crystallization and typical of igneous gabbros (Mehnert, 1968).

Features suggesting solid-state recrystallization are as follows:

(i) General appearance of textural equilibrium and rarity of zoning in plagioclase or exsolution in pyroxene (except in the Keerbank body)

(ii) General lack of euhedral crystals, with the exception of pyroxene in most rocks and plagioclase in the Keerbank body

(iii) Lack of Carlsbad twinning except for plagioclase in the Keerbank body

(iv) Very strong pleochroism of hypersthene, typical of metamorphic rocks formed under pressures higher than those characteristic of normal igneous rocks

(v) The presence of diopside in the intermediate charnockites which is not characteristic of intermediate igneous rocks.

In summary, therefore, textural and mineralogic evidence for crystallization from a liquid is strong for the Keerbank body; but the weight of evidence for the other charnockite bodies suggests that *in their present state* they are metamorphic rocks that crystallized in the solid state.

8. Relative Age

The Jakkalskop charnockite is younger than the Garub sequence and layered biotite gneiss. It is older than the pegmatoid migmatite neosomes, the biotite granite gneiss and, most probably, the Aus granite gneiss. Contacts with the Tsirub gneiss are not exposed.

9. Correlation

Possible correlates of the Jakkalskop charnockite elsewhere in the Namaqua belt are described in Section 4.6. The lithology and field relations of the very large Signalberg charnockite near Klein Karas are closely similar to those of the Jakkalskop charnockite. The Stolzenfels charnockite near Onseepkans (Toogood, 1976) is another possible correlate although it is more mafic in composition than are the Jakkalskop and Signalberg charnockites. In all three areas the charnockites represent one of the oldest syntectonic intrusive rocks.

3.5. MAGNETTAFELBERG SERPENTINITE

Map unit: *GnM Magnettafelberg serpentinite*

1. Origin of name

This map unit is named after the flat-topped hill situated 21 km due north of Garub Station in the Diamond Area (D2). The explorer Klinghardt, after noting an anomalous magnetic field in the vicinity of the hill, collected rock specimens in 1910 that were subsequently identified as essexite (alkali gabbro) by Beetz (1924) and as dioritic gabbro and serpentinite by Kaiser (1926)

2. *Distribution and Size*

Bodies of serpentinite are rare but widely scattered over the northern part of the study area. The largest of these bodies is Magnettafelberg which is of ovoid shape in plan with its long axis trending northwest. The body has dimensions of 1000 m by 400 m; its depth is not known.

Smaller bodies of serpentinite are present in the northeastern part of Aus Townlands (F5) and in the Bienenstich hills (E7). A lenticular body of larger size, some 3 km in length, is present on the farm Excelsior (B6, B7); the extremely strong disturbance of the local magnetic field (which necessitated azimuth readings to be estimated by the position of the sun) suggests that large parts of this body are unexposed.

3. *Lithology*

The core of Magnettafelberg (D2), which forms the main part of the body, is composed of fine-grained red-brown or black biotite-bearing serpentinite. Surrounding the core is a thin zone of very coarse-grained amphibolite which, in turn, is enclosed in an outer casing of very resistant coarse-grained green-grey hornblendite which has been partially serpentinized. No concentrations of chromite, magnetite or sulphides were found.

The two small bodies of serpentinite northeast of Aus Village are of similar appearance: black fine-grained very tough serpentinite contains scattered patches of talc-chlorite schist. The small exposure at Bienenstich (E7) contains a wide variety of ultramafic rocks: green and black serpentinites, dark-green and light-green hornblendite and pegmatitic biotite-plagioclase breccia are intermixed. The serpentinite on Excelsior (B6,B7) is very fine grained and dark green-grey in colour.

4. *Internal Structure*

Most of these serpentinites show no penetrative linear or planar fabric; they have apparently reacted incompetently during deformation. The contact zone of the Magnettafelberg body is, however, strongly lineated, with the lineation being parallel to that in the surrounding biotite gneiss. The borders of the serpentinite are well foliated, but this foliation does not persist inwards. Nevertheless the inner parts of the body have been cut by numerous shear planes or irregular veins of pale-green antigorite and white magnesite which have apparently formed relatively late in the tectonic history.

The Excelsior serpentinite is situated on the southern margin of the major mylonite belt of the same name. The rock has been profoundly affected by intense shearing. The serpentinite breaks into extremely long and splintery mullions parallel to a penetrative mineral lineation in the adjoining amphibolites. That part of the serpentinite body closest to the core of the shear zone consists of rounded nodules of serpentinite set in a matrix of fine-grained dark-purple mylonite.

5. External Structural Relations

Contacts with the surrounding rocks are best displayed at Magnettafelberg. This ovoid body is surrounded on three sides by Garub metasediments and biotite gneiss; the strike of the layered rocks is roughly parallel to the contact with the enclosed body, which occupies the core of a large early isoclinal fold and has apparently controlled the pattern of deformation around it. Detailed mapping around the contact, however, revealed that individual units of the surrounding rocks terminate against a transgressive contact with the serpentinite (refer to geological map, Annexure 1). Thin concordant strips of ultrabasic rock are present within the layered country rocks some distance beyond the borders of the intrusion, but it was not possible to determine if these were intrusive 'sills' or tectonic 'slices' introduced during deformation.

Exposed contacts of the other serpentinite bodies are all concordant with the foliation and layering of the country rocks.

6. Mode of Origin

The serpentinites appear to be the metamorphosed and deformed remnants of intrusive rocks of predominantly ultramafic composition. It is possible to speculate on the original nature of the Magnettafelberg intrusion: the core of serpentinite may have been derived from peridotite, the inner casing of amphibolite from gabbronorite, and the outer casing of hornblendite from pyroxenite. This zonation may originally have been vertical and produced by gravitational differentiation; or it may have been originally lateral and produced by the successive intrusion of different magmas to form a ring structure; without a detailed study no firm conclusions can be drawn

7. Relative Age

The serpentinites appear to represent intrusions emplaced early in the tectonic development of the area. They have been intruded into the layered rocks of the Garub sequence. Unfortunately contacts with the two other early-syntectonic intrusive rocks, the Tsirub gneiss and the Jakkalskop charnockite, are not exposed.

3.6. KUBUB GRANITE GNEISS

Map unit: *GnK Kubub granite gneiss*

1. *Origin of Name*

The Kubub granite gneiss is named after the mountains south of Aus Village in the western part of the farm Kubub (G4, H4) where the most extensive exposures of this rock type are situated.

2. *Distribution*

The Kubub granite gneiss is situated almost entirely in the centre of the Aus area, where it has a wide distribution and is the dominant rock type. It forms the granitic massif that extends southwards from Aus Village for 16 km; the maximum east-west exposure of these rocks is 30 km. Elsewhere only small exposures are preserved.

3. *Lithology*

The Kubub granite gneiss is composed of leucocratic heterogeneous rocks. Although it is fairly uniform on a regional scale, the Kubub granite gneiss is extremely variably in appearance at individual outcrops. The Kubub granite gneiss was differentiated into two varieties: a medium-to-coarse-grained granite gneiss GnK_1, which is usually foliated, and a pegmatoid non-foliated variety GnK_2. The two varieties are intermingled and have gradational contacts but usually one variety predominates at individual outcrops. Thus GnK_1 is more common generally but GnK_2 predominates in the eastern Kubub Mountains and in the outlying parts of the study area.

The medium-grained GnK_1 rocks are pale grey when fresh and weather to form pale-brown boulders or slabs depending on the degree of foliation. The granite gneiss contains small amounts of biotite, typically concentrated as schlieren (Plate 17); garnet is often present in the form of trains or large (up to 15 mm) porphyroblastic aggregates which are surrounded by leucocratic diffusion coronas. Banding is weakly defined by schlieren and does not continue laterally for more than 10 or 20 cm.

The pegmatitic GnK_2 variety is almost entirely devoid of mafic minerals except for 1% of pink garnet porphyroblasts.

In thin section the Kubub granite gneiss is shown to be of granitic composition: the plagioclase/(total feldspar) ratio varies between 0,15 and 0,30. The colour index varies between 1% and 4%. Biotite is present in every specimen (even though in very small amounts), whereas garnet and sillimanite are rare.

The texture of these rocks is inequigranular and granoblastic (not hypidiomorphic, which is characteristic of granites).

Potassic feldspar constitutes half of the rock and is usually present as large xenoblasts of microcline and more rarely as orthoclase with very fine-

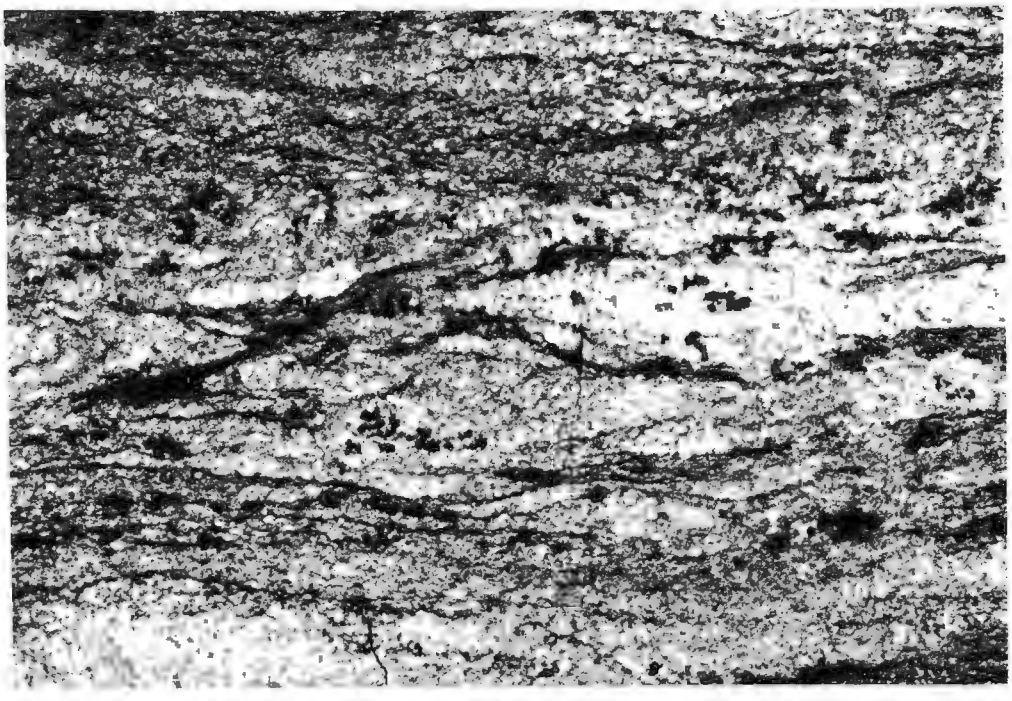

Plate 17. Texture of Kubub granite gneiss showing typical biotite-rich schlieren with scattered porphyroblasts of garnet. Area shown in 30x45 cm. 1 km NE of Kububer Horn (H4)

Plate 18. Partially absorbed inclusions of Tsirub gneiss (dark) in Kubub granite gneiss (light) showing dissemination or concentration of biotite from palaeosome into schlieren. 1 km NE of Kububer Horn (H4)

scale perthite structure of string or bead form; the plagioclase component of the perthite is sufficiently large for the grains to be classed as mesoperthite.

Plagioclase usually occurs in the form of subidioblastic laths, often of considerable size, with fairly smooth margins. It is rarely antiperthitic with irregular patch-perthite inclusions of microcline. Myrmekitic textures are common. A large proportion of crystals show deformation twinning and partial saussuritization.

Quartz comprises 30-50% by volume of the specimens examined. The mineral is generally in the form of irregular intergranular xenoblasts but it also takes the form of rounded or hexagonal inclusions within the much larger K-feldspar crystals. This type of inclusion is interpreted by Mehnert (1968, p.58) as relicts of the palaeosome that became trapped within younger feldspars growing by blastesis.

Biotite has the form of scattered disorientated subidioblastic flakes. Where it is locally concentrated into schlieren a strong foliation is present. Where fresh the biotite has a red-brown Z absorption colour, but the mineral is commonly chloritized.

Garnet is colourless in thin section and chloritized in places. Sillimanite is rare but is locally concentrated in the form of trains where it defines a foliation.

4. *External Structural Relations*

The Kubub granite gneiss has intruded rocks of the Garub sequence and the Tsirub gneiss. Fragments of the Garub biotite schist and aluminous gneiss are partially absorbed and the mafic constituents are distributed through the granite gneiss or concentrated as schlieren. Garub rock types such as amphibolite and metaquartzite are less easily absorbed and are preserved as lenticular xenoliths. Tsirub gneiss fragments are preserved as angular xenoliths which have been partially absorbed by the granite gneiss at their margins (Plate 18). At least two periods of deformation predate the intrusion of the Kubub granite gneiss; the inclusions contain a foliation which has been folded isoclinally.

The Kubub granite gneiss is cut by veins of biotite granite gneiss, which has formed late in the sequence of migmatization.

5. *Mode of Origin and Relative Age*

The inclusions of older rocks within the Kubub granite gneiss have been mentioned above. Field evidence for derivation of this rock type by anatexis is summarized in Chapter 5. The high-temperature metamorphic character of this rock unit is suggested by its granoblastic texture, the presence of microperthite and mesoperthite, the red colour of the biotite (which defines the foliation), the drop-like inclusions of quartz in feldspar, the presence

of sillimanite and garnet and the absence of muscovite. The Kubub granite gneiss is thought to have formed syntectonically by partial melting of pretectonic rocks on a regional scale followed by crystallization of the rock under conditions of high-grade metamorphism.

The Kubub granite gneiss is contemporaneous with Aus granite gneiss and the quartzofeldspathic magmatite neosomes that cut the pretectonic rocks. It postdates the Garub sequence, the Tsirub gneiss and, probably, the syntectonic Jakkalskop charnockite. It predates the syntectonic biotite granite gneiss.

6. Correlation

In the field the Kubub granite gneiss is indistinguishable from non-megacrystic varieties of the group of leucocratic granite gneisses mapped by Blignault (1976, Annexure 1) as 'megacrystic granite gneiss' and Genis (*in* Blignault, 1975) as 'Grabwasser Granite Gneiss' in the Klein Karas area, some 200 km southeast of Aus; megacrystic portions of the Grabwasser granite gneiss are equivalent to the Aus granite gneiss (see following section). The Grabwasser granite gneiss intrudes a sequence of biotite schists and aluminous gneisses known as the Grünau sequence (ibid.) which is a probable correlate of the Garub sequence at Aus.

3.7. AUS GRANITE GNEISS

Map Unit: *GnA Aus granite gneiss*

1. Origin of Name

The Aus granite gneiss is a megacrystic rock forming the large domed inselbergs north of Aus Village. It is the dominant rock type on Aus Townlands (G4) and was referred to as the Aus granite by Beetz (1924, p.22) who included it in his youngest group of granites (Red Granite) and mentioned the large characteristic 'phenocrysts' of feldspar.

2. Distribution

The Aus granite gneiss forms a large body at least 21 km in width north of Aus Village. Smaller bodies underlie the Nama escarpment in the east-centre of the study area: on the farm Jakkalskop (G7) and Tsachanabis (I8) Aus granite gneiss is associated with the Jakkalskop charnockite; another body of granite gneiss is present on the farm Duinsig (D8). Beetz (1924, p.22) noted the virtual restriction of megacrystic granite gneiss to areas

north of the railway around Aus (Annexure 1).

3. *Lithology*

The Aus granite gneiss is a coarse-grained leucocratic rock containing white tabular crystals of K-feldspar up to 5 cm in length but seldom more than 1 cm in width. Garnet is ubiquitous and is present in quantities of 1-2% in the form of small porphyroblasts, scattered or arranged in trains. Biotite is commonly present in quantities of 1-2% but the biotite-rich schlieren typical of the Kubub granite gneiss are rare in the Aus granite gneiss. The plagioclase/(total feldspar) ratio of the specimens varies from 0,08 to 0,20; quartz varies from 35 to 45 modal per cent.

Aus granite gneiss has a consistent appearance except in the immediate vicinity of other rocks such as charnockite or, rarely, amphibolite. Plate 19 shows the darkening of the granite gneiss by contamination with Jakkalskop charnockite. The contaminated granite gneiss contains greater amounts of biotite (approximately 10%) but the appearance of the white feldspar megacrysts is unchanged. In places the Aus granite gneiss has been affected by retrograde epidotization which has resulted in the formation of a green matrix.

The megacrysts consist of orthoclase and microcline; they are commonly perthitized and form a very fine-scale bead or string perthite. These crystals are lath-like but are not bounded by their crystal faces and their margins are irregular. The borders of the megacrysts are crowded with inclusions of quartz and plagioclase, whereas the central parts are free of inclusions. Smaller xenoblastic grains of microcline are present in the matrix of the rock.

Small xenoblasts of plagioclase are also present in the matrix. Reaction zones of myrmekite have developed where the mineral is in contact with K-feldspar. Quartz forms xenoblastic intergranular crystals of varying size.

Pale-pink or neutral garnet commonly has the form of small (<1 mm) rounded crystals, but grains may also be of amoeboid shape. The mineral is usually associated with small well-oriented laths of reddish biotite which is commonly chloritized. Minute rounded grains of zircon were observed in one specimen.

4. *Internal Structure*

The Aus granite gneiss usually has a foliation defined by the preferred orientation of megacrysts and biotite laths which is parallel to garnet trains. This foliation is strongest in the outer parts of the main body; in the eastern part of the body the parallel trend of the long axes of the megacrysts defines a lineation, as well as a foliation, whereas in the west the megacrysts all lie within a foliation plane but do not trend in any particular direction. In contrast the megacrysts in the centre of the main body show little or no preferred orientation; they are arranged in apparently random

Plate 19. Aus granite gneiss showing abnormal darkening of matrix by contamination with older Jakkalskop charnockite in contact zone. Note strong preferred orientation of white K-feldspar megacrysts. 4 km NW of Schakalskuppe Station (G7)

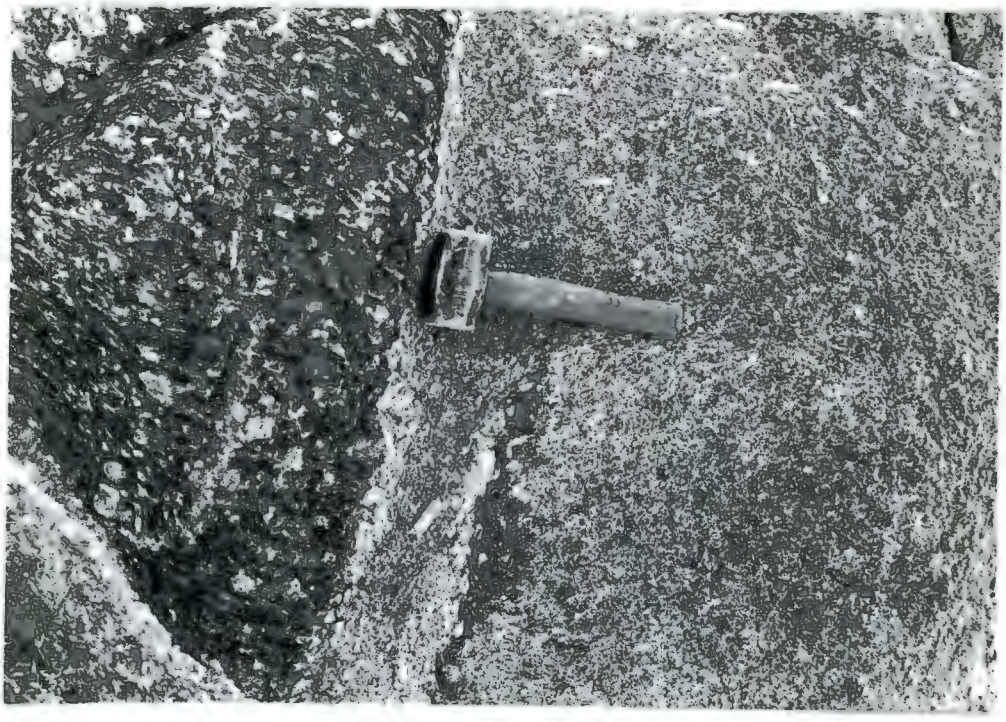

Plate 20. Xenolith of Tsirub gneiss (dark) in Aus granite gneiss. Note foliation in *GnT* crosscut by younger foliation in *GnA* at contact. Incompletely absorbed remnant of *GnT* below hammer handle. 1 km E of Kanupsforte (F4)

fashion or in groups of crystals showing a preferred orientation that changes erratically over a few metres.

5. *External Structural Relations*

The Aus granite gneiss contains numberous inclusions of older rocks in the hills north of Aus Village (G4). Contacts with older rocks are fairly sharp but are not chilled. Southwest of Kanusbank Hill large rafts of marble, calc-granofels, granofels and amphibolite of the Garub sequence are present within the megacrystic granite gneiss (see Annexure 1). On Swartaus Hill (G5) Aus granite gneiss contains disoriented xenoliths of Tsirub gneiss (Plate 20) which contain an older fabric. But at the main contact of the two rock types a few metres away Tsirub gneiss has been refoliated parallel to the foliation in the Aus granite gneiss. At the contact the Tsirub gneiss contains smaller amounts of mafic minerals than elsewhere and the Aus granite gneiss contains garnet trains parallel to the contact.

The field relations between the Aus granite gneiss and the Jakkalskop charnockite are described in Section 3.4. The Aus granite gneiss has gradational contacts with the Kubub granite gneiss and the pegmatoid mobilizates that were produced during regional migmatization.

6. *Mode of Origin*

The transgressive contacts with the country rocks, the numerous inclusions contained within it and its lithologic homogeneity suggest that the Aus granite gneiss is of igneous origin. In Chapter 5 the hypothesis is advanced that this rock unit was derived by regional anatexis and, during intrusion, moved only a relatively small distance through the crust to its present position.

The megacrysts may be phenocrysts or porphyroblasts. Support for the former hypothesis, which would be applicable to a non-recrystallized igneous rock, is given by the orientation of the megacrysts in the vicinity of angular inclusions. At the contact with these inclusions the feldspar megacrysts are in many places aligned parallel to the borders of the inclusions and oblique to the main direction of preferred orientation. The well-developed orientation at the borders of the main body and the absence of this alignment at the centre could be ascribed to magmatic flow which is strongest at the contacts. In this case the presence of garnet and sillimanite would have to be ascribed to a former metamorphic event; their preservation would be due to their refractory nature.

Alternatively the megacrysts are porphyroblasts; their growth would then be a metamorphic event postdating the intrusion. The foliation defined by the alignment of megacrysts, garnet trains and biotite flakes would have been produced entirely during this metamorphic event.

The writer favours a combination of these two hypotheses. Because the megacrystic granite gneiss was undoubtedly intrusive in origin and was intruded syntectonically during a period of high-grade regional metamorphism and migmatization (Section 4.5, 5), it is likely that the rock crystallized under conditions of stress and high temperature. It seems probable therefore that the megacrysts are of primary origin but grew by blastesis; this is suggested by their irregular inclusion-filled borders in thin section and the common occurrence of similar porphyroblasts in other rock units adjacent to the Aus granite gneiss. Because stress is commonly concentrated at the borders of rock bodies it follows that the foliation would be more strongly developed near the contacts (Strömgård, 1973, p.236).

Because the inclusions of Tsirub gneiss show evidence of absorption by the megacrystic granite gneiss (Plate 20), it is likely that many of the garnet trains near the inclusions represent refractory remnants of the Tsirub gneiss; but the evenly-distributed garnet porphyroblasts situated many kilometres away from the contact are more likely to have formed during crystallization of the granite gneiss.

7. *Relative Age*

The Aus granite gneiss postdates the Garub sequence and the Tsirub gneiss; it probably postdates the Jakkalskop charnockite (Section 3.4) and is contemporaneous with the Kubub granite gneiss and the quartzofeldspathic pegmatoid neosomes produced during migmatization.

8. *Correlation*

The Aus granite gneiss is lithologically identical to the megacrystic varieties of Blignault's (1976, Annexure 1) 'megacrystic granite gneiss', which is also known as the Grabwasser granite gneiss (Genis *in* Blignault, 1975) in the Klein Karas area 200 km to the southeast of Aus. Both granite gneisses contain the characteristic tabular megacrysts of K-feldspar and very small amounts of garnet and biotite; both contain large amounts of K-feldspar and quartz. Both rocks were intruded relatively late in the tectonic development of the Klein Karas (Blignault, 1976, Annexure 1) and Aus areas.

The writer is not in favour of the correlation of these megacrystic granite gneisses with the Beenbreek (Toogood, 1976) and Eendoorn (Beukes, 1973) granite gneisses of the Warmbad District as suggested by Blignault et al. (1974). The Eendoorn and Beenbreek granite gneisses are darker rocks containing an average of 18 (Beukes, 1973, p.211) and 17±5 (Toogood, 1976) modal per cent of biotite; in contrast the Aus granite gneiss contains an average of 2 modal per cent of biotite. Furthermore both the Beenbreek and Eendoorn granite gneisses have been intruded early in the tectonic development of the Warmbad District (Toogood, 1976; Beukes, 1973, p.ix) in contrast to the Aus and Grabwasser granite gneisses.

3.8. BIOTITE GRANITE GNEISS

Map units: *GnBh Biotite granite gneiss*
GnBs Streaky biotite gneiss
GnB Undifferentiated biotite gneiss

1. Nomenclature

The name 'biotite granite gneiss' refers to lithologically homogeneous greyish foliated biotite granites. Those varieties of biotite gneiss not displaying evidence of intrusion were mapped as 'undifferentiated biotite gneiss' in order to indicate the possibility of correlation with the undifferentiated biotite gneisses of similar appearence associated with the pretectonic layered gneisses. 'Streaky biotite gneiss' is characterized by streaky aggregates of biotite and is present in areas where a linear structural fabric predominates over a planar fabric.

2. Distribution

Unlike layered biotite gneiss, which is widespread in the south, biotite granite gneiss is found mainly in the centre-north of the Aus area. Undifferentiated biotite gneiss is the dominant rock type along the escarpment (E8, D8) in the north; the less common biotite granite gneiss is well developed in the hills around Groot Löwenberg (E4, F4) where it forms large bodies or small dykes, which are often folded, and stocks.

3. Lithology

Even in the form of narrow dykes the biotite granite gneisses are medium grained and lack chilled margins. They consist mainly of K-feldspar and quartz with subordinate amounts of plagioclase. Biotite is the main mafic mineral and comprises 1-10% of the rock; garnet is common but hornblende was not found. These rocks are even-grained and are homogeneous or, more usually, nebulitic with faint layering or discontinuous schlieren. Garnet can form porphyroblastic aggregates up to 10 cm in diameter (Plate 21). Differentiation of this type can only take place in situ and the garnet is therefore not a relict of a pre-intrusive metamorphic event.

4. Internal Structure

Biotite granite gneiss almost invariably shows some degree of foliation,

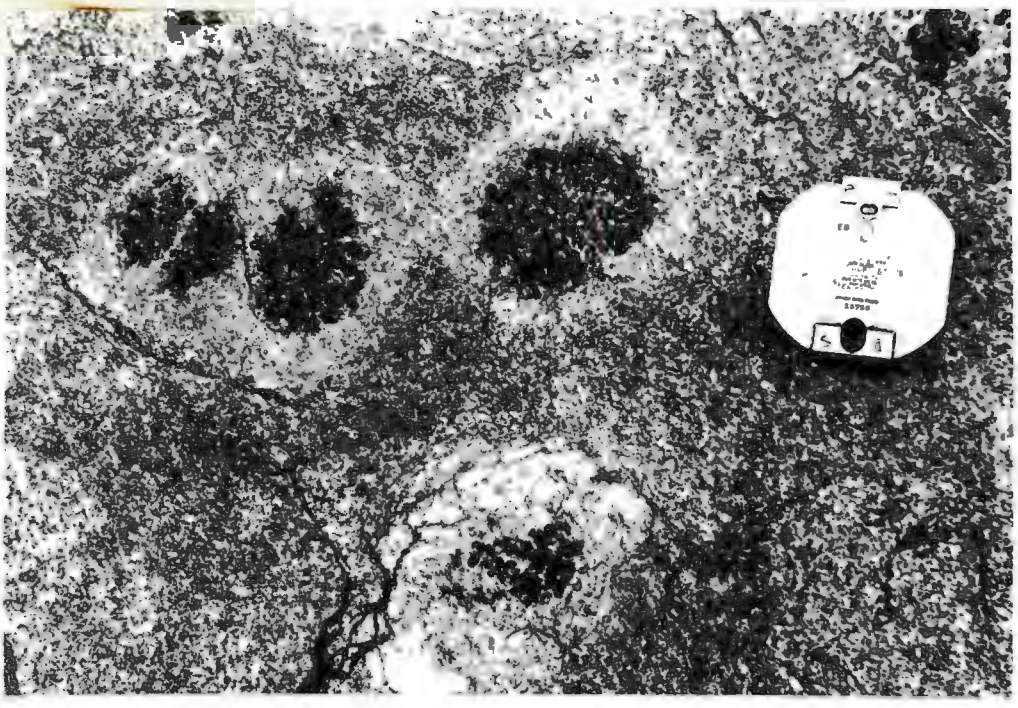

Plate 21. Porphyroblastic aggregates of garnet with leucocratic diffusion coronas in biotite granite gneiss. Northern foothills of Festung Mountain (G2).

Plate 22. Contact between younger porphyritic mafic dyke (dark) and older biotite granite gneiss (light) illustrating the Sederholm effect; remobilization of granite gneiss country rock has produced intrusive tongues of granite. N end of Bienenstich Hills (E7)

even when in the form of narrow dykes. This foliation is defined by the preferred orientation of biotite flakes and is commonly oblique to the strike of the nebulitic inclusions within the granite gneiss. In the hinge zones of major early folds deformation has resulted in the development of a penetrative linear fabric which is indicated by the aggregation of biotite flakes into cigar-shaped segregations giving rise to a streaky appearance at outcrop.

5. *External Structural Relations*

The relation of the dykes and stocks of biotite granite gneiss to their country rocks is unambiguous: the intrusive rocks cut through the banding of the country rocks and the foliation of the granite gneiss is commonly oblique to the older foliation in the layered rocks. Contacts are generally sharp, but there are no chilled margins. These dykes commonly cut rocks of the Garub sequence and the Tsirub gneiss; the Aus granite gneiss is intruded by biotite granite gneiss on Kanusbank (F4).

Inclusions of Garub rocks within the biotite granite gneiss are generally lenticular and are roughly concordant with the nebulitic layering of the granite gneiss. They commonly exceed 40 m in length but range in size down to schlieren only a few millimetres wide. The biotite granite gneiss cuts the foliation and folding associated with early deformation and also the quartz-feldspar migmatite neosomes. In numerous localities the biotite granite gneiss crosscuts the pretectonic layered biotite gneiss and on the farms Kwessipoort (F6) and Duinsig (E8) veins of biotite granite gneiss cut the Jakkalskop charnockite.

There is evidence for remobilization of the biotite granite gneiss after its initial crystallization. Thus Plate 22 illustrates the Sederholm effect (Eskola, 1961): a late-tectonic porphyritic basic dyke was intruded into the biotite granite gneiss, but remobilization of the granite gneiss has resulted in its intrusion into the basic dyke; the granite gneiss is thus partially older and partially younger than the rock which it contains.

6. *Origin*

The possible origin of the biotite granite gneiss is discussed in Section 5.3; it is concluded that these rocks most probably formed by diatexis (melting of the quartz-feldspar-biotite fraction of older rocks) during regional migmatization.

how does it really differ from partial melting or anatexis! Jargon

7. *Relative Age*

The biotite gneiss is younger than the Garub sequence, the layered biotite gneiss, the Tsirub gneiss and the Jakkalskop charnockite. It is most probably

also younger than the Kubub and Aus granite gneisses.

8. Correlation

Rocks greatly resembling the biotite granite gneiss are present at the coast to the west of the Aus area. The 'orthogneiss' of Kröner and Jackson (1974, p.83), which is the dominant rock type at Hottentot Bay, shows many similarities in lithology to the rocks described here and occupies a similar tectonic position. The 'mixed gneiss' of Greenman (1966) around Lüderitz is also of similar appearance. Other rock types of similar appearance mapped elsewhere in the Namaqua belt as part of the 'mixed gneiss' or 'grey gneiss' units (Blignault et al., 1974; von Backström, 1964) are possible correlates; but since these sack-names describe rocks that are both pretectonic and syntectonic, well-founded correlations cannot be made. — So 2ac GnB1!

3.9. ANIB GRANITE GNEISS

Map unit: *GnAn Anib granite gneiss*

1. Origin of Name and Distribution

This rock unit is named after the farm Anib (M6) where the rocks are best exposed. Anib granite gneiss is restricted to the farms Grens, Anib, Anusi and Pockenbank in the extreme southeast part of the study area (M5, M6). The eastern, western and southern parts of the granite gneiss are overlain by sediments of the Nama Group and it is not known how far the Anib granite gneiss extends beneath this cover.

2. Lithology

The Anib granite gneiss is lithologically uniform throughout the area in which it is exposed. It is a leucocratic pink-green granitoid which weathers to form pink-grey rounded boulders. The rock is coarse grained and often porphyroblastic but these blasts are not as well formed or regularly developed as those of the Aus granite gneiss. Specimens of Anib granite gneiss have a plagioclase/(total feldspar) ratio of ∿0,10 and contain large amounts of quartz (50-60%) but only 1-2% biotite. Compositionally, therefore, the rock is a quartz-rich leucogranite.

K-feldspar occurs as both microcline and perthite; the latter has the coarse irregular texture typical of replacement perthites. The grains are commonly in the form of aggregates or porphyroblasts. Large xenoblastic

crystals of quartz are set in a matrix of smaller grains. Chloritized biotite is the only mafic mineral present. Retrograde muscovite has formed by breakdown of microcline. Slight concentrations of biotite define a nebulitic layering.

3. *Internal Structure*

Because it contains such a low proportion of biotite, the Anib granite gneiss does not usually display a strong foliation, but where the biotite has been concentrated in the form of schlieren a foliation is apparent.

The Anib granite gneiss has been cut by the Kuckaus mylonite belt. In the vicinity of the mylonites the development of a cataclastic foliation is shown by weathering in the form of pinnacles instead of the spheroidal boulders typical of the unsheared rock. In the core of the shear zone fine-grained laminated rocks were formed by mylonitization.

implies crushing & granulation - i.e. physical separation Can you be sure not simply annealing?

4. *External Structural Relations*

All contacts with other rock units are obscured by a cover of sand or by sediments of the Nama Group. Inclusions of other rock types are present: on Arasab Berg (M5) nebulitic inclusions of layered biotite gneiss are common and on the farm Anusi (N7) a large xenolith of Garub amphibolite (see Annexure 1) has been migmatized by pegmatoid from the granite gneiss.

5. *Origin and Relative Age*

The strikingly uniform lithology and the xenoliths it contains suggest an intrusive origin for the Anib granite gneiss. The nebulitic portions are interpreted as incompletely absorbed relicts of country rock.

The Anib granite gneiss is younger than the rocks of the Garub sequence and layered biotite gneiss. Its relation to other syntectonic intrusive rocks is not known.

3.10 PYRAMIDE GRANITE GNEISS

Map Unit: *GnP Pyramide granite gneiss*

1. *Origin of Name and Distribution*

1. *Origin of Name and Distribution*

The Pyramide granite gneiss is named after two hills in the southern part of Kubub Farm - the Grosse Pyramide and Kleine Pyramide (I4) - where the rock type is particularly well exposed.

The Pyramide granite gneiss is not common and all outcrops are in the form of small stocks. Nevertheless, it is widespread in the south of the study area and outcrops are present in the following places: in the southern part of Kubub Farm (I4), south of Oisib peak in the Kuckaus Mountains (K3, K4), at Ganaam waterhole (I3), on the southern part of Arasab Farm (J6), the northern part of Kokerboomkloof Farm (K6) and west of Heiderberg (H8).

2. *Lithology*

Pyramide granite gneiss comprises mesocratic pink-grey granites which weather to form greyish boulders; they are medium grained or coarse grained and generally equigranular. A weak foliation is usually present but on Arasab Farm a strong foliation is developed. Pink feldspar megacrysts with rectangular or oval shape (up to 1 cm long) are present on the farms Kokerboomkloof and Arasab. Spheroidal porphyroblasts of garnet are rare.

The Pyramide granite gneiss contains approximately equal amounts of microcline (often with coarse perthetic inclusions) and plagioclase, about 30% quartz and up to 20% biotite. These rocks are distinguished from the biotite granite gneisses and gneisses by their pink-grey colour.

3. *External Structural Relations*

Numerous contacts with biotite schist and amphibolite of the Garub sequence show that the contacts and foliation of the Pyramide granite gneiss cut the foliation, banding, neosome veins and early folds of the older rocks. South of Kuckaus Mountains (K3) the granite gneiss transects banding and foliation of layered biotite gneiss.

On Arasab Farm the Pyramide granite gneiss is cut by veins of garnetiferous quartzofeldspathic neosome; it was not possible to determine if the foliation in the granite gneiss predated the intrusion of the neosome because of the lack of foliation in the latter.

4. *Origin and Relative Age*

The sharp intrusive contacts with the country rocks and the distinctive appearance of the Pyramide granite gneiss suggest that the rock was not formed in situ but was intruded after the initial migmatization of the pretectonic rocks but before the processes of migmatization and deformation had ceased. It may be contemporaneous with the Anib granite gneiss.

5. Correlation

The Pyramide granite gneiss closely resembles the late-syntectonic 'adamellite' at Lüderitzbucht (Greenman, 1966) and the pink-grey granite at Douglas Bay farther north (Kröner and Jackson, 1974). Preliminary minimum U/Pb zircon ages determined by Dr. A.J. Burger for the two coastal rock types are 1082 Ma and 1114 Ma respectively (Kröner, 1975, p.56).

3.11 TIRAS GNEISS

Map unit: *GnTa Tiras gneiss*

1. Origin of Name and Distribution

This rock unit was named by von Brunn (1967) after the Tiras mountains (B7). The rock is referred to as 'gneiss' rather than 'granite gneiss' in order to emphasize its uncertain origin and stratigraphic position. The Tiras gneiss is restricted to the northeast of the study area, where it is widespread. It builds the Tiras Mountains (A6, B7) and underlies large areas of the Tiras Plateau (B8). The formation is situated almost entirely north of the Excelsior mylonite belt except on the farm Neisip (C8) where it extends a few kilometres south of the mylonites.

2. Lithology

The Tiras gneiss is a fine-grained leucocratic reddish-pink granitoid. The petrography of this rock was described by von Brunn (1967, p.111-112) and need not be repeated here.

In parts of the Tiras Mountains the rock is so fine grained that it resembles an acid lava; but since the rocks are highly sheared, these varieties may represent silicified cataclasites. In thin section these rocks resemble blastomylonites (partially recrystallized mylonites) and consist almost entirely of minute grains of quartz and feldspar in which are set larger grains of strained K-feldspar. The rock is cut by veins of pink aplite and pegmatite which may be a later phase of the same intrusion.

3. Internal Structure

As reported by von Brunn (1967, p.110), the Tiras gneiss is unfoliated or weakly foliated in the extreme northeast of the area (A8) and could thus

be classed as granite gneiss but in the Tiras Mountains, which border the Excelsior mylonite zone, the Tiras gneiss is strongly foliated. Here alignment of biotite flakes defines a foliation and a lineation that trends parallel to those in the adjoining mylonites.

4. *External Structural Relations*

On the northern margin of the Tiras Mountains (B7, A7) the Tiras gneiss contains lensoid mappable bodies and small rafts of Garub granofels, amphibolite and biotite schist (see Annexure 1). The gneiss has intruded the Garub rocks in lit-par-lit fashion. Contacts with biotite granite gneiss (restricted to Neisip Farm) are highly sheared and ambiguous. The relation between the Tiras gneiss and younger rocks of the Naisib River Complex is discussed in the following section.

5. *Origin*

Von Brunn (1967, p.114) suggested that the Tiras gneiss represented an early intrusive phase of the Tumuab granite (correlated by Watters, 1974, with the Sinclair Group and described in the present report in Section 3.13), which is situated on the northern fringe of the study area (see Annexure 1). The well-foliated and metamorphic nature of the Tiras gneiss was ascribed to two possible processes (ibid.):

(i) Deformation due to the pressure exerted by later granitic intrusions (including the Tumuab granite) just north of the present study area (the exposed width of these batholiths exceeds 80 km)

(ii) Deformation due to shearing related to the formation of the Excelsior mylonite belt

The present writer favours the second possibility because:

(i) The structures in the well-foliated parts of the gneiss are parallel with those in the adjoining mylonites.

(ii) The foliation and lineation within the gneiss are most strongly developed in the vicinity of the mylonite belt; northwards from here the foliation is less marked or absent.

Isoclinally folded layering, which may represent primary stratification, is visible on colour aerial photographs of the northern flank of the Tiras Mountains; no sign of layering is visible in the field. But at least part of the Tiras gneiss is of intrusive origin (Section 4, above).

6. Relative Age

Von Brunn (1967, p.110) recorded that 'The exact stratigraphic position of gneissic rocks that build the Tiras mountains still remains uncertain'. This conclusion was also reached by the present author. As noted by von Brunn, the Tiras gneiss is certainly younger than the Garub rocks ('meta-Kheis' of von Brunn) but apart from this conclusion there is some doubt as to its relative age. The Tiras gneiss is not in contact with the syntectonic granite gneisses that are extensively developed in the central part of the Aus area (Aus granite gneiss, Kubub granite gneiss) and contacts with biotite granite gneiss are too sheared to provide a sound conclusion. Furthermore the Tiras gneiss is not in contact with rocks of the Sinclair Group, which is situated immediately north of the study area (von Brunn 1967; Watters, 1974, Fig. 33).

3.12 NAISIB RIVER COMPLEX

Map Units:
- *GT* *Tierkloof diorite*
- *GTv* *Tierkloof rhyolite and dacite*
- *gd* *Granodiorite dyke*
- *GK* *Klein Tiras granite*
- *GH* *Houmoed granodiorite*

The Naisib River Complex comprises a suite of late-syntectonic intrusive granitoids and felsic extrusives restricted to the northeastern part of the study area. It has intruded older rocks of the Namaqua Metamorphic Complex, but it predates the Sinclair Group, as defined by Watters (1974).

The Naisib Complex is composed of three formations: Tierkloof diorite, Klein Tiras granite and Houmoed granodiorite. None of the three formations are in contact with each other. The igneous complex is named after the large riverbed in the plain separating the Houmoed granodiorite from other formations in the complex.

1. Tierkloof Diorite

The Tierkloof diorite is named after the narrow valley on the northern margin of the body. It was mapped by von Brunn (1967) as 'hybrid rocks' consisting of 'granite and Kheis (?) metabasalt' and referred to by the present writer in a preliminary report (Jackson, 1974) as part of an 'intrusive suite'.

The formation builds the Nausspitzkopf Mountain in the northeast part of Excelsior Farm (A6). The exposed areal extent of the body is about 35 km^2.

The Tierkloof diorite comprises coarse-grained equigranular plutonic rocks which are predominantly mesocratic and dark-weathering. The dark-weathering rocks grade into lighter-coloured varieties which are more common in the

western part of the body. Large (up to 6 cm in length) phenocrysts of plagioclase are present in a porphyritic border zone about 5 m wide on the northern margin of the body in Tierkloof; the porphyritic zone grades into the massive diorite.

Most of the specimens of Tierkloof diorite are quartz monzodiorites: they contain 5-10% quartz, and plagioclase constitutes 80-90% of the feldspars. The texture of these rocks is coarse-grained hypidiomorphic granular. The chief mafic minerals are biotite (7-10%) and hornblende (∿20%). Hornblende is usually chloritized and the ragged borders found in some grains suggest that at least some of the hornblende is secondary. In one specimen hornblende has clearly formed from clinopyroxene which is preserved in some hornblende pseudomorphs. Some of the biotite has formed by breakdown of pyroxene but much of it appears to be primary. Plagioclase is present as well-formed euhedral laths; microcline is in the form of anhedral crystals of irregular shape which display the coarse intergrowths typical of replacement perthites.

Inclusions of volcanic rocks (map unit *GTr*) are scattered throughout the diorite body and some of these are shown on the map (Annexure 1). They are well preserved at the southeastern end of Tierkloof where they are intruded by diorite. An older variety is a fine-grained dark grey-green dacite porphyry containing phenocrysts of plagioclase. Chloritized biotite (∿15%) and opaque minerals are the mafic components. The lavas contain rounded clasts of quartz-feldspar fragments arranged in layers (Plate 23). These clasts may be of tectonic origin because much of this rock is cataclastic and has a mortar structure: rounded grains of plagioclase (∿ 1 mm in diameter) constitute about 75% of the rock and are cemented by a very fine-grained aggregate of quartz and feldspar.

The dacite is subordinate in volume to a younger rhyodacite which cuts the banding in the dacites. The rhyodacite, which is well exposed at the southeast end of Tierkloof, is a leucocratic but dark-coloured, pink-grey volcanic rock with well-developed flow structure defined by pink or grey bands and dark streaks of mafic minerals. The rock contains dark-grey lensoid inclusions up to 3 cm in length. The banding curves around these inclusions and thins at the thickest parts of the inclusions, indicating flattening. The rock fractures into spindle-shaped or bladed fragments which are elongated parallel to the banding and the long axes of the inclusions. The matrix of this rock consists of a very fine-grained mixture of quartz and feldspar. The inclusions comprise lensoid aphanitic lithic clasts, which are suggestive of flattened pumice fragments, and small phenocrysts or clasts of plagioclase and quartz. The dark streaks visible in hand specimen comprise aggregates of minute needles of green amphibole.

The main mass of the Tierkloof diorite is unfoliated; only in the extreme southern and northern parts of the body is the foliation developed. In the south the diorite is in sheared contact with amphibolite of the Garub sequence; foliated diorite, sheared volcanic rock and retrogressively metamorphosed sheared amphibolite are intercalated. The northern margin of the body is bounded by the Excelsior mylonite belt and the rocks have been affected to varying degrees by shearing. A non-pervasive foliation is present up to 2 km away from the mylonites; the intensity of foliation increases towards the

Plate 23. Tierkloof dacite containing white clasts of quartz-feldspar rock arranged in layers. SE end of Tierkloof (B6)

Plate 24. Xenoliths of Garub amphibolite in unfoliated Houmoed granodiorite. 5 km E of Kalk beacon (B8)

centre of the shear zone and the diorite is penetratively foliated immediately adjacent to the mylonites at the northwestern end of Tierkloof. Here the diorite is porphyritic and the degree of flattening shown by the phenocrysts provides a measure of the extent of deformation in the rock. The phenocrysts are in random orientation as close as 100 m away from the mylonites, but these zones of unsheared diorite alternate with sheared rock in which the phenocrysts are drawn out into flattened oval crystals; the long axes of the deformed crystals define a lineation and their flattened shape defines a foliation. With increasing strain the phenocrysts have been shattered and partly dispersed in the form of trails of broken fragments; the matrix of the rock is dark and schistose. Within the mylonite zone itself poorly-defined white streaks are all that remain of the plagioclase phenocrysts and at this stage the matrix of the rock is so fine grained that it resembles mafic lava. Intercalated with these mylonites are tectonic slices of unsheared dark-green dacitic lava containing euhedral phenocrysts of plagioclase. The foliation and lineation of the sheared porphyritic diorite roughly parallels that of the mylonites in the core of the shear zone.

The lenticular fragments within the pink rhyodacites are strongly aligned parallel to the lineation in the nearby mylonites and Tiras gneiss at the south-east end of Tierkloof; this fact, together with the textural evidence for flattening, suggests that the fabric of these extrusive rocks developed largely as a result of deformation by elongation and realignment of the inclusions in a similar manner to the deformed phenocrysts in the diorite. Some degree of preferred orientation of the inclusions could be expected to arise from primary flow, but it is not known to what extent this process has contributed to the preferred orientation now observed.

Direct evidence for the relation of the Tierkloof intrusive and extrusive rocks to the other lithologic units is not present because both contacts to the north and south of the body are highly sheared. No xenoliths of other rocks, apart from the volcanic inclusions, were found in the Tierkloof diorite. Dykes of fine-grained dark-grey hornblende granodiorite (map unit *gd*), which may be related to the Tierkloof diorite, cut through biotite granite gneiss and migmatized biotite schist of the Garub sequence a few kilometres south of the diorite body.

2. *Klein Tiras Granite*

The Klein Tiras granite is named after the small hill at the southeastern end of the Tiras mountain range. This rock is restricted to the southwest part of Tiras Farm (B7). It occurs in the form of two small stocks, with an exposed width of 2 and 4 km respectively adjoining the Tiras gneiss. The Klein Tiras granite is medium-to-coarse grained, leucocratic and pale grey in colour. The eastern body is predominantly even-grained,whereas the western body is porphyritic and contains tabular phenocrysts (up to 5 cm in length) of K-feldspar.

The non-porphyritic varieties display allotriomorphic-granular textures in thin section. The plagioclase/(total feldspar) ratio in the specimens is about

0,20 and quartz is present in quantities of about 25%. One per cent chloritized biotite and secondary epidote are the sole mafic components.

The Klein Tiras granite is largely unfoliated but a weak foliation is present in the extreme south of the eastern exposure in the vicinity of the mylonite belt. The granite cuts across the foliation in the adjoining Tiras gneiss; this relation indicates that the granite was intruded after the main deformation had taken place, but before large-scale movement had ceased.

3. *Houmoed Granodiorite*

The Houmoed granodiorite was referred to by von Brunn (1967) as the 'grey granodiorite'. Its name has been changed (Jackson 1975) to Houmoed granodiorite in order to conform with the lithostratigraphic nomenclature recommended by the ISSC (Hedberg, 1970). The name is taken from the farm where the largest outcrop of this rock is present.

The Houmoed granodiorite occurs only in the extreme northeastern part of the study area (Annexure 1) but according to von Brunn (1967) this body extends farther eastwards and occupies an area of about 79 km^2; smaller bodies are also present to the north of the study area.

The Houmoed granodiorite is a medium-grained leucocratic grey rock which greatly resembles the paler varieties of the Tierkloof diorite. Biotite and hornblende are commonly in the form of small aggregates of crystals or larger clots. In common with other plutonic rocks (e.g. the Jakkalskop charnockite and the Tierkloof diorite) the granodiorite has a striking mode of weathering which gives rise to prominent irregular patches of dark-coloured desert varnish on outcrop surfaces.

The texture of the granodiorites is allotriomorphic granular and the grain size is seriate. Crystals of quartz and feldspar are extremely ragged and riddled with inclusions of mafic minerals. Cataclastic specimens have a mortar structure. Very small amoeboid crystals of blue-green hornblende in modal quantities of 1-3% commonly occur in aggregates; subhedral flakes of olive-brown biotite in modal quantities of 2-15% are evenly scattered through the rock. Idioblastic grains of zoisite and epidote (3-7%) are concentrated in the form of veins. Glomeroporphyritic aggregates of sphene and skeletal opaque crystals with subhedral form are commonly present in modal quantities of up to 3%.

Plagioclase crystals are largely altered to a mixture of epidote and sericite; crystals of plagioclase, microcline (commonly of smaller size) and quartz are all anhedral. The plagioclase/(total feldspar) ratio of the specimens varies between 0,8 and 1,0. Chemical analyses of the Houmoed granodiorite by von Brunn (1967, p.48) show close similarity with the composition of Nockolds' (1954, p.1014) average granodiorite.

The Houmoed granodiorite is largely unfoliated,but discontinuous zones of sheared rock are found throughout the exposures on Houmoed Farm (A8, B8). Two specimens of foliated granodiorite from its northernmost exposure at the Aus-Helmeringhausen road have a weakly cataclastic mortar texture. There is no

systematic increase in foliation development southwards and the Houmoed granodiorite is unfoliated at its southernmost exposure in the area (Plate 24).

Mafic inclusions are characteristic of the Houmoed granodiorite; these consist of amphibolite and mafic lavas. At the southern margin of the granodiorite a few kilometres west of Houmoed farmhouse on the eastern border of the study area (B8) the formation is in contact with amphibolites correlated with the Garub sequence. The granodiorite has a contact zone about 20 m wide which is crowded with disoriented angular xenoliths of amphibolite (Plate 24) that are of identical lithology to those on Excelsior Farm (B7) farther south. The xenoliths are foliated and lineated; some show banding and isoclinal folds which are truncated by the unfoliated granodiorite. Small inclusions of fine-grained mafic lavas are common in the central parts of the granodiorite body; some of them are porphyritic and amygdaloidal. These lavas contain needles of blue-green hornblende, chlorite and epidote-zoisite. If present, the phenocrysts are euhedral plagioclase grains. In summary, therefore, the Houmoed granodiorite contains inclusions of two types: (i) amphibolite-facies tectonized amphibolite of the Garub sequence; (ii) greenschist-facies non-tectonized volcanic rock.

Field relations between the Houmoed granodiorite and the Tiras gneiss are ambiguous. Von Brunn (1967, p.7; written comm., 1975) reports that at a number of places on the farms Houmoed and Nuweplaas (east of Houmoed) on the Tiras Plateau fine-grained pink granitoid correlated with Tiras gneiss intrudes grey granitoid correlated with Houmoed granodiorite; examination of contacts in this area by the writer revealed gradational contacts between the two rock types. It would thus appear that on the Tiras Plateau, at least, the Houmoed granodiorite is postdated by, or contemporaneous with, a granite resembling the Tiras gneiss. However, the reverse relation is present farther south 4 km east of Kalk trigonometrical beacon (B8). Here, unfoliated Houmoed granodiorite is separated by 100 m of unexposed ground from strongly foliated Tiras gneiss containing inclusions of equally strongly foliated Garub amphibolite. The most likely explanation for this relation is that the intrusion of the Tiras gneiss into the Garub amphibolites was followed by a period of tectonism after which the Houmoed granodiorite was intruded.

It would appear from the above observations that rocks correlated with the Tiras gneiss are both older and younger than the Houmoed granodiorite and that there are therefore at least two types of Tiras gneiss; an older strongly foliated gneiss (typical of the Tiras Mountains) and a younger granite in which a foliation is only weakly developed or absent (typical of the Tiras Plateau). There is also the possibility of more than one age for the Houmoed granodiorite as suggested by von Brunn (written comm., 1975).

4. *Discussion on the Correlation and Age of Formations in the Naisib River Complex*

Although none of the formations that make up the Naisib River Complex are in contact with each other, their correlation is suggested by similarities in lithology, associated rock types, tectonic category and stratigraphic position.

These similarities are briefly summarized below.

Pale varieties of the Tierkloof diorite are indistinguishable in appearence from the Houmoed granodiorite. Porphyritic rock types are a feature of both the Klein Tiras granite and the Tierkloof diorite. Low-grade, largely undeformed (outside the mylonite belt) extrusive rocks are present as inclusions in both the Houmoed and Tierkloof formations. All three formations of the Naisib River Complex are largely unfoliated but in each case a cataclastic foliation is present in certain parts of the intrusions: intermittently developed in the Houmoed granodiorite and restricted to the mylonite belt or contacts of the other bodies. The Tierkloof diorite was intruded before the formation of the Excelsior mylonite belt. The Houmoed granodiorite postdates the deformation and metamorphism of the Garub amphibolites; dykes correlated with the Tierkloof diorite have intruded both the Garub formation and biotite granite gneiss.

The Houmoed granodiorite underlies the Nagatis Formation of the Sinclair Group just north of the study area (von Brunn, 1967, p.7; Watters, 1974, Table 22): the Nagatis Formation has not yet been dated but the younger Tumuab granite (A8), which intrudes it, has yielded two unreliable Rb/Sr isochrons, based on two specimens each, with slopes corresponding to ages of 1020±80 Ma and 1290±80 Ma respectively (von Brunn and Dodson, 1967). The nearby Rooikam granite of equivalent stratigraphic position to the Tumuab granite (von Brunn, 1967) has yielded a more reliable U/Pb minimum zircon age of 1360±50 Ma (Burger and Clifford *in* Burger and Coertze, 1973, p.23). On the basis of this age obtained from the Rooikam granite, which is younger than the Nagatis Formation, which in turn rests on the Houmoed granodiorite, the age of the Houmoed granodiorite must be greater than this. Yet the radiometric age yielded by the Houmoed granodiorite is only ∿1078 Ma (Appendix 7); it is strikingly similar in appearance to the 1900 Ma-old Vioolsdrif granite and was tentatively correlated with it by von Brunn (1967, p.48) on the basis of chemical similarities.

Rocks of the Naisib River Complex may be correlates of pre-Sinclair rocks farther north. The pre-Sinclair Kumbis Complex north of Sinclair Mine includes certain granitoids that were correlated by Watters (1974, Table 1) with the Houmoed granodiorite. Similarly Schalk (pers. comm., 1975) reports that rocks closely resembling the Tierkloof diorite are widespread in the area north of that mapped by Watters, where they underlie rocks of the Sinclair Group. The presence of inclusions of volcanic rock in the Naisib River Complex, which predates the Nagatis Formation (von Brunn, 1967, p.7), is evidence for the existence of extrusive and intrusive igneous activity before the formation of the Sinclair Group. This pre-Nagatis igneous event is postulated to have been the precursor of the very much more extensive igneous activity that resulted in the formation of the Sinclair rocks. Table 16 shows the stratigraphic succession of this region (Excelsior area) determined by von Brunn (1967) compared with that proposed here in the light of the above observations.

TABLE 16

Comparison of stratigraphic columns suggested for the Excelsior area

VON BRUNN (1967)	JACKSON (this report)	
Tumuab granite	Tumuab granite	Sinclair Group (Watters, 1974)
Tiras gneiss	Nagatis Formation	
Nagatis Formation		
	Klein Tiras granite	Naisib River Complex (Jackson 1975)
Grey granodiorite	Houmoed granodiorite	
	Tierkloof diorite extrusive rocks	
	Tiras gneiss	Namaqua Metamorphic Complex
	Biotite granite gneiss	
Kheis (?)	Garub sequence	

3.13 TUMUAB GRANITE

Map Unit: *GTb Tumuab granite*

The Tumuab granite was named by von Brunn (1967) after the trigonometrical beacon on Tumuab Mountain which is situated about 15 km east of the northeastern corner of the present study area. The granite is restricted to the northern fringe of the study area but its outcrops extend northwards and cover an area of approximately 720 km^2 west of Helmeringhausen Village (ibid.).

The petrology and field relations of the Tumuab granite have been fully described by von Brunn (1967). The Tumuab granite is a leucocratic alkali-rich red granite emplaced in the form of a composite batholith; it has intruded the Houmoed granodiorite and the Nagatis Formation but is not in contact with the Tiras gneiss.

The Tumuab granite is unfoliated except in the western end of the Koiimasis-Namtib Mountains where the rock has been sheared along planes striking west-northwest (ibid.). The granite is younger than the main phase of shearing: the Excelsior mylonite belt does not continue on its northwest trend into the large mass of Tumuab granite that builds the Koiimasis-Mantib Mountains. According to von Brunn (pers. comm., 1975) coarse-grained alkali granite (possibly Tumuab granite) intrudes the mylonites on the eastern flank of Springbok Vlakte which lies west of Nausspitzkopf Mountain (A6). It would therefore appear that the weak shearing in Tumuab granite at the western end of the Koiimasis-Namtib mountains is due to post-mylonite deformation of smaller magnitude (displacement along the Excelsior mylonite belt continued in post-Nama times).

The geochronology of the Tumuab granite was discussed in the previous section. These radiometric data provide unreliable minimum ages for the deformation which formed the Excelsior mylonite belt. The Tumuab granite was correlated by Watters (1974, Table 22) with the Nubib granite of the Sinclair Group.

3.14 MINOR INTRUSIVE ROCKS

Map units:

ap	*pink aplite*
pp	*pink pegmatite*
pd	*porphyritic basic dyke*
d	*basic dyke*
md	*monzodiorite dyke*
td	*phonolite dyke*
q	*quartz vein*
qb	*brecciated quartz vein*

Almost all of the minor intrusions are in the form of dykes; most of them are unfoliated and were formed late in the geological history of the area.

1. Pink Aplite and Pegmatite

Pink aplites and pegmatites are rare but are distributed widely throughout the area. *Pink aplite* is present as mappable bodies of irregular shape on the farms Augustfelde (F6) and Neisip (C7). These bodies have intruded Garub granolite, Jakkalskop charnockite and biotite granite gneiss on Augustfelde; the aplite body on the northwest part of Neisip contains rafts of Garub amphibolite and biotite schist. Contacts with the country rocks are invariably sharp. Dykes or veins of pink aplite are commonly in the form of dyke swarms, as in the southeastern part of Neisip Farm (C8). These dyke swarms are small and poorly developed, but a large NNW-trending swarm is exposed west of Dicker Willem Mountain just beyond the western border of the study area.

The aplite is a fine-to-medium-grained leucocratic alkali-rich granitoid characterized by a strong pink or pink-yellow colour. Weak foliation is present in places and is defined by small amounts of chloritized biotite. In hand specimen the aplite resembles both the Garub pink quartz-feldspar rock (*Gb7*) and the Tiras gneiss (*GnTa*). The pink Garub rocks, however, have the same fabric as the other Garub rocks with which they are intercalated, whereas the pink aplites are non-foliated or weakly foliated with a younger fabric and they clearly intrude the Garub rocks and the biotite granite gneisses. Nevertheless local remobilization of the pink quartz-feldspar rock has formed an intrusive pink granitoid that is indistinguishable from coarser varieties of the pink aplite.

Pink Pegmatites crosscut all the pretectonic and syntectonic rocks. They are commonly in the form of straight dyke-like bodies and are seldom more than a few metres wide. The pegmatite dykes have chilled margins and sharp contacts and contain crystals up to 1 m in width. These pegmatites consist almost entirely of quartz and K-feldspar, but north of Am Einschnitt Mountain (E3) an oval body of pink pegmatite contains abundant pyrite. The pink pegmatites intrude the pink aplites, but because of the similar composition and field relations the pegmatites are thought to represent a late phase of the same period of intrusion.

2. *Beryl Pegmatites*

The beryl pegmatites are largely restricted to an east-trending zone, 2-3 km wide and 25 km long on the farms Keerbank and Harris (J7, J8). Irregular veins of pegmatite, seldom more than 100 m in length, are abundant within this zone.

The pegmatites consist of quartz and white feldspar with subordinate amounts of muscovite in the form of large books. Many of these pegmatites contain euhedral prisms of beryl concentrated at the junction of quartz and feldspar crystals. Some of the pegmatites show a crude zonation.

3. *Basic Dykes*

Included in this group are the porphyritic basic dykes, basic dykes, monzodiorite dykes and phonolite dykes.

Porphyritic Basic Dykes

Porphyritic basic dykes are sparsely distributed through the centre of the area. These dykes are not concentrated into swarms and do not have a consistent trend. Some, such as the intrusion near Sesselberg (G2), are sub-horizontal.

These dykes are, in some places, folded by late-stage deformation and must have formed early in the history of the area because they have been intruded by remobilized host rock (Plate 22). These dykes have also been intruded by the pink aplite.

The porphyritic basic dykes are generally medium grained but usually have chilled margins against the country rocks. The plagioclase phenocrysts are large and euhedral,or small and rounded. They are set in a melanocratic felty matrix of ferromagnesian minerals and plagioclase; dark flecks of chloritized and uralitized pyroxene (up to 8 cm long) are sometimes visible in hand specimen.

Basic Dykes

Basic dykes occur in swarms in the extreme south and north of the study area. The trend of these dyke swarms is north-northeast or north. The dykes are narrow and straight and their dip is invariably near-vertical. The dykes vary in width between 1 and 10 m but they may be several kilometres in length. They are all of pre-Nama age but they cut across the mylonites in the core of the Kuckaus shear zone (M6). The dykes consist of fine-grained dark-green dolerite and are invariably altered.

These basic dyke swarms have possible correlates both north and south of the Aus area. Their trend is parallel to that of the basic feeder dykes of the Guperas Formation near Sinclair Mine, some 40 km north of the present study area (Watters, 1974, p.73) and their size is similar. The Guperas Formation has been intruded by the Rooiberg granite, which has yielded a minimum U/Pb age of 1270 Ma (ibid., p.182).

A possible correlate of the southern dyke swarm is the Gannakouriep dyke suite (de Villiers and Söhnge, 1959), which has a closely similar trend, and is well developed to the southeast of the study area in the Ai-Ais area (Blignault, 1976, Annexure 1) and in the northern Richtersveld;

Monzodiorite Dykes

Dykes of monzodiorite are extremely rare in the Aus area and were only found in the northern part of Kokerboomkloof Farm (K6). Three monzodiorite dykes, which trend northeast, are short but broad and do not have chilled margins. The monzodiorite is medium grained and heavily altered by veins of epidote and pink K-feldspar.

Phonolite Dykes

Phonolite dykes are rare and were only found in the plain east of Dicker Willem Mountain. Specimens of these dykes were collected by the explorer Klinghardt and described by Kaiser (1926) as 'tinguaite', a textural variety of phonolite. Narrow dykes, about 10 m wide, trend northwards and do not appear to be structurally related to the nearby Dicker Willem carbonatite.

The phonolite is a dark grey-green porphyritic aphanite consisting of phenocrysts of lath-like orthoclase and equant zeolitized nepheline and pyroxene set in an extremely fine-grained matrix. These phonolites may be of equivalent age to the Early-Cretaceous Pomona Syenite Complex south of Lüderitz which is part of the Lüderitz Alkaline Province (Marsh, 1973).

4. Quartz Veins and Quartz-Breccia Veins

Quartz veins large enough to be shown on the accompanying geological map (Annexure 1) are extremely numerous. They are coarse-grained and consist almost entirely of quartz, in places with minor amounts of pyrite and submicroscopic inclusions. There are three main types of quartz vein in the Aus area and these are briefly described below in order of decreasing age.

Coloured quartz veins are pink or blue-grey and are in the form of irregular segregations, often associated with Garub marbles (as in the vicinity of Am Einschnitt Mountain (E3).

Quartz veins are present in the Kuckaus mylonite belt as long dyke-like bodies with a strike parallel to that of the surrounding mylonites (Plate 25). The margins of these intrusions are strongly lineated parallel to the lineation in the mylonites. North of Magnettafelberg (C2) the Solo Hill marks the southeast end of a 13 km long vein of quartz breccia outlining a mylonite zone which is parallel to the much larger Excelsior and Kuckaus mylonite belts to the north and south. The quartz breccias represent quartz veins that have been broken up by renewed movement after initial cooling and have become recemented by vein quartz.

Quartz veins in faults are of post-Nama age in contrast to the mylonite quartz veins. They mark the site of north-or northeast-trending faults and small shear zones. The veins are usually straight and narrow but some are anastomosing. Quartz-breccia veins are present east of Dicker Willem and may be part of a fracture system produced during the emplacement of the carbonatite (Section 3.16).

3.15 NAMA GROUP

Sediments of the lower Nama Group overlie the basement rocks in the east of the area where they form a plateau bounded on its western margin by an escarpment. The stratigraphy and lithology of the lower Nama Group in southern South West Africa have been described in detail by Germs (1972) and were not studied during the present survey. Nevertheless because the Nama Group is present in large parts of the study area, it was thought advantageous to subdivide it by photogeological interpretation on the basis of the stratigraphic succession established by Germs (1972) as shown in Table 17.

The carbonate members of this succession were used as marker horizons in the photogeological study because of their characteristic mode of weathering. The middle carbonate member of the Kuibis Formation is more than 15 m thick in the south of the area but was not mapped separately because it pinches out northwards owing to a facies change.

TABLE 17

Stratigraphic succession of the lower Nama Group in the Aus area (after Germs, 1972) showing the lithologic units mapped in the present study

Formation	Member (Germs)	Dominant Lithology	Map unit (Jackson)
SCHWARZRAND FORMATION	Huns limestone member	limestones	N_{2b}
	Nasep quartzite member	quartzites and sandstones	
	Basal clastic member	shales overlying quartzites overlying shales	N_{2a}
KUIBIS FORMATION	Schwarzkalk limestone member	limestones	N_{1b}
	Upper clastic member	shales overlying quartzites with basal conglomeratic sandstone	
	Middle carbonate member	limestones and dolomites	N_{1a}
	Basal clastic member	quartzites overlying conglomerates or conglomeratic sandstones	

3.16 DICKER WILLEM CARBONATITE

Map Units: *C* *Dicker Willem carbonatite*
Cb *Carbonatite breccia*
Cd *Carbonatite dyke*

1. Nomenclature and Historical Background

Dicker Willem is a solitary steep-sided mountain rising 650 m above the

Plate 25. Kuckaus mylonite belt showing mylonites (dark) and associated quartz veins (pale) with cataclastic biotite gneiss in background. View southwards of north face of Kuckaus Mountains (J3)

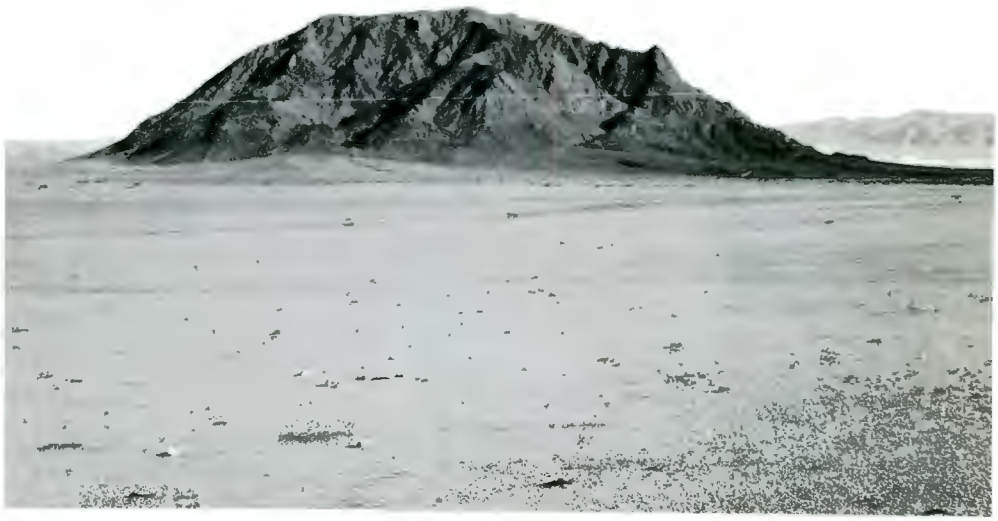

Plate 26. View SE of Dicker Willem carbonatite. The mountain is 650 m high and more than 3 km in diameter. Diamond Area (E2)

surrounding desert plain in the Diamond area (E2) (Plate 26). Its distinctive profile serves as a prominent landmark for the surrounding area and a painting of the hill forms the frontispiece of Kaiser's monumental work *Die Diamantenwüste Südwestafrikas* (Vol. 1, 1926).

The name 'Dicker Willem' is taken from an early topographic map published by Dietrich Reimer, Berlin, and this is the name used by the inhabitants and farmers of Aus. The mountain is also known as Garub Berg and Great Tigerberg. The name 'Garub Berg' is that officially designated to the mountain on recent topographical maps but it is not used in the present study in order to avoid confusion with:

(i) the basement metasediments at Garub Station 12 km to the south which have been named the Garub sequence

(ii) the Garub carbonatite diatremes in the Great Karas Mountains (Haughton, 1969, p.228)

Beetz (1924, p.27) reported that the upper part of Dicker Willem consisted of limestone which he tentatively correlated with the Nama 'System'. Kaiser (1926) reported that quartzite and limestone were deposited onto basement rocks at Dicker Willem. Possibly as a result of these early reports Dicker Willem is erroneously designated on the official geological map of South West Africa (1963) as a correlate of the Late-Precambrian Gariep 'System'.

2. *Form*

Dicker Willem is a large well-exposed circular diatreme 3,5 km in diameter. The lower slopes of the mountain are largely obscured by talus debris and outcrops are extremely scarce in the surrounding plain (Plate 26). A thick formation of dunes has accumulated against the eastern flank of the mountain; the western side is obscured by a thick outwash deposit of boulders. To the north and south calcrete deposits obscure the underlying rocks. Thus it is not certain how far the intrusion extends outward beneath the superficial cover. However, because of the resistant nature of the carbonatite in the arid climate, it is probable that the intrusion does not extend much beyond the present limits of the mountain. Small outcrops of silicified carbonatite are present up to 3 km from the base of the hill but these are almost certainly part of the radial dyke system described below.

3. *Lithology*

General

The main rock type, which forms the bulk of the mountain, is a siderite-bearing sövite (calcite-rich carbonatite). The rock is fine grained and varies in colour from buff to yellow brown and dark brown. Iron-rich varieties

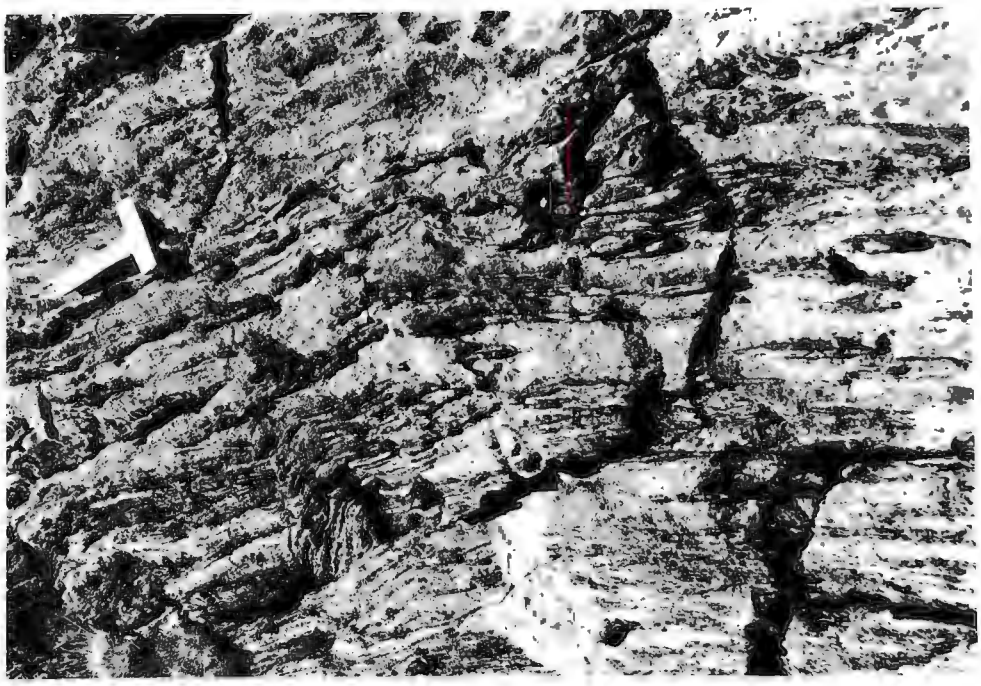

Plate 27 Flow-banded carbonatite; layering is concentric around centre of intrusion and dips vertically. NW part of Dicker Willem Mountain, Diamond Area (E2)

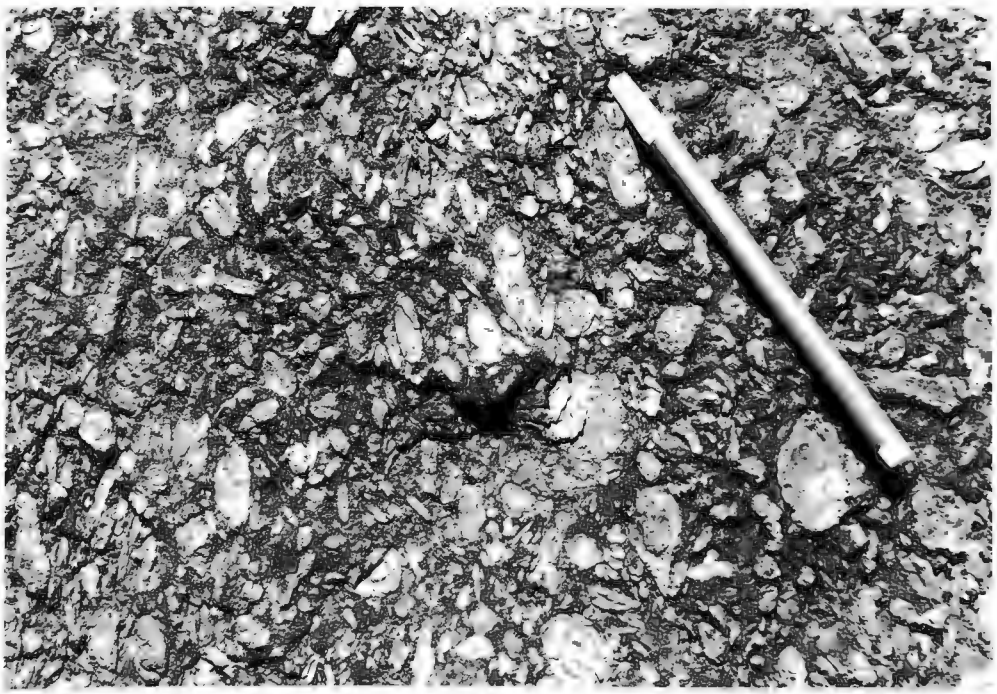

Plate 28. Pellet breccia, possibly of pyroclastic origin, consisting of pale-yellow beforsite clasts in matrix of dark-orange sövite. Near S contact of Dicker Willem carbonatite, Diamond Area (E2)

weather to a black colour and define a mesoscopic layering which is concentric and near-vertical, resembling that of high-grade metasediments (Plate 27) but which is probably due to magmatic flow (Hyndman, 1972, p.221). Black-weathering silicified gossan forms cappings to many ridges on the mountain-side. Magnetite is a common accessory mineral. The outer zones of the body and many of the outlying dykes have been largely silicified. No large-scale concentric zonation was observed during a traverse to the summit of the mountain, but breccias are more common in the outer parts of the body than in the centre.

Breccia Structures

Breccias cut across the flow-banded carbonatite. Three types of breccia are present:

(i) *Pellet breccia*: moderately well-sorted oval or spheroidal clasts (generally less than 3 cm in length) of yellow beforsite (dolomite-rich carbonatite) are set in a matrix of fine-grained dark-orange sövite (Plate 28). These are rare and may represent xenoliths of agglomeritic extrusive rock from a higher level of the original intrusion.

(ii) *Boulder breccia* is extremely common and contains a wide variety of poorly-sorted clasts which are well rounded or subangular and range in size from minute fragments to boulders several metres in diameter. The high degree of rounding shown by some of the clasts (Plate 29) suggests abrasion during transport in a fluid medium during emplacement.

(iii) *Talus breccias*, which are cemented by calcrete, are common in rubble-choked gullies on the mountain-side. Although they of secondary origin and produced merely by weathering, they are strikingly similar in appearance to the primary boulder breccias described above. However, the primary breccias have a matrix consisting of bright-orange sövite rather than dirty-white calcrete and are commonly cut by dykes of carbonatite (Plate 30).

Carbonatite Dykes

Intersecting dykes and veins of carbonatite are common at the base of the mountain. The dykes are up to several metres in width and three or four generations of veins can usually be distinguished at any one outcrop. These veins consist of extremely fine-grained yellow or orange sövite. Many of the larger dykes show irregular lensoid segregations of black iron-rich material and small blebs of quartz. These dykes crosscut the carbonatite breccias described above. Carbonatite dykes crop out in the plain southeast of Dicker Willem. They are poorly exposed but appear to be radially arranged; they may represent part of a large unexposed radial-dyke system. The dykes crosscut the north-trending quartz-breccia veins to the east of the mountain.

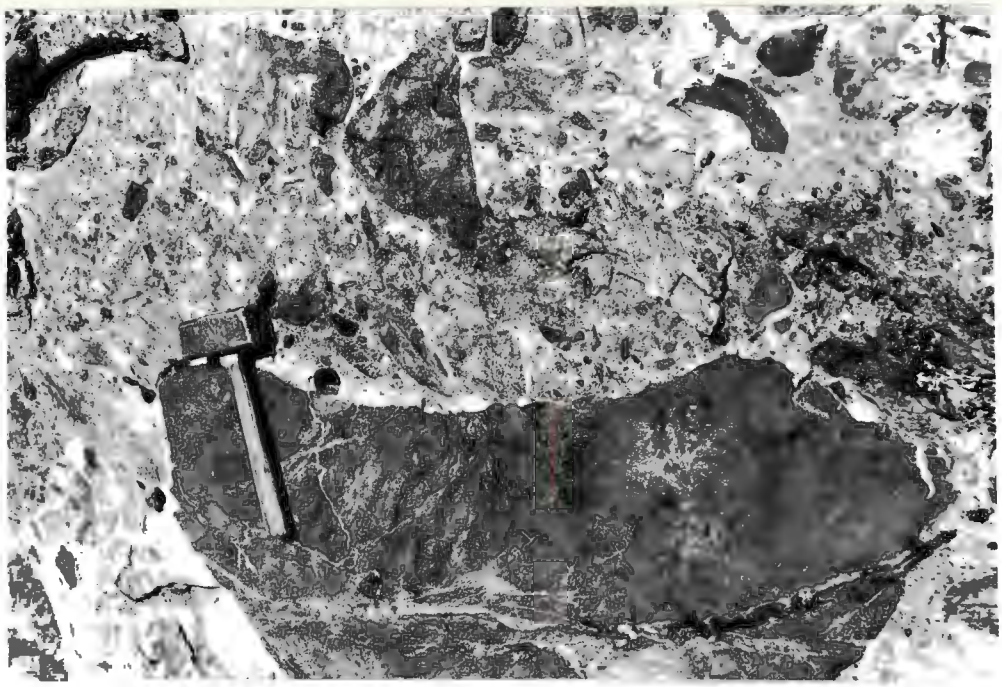

Plate 29. Boulder breccia consisting of clasts of various carbonatite lithologies in matrix of sövite carbonatite. Some clasts show high degree of rounding, possibly resulting from fluidization during emplacement. S margin of Dicker Willem carbonatite, Diamond Area (E2)

Plate 30. Sövite dyke crosscutting carbonatite pellet breccia. S margin of Dicker Willem carbonatite, Diamond Area (E2)

In many parts of the main body shear zones filled with orange carbonatite have disrupted primary layering. Veins of white coarsely-crystalline calcite ramify in all directions and cut the shear zones.

4. *Internal Structural Relations*

On the basis of the few measurements of linear structures within the body it appears that the primary layering and the shear zones are arranged concentrically about the centre of the intrusion, whereas the small faults and calcite veins radiate from the centre of the body. The evolution of the intrusion was determined as follows:

(i) flow-banded carbonatite

(ii) pellet breccia

(iii) boulder breccia consisting of (i) and (ii) in carbonatite matrix, together with concentric shearing

(iv) dyke system of carbonatite together with radial fracturing

(v) calcite veining

5. *External Structural Relations*

The only well-exposed contact of the carbonatite with neighbouring rocks is on the southern margin of Dicker Willem mountain. This contact is characterized by slices of basement rocks separated and intruded by the carbonatite. Silicified carbonatite and Garub marble are in contact 2,5 km southeast of the base of the mountain.

No large-scale fenitization of the country rocks was found, but in one place hybrid rocks grade into both carbonatite and basement gneiss in a 50 m contact zone. Apart from the phonolite dykes to the east, which may be entirely unrelated to the carbonatite, no alkali rocks, typically related to carbonatites, were found in the vicinity of the Dicker Willem intrusion.

6. *Dicker Willem and Other Carbonatites in Southern Africa*

The two largest of the 32 carbonatite bodies in southern Africa reviewed by Verwoerd (1966) are both northwest of Pretoria in the Transvaal; they are Nooitgedacht, 3,5 km in diameter, and Tweerivier, 3,0 km in diameter. The former carbonatite body is very poorly exposed and may include other rock types (ibid., p.152). The average diameter of carbonatite pipes in southern Africa is given (ibid.) as one mile (1,6 km). By comparison the Dicker Willem carbonatite is at least 3,5 km in diameter and thus may well be one of the largest bodies of

carbonatite in southern Africa.

Apart from its large size Dicker Willem differs from most other southern African carbonatites in two other important respects:

(i) *Circular shape:* only two other major carbonatites have this property, one of which is Nooitgedacht (ibid., p.170)

(ii) *Lack of associated intrusions*: only two other large carbonatite complexes cited (ibid.) consist solely of carbonatite - Tweerivier and Nooitgedacht.

The large size and circular shape of Dicker Willem and the lack of associated intrusives suggest the possibility that this body represents the vent of a deeply eroded igneous complex from which the upper parts (possibly consisting of extrusive and intrusive alkali rocks) have been removed.

6. *Age and Correlation*

Because Dicker Willem intrudes basement rocks of unknown age, it cannot be dated by field relations. Marsh (1973, p.2) speculated that Dicker Willem may be a correlate of the Early-Cretaceous Lüderitz Alkaline Province some 100 km to the southwest. According to geologists of Consolidated Diamond Mines Limited in Oranjemund a small carbonatite is present 20 km southwest of Dicker Willem, just west of the Garub station marble body. In addition to this occurrence fragments of carbonatite were found by the writer south of Koichab Pan 40 km west of the study area. These occurrences may form part of the same suite.

Chapter 4

METAMORPHISM

The metamorphic grade of the Aus area is predominantly that of the amphibolite facies; the grade increases towards the centre of the study area, where granulite facies metamorphites are preserved. Retrograde metamorphism, in the form of chloritization and epidotization, has superimposed a weak metamorphic imprint on the pattern of high-grade metamorphism. Since evidence of this retrogressive metamorphic event is sparse and widely scattered, this event has not been studied.

Rocks of the Garub sequence have been used in the determination of metamorphic grade because of their lithologic diversity. A metamorphic zonation is described with respect to four compositional groups, viz. mafic, semi-pelitic, pelitic and calcareous. This is followed by a summary of the evidence for amphibolite facies metamorphism. The summary is followed by a discussion on granulite metamorphism in the Aus area and elsewhere in the Namaqua Mobile Belt.

4.1. METAMORPHISM OF MAFIC ROCKS

The metamorphism of the amphibolites and hypersthene granolites is described in this section. These rocks are loosely termed 'metabasites' (*after* Miyashiro, 1973); the term is used here to describe metamorphosed rocks of igneous or sedimentary origin that are rich in ferromagnesian minerals. The

metamorphism of these rocks provides a frame of reference for the other rock types because of their abundance and wide distribution.

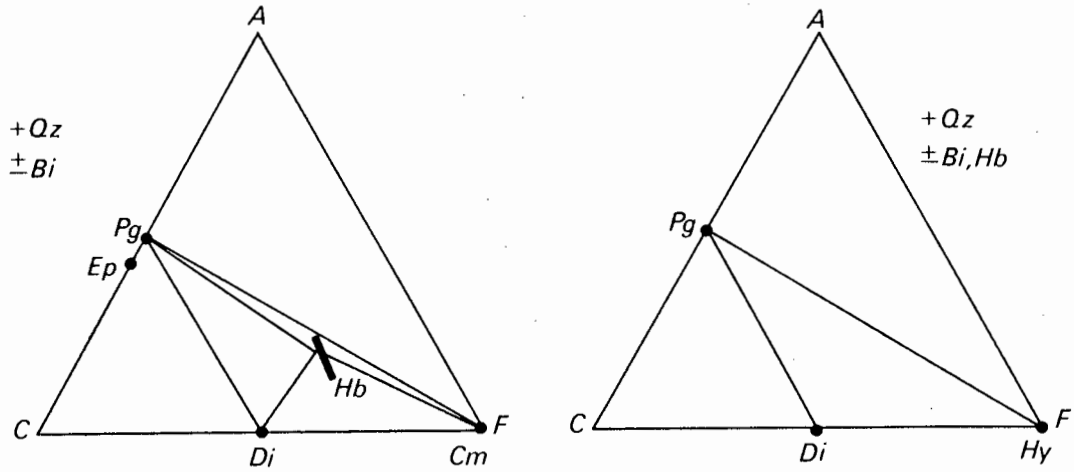

Figure 24. ACF diagrams showing mineral parageneses in the Garub metabasites Bi biotite, Cm cummingtonite, Di diopside, Ep epidote, Hb hornblende, Hy hypersthene, Qz quartz

1. Mineral Parageneses and Metamorphic Zones

The mineral parageneses for metabasites are shown in Figure 24. In amphibolite facies metabasites (amphibolites) hornblende is ubiquitously present, whereas in the granulite facies metabasites (granolites) hypersthene is diagnostic (after de Waard, 1965b; Winkler, 1974).

The zone of granulite facies metamorphism is situated in the east-central part of the Aus area and its distribution is shown in Figure 25. The zone of amphibolite facies metamorphism extends over a much larger area, many thousands of square kilometres in extent. However, as shown below, it is possible to further subdivide this very large metamorphic zone into subunits. The colour of the hornblende in specimens from the extreme north and northwest of the area is almost invariably blue green in contrast to the brown varieties nearer the centre of the study area. Furthermore many of the metabasites with blue-green hornblende contain the paragenesis 'epidote + quartz'. According to Miyashiro (1973, p. 218) epidote is the predominant calcium-aluminium silicate in the low-temperature zones of many low-to-medium pressure metamorphic terrains. It was therefore decided to investigate the possibility that the amphibolites containing blue-green hornblende and epidote represent a lower metamorphic grade than the other amphibolites.

Similarly the presence of diopside in the amphibolites is restricted to

certain areas; it is absent from the north but is common in the area adjoining the granulite zone. In the presence of calcite diopside is stable at relatively low temperatures of the amphibolite facies, but in the absence of calcite diopside is present only in the middle or upper part of the amphibolite facies (Miyashiro, 1973, p. 260). The occurrence of diopside in metabasites of the upper amphibolite facies in metamorphic zones transitional with the granulite facies has been reported by Engel and Engel (1962a), Wenk and Keller (1969) and Bard (1969). It is therefore possible that the diopside-bearing amphibolites at Aus represent a distinct metamorphic zone.

The above observations therefore indicate the possibility of four metamorphic zones:

Zone A: 'epidote-hornblende zone', characterized by blue-green hornblende and 'epidote + quartz'

Zone B: 'hornblende zone

Zone C: 'diopside-hornblende zone', characterized by the presence of diopside

Zone D: 'hypersthene zone', characterized by the presence of hypersthene and, commonly, diopside

Zones A, B and C represent the amphibolite facies; Zone D represents the granulite facies. The validity of the threefold subdivision of the amphibolite facies is examined with respect to the following properties:

(i) Spatial relations of the metamorphic zones

(ii) Geochemical trends in the mineralogy of certain minerals

(iii) Mineral parageneses and possible reactions in the different metamorphic zones

2. *Distribution of Metamorphic Zones*

Each metamorphic zone occupies a distinct area (Fig. 25). The granulite-facies rocks (zone D) occupy large areas east of Aus Village but are largely overlain by the Nama Group. The estimated width of the granulite zone (disregarding the narrow strip of amphibolite facies rocks in the centre) is at least 60 km. Both the northern and southern parts of the granulite zone appear to extend in a west-northwestern direction, but the shape of the northern zone is largely speculative because of the poor degree of exposure.

Zone C is also divided into two parts which are even more markedly extended in a west-northwesterly direction. Zone B extends southwards to the southern limits of the area and northwards to the Excelsior mylonite belt. The amphibolites of zone A are most common in the extreme north of the area, where they occur on both sides of the Excelsior mylonite belt. This could suggest that their relatively low grade is the result of shearing-induced retrogression. However, the amphibolites are only cataclastic within 1 km of the

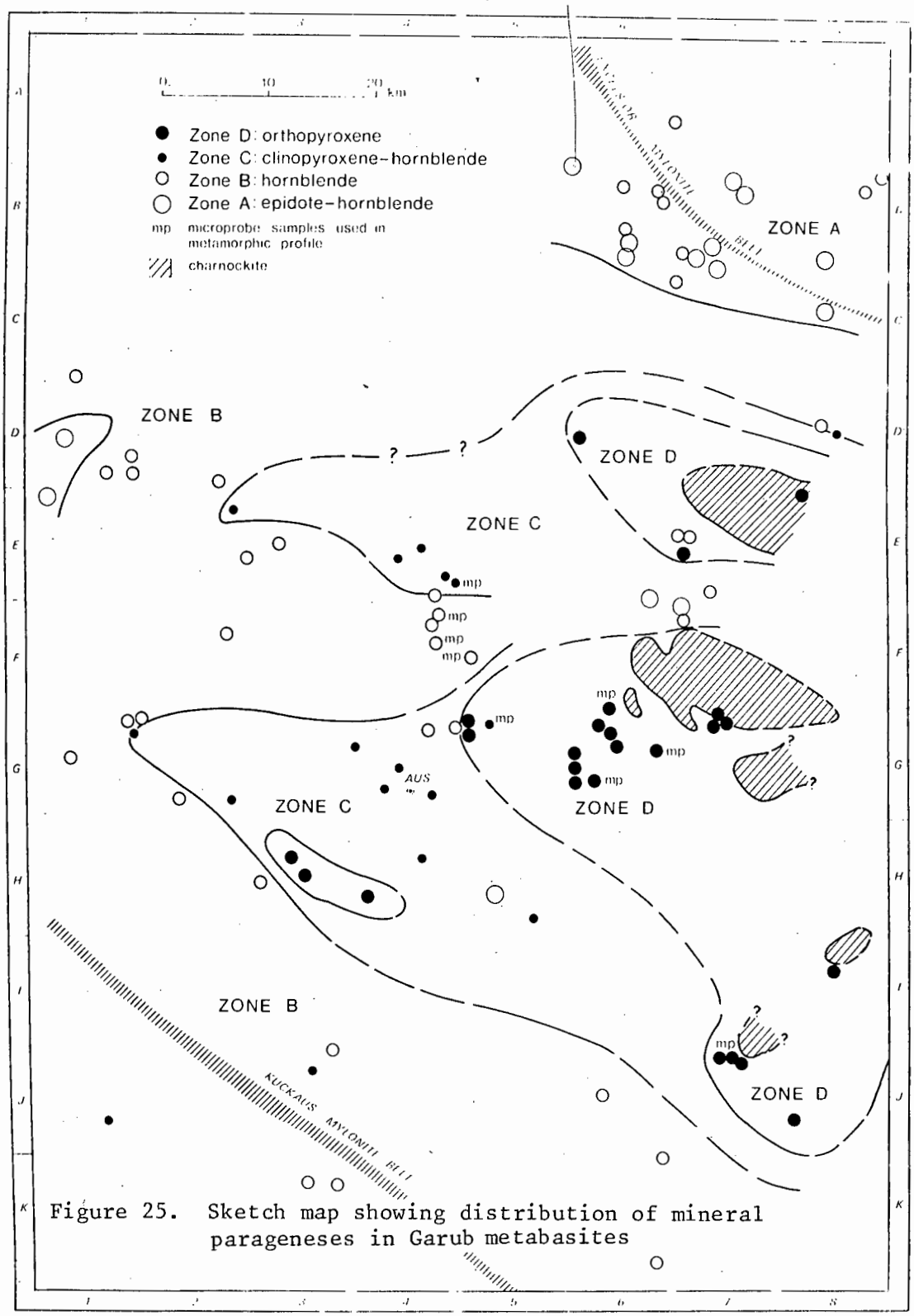

Figure 25. Sketch map showing distribution of mineral parageneses in Garub metabasites

mylonite zone. Furthermore, just west of Magnettafelberg (D1), zone A amphibolites also occur in a small area - whose westward extent has not been mapped. These observations suggest that zone A amphibolites are the result of prograde regional metamorphism (no relics of higher grade minerals were found) rather than of localized retrograde metamorphism.

In summary, therefore, the distribution of the four metamorphic zones indicates an increase in metamorphic grade from the north, south and west towards the centre of the area. This regional trend is consistent with the hypothesis advanced that the epidote-hornblende zone (zone A) represents a zone of lower-grade metamorphism; but the diopside-hornblende zone C is not clearly related to the granulite zone D.

3. *Colour Changes in Hornblende and Biotite*

Apart from variations in the modal proportions of minerals, there are also changes in mineral composition and appearance between the different metamorphic zones. One type of change occurs in the Z absorption colour of hornblende and biotite.

Hornblende

The correlation of hornblende colour with metamorphic grade has been known for several decades and a number of studies in a wide variety of metamorphic terrains have made use of hornblende colour changes in assigning metabasites to various metamorphic zones (e.g. Wiseman, 1934; Billings and White, 1950; James, 1955; Miyashiro, 1958; Shido, 1958; Engel and Engel, 1962a,b; Binns, 1965; Katada, 1965; Gemuts, 1965; Fabriès, 1968; Bard, 1970). A general trend of blue-green → green → brown can be linked to rising metamorphic grade. Binns (1965) correlated these colour changes with increasing Ti and decreasing Fe^{3+} contents of the hornblendes.

In the Aus area the hornblendes from metabasites show the full range of colour changes. Hornblendes in some ninety metabasite specimens were examined by the method outlined in Appendix 3. Hornblende colour was graded into three categories:

(i) blue-green (20 specimens)

(ii) green-brown and green (34 specimens)

(iii) brown (31 specimens)

Six hornblende specimens were completely altered to chlorite and these have been omitted from the study.

Biotite

Binns (1969) reported small increases in the Ti content and the Mg/(Mg + Fe) ratio in biotites of metapelites from different metamorphic zones in the

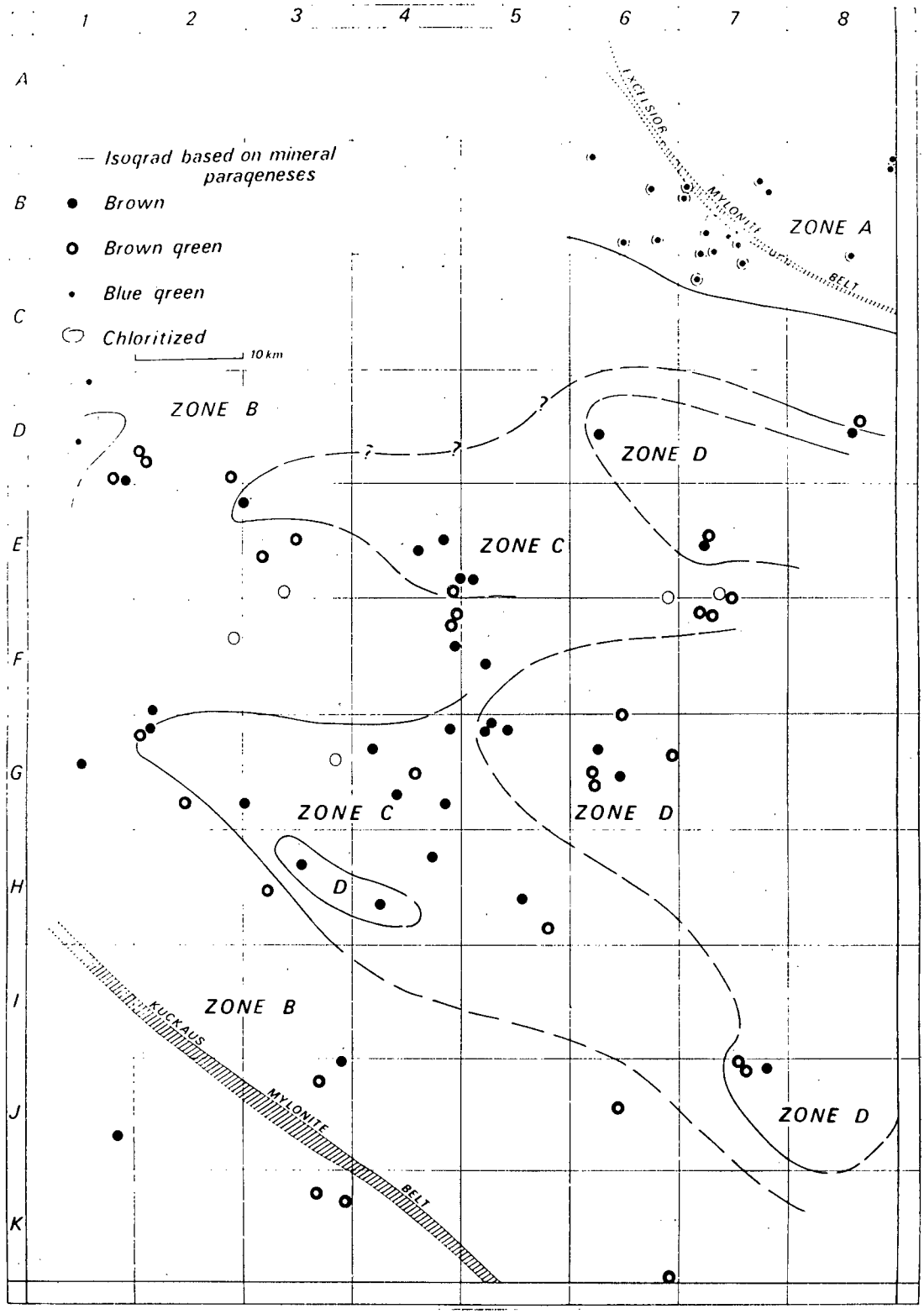

Figure 26. Sketch map showing distribution of different-coloured hornblendes from Garub metabasites and their relation to metamorphic zones

Broken Hill area, New South Wales; the increases were correlated with increasing metamorphic grade. In the Aus area approximately 45 metabasite specimens from all metamorphic zones contain biotite, the colours of which were recorded in a similar manner to those of the hornblendes. No green biotites were observed and colours are either:

(i) brown

(ii) red or red-brown

4. *Distribution of Colour Variations in Hornblende and Biotite*

Hornblende

The distribution of the different-coloured hornblendes in metabasites from the Aus area is shown in Figure 26 which also shows the isograds defined by mineral parageneses.

Blue-green hornblende characterizes the metabasites from zone A and is restricted to areas in the extreme north and northwest of the study area. There is less correlation of the other colour groups with metamorphic grade. Zone B hornblende is chiefly green-brown, whereas that of zone C is mainly brown. The blue-green colour persists up to the 'epidote + quartz out' isograd separating zones A and B. Greenish hornblende colours are separated from brownish ones by the 'clinopyroxene-in' boundary which divides zones B and C. Within zone D, however, there is no consistency in hornblende colour: brown grains, typical of granulite facies, are present in the same outcrop as green-brown ones.

Biotite

Colour changes in biotite are described in the section dealing with the metamorphism of semi-pelitic rocks because biotite is more common in these rocks than in the metabasites. The relevant conclusions in section 4.2 are: in metabasites biotite changes from brown to red-brown between zones A and B.

5. *Compositional Variations with Metamorphic Grade*

Certain compositional trends in some minerals are thought to be sensitive to PT conditions at the time of their formation. If it can be established that these trends are largely independent of host-rock composition, they provide an estimate of the grade of metamorphism that prevailed at the time of recrystallization.

Hornblende and plagioclase in the Garub metabasites were selected for studies of their composition because these minerals are present at all metamorphic grades. Twenty-six metabasites from the four metamorphic zones were

TABLE 18

Equality of variances between different pairs of samples (variation of anorthite content with metamorphic zone) determined by means of the F test. Values in italics represent pairs of samples that show differences in variances above acceptable limits for t testing (at 5% level of significance)

SAMPLE PAIRS	ν_1	ν_2	F (α=0,05)	F sample pairs
A and B	17	30	1,98	1,09
B and C	30	8	3,08	*3,33*
C and D	8	11	2,95	1.55

TABLE 19

Results of t and t' tests (variation of anorthite content with metamorphic zone). A significant difference between each sample mean is proven at a level of 5% significance if $t_{sample} > t_{(\alpha=0,05)}$

SAMPLE PAIR	ν_1	t (α=0,05)	t sample	t' sample	t sample or t' sample > t(α=0,05)
A and B	47	2,02	2,22		yes
B and C	38	2,03		3,03	yes
C and D	19	2,09	2,97		yes

t test for comparison of two samples with similar variance after Davis (1973, p.98)
t' test for comparison of two samples with dissimilar variance after Guenther (1965, p.146)

studied. Every rock specimen contains fresh hornblende and all except two contain unaltered plagioclase. From these specimens 71 plagioclase grains and 92 hornblende grains were analysed by electron microprobe. Specimen localities are given in Appendix 6 and full analyses are listed in Appendix 5.

Plagioclase

A rise in anorthite content of plagioclase with increasing metamorphic grade is well known (Deer, Howie and Zussman, 1966, p.336). The effect of metamorphic grade and mineral parageneses on plagioclase compositon was extensively studied by Wenk and Keller (1969) in their examination of more than 700 amphibolites in the central Alps. More recently Braun and Müller (1975) reported the results of 34 000 microprobe analyses of plagioclase from various metamorphic grades and found that only in the upper-amphibolite-facies (anorthite-rich) plagioclase could geothermometry be applied because compositional variations at lower grades were so wide.

The variation in anorthite content of plagioclase from the four metamorphic zones of the Aus area is shown in Figure 27. The histograms show considerable overlap of values between the zones, but if the means and standard deviations of the samples are calculated (top of figure), a consistent trend of increasing anorthite content from zones A→B→C→D is apparent: the average An percentage for plagioclase from the zones A, B, C and D is 56, 67, 75, and 82 respectively. Standard deviations indicate that there is less variation in plagioclase composition at higher grades (in agreement with Braun and Müller, 1975). The results of F and t tests (Tables 18 and 19) indicate that a statistically significant difference exists between the means of all four samples at a confidence level of 95%.

The variation in anorthite content of plagioclase within the same rock specimen is illustrated in Figure 28. Differences in anorthite content vary between a minimum of about 2% to a maximum of 15% and average 6%. Inhomogenieties of single crystals were studied and it was found that the anorthite content of individual grains varies within 5%, producing reversed zoning. Braun and Müller (1975) reported a similarly small variation of 6,5% An in plagioclase grains within the compositional range 69-79%. Thus the effect of zoning on the study is not particularly large - as would be expected in metamorphic rocks which have crystallized under conditions of chemical equilibrium. Nevertheless only the cores of the larger crystals were examined in order to minimize the effect of any possible zoning on the analyses.

The correlation between plagioclase composition and metamorphic index minerals in the Garub metabasites is very similar to that described by Wenk and Keller (1969) although the metamorphism in the Central Alps was characterized by higher pressure and lower temperature than in the Aus area. Thus in the central Alps epidote is abundant in rocks with plagioclase compositions up to An_{30} but is scarce in rocks containing plagioclase compositions of An_{30-50}; clinopyroxene is only present in amphibolites with a plagioclase composition greater than An_{50}; biotite is present in metabasites of all grades.

The anorthite content of plagioclase in the Garub metabasites is higher than the values given for the central Alps (ibid.): the minimum value recorded in the Aus area was An_{35} and the plagioclase in metabasites of zone A averaged

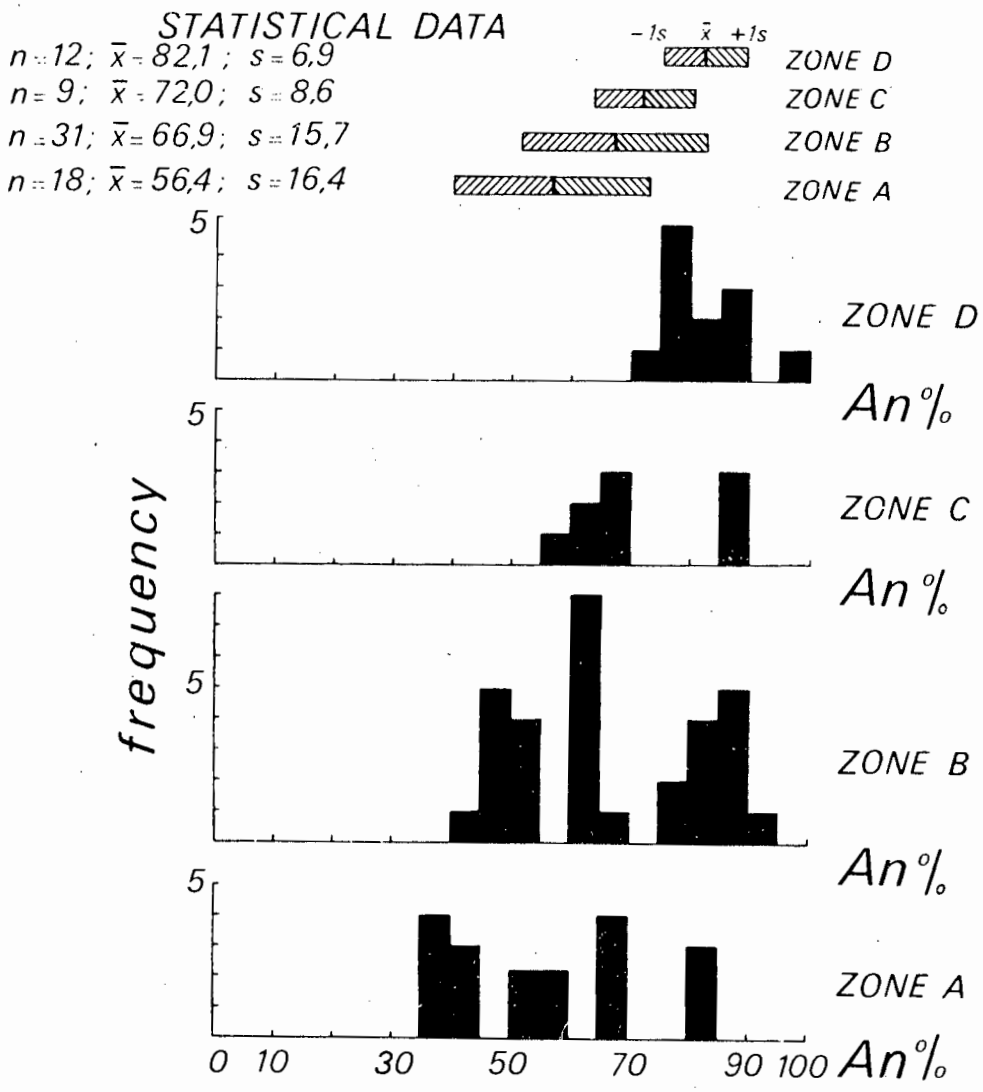

Figure 27. Variation in anorthite content of plagioclase in Garub metabasites with metamorphic grade

An_{55}. These anorthite contents are very much higher than the abrupt compositional change (at An_{5-17}) characteristic of the greenschist-amphibolite transition (Winkler, 1974, p.74). The plagioclase compositions therefore indicate that even the lower-grade metabasites of the Aus area are situated well within the amphibolite facies. The maximum values found are in excess of An_{90} (in the granulite facies) which indicate an extremely advanced state of calcium substitution, attributable to high metamorphic grade. No carbonate minerals were found in any metabasites thus indicating that the rocks are not saturated in calcium.

Hornblende

Despite the large amount of detailed work on the subject there are still many uncertainties as to the factors controlling the composition of the amphiboles. Leake (1968, p.3) described their composition as 'undoubtedly the most

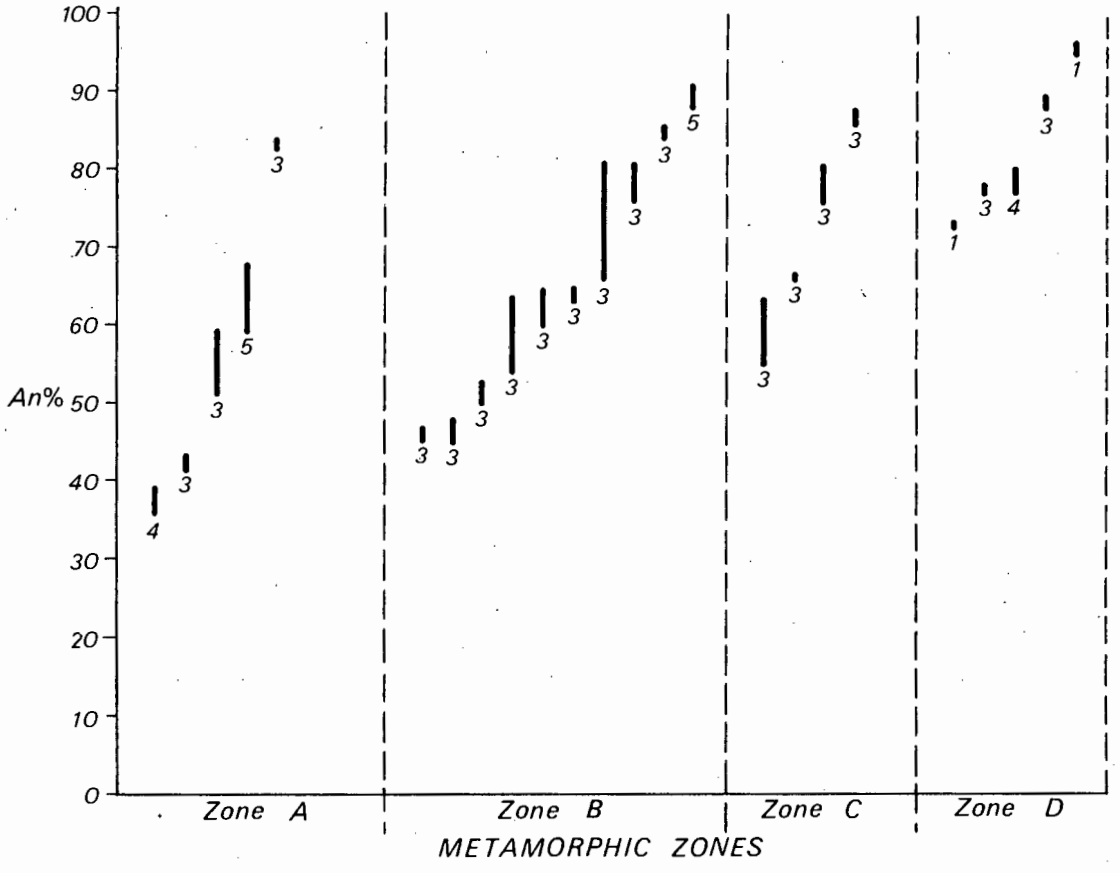

Figure 28. Range of variation in anorthite content of plagioclase in Garub metabasites. Each bar represents the range of An% variation in a single rock specimen; figures below each bar represent the number of grains analysed in each rock specimen

complex and variable of all the rock-forming minerals'; Ernst (1968, p. 1) vouched a similar opinion. Their complexity is reflected in the 27 end members required to define the variations of the amphibole group (ibid., Table I).

The majority of chemical variations in the amphiboles can be ascribed to changes in the bulk composition of the parent rock. The aim of this section is to examine the relatively small number of variations that can be related to the physical conditions of metamorphism.

On the basis of their chemical analyses, all amphiboles from the Aus area can be described as calcic (Ca = 1,5-2,0 cations per 23 oxygen anions). Calcic amphiboles can be divided into two general groups, viz. hornblende and actinolite, of which only the first has been found in metabasites of the Aus area. The general chemical formula for hornblende can be written as follows (Miyashiro, 1973):

$$(Ca,Na,K)_{2-3}(Mg,Fe,Al)_5Si_6(Si,Al)_2O_{22}(OH)_2$$

This formula includes the hydrous components and therefore contains 24 anions oxygen. However, in the present study hornblende formulae were calculated on an anhydrous basis (23 oxygens) as suggested by Borg (1963) and carried out by Binns (1965), Bard (1970), Raase (1974) and Grapes (1975).

Ignoring the water and fluorine contents, the structural formula of hornblende may be written (Ernst, 1968, p.7):

$$W_{0-1}\ X_2\ Y_5\ Z_8\ O_{23}$$

where 'Z' represents tetrahedrally-coordinated cations (Si and Al^{IV}) in the sites Si_I and Si_{II}; 'Y' represents 6-fold coordinated cations in the M_1, M_2 and M_3 sites (Mg, Fe, Al^{VI}, Ti, Mn); 'X' represents 6-or-8-fold coordinated cations (mainly Ca) in the M_4 site; 'W' represents 10-to-12-fold coordinated cations (Na + K + Ca) which cannot be accommodated in the X group and are therefore accommodated in the A site. Commonly completely vacant or only partially filled, the A site provides a convenient locality for excess cations from the M_4 sites adjacent to it and for the incorporation of entirely new elements (typically alkalis) into the crystal structure.

Two types of variation in site occupancy take place. The first of these is a substitution of aluminium for silica which results in a decrease in Al^{VI} and Si, and an increase in Al^{IV}; this trend is known as *tschermakitic* substitution. *Edenitic* substitution refers to the accommodation of sodium and potassium in the vacant A site. As will be described later both these substitution trends are linked with variations in metamorphic grade.

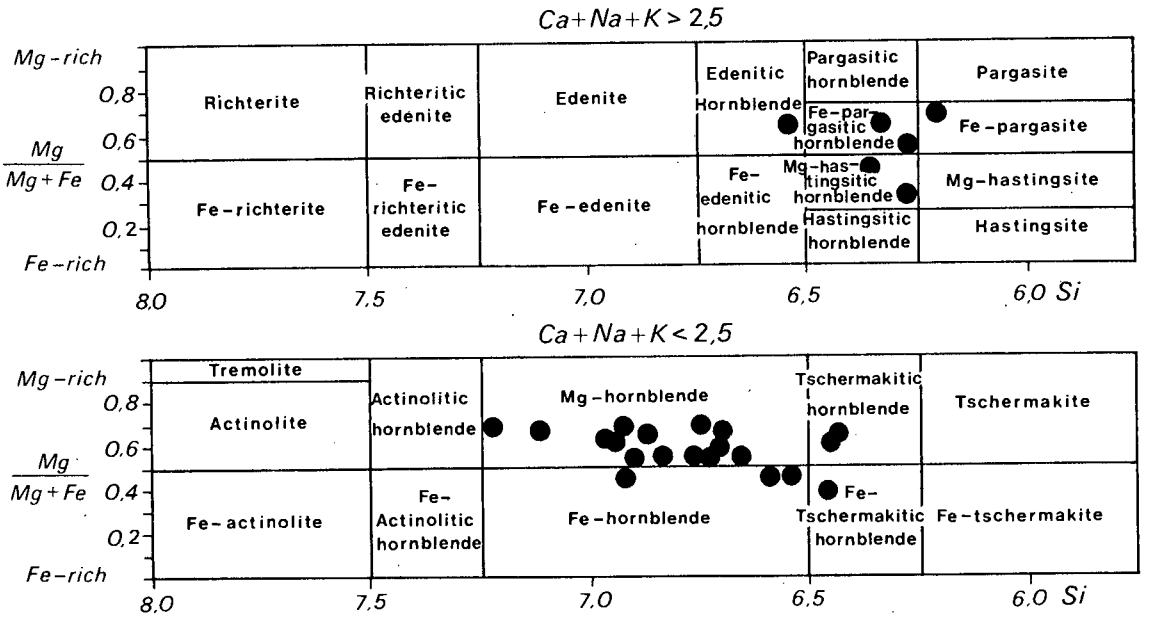

Figure 29. The nomenclature of hornblende in Garub metabasites in terms of Leake's (1968) classification. Each dot represents the average value of 3-5 hornblende grains in each rock specimen

Leake (1968) recommended a system of nomenclature for the calcic and sub-calcic amphiboles which is reproduced in part as Figure 29. The compositions of hornblende in the 26 analysed specimens from the Aus area are shown in the diagram. Most of the analysed hornblendes contain an excess of magnesium over iron, but there is no systematic variation of this ratio with metamorphic grade. The Mg/(Mg+Fe) ratio is therefore discarded as an indicator of metamorphic grade and all the hornblendes may be referred to by the names of the magnesium-rich member without loss of identity.

Figure 30 shows the compositions of the analysed hornblendes from the Aus area plotted on a graph with the variables of Si, reflecting the tschermakitic trend, and (Ca+Na+K), reflecting the edenitic trend (*after* Miyashiro, 1973). The hornblende from zones C and D is more edenitic and less tschermakitic than that of the lower-grade metamorphic zones.

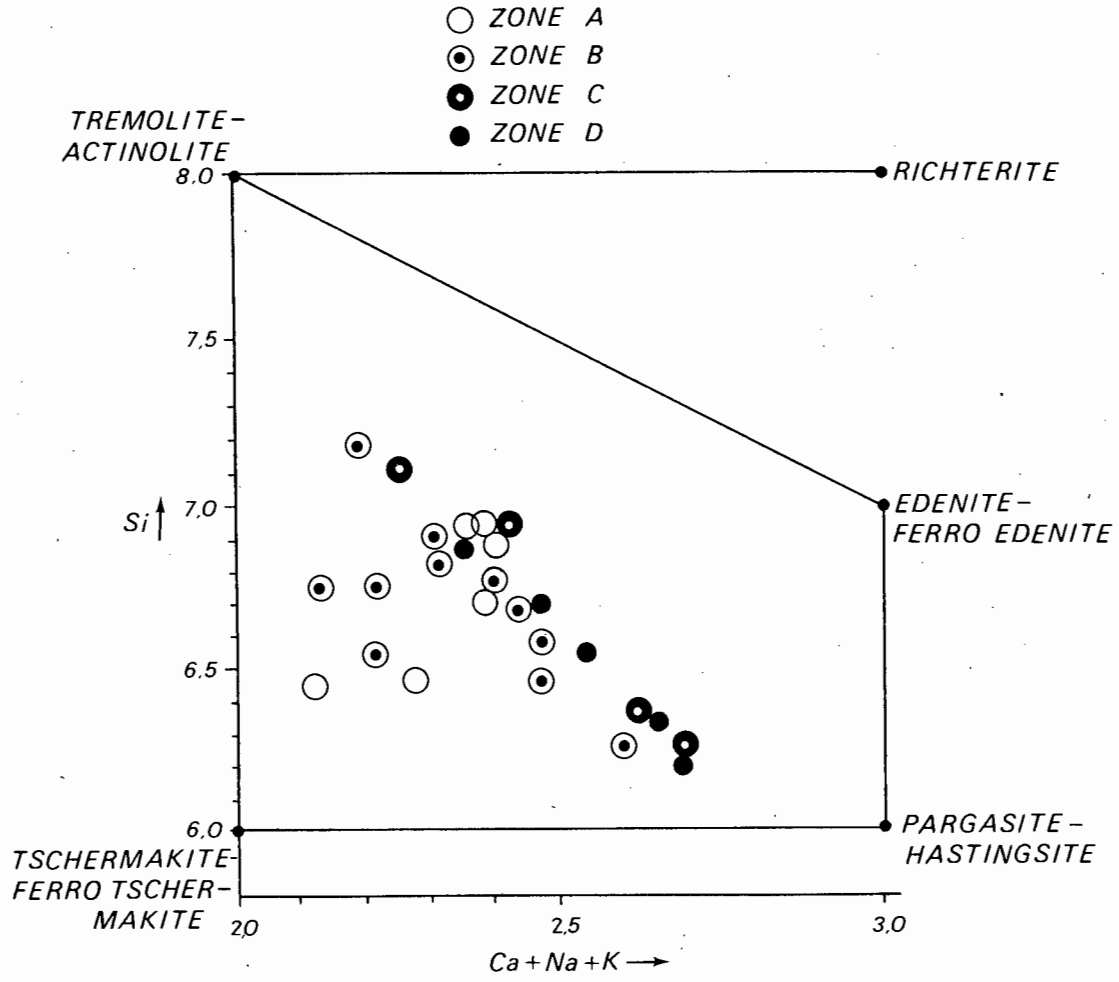

Figure 30. The composition of hornblendes in Garub metabasites plotted according to the classification of Miyashiro (1973, p.252). Each symbol represents the average value of 3-5 hornblende grains in each rock specimen. Values represent number of cations per 23 oxygen anions

Tschermakitic substitution (substitution of Al^{IV} for Si) is reflected in the variation of silica content shown in Figure 30. On the basis of 850 published analyses of hornblende Leake (1965) reported that metamorphic hornblendes generally have higher values of Al^{VI} than hornblendes of igneous origin (i.e. metamorphic hornblendes are less tschermakitic). He noted that the hornblendes associated with high-pressure metamorphic minerals (e.g. kyanite, jadeite or glaucophane) that formed over a wide range of temperature contain close to the maximum possible amount of Al^{VI}. Leake therefore concluded that the variation in Al^{VI} is, to a large degree, a function of pressure.

The pressure dependancy of Al^{VI} content was further elaborated by Raase (1974). He investigated hornblendes of metamorphic origin which he divided into low-pressure and medium-to-high-pressure groups on the basis of the facies series that characterized them. When plotted on a Al^{VI}/Si graph, each group formed two well-defined fields which could be separated by a line dividing metamorphic pressure-zones of less than and greater than 5 kb (ibid.). Hornblendes from higher-pressure régimes are therefore characterized by less advanced tschermakitic substitution.

The compositions of analysed hornblendes from the Aus area are plotted on a Al^{VI}/Si graph similar to that of Raase (1974). Figure 31 shows that almost all values fall in the field of low-pressure regional metamorphism (an environment also suggested by mineral parageneses in other rock types - see section 4.5).

Edenitic substitution (enrichment of alkalis in the A site of hornblendes) was originally linked with rising metamorphic grade by Shido (1958) in the Abukuma Plateau. Since then other studies have shown that enrichment in alkalis is a well-defined trend in other low-pressure metamorphic terrains (Bard, 1970, p. 133; Engel and Engel, 1962b; Binns, 1965, p.324). Binns (1965) stressed that only the alkali enrichment in the A site ('edenitic alkalis') is controlled by metamorphic grade. In many published crystal-structure analyses of hornblende (Leake, 1965; Binns, 1965; Bard, 1970) there is insufficient calcium incorporated in the hornblende to completely fill the M_4 site and this space is therefore filled by alkalis; the remaining alkalis occupy the adjacent A site. The hornblendes of the Garub metabasites, however, contain more calcium than can be accommodated in the M_4 site (see structural formulae in Appendix 5) and any alkalis that are incorporated during metamorphism must consequently be accommodated in the A site. Thus all the alkalis in these hornblendes are edenitic and the total (Na+K) is sufficient to plot the extent of edenitic substitution. Although the total (Ca+Na+K) was used by Miyashiro (1973), calcium content is independent of metamorphic grade (in agreement with Bard, 1970, p.125) in the Aus area: the average calcium content (per 23 oxygen anions) in hornblende from zones A, B, C and D is 1,88, 1,82, 1,88 and 1,89 (see structural formulae in Appendix 5).

The variation of alkali content of hornblende from the four metamorphic zones in Aus area is shown in Figure 32. Within each metamorphic zone there is a wide variation in alkali content which increases to a maximum in zone C. The mean and standard deviations of the samples indicate a steady enrichment in alkali content from zone A to zone C, beyond which there is no increase. The results of F and t testing (Tables 20 and 21) show that a statistically significant difference (at 5% significance) exists between the mean values of

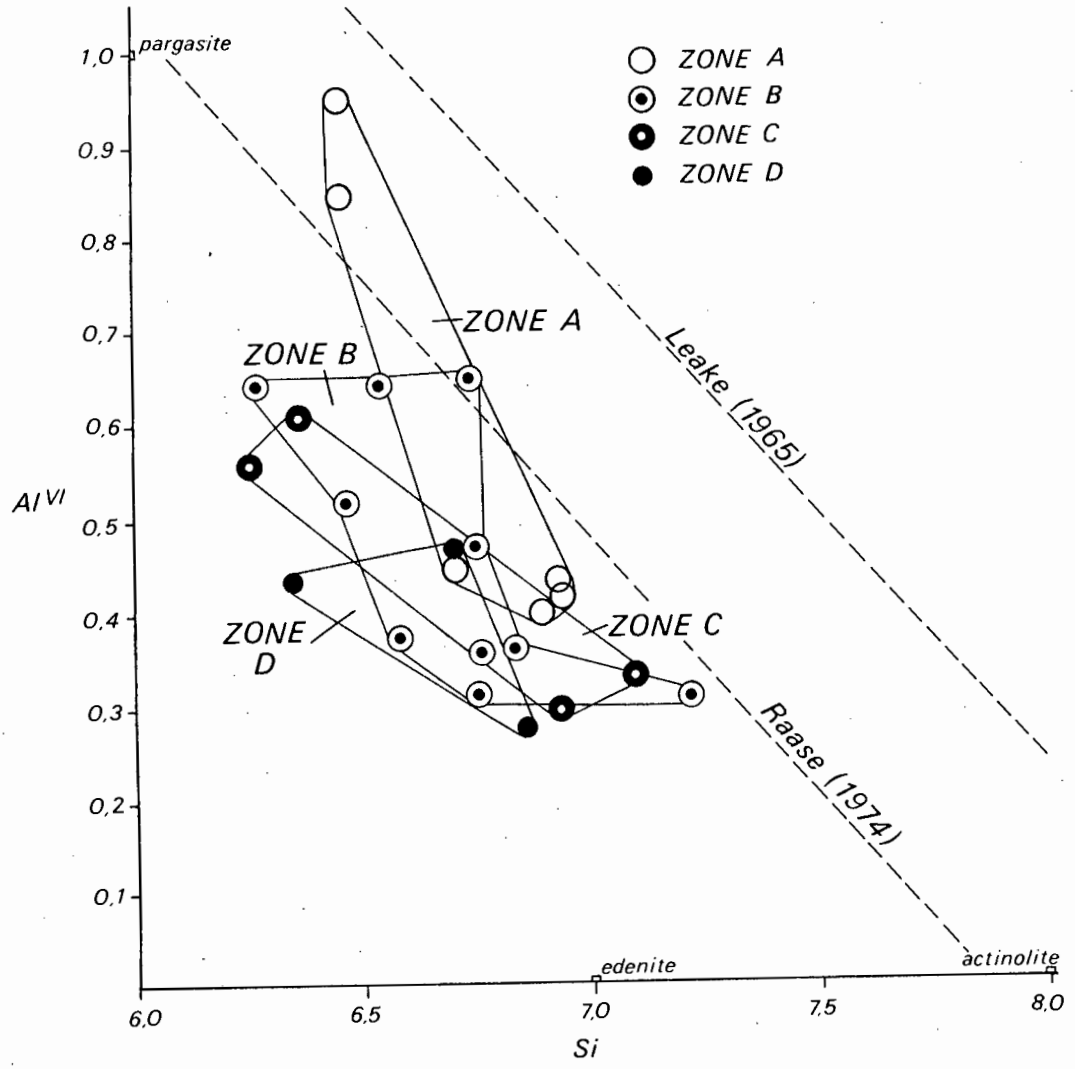

Figure 31. Relation between Al^{VI} and Si (cations per 23 oxygen anions) contents of hornblendes in Garub metabasites. Each symbol represents the average value of 3-5 hornblende grains in each rock specimen. Upper diagonal line (after Leake, 1965) indicates maximum possible amounts of Al^{VI}. Lower diagonal line (after Raase, 1974) indicates division between hornblendes from low-pressure regional metamorphic terrains (below) and higher-pressure metamorphic terrains (above)

hornblende from zones A and B, and zones B and D; no significant difference in alkali content of hornblende was proven between zones B and C, and C and D.

The above results show that hornblendes of the epidote-zone (zone A) contain statistically significantly smaller amounts of alkalis than those from zone B, which are not associated with epidote. Similarly hornblendes from the granulite facies (zone D) are significantly more enriched in alkalis than the hornblendes from zone B. These observations are compatible with the hypothesis

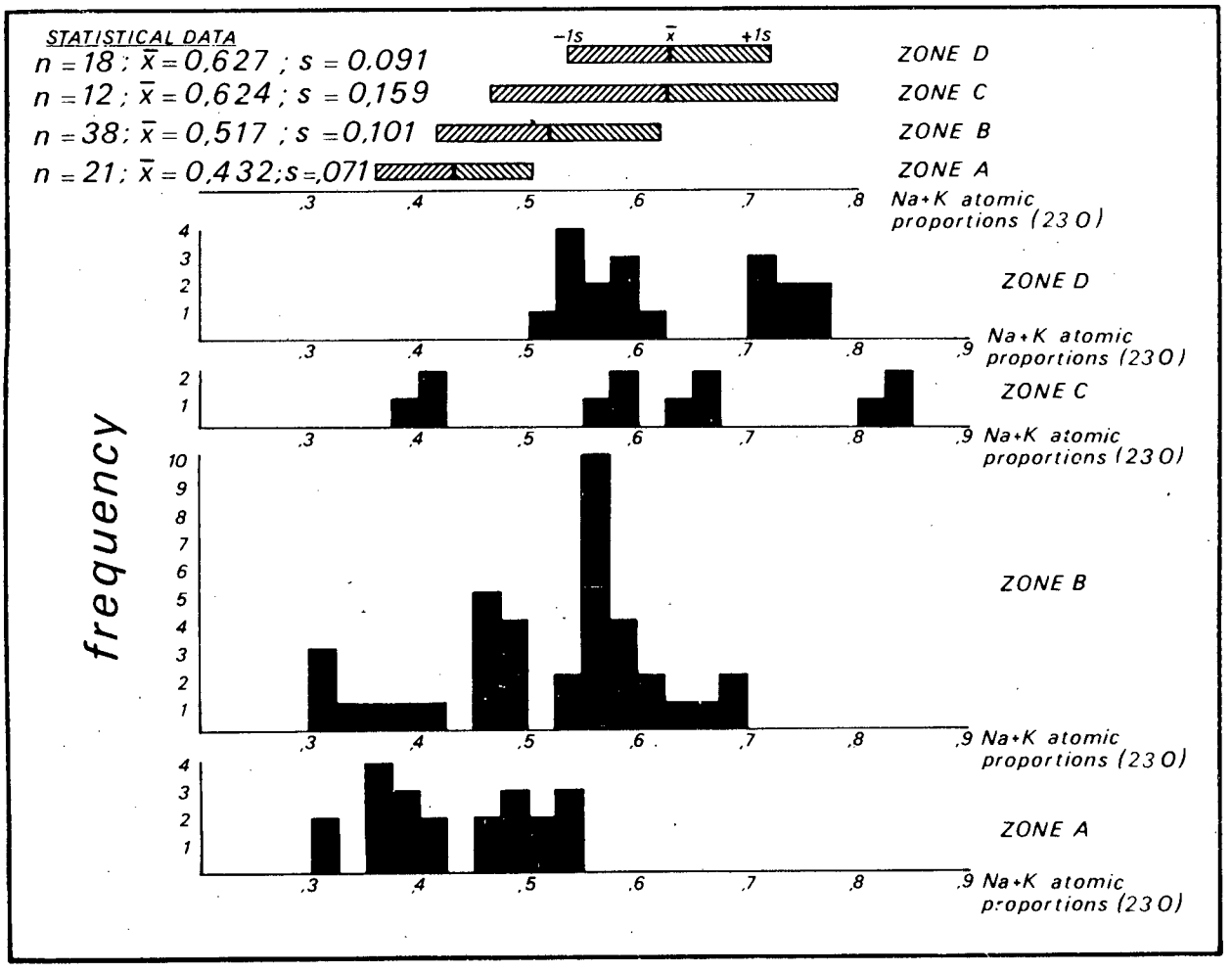

Figure 32. Variation in alkali content of hornblende from Garub metabasites in the different metamorphic zones

that enrichment of hornblende in alkalis is a feature of increasing metamorphic grade. In contrast the identity in alkali content of hornblende from the diopside-hornblende (zone C) and hypersthene (zone D) zones, suggests that there is little difference in metamorphic grade between the two zones. It is possible that the supply of sodium to the hornblende was restricted by a slow breakdown of the albite component of plagioclase (which is suggested by the relatively small difference in the mean anorthite content of plagioclase from zones C and D as shown in Figure 27).

Titanium enrichment: both Engel and Engel (1962b, p.1504) and Binns (1965, p. 312; 1964, Tables 2 and 3) reported increases in the titanium content of hornblende with increasing metamorphic grade which were independent of the titanium content of the host rock. Leake (1965, p.301) postulated that this titanium enrichment was a function of temperature of crystallization. Raase (1974, p. 324) summarized the titanium values of hornblendes from various metamorphic facies series and demonstrated that there is a general rise in maximum

TABLE 20

Equality of variances between different pairs of samples (titanium and alkali contents of hornblende) determined by means of the F test. Values in italics represent pairs of samples that show differences in variances above acceptable limits for t testing (at 5% level of significance

PARAMETERS	SAMPLE PAIRS	v_1	v_2	F (α=0,05)	F sample pairs
Hornblende alkalis, Metamorphic zone	A and B	37	20	2,02	*2,04*
	B and C	11	37	2,06	*2,48*
	C and D	11	17	2,41	*3,05*
	B and D	37	17	2,12	1,23
Hornblende titanium, Hornblende colour	BlGr and GrBr	23	28	1,92	1,58
	GrBr and Br	33	23	1,95	*2,06*
Hornblende titanium, Metamorphic zone	A and B	36	26	1,87	*2,42*
	B and C	12	36	2,03	*2,18*
	C and D	12	14	2,53	1,42

titanium content with metamorphic grade from 0,08 (cations per 23 oxygen anions) in the transition zone between greenschist and amphibolite facies, 0,13 in lower amphibolite facies, 0,20 in upper amphibolite facies and 0,29 in granulite facies. Bard (1970, p. 124) reported a similar enrichment of hornblende in Ti with increasing metamorphic grade and ascribed this mainly to temperature increases. However, he concluded that this trend was not as systematic as that of the alkali enrichment described above because many low-grade hornblendes had higher titanium contents than those of higher grade.

Titanium contents of hornblende from Garub metabasites were determined by microprobe analysis to find out whether colour changes in the mineral could be correlated with its chemistry. Figure 33 shows the titanium content of hornblende from the different colour groups (blue-green, green-brown and brown) which increases from 0,06 through 0,11 to 0,16 (cations per 23 oxygen anions). Tables 20 and 21 show that a statistically significant difference exists between the mean titanium values in each sample. Maximum values in each statistical sample increase in a similar fashion from 0,13 through 0,19 to 0,26 (Fig. 33). The standard deviation of each sample also increases with increasing

TABLE 21

Results of t and t' tests (titanium and alkali contents of hornblende). A significant difference between each sample mean is proven at a level of 5% significance if t_{sample} *or* $t'_{sample} > t_{(\alpha=0,05)}$

PARAMETERS	SAMPLE PAIRS	ν_1	$t_{(\alpha=0,05)}$	t_{sample}	t'_{sample}	t_{sample} or t' sample > $t(\alpha=0,05)$
Hornblende alkalis, metamorphic zone	A and B	57	2,00		2,44	yes
	B and C	48	2,01		1,01	no
	C and D	28	2,05		1,40	no
	B and D	54	2,01	3,93		yes
Hornblende titanium, hornblende colour	BlGr and GrBr	51	2,01	5,05		yes
	GrBr and Br	56	2,00		2,40	yes
Hornblende titanium, metamorphic zone	A and B	62	2,00		6.40	yes
	B and C	61	2,00		-1,03	no
	C and D	26	2,06	2,23		yes

t test for comparison of two samples with similar variances after Davis (1973, p.98)
t' test for comparison of two samples with dissimilar variances after Guenther (1965, p.146)

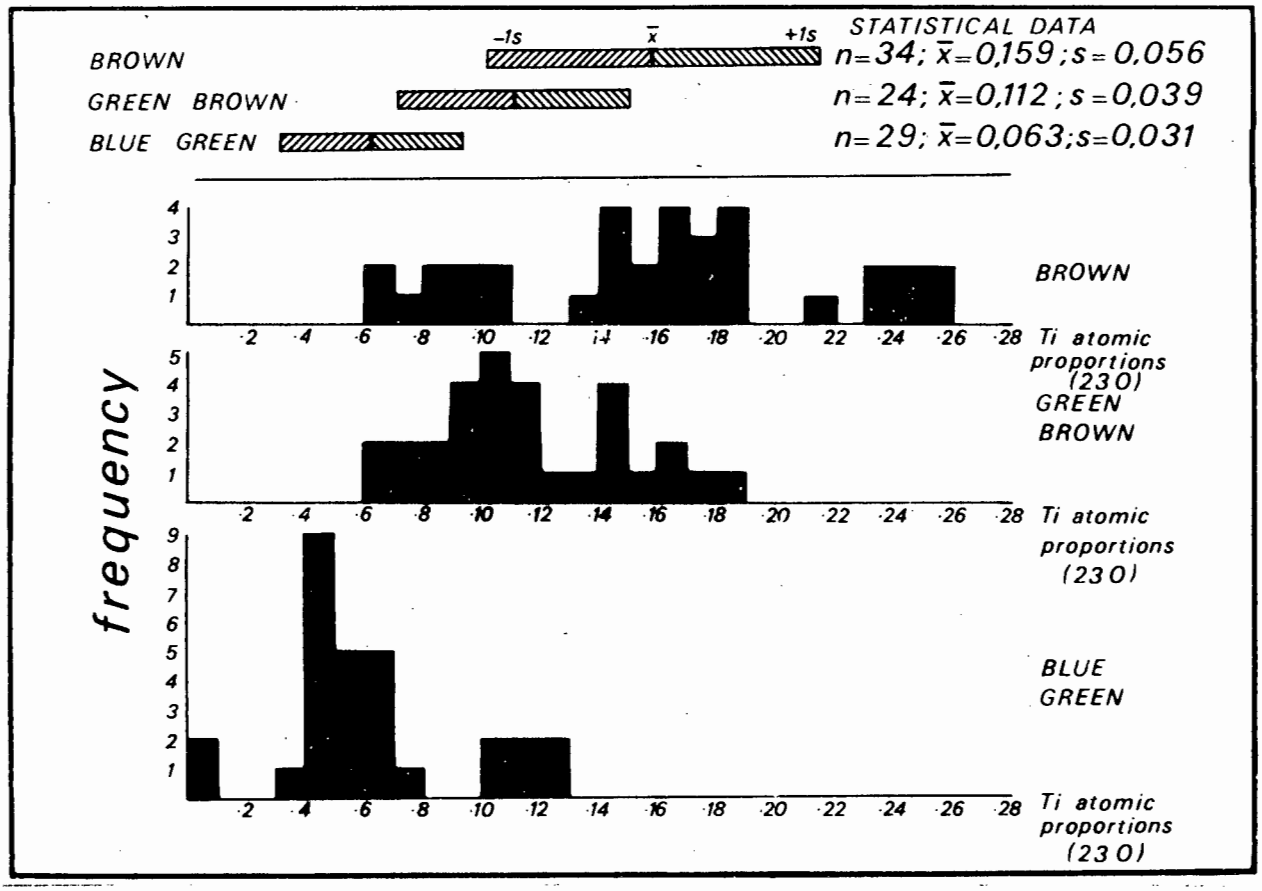

Figure 33. Variation in titanium content with Z absorption colour of hornblende in Garub metabasites

grade. It can therefore be concluded from these results that differences in titanium content may be a major factor in producing the observed colour changes in hornblende (in agreement with Binns, 1965).

Figure 34 shows the titanium content of hornblende plotted according to the four metamorphic zones. The hornblendes of zone A comprise a statistical sample with a low standard deviation and a mean value that is significantly lower than that of the other samples (Tables 20 and 21). Similarly, the mean value of the zone D sample is significantly higher than that of the samples from other zones. There is no significant difference between the samples from zones B and C (Table 21). The relatively low-grade hornblendes of zone A and the granulite-grade hornblendes of zone D are thus characterized by the titanium contents significantly lower and higher than those of the intervening zones B and C, which are not as clearly differentiated.

Most workers in this field (e.g. Engel and Engel, 1962b; Leake, 1965; Binns, 1965) have reported that, providing sufficient titanium is available in the rock, the trend of titanium enrichment in hornblende is independent of variations in host-rock composition. The presence of the titanium-bearing minerals sphene and ilmenite indicates titanium saturation in three quarters of

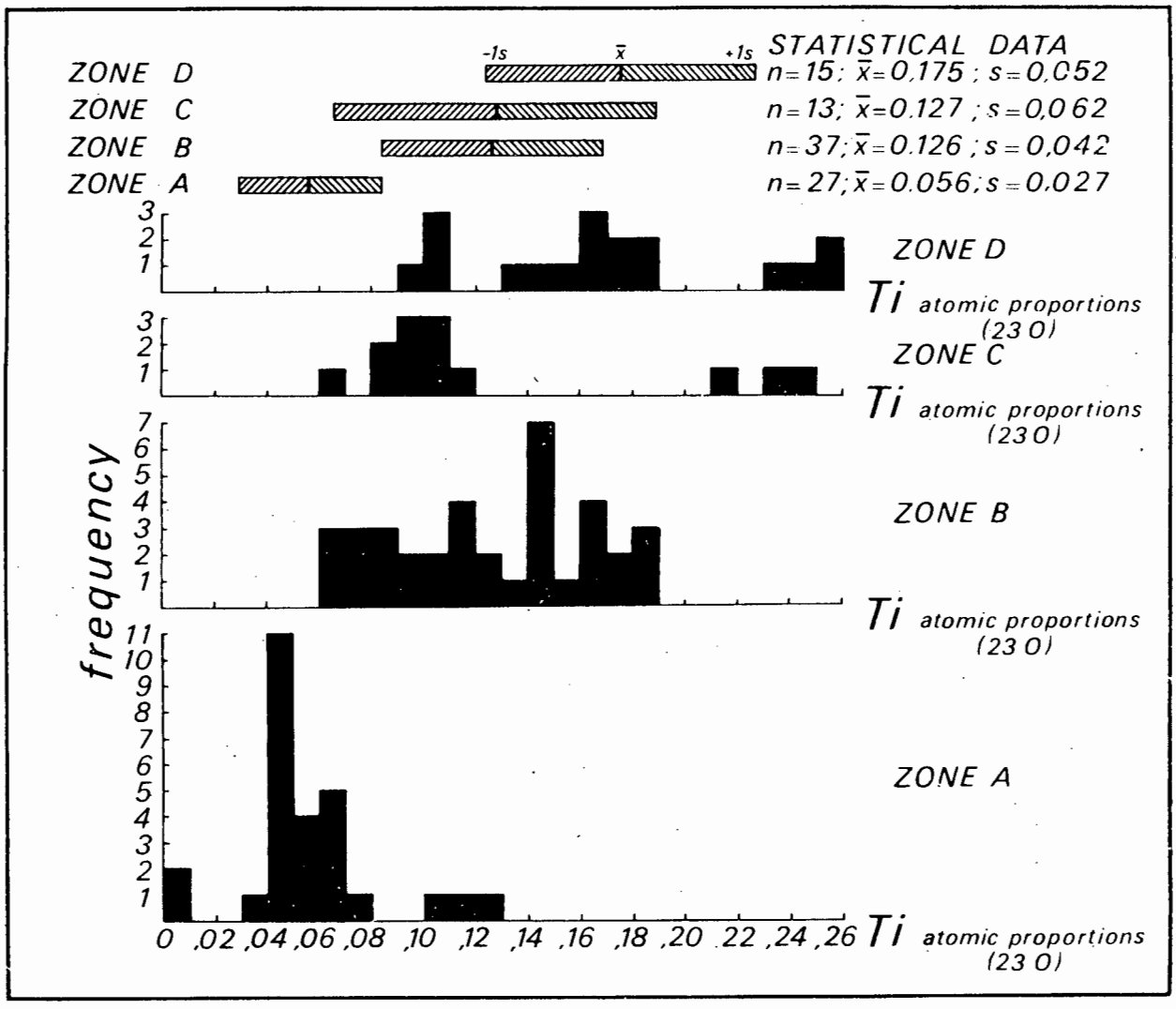

Figure 34. Variation of titanium content of hornblende in Garub metabasites in the different metamorphic zones

the specimens from zones A, B and C but only half from zone D. Furthermore biotite is present in larger amounts in the zone D metabasites (Fig. 36); this mineral has a greater affinity for titanium than does hornblende (Leake, 1965, p. 305). These facts suggest that the supply of titanium to hornblende in zone D was restricted and that had titanium been more freely available, its enrichment in hornblende would have been more marked than these results indicate.

Comparison of Geochemical Differences in Plagioclase and Hornblende from Different Metamorphic Zones

Figure 35 illustrates the composition of hornblende plotted according to titanium and alkali content. The blue-green hornblendes of zone A form a geochemically distinct group characterized by low titanium contents. The groups from other zones show considerable overlap but their mean values, in-

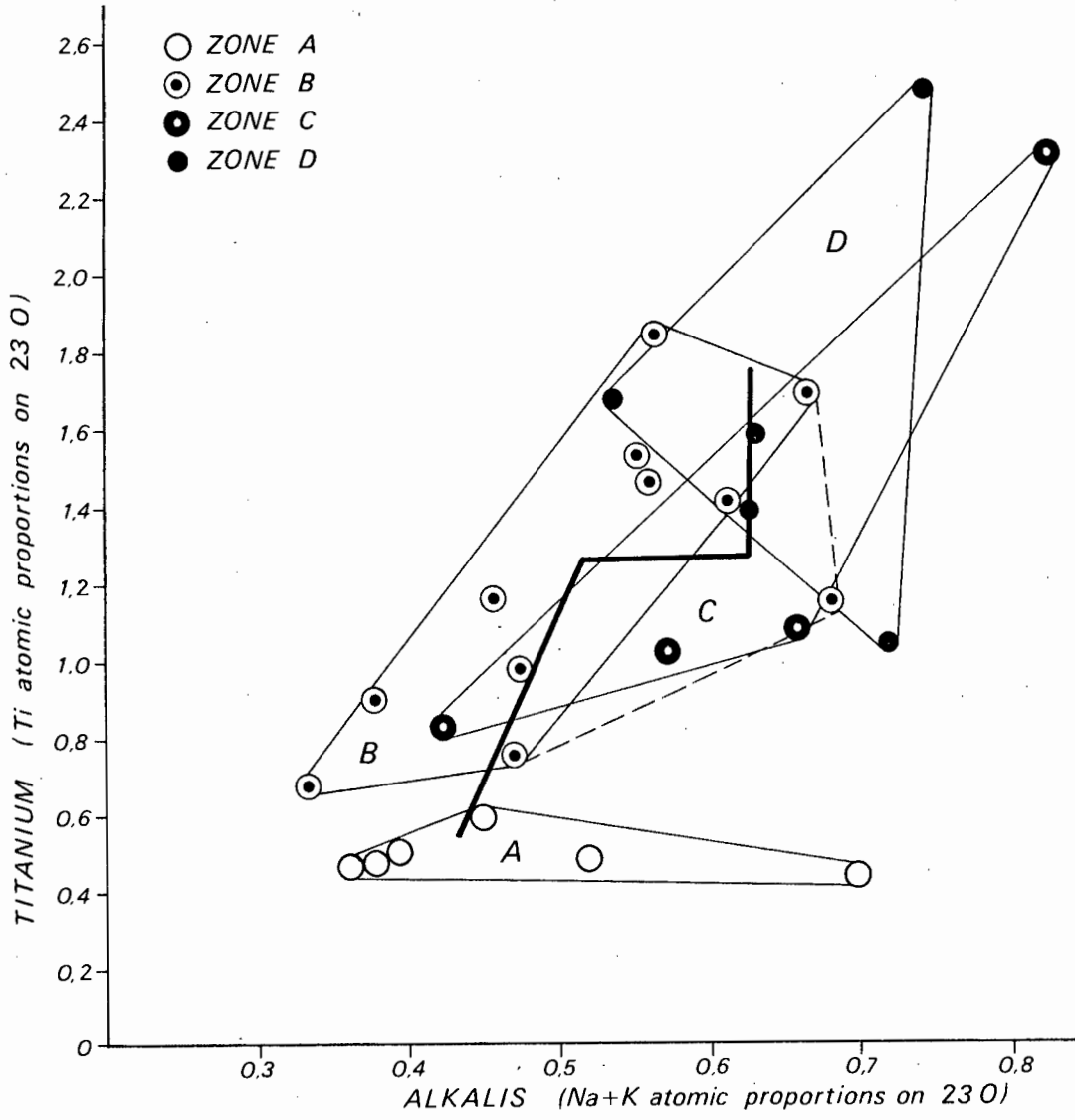

Figure 35. Variation of titanium and alkali content of hornblende in Garub metabasites of different metamorphic zones. Each symbol represents the average value of 3-5 grains in each specimen

dicated in the diagram by the heavy line, show an increase with metamorphic grade.

The statistical significance of these compositional trends in hornblende is shown in a significance truth table that summarizes the results of t testing of the variation in alkali and titanium content (Table 22). Both parameters indicate that the blue-green hornblendes of zone A are significantly different from those of higher metamorphic grade. No significant difference was proven between the hornblendes of zones B and C. The hornblendes of the granulite facies (zone D) contain statistically significantly higher amounts of titanium than those of all other samples from zones A, B and C, whereas the alkali

content of granulite facies hornblendes is not significantly higher than that of hornblendes in diopside-amphibolites but is significantly higher than that of hornblendes in diopside-free amphibolites.

TABLE 22

Significance truth table for differences in mean values of titanium and alkalis in hornblende samples from zones A,B,C and D. Results compiled from Table 21; s=significant difference proven at 5 probability; n=significant difference not proven at 5% probability

Zones (Titanium) \ Alkalis	A	B	C	D
A		*s*	*s*	*s*
B	*s*		*n*	*s*
C	*s*	*n*		*s*
D	*s*	*s*	*n*	

In contrast the anorthite content of plagioclase increases significantly with metamorphic grade. Table 19 shows that the mean anorthite content of each statistical sample from the four metamorphic zones is significantly different.

In summary, the results indicate that the epidote-bearing amphibolites of zone A are of significantly lower metamorphic grade than other metabasites; there is thus good justification for differentiating blue-green hornblende from hornblende of other colours. The granulite facies metabasites from zone D contain plagioclase with significantly higher anorthite contents and hornblende with significantly higher titanium contents than those in the amphibolite facies metabasites from zone C. The plagioclase composition in the diopside amphibolites (zone C) indicates a higher metamorphic grade than that in the amphibolites of zone B,but this conclusion is not supported by compositional differences in hornblende; on this basis there is little justification in regarding the presence of diopside in amphibolites as indicating higher metamorphic grade than those that are diopside-free.

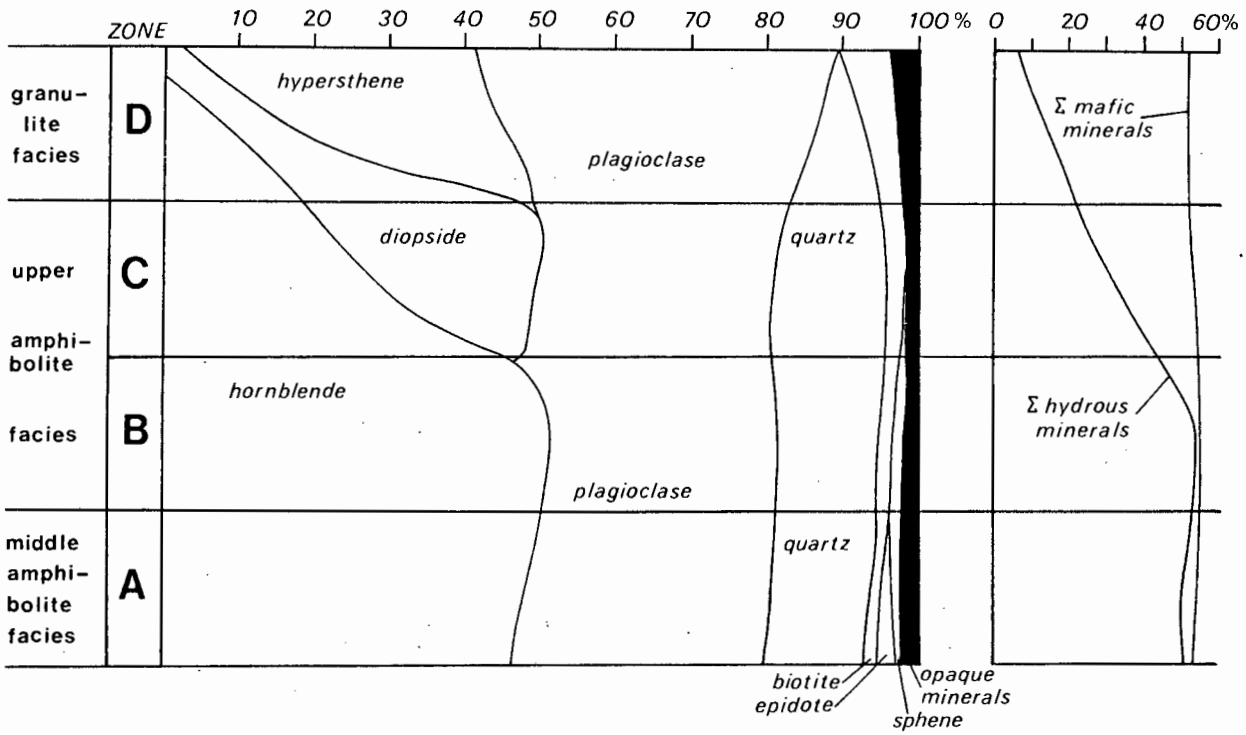

Figure 36. Variations of the modes (in volume %) of Garub metabasites from the four metamorphic zones

7. *Discussion on the Metamorphic Zonation Defined by the Metabasites*

Variations in the Mode of Metabasites from the Four Metamorphic Zones

An examination of the estimated modes of metabasites from the four metamorphic zones provides a qualitative guide to the reactions that may have taken place during the formation of the present mineral assemblages. The following observations may be made from Figure 36:

(i) the percentage of mafic minerals in each zone is virtually unchanged (range 53-55)

(ii) the steady decline in the proportion of hydrous minerals from ∿50% in the middle amphibolite facies to 12% in the granulite facies is in harmony with the progressive dehydration that occurs with prograde metamorphism

(iii) the decline in the modal percentage of hornblende with increasing grade corresponds to the formation of diopside in zone C and hypersthene in zone D. Hypersthene takes the place of both hornblende and diopside

(iv) in the granulite facies there is an increase in plagioclase content and a decrease in quartz content

Zone A: A Greenschist/Amphibolite Transition Facies?

The widespread presence of blue-green hornblende in this area, together with the presence of minor epidote, suggest that zone A may represent the epidote-amphibolite facies (Eskola, 1939), which is transitional between the greenschist and amphibolite facies. The epidote-amphibolite facies is characterized by the parageneses:

hornblende + albite + epidote

actinolite + oligoclase + epidote

The paragenesis in the zone A metabasites of the Aus area is:

hornblende + andesine/labradorite + quartz ± epidote

According to Miyashiro (1973, p.248) epidote is the dominant calcium-aluminium silicate (in place of anorthitic plagioclase) in low-temperature zones of many medium-and low-pressure metamorphic terrains. Epidote in the zone A metabasites, however, averages only 1,5% by volume and is absent from more than half the rocks examined. This fact, combined with the large proportion of anorthite component in the plagioclase, suggests that the bulk of the epidote has broken down to release Ca and Al which formed the anorthite component of plagioclase (ibid.) according to the reaction:

(1) Na-rich plagioclase + Na-poor hornblende + epidote → Ca-rich plagioclase + Na-richer hornblende

The high proportion of anorthite (>50%) in the plagioclase in zone A metabasites, together with the paucity of epidote, suggests that zone A does not represent a facies transitional with the greenschist facies but is equivalent to middle-amphibolite facies.

Further evidence is given by the presence of cummingtonite in the more magnesian metamorphites of the Garub sequence in zone A. According to Shido (1958) cummingtonite is typical of high-temperature/low-pressure metamorphic terrains. With increase of pressure the mineral breaks down by the volume-reducing reactions 2 and 3:

(2) 14 anorthite + 3 cummingtonite + 4 H_2O → 7 tschermakite + 10 quartz

(3) 14 albite + 3 cummingtonite + 4 H_2O → 7 glaucophane + 10 quartz

Low-pressure regional metamorphism is further suggested by the absence of garnet from the Garub metabasites of all grades. Almandine is a common constituent of amphibolite-facies metabasites from medium-pressure or high-pressure facies series (Wiseman, 1934; Mason, 1962; Lee et al., 1963; Banno, 1964; Ernst, 1965; Wenk and Keller, 1969; Cooper, 1972). In contrast, as pointed out by Miyashiro (1973, p. 279), almandine is absent or very rare in metabasites from low-pressure facies series (Eskola, 1914; James, 1955; Miyashiro, 1958; Katada, 1965; Bard, 1969).

In summary the mineral compositions and parageneses of the metabasites in zone A (namely the paucity of epidote, the presence of cummingtonite, the absence of garnet, and the high anorthite content of plagioclase) suggest that these rocks were metamorphosed to middle amphibolite facies in a low-pressure environment (this is confirmed by the associated semi-pelitic rocks which contain parageneses characteristic of the upper part of Winkler's (1974) medium-grade and the lower part of his high-grade).

Zone B

Apart from the absence of epidote-group minerals in Zone B metabasites there is no difference in the parageneses of metabasites from zones A and B. Nevertheless chemical analyses indicate that breakdown of albite has yielded a component of newly-formed plagioclase with higher anorthite content (zone A, 56% An; zone B, 67% An mean). The calcium component of this anorthitic plagioclase was derived from the breakdown of epidote and hornblende (zone A, Ca = 1,88 cations; zone B, Ca = 1,82 cations). The sodium derived from breakdown of albite was incorporated in the vacant sites of hornblende (zone A (Na+K) = 0,43; zone B, (Na+K) = 0,53 cations).

Zone C: The Formation of Diopside

As described in the end of Section 4.1.5 there is some doubt as to whether the rocks of zone C reflect a higher metamorphic grade than those of zone B. The presence of diopside in the zone C metabasites may therefore be due to possible compositional differences between these rocks and those of zone B or to a lower water pressure ($P_{H_2O} < P_t$) in zone C. The much lower proportion of hydrous minerals in zone C is compatible with progressive dehydration during prograde metamorphism (Figure 36).

However, the commonly observed intergrowth between hornblende and diopside in zone C metabasites implies that diopside has formed by breakdown of hornblende; Figure 36 suggests that this reaction has taken place without net change in the percentages of quartz or plagioclase.

Differences in mineralogy between plagioclase and hornblende of zones B and C show that there has been further exchange of alkalis and calcium between the two minerals which become more anorthitic and edenitic respectively.

Zone D: The Granulite Zone

Further dehydration and major changes in modal proportions characterize the metabasites of zone D. Orthopyroxene appears to have formed by breakdown of both hornblende and diopside (Figure 36). There is abundant textural evidence for the breakdown of hornblende to form hypersthene but not for the breakdown of diopside. Figure 36 shows that the proportion of plagioclase has increased at the expense of quartz. The reactions below

(4) 1 hornblende + 1 quartz → 3 orthopyroxene + 2 anorthite + H_2O (De Waard, 1965a)

(5) 1 hornblende + 3 quartz → 1 orthopyroxene + 1 clinopyroxene + 1 plagioclase + H_2O (Sen and Ray, 1971a)

account for the breakdown of quartz and hornblende and the accompanying formation of orthopyroxene and (anorthitic) plagioclase indicated in Figure 36; but the decrease in clinopyroxene is not accounted for. It can therefore be postulated that this is due to Ca deficiency in the granulute facies metabasites. Considerable calcium must have been liberated during the breakdown of hornblende which was accommodated in anorthite; this explains both the increase in the modal percentage of plagioclase and its progressively more calcic character (An_{75} in zone C to An_{82} in zone D). The enrichment in titanium (0,13 in zone C and 0,18 cations in zone D) is mainly due to the breakdown of hornblende.

A full discussion on the granulite zone and PT estimates for the metamorphism are given in Section 4.6.

4.2. METAMORPHISM OF SEMI-PELITIC ROCKS

In this section all rocks of semi-pelitic composition are discussed together. This group comprises biotite schists and gneisses but also includes micaceous metaquartzites and hornblende schists. The term 'semi-pelitic' is used in a broad sense to refer to rocks of composition intermediate between pelites and psammites that contain small amounts of micas together with quartz and feldspar. The metamorphism of pelitic rocks, which consist primarily of aluminous minerals, is disucssed in Section 5.3.

1. Mineralogical Variations in Biotite

Although predominantly present in the biotite schists and gneisses examined (51 specimens), biotite is also present in many metabasites (38 specimens) and in all metapelites (22 specimens). The *Z* absorption colour of biotite in all three rock types was examined (see Appendix 3) to determine whether colour variations in this mineral could be linked with changing metamorphic grade (cf. hornblende). Biotite colour could be resolved into two varieties: (i) brown or (ii) red/red-brown. No green biotite was found in the area (except where this mineral had been chloritized). These two varieties are referred to as 'brown' and 'red' and their distribution in the biotite schists, metapelites and metabasites is shown in Figure 37; biotite from the three compositional groups is symbolized by circles, squares and triangles, respectively; completely chloritized biotite of indeterminate original colour is present in a few specimens and is depicted as rhombs.

Biotite from the metabasites shows a colour transition from brown to red in the northwestern and northeastern parts of the study area. This change corresponds approximately to the 'muscovite + quartz + plagioclase out' isograd in the

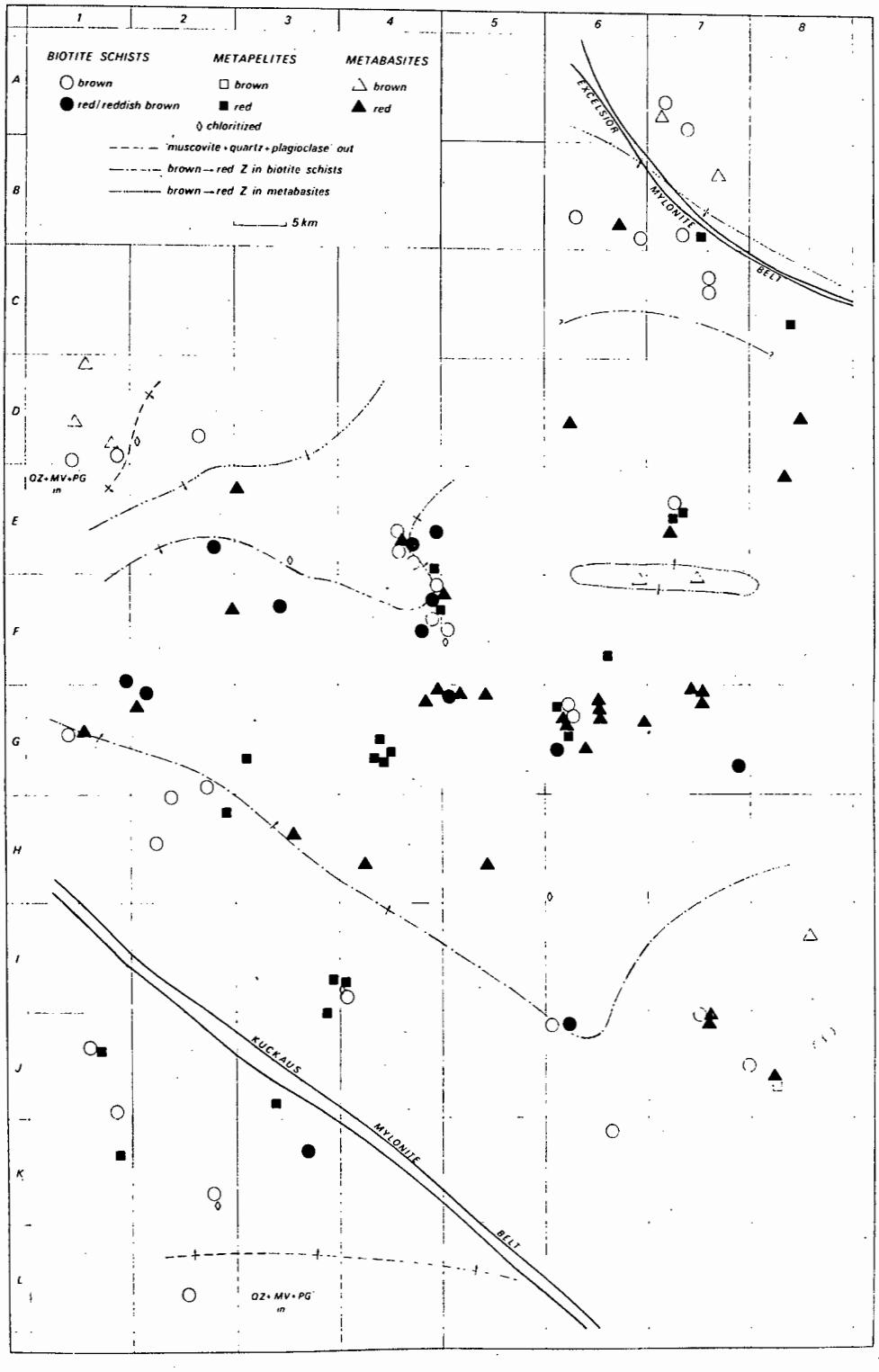

Figure 37. Sketch map showing variations in the Z absorption colour of biotite in biotite schists, metapelites and metabasites of the Garub sequence and biotite gneisses in the Aus area

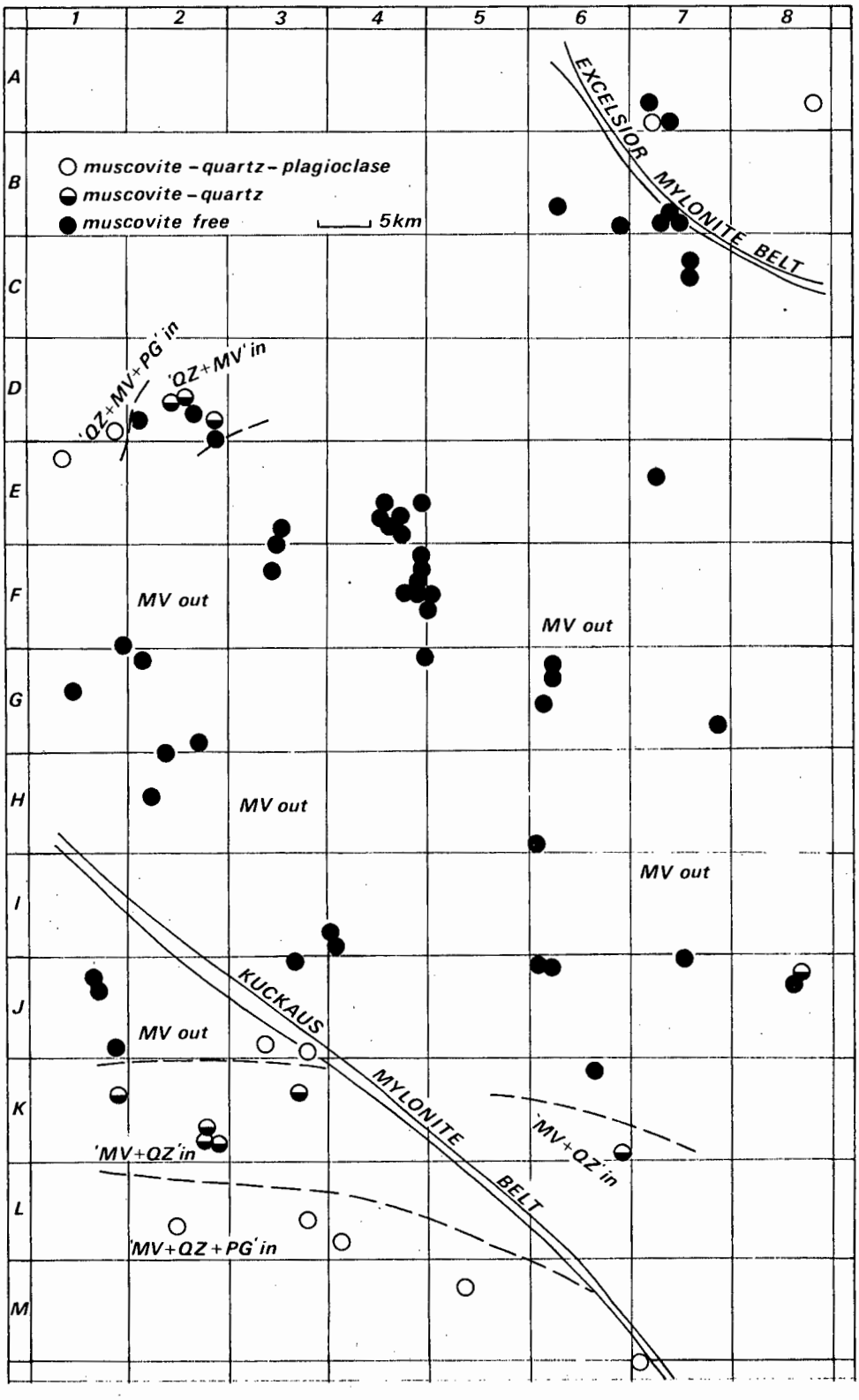

Figure 38. Sketch map showing distribution of mineral parageneses in biotite schists, gneisses and metaquartzites of the Aus area

Mv - muscovite in
opite of abbreviations
p. viii

biotite schists (see below) and with the change from blue-green to green-brown hornblende in the metabasites.

The semi-pelitic rocks, although widespread, do not show the same regular change in biotite colours as do the metabasites. What is clear, however, is that the biotite colour change from brown to red appears to take place at higher grades in this group than in the metabasites; the colour-change 'isograds' are displaced more towards the high-grade centre of the area than those of the metabasites. But there is much colour variation in the centre of the area. Some biotite in the biotite schists of the granulite zone is brown. On the farms Tsirub and Heinrichsfelde (G1,G2), however, there is a better-defined change from brown to red biotite which corresponds to the 'clinopyroxene-in' isograd of the metabasites. The metapelites do not contain brown biotite and virtually all the biotite examined is red in these rocks, even near the lower-grade borders of the area. This indicates that the brown-to-red change in the metapelites takes place at lower grades than in metabasites or semi-pelitic rocks.

In summary therefore the brown-to-red change of biotite in metabasites takes place at the approximate boundary between zones A and B, whereas the equivalent change in semi-pelitic rocks takes place at the transition between zones B and C. The equivalent change in the metapelites appears to take place at lower grades than in either the metabasites or the biotite schists. Binns (1969, p.328) reported that metapelites from the Broken Hill area, New South Wales, contain larger amounts of Ti and Mg/(Mg+Fe) than do semi-pelitic rocks from the same area. The proportion of these cations also increases with metamorphic grade (ibid., p.329).

2. *The Distribution of Mineral Parageneses*

Mineral parageneses of metamorphic significance fall into three major groups:

Group 1: muscovite + quartz + plagioclase (+ biotite + K-feldpsar)

Group 2: muscovite + quartz (+ biotite + K-feldspar)

Group 3: quartz + plagioclase (+ biotite + K-feldspar ± almandine, hornblende, diopside)

Figure 38 illustrates the distribution of these three groups. The 'muscovite + quartz + plagioclase' paragenesis is widespread south of the Kuckaus mylonite belt. Outcrops in this area are limited but the northern boundary of this zone appears to coincide with the mylonite belt except in the west, around Agub Mountain (J1), where muscovite-free biotite schists are present south of the mylonite belt. Within the Kuckaus mylonite belt the mylonites contain abundant well-formed flakes of muscovite in apparent equilibrium with quartz and plagioclase. The muscovite has recrystallized within the mylonite foliation plane and was produced after the regional metamorphism had taken place.

The group 1 paragenesis is also present in a small area farther north to the west of Magnettafelberg (D1). Similarly this paragenesis appears to be stable to the north of the Excelsior mylonite belt (A7,A8); unfortunately this area contains few semi-pelitic rocks and the sampling density is too low to be certain of a metamorphic change across the mylonite belt.

The group 2 paragenesis, 'muscovite + quartz', is present in the metaquartzites of the Magnettafelberg area (D2). Plagioclase-bearing mica schists in the same area are devoid of muscovite. North and south of the Kuckaus mylonite belt (K2,K6) 'muscovite + quartz' is present in metaquartzites and quartz-mica schists devoid of plagioclase or where muscovite is isolated from plagioclase by being interleaved with biotite or enclosed within quartz grains.

The group 3 paragenesis is present in micaceous rocks throughout the large area bounded approximately in the north and south by the Excelsior and Kuckaus mylonite belts (Fig. 38); in this central zone all rocks (with the exception of the mylonites) are completely devoid of muscovite.

3. *Discussion on the Stability of Muscovite*

The three different parageneses within the semi-pelitic rocks reflect the progressive breakdown of muscovite with increasing metamorphic grade. The areas occupied by the parageneses of groups 1, 2 and 3 (above) can be referred to in this section as metamorphic zones 1, 2 and 3 respectively. Zone 1 represents a metamorphic environment where muscovite is stable in all combinations. In zone 2, muscovite coexists with quartz in plagioclase-free rocks but is not stable in contact with quartz and plagioclase. The complete absence of muscovite from all rock types in zone 3 suggests that the mineral is not stable in any combination.

Winkler (1974, Fig. 7-3) has summarized experimental results on the breakdown of muscovite. This diagram is reproduced here, in part, as Figure 39. Winkler (1970) suggested that at water pressures below 3,5 kb muscovite would disappear by reaction 6 (curve 6a):

(6) muscovite + quartz → K-feldspar + Al_2SiO_5 + H_2O

In this pressure range, reaction 6 defines the change from Winkler's (1970) medium-grade to high-grade metamorphism.

According to data presented in the following section on the metapelites, P_{H_2O} during metamorphism was not as low as 3,5 kb anywhere in the Aus area. This is confirmed by the distribution of migmatites (see Fig. 64), which extend to lower-grade areas than the 'muscovite + quartz out' isograd. Reference to Figure 39 indicates that this relation is to be expected where P_{H_2O} is greater than 3,5 kb.

At water pressures in excess of 3,5 kb a number of reactions are possible for the breakdown of muscovite in the presence of quartz and plagioclase (Winkler, 1974, p.84):

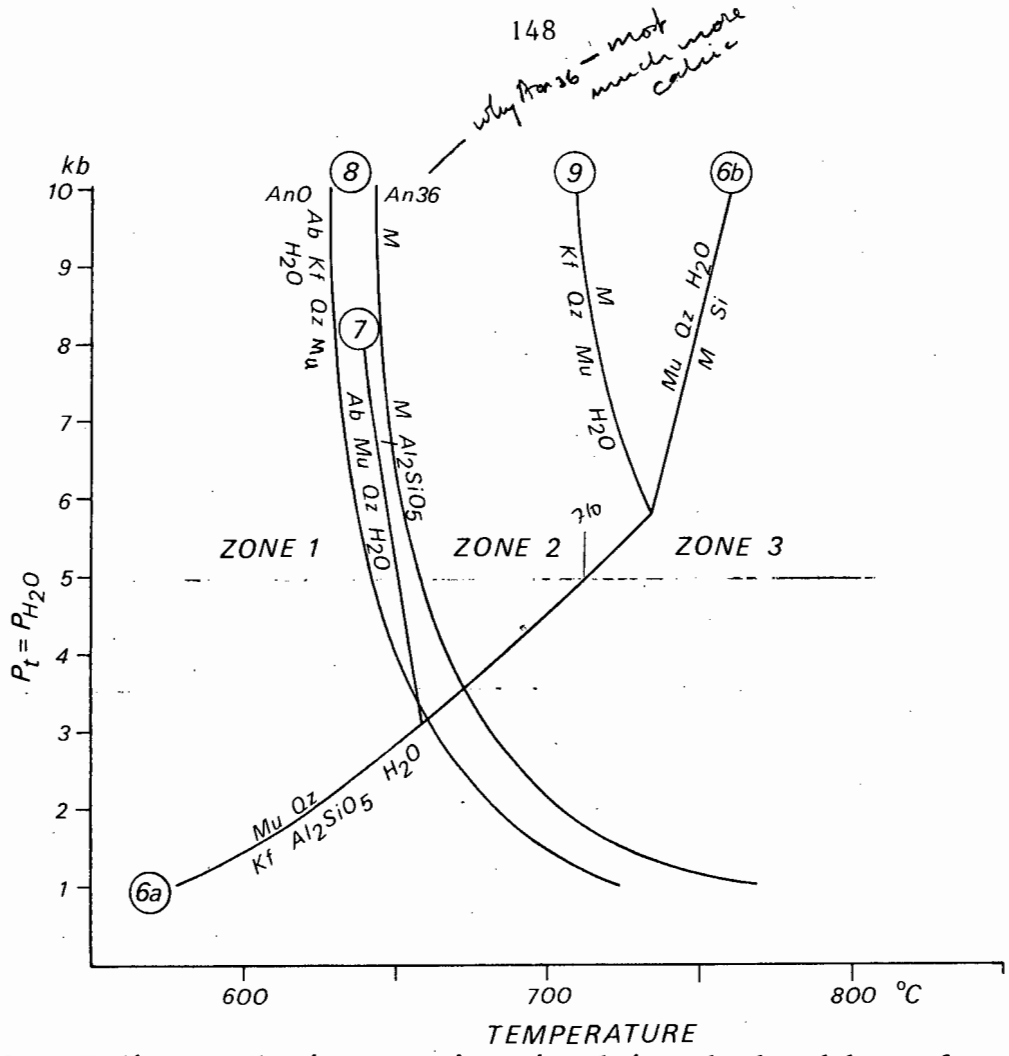

Figure 39. PT diagram showing reactions involving the breakdown of muscovite with quartz
Ab albite, An anorthite, Kf K-feldspar, Mu muscovite, M melt, Qz quartz, Si sillimanite.
(6a) Althaus et al. (1970); (6b) Storre and Karotke (1972); (7) Storre and Karotke (1971); (8) Winkler (1970); Lambert et al. (1969)

(7) muscovite + quartz + albite + H_2O → sillimanite + melt

(8) muscovite + quartz + albite + K-feldspar + H_2O → melt

In the absence of plagioclase muscovite is stable in the presence of quartz to much higher temperatures [at which point the] combination becomes unstable and muscovite melts according to the following reactions:

(6) muscovite + quartz → K-feldspar + sillimanite + H_2O

(9) muscovite + quartz + K-feldspar + H_2O → melt

The breakdown of muscovite with quartz therefore takes place at about 650°C if plagioclase is present and at about 710°C if plagioclase is absent (P_{H_2O}=5 kb). The paragenesis of 'Mv + Qz + Pg' in zone 1 suggests that the PT field for this metamorphic grade is situated to the left of curve 7 in Figure 39; the stability

of 'Mv + Qz' in zone 2 suggests PT conditions in the field between curves 7 and 9/6a; the complete absence of muscovite from zone 3 indicates temperatures exceeding those of curve 6b.

It is significant that most of the reactions cited above for the breakdown of muscovite involve the formation of sillimanite because this mineral is absent from the high-grade semi-pelitic rocks of zone 3. However, even in the lowest-grade rocks (zone 1) only very low quantities of muscovite are present (1-3 modal%) which suggests that the composition of these rocks is not favourable for the presence of muscovite. Figure 40a shows the suggested composition of the biotite schists in zone 1.

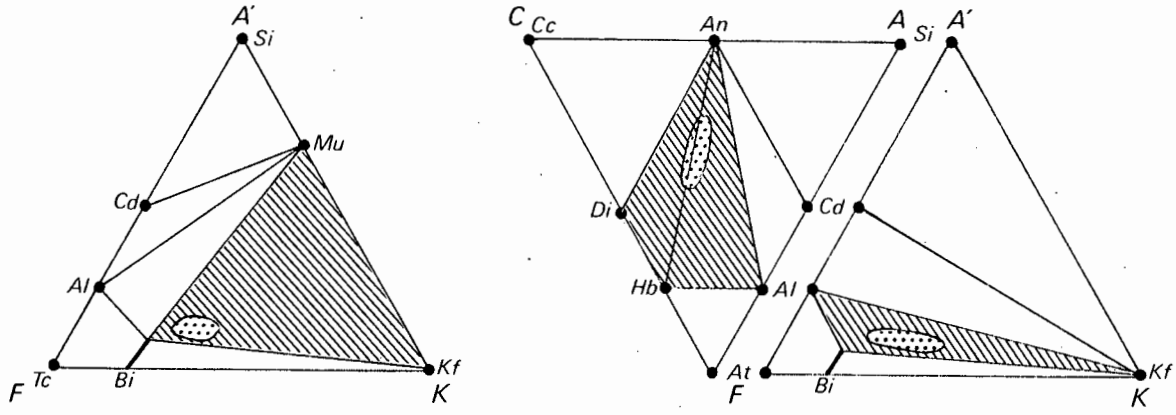

(a) zones 1 and 2 (b) zone 3

Figure 40. Ternary diagrams illustrating the mineral parageneses in semi-pelitic rocks. Hatched areas show parageneses present in Garub biotite schists; stippled areas show composition of these rocks estimated from their modes
An anorthite, Al almandine, At anthophyllite, Bi biotite, Cc calcite, Cd cordierite, Hb hornblende, Kf K-feldspar, Mu muscovite, Si sillimanite, Tc talc

The amount of aluminium released by the breakdown of this minute amount of muscovite at higher metamorphic grades would have been correspondingly small. Figure 40b suggests that this small amount of aluminium would have been incorporated in recrystallizing almandine or plagioclase rather than sillimanite because the biotite schists lack cordierite. Many of the high-grade biotite schists contain more K-feldspar than can be accounted for by the breakdown of 1-3% muscovite. These rocks are therefore more potassic than those of zone 1; other possible differences in bulk composition may account for the lack of sillimanite in the rocks of zone 3 (sillimanite and K-feldspar are abundant in metapelites of zone 3).

It can therefore be concluded that although the biotite schists and related rocks are widespread and abundant, on their own they offer a limited amount of data on the PT conditions of their metamorphism because of their unsuitable bulk compositions. However, the reactions suggested in this section for the

metamorphism of the semi-pelitic rocks are known to have taken place in the metapelites of the same area. Furthermore, geothermometric data derived from the calcareous rocks (Section 4.4.) are in complete agreement with the temperature range shown in Figure 39.

4.3. METAMORPHISM OF PELITIC ROCKS

This section describes the metamorphism of the aluminous gneisses, which are referred to as metapelites (*after* Miyashiro, 1973). The term is used here to describe metamorphites of pelitic composition, not necessarily of sedimentary origin, that consist largely of aluminous minerals such as sillimanite, garnet, cordierite and biotite, together with quartz and feldspar. These rocks have a relatively restricted distribution in the Aus area and are largely confined to the zone of high-grade metamorphism in the centre of the area. No isograds are defined by the metapelites and changes in mineral parageneses appear to be due to variations in bulk composition rather than metamorphic grade. However, the metapelites are of significance because their mineral parageneses - particularly the coexistence of cordierite and garnet - provide useful estimates of the pressure conditions of metamorphism where the rocks are present.

1. Mineral Parageneses

Many of the Garub metapelites are composed of up to nine mineral phases and most of these rocks contain six or more (Table 5). In order to simplify and clarify the significant parageneses, the following minerals common to all the metapelites (except the rocks consisting solely of sillimanite) will be omitted: quartz, plagioclase, magnetite, ilmenite and, usually, K-feldspar.

The mineral assemblages in the metapelite specimens are listed in order of decreasing frequency of occurrence:

'cordierite + garnet + sillimanite + biotite'
'cordierite + garnet + biotite'
'cordierite + sillimanite + biotite'

Examination of the textural relations of the Garub metapelites confirmed that in every case the four-component assemblage referred to above was not a true paragenesis (in agreement with Reinhardt, 1968) because all four minerals are not in contact, commonly because of segregation banding. This assemblage was found to consist of two of the following four parageneses in every thin section examined:

'cordierite + almandine + sillimanite'
'cordierite + almandine + biotite'
'cordierite + sillimanite + biotite'
'almandine + sillimanite + biotite'

These parageneses are illustrated in Figure 41 (mineral compositions based on Reinhardt, 1968).

2. *Distribution of Mineral Assemblages*

The distribution of the mineral assemblages in the Garub metapelites is shown in Figure 43. All the metapelites are situated in the zone of high-grade metamorphism. Sillimanite is widespread within the metapelites of this central high-grade zone; it is also abundant in the metaquartzites of the medium-stage zone in the northwest of the study area (not shown in Fig. 43) and therefore provides a useful minimum temperature estimate for this zone, which has the lowest regional metamorphic grade in the study area. The Al_2SiO_5 triple point was determined by Richardson et al. (1968, 1969) to be situated at 625°C and by Althaus (1967, 1969) at 595°C (point 10, Fig. 42). Neither kyanite nor andalusite were found within the Aus area.

Muscovite is absent from all specimens except one from the southwest of the area (K1) which contained traces of the mineral not in contact with plagioclase. The metapelites are strongly migmatized and commonly surrounded by anatectic granitoids such as the Kubub granite gneiss or the biotite granite gneiss. The mineral assemblages of the metapelites are compatible with those of restites, as suggested by Mehnert (1968, p.336). It is suggested that concentration of Al, Fe and Mg in the restites must have taken place during regional migmatization and their composition is therefore not that of the original parent rock. Nevertheless their highly aluminous nature cannot be solely ascribed to concentration during migmatization because although biotite schists in the same area are equally strongly migmatized, a similar concentration of aluminous minerals has not taken place.

The almost ubiquitous presence of migmatite neosomes and the low proportion of K-feldspar in some metapelite specimens containing silliminate suggest that the melting reactions 7, 8 and 9 have taken place:

(7) muscovite + quartz + albite + H_2O = sillimanite + melt

(8) muscovite + quartz + albite + K-feldspar + H_2O = melt

(9) muscovite + quartz + K-feldspar + H_2O = melt

The experimentally-determined reaction boundaries are shown in Figure 42.

Some of the metapelite outcrops are situated within the granulite zone but not all are at granulite grade. Metapelites that are unmigmatized and interlayered with hypersthene granolites reflect granulite-grade metamorphism, whereas those metapelites that have been strongly migmatized or intruded by the syntectonic granite gneisses are assumed to reflect amphibolite-grade metamorphism which followed the granulite-grade metamorphism. No differences in mineralogy were found between the two groups of metapelite; both contain coexisting garnet and cordierite, and both are free of hypersthene.

The absence of hypersthene from these granulite-grade metapelites requires some explanation in view of the fact that metapelites of similar

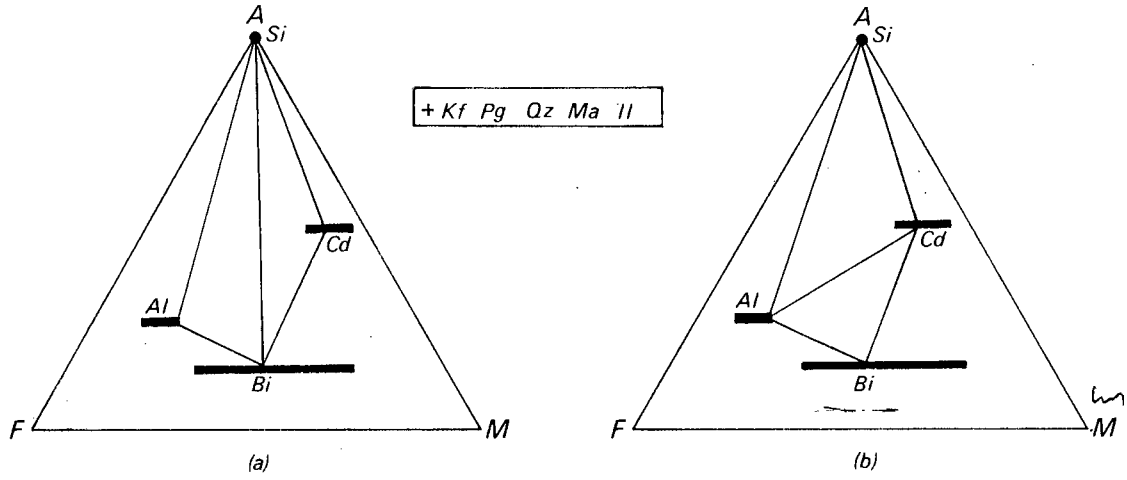

Figure 41. AFM diagrams for mineral parageneses in the Garub metapelites (after Reinhardt, 1968). Diagrams projected through K-feldspar

$A = Al_2O_3-(K_2O+NaO+CaO)$

$F = FeO-(Fe_2O_3-TiO_2)$

$M = MgO$

Al almandine, Bi biotite, Cd cordierite, Kf K-feldspar, Il ilmenite, Pg plagioclase, Qz quartz, Ma magnetite, Si sillimanite

grade contain hypersthene in the Warmbad (Beukes, 1973) and Nababeep (Clifford et al., 1975b) areas to the southeast. Hensen and Green (1971, 1972, 1973) concluded that in metapelites where the $(MgO + FeO)/Al_2O_3$ ratio was less than 1, sillimanite would form with cordierite, almandine and quartz; where this ratio was greater than 1, hypersthene would form in place of sillimanite. Furthermore the association of hypersthene and sillimanite is not possible in almandine-bearing and biotite-bearing metapelites (Reinhardt, 1968) because hypersthene and sillimanite are situated at opposite ends of the AFM triangle and are separated by the almandine-biotite tie-line (see Fig. 44). It would thus appear that the Garub metapelites in the granulite facies are too aluminous for the formation of hypersthene.

The coexistence of cordierite and garnet in most of the metapelite specimens provides a valuable indication of the pressure during metamorphism. Cordierite is extremely widespread and is present in approximately 90% of the specimens. Garnet is present in about 70% of the specimens and is always accompanied by cordierite (except in rocks consisting almost entirely of sillimanite). The metapelites of the Aus area thus fall into two groups which contain (i) 'cordierite + garnet' and (ii) cordierite alone. The former group is shown as solid symbols in Figure 43.

The cordierite-garnet association has been reported from many high-grade metmorphic terrains (summarized by Wynne-Edwards and Hay, 1963: more recent reports from the Grenville Province, Canada, include those by Reinhardt, 1968; Currie, 1971; Lal and Moorhouse, 1969; Hutcheon et al., 1974; and Dostal, 1975: and from the Namaqua belt by von Backström, 1964; Joubert, 1971; Beukes, 1973; Blignault et al., 1974; and Toogood, 1976). Experimental

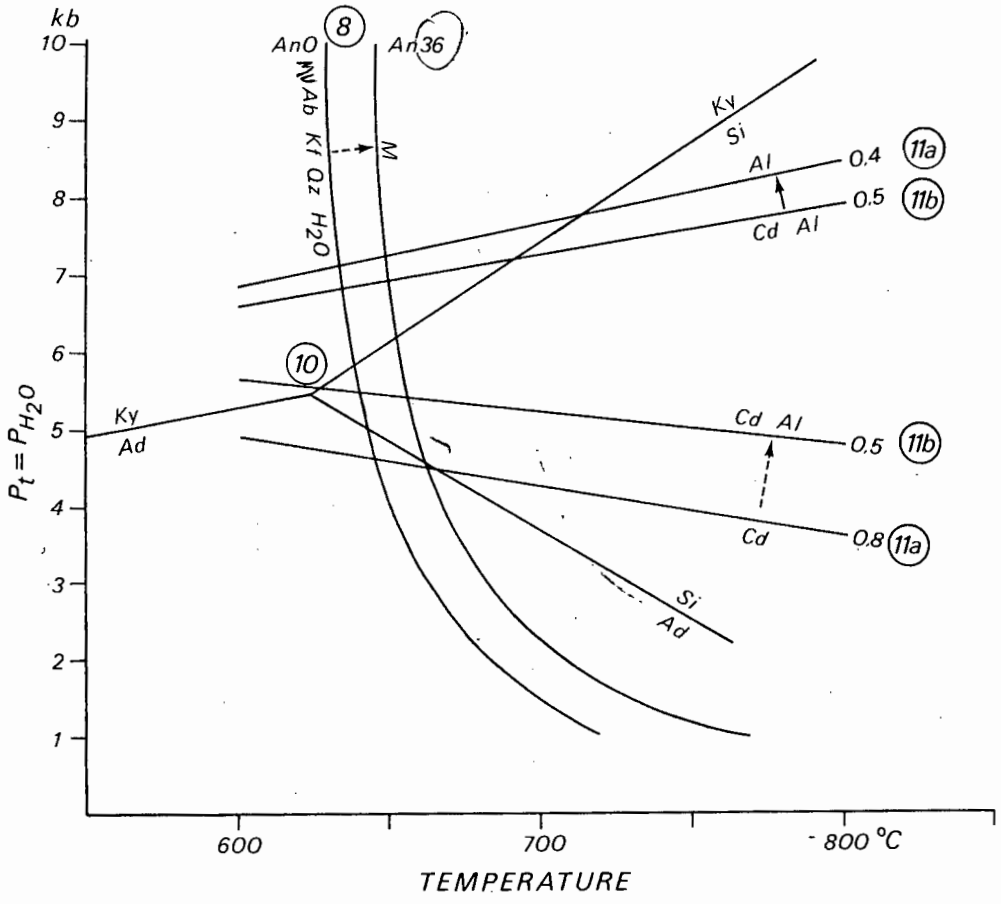

Figure 42. PT diagram showing experimental data relevant to the Garub metapelites
(8) minimum anatexis curves for gneisses with plagioclase An 0-36 (Winkler, 1970) — yours are nearer An50
(10) Al_2SiO_5 triple point (Richardson et al., 1968, 1969).
(11ab) maximum and minimum pressures for coexistence of cordierite and almandine in metapelites with FeO/(FeO+MgO) ratios of 0,8 and 0,5 (Currie, 1971)

studies (Hensen and Green, 1971, 1972, 1973; Hirschberg and Winkler, 1968; Currie, 1971; Hutcheon et al., 1974) have been carried out to determine the PT conditions under which cordierite and garnet coexist.

The data of Currie (1971) appear to be widely accepted in recent literature and are reproduced, in part, in Figure 42. The upper and lower stability limits of both cordierite and almandine are affected by the FeO/(MgO+FeO) ratio of the host rock. The upper- and lower-pressure limits for the coexistence of these two minerals is demarcated by the stability of iron-rich cordierite and magnesium-rich almandine respectively; according to Winkler (1974, p.224) metapelites in which garnet and cordierite coexist most commonly have FeO/(FeO+MgO) ratios between 0,5 and 0,6; in the absence of chemical analyses of the Garub metapelites therefore, these rocks have been assigned an 'average' value of 0,5 which serves as an approximate guide to their composition.

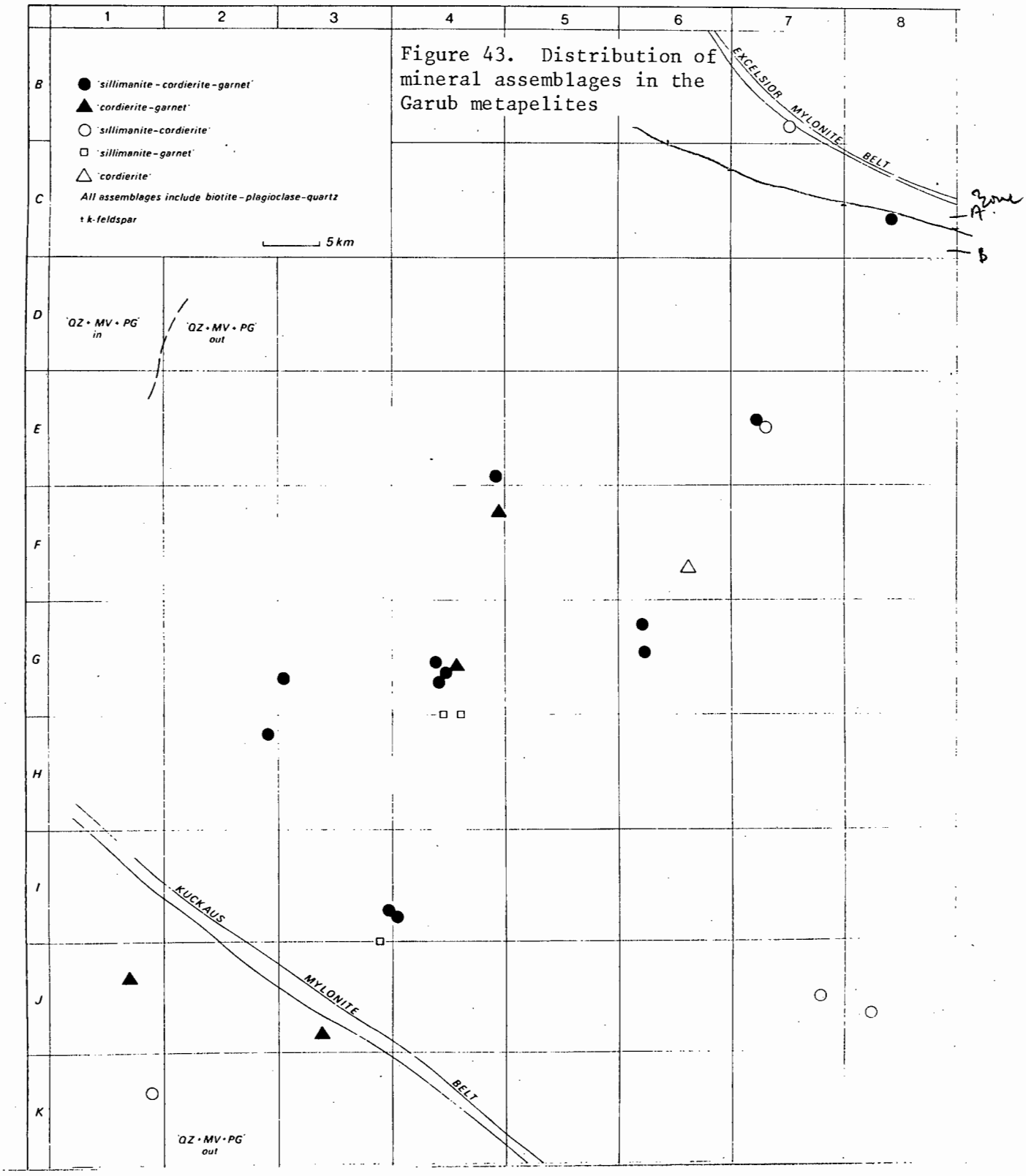

Figure 43. Distribution of mineral assemblages in the Garub metapelites

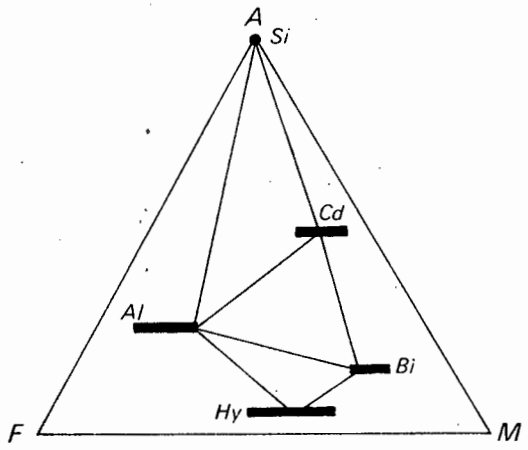

Figure 44. AFM diagram showing the incompatibility of sillimanite and hypersthene in biotite-bearing metapelites of the granulite facies (*after* Reinhardt, 1968)
Al almandine, Bi biotite, Cd cordierite, Hy hypersthene, Si sillimanite

Hirschberg and Winkler (1968) reported a PT field for the coexistence of cordierite and garnet that was even more wedge-shaped than that of Currie (1971); the point of this wedge provides a minimum temperature of 630°C for the coexistence of garnet and cordierite which can be applied to almost the entire area in which the Garub metapelites are exposed (Fig. 43).

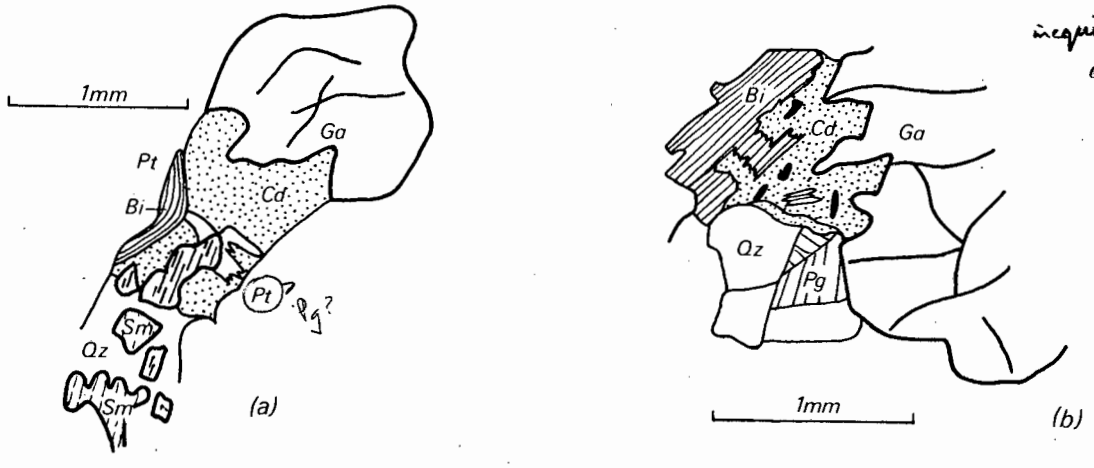

Figure 45. Sketches of textural relations in Garub metapelites
(a) Texture illustrating the formation of cordierite by reaction of garnet, sillimanite and quartz
(b) Texture illustrating the formation of cordierite by reaction of garnet and biotite

In the Garub metapelites the coexistence of cordierite and garnet appears to be partly due to the breakdown of garnet to form cordierite. Figure 45a shows textural evidence of this reaction, which is widespread in these rocks. Coarsely-crystalline sillimanite and quartz are shown co-existing in the bottom of the diagram; closer to the garnet, cordierite has formed. However, in cases where the garnet is surrounded by perthite in which are set numerous sillimanite grains there is no reaction forming cordierite and the garnets are free of corrosion. These textures suggest that the following reaction has produced the cordierite:

(12) 1 garnet + 4 sillimanite + 5 quartz → 3 cordierite

This reaction was reported by Richardson (1968), Hirschberg and Winkler (1968) and Currie (1971). There is, furthermore, textural evidence (Fig. 45b) for the reaction below which has also resulted in the formation of cordierite:

(13) garnet + biotite → cordierite + magnetite + K-feldspar

Because the proportion of cordierite in the Garub metapelites is independent of that of sillimanite and garnet, it can be deduced that reactions 12 and 13 are not solely responsible for the formation of the cordierite in these rocks. The complex textural relations suggest that the formation of cordierite is likely to have taken place by a complex series of reactions (involving biotite, sillimanite, garnet and earlier-formed cordierite) documented by Carmichael (1969), Reinhardt (1968), Hutcheon et al. (1973) and Hensen and Green (1971, 1972, 1973). Cordierite is commonly found as a mantle around garnet grains in the Garub metapelites. According to Currie (1971, p.221) metapelites relatively enriched in Mg (i.e. FeO/(FeO+MgO) = 0,4) are garnet-free at pressures of up to 5,5 kb within the temperature range 650-800°C (Fig. 42). It is therefore possible that the garnet-free metapelites are merely more magnesian than the garnet-bearing varieties.

In summary therefore the coexistence of cordierite and garnet indicates minimum pressures of 5,0-5,5 kb between temperatures of 650 and 800°C if the composition of an 'average' pelite (FeO/FeO+MgO = 0,5) is assumed; maximum pressure estimates under these same temperature conditions are 7-8 kb. These temperature limits are further discussed in the following section.

The presence of a dark-green variety of spinel, with the optical properties of hercynite, suggests high-temperature metamorphism. In one metapelite specimen from the granulite zone in the east and in two from the central part of the study area (see Fig. 46) numerous grains of spinel are present which poikiloblastically enclose sillimanite needles; quartz forms an additional phase in some cases. The stability of the paragenesis:

'hercynite + sillimanite + quartz'

was experimentally investigated by Richardson (1968) who suggested a minimum temperature limit of 780°C for this paragenesis. The experiment was carried out under conditions of $P_{H_2O} = P_t$, but since the composition of the fluid phase during the metamorphism of the Garub metapelites is not known (graphite is present at two of the localities and the fluid phase might have been appreciably diluted by CO_2), not too much reliance is placed on this paragenesis as evidence for minimum temperature conditions. However, it is significant

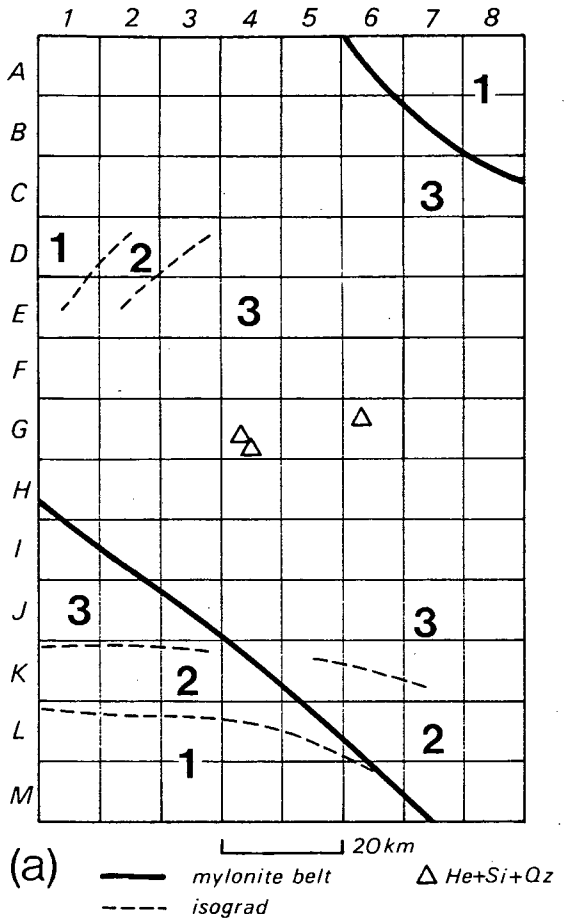

Figure 46. (a) Key map showing distribution of metamorphic zones 1, 2 and 3 defined by pelitic and semi-pelitic rocks; small triangles represent location of 'hercynite + sillimanite + quartz' parageneses (b) PT diagram showing synthesis of experimental data on semi-pelitic and pelitic rocks and PT fields estimated for zones 1, 2 and 3

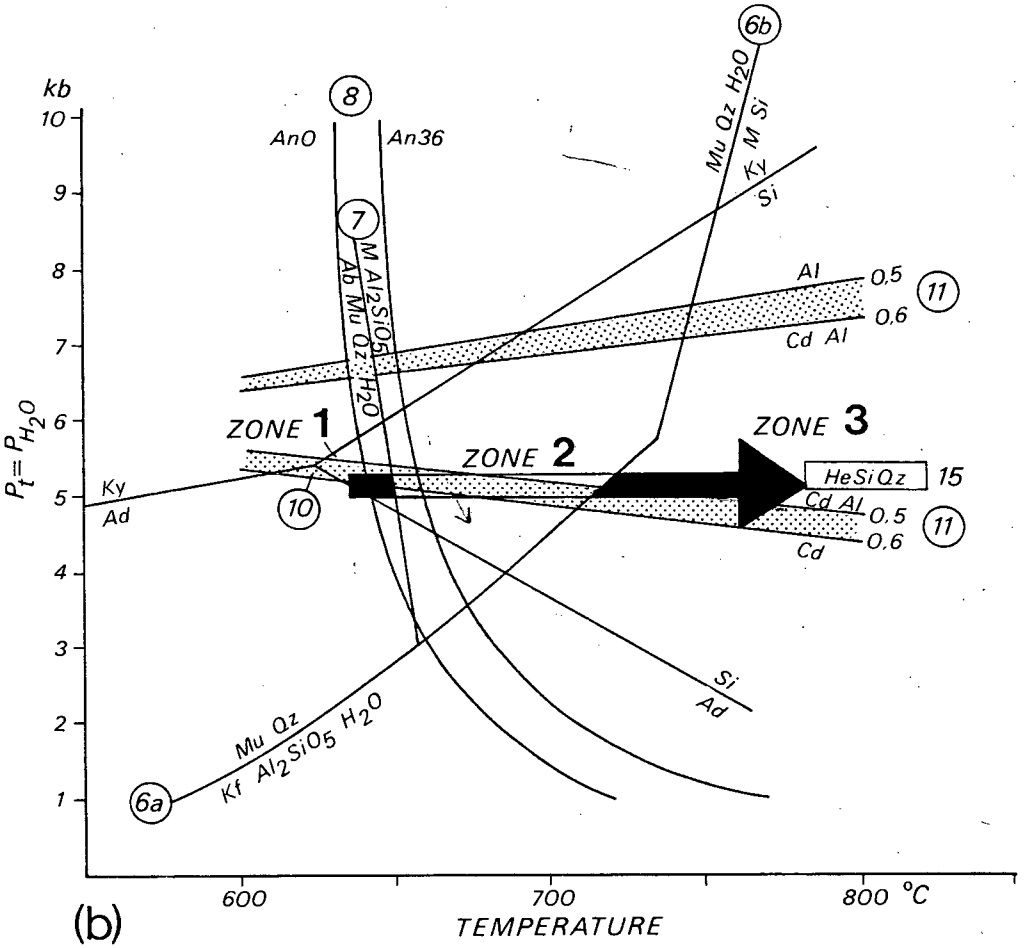

(6a) Althaus et al., 1970; (6b) Storre and Karotke, 1972; (7) Storre and Karotke, 1971; (8) Winkler, 1970; Richardson et al., 1968, 1969; (11) maximum and minimum pressures for coexistence of cordierite and almandine in rocks with FeO/(FeO+MgO) ratios of 0,5 and 0,6 (Currie, 1971); (15) Richardson, 1968

Ab albite, Ad andalusite, Al almandine, An anorthite, Cd cordierite, He hercynite, Kf K-feldspar, Ky kyanite, M melt, Mu muscovite, Qz quartz, Si sillimanite

that this minimum value is in close agreement with the minimum temperature estimate of 780°C (at P_t = 5 kb) for calcareous rocks nearby (see Section 4.4).

3. *Summary of the Metamorphism of Pelitic and Semi-pelitic Rocks*

The physical conditions prevailing during the metamorphism of these rocks can be determined with more accuracy if the data relevant to both rock groups are combined. Figure 46b illustrates experimental data and PT fields estimated for the three metamorphic zones defined by the semi-pelitic rocks. The reactions leading to the complete disappearance of muscovite in the central zone (zone 3) were not established beyond doubt in the case of the semi-pelitic rocks; but examination of the pelitic rocks confirmed that the reactions shown in Figure 46b had indeed taken place. The distribution of the metamorphic zones is shown in the sketch map, Figure 46a. The characteristic features of each metamorphic zone are briefly summarized below.

Zone 1 (medium stage)

$$P_t = 5\text{-}6 \text{ kb}; \quad T = 625\text{-}650^{\circ}C$$

The PT conditions for zone 1, which occupies the fringe of the area, are indicated by:

(i) stability of sillimanite within two kilometres of the borders of this zone (D2, K2); no Al_2SiO_5 mineral was found within zone 1 itself

(ii) coexistence of muscovite, quartz and plagioclase

Since metapelites are absent from this zone, it is not known whether cordierite and garnet coexist or whether cordierite alone is stable; from Figure 46b it appears that both parageneses are possible. In this PT régime only limited melting could take place and this is confirmed by the scarcity of migmatites in zone 1 (see Fig. 64).

Zone 2 (high stage)

$$P_t = 5\text{-}7{,}5 \text{ kb}; \quad T = 650\text{-}725^{\circ}C$$

This metamorphic zone occupies relatively small areas adjoining zone 1. The metamorphic features of this zone are:

(i) sillimanite is stable

(ii) cordierite and garnet do not coexist in the single specimen of metapelite examined from this zone

(iii) muscovite is stable with quartz, only in plagioclase-free rocks

(iv) migmatites are abundant

Zone 3 (high stage)

$$P_t = 5\text{-}8 \text{ kb}; \quad T = 725\text{-}?800^{\circ}C$$

This metamorphic zone occupies the bulk of the study area and is loosely referred to as the central zone. Here muscovite has not been found in regional metamorphic rocks of any composition. In this zone migmatites are widespread and the geology is dominated by large masses of anatectic granitoids. The arrow indicating the path of prograde metamorphism (in Fig. 46b) has been drawn close to the lower limit of the coexistence of cordierite and garnet because a minority of metapelites contain only cordierite. Because the arrow is subparallel to the x axis of the graph, the metamorphic facies series from zone 1 to zone 3 appears to have been approximately isobaric.

As previously mentioned, the paragenesis:

'hercynite + sillimanite + quartz'

may indicate minimum temperatures of 780°C (Richardson, 1968). This paragenesis is shown in Figure 46 and may provide a minimum estimated temperature for metamorphism in the central part of the study area.

4.4. METAMORPHISM OF CALCAREOUS ROCKS

The metamorphism of calcareous rocks is described with reference to the following rock types: marbles, calc-granofelses, calc-silicate segregations and granofelses. These rock types are largely restricted to a west-trending zone situated in the north-centre of the study area. This compositional group therefore supplies metamorphic data for only part of the area (as do the metapelites). Nevertheless calcareous rocks are present in all the metamorphic zones and have supplied invaluable geothermometric data.

The calcareous rocks are discussed in order of increasing chemical complexity, starting with pure marbles and ending with a system containing the oxides and carbonates of Ca, Mg, Si, Al and K; all systems include CO_2 and H_2O as fluid components. All reactions are initially discussed using the variables T and X_{CO_2} for the condition P_t= 5 kb in order to arrive at conservative estimates of temperature (pressure limits were estimated at 5-7 kb in the previous section). At the end of this section the significant data are plotted on a PT diagram. All observed and theoretically possible mineral parageneses are shown in Figure 47.

1. *System* $CaCO_3 - CaMg(CO_3)_2$

Marbles consisting entirely of calcite have not been found in the Aus area. All pure marbles examined consist almost entirely of dolomite. Dolomite marbles, if pure, are stable up to the highest grades of metamorphism, changing

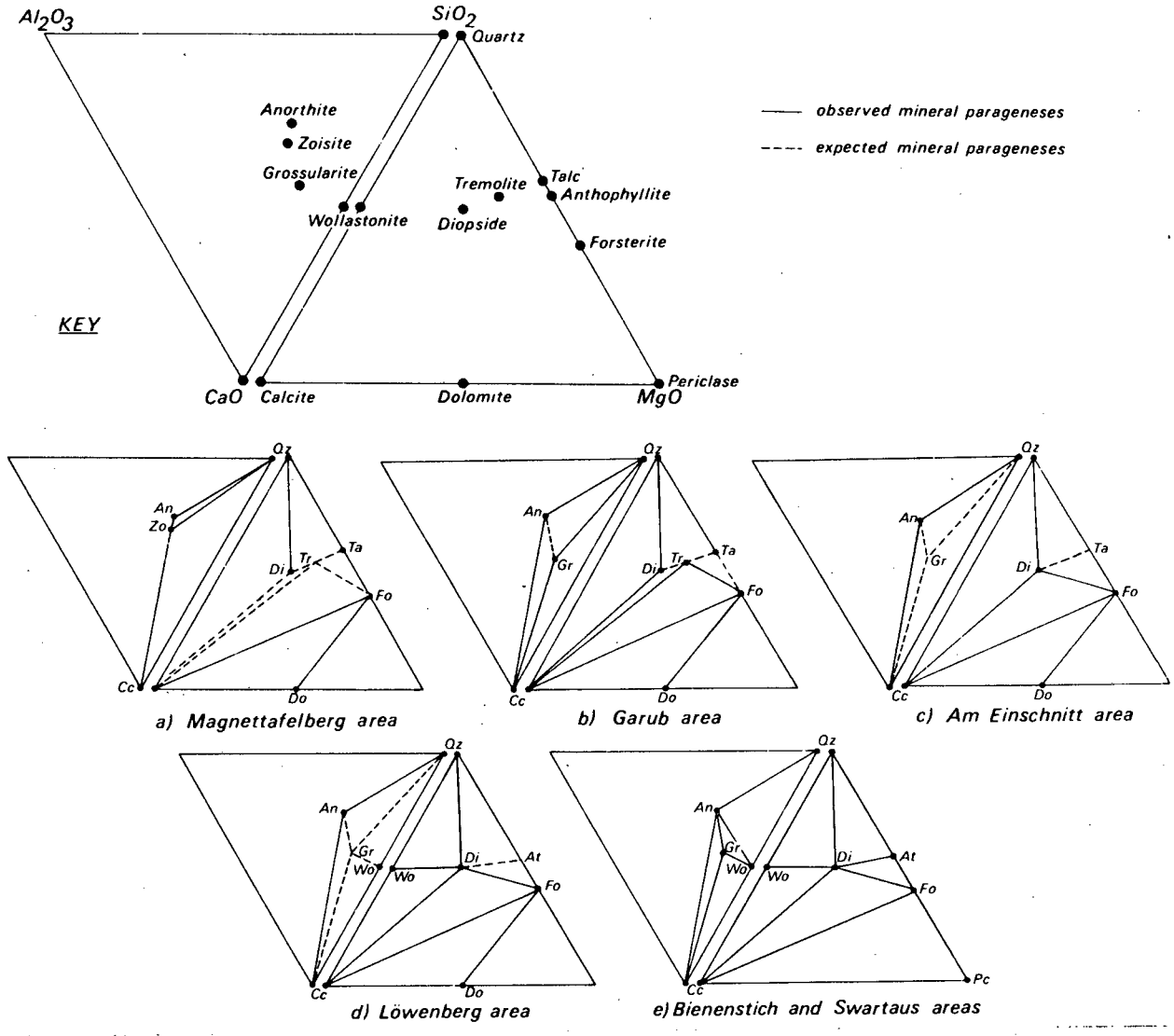

Figure 47. Ternary diagrams showing observed and theoretically possible mineral parageneses in calcareous rocks of the Garub sequence

little in response to rising temperatures except for an increase in grain size. The pure marbles around Aus and farther west are coarsely crystalline with grain size up to 10 mm.

If a dolomite marble body is sufficiently thin or small and is surrounded by pelitic or granitic rocks, its CO_2 fluid phase will be diluted by water. If the concentration of CO_2 in the fluid phase (X_{CO_2}) is reduced sufficiently, then dolomite will break down at elevated temperatures according to the following reaction:

(16) 1 dolomite → 1 periclase + 1 calcite + CO_2

The T-X_{CO_2} conditions (at P_t=5 kb) for the formation of periclase by this re-

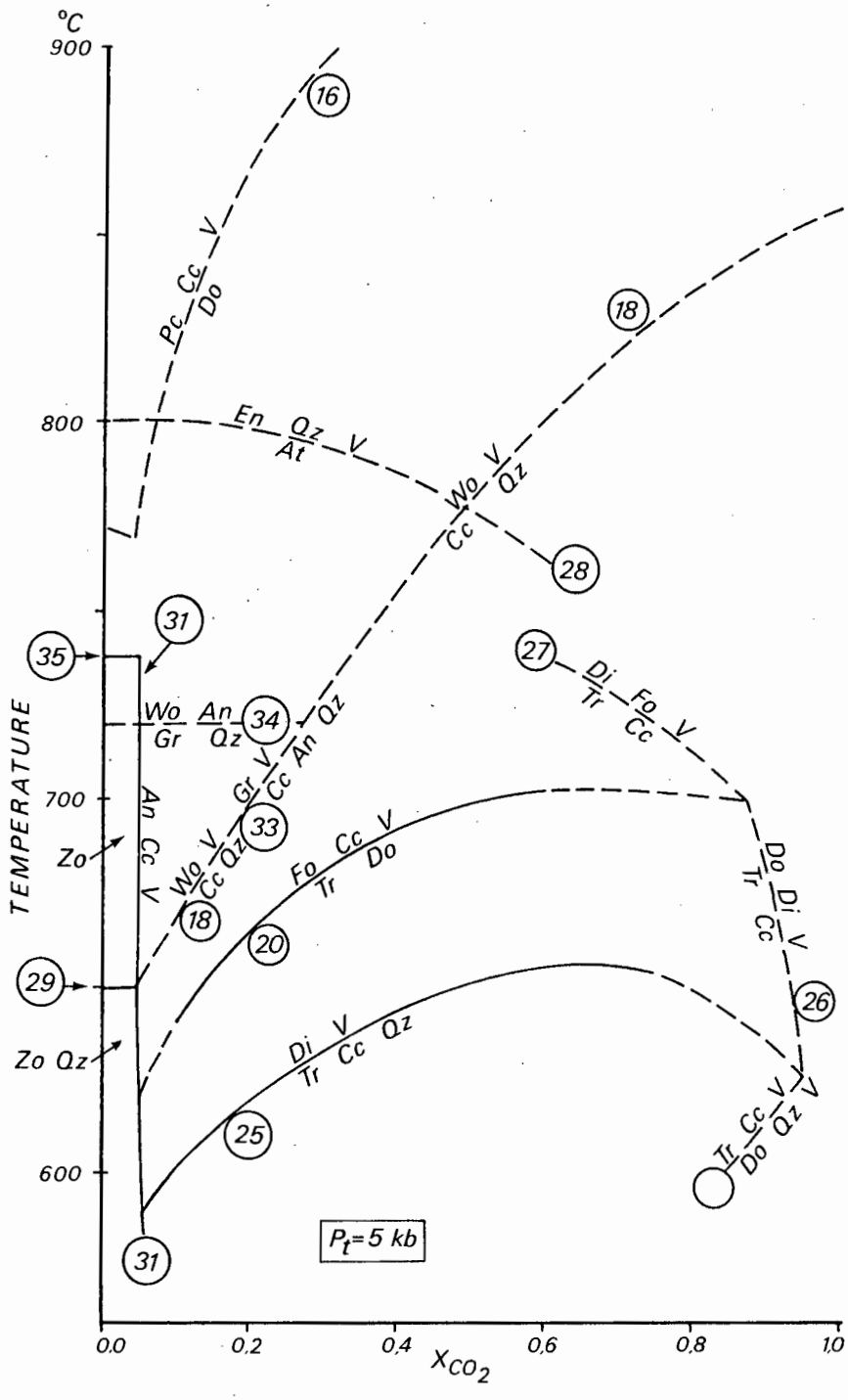

Figure 48.

Isobaric T-X_{CO_2} diagram at P_t= 5 kb for reactions in calcareous rocks discussed in the text (see text for sources)
An anorthite, At anthophyllite, Cc calcite, Di diopside, Do dolomite, En enstatite, Fo forsterite, Gr grossularite, Pc periclase Qz quartz, Tr tremolite, V vapour, Wo wollastonite, Zo zoisite

action are shown as curve 16 in Figure 48 (graphically extrapolated from the data of Harker and Tuttle (1955) and Metz (1967) valid for P_t= 1 kb). It is obvious that periclase can only form at extremely low X_{CO_2} (probably <0,2). This extrapolation implies a minimum temperature of approximately 770°C at P_t= 5 kb. Periclase can also form by another decarbonation reaction at about 50°C lower temperature:

(17) 1 magnesite → 1 periclase + CO_2 (Johannes and Metz, 1968)

but since magnesite disappears at comparatively low grades and the reaction only takes place in rare rocks consisting solely of magnetite and dolomite (Winkler, 1974, p.128), this reaction is not applicable to the area under discussion.

A calcite marble containing periclase (specimen MJ46) is present near Swartaus (G4) (see Fig. 50). This is a very small pod of marble a few metres in length which is surrounded by pegmatoidal mobilizate produced during the regional migmatization. In this case it appears that the fluid phase of this small pod was swamped by water from surrounding rocks so that periclase was able to form.

2. *System* $CaCO_3$ - SiO_2

Calcite and quartz are stable up to the highest temperatures of regional metamorphism provided that X_{CO_2} is sufficiently high. If the fluid phase is sufficiently hydrous, however, wollastonite will form by reaction of calcite and quartz. The reaction:

(18) 1 calcite + 1 quartz → 1 wollastonite + CO_2

was experimentally studied by Harker and Tuttle (1956) and Greenwood (1967) who found that the reaction temperature was greatly dependant on X_{CO_2}. This reaction (extrapolated from P_t= 2 kb to 5 kb) is shown as curve 18 in Figure 48. No meaningful quantitative conclusions can be drawn because of the wide range of reaction temperature (650-840°C at X_{CO_2}<0,80) controlled by the partial pressure of CO_2.

Wollastonite formed by reaction 18 is present in two localities north of Aus (refer to Fig. 50): 2 km west of Groot Löwenberg (F4) and 7 km northwest of the same mountain (E4). The parageneses are:

'wollastonite + diopside + sphene'
'diopside + wollastonite + quartz'

Quartz (5% by volume) is present in the form of small scattered blebs; the excess quartz remained after all the available calcite had been consumed during the formation of wollastonite.

3. *System* $CaCO_3$ - SiO_2 - $MgCO_3$

Siliceous dolomites are capable of forming the following silicate minerals

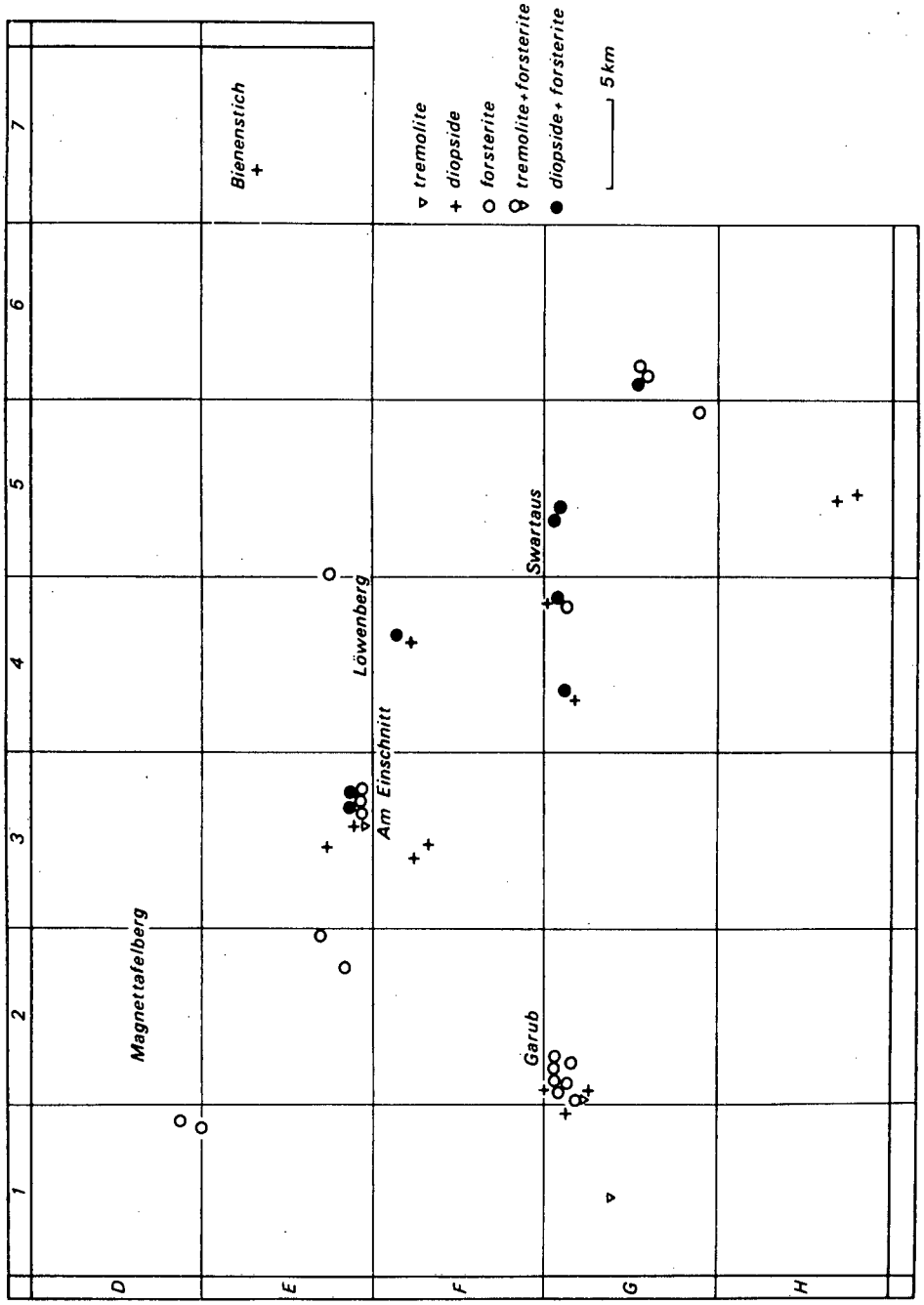

Figure 49. Sketch map showing distribution of tremolite, diopside and forsterite in the Garub marbles and calc-granofelses

during metamorphism: talc, tremolite, diopside, forsterite and anthophyllite. Most of these minerals are likely to contain traces of Fe^{2+}, but according to Metz (1973, *in* Winkler, 1974, p. 124), even high amounts of Fe^{2+} will not reduce reaction temperatures by more than $10^{o}C$.

The Breakdown of Talc

Talc was found to be stable together with forsterite and calcite in the lower-grade areas in the west. At Am Einschnitt Mountain 'forsterite + talc' are stable. The stability of talc and forsterite is limited by the reaction:

(19) 9 talc + 4 forsterite → 5 anthophyllite + H_2O

which takes place at P_t= 2 kb between the temperature limits of 550-670^{o}C, depending on X_{CO_2} (Johannes, 1969). At 5 kb this reaction takes place at approximately 690^{o}C (Winkler, 1974, p.158) thus providing an approximate upper temperature limit for the Am Einschnitt area.

The Distribution of Tremolite, Diopside and Forsterite

The distribution of tremolite, diopside and forsterite in Garub marbles and calc-granofelses is illustrated in Figure 49. The following points are evident:

(i) Forsterite is the most abundant of the three minerals and is present in about 70% of the specimens, whereas diopside is present in about 50% of the rocks examined

(ii) Coexisting forsterite and diopside are present in only 20% of the specimens and these rocks are all from the centre of the study area

(iii) Tremolite is extremely rare

The Breakdown of Tremolite

The equilibrium paragenesis:

'tremolite + dolomite + forsterite + calcite'

is present at Garub Station (G2). Both tremolite and forsterite are in the form of large well-developed crystals separated by a zone of fine-grained dolomite and calcite (specimen MJ23). As described by Trommsdorff (1966) this assemblage represents the reactants and products of the following reaction:

(10) 1 tremolite + 11 dolomite → 8 forsterite + 13 calcite + 9 CO_2 + 1 H_2O

The PT conditions for this reaction at P_t= 1 kb were determined by Metz and Trommsdorff (1968) and Metz (1970). As determined for P_t= 5 kb (Metz, 1973) this reaction is depicted as curve 20 in Figure 48. The reaction temperatures are 680 and 700^{o}C where X_{CO_2} is 0,3 and zero respectively. This is the estimated temperature range for the marbles at Garub Station and the minimum temperature range at which forsterite can form (P_t= 5 kb).

Three other reactions:

(21) 1 talc + 5 dolomite → 4 forsterite + 5 calcite + 5 CO_2 + 1 H_2O

(22) 11 talc + 10 calcite → 5 tremolite + 4 forsterite + 10 CO_2 + 6 H_2O

(23) 11 talc + 10 domomite → 5 tremolite + 12 forsterite + 20 CO_2 + 8 H_2O

involving the formation of forsterite (Metz and Trommsdorf, 1968) are not likely to occur at P_t> 2 kb (Winkler, 1974, p.122) and can therefore be disregarded in this study.

The Formation and Coexistence of Forsterite and Diopside

Forsterite is also present in areas of lower grade than Garub Station. The assemblage 'forsterite + calcite' is found in marbles southwest of Magnet-tafelberg (D1). This assemblage is most likely to have formed by reaction 20 which was discussed with reference to the breakdown of tremolite. The formation of forsterite in this relatively low-grade area is undoubtedly due to a low concentration of CO_2 in the fluid phase during metamorphism. The layers of forsterite marble are thin and surrounded by biotite schist which would have diluted the fluid phase with water, thereby enabling the formation of forsterite at the relatively low temperatures of 640-660°C (at X_{CO_2}= 0,1-0,2; P_t= 5 kb)(see Fig. 48, curve 20, *after* Metz, 1973).

The reactions leading to the formation of diopside in the forsterite-free marbles are not known with certainty because no trace of the reactants has been found in these rocks (which indicates that temperatures at the peak of metamorphism exceeded the reaction temperatures by a sufficient margin). Three reactions are possible for the formation of diopside (Metz and Trommsdorf, 1968; Metz, 1970):

(24) 1 dolomite + 2 quartz → 1 diopside + 2 CO_2

(25) 1 tremolite + 3 calcite + 2 quartz → 5 diopside + 3 CO_2 + 1 H_2O

(26) 1 tremolite + 3 calcite → 1 dolomite + 4 diopside + 1 CO_2 + 1 H_2O

On the basis of field observations on the appearance of diopside, Winkler (1974, p.119) suggested that reaction 25 is the most likely. The PT conditions for this reaction at P_t= 5 kb are shown as curve 25 in Figure 48. However, since no tremolite has been found together with diopside anywhere in the area, this temperature (approximately 650°C) must have been exceeded by a substantial amount.

The coexistence of forsterite and diopside in the same marble is widespread throughout the centre of the study area but is absent west of the Diamond Area boundary. The coexistence of these two minerals is brought about by the reaction:

(27) 3 tremolite + 5 calcite → 11 diopside + 2 forsterite + 5 CO_2 + 3 H_2O

The fact that tremolite is absent from all marble specimens containing 'diopside + forsterite' suggests that the equilibrium temperature of reaction 27 was greatly exceeded. Curve 27 in Figure 48 therefore indicates an approximate minimum temperature of 700-730°C for metamorphism of the forsterite-diopside marbles at P_t= 5 kb; the exact temperature has not been experimentally

determined (Winkler, 1974, p.121).

On Am Einschnitt Mountain, where the marbles contain coexisting forsterite and diopside, the retrograde assemblage 'tremolite + calcite' has formed by the reverse of reaction 27 in a few places. The tremolite is ragged and decussate and probably formed after the peak of metamorphism in this area.

The Significance of Anthophyllite

The reaction

(28) 1 anthophyllite → 7 enstatite + 1 quartz + 1 H_2O

defines the upper temperature limit for the stability of anthophyllite. The data of Fyfe (1962), Greenwood (1963) and Zen (1971) indicate that anthophyllite breaks down at just below 800°C at 5 kb. Being a dehydration reaction, this decomposition takes place at lower temperatures than 800°C if P_{H_2O} is less than P_t (as shown in Fig. 48, curve 28, *after* Johannes, 1969); such a condition prevails if the fluid phase is partially composed of CO_2. However, this study is concerned with the *maximum* stability limit of anthophyllite and it is therefore assumed that P_{H_2O} is approximately equal to P_t.

The upper temperature limit of anthophyllite also depends on its Mg/(Mg+Fe) ratio. Ravoir and Hinrichsen (1975) reported that Mg-rich synthetic anthophyllite (ratio 0,8) was stable at temperatures of 40°C higher than the less Mg-rich anthophyllite (ratio 0,6) at 6 kb. A natural Al-bearing anthophyllite (ratio 0,9) was stable to temperatures of 835°C at 6 kb, which is some 60°C higher than the synthetic anthophyllite (ratio 0,8).

Anthophyllite is present near Swartaus (G4) in the following assemblage (MJ1093A):

'anthophyllite + diopside + vesuvianite'

and at Bienenstich (E7) as a monomineralic rock (specimen MJ941) (see Fig. 50). The temperature limit defined by reaction 28 (800°C at P_t= 5 kb) can be taken as the maximum temperature prevailing during metamorphism. The outcrop at Swartaus is surrounded by anatectic mobilizate and augen gneiss (Fig. 5), so X_{CO_2} is unlikely to have been particularly high. The Bienenstich outcrop is not associated with marbles, so the same conclusion can be drawn. Thus for both localities 800°C provides a high temperature limit at P_t= 5 kb (possibly reaching 820°C at P_t= 7 kb) that is applicable for amphibolite facies metamorphism throughout the area.

4. *System* $CaCO_3$ - SiO_2 - $MgCO_3$ - Al_2O_3

With addition of Al_2O_3 to the system, the formation of the following additional minerals is possible (iron components omitted): zoisite, grossularite, vesuvianite, anorthite and calcic scapolite (meionite).

Of the above minerals, zoisite is formed at the lowest temperature and its breakdown in the presence of quartz involves the formation of minerals such as anorthite and grossularite. Epidote is stable in the calcareous rocks in the

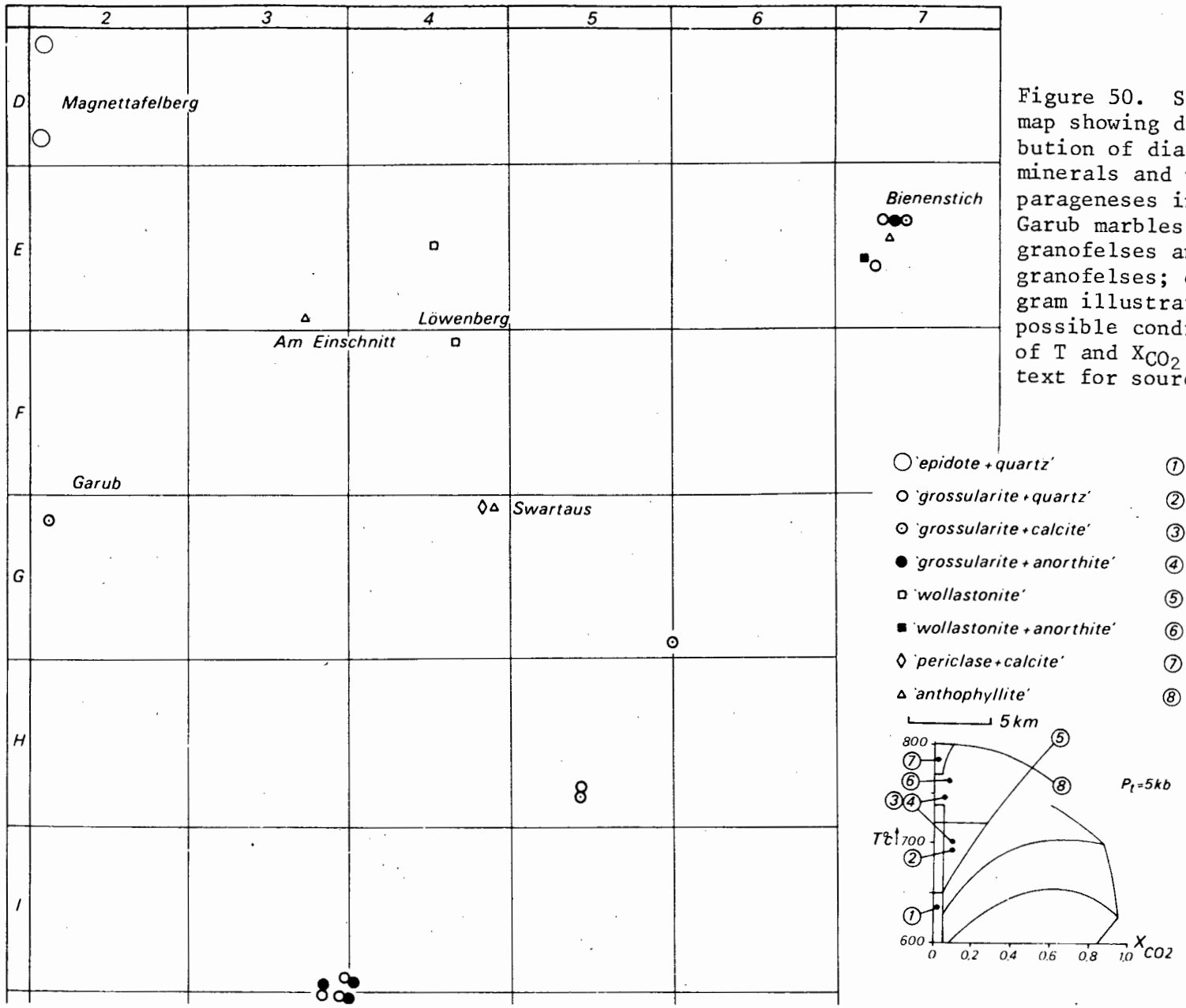

Figure 50. Sketch map showing distribution of diagnostic minerals and mineral parageneses in the Garub marbles, calc-granofelses and granofelses; diagram illustrates possible conditions of T and X_{CO_2} (see text for sources)

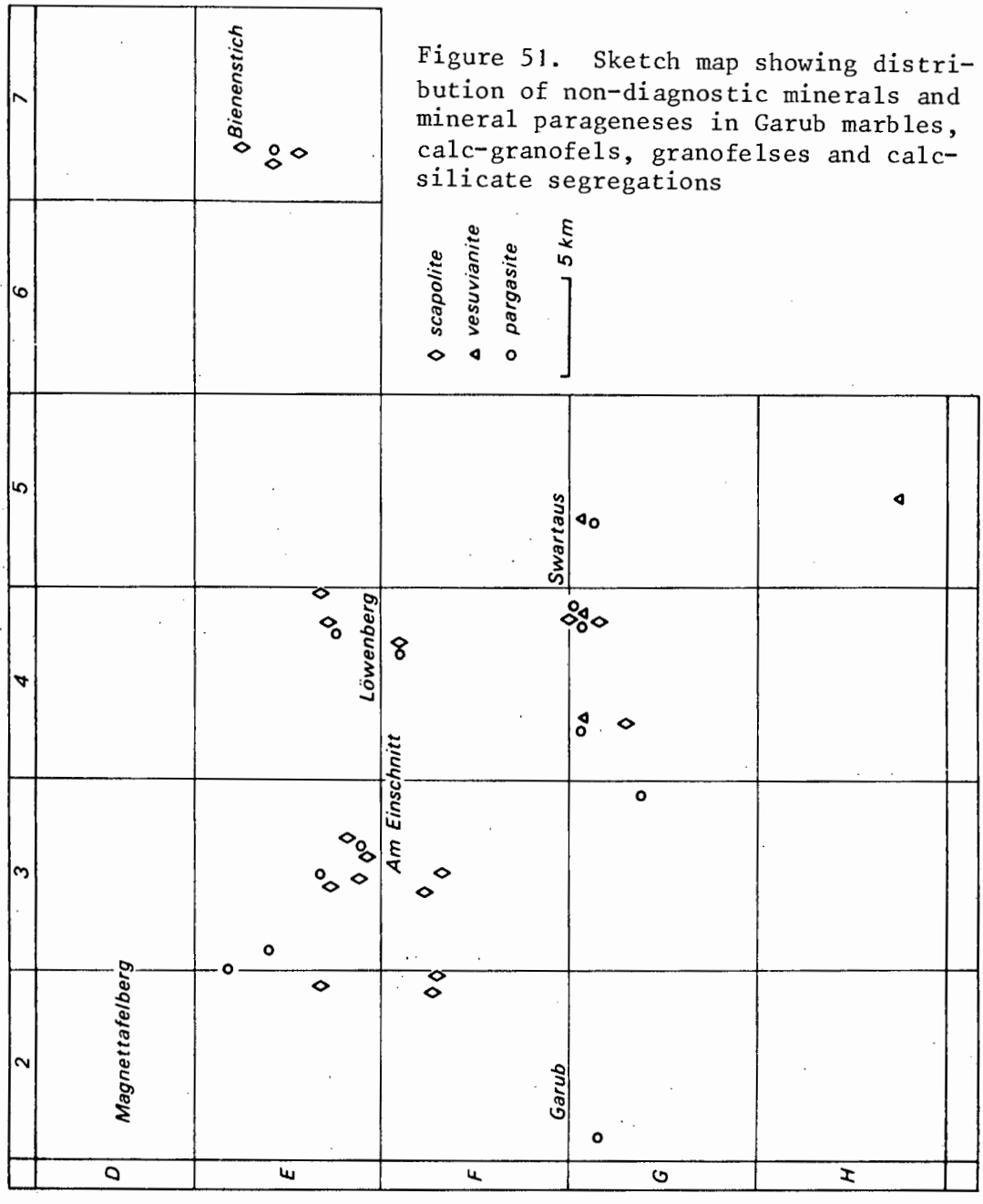

Figure 51. Sketch map showing distribution of non-diagnostic minerals and mineral parageneses in Garub marbles, calc-granofels, granofelses and calc-silicate segregations

extreme northwest of the study area (around Magnettafelberg, D1, D1). The metabasites in the same area contain blue-green hornblende and epidote which indicate a relatively low metamorphic grade (Section 4.1). The granofelses contain the paragenesis:

'plagioclase + quartz + epidote + sphene'

Reaction 29 provides a maximum limit for the coexistence of epidote and quartz:

(29) 4 zoisite + 1 quartz → 5 anorthite + 1 grossularite + 2 H_2O

This reaction has been studied experimentally by several workers (Nitsch and Winkler, 1965; Newton, 1966; Holdaway, 1972; Boettcher, 1970; and Liou, 1973). The data of Holdaway (1972) and Liou (1973) agree within close limits that reaction 29 takes place at about 650°C at P_t= 5 kb, whereas Boettcher (1970) and Newton (1966) recorded temperatures some 25°C lower. The reaction takes place at low concentrations of CO_2 (X_{CO_2}<0,03), as indicated by curve 29 in Figure 48 (extrapolated from Storre and Nitsch, 1973). Assuming a total pressure of 5 kb it is therefore unlikely that the temperature attained during metamorphism in the Magnettafelberg area (D1,D2) exceeded 650°C.

In the remainder of the area where calcareous rocks are exposed epidote and zoisite have reacted with quartz or calcite where the latter minerals are present. The most likely reactions leading to the disappearence of zoisite are:

(29) 4 zoisite + 1 quartz → 5 anorthite + 1 grossularite + 2 H_2O

(30) 2 zoisite + 5 calcite + 3 quartz → 3 grossularite + 5 CO_2 + 1 H_2O

(31) 2 zoisite + 1 CO_2 → 3 anorthite + 1 calcite + 1 H_2O

Reaction 29 has been discussed above. According to Storre and Nitsch (1973) reaction 31 (curve 31 in Fig. 48) takes place in a temperature range in excess of 150°C; reaction 30 (omitted from Fig. 48 through lack of space) takes place at a temperature of approximately 650°C at the same total pressure of 5 kb. All three reactions take place at very low partial pressures of CO_2. Other reactions for the breakdown of zoisite listed by Storre and Nitsch (1973) involve the formation of corundum, which has not been found in the Aus area. Both the assemblages 'anorthite + grossularite' and 'anorthite + calcite' are present in the Aus area (Fig. 50), so both reactions 29 and 31 are likely to have taken place with the disappearance of epidote/zoisite.

With increase of temperature scapolite is likely to have formed by reaction of anorthite and calcite (reaction 32) because where scapolite is present in the Aus area, calcite and quartz do not coexist.

(32) 3 anorthite + 1 calcite → 1 meionite

This reaction (Deer, Howie and Zussman, 1966) has not been experimentally investigated and as scapolite is stable in both medium-stage and high-stage metamorphism (Winkler, 1974, p.125), it is non-diagnostic in the present discussion (see Fig. 51).

The grossularite component of grandite can also be formed by reaction of calcite and anorthite (curve 33, Fig.48) as reported by Mukherjee and Rege (1972).

The garnet may also form by breakdown of zoisite (reactions 29 and 30).

(33) 2 calcite + 1 anorthite + 1 quartz → 1 grossularite + 1 CO_2

Parageneses resulting from reactions 29,30 and 33 are:

'grossularite + calcite'
'grossularite + anorthite'
'grossularite + quartz'

and are all stable above a certain minimum temperature range (defined by curves 29 and 33 in Fig. 48). However, grossularite is stable together with calcite or anorthite up to the highest temperatures reached during the metamorphism of the marbles, so that no maximum temperature estimates are meaningful. According to Boettcher (1970) grossularite persists in the absence of quartz to at least 875°C at P_t= 2 kb.

The assemblage 'anorthite + calcite' produced by reaction 31 is stable over an extremely broad range of temperature and X_{CO_2} extending throughout most of the T-X_{CO_2} field in Figure 48; the assemblage is therefore not diagnostic and is not included in Figure 50.

In the presence of quartz grossularite decomposes according to the reaction:

(34) 1 grossularite + 1 quartz → 2 wollastonite + 1 anorthite

Reaction 34 has been experimentally studied by Newton (1966), Boettcher (1970) and Gordon and Greenwood (1971). The data show that at P_t= 2 kb the reaction takes place at just below 600°C independently of X_{CO_2} providing X_{CO_2} is less than 0,2. Extrapolated to P_t= 5 kb (Newton, 1966, p.211; Boettcher 1970, p.352; Gordon and Greenwood, 1971, p.1685) this reaction takes place close to 725°C (shown as curve 34 in Fig. 48).

The assemblage 'wollastonite + anorthite', which results from reaction 34, has only rarely been reported from regional metamorphic terrains and Newton (1966, p.204) states that the appearance of this assemblage 'may be considered to mark the highest temperatures encountered by rocks in solid-state regional metamorphism'. Misch (1964) first reported the assemblage from the Nanga Parbat peak (northwest Himalayas) and the same assemblage was subsequently reported from the Eastern Ghats, India, by Mukherjee and Rege (1972).

The paragenesis 'wollastonite + anorthite' is present in the Aus area at Bienenstich (Fig. 50). The petrography of this rock (specimen MJ500) is described in Section 3.1 but the salient features will be summarized here (refer to Plate 2 for the general appearance of the rock). Large poikiloblasts of garnet are sieved with small diopside, wollastonite and plagioclase crystals to form a net structure. These porphyroblasts are set in a matrix of wollastonite and plagioclase with small amounts of diopside. The paragenesis is:

'wollastonite + anorthite + grossularite + diopside'

No quartz or carbonate are visible. It thus appears that the original garnet crystals scattered through the rock reacted with quartz in the presence of

a fluid phase with $X_{CO_2} < 0,2$ to produce anorthite and wollastonite. When all the quartz in the rock had reacted the remaining garnet was concentrated to form large scattered porphyroblasts.

Minute grains of epidote are contained within the porphyroblastic garnet and are therefore isolated from the remaining components of the rock. At P_t= 2 kb zoisite decomposes by reaction 35 at a temperature some 25°C lower than the formation of 'wollastonite + anorthite' (Storre and Nitsch, 1973) which is present in the same rock.

(35) 6 zoisite → 6 anorthite + 1 grossularite + 1 corundum + 1 H_2O

However, according to the data of Boettcher (1970) at pressures greater than 4 kb the 'zoisite out' reaction (35) takes place at higher temperatures than the 'grossularite + quartz' reaction. Thus at P_t= 5 kb 'zoisite out' occurs at temperatures about 20°C higher than the reaction 'grossularite + quartz out'; at P_t= 7 kb (the estimated upper pressure limit) the temperature difference is about 50°C. The preservation of epidote therefore suggests firstly that pressures were greater than 4 kb and secondly, that very low X_{CO_2} must have been present in the immediate vicinity of the epidote for the mineral would have decomposed by reaction 31 to form anorthite and calcite.

Two kilometres north of the 'wollastonite + anorthite' assemblage another calc-granofels (specimen MJ530) contains the assemblage 'grandite + quartz' (the reactants leading to the formation of 'wollastonite + anorthite' by reaction 34). The garnet-quartz rock is in the form of thin, competent bands surrounded by a matrix of white wollastonite (Plate 31). The coexistence of wollastonite with the assemblage 'grossularite + quartz' is possible because curve 18 (Fig. 48), which defines the formation of wollastonite by reaction 18 from 'calcite + quartz', coincides with curve 33 (Storre and Nitsch, 1973), which defines the formation of grossularite by reaction 33. It would therefore appear that in this case wollastonite was formed not by the breakdown of grossularite and quartz but by the breakdown of calcite and quartz. The assemblage 'wollastonite + anorthite' 2 km farther south (specimen MJ500) could not have reached temperatures very much higher than the minimum defined by curve 34 in Figure 48 (i.e. 725°C at P_t= 5 kb).

Other minerals characteristic of the system $CaCO_3$-$MgCO_3$-SiO_2-Al_2O_3 such as meionite and vesuvianite are common but little or no experimental work has been done to determine their stability limits. The distribution of these minerals which do not provide meaningful quantitative data is shown in Figure 51. 'Diopside + vesuvianite' assemblages have been reported from amphibolite facies rocks by Tilley (1927) and Trommsdorff (1968). Scapolite is known from both medium-grade and high-grade terrains (Winkler, 1974, p.125). Fyfe, Turner and Verhoogen (1958, p.160-161) suggested an upper temperature limit for the stability of scapolite of 800°C - providing P_{H_2O} was high.

5. *System* $CaCO_3$ - SiO_2 - $MgCO_3$ - Al_2O_3 - K_2O

The addition of potassium to the system makes possible the formation of

the minerals phlogopite, biotite and K-feldspar, all of which are rare in the calcareous rocks of the Aus area. The paragenesis 'phlogopite + calcite' occurs in four specimens collected from around Am Ainschnitt (E3) and Magnettafelberg (D1) and in one specimen west of Löwenberg (F4)(Tables 2 and 3). This paragenesis suggests the reaction (Winkler, 1974, p.114):

(36) 3 dolomite + 2 K-feldspar + 1 H_2O → 1 phlogopite + 3 calcite + 3 CO_2

Experimental data on the stability of the 'phlogopite + calcite' assemblage are not available.

Pargasite (see Fig. 51) is stable up to the highest temperature limits of the Aus area. According to Boyd (1959) its upper stability limit is 1040°C at pressures as low as 1 kb where $P_{H_2O} = P_t$; pargasite is the most refractory of the amphiboles (Ernst, 1968).

6. *Résumé of Mineral Parageneses in Calcareous Rocks*

The scattered outcrops of calcareous rocks can be grouped into type areas characterized by different mineral parageneses (see Fig. 47). These type areas serve to illustrate the path of prograde metamorphism from the northwest (Magnettafelberg) to the centre of the study area (Swartaus); their localities are shown in Figures 49 and 50.

The significant changes in the mineral parageneses shown in Figure 47 can be summarized as follows:

(i) *Magnettafelberg area*: 'epidote + quartz' stable; 'forsterite + talc' stable; tremolite probably stable.

(ii) *Garub area*: grossularite becomes stable and coexists with calcite, quartz and, probably, anorthite; 'epidote + quartz' unstable in consequence; tremolite metastable with forsterite; talc probably stable; forsterite and diopside both present but do not coexist

(iii) *Am Einschnitt area*: tremolite becomes unstable; coexisting 'forsterite + diopside'; 'talc + forsterite' unstable; anthophyllite stable

(iv) *Löwenberg area*: wollastonite stable and 'calcite + quartz' unstable

(v) *Bienenstich area*: 'grossularite + quartz' unstable and 'wollastonite + anorthite' stable

(vi) *Swartaus area*: dolomite unstable and 'calcite + periclase' stable

Some very important and common assemblages such as 'forsterite + calcite' and 'diopside + calcite' occur in all metamorphic zones in the Aus area (refer to Fig. 47) and have therefore not been mentioned in the foregoing summary.

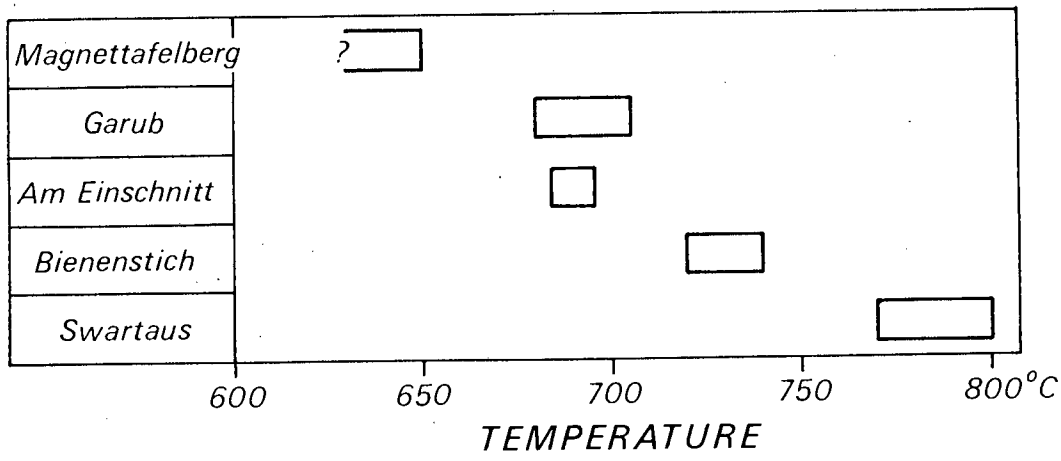

(a)

Figure 52. (a) Estimated temperature limits for selected areas, P_t= 5 kb
(b) Minimum temperature estimates for part of the Aus area, showing progressive increase in temperature from the north-west to the centre of the study area, P_t= 5 kb

(b)

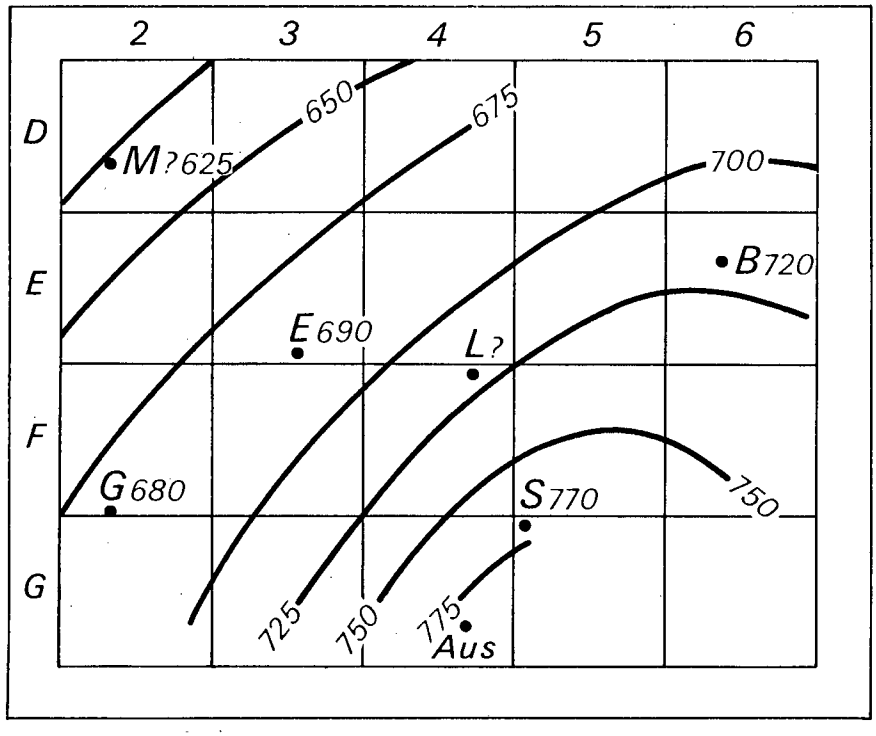

- M Magnettafelberg area
- G Garub area
- E Am Einschnitt area
- L Löwenberg area
- B Bienenstich area
- S Swartaus area

Figures represent minimum temperature estimates in degrees Celsius.

7. *Estimated Temperature Conditions*

On the basis of the reactions considered it is possible to construct maximum and minimum temperature estimates for each of the type areas described above assuming a constant pressure. Table 23 summarizes these temperature limits and the reactions from which the estimates were made (omitting the Löwenberg area because temperature limits of the stability of wollastonite there are greatly dependent on X_{CO_2}). Figure 48 should be consulted in conjunction with this table.

TABLE 23

Estimated temperature limits derived from calcareous metamorphites for selected areas, P_t = 5kb

AREA	TEMP. LIMITS °C		SOURCE
Magnettafelberg	Min.	?	not provided
	Max.	650	(reaction 29) 'epidote + quartz' stable
Garub Station	Min.	680	(reaction 20) 'tremolite + forsterite' metastable in marble (X_{CO_2}= 0,3)
	Max.	705	(reaction 20) 'tremolite + forsterite' metastable in marble (X_{CO_2}= 0,8)
Am Einschnitt	Min.	690	(reaction 27) coexisting 'forsterite + diopside'
	Max.	690	(reaction 19) coexisting 'forsterite + talc'
Bienenstich	Min.	720	(reaction 34) 'grossularite + quartz' unstable
	Max.	740	(reaction 35) epidote stable
Swartaus	Min.	770	(reaction 16) dolomite unstable
	Max.	800	(reaction 28) anthophyllite stable

These temperature estimates are illustrated graphically in Figure 52a. Because they are based on a total pressure of 5 kb and the estimated pressure range for the Aus area lies between 5 and 7 kb, temperatures quoted are conservative estimates and would be raised by some 40-80°C at P_t= 7 kb. Furthermore it should be remembered that much of the experimental data has been extrapolated from 2 kb (see text) and should thus be treated with caution.

Figure 52b illustrates a progressive rise in the estimated range of temperature from the northwest to the centre of the study area. A crude thermal dome is centred on Swartaus in the centre of the study area. The relation of this thermal dome, which is defined by calc-silicate minerals, to the zonation defined by the metabasites is described in Section 4.5.

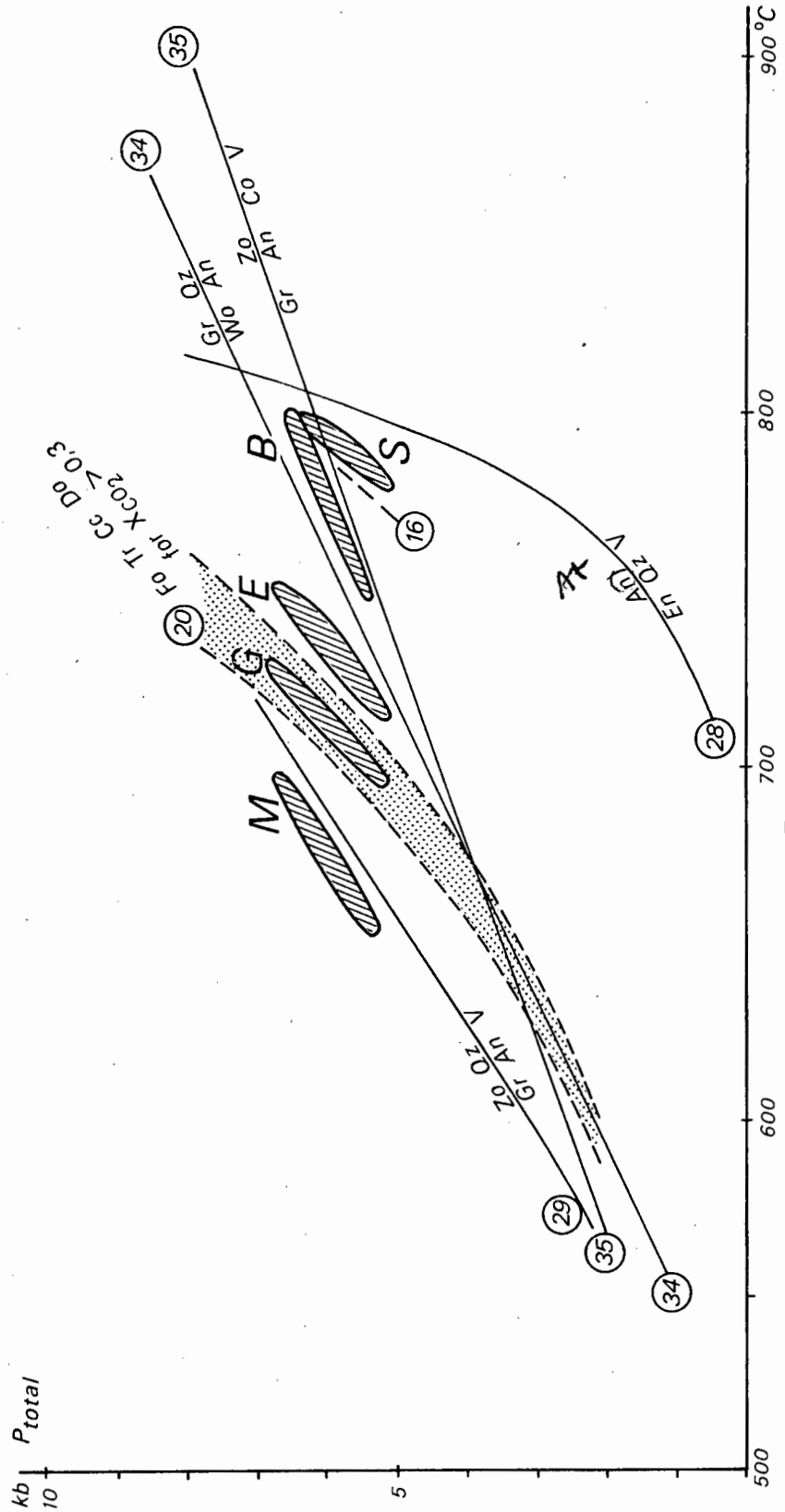

Figure 53. PT diagram of selected reactions in calcareous rocks showing PT domains estimated for selected areas, assuming pressure limits of 5-7 kb
M Magnettafelberg area, G Garub Station, E Am Einschnitt, B Bienenstich, S Swartaus
An anorthite, Cc calcite, Co cordierite, Do dolomite, En enstatite, Fo forsterite,
Gr grossularite, Qz quartz, V vapour, Zo zoisite
Experimental data sources: (16) Winkler (1974); (29) Holdaway (1972) and Liou (1973); (20) Winkler (1974); (28) Greenwood (1963); Fyfe (1962) and Zen (1971); (34) Gordon and Greenwood (1971), Kerrick (1970) and Newton (1966); (35) Boettcher (1970)

8. Summary of Pressure-Temperature Estimates from Calcareous Rocks

As mentioned in the introduction to this section all metamorphic reactions have been considered with respect to only two variables, T and X_{CO_2}; P_t has been fixed at 5 kb. In order to integrate the data derived from the calcareous rocks with that derived from the metapelites and metabasites (see Section 4.1-4.3), it is necessary to summarize the data of the present section in terms of the variables T and P_t. This is only possible for reactions that are independent of X_{CO_2} or that take place within a restricted range of X_{CO_2} so that the concentration of CO_2 need not be considered as a variable. Other reactions may be represented on a PT diagram if they supply only a maximum or minimum temperature value (such as reaction 28 'anthophyllite out'). These results are depicted in Figure 53. Reactions are numbered according to the same system as in Figure 48, but in some cases the experimental data have been drawn from different sources and these are acknowledged in the diagram.

The most significant feature in the PT diagram is the intersection of curves 28 and 34 at a pressure slightly greater than 7 kb. This provides a maximum pressure estimate for the highest grade metamorphism; the estimate agrees well with the estimated pressure range of 5-7 kb derived from a study of the metapelites (section 4.3). The metamorphic petrology of the metapelites indicates a facies series from the outer part of the area towards the centre that followed an essentially isobaric path (Fig. 46b). Using these pressure estimates the PT fields occupied by assemblages from the five type areas are shown in Figure 53 (the minimum temperature for the Magnettafelberg area is not indicated by the calcareous rocks and it is not known whether zoisite is stable in the Swartaus type area).

In summary the mineral parageneses of the calcareous metamorphites provide valuable data on the varying T, P_t and X_{CO_2} conditions during metamorphism in different parts of the Aus area. A large number of different parageneses are present in these complex rocks, but only a small number of reactions and assemblages provide temperature estimates within comparatively small ranges for different type areas. Assuming an essentially isobaric facies series these estimates indicate a well-defined and consistent increase in temperature from a minimum of slightly less than 650°C in the northwest to a maximum of 770-800°C in the centre of the area.

4.5. SUMMARY OF AMPHIBOLITE FACIES PT CONDITIONS IN THE AUS AREA

The PT estimates for amphibolite facies metamorphism of the mafic, pelitic and calcareous metamorphites of the Garub sequence are synthesized in this section.

Table 24 shows mineral changes in the Garub metamorphites with reference to the metamorphic zones defined by metabasites (zones A,B and C) and metapelites (zones 1, 2 and 3). These metamorphic zones have been combined to

TABLE 24.

Chart showing progressive mineral changes and amphibolite facies metamorphic zones in the Aus area

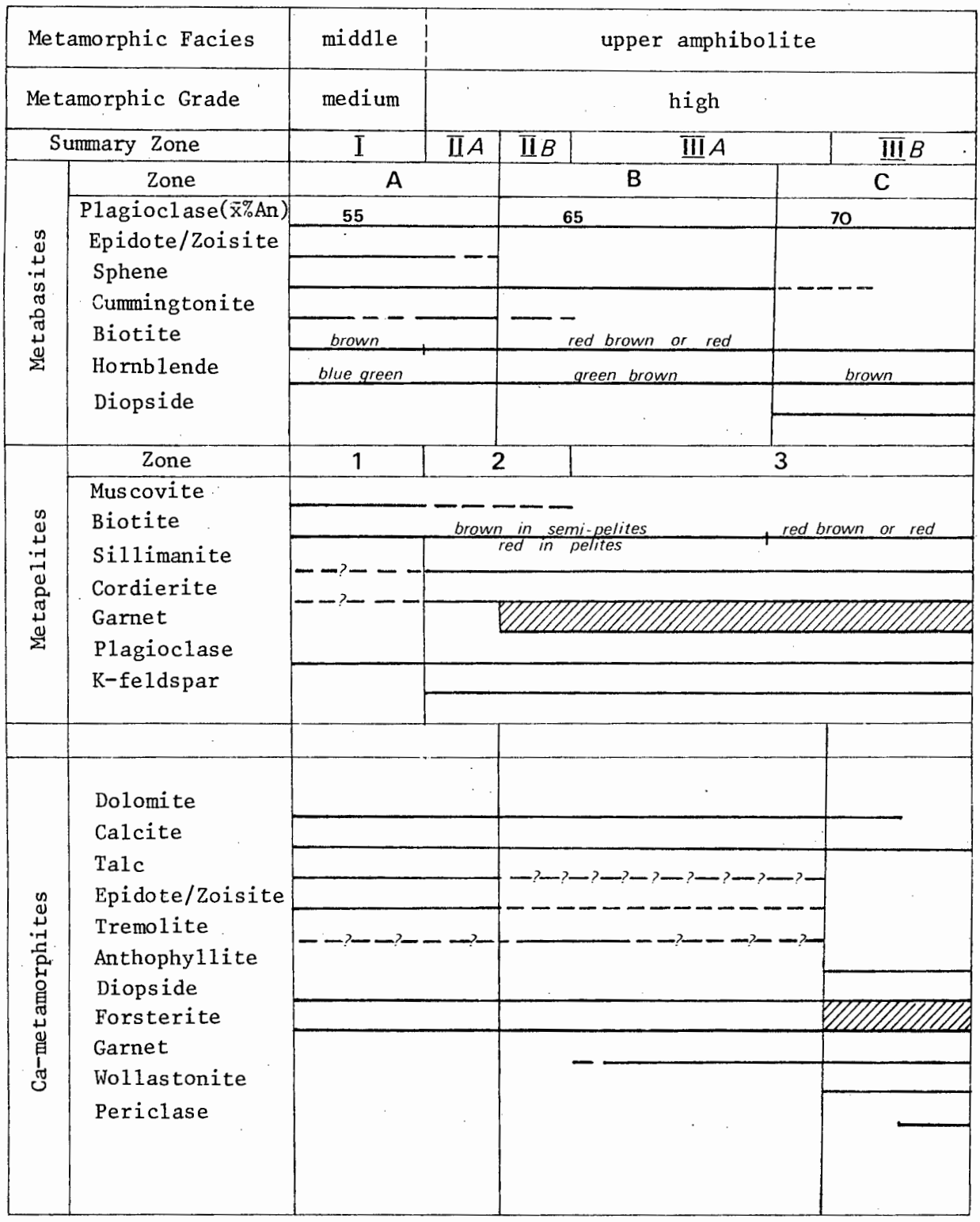

construct a 'summary zonation' comprising the metamorphic zones I, II and III. The relation of these metamorphic zones to the facies classification and to Winkler's (1970) grade classification is shown in the table; most of the metamorphites are of high-grade or upper-amphibolite facies metamorphism. The table shows the stability zones of individual minerals and compositional trends in plagioclase, hornblende and biotite. The coexistence of 'cordierite + almandine' and 'diopside + forsterite' is indicated by hatched lines; for details of all other parageneses, Figures 24, 41 and 47 should be consulted.

A selection of the most significant reactions and mineral parageneses is used to estimate the PT conditions for the metamorphic zones I, II and III. In Figure 54 dashed lines enclose the probable PT field which is estimated from the reaction curves shown and from other data mentioned in the text (particularly in the previous section on calcareous metamorphites).

Table 25 shows the minerals and mineral parageneses that are diagnostic for (shown in italics) or typical of each metamorphic zone; it also shows the type area for each metamorphic zone and the associated type of migmatization in each zone (see Chapter 5). The areal distribution of each zone is shown in Figure 55 which was compiled from Figures 25, 38, 42, 46, 49 and 52.

Figure 56 shows the estimated PT field for the Aus amphibolite metamorphism in relation to various geothermal gradients; the PT field suggests geothermal gradients of 30-50 ^{o}C/km. According to Miyashiro (1973, p.396), low-pressure metamorphic belts are formed with geothermal gradients probably higher than 25 ^{o}C/km, whereas high-pressure metamorphic belts are characterized by geothermal gradients of less than 10 ^{o}C/km (ibid., p.394). The estimated PT field of the lowest-grade and highest-grade zones of amphibolite facies therefore defines a metamorphic facies series of the low-pressure/high-pressure type.

In addition to these PT estimates there are a number of geological features that also support a low-pressure/high-temperature facies series. Characteristic features of low-pressure metamorphic belts elsewhere that are also present in the Aus area are:

(i) Evidence of widespread melting and abundance of syntectonic granitoids (ibid., p.396)

(ii) Rarity of basaltic magmatism and extreme rarity of peridotite and serpentinite (ibid., p.397)

(iii) Presence of mature pelitic rocks (ibid.)

(iv) Presence of cummingtonite and clinopyroxene in high-temperature metabasites (see Section 4.1)

(v) Low values of Al^{VI} and Si in hornblendes in the metabasites (Raase, 1974)

(vi) Absence of garnet from all metabasite specimens (see section 4.1)

(vii) Absence of kyanite at lower grades; presence of sillimanite

(viii) Cordierite and almandine coexisting in most metapelite specimens; almandine alone not present in metapelites

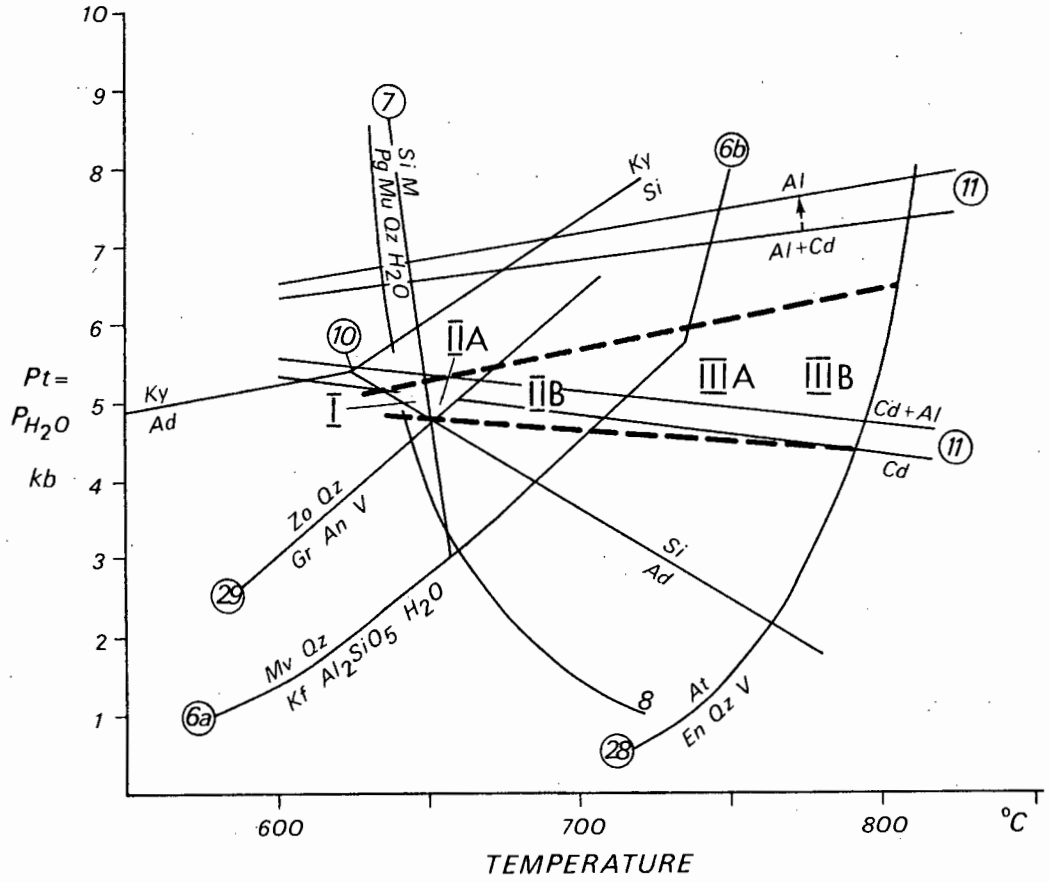

Figure 54. Summary diagram showing PT estimates for the amphibolite facies metamorphic zones of the Aus area. Dashed lines outline estimated PT field for summary zones I, II and III
Ad andalusite, Al almandine, An anorthite, At anthophyllite, Cd cordierite, En enstatite, Ky kyanite, M melt, Pg plagioclase, Qz quartz, Si sillimanite, V vapour, Zo zoisite
(6a) Althaus et al. (1970); Storre and Karotke (1972); (7) Storre and Karotke (1971); (8) minimum melting after Winkler (1970); (10) Richardson et al. (1968, 1969); (11) upper and lower pressure limits for coexistence of 'Cd + Al' in metapelites with MgO/(MgO+FeO) = 0,5 - 0,6 (Currie, 1971); (28) Fyfe (1962), Zen (1971) and Greenwood (1963); (29) Holdaway (1972) and Liou (1973)

(ix) Presence of wollastonite, grandite, diopside and vesuvianite in calcareous metamorphites (Miyashiro, 1973, p.300)

High metamorphic temperatures are indicated by the following features in the Aus area:

(i) Widespread melting and abundance of syntectonic granitoids (see Chapter 5)

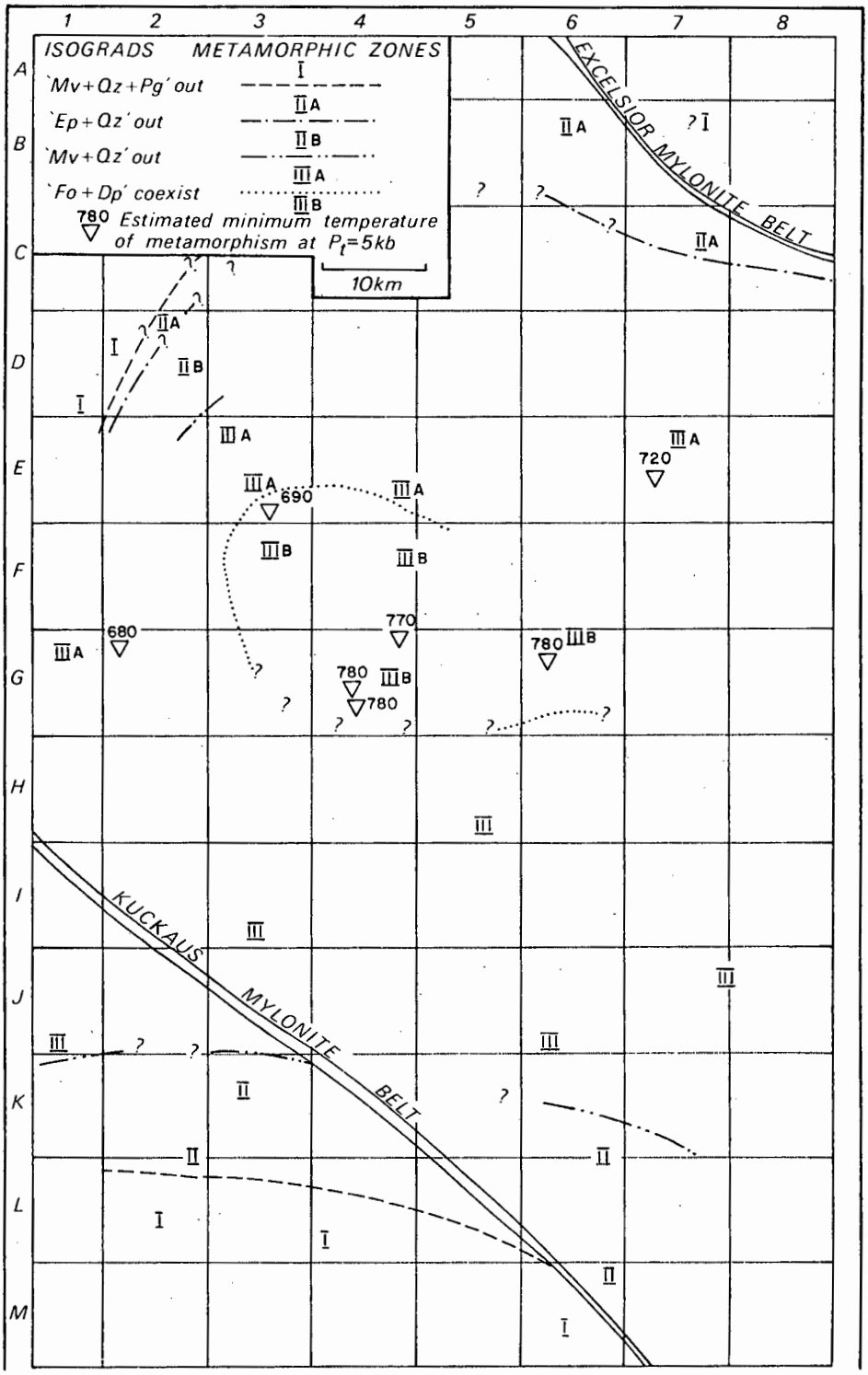

Figure 55. Distribution of amphibolite facies metamorphic zones in the Aus area as indicated by mineral parageneses in calcareous, mafic and semi-pelitic rocks of the Garub sequence

TABLE 25

Summary of amphibolite facies metamorphism and associated migmatization of pelitic, mafic and calcareous rocks of the Garub sequence. Italicized parageneses are diagnostic for each zone

ZONE	TYPE AREA(S)	METAMORPHIC PARAGENESES	MIGMATIZATION
I	Tsaus Mountain and Glockenberg (extreme SW and NW of area)	1. *Mu+Qz+Pl stable* 2. no metapelites 3. Ep+Qz stable in metabasites 4. Tc+Fo stable; Tr, Di stable	little or no anatexis; injection neosomes present
IIA	Excelsior area, Urus Mountain and E. of Magnettafelberg N,NW and SW of area	1. *Mu+Qz+Pl unstable, Mu+Qz stable* 2. Sm, Cd stable 3. metabasites, as in zone I 4. calcareous rocks, as in zone I	metatexis
IIB	NE of Dicker Willem Mountain	1. semi-pelitic rocks, as in zone IIA 2. metapelites, as in zone IIA 3. *Ep+Qz not stable* 4. calcareous rocks as in zone I	widespread metatexis
IIIA	Tsirub, Paddaputs Farms	1. *Mu not stable* 2. *Cd+Al coexist* 3. Di stable in metabasites 4. Ga stable in calcareous rocks, Tr metastable	vast amounts of metatectic melt, diatexis locally
IIIB	Aus Townlands	1. semi-pelitic rocks, as in zone IIIA 2. Cd+Al coexist; locally *He+Si+Qz* 3. metabasites, as in zone IIIA 4. *Fo+Di coexist*; Ga and At stable; Wo and Pe locally formed	widespread diatexis and intrusion of granitoid melts

(ii) In calcareous rocks: presence of wollastonite formed by reaction of 'calcite + quartz' and 'grossularite + quartz'; presence of periclase formed by decomposition of dolomite; coexistance of 'forsterite + diopside' in marbles (see Section 4.4)

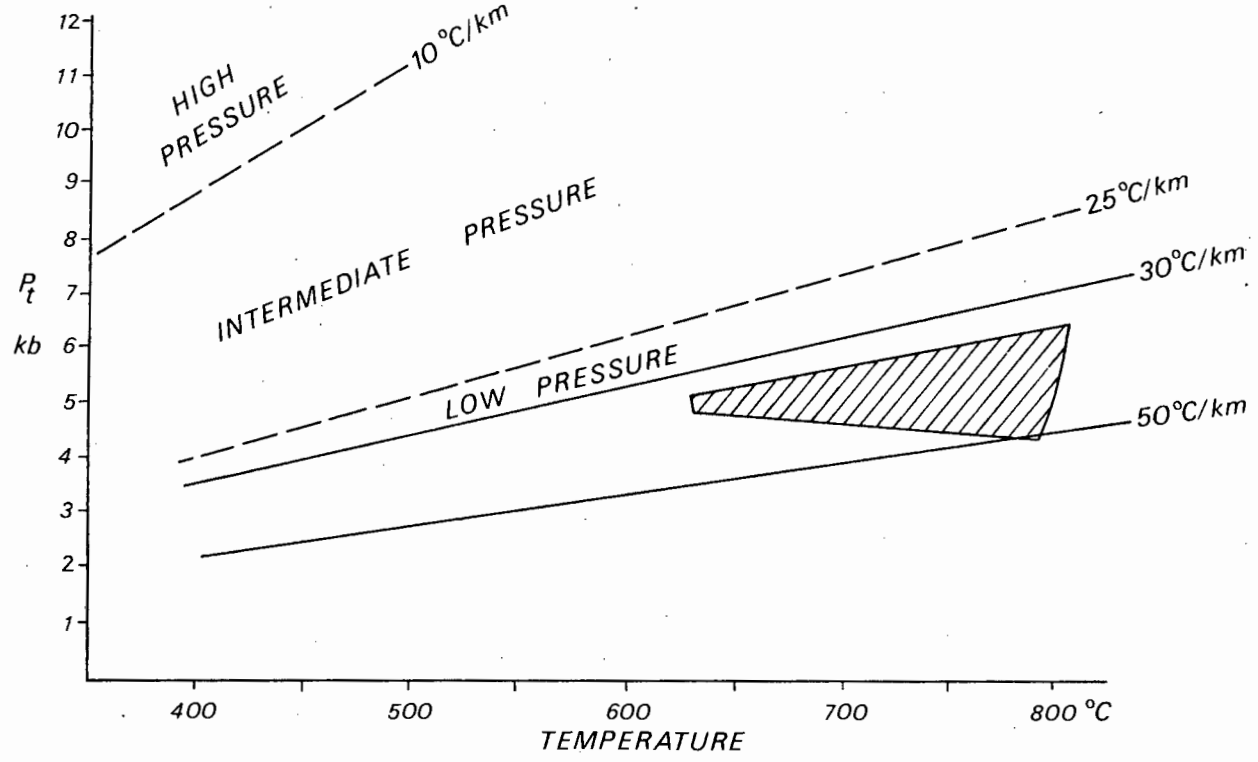

Figure 56. PT diagram showing field of Aus amphibolite facies metamorphism (hatched) with respect to various geothermal gradients and Miyashiro's (1973) facies series. A low-pressure/high-temperature facies series is suggested to have formed under high geothermal gradients of 30-50°C/km

(iii) In pelitic rocks: absence of muscovite; presence of K-feldspar and sillimanite; presence of 'hercynite + sillimanite + quartz' (see Section 4.3)

(iv) In metabasites: high anorthite values of plagioclase (An_{40}-An_{95}); advanced titanium and edenitic enrichment in hornblendes (see Section 4.1)

4.6 GRANULITE METAMORPHISM AND THE ROLE OF THE CHARNOCKITES

In the zone of highest metamorphic grade defined by the metabasites (zone D) orthopyroxene is present in metamorphic rocks on a regional scale (Fig. 59). The isograd marking the first appearance of orthopyroxene is taken as the boundary of the granulite facies domain, regardless of the rock type or nature of the reaction producing the orthopyroxene (de Waard, 1965a; Winkler, 1974); the granulite zones in the Aus area are thus synonymous with zone D.

Although granolites and their associated charnockites have long been the subject of intensive study and speculation in other Precambrian terrains, they have not received this attention in the Namaqua belt. This is largely due to the lack of regional mapping in most of this terrain until recent years. In this section possible physical conditions for the granulite metamorphism in the Aus area are discussed and the original extent of the granulite zone in this area is speculated on. Following this the petrological and field evidence for the origin of the charnockites near Aus and their relation to the granolites is described. The granolite/charnockite association in other parts of the Namaqua Metamorphic Complex is reviewed with reference to recent - mostly unpublished - studies in this area.

1. *Stability of Hydrous Minerals in the Aus Granolites*

The granolites of the Aus area contain both biotite and hornblende in quantities averaging 5% and 9% respectively. The question arises: are these hydrous minerals in the granolites *prograde* and therefore indicative of certain minimum water pressures during granulite metamorphism or *retrograde*, having been produced by the introduction of small amounts of water after the original granulite metamorphism?

There is no textural evidence in the granolites for the retrograde character of biotite; nor is there any K-feldspar in these rocks from which biotite could form by retrogression. Similarly there is no textural evidence of a retrograde origin for much of the hornblende. High-titanium brown hornblende grains with polygonal outlines are unlikely to be retrograde (Leake, 1965; Spry, 1969), but in cases where the mineral has obviously reacted with hypersthene it is not always clear whether this reaction is prograde or retrograde.

The stability of hornblende and biotite in the granulite facies has been well documented elsewhere (Cooray, 1962; Binns, 1965; Davidson, 1968; Ramaswamy and Murty, 1973; Howie, 1955; Philpotts, 1966; Saxena, 1969; Engel & Engel, 1962a; Schrijver, 1973). De Waard (1965b) proposed a subdivision of the granulite facies based on the presence or absence of hornblende: the 'hornblende granulite' and 'pyroxene granulite' subfacies. Granolites completely lacking hydrous minerals are extremely rare, and the majority of the world's granulite facies rocks fall into the hornblende granulite subfacies (ibid., p.456).

Sen and Ray (1971b) reported that most of the granolites from the Madras area in India (the type area of charnockite) are hornblende bearing and that the hornblende is prograde. They concluded that the presence of hornblende was stabilized by a lack of quartz; this appeared to be the limiting factor for the stability of hornblende in the granulite facies (Sen and Ray, 1971a). This view is at variance with that of Winkler (1974) who, following Buddington (1963), attributed the occurrence of granolites with or without hornblende to differing amounts of water in the original rock.

The formation of orthopyroxene in the granulite facies is commonly attributed to the breakdown of either hornblende or biotite. The breakdown of these minerals to form hypersthene is controlled by 'sliding reactions' (Winkler, 1974, p.254); both reactants and products coexist over a range of temperature but their proportions change throughout this range. The occurrence of hydrous minerals together with orthopyroxene can be attributed to this co-existence of equilibrium phases.

Breakdown of hornblende is thought to be the main mechanism by which the pyroxenes were formed in the Garub metabasites. As pointed out previously, the average modal percentage of hornblende is 57% in diopside-free amphibolites and 28% in the diopside amphibolites; in the hypersthene granolites the average hornblende content is only 9%. The breakdown reaction of hornblende as established by de Waard (1965a) is:

(4) 1 hornblende + 1 quartz → 3 hypersthene + 2 anorthite + H_2O

This reaction has been studied quantitatively in detail by Sen and Ray (1971a), based on analyses of hornblende and pyroxene from a number of granulite terrains. The calculated reactions involved the formation of clinopyroxene as well as magnetite and ilmenite. The reactions for rocks from the Madras, Salem and Adirondack areas can be simplified in the form of reaction 37 (ibid):

(37) hornblende + (2,5-3,5) quartz → (1,0-1,5) orthopyroxene + (1,0-1,5) clinopyroxene + labradorite + magnetite + ilmenite

There is strong evidence that the hypersthene was not formed from breakdown of biotite. Firstly in contrast to the modal percentage of hornblende, that of biotite remains fairly constant in metabasites from different metamorphic zones. Secondly, the prograde breakdown of biotite must involve the formation of K-feldspar, which is absent from the granolites. De Waard (1965b, p.456) gives the following reaction for the breakdown of biotite in the granulite facies:

(38) 1 hornblende + 2 biotite + 17 quartz → 15 orthopyroxene + 4 K-feldspar + 1 albite + 2 anorthite + 5 H_2O

There is no evidence of instability of biotite in either the metabasites or the metapelites in the granulite zone of Aus. Indeed, Reinhardt and Skippen (1970) have stressed the necessity of biotite as a stable phase in the granulite zone. If it were not present, this would entail the coexistence of sillimanite and hypersthene which is extremely rare (refer to Fig.44).

In summary therefore it appears that both diopside and hypersthene have formed by breakdown of hornblende, but that hornblende is present as a prograde mineral in many of the Garub granolites. Biotite is stable in both the metabasites and metapelites in the granulite zone and does not appear to have contributed to the formation of the pyroxenes.

2. *The Role of Water in Granulite Facies Metamorphism*

The composition and pressure of the fluid phase in non-calcareous rocks has been a rather neglected field of the study of reactions at elevated temperatures and pressures until recently. Winkler (1967) stressed that granolites do not require exceptionally high temperatures or pressures for their formation and that they form at PT conditions characteristic of normal high-grade metamorphism (upper amphibolite facies) provided that P_{H_2O} was much lower than P_t. The experimental work of Yoder (1955) and Althaus (1968) has shown the great influence of the partial pressure of water on all reactions involving water. Under conditions of fixed P_t reactions yielding water (dehydrating), such as the breakdown of amphiboles or biotite to form orthopyroxene, take place at much lower temperature if the P_{H_2O} is reduced. Conversely reactions consuming water, such as anatexis, take place at greatly elevated temperatures if P_{H_2O} is reduced.

Anhydrous conditions, produced by P_{H_2O} being much lower than P_t, can occur in two ways: either by the metamorphism of 'dry' rocks which have either been dehydrated during earlier metamorphism or were originally anhydrous such as mafic magmatic rocks; or by dilution of the water-rich fluid phase by other fluids such as CO_2, so that the fluid pressure remains high, but anhydrous conditions are nevertheless present. Likely estimates of P_{H_2O} and P_t during the Aus granulite metamorphism are given in the following section.

3. *Estimated PT Conditions of Granulite Metamorphism in the Aus Area*

The experimental data relevant to the granulite facies PT conditions for the Aus area are shown in Figure 57. In their classic experimental work, Green and Ringwood (1967) subdivided the granulite facies into three geobarometric types:

(i) *Low-pressure:* characterized by the stable association of 'olivine + anorthite'

(ii) *Low intermediate-pressure*: 'olivine + anorthite' unstable; garnet unstable

(iii) *High intermediate-pressure*: garnet stable, first in undersaturated iron-rich rocks; then, with increasing pressure, in oversaturated iron-poor rocks; decrease in plagioclase proportion with increasing pressure

At still higher pressures (eclogite facies) plagioclase is no longer stable and the paragenesis 'diopside + pyrope' becomes stable.

The appearance of garnet in the high intermediate-pressure granolites is governed by the reactions:

(39) 4 orthopyroxene + 1 anorthite → almandine-pyrope + 1 clinopyroxene + 1 quartz

(40) 2 orthopyroxene + 1 anorthite → grossular-almandine-pyrope + 1 quartz

These reactions (ibid.) therefore involve not only the formation of garnet but also the breakdown of orthopyroxene in the presence of plagioclase. The lower stability limit of garnet in quartz tholeiites (ibid.) is shown as curve 9 in Figure 57. Kushiro and Yoder (1966) studied the experimental conditions for the appearance of garnet by breakdown of orthopyroxene and plagioclase at lower temperatures than Green and Ringwood (1967) who worked in the temperature range 1000-1250°C and extrapolated their data to lower temperatures. The results of Kushiro and Yoder (1966) therefore are probably more applicable to the present study. Their data indicate a lower pressure limit for the stability of garnet (curve 8, Fig. 57).

The Aus granolites are quartz-bearing mafic rocks and they therefore fall into the compositional field of quartz tholeiites. All the granolite specimens from the Aus area are free of garnet and therefore formed below the stability limit of garnet in metabasites. Curves 8 and 9 in Figure 57 therefore define the upper pressure limit for granulite metamorphism in the Aus area.

An additional upper pressure limit is provided by the coexistence of cordierite and garnet in the granulite facies metapelites. This limit is shown as curve 4 in Figure 57 (*after* Currie, 1971). As previously stated, in the absence of chemical anlyses of the Garub metapelites an 'average' (Winkler, 1974, p.224) FeO/(FeO+MgO) ratio of 0,5 has been assumed.

With reference to the three geobarometric granolite types of Green and Ringwood (1967) both the curves for the lower stability limit of garnet in metabasites and the upper stability limit for the coexistence of cordierite and garnet in metapelites indicate that the Aus granulite metamorphism was of the intermediate-pressure type.

In their review of intermediate-pressure granulites Green and Ringwood (1967) concluded that mafic granolites of this type characteristically contain orthopyroxene, clinopyroxene and plagioclase if they are saturated with quartz (Groves, 1935; Subramanian, 1956; Wilson, 1959; O'Hara, 1961; Banno et al., 1963; Binns, 1964; de Waard , 1964). However, granolites of intermediate-

Figure 57. P_tT diagram showing experimental data relevant to the Aus granulite metamorphism. Hatched field represents estimated P_tT conditions
Ad andalusite, Al almandine, An anorthite, Cd cordierite, Cp clinopyroxene, Di diopside, En enstatite, Ga garnet, Ky kyanite, M melt, Ol olivine, Op orthopyroxene, Or orthoclase, Qz quartz, Si sillimanite
(1) Al_2SiO_5 triple point (Althaus et al., 1967, 1969; Richardson et al., 1968, 1969; *in* Winkler, 1974); (2a,2b) minimum anatexis for gneisses with plagioclase An_0 and An_{36} (Winkler, 1970); (3,4) lower and upper limits for coexistence of 'Cd+Al' in metapelite with MgO/(MgO+FeO) = 0,5 (Currie, 1971); (5,6,7) upper limits for coexistence of 'Ol+An' (Green and Ringwood, 1967; Irving and Green, 1970; Kushiro and Yoder, 1966); (8) lower limit of Ga in mafic rocks (Kushiro and Yoder, 1966); (9) lower limit of Ga in quartz tholeiite (Green and Ringwood, 1967); (10,11) maximum and minimum temperature limits for hornblende-bearing granolites (Hewins, 1975)

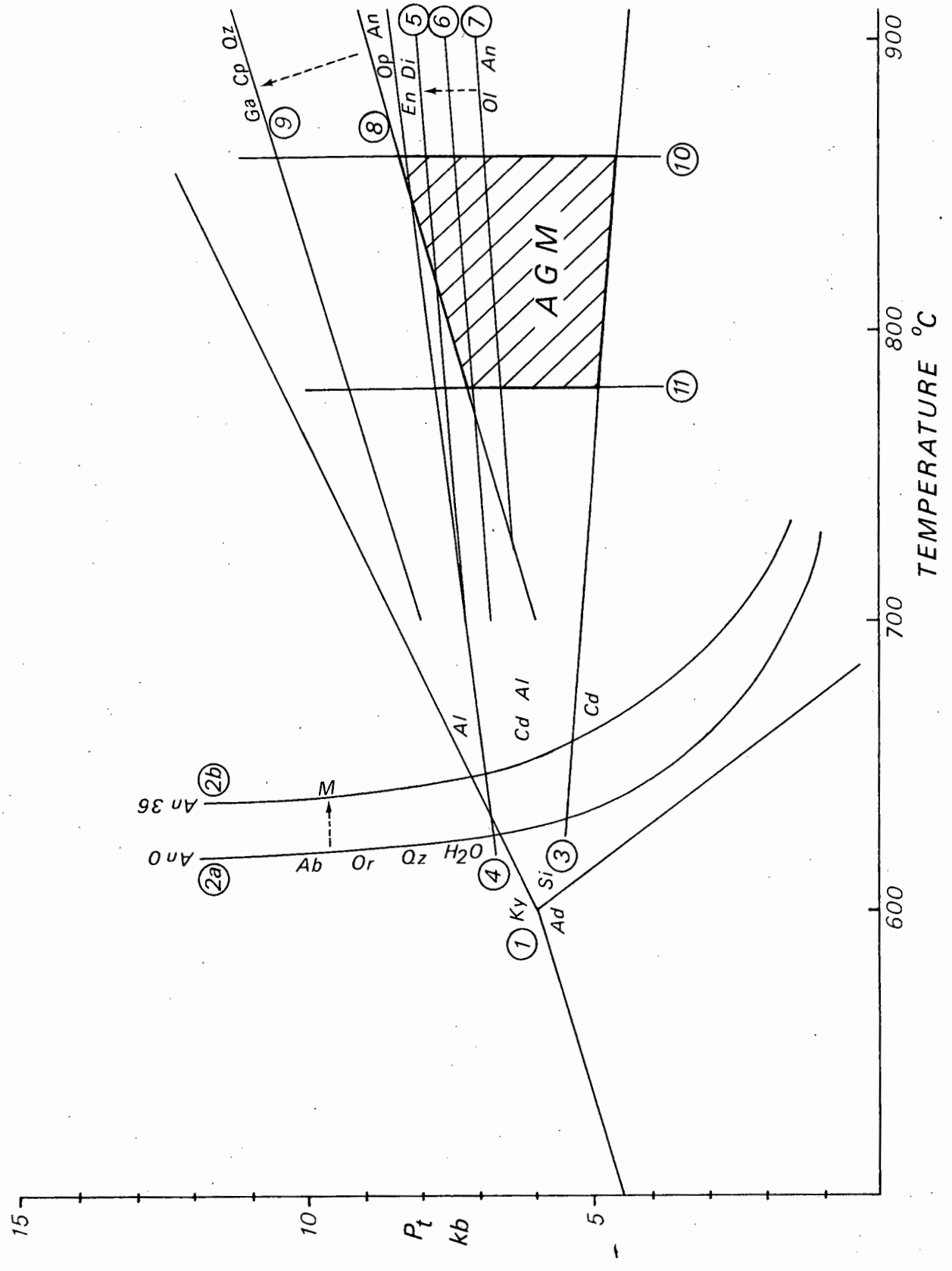
Ga Cp Qz
Op An
En Di
Ol An
AGM
Al
Cd Al
Cd
An 36
An 0
M
Ab Or Qz H2O
Ky
Si
Ad
TEMPERATURE °C
900
800
700
600
15
10
5
Pt kb

pressure type that are undersaturated contain garnet instead of olivine (Green and Ringwood, 1967).

The Garub granolites are quartz-bearing saturated rocks containing coexisting pyroxenes and coexisting orthopyroxene and plagioclase; these are parageneses characteristic of intermediate-pressure granulite metamorphism. However, one of the charnockite bodies is undersaturated and ultramafic. This charnockite is the Keerbank body, which contains the paragenesis 'forsterite + enstatite + plagioclase'. Although the olivine is highly serpentinized and plagioclase is rather rare in the olivine-bearing part of the rock, there is no textural evidence of reaction between the olivine and plagioclase.

The reactions:

(41) 2 olivine + 2 anorthite → Al-diopside + 2 Al-enstatite

(42) 2 olivine + 1 anorthite → 1 diopside + 2 enstatite + spinel

mark the boundary between the low-pressure and the intermediate-pressure granulite fields of Green and Ringwood (1967). The upper stability limit of 'olivine + plagioclase' was experimentally determined by Kushiro and Yoder (1966), Green and Ringwood (1967) and Irving and Green (1970). Their respective results are shown as curves 7, 5 and 6 in Figure 57. As in the case of lower stability limit of garnet, the upper stability limit of olivine as determined by Green and Ringwood (1967) is somewhat higher than that determined by Kushiro and Yoder (1966), whereas that of Irving and Green (1970) is intermediate between the two. These results are in good agreement with the upper stability limit of 'cordierite + garnet' shown as curve 4 in Figure 57 which provides an upper pressure limit for the granulite metamorphism.

If the coexistence of olivine and plagioclase in the ultramafic charnockite can be taken as representative of the granulite facies, then the granolites would be classed as low-pressure after Green and Ringwood (1967). However, this evidence is taken from a single outcrop of charnockite and should be weighed against the extremely widespread coexistence of orthopyroxene and clinopyroxene in the mafic granolites which is an association typical of low-intermediate-pressure granulite metamorphism. Furthermore the paragenesis 'hypersthene + diopside + plagioclase + spinel + magnetite' in a granolite specimen from Aus suggests that reaction 42 has indeed taken place. This rock is quartz-free and this undersaturated composition is compatible with the presence of olivine in the same rock at lower pressures. Since all other quartz-free granolites containing coexisting orthopyroxene and clinopyroxene which form the majority of this group also do not contain olivine, this is strongly indicative that the Garub granolites were produced under conditions of low intermediate-pressure metamorphism at pressures greater than those in which 'olivine + anorthite' are stable.

The lower pressure limit for this metamorphism is provided by curve 3 in Figure 57 which marks the lower limit for the coexistence of cordierite and garnet in metapelites with FeO/FeO+MgO = 0,5 (Currie, 1971). For this ratio the lower limit of coexistence at 800°C is about 5 kb, while for ratios of 0,3 and 0,7 the pressure limits are approximately 4 kb and 6 kb respectively.

Some of the Garub metapelites within the granulite zone near Aus contain only cordierite, implying pressures even below those defined by curve 3. But since these metapelites are strongly migmatized and intruded by the granite gneisses, their mineralogy probably reflects the later period of amphibolite facies metamorphism.

Curves 3 to 8 therefore outline a relatively low pressure field for the granulite metamorphism in the Aus area. The absolute pressure limits depend on the estimated temperatures. A large amount of geothermometric data exists on the probable temperature limits of granulite metamorphism in granulite terrains around the world. The data, which have been recently summarized by Touret (1974, p.8) and Hewins (1975, p.207) are based on a number of different studies including pyroxene geothermometry, fluid inclusions and experimental study of the stability of various parageneses. The different methods give temperature estimates that are remarkably consistent. Hewins (1975) gave temperature limits of 780-860^{o}C for hornblende-bearing granolites. If applied to the Garub granolites, these limits (curves 10 and 11) fix the pressure limits defined by the various curves in Figure 57 between 4,5 and 8 kb; these are maximum and minimum pressure limits and the likely pressure limits (defined by curves 3 and 7) are 5 and 7 kb respectively. The hatched zone in Figure 57 therefore defines the estimated P_tT field for the Aus granulite metamorphism (AGM). These estimates are conditional on the FeO/MgO ratio of the metapelites and, to a lesser extent, the CaO/NaO ratio the metabasites. These estimates also assume temperature limits typical of hornblende-bearing granolites elsewhere around the world. The estimates should therefore be treated with due caution.

The P_tT limits above have been estimated independently of the third variable, P_{H_2O}. In the previous section it was concluded that the fluid phase was only partly hydrous during granulite metamorphism. Using the P_tT estimates in the preceeding paragraph it is possible to determine semi-quantitatively the third variable, P_{H_2O}.

The hatched zone in Figure 57, which represents the estimated P_tT field of granulite metamorphism, has been reproduced in Figure 58, together with the experimentally determined curves for the following reactions:

(8a) minimum anatexis, An_0

(8b) minimum anatexis, An_{36}

(43) gedrite + quartz → hypersthene + cordierite + H_2O

(44) hornblende → enstatite + anorthite + diopside + H_2O

The curves 43 and 44 delimit a stippled area corresponding to the upper stability limits of the complete range of amphibole compositions (Althaus, 1968). The breakdown of hornblende to hypersthene is governed by a sliding equilibrium and the two minerals coexist within the stippled field bounded by curves 43 and 44.

Figure 58a illustrates the conditions of $P_{H_2O} = P_t$. Under these conditions of water saturation complete breakdown of hornblende requires extremely high temperatures (850-1000^{o}C at 5 kb) that are not realised during granulite metamorphism (Winkler, 1974). This shows why anhydrous or partially anhydrous conditions are necessary for the formation of hypersthene during regional

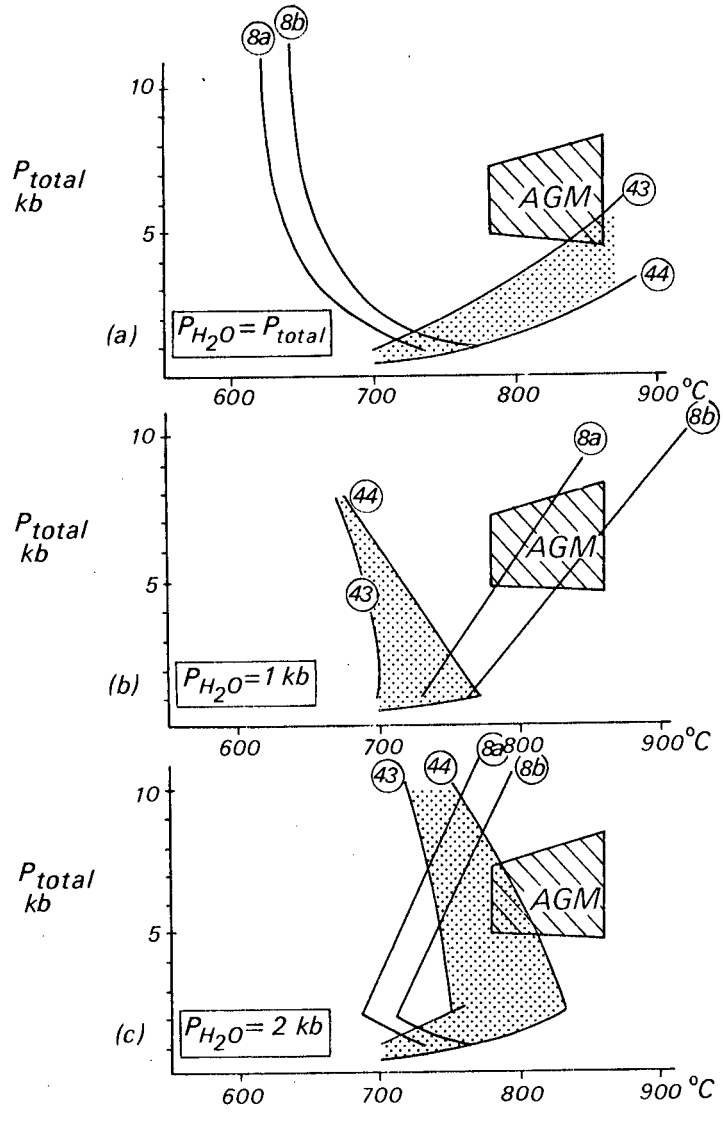

Figure 58. Estimated water pressures during the Aus granulite metamorphism. AGM represents estimated P_tT field for the Aus granulite metamorphism from Figure 57
(8a) minimum anatexis (Althaus, 1968); (8b) anatexis in gneiss with An_{36} (Fig. (a) *after* Winkler, 1970; Figs. (b,c) extrapolated *after* Winkler, 1970 and Althaus, 1968); (43,44) stippled field defines coexistence of hornblende and hypersthene (Althaus, 1968)

metamorphism. Under the conditions of $P_{H_2O} = P_t$ the hatched zone is situated well within the zone of anatexis (lower PT limits defined by curves 8a and 8b).

Figure 58b illustrates the condition of P_{H_2O} = 1 kb which represents virtually anhydrous conditions at P_t = 5 kb. The hatched zone is situated well on the high-temperature side of the field for the coexistence of hornblende and hypersthene. Thus hornblende could not exist under these conditions. At a partial pressure of water as low as this, anatexis can only take place at very high temperatures. The hatched zone is transected by the curve (8a) of minimum anatexis, but it is unlikely that melting could have taken place in gneisses with plagioclase as calcic as An_{36} (curve 8b). — and gneisses are more calcic

Figure 58c illustrates the condition of P_{H_2O} = 2 kb; at intermediate pressures this represents partially anhydrous conditions. The hatched zone is situated partly above the field of coexistence of hornblende and hypersthene and partly within it. It is also situated entirely within the zone of anatexis for gneisses of intermediate composition.

Figure 58 suggests a water pressure of approximately 2 kb during the granulite metamorphism around Aus. Evidence for this is summarized as follows.

All granolites contain prograde hydrous minerals (biotite or hornblende) in small amounts, suggesting that conditions were not completely anhydrous although the water pressure was relatively low. Two thirds of the granolites examined contain hornblende, which suggest that the PT conditions for the formation of the granolites straddled the upper limits of the hornblende-hypersthene field of coexistence. This situation corresponds with the condition of P_{H_2O} = 2 kb (Fig. 58c). With a water pressure of only 1 kb (Fig.58b) no hornblende could be stable.

Xenoliths of biotite schist within the charnockites have been migmatized; the neosomes are thin and discontinuous but fairly extensive. It would thus appear that the conditions for anatexis of the biotite schist were attained but not greatly exceeded during the intrusion of the charnockites. The melting curve of the xenolithic schist, which contains plagioclase of An_{38}, therefore approximates curve 8b. With a water pressure of 2 kb minimum anatexis of the schist would take place some 10 or 20°C below the low-temperature limits of the hatched zone; the schist would therefore be expected to show the effects of incipient melting. With a water pressure of only 1 kb biotite schist would begin to melt only in the very high temperature part of the hatched zone.

The estimated physical conditions of the Aus granulite metamorphism can therefore be summarized as follows. In the absence of geothermometric data from the area the temperature limits of 780-860°C for hornblende-bearing granolites around the world (Hewins, 1975) are applied to the Garub granolites. Within these temperature limits the mineral parageneses present in rocks of mafic ultramafic and pelitic composition suggest extreme limits of P_t between 5 and 8 kb and probable limits of 5-7 kb. The coexistence of hornblende and hypersthene and the melting of biotite schist by the charnockites suggest that the partial pressure of water during granulite metamorphism was approximately 2 kb.

4. *Original Extent of the Granulite Zone in the Aus Area*

The distribution of the granulite facies rocks is shown in Figure 59. Beyond the main granulite zones in the east there is only one other occurrence of hypersthene-bearing rocks within the study area. This is a small area containing granolites associated with metapelite and biotite schist and surrounded by the syntectonic Kubub granite gneiss

The remarkable freshness of the granolites through the area, together with the complete absence of higher-grade relict minerals in any of the amphibolite specimens from the zones of amphibolite facies, suggest that the amphibolite facies metabasites were never at a higher grade. If the granulite zone was ever more extensive than at present, then the granolites must have been retrograded so thoroughly during the migmatization that followed that not even minute relicts of the hypersthene remain in the specimens examined. It thus appears that the present-day distribution of the granolites corresponds to their original extent and that the granulite zone was never more extensive.

5. *The High-Temperature Character of the Jakkalskop Charnockites*

In a summary of the petrographic features of the Jakkalskop charnockites (Section 3.4) it was tentatively concluded that the specimens of intermediate composition have textures more typical of metamorphic rocks than of igneous rocks, whereas the mafic-ultramafic Keerbank body has an igneous texture. However, in spite of their apparent metamorphic textures, the intermediate charnockites show field evidence of once being molten because they contain angular fragments of country rock that have been cut by veins of charnockitic material.

There is abundant evidence for high-temperature conditions during the crystallization of the charnockites (whether in the solid state or liquid). This evidence is supplied by the presence of hypersthene, the extreme elongation of apatite and zircon and the presence of microperthite and mesoperthite.

Hypersthene is stable only at high temperatures and its stability limits depend greatly on the water pressure. Because there was sufficient water pressure to stabilize biotite and induce melting in xenoliths of biotite schist (Fig. 58c), temperatures were probably in excess of 800°C. Hypersthene is also present in xenoliths of metabasite in the charnockite.

The extreme elongation of apatite and zircon crystals further suggests a high temperature of crystallization. Wyllie et al. (1962) argued that acicular apatite crystals could be used as criteria for crystallization from a high-temperature magmatic state. Mehnert (1963) showed that the elongation ratio (length/width) increased with the temperature of formation of Black Forest granitoids from 5/1 in granites to 15/1 in syenites and diorites; migmatites and pegmatites contained apatites with a ratio of less than 5/1. The elongation ratio of 40/1 measured in apatite from the Jakkalskop charnockites therefore suggests very high temperatures of crystallization. Mehnert (1968, p.114) suggested that the same conclusions can be drawn from zircon crystals.

Zircons from metamorphic rocks of sedimentary origin generally have elongation ratios of less than 2/1, whereas igneous zircons have ratios of up to 4/1. The elongation ratio of 13/1 displayed by zircons in the Jakkalskop charnockites suggests temperatures of crystallization much greater than those of granite. These elongation ratios might possibly be interpreted as evidence of magmatic rather than metamorphic crystallization, but quantitative conclusions should not be drawn from these data because other effects besides high temperatures could be responsible for this extreme elongation.

The occurrence of microperthite and mesoperthite in the charnockites is further evidence for the high-temperature crystallization of these rocks. The system must have exceeded the solvus maximum temperature, which is between the limits of 660 and 715^{o}C (depending on water pressure and An-content of plagioclase) for unmixing to take place (Mehnert, 1968, p.102).

6. *The Relation of the Jakkalskop Charnockites to the Granulite Zone*

The absence of chilled contacts with the country rocks suggests that the charnockites were emplaced into a hot environment. The charnockites were therefore either intruded as relatively anhydrous high-temperature melts into an equally hot anhydrous environment (the charnockites are surrounded by granolites) or they recrystallized together with the country rocks during granulite metamorphism. These possibilities are now discussed in more detail.

Hypersthene may form under conditions of rising temperature (metamorphic heating) or falling temperature (magmatic cooling); the PT conditions for both origins will be similar (Cooray, 1969). The mineralogy of the charnockites is compatible with the estimated PT conditions for the formation of the granolites (Section 4.6.3) and both rock types could be termed charnockitic on the basis of their mineral assemblages.

The close relation between the charnockites and the granolites is emphasized by their strong spatial association. Figure 59 illustrates the relation between the charnockites and the orthopyroxene isograds as defined by the metabasites. *The charnockites are widespread within, but entirely restricted to, the granulite zone.* Furthermore *every metabasite xenolith collected from the charnockites is a hypersthene granolite.* Thus not only are the charnockites surrounded by a broad zone of granolites, but they also contain inclusions of these rocks.

7. *The Amphibolite/Granolite/Charnockite Metamorphic Profile*

In order to throw light on the relation between the charnockites and granulite metamorphism it was decided to integrate the study of this problem with that of the regional study of hornblende compositions in the metabasites. These hornblendes show grade-dependant chemical variations and are progressively enriched in alkalis and titanium with increasing metamorphic grade (Section 4.1). Accordingly these compositional variations are used to provide an

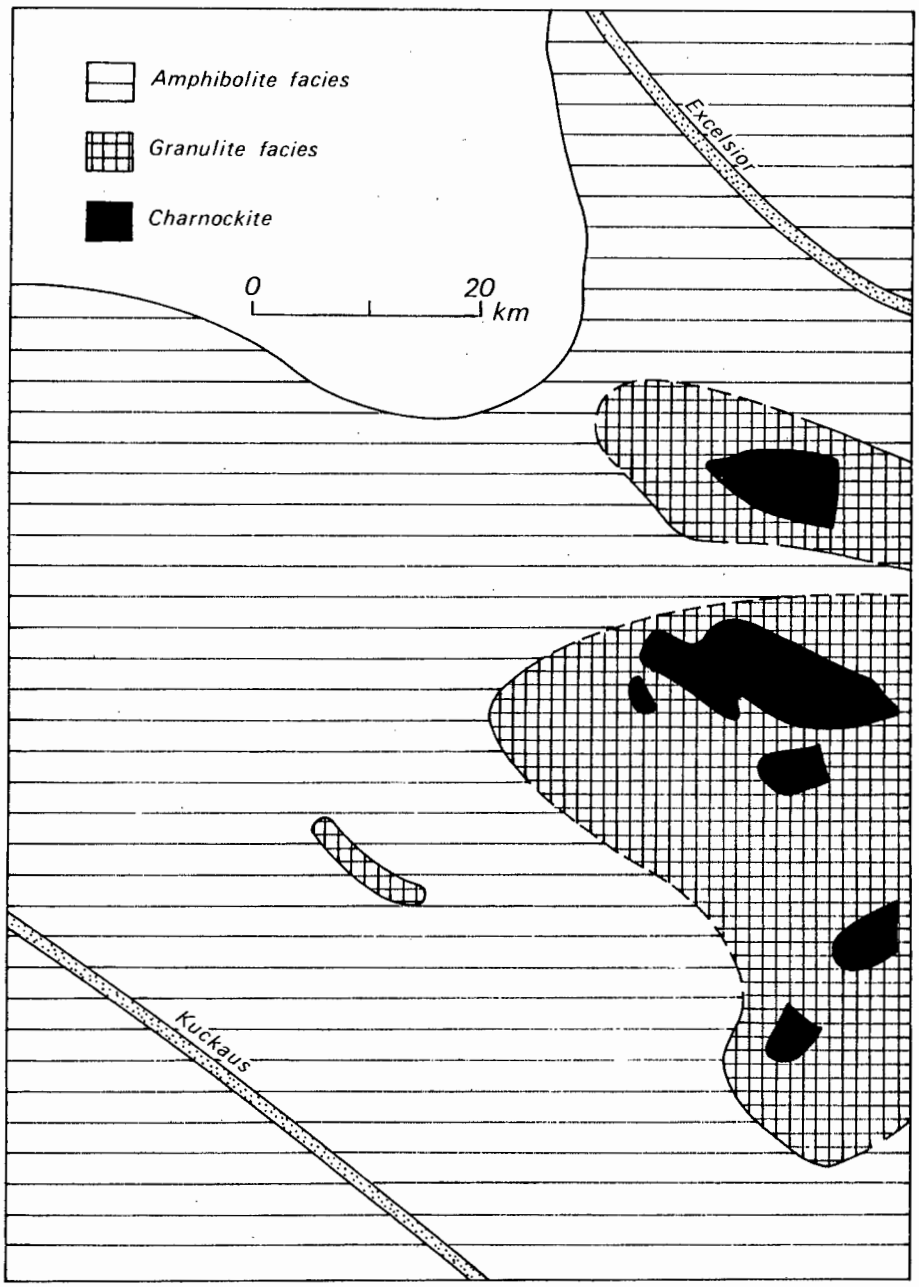

Figure 59. Sketch map showing relation of Jakkalskop charnockites to the zone of granulite facies metamorphism in the Aus area

estimate of the metamorphic transition from the amphibolite facies to the granulite facies in a small part of the Aus area. The chemical data of this study were derived from microprobe analyses of hornblende in metabasites from a geochemical traverse some 25 km in length (see Fig. 25). This traverse covers the critical zone of the amphibolite/granulite transition and the area between this transition zone and the charnockites. Using the parameters of (Na+K) and Ti as indicators of metamorphic grade it is possible to draw up a metamorphic profile across the zone.

Variation of Ti and (Na+K) content of hornblende with metamorphic grade and distance from charnockites

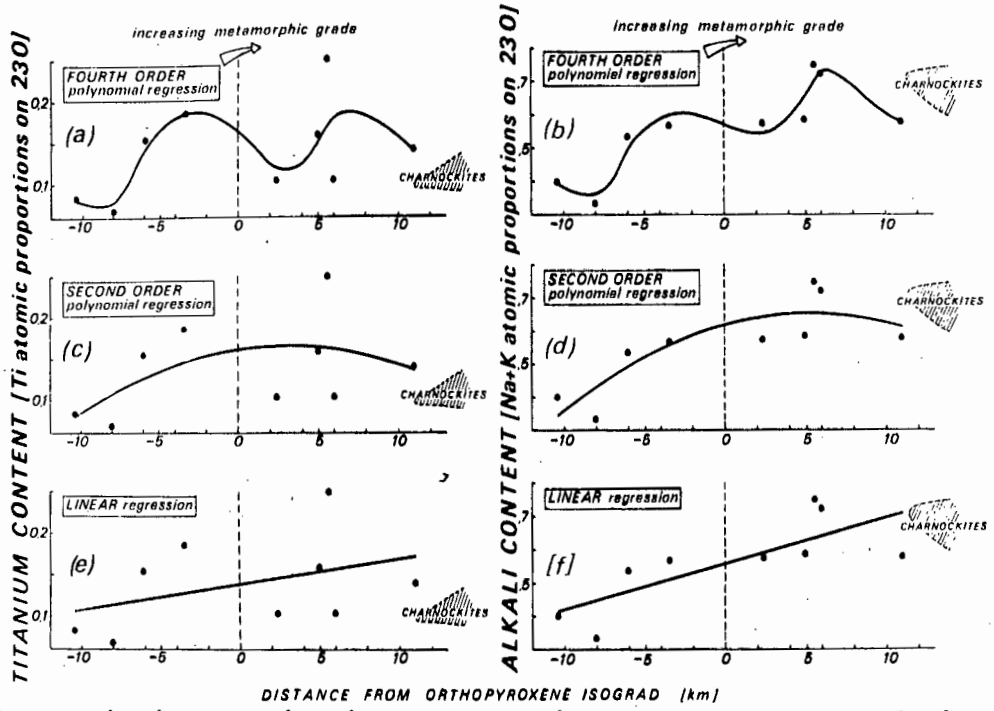

Figure 60. Variation of titanium and alkali content of hornblende in Garub metabasites with metamorphic grade and distance from charnockites

This metamorphic profile is illustrated in Figure 60. The nine plotted points in the six graphs each represent the average value of 3-5 hornblende crystals in each rock specimen. The positions of the sample points is shown in a sketch map in Appendix 6 and Figure 25. Calculations for polynomial regression were carried out by computer (program BMD05R University of California, Los Angeles, 1966).

Figure 60a and b show best-fit curves determined by fourth-order polynomial regression. They illustrate little except the degree of variability between the specimens. The regression lines in Figures 60e and f are produced by simple linear regression. They show that a marked increase in alkalis and a slight increase in titanium occurs in specimens nearer the charnockites. Correlation coefficients calculated for these values indicate that there is a correlation between this increase of alkalis and proximity to the charnockites that is statistically meaningful, but that this is not the case with the titanium values. Accordingly no meaningful conclusions on the metamorphic profile can be drawn from the distribution of titanium. Bard (1970) came to a similar conclusion that variations in alkali content appear to be a much more sensitive indicator of metamorphic grade than variations in titanium content.

The second-order curve for alkalis (Fig. 60d) climbs steeply on approaching the orthopyroxene isograd and its flattening opposite the amphibolite-granolite transition suggests that similar conditions of temperature and total pressure existed in the upper amphibolite facies and the granulite facies.

TABLE 26

Correlation coefficients calculated for correlation between distance from orthopyroxene isograd and alkali (r_a) and titanium (r_t) contents of hornblende in 9 Garub metabasite specimens in comparison with correlation coefficients at 5% and 1% significance

r_a	r_t	r at 5%	r at 1%
0,768	0,391	0,666	0,798

The apparent equivalence of temperature and pressure between the amphibolite and granulite zones is in agreement with experimental work on the PT conditions of granulite metamorphism (Winkler, 1967; Althaus, 1968).

The conclusions drawn from this metamorphic profile bring into focus two main problems which can now be discussed:

(i) How did the relatively anhydrous conditions arise?

(ii) What was the role of the charnockites during this granulite metamorphism - are they the cause or the result of the anhydrous conditions? Either the granulite zone developed independantly of the charnockites, which would thus represent magma intruded and crystallized under the PT conditions characteristic of granulite metamorphism; or, alternatively, the charnockites themselves were in some way responsible for the granulite facies conditions that developed around them.

To answer these questions it is necessary to discuss a somewhat neglected aspect of the granulite problem - the role of CO_2.

8. *Composition of the Fluid Phase During Granulite Metamorphism*

During metamorphism, heated fluids (composed of a homogeneous mixture of liquid and gas) may be trapped as inclusions within certain minerals, most commonly quartz. Apart from minute traces of hydrocarbons such as methane, this fluid phase is almost entirely composed of water or carbon dioxide (Touret, 1974). The proportion of H_2O/CO_2 is of great significance because if a fluid is composed predominantly of CO_2, it will be relatively anhydrous; therefore even under conditions of $P_f=P_t$ the water pressure would be low so that P_{H_2O} is much less than P_t.

Thus, anhydrous conditions may be produced not only by the removal of water from the system but also by dilution of the hydrous fluid phase by carbon dioxide. Because all water-consuming and water-producing reactions are affected by P_{H_2O}, the presence or absence of CO_2 in the fluid phase is capable of profoundly influencing these reactions, even if CO_2 is not one of the reactants or products of the reaction.

Touret (1972) found that both CO_2 and H_2O are commonly present in fluid inclusions in both the amphibolite and granulite facies but that their proportions are very different in each case. Fluid inclusions in granolites are predominantly carbonic, whereas those in amphibolite facies rocks are predominantly hydrous. Al Khatib and Touret (1973) reported that the numbers of carbon dioxide bubbles released by crushing of quartz in anhydrous glycerine was several orders of magnitude higher in quartz from granulite zones than from amphibolite zones nearby. Touret (1972) suggested the use of fluid inclusion data to map the orthopyroxene isograd, which is marked by a rapid rise in CO_2 content of the inclusions. Such a method could be advantageous in predominantly quartzofeldspathic terrains where quartz (containing inclusions) is widespread and orthopyroxene is restricted to metabasites or low-alumina metapelites. Specimens of granolite from all over the world invariably contain high-density fluid inclusions rich in carbon dioxide, provided there has been no post-metamorphic recrystallization of quartz (Touret, 1974).

During preliminary studies of fluid inclusions from the Aus area carbon dioxide-rich fluids were identified in the quartz grains of charnockites and granolites on the basis of their dark colour (Touret, pers. comm., 1975). These inclusions are abundant and widespread. Their identification was subsequently confirmed by an examination of the thin sections by Prof. Touret. Quantitative studies on the composition of the fluid phase in the charnockites and granolites have been started but the results are not available at this stage. From estimates of the distribution density of the CO_2 and H_2O inclusions, however, it appears that the proportion of carbon dioxide is somewhat higher in the charnockites than in the surrounding granolites; no carbonic inclusions were found in rocks of similar composition outside the granulite zone.

What is the source of the carbon dioxide that was apparently present in abundance during the granulite metamorphism? Touret (1971) suggested three possible sources:

(i) Calcareous rocks

(ii) Pelitic rocks containing graphite which combined with O_2 to form CO_2

(iii) juvenile CO_2

and is now of the opinion (Touret, pers. comm., 1975) that the last source is much more significant than the first two. The latter are unlikely to have provided sufficient quantities of CO_2 during metamorphism in the Aus granulite zone because both calcareous and pelitic rocks are more common *outside* the granulite zone. Carbon dioxide pressure was undoubtedly high in those areas with thick bodies of marble but this was insufficient to result in the formation of hypersthene in the surrounding metabasites. However, oxidation of graphite in the metapelites could be responsible for the presence of anhydrous conditions in the small area (H3) where hypersthene granolites have formed outside the main granulite zone.

The third source - juvenile carbon dioxide - appears most likely for the Aus area. The abundance of charnockitic rocks within the granulite zone and the development of granolites within and around the charnockites suggests that the charnockites themselves provided the carbon dioxide. This hypothesis is in agreement with the apparently greater abundance of CO_2 in the charnockites than in the surrounding granolites (described above). Evidence for an intrusive origin for the charnockites is given in Section 3.4. It is suggested that the charnockites were intruded during conditions of high-grade regional metamorphism and that abundant CO_2 was introduced together with them as a volatile constituent of the magma. This carbon dioxide-rich fluid phase permeated the already-heated country rocks and diluted the water-rich fluids there thus producing largely anhydrous conditions which resulted in the decomposition of hornblende to produce orthopyroxene over a wide area around the charnockites. It must be emphasized, however, that there is no evidence that the charnockites were at a higher temperature than the rocks which they intruded or for any form of contact metamorphism. The influence of the charnockites on the metamorphic evolution is restricted to the postulated emanations of carbon dioxide.

The partial pressure of CO_2 can be deduced from the PT conditions estimated in Section 4.6.3. Water pressure was estimated at 2 kb and P_t, between 5 and 7 kb. Assuming that the fluid phase contained negligable amounts of volatiles other than H_2O and CO_2 (Touret, 1974), the partial pressure of CO_2 would have been between 3 and 5 kb under the condition, $P_f=P_t$.

Consideration of the ultimate source of the carbon dioxide is not within the scope of this study. However, Touret (1974) suggested that CO_2 is concentrated in the lower part of the crust between the Conrad and Mohorovicic discontinuities. A possible reason for this concentration is that water is preferentially dissolved in magmatic masses; fluids would thus be enriched in carbon dioxide which, being extremely dense, would tend to sink to lower levels (ibid.).

9. Distribution of Charnockites in the Namaqua Metamorphic Complex

The discussion on the role of the charnockites in granulite metamorphism is here extended beyond the Aus area to cover the association between charnockites and granolites in other parts of the Namaqua Metamorphic Complex in southern South West Africa and the northwestern Cape.

The charnockites discussed here include all orthopyroxene-bearing plutonic rocks in the Namaqua Metamorphic Complex - irrespective of their age or whether they are of magmatic or metamorphic derivation. All these bodies are loosely referred to by the general term 'charnockite' (Turner, 1968, p.33; Clifford, 1974, p.3) but their formal or detailed nomenclature in this section follows that of Tobi (1971, 1972). Many of these charnockites have been retrogressed by later periods of hydrous metamorphism that were typically accompanied by this later metamorphism, but relicts of orthopyroxene are preserved in those parts that remained anhydrous.

definition would not generally be acceptable

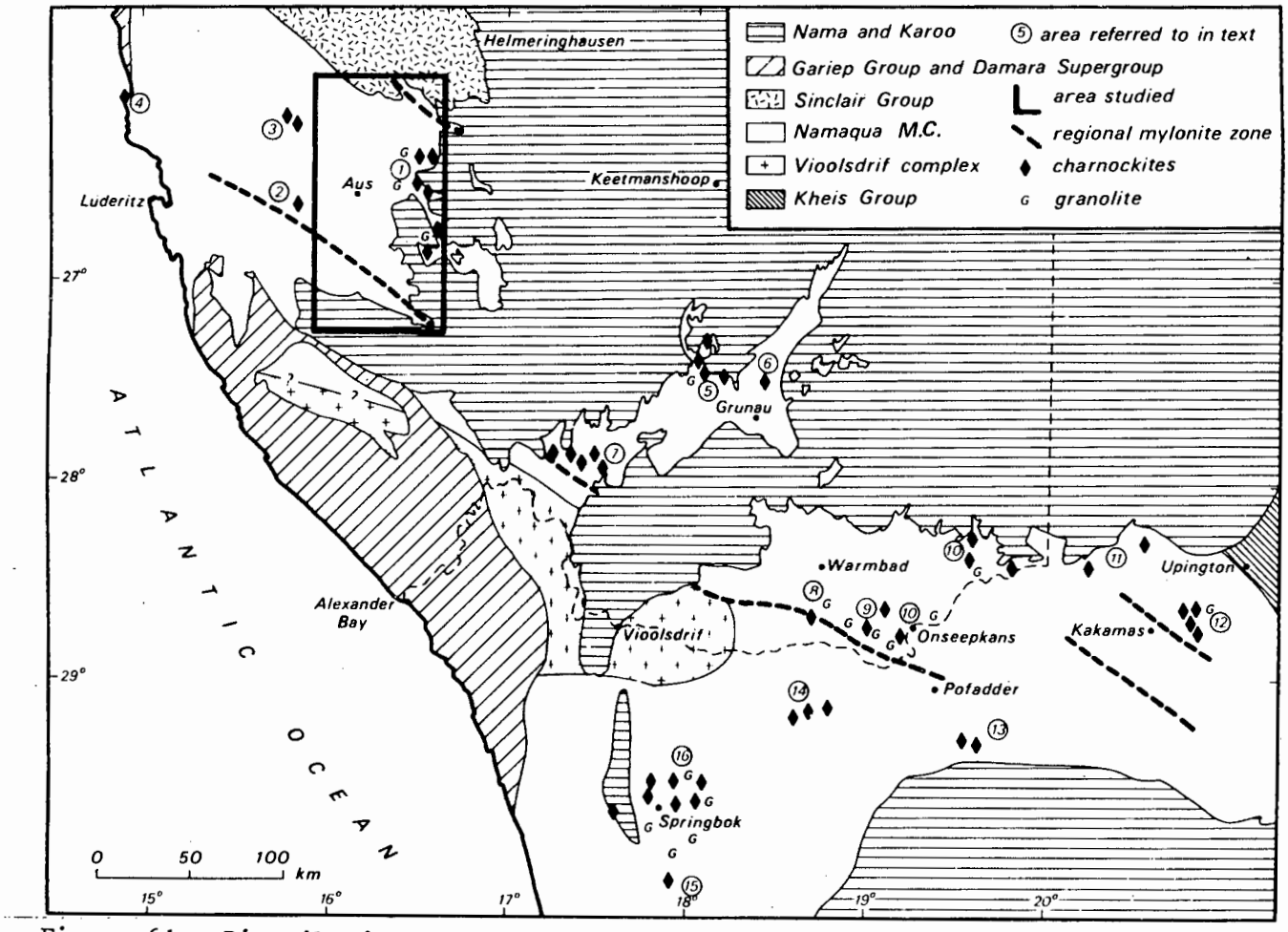

Figure 61. Distribution of charnockites and granolites in the Namaqua Metamorphic Complex (sources in text)

All charnockite occurrences in the Namaqua Metamorphic Complex known to the writer are shown in Figure 61. The individual occurrences and their sources of information are briefly summarized below. Most of the South West African occurrences have not been reported before so these will be described in more detail than those such as the O'Okiep charnockites which are better known.

In the eastern Lüderitz district of South West Africa the charnockites around Aus have already been described (area 1 on Fig. 61). Just west of the study area is the ultramafic Letterkuppe body (area 2) which has also been described in this report. Reconnaissance mapping by the writer and J. McDaid to the northwest (area 3) has revealed a large norite body, some 12 km long, which is partly amphibolitized. Other occurrences of charnockite in this area may be revealed by further mapping. Farther west (area 4) an outcrop of norite situated on the headland at Hottentot Bay (Kröner and Jackson, 1974, p.83) is almost entirely altered to amphibolite. It is the oldest intrusive rock in the area.

Just north of Klein Karas (area 5) is one of the largest masses of charnockitic rocks in the Namaqua belt - possibly in excess of 25 km wide (Blignault

et al., 1974, Annexure 1). Five handspecimens collected from different parts of this body indicate wide variations in composition from charnockite sensu stricto to charno-enderbite and monzonorite. The charnockite has been intruded by granite gneisses but is well preserved away from the contacts. Just east of Klein Karas (area 6) on the National Road some 11 km north of Grünau the writer found an outcrop of charno-enderbite. Mapping may reveal further bodies in the area.

To the southeast (area 7) is the large Ai-Ais complex (Blignault, 1976, Annexure 1), which consists mainly of 'metagabbro' with remnants of orthopyroxene; it may represent the amphibolitized remains of older charnockites.

In the Warmbad District hypersthene-bearing bodies are abundant and widespread though generally below 5 km in maximum dimension. The Tantalite Valley body (area 8) is a norite consisting of orthopyroxene, clinopyroxene and olivine (Beukes, 1973). It is situated in the core of the Pofadder Lineament (Joubert, 1974a) which transects southern South West Africa and the body is surrounded by highly cataclastic rocks (A.C. Moore, pers. comm., 1974; Toogood, 1976); its relation to the other rock units is therefore not known. The Kumkum body (area 9) is of similar composition (Beukes, 1973; Toogood, 1976).

Farther east (area 10) in the area around Onseepkans, charnockites of noritic and enderbitic composition constitute six bodies (Toogood, 1976). These bodies as well as the Kumkum body, are the oldest intrusive rocks in the area and contain xenoliths of the paragneiss sequence.

Still farther east in an adjoining area of the northwest Cape (area 11) Geringer (1973) reported the occurrence of charnockite sensu stricto from the Cnydas complex. The stratigraphic position of the charnockite is, unfortunately, not clarified (ibid., p.117 and folder 3). Geringer's Kourop River granite is also charnockitic in places, but the pyroxene is reported as 'diopside' (ibid., p.107), a mineral which is extremely unlikely in a granite and has probably been mis-identified for hypersthene.

To the southeast (area 12) between Kakamas and Upington are the well known charnockites described by Poldervaart and von Backström (1949), Poldervaart (1966) and von Backström (1964). A present study on the petrology of these charnockites suggests that much of the 'charnockitic adamellite' is hypersthene free (R. Schultz, pers. comm., 1975) so the outcrops of true charnockite in the area have been somewhat reduced in the sketch map (Fig. 61).

In Bushmanland a number of charnockites have been reported by Joubert 1974b, p.26). South of Pofadder at Nouzees (area 13) are norite bodies, some of which contain olivine. Other mafic charnockites are present north of the Haramoep range farther west (area 14).

In Namaqualand Joubert (1971) mapped similar bodies near Gamoep as 'pyriclasites' (area 15). North of here in the Springbok area (area 16) are the most intensively studied charnockitic rocks in the Namaqua belt. These rocks constitute the copper-bearing 'noritoid suite' which consists largely of diorite with lesser amounts of norite, hypersthenite and anorthosite (Clifford et al., 1975a, p.166); all these rock types would be represented as norites in terms of Tobi's classification of charnockites (1971). More than 700 of these

relatively small bodies were discovered in the O'Okiep copper district (van Zyl, 1975, p.166). These bodies were described by Benedict et al. (1964) and more recently several other studies have been carried out (e.g. Steyn, 1975; Stumpfl and van Zyl, 1975; van Zyl, 1975). These bodies show intrusive contacts with the country rocks but there is some doubt as to whether they differentiated at depth or whether they formed in situ by remobilization during very high grade metamorphism (Stumpfl and van Zyl, 1975). These charnockites postdate the M_2 metamorphism of Joubert (1971) and the intrusion of the Rietberg and Concordia granites (Clifford et al., 1975a).

10. Association of Charnockites with Granolites in the Namaqua Metamorphic Complex

The foregoing summary includes all orthopyroxene-bearing rocks of igneous appearance, regardless of their origin or relative age. In some cases, these rocks have been described as relatively late phenomena (von Backström, 1964; Benedict et al., 1964; Beukes, 1973; Clifford et al., 1975a), but there is increasing evidence that many of the charnockites played an integral role in the early metamorphic evolution of the terrains in which they are presently situated.

As has already been described there is a close association of early syntectonic charnockites with the granulite zone in the Aus area; the granolites appear to have been metamorphosed on a regional scale during the intrusion of the charnockites. A closely similar situation prevails in the Onseepkans area (area 10) where charnockites are the oldest intrusive rocks and are intimately associated with foliated hypersthene granolites of identical composition (Toogood, 1976). Similar hypersthene granolites are also developed away from the charnockites but these have been largely amphibolized by later hydrous metamorphism.

South of Warmbad Village (area 8) Beukes (1973, p.175) reported hypersthene-sapphirine metapelites from his Arus Formation, which he assigned to de Waard's (1965b) 'hornblende-orthopyroxene-plagioclase granulite' subfacies. Similar metapelites of granulite grade in the neighbourhood of the Kumkum body (area 9) were tentatively attributed to contact metamorphic effects of the intrusion by Beukes (1973). But in view of the more recent work by Toogood (1976) in the same area, it appears more likely that these are granolites developed on a regional scale early in the metamorphic history. Farther east, in the Onseepkans area, sillimanite takes the place of hypersthene in the granulite grade metapelites (Toogood, 1976); this is probably due to a higher alumina content in these rocks (Hensen and Green, 1973). Thin strips of hypersthene-bearing metabasites within the 'grey gneiss' some 10 km north of the Tantalite Valley body (area 8) that were mapped as 'hypersthene gabbro' by Beukes (1973) may be equivalent to the widespread retrogressed mafic granolites reported by Toogood (1976) farther east in the Onseepkans area.

The large charnockite body north of Klein Karas (area 5) is also associated with granolites. Inclusions within the charnockite include fine-grained hypersthene granolites, some of which have a strong fabric. Metapelites that contain coexisting cordierite and garnet are also found as inclusions at the same

locality; this paragenesis implies certain pressure limits which are not characteristic of contact metamorphism (Currie, 1971; see also Section 4.3). The hypersthene-bearing rocks are therefore produced by regional metamorphism and cannot be attributed merely to contact metamorphism by the charnockite.

Granolites are also associated with the charnockite near Kakamas, which was reported by von Backström (1964) to have intruded a terrain of low-grade and medium-grade metamorphic rocks. However, recent mapping by J. van Bever Donker and R. Schultz of the Precambrian Research Unit has shown the presence of remnant sillimanite and diopside within the chlorite zone (R. Schultz, pers. comm., 1975). The chlorite and muscovite zones appear to be retrogressive and were produced by the pronounced northwest-trending shearing in the area. Some of the rocks interpreted by von Backström (1964) as having formed in contact metamorphic aureoles apparently represent remnants of much higher grade regional metamorphism. Thus wollastonite is present in numerous localities up to 5 km away from the charnockites and is separated by a 'chlorite zone' from them. These wollastonite-bearing rocks are associated with hypersthene-cordierite-garnet metapelites (R. Schultz, pers. comm., 1975). The coexistence of cordierite and garnet is possible only at pressures characteristic of regional metamorphism (Currie, 1971) and it is most likely that these hypersthene-bearing rocks are of granulite grade.

Cornell (1975, p.25) reported the presence of granolites from the Marydale Formation of the Kheis Group on Happy Valley Farm. These rocks are unfoliated granoblastic, hypersthene-pyroclase granolites; in the foliated varieties, poikiloblastic garnet is present. Vajner (1974, p.178) recorded the assemblage 'clinopyroxene + almandine' from nearby but, on the basis of field evidence he mapped the two-pyroxene granolite as metagabbro. According to Cornell (1975, p.27), cataclastic hypersthene-pyroclase granolites are also present on the neighbouring farm, Irene, and these rocks grade into hypersthene-bearing intermediate rocks, which he regarded as metamorphic. There exists the possibility that the latter rocks form part of a charnockitic suite.

The noritoid suite of the O'Okiep area is situated in a broad zone of granolites of mafic and pelitic composition (Joubert, 1971). The compositions of some of the charnockites are identical to that of the mafic granolites (T.N. Clifford, pers. comm., 1975). Clifford et al. (1975b) have tentatively suggested that the charnockites were derived by partial fusion of metabasites during the M_2 metamorphism and were intruded into their present position. Despite a discrepancy of some 200 Ma between the radiometric ages of the charnockites and the M_2 metamorphism, it is possible that these rocks form a genetically-related charnockite-granolite association (T.N. Clifford, pers. comm., 1975).

In summary therefore, granulite facies metabasites and metapelites are associated with charnockitic rocks in the areas around O'Okiep, Marydale, Kakamas, Onseepkans, Warmbad, Klein Karas and Aus. There exists the very strong probability that detailed mapping in other parts of the mobile belt will reveal more associated charnockites and granolites.

11. *Regional Variations in Granulite PT Conditions in the Namaqua Metamorphic Complex*

If the PT estimates based on mineral parageneses and chemistry for the O'Okiep, Warmbad and Aus areas are compared, then certain differences become apparent. These three areas all contain the assemblage 'orthopyroxene + clinopyroxene + plagioclase' which is indicative of medium-pressure granulite metamorphism (Green and Ringwood, 1967). However, as shown below there is a successive reduction in pressure estimates for the granulite metamorphism in a northward direction.

South of the O'Okiep area Joubert (1971, p.45) reported the presence of the assemblage 'clinopyroxene + almandine + plagioclase' in a restricted area between Springbok and Gamoep. This was reported (ibid., p.121) to be the highest metamorphic zone (zone E) in Namaqualand. This assemblage suggests relatively high-pressure granulite metamorphism (de Waard, 1965b). According to the data of Green and Ringwood (1967) the minimum pressure for the appearance of almandine in rocks of quartz tholeiite composition at a temperature of 850°C is approximately 10 kb, depending on the $Mg/(Mg + Fe^{+2})$ ratio. Kushiro and Yoder (1966) suggest a pressure of more than 8 kb at 850°C for the lowest stability of almandine in these rocks. Such granolites are in the highest pressure classification of Green and Ringwood (1967) and de Waard (1965b) where orthopyroxene is not stable with plagioclase. Because the curve of the garnet-forming reaction has a positive and relatively flat slope the assemblage 'clinopyroxene + almandine' would indicate that the area in which it is found was the site of deep-seated high-pressure granulite metamorphism, rather than a regional thermal dome; increase of temperature would *discourage* the formation of this assemblage. However, it is probable that the garnet in Joubert's (1971, p. 45) 'garnet granulite' is not almandine-rich but is grandite because it is associated with the calcareous minerals, clinopyroxene, bytownite and sphene and because orthopyroxene and plagioclase coexist in the same area (ibid. Tables 7, 8, 9; Folder 2). Thus the granolites of zone E were probably not formed under higher pressure than those of zone D.

In the O'Okiep area almandine is absent from the metabasites (T.N. Clifford, pers. comm., 1975). The PT conditions of the granulite metamorphism in this area have been estimated by Clifford et. al., 1975b) as follows. The high alumina content (7%) of orthopyroxene in the metabasites suggests that temperatures of 900-1000°C may have prevailed (Anastasiou and Seifert, 1972). The high pyrope content of garnet in the metapelites (25%) suggests high pressures. These data, together with the paragenesis 'hypersthene + diopside + plagioclase', suggest that temperatures of 800-1000°C and pressures of 6-8 kb prevailed during granulite metamorphism. E.F. Stumpfl (pers. comm., 1975) has suggested pressures of up to 10 kb for the granulite metamorphism.

Beyond the Orange River in the Warmbad District Toogood (1976) has estimated a pressure range of 8-9 kb, assuming a temperature range of 780-860°C (based on the geothermometric data of Hewins, 1975) for the granulite metamorphism. These pressure estimates are based on the upper pressure limit of 8 kb for the stable coexistence of olivine and plagioclase, which have reacted together to produce corona structures in the charnockites. Cordierite was apparently not stable during the granulite metamorphism because almandine in

metapelite inclusions in the charnockites is rimmed by later cordierite. An upper pressure limit of 9 kb is provided by the stable coexistence of orthopyroxene and clinopyroxene and the consequent absence of almandine from the metabasites (Kushiro and Yoder, 1966).

In the Aus area farther north the pressure estimates for the granulite metamorphism are lower because 'cordierite + almandine' is stable in the granulite facies metapelites. However, the widespread metabasite mineral paragenesis 'orthopyroxene + clinopyroxene + plagioclase' suggests low intermediate-pressure granulite metamorphism (Green and Ringwood, 1967). Estimates of P_t for the Aus granulite metamorphism are 4,5-8 kb (probably 5-7 kb) within the probable temperature range of 780-860°C for hornblende-bearing granolites (Hewins, 1975).

In summary therefore there are slight reductions in the pressure estimates for granulite metamorphism in a northward direction if the *maximum* estimates are considered: in the Springbok area, 8 or 10 kb; in the Onseepkans area, 9 kb; and in the Aus area, 7 or 8 kb.

12. *Regional Variations in the Charnockite Compositions in the Namaqua Metamorphic Complex*

In a previous section describing the distribution of the charnockite bodies in the Namaqua Metamorphic Complex, the composition of these bodies was briefly referred to. If these compositions are plotted on a sketch map (Fig. 62), regional variations are immediately apparent. Because few chemical analyses are available for the majority of these bodies, it was decided to differentiate the charnockites into three groups on the basis of their quartz content:

(i) *quartz-free*, usually olivine-bearing (olivine norites, orthopyroxene-bearing peridotites, pyroxenites etc.)

(ii) *quartz 0-20%* (quartz norites, monzonorites)

(iii) *quartz>20%* (enderbites, charno-enderbites, charnockites sensu stricto)

These three compositional groups are plotted in Figure 62. They will be referred to sensu lato as '*ultrabasic*', '*basic*', and '*intermediate*', respectively. The plotted points represent charnockites for which data on modal composition are available (sources of data are given below); charnockites of unknown composition are represented by question marks.

Reference to Figure 62 indicates marked regional variations in the composition of the charnockites. If the major structural dislocation known as the Pofadder Lineament (Joubert, 1974a) is used as base-line, the charnockites become increasingly more acidic away from the lineament in a northeasterly direction. Quartz-free olivine-bearing norites are widespread in the vicinity of the lineament south of Warmbad (Beukes, 1973; Toogood, 1976) and bodies closest to the lineament in the Aus area are also quartz-free.

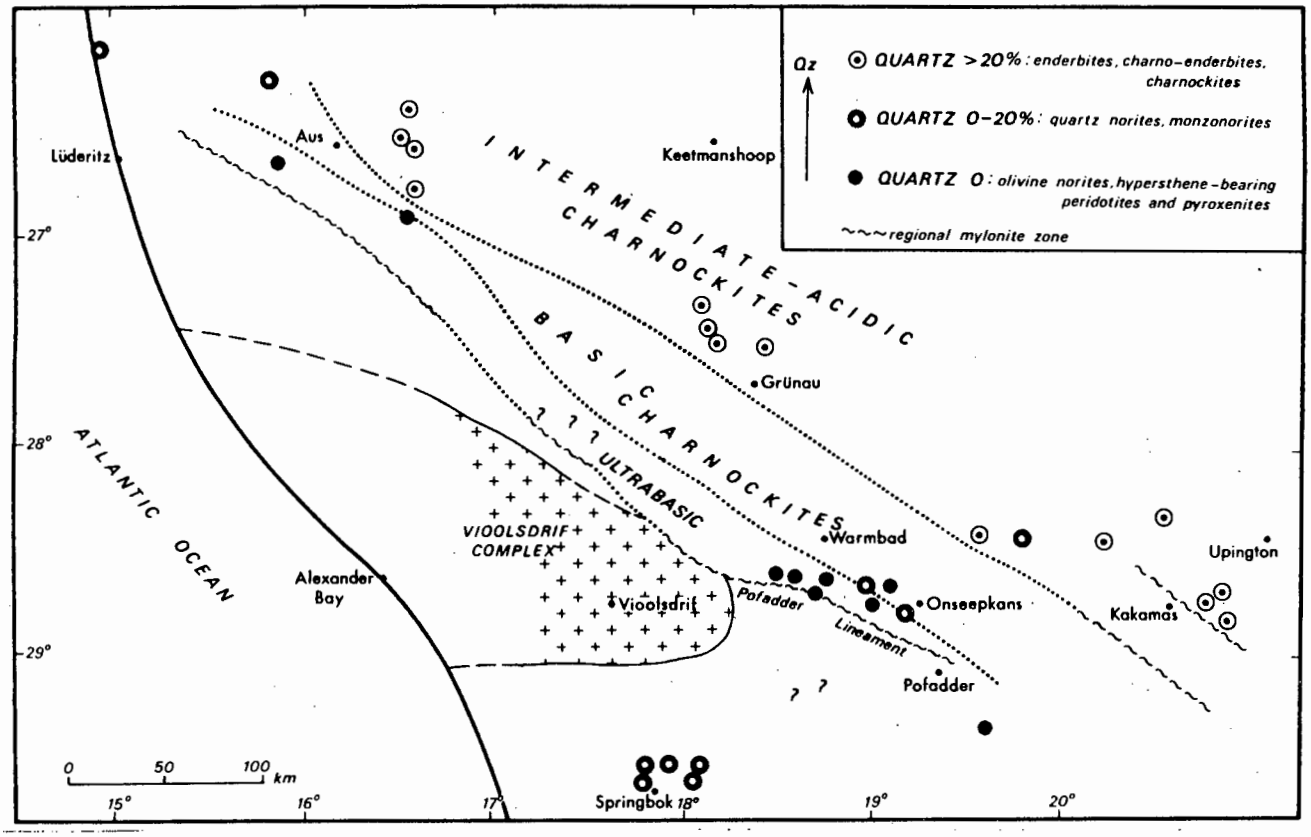

Figure 62. Regional variations in the composition of charnockitic rocks in the Namaqua Metamorphic Complex

Quartz-norites representing the 'basic' group are present to the south-east and east of Warmbad at a greater distance from the Pofadder Lineament than the 'ultrabasic' group in this area. They are also present to the north and northeast of Lüderitz. Most of the charnockitic rocks in the O'Okiep area are quartz-bearing; of the great many bodies examined only the minority are olivine-bearing or contain quartz in quantities greater than 20% (C.J.V. Wheatley, pers. comm., 1975). They thus fall into the 'basic' category.

'Intermediate' charnockites (quartz content> 20%) are widespread away from the Pofadder Lineament. They are especially common east of Aus, north-west of Grünau and southwest of Upington. There is also a trend of increasing potassium content of these rocks away from the shear zone as reflected by the increasing content of K-feldspar: enderbite (plagioclase/(total feldspar) > 0,9) is present near the southern margin of the 'intermediate' zone east of Warmbad (Toogood, 1976); charno-enderbite (plagioclase/(total feldspar) = 0,65-0,9) constitutes most of the 'intermediate' zone; charnockite sensu stricto (plagioclase/(total feldspar) < 0,65) is present in one of the northernmost charnockites near Aus and is dominant in the area east of Upington (Geringer, 1973) which is situated farthest from the trend of the Pofadder Lineament.

There is thus a trend of increasing acidity (as indicated by rising quartz content) and of increasing K_2O content (as indicated by rising K-feldspar content) in the charnockites northeastwards from the trend of the Pofadder Lineament. It is suggested that such compositional changes can be correlated with the variations in PT estimates described in the preceding section. According to Lambert and Heier (1968, p.43), granulite metamorphism results in an upward migration of K, Si, Rb, Pb, Th and U into regions of lower pressure, while the deeper regions are enriched in Ca, Fe, Mn and Ti. Lower-pressure granulite zones would thus be expected to be comparatively enriched in the elements K and Si, whereas higher pressure granulite zones would be enriched in the elements Ca, Fe and Mn.

It is therefore possible that the observed compositional differences in the charnockites in southern South West Africa and neighbouring areas may be explained by a decrease in pressure during the granulite metamorphism within the crustal levels presently exposed; successively higher levels of crust may be exposed in a northeasterly direction from the trend of the Pofadder Lineament. The granulite metamorphism predates the lineament but this major dislocation has altered the present distribution of regional metamorphic zones by bringing into juxtaposition different crustal blocks; a medium-stage (Winkler, 1974) metamorphic zone on the southern side is in contact with a high-stage zone on the northern side (Toogood, 1976). Tilting of the northern block in a northeasterly direction would result in the exposure of deeper areas of the crust immediately north of the lineament and successively higher crustal levels towards the northeast. In this way, higher-pressure charnockites (enriched in Ca, Fe, and Mn) would be exposed near the lineament and lower-pressure charnockites (enriched in Si and K) would be exposed away from it.

The evidence cited indicates a general decrease in the estimated temperature limits for granulite metamorphism from south of Springbok to Aus. It is possible that the higher pressure estimates for the Warmbad area with respect to the Aus area are due to the proximity of the former area to the Pofadder Lineament. The pressure estimates for the Onseepkans area were derived from mineral parageneses in the vicinity of the Kumkum charnockite body (D.J. Toogood, pers. comm., 1975) about 6 km north of the lineament. In contrast estimates for the Aus area are based on areas situated 30-50 km from the lineament.

It is not yet known how widely this model (higher pressure granolites/basic charnockites, lower pressure granolites/intermediate charnockites) can be applied. The O'Okiep area, for example, which shows evidence of higher-pressure granulite metamorphism, is dominated by 'basic' charnockites, rather than olivine-bearing varieties as would be expected. However, the hypothesis does explain the absence of the more acidic charnockites in the O'Okiep area.

13. Summary of Conclusions

Both diopside and hypersthene in the Garub granolites appear to have formed by breakdown of hornblende although hornblende is stable in many of these rocks. Biotite is stable in both the metabasites and the metapelites in the the granulite zone and does not appear to have contributed to the formation of the pyroxenes.

Within the temperature limits typical of hornblende-bearing granolites around the world (780-860°C) suggested by Hewins (1975), the mineral parageneses in rocks of mafic, ultramafic and pelitic compositions from the Aus area suggest extreme limits of P_t between 4,5 and 8 kb, probable limits of 5-7 kb, and P_{H_2O} equal to 2 kb. The environment was therefore largely anhydrous during the granulite metamorphism.

Although their present textures are predominantly metamorphic, the field relations of the Jakkalskop charnockites indicate that they were originally at least partially molten. The presence of hypersthene and micro-perthite, and the extreme elongation ratios of apatite and zircon grains suggest high temperatures of crystallization for these charnockites.

The Jakkalskop charnockites have mineral parageneses characteristic of the granulite facies and are widespread within but entirely restricted to the granulite zone, which extends over a broad area around them. Abundant CO_2-rich fluid inclusions within the quartz grains of the charnockites and the surrounding granolites suggest that dilution of the hydrous fluid phase by CO_2 created the largely anhydrous conditions necessary for granulite metamorphism (in this case, P_{H_2O}= 2 kb, P_{CO_2}= 3-5 kb). It is speculated that the CO_2 was most likely to have been juvenile and supplied when the charnockites were emplaced during high-grade regional metamorphism. CO_2- rich fluids are postulated to have permeated the already-heated country rocks and stabilized the formation of orthopyroxene in metabasites around the charnockites.

Elsewhere charnockites are found to be present in at least 16 widely scattered localities in the Namaqua mobile belt in southern South West Africa and the northwest Cape. In a number of these localities (viz. the Aus, Klein Karas, Warmbad, Onseepkans, Kakamas, Marydale and O'Okiep areas) granolites are also shown to be present. It would appear therefore that the charnockite-granolite association, which is widespread throughout central and northern Africa (Clifford, 1974) is also well represented in the Namaqua mobile belt.

There is a slight northward reduction in the maximum pressure estimates in the three areas where the PT conditions of granulite metamorphism have been estimated: in the O'Okiep area, 8 or 10 kb (Clifford et al., 1975b); in the Onseepkans area, 9 kb (Toogood, 1976); in the Aus area, 7-8 kb.

If the compositions of the charnockites throughout the Namaqua Metamorphic Complex are divided into three groups on the basis of their quartz content, there is a well-defined trend of increasing acidity northeastwards from the Pofadder Lineament. A similar rise in the proportion of K-feldspar is also shown. Following Lambert and Heier (1968) it is suggested that these compositional trends reflect different prevailing pressures in the environment where the charnockites formed. It is speculated that tilting of crustal blocks during the major shearing that formed the Pofadder Lineament resulted in the exposure of successively more shallow crustal levels northeastwards from the lineament; this may be responsible for the decrease in pressure estimates for the granulite metamorphism referred to in the previous paragraph.

Chapter 5

MIGMATIZATION

Migmatites are distributed over most of the Aus area and the process of migmatization has profoundly affected pre-existing rocks and generated new rocks. Because of this widespread and profound effect, any investigation of the geology of this terrain would be incomplete without a study of the nature and causes of migmatization.

Processes such as metamorphic differentiation, metasomatism and magmatism may well have contributed to the formation of migmatites. These rocks are complex and no simple explanation or model is completely adequate to explain their formation. However, it is felt that an anatectic model best explains the formation of migmatites in the Aus area and the descriptions and discussions in this chapter are therefore centred around this concept.

5.1. ANATECTIC PROCESSES IN THE LIGHT OF EXPERIMENTAL STUDIES

Read (1951) and Simonen (1960) described the intimate association between high-grade metamorphism and the formation of granitic melts. The inevitability of large-scale partial melting of suitable rocks during high-grade regional metamorphism has been confirmed and strengthened by the results of recent experimental work (Mehnert, 1968, 1971, p.350; Fyfe, 1973, p.13; Winkler, 1974, p.299). Within the last decade experimental evidence has been accumulated to show that quartz-K-feldspar-mica gneisses and schists begin to melt under pressure at temperatures well below those attained during high-grade metamorphism, providing sufficient H_2O is present to saturate the melt.

Under these conditions of water saturation the temperature at which melting takes place at a given pressure depends both on the proportions of quartz/alkali feldspar/plagioclase in the rock and on the anorthite composition of plagioclase (Winkler and von Platen, 1961). At the critical temperature of

minimum melting, quite small differences in anorthite content of the plagioclase in otherwise very similar rocks will determine whether a pelitic gneiss will be half-melted (plagioclase An_{13}) or unaffected by melting (plagioclase An_{30}) (ibid.). However, most gneisses in high-grade terrains contain plagioclase between the compositional limits of An_{10} and An_{35} (Winkler, 1974, p.281) and the minimum melting curves for rocks of these compositions define a relatively narrow band.

The initial melt consists of a water-saturated cotectic mixture of An-Ab-Or-Qz (ibid., p.280). After one of these components has been completely melted (typically a feldspar) higher temperatures are required for the production of melts of more simple composition which coexist with (unmelted) quartz and the remaining feldspar. If the unmelted feldspar is plagioclase, it is likely to be more anorthitic than it was before anatexis (Steuhl, 1962). Further increase in temperature will melt all the plagioclase, and quartz only will be left in the melanosome. Higher temperatures are required to melt the ferromagnesian components of the melanosome - first biotite, then hornblende, then garnet, then the opaque minerals. These minerals are increasingly refractory and it is doubtful whether sufficient temperatures are produced during regional metamorphism to melt more than the hydrous minerals mentioned.

By this process of selective melting, large amounts of quartzofeldspathic material may be produced, providing $P_{H2O} = P_t$. Winkler (1974, p. 306) cites figures of 50% melt produced by pelitic rocks and 70-95% melt produced from greywackes, which have a composition nearer to that of the cotectic melt.

However, it is probable that the condition of $P_{H_2O} = P_t$ may not always apply to the melting of natural rocks. The widespread occurrence of garnet in the neosomes of the Aus migmatites suggests that the melt was not always saturated with water and was wholly or partially anhydrous (Fyfe, 1971, p.204). As pointed out by Mehnert (1968, p.242) the original water content of the rock during melting is difficult to determine because all chemically uncombined water is driven out during crystallization. But if almandine is present in the neosome, it is probably safe to assume anhydrous conditions (otherwise biotite would have formed instead from the available Fe, Mg, and Al). However, this assumption only holds true if the garnet is known to have crystallized from the neosome melt. In many places garnet is concentrated into trains which commonly border the palaeosome of the migmatite. This suggests that the mineral represents that part of the palaeosome which was not dissolved in the melt because of the mineral's refractory nature (the quartz, feldspar, and biotite in the palaeosome being entirely melted). In melanocratic rocks there is a large temperature range between initial and complete melting of all the components so that a melanosome enriched in Mg, Fe, Ti, and Al is left as a restite.

If the melt is not saturated with water and P_{H2O} is less than P_t, the minimum melting curves are not applicable. If no water is added from an external source, would melting take place in dry rocks of semi-pelitic and pelitic composition under the PT conditions estimated for amphibolite facies metamorphism in the preceeding chapter? Figure 63 shows the melting curves for dry rocks from Fyfe (1971, p. 212) and Winkler (1974), p.293). The melting of muscovite, biotite and hornblende requires progressively higher temperatures and the reactions yield progressively smaller amounts of water (Fyfe, 1971, p.210). From the position of the estimated PT field for the Aus amphibolite

metamorphism (hatched field in Fig. 63), which accompanied migmatization, it would appear that melting of the muscovite component would have taken place throughout almost the entire study area and that temperatures were sufficient to melt dry biotite granite in parts of metamorphic zone III, which covers the very large central zone of the study area (Fig. 55). Under these conditions a biotite schist or gneiss would be capable of melting completely (except for its refractory content of garnet, sillimanite, etc).

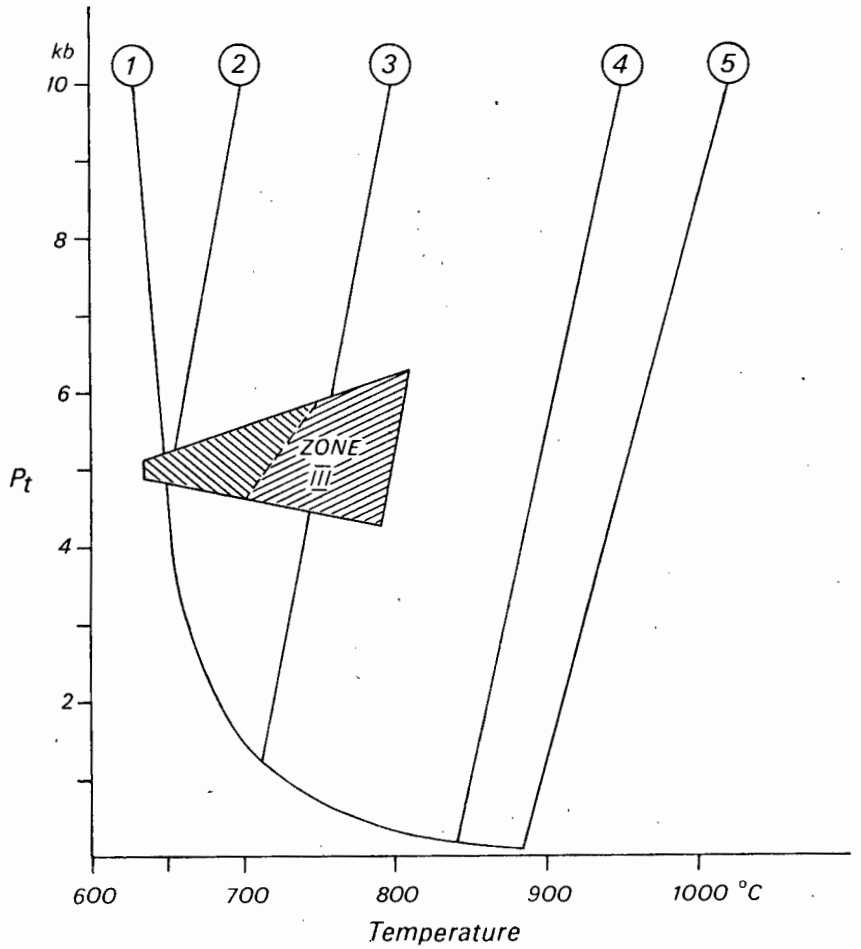

Figure 63. PT diagram showing melting curves for various hydrous minerals in dry rocks compared to the minimum melting curve. Hatched area represents estimated PT field of Aus amphibolite metamorphism
(1) minimum melting in Qz-Ab-Or system, $P_{H_2O} = P_t$
(2) beginning of melting in dry muscovite granite, Mu is sole OH-mineral
(3) beginning of melting in dry biotite granite, Bi is sole OH-mineral
(4) beginning of melting in dry hornblende granitoid, Hb is sole OH-mineral
(5) melting in dry Qz-Ab-Or system, no OH-minerals present
Curves 2 and 4 *after* Fyfe (1971); curves 1, 3 and 5 *after* Winkler (1974)

Plate 31. Thin layers of grandite-quartz rock (dark) in matrix of wollastonite (light). Specimen MJ530, Garub sequence. Bienenstich Hills (E7)

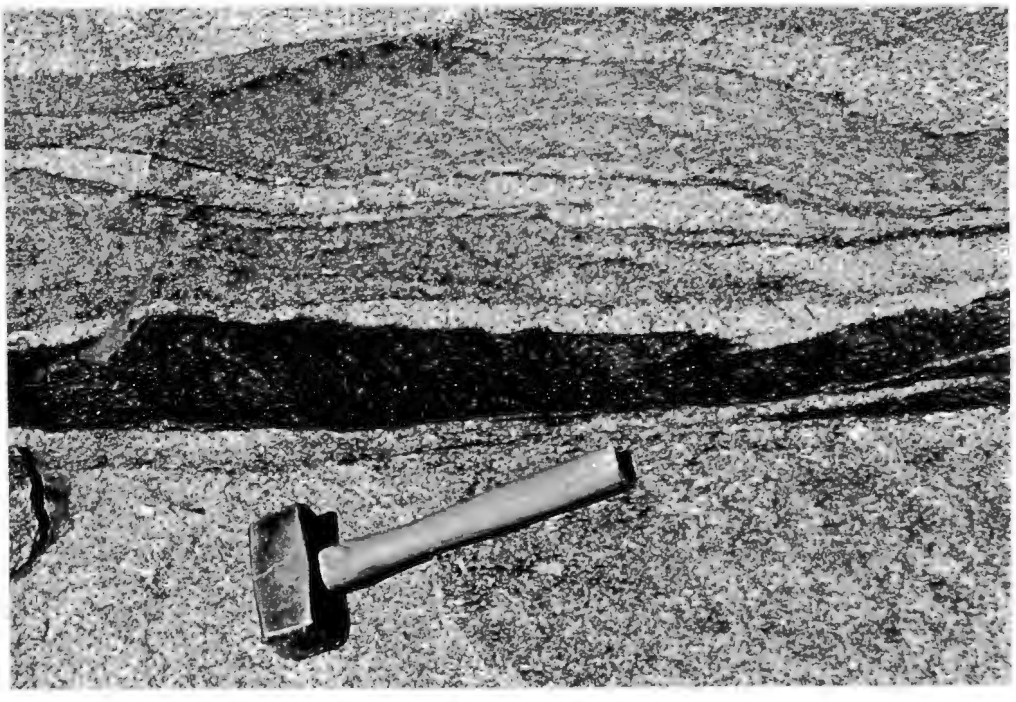

Plate 32. Remnants of Garub rocks in biotite granite gneiss, showing selective melting; biotite-hornblende schist (dark grey) has been depleted of biotite content by melting, leaving hornblende grains defining nebulitic structure; amphibolite (black) has not melted. 4 km W of Löwenberg (E4)

Figure 63 suggests that melting of hornblende is not possible within the PT field estimated for the amphibolite facies metamorphism. Any hornblende present in the biotite schists could therefore not be dissolved in the melt. An example of this selective melting of biotite from the Aus area is illustrated in Plate 32. Syntectonic biotite granite gneiss surrounds two different Garub rock types. A strip of dark amphibolite near the hammer is unaffected by the surrounding melt. Above the amphibolite are two strips of paler hornblende-biotite schist which have been depleted of their biotite content by selective melting; only the hornblende remains as a nebulitic structure showing the outlines of the schist. At the end of the central strip hornblende is dispersed in the melt or concentrated into schlieren. The melting of biotite is further suggested by the presence of flecks of cordierite in the surrounding granite gneiss at the same locality. On incorporation into the melt biotite melts incongruently (von Platen and Höller, 1966) to form cordierite and K-feldspar. On crystallization under high grades of metamorphism some of the cordierite will form stichtolithic segregations rich in biotite and cordierite.

As shown in Figure 63 the maximum estimated PT field for melting in the Aus area straddles the curve for the melting of dry biotite granite. Even if the biotite melts completely - which seems unlikely - then this process will probably not supply sufficient water to form a water-saturated melt (Lundgren, 1966). Mehnert (1968, p. 243) is of the opinion that introduction of H_2O into the system is necessary for anatexis to take place. The amount of water required for saturation of the melt is, however, relatively small, even for large quantities of melt. Thus 5% H_2O permeating a rock, if dissolved in a melt constituting 50% of the rock, would produce a 10% water content in the melt; this is the saturation limit for a pegmatoidal melt (Mehnert, 1968, p. 242).

Part of the water in the melt would be chemically bonded into hydrous minerals (mainly biotite) during crystallization; the remainder would be expelled during this process. If it migrated, this expelled water could then be used in other melting reactions elsewhere. In this manner, given sufficient time, a large mass of rocks could be melted and recrystallized to produce anatectic granitoids. If the temperature of the granitic melt is appreciably higher than its solidus temperature, then the magma is capable of rising a substantial amount before a lowering of pressure raises the solidus temperature sufficiently to induce crystallization, especially if the magma is water deficient (Fyfe, 1971, p. 210). Large masses of granitoid melts may therefore be intruded into areas adjacent to the zones of melting where amphibolite facies metamorphism prevails.

5.2. APPROACH ADOPTED IN THE PRESENT STUDY

In this study the concept of 'migmatitic grade', which is based on the anatectic model described above, is employed. The grade of migmatization does not simply reflect the local abundance of migmatitic neosome, which is largely dependent on the bulk composition of the rock undergoing melting. Nor is it a straightforward correlate of metamorphic grade because it is influenced by

the factors of bulk composition and availability of water. Migmatitic grade is a measure of the degree of homogeneity attained by a rock during progressive melting. This degree of homogenization reflects the extent to which the process of anatexis has advanced in any one area.

The aim of the present study is the production of a map showing not only the extent of the migmatites in the Aus area but also variations in the grade of migmatization in different parts of this area. The map is based on descriptive features recorded in the field and lays the groundwork for detailed geochemical and petrofabric studies in much smaller areas (e.g. Sharma, 1969; Harris, 1974) which have not been attempted here.

The migmatite nomenclature used in this study follows that of Dietrich and Mehnert (1960) to which paper the reader is referred for definitions. The non-genetic term 'neosome' is applied only to the migmatite component that shows evidence of being younger than the palaeosome and not simply to gneissic layering.

5.3. FIELD OBSERVATIONS

Where migmatites were observed in the field a simple set of characteristics was recorded (Appendix 1):

(i) *lithology of neosome*: three types were present: (1) quartz-feldspar pegmatoid, (2) fine-grained biotite granite gneiss, and (3) coarse-grained megacrystic leucocratic granite gneiss

(ii) *abundance of neosome*: this was recorded semi-quantitatively as 1-10%, 10-30%, 30-60%, and >60%.

(iii) *style of migmatization*: the ten migmatite styles of Mehnert (1968) were used as a basis.

Although it is a commonly recorded attribute of migmatites, style is the result of the complex interaction of a number of factors:

(i) the abundance and character of the neosome

(ii) the lithology of the palaeosome

(iii) viscosity contrast of palaeosome and neosome during deformation

(iv) the stress environment, which covers the type and degree of deformation.

Thus details of migmatitic style are difficult to interpret without a thorough study of all these factors.

There is, however, a general dichotomy between the predominantly *metatectic* styles (blastic, stromatic and phlebitic) and the predominantly *diatectic* styles (schlieric, nebulitic and homophanous). Mehnert (1968) suggested that

Plate 33. Quartz-feldspar blastesis in Garub biotite schist. Garub Station, Diamond Area (G2)

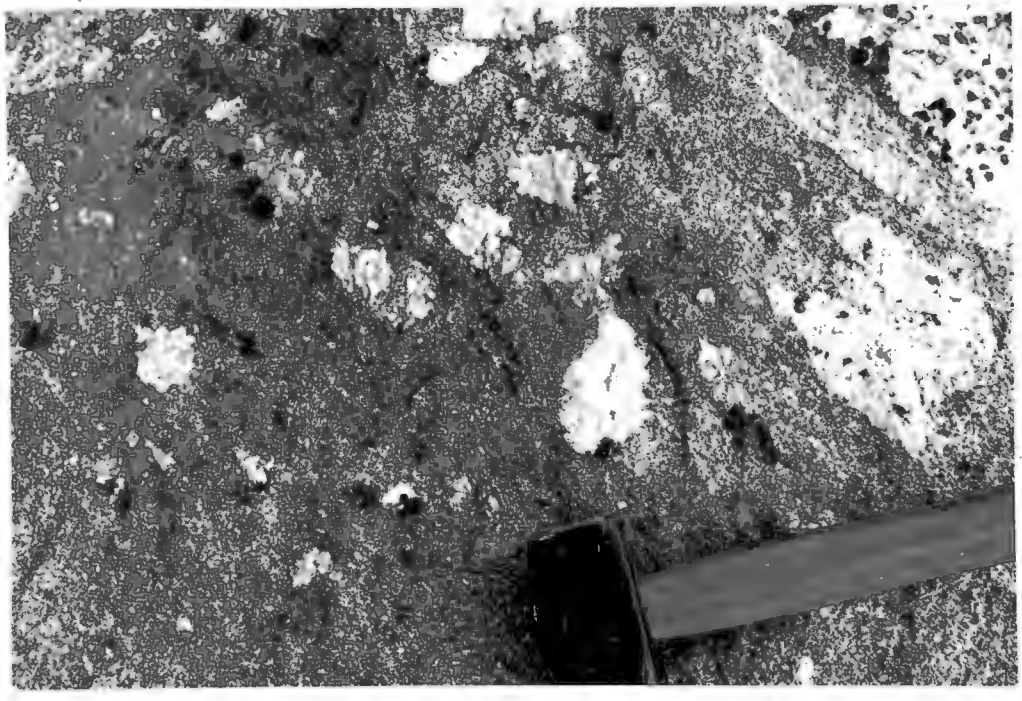

Plate 34. Quartz-feldspar-garnet blastesis in biotite granite gneiss. 1 km SE of Klein Aus farmstead (G4)

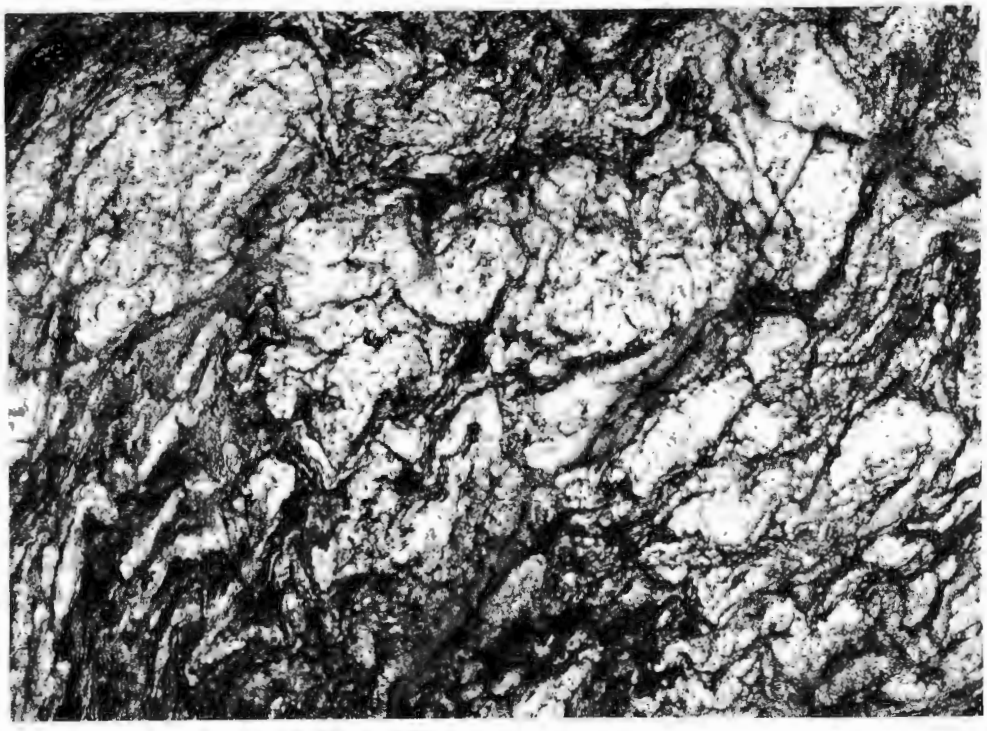

Plate 35. Veined migmatite: extensive and irregularly developed metatectic neosome of venitic origin in Garub biotite schist. Area shown is 40x30 cm. 1 km NE of Kububer Horn (H4)

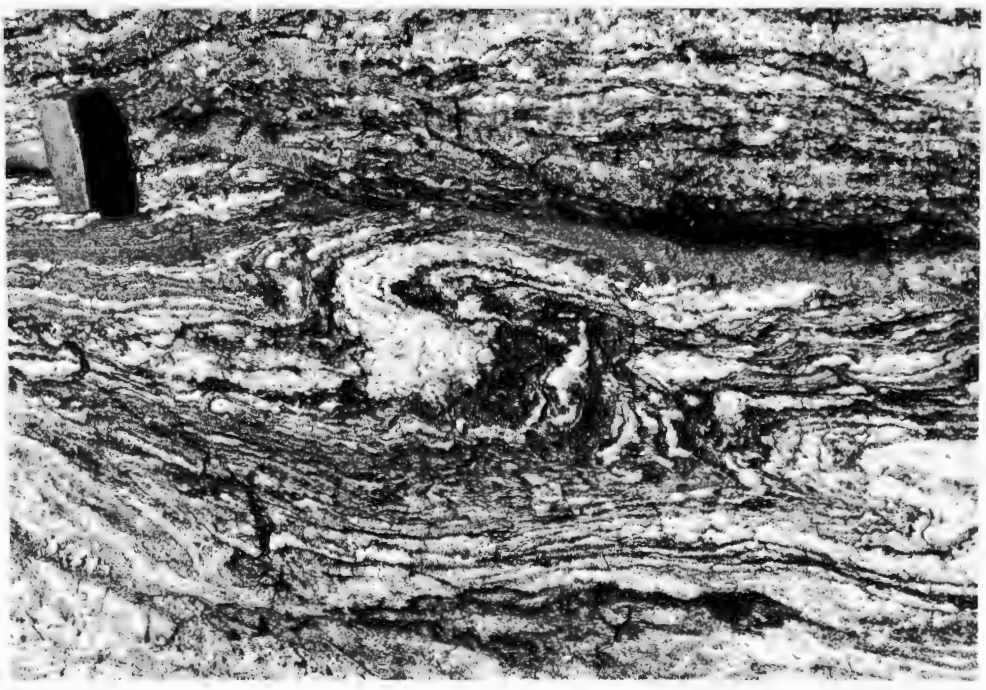

Plate 36. Venitic metatectic migmatite folded during D_2. Garub biotite schist. 1 km NE of Kububer Horn (H4)

the metatectic styles are characteristic of the outer parts of anatectic massifs and the diatectic styles, of the inner parts.

At an early stage in the present field work it became apparent that the stromatic or veined types are common throughout most of the Aus area. In the centre of the area these migmatitic styles are followed by, and partly obliterated by, schlieric or nebulitic granitoids. A simple example of this is an inclusion of veined migmatite within schlieric granitoid. The granitoids, typified by the Kubub granite gneiss, show field evidence for derivation by anatexis and homogenization of older rocks. This suggests a migmatitic sequence from metatexis to diatexis such as one would expect under conditions of prograde metamorphism. In this model metamorphic rocks of suitable composition are converted to heterogeneous migmatites by selective melting of their quartzofeldspathic component (metatexis) and then to nearly homogeneous granitoids by melting of their biotite component (diatexis). The migmatitic sequence from blastesis to nearly complete melting is described below and illustrated by photographs of field relations.

1. *Blastic Migmatites*

Isolated quartzofeldspathic segregations (blasts) are not a common feature of the Aus migmatitic terrain. However, limited blastesis has taken place in both the Tsirub gneiss (Plate 41) and in the Garub rocks (Plate 33). It has also taken place in much younger rocks: Plate 34 shows a granitic mobilizate (representing the culmination of migmatization) that has undergone later blastesis.

The formation of the augen in the Tsirub gneiss was ascribed to blastesis in a preliminary report (Jackson, 1974), but strong evidence has since been assembled (Section 3.3) that contradicts this hypothesis. The bulk of the augen are now thought to represent the deformed and recrystallized phenocrysts of a porphyritic intrusive rock.

2. *Veined Migmatites*

The neosome of veined migmatites may be *venitic* (arising in situ by partial melting of a rock) or *arteritic* (the mobilizate is formed elsewhere and injected, usually as a melt). Both types of neosome are present in the Aus area. Plate 35 shows many of the features typical of venitic neosomes. Here, originally homogeneous biotite schist has segregated into a quartz-feldspar fraction (leucosome) and a mafic fraction (melanosome) that has been concentrated into thin schlieren. As is typical of venites, the development of neosome is patchy and irregular, yet at the same time extensive.

Plate 37. Arteritic veined migmatite with transgressive and concordant metatectic neosomes. Note sharp contacts and lack of mafic selvage. Garub biotite schist. 3 km NW of Namies Hochberg, Heinrichsfelde 10 (H3)

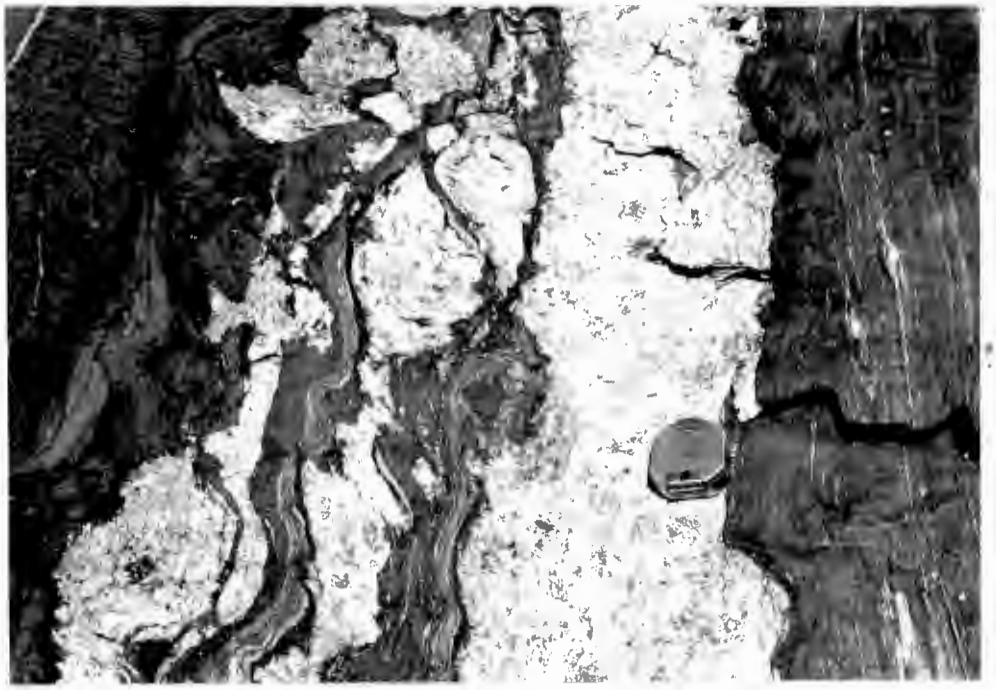

Plate 38. Melanosome produced by partial melting of palaeosome after injection of metatectic neosome. Garub biotite schist. 6 km NW of Am Einschnitt Mountain, Diamond Area (E3)

The relation of this type of venitic migmatite to deformation is illustrated in Plate 36. The neosomes have clearly been folded and there is good separation of the neosome into leucosome and melanosome. A relatively unmigmatized part near the hammer head shows incipient blastesis and the coalescing of the 'tails' of the blasts to form veins parallel to the foliation.

Arterites contain injected mobilizates forming largely continuous neosomes which are often transgressive to the foliation, though usually near-parallel. Contacts are typically sharp and do not normally have mafic selvages on the borders of the neosome (Plate 37).

The presence of a melanosome, or mafic rim, does not necessarily signify a venitic origin for the neosome. Such features can be produced in arterites by partial melting of the host rock by the injected neosome. Such a case is shown in Plate 38 where thick leucosomes are rimmed by a narrow selvage of biotite-rich melanosome. The quantity of leucosome in this case, is completely out of proportion to that of the melanosome and such a combination could not have been produced by melting of the host rock. The leucosome must have been introduced from elsewhere and is therefore of arteritic origin. This injection and its accompanying supply of heat and water has caused local metatexis along the contacts of the palaeosome to form the narrow melanosome.

A more straightforward example of injection is illustrated in Plate 39. Pegmatoidal mobilizate has been introduced into the fractured Tsirub gneiss to form an agmatite. The contact between neosome and palaeosome is in most places very sharp and devoid of a mafic rim, but a melanosome is rarely developed (Plate 40) by melting of the palaeosome by the arteritic neosome.

However, in many cases it is not possible to make a clear distinction between venitic and arteritic types of migmatite with concordant neosomes. This is especially so where post-migmatization deformation has destroyed the original relation of palaeosome and neosome. For this reason, the arteritic and venitic types of veined migmatite have been classified in the same group in the present study although these two types of migmatite have a rather different significance. Venites imply anatexis within the migmatites themselves whereas arterites imply merely access to mobilizates which may have originated in a zone of melting some distance away from the migmatites in which they crystallized.

3. Agmatitic Migmatites

These are breccia-like migmatites produced by the introduction of mobilizate into the shattered palaeosome. With increase in the proportion of neosome, these migmatites grade into raft structures.

Several features typical of agmatites are present in Plate 39. Narrow veins of neosome have penetrated the palaeosome along planes aligned in several directions. The smaller veins have perfectly matched walls, but there appears to have been limited movement between some of the larger fragments of palaeosome. All contacts are sharp and angular. At the outcrop illustrated in Plate 41 the neosome, which cuts the foliation obliquely, appears to be responsible for the

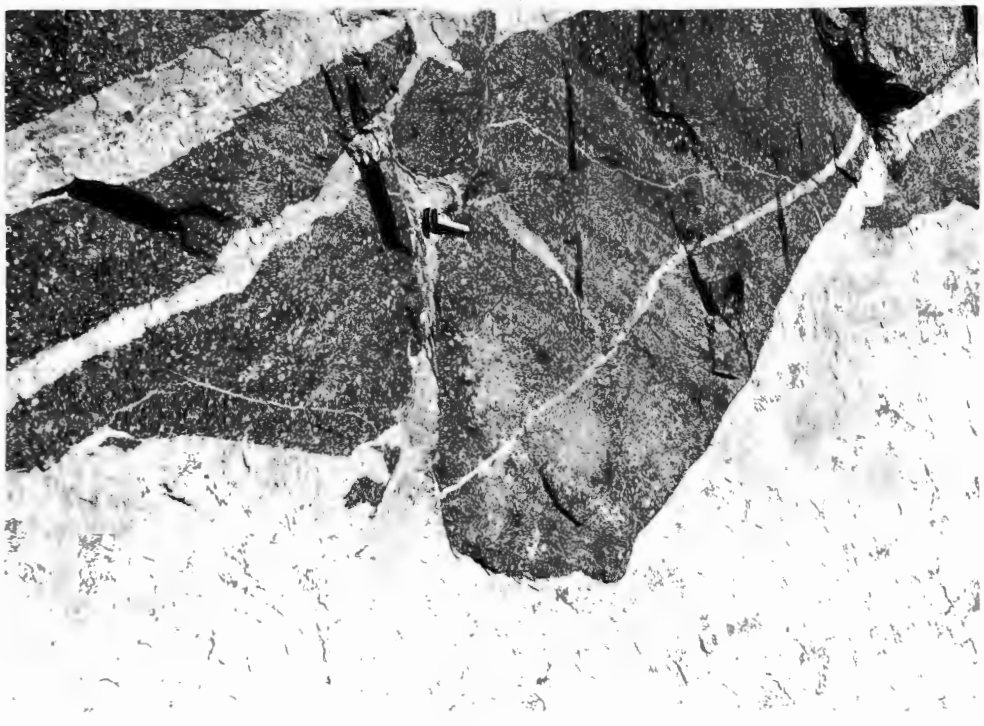

Plate 39. Agmatite produced by injection of metatectic neosome into fractured Tsirub gneiss. Note sharp contacts and matching walls of neosome veins. North face of Kahlerberg (G5)

Plate 40. Development of melanosome at contact between palaeosome (Tsirub gneiss) and injected neosome (quartz-feldspar pegmatoid) in agmatite. Same locality as Plate 39.

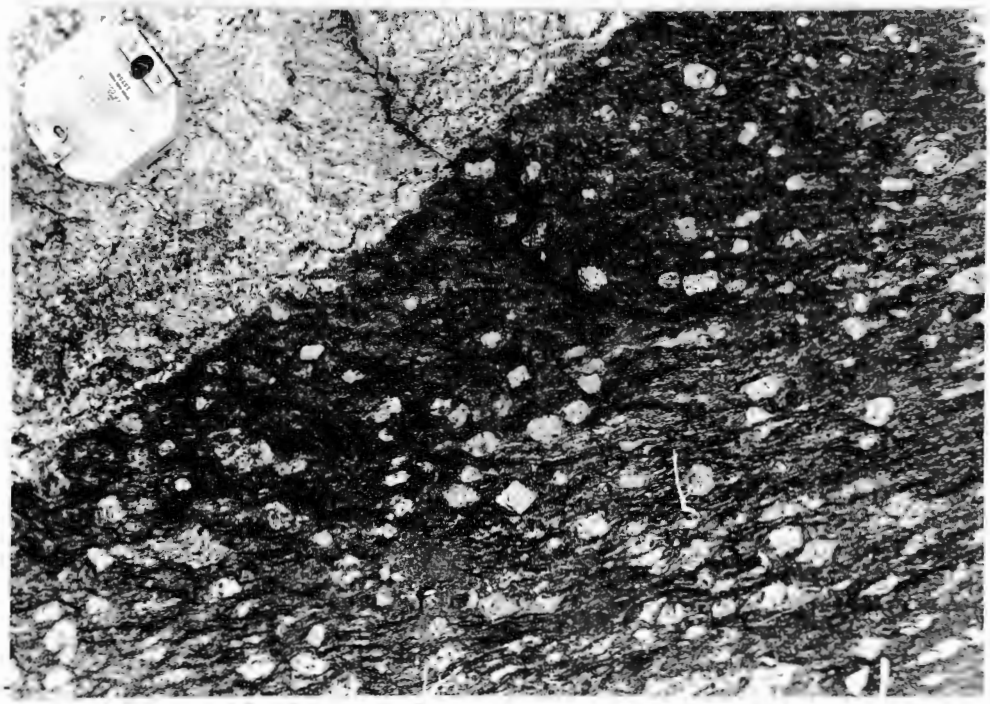

Plate 41. Development of K-feldspar blasts in contact zone between palaeosome (Tsirub gneiss) and injected neosome (quartz-feldspar pegmatoid) transgressive to foliation. Note idioblastic shape of blasts (centre) and oval shape of deformed augen (bottom right). Rooibank (G5)

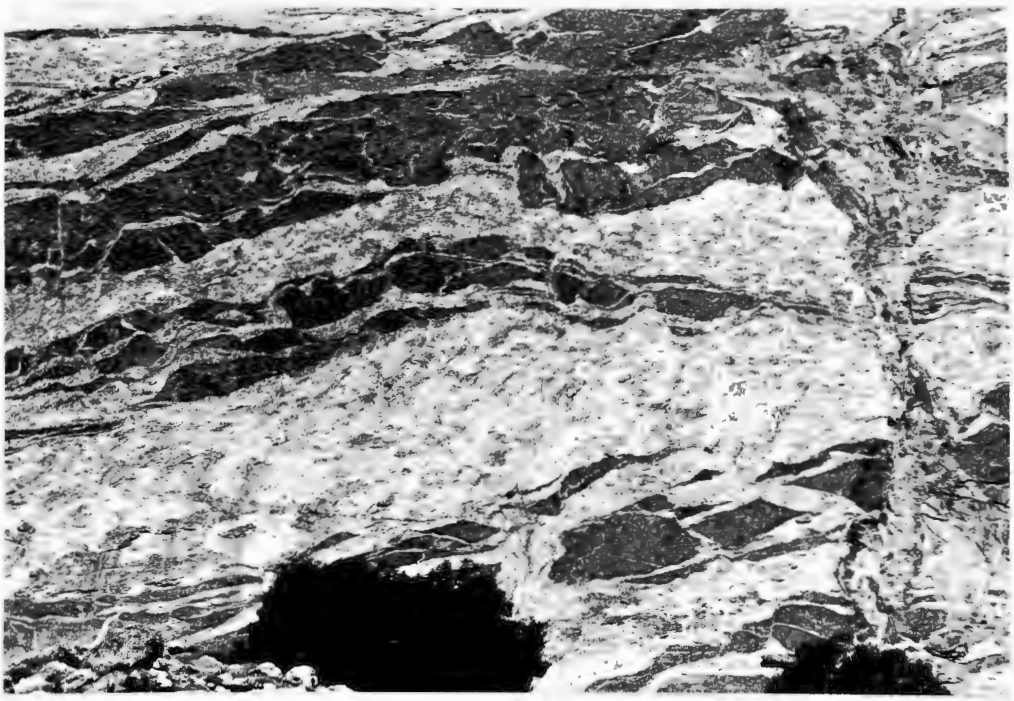

Plate 42. Large-scale agmatite with high proportion of neosome. Original layering in palaeosome is preserved, but adjacent fragments have few matching walls. Tsirub gneiss. Trees at base of cliff are approximately 5 m high. 4 km S of Elefantenberg, Tsirub Farm (H3)

blastic growth of idioblastic feldspar crystals in a 15 cm-wide contact zone. The shape of these crystals contrasts with that of the strongly oriented augen within the gneissic palaeosome.

With an increase in the relative quantity of neosome there is increased movement between the palaeosome fragments. As illustrated in Plate 42 the fragments are preserved in their approximate original positions to form layers parallel to the foliation, but there are few matching walls between the adjacent fragments and the ends of the fragments have become attenuated and crumpled by deformation.

All the above relations between palaeosome and neosome in the agmatites suggest that the neosome was injected into fragmented and deforming palaeosome. Although these rocks are true migmatites, they do not represent anatexis in situ or, necessarily, high-grade metamorphism since such structures are also extremely common in the contact zones of high-level plutons. The mobilizate was derived from elsewhere and introduced into its environment of crystallization.

However, in many outcrops the agmatitic migmatites grade into layered migmatites and it is not possible to determine by field observations whether the neosome was derived in situ. For this reason and because of the regional nature of the mapping, it was decided not to separate agmatites from layered migmatites but to group together all migmatites with metatectic neosomes, whether or not they were derived in situ.

The next stage of migmatization involves the formation of schlieric and nebulitic rocks by diatexis during which mafic,as well as quartzofeldspathic, constituents of the rock are melted.

4. Schlieric and Nebulitic Migmatites

The Kubub granite gneiss typifies the schlieric rocks of the Aus area. Abundant field evidence indicates that its formation to a large degree involves melting of pre-existing rocks during deformation and high-grade metamorphism. These older rocks were broken up and dispersed, then partially or completely absorbed by the granitic melt.

The formation of schlieric leucocratic granite gneiss by absorption of Garub rocks and Tsirub gneiss is illustrated in Plates 43 and 18 respectively. The mafic components are redistributed within the neosome or are concentrated as schlieren. Contacts between palaeosome and neosome are vague and irregular. The nature of the schlieren and the pinching out and attenuation of the ends of the fragments indicate deformation in a solid but relatively incompetent matrix. The fragments are thus not merely xenoliths in a liquid medium.

Schlieric structures are also present in the biotite granite gneiss although they are less common than in the Kubub granite gneiss. Plate 32 illustrates mafic layers of biotite-hornblende schist which pass laterally along the strike of their foliation into schlieric granite gneiss. Both lit-par-lit injection and

Plate 43. Transformation of Garub aluminous gneiss (dark) to schlieric Kubub granite gneiss (light) by diatexis. During melting biotite is dispersed or concentrated into schlieren together with unmelted garnet to define a nebulitic layering. Klein Kubub (H4)

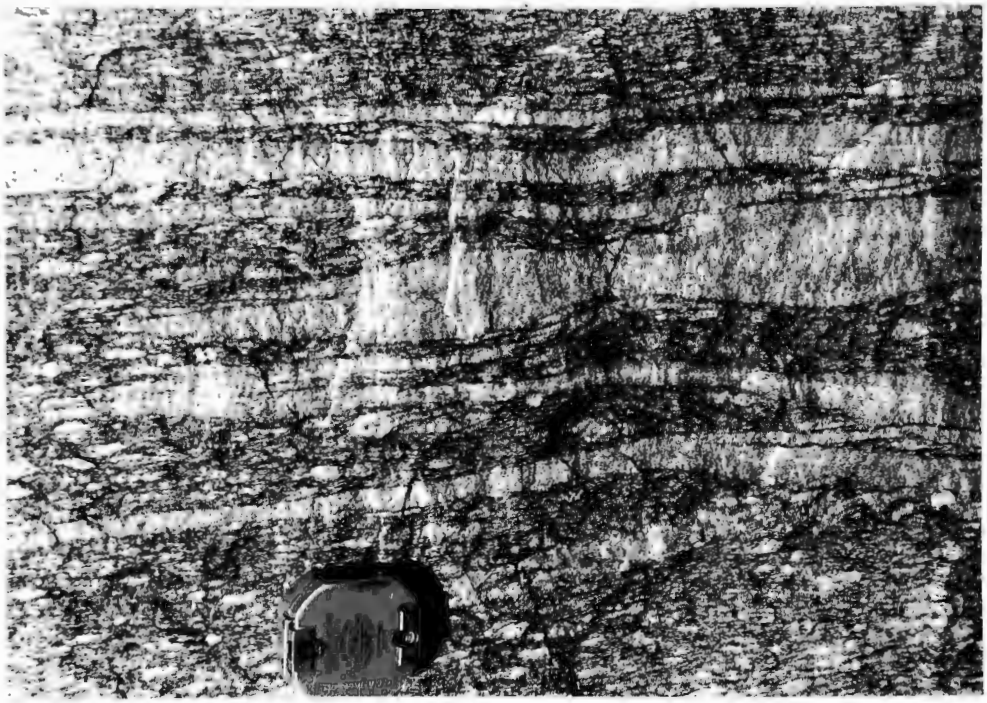

Plate 44. Diatexis of Tsirub gneiss resulting in formation of biotite granite neosomes in situ. 1 km SE of Klein Tiger Berg, Diamond Area (E2)

diatexis appear to have been operative in this case; biotite in the mafic horizon has joined that of the melt and left the more refractory hornblende as a residue.

Nebulitic granite gneisses are common in the northern half of the area. Over small outcrop areas the biotite granite gneiss appears fairly homogeneous but its nebulitic nature becomes apparent if large outcrop areas are examined.

Homogeneous biotite granite gneiss may arise in situ by diatexis. Such a case is shown in Plate 44 where discontinuous wisps of fine-grained granite gneiss have formed subparallel to the foliation of the augen gneiss. Fine-grained granitic mobilizate has been injected into other rocks to form agmatites, dykes and small stocks especially around Groot Löwenberg (E4,F4). The intrusions are homogeneous but differ from high-level igneous intrusions by their gradational contacts and lack of chilled margins. Their high-grade metamorphic environment is also indicated by their gneissic fabric and development of such minerals as cordierite and garnet within them.

5. *Polymigmatization*

Repeated migmatization in the Aus area is indicated by the superimposition of younger migmatite structures onto older migmatites. Plate 45 shows a migmatized biotite schist in which the neosome has been isoclinally folded. This earlier-formed migmatite is truncated by a younger neosome in the centre of the photograph. On Groot Löwenberg numerous outcrops are present in which homogeneous biotite granite neosome crosscuts earlier-formed migmatites characterized by agmatitic, schlieric or nebulitic structures. In places this younger neosome has differentiated into melanosome (porphyroblastic clusters of garnet) and leucosome (quartz-feldspar coronas) as shown in Plate 21.

The above evidence points to a sequence of increasing grade of migmatization in migmatites of the Aus area which involved the following successive stages: metatexis in situ, injection of metatectic neosome, schlieren development by diatexis, homogenization and injection of diatectic melt. Plate 46 shows an excellent exposure which illustrates in one outcrop most of the above stages of progressive migmatization:

(i) Thin,discontinuous,but roughly concordant,veins of metatectic neosome in biotite schist have been isoclinally folded

(ii) the gneiss has been further migmatized by injections of discordant pegmatoidal quartz-feldspar neosome which has acted competently during deformation with respect to the palaeosome

(iii) homogeneous granitic neosome has cut across the earlier structures and migmatites

(iv) late-stage pegmatoidal neosomes (in a reversal of the migmatite sequence) have intruded the granitic neosome as narrow veins; in the surrounding area this young neosome is present in much larger amounts and 'trains' of garnet have preserved the nebulitic outline of the palaeosome

Plate 45. Tightly folded pre-D_2 migmatite neosomes crosscut by post-D_2 neosomes of similar lithology. Biotite schist. 600 m SE of Klein Aus farmstead (G4)

Plate 46. Four episodes of migmatization preserved in a single outcrop of migmatized biotite schist (see text for description). 4 km NNE of Groot Löwenberg, just below marble body

The examples described in this chapter provide field evidence for a migmatite sequence reflecting a progressive rise in the grade of migmatization. This has resulted in the re-migmatization and partial or complete obliteration of earlier migmatites by a process of polymigmatization. Migmatization appears to have continued for some time in this part of the crust and has spanned more than one deformational event. Anatectic conditions during high-grade metamorphism appear to have been a protracted feature of this area and the various episodes of migmatite formation may have been promoted by nothing more than the passage of water through different parts of a continually heated crust, rather than by episodes of rising temperature.

5.4 THE PRACTICAL DETERMINATION OF MIGMATITIC GRADE

Mehnert (1968, p.344) states that 'a petrographic classification of mixed rocks must primarily rely on the composition of the *neosome*' because immobile resistors remain unchanged and in disequilibrium with the newly-formed components of the migmatite. The migmatite structure (the form of interpenetration of the neosome and palaeosome) is of secondary importance in the classification of migmatites; it depends largely on the abundance of neosome, viscosity contrast between palaeosome and neosome, and the mechanical behaviour of the palaeosome.

The quantity of neosome produced during melting is strongly dependent on the composition of the palaeosome. Winkler (1974) has shown that quite delicate variations in host-rock composition within the same lithological group have a marked effect on the melting temperature of the rocks and hence, on the amount of melt produced. Therefore, mere quantity of neosome is not a sufficient indication of grade of migmatization. Field work in the Aus area involved the systematic recording of the type and quantity of neosome in all localities where migmatites were observed. This study confirmed that the quantity of neosome developed during migmatization was strongly dependent on palaeosome composition. For instance, biotite schists and metapelites were capable of producing abundant neosome, whereas in the same outcrops mafic or largely monomineralic rocks such as metaquartzites, marbles and- to a lesser extent - granofelses and metabasites had lesser amounts of neosome or were entirely non-migmatized.

Migmatitic grade - as indicated by the degree of homogenization achieved - should not be taken as equivalent to metamorphic grade (Mehnert, 1968, p.345). Metamorphic grade is independent of bulk composition (but dependent on the composition of the fluid phase), whereas migmatitic grade is strongly dependent on host-rock composition. However, a certain minimum metamorphic grade, equivalent to Winkler's (1970) high stage (upper amphibolite facies) is necessary for the formation of migmatites by melting. The pattern of migmatitic grades depicted on a map cannot be expected to be identical to the configuration of of the metamorphic isograds associated with the migmatization.

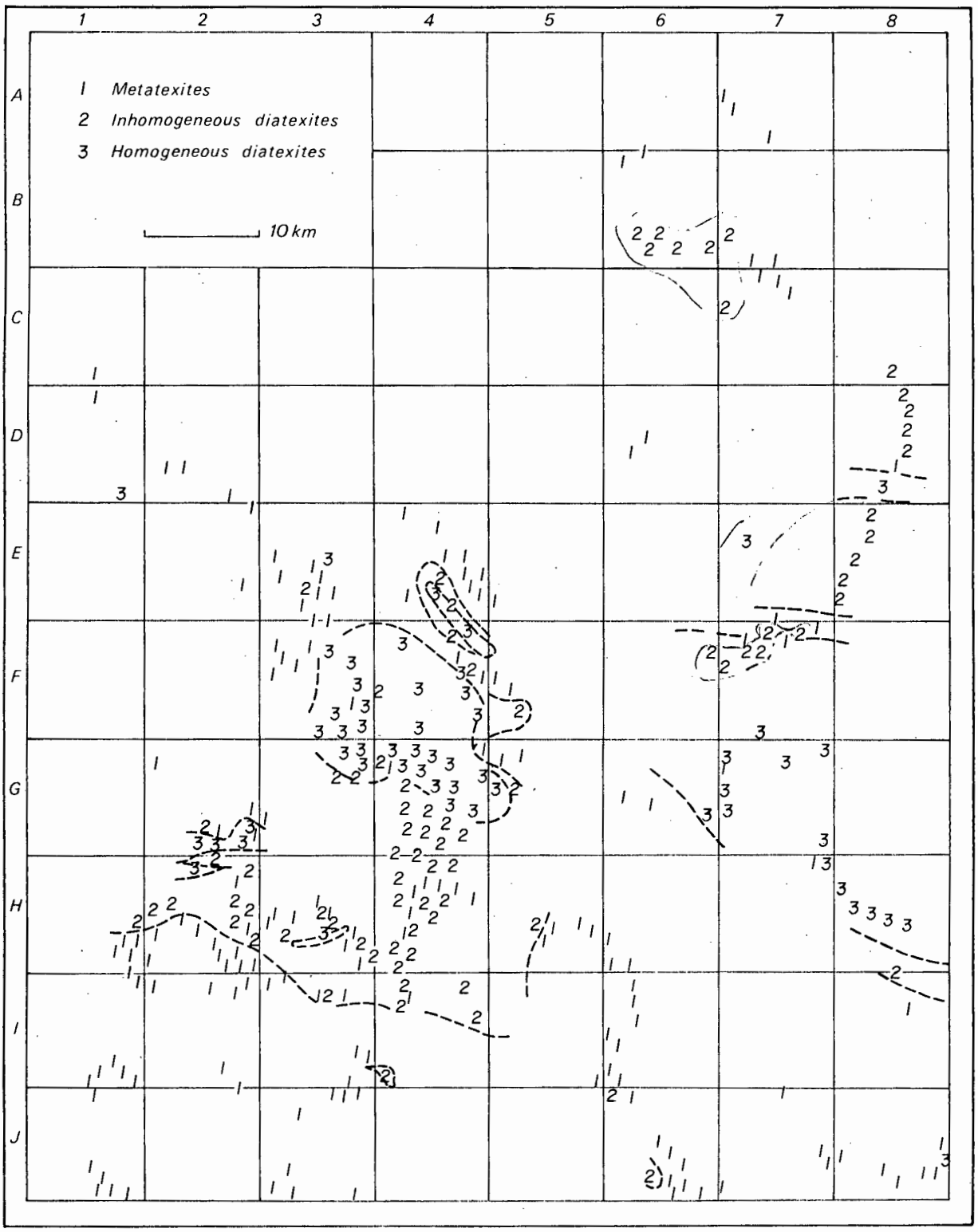

Figure 64. Sketch map showing variations in the grade of migmatization in the Aus area, as indicated by degree of homogeneity of migmatites. Migmatitic grade increases from 1-3

In constructing the map showing migmatitic grade (Fig. 64), the effect of polymigmatization (described in the previous section) has been taken into account. Where migmatitic structures of more than one generation are present in a single outcrop the highest migmatitic stage is represented on the map. Garub rocks, migmatized up to the metatectic stage, are commonly surrounded by diatectic granite gneisses. If the metatectic remnants are sufficiently large, they are represented on the map; otherwise they are omitted and only the surrounding diatectic migmatites are shown. The same rule of generalization applies to isolated intrusions of granitic (diatectic) neosome intruding large areas of lower-grade migmatites.

The migmatite map does not cover the southern parts of the study area. The reason for this omission is partly the paucity of outcrop in this region and partly the difficulty in determining the migmatitic grade there because layered biotite gneisses in this area are easily confused with nebulitic or schlieric biotite gneisses produced by partial homogenization of banded migmatites. Thus the true extent of migmatization in this region and the southern boundary of migmatization cannot be accurately depicted on the map.

It should be emphasized that the migmatite map is based solely on field observations over a very large area. The conclusions reached cannot therefore be treated with the same confidence as those derived by detailed petrologic studies of much smaller areas. A point of possible controversy is the status of homogeneous plutonites in the centre of the area (typified by the Aus granite gneiss and the biotite granite gneiss of Groot Löwenberg). Although there is considerable field evidence that these rocks were derived by anatexis of earlier rocks, it is not impossible that they represent the products of magmatic differentiation and igneous intrusion. However, a detailed study of the origin of these plutonites is beyond the scope of the present study. It is felt that the origin of these rocks must always remain in some doubt because of the nature of their setting within a high-grade metamorphic terrain. The conditions of formation of these plutonites, whether they are magmatic differentiates or anatectic mobilizates, will ultimately be the same at depth. Mehnert (1968, p.348) has pointed out that this convergence in character and origin within the high-temperature parts of the crust 'renders the ultimate distinction between "juvenile" and "palingenetic" magmatites impossible'.

5.5 AREAL DISTRIBUTION OF MIGMATITIC GRADES

On the sketch map of migmatitic grades (Fig. 64) three main classes of migmatites are represented. Non-migmatized areas are depicted by a lack of symbols; here the rocks were not of suitable composition to generate quartzofeldspathic neosomes by melting or were not injected by mobilizates. Only rarely are these non-migmatized areas actually situated outside the zone of regional migmatization.

The migmatites are classified in the following stages:

(i) *metatexites*: comprising pretectonic rocks migmatized by quartzo-feldspathic neosomes; this migmatitic style may be blastic, stromatic, veined or agmatitic

(ii) *inhomogeneous diatexites*: rocks partially homogenized by conversion to schlieric and nebulitic granite gneisses (such as the Kubub granite gneiss and the schlieric biotite granite gneiss); or pretectonic palaeosomes with neosomes of this type

(iii) *homogeneous diatexites*: plutonitic Aus granite gneiss and biotite granite gneiss; pretectonic palaeosomes with neosomes of these rock types

The sketch map (Fig. 64) shows that the distribution of these migmatitic types is fairly erratic in detail (as would be expected from the many factors which influence the melting behaviour of these rocks). However, on a regional scale a distinct pattern is visible.

The centre of the study area is dominated by stage-3 migmatites, chiefly the Aus granite gneiss. Southwards from here a broad zone of schlieric stage-2 migmatites is terminated along a fairly even southern boundary (around level H on the coordinate grid). Within this stage-2 zone the migmatitic grade is fairly consistent with the exception of Festung Mountain (G2). Here all three migmatitic grades are present; nebulitic biotite granite gneisses (stage 2) alternate with Garub rocks which are cut by neosomes of quartzo-feldspathic pegmatoid (stage 1) or fine-grained biotite granite gneiss (stage 3). The eastern boundary of this large stage-2 zone is situated on the central part of Kubub Farm (H5).

South of this zone, stage-1 migmatites and non-migmatized rocks are present, but, as mentioned above, the southern boundary of migmatization could not be accurately fixed.

Northwards from the central plutonites of stage 3 there is no broad zone of stage-2 migmatites as in the south and the migmatitic grade is predominantly that of stage 1. An exception to this is Groot Löwenberg where Garub rocks have been migmatized to produce nebulitic and schlieric granite gneisses (stage 2) and small areas of homogeneous biotite granite gneiss (stage 3). Northwest of here migmatites are less common. Beyond the western boundaries of the study area, however, migmatites become increasingly common and spectacular stage-1 migmatites are a feature of the area around Koichab Pan and along the coast between Lüderitz and Hottentot Bay (Greenman, 1966; Jackson, 1974; Kröner and Jackson, 1974).

In the eastern part of the study area along the Nama escarpment, which is more or less isolated from the inselbergs of the centre-west, the pattern of migmatization is slightly different. Here high-grade migmatization has extended much farther north. Schlieric and nebulitic biotite granite gneisses constitute a broad zone of stage-2 migmatites in the north. Stage-1 migmatites are preserved in the east-trending synform on Kwessiepoort Farm (E7, F7). In the central part of this eastern area (G7) a stage-3 zone of homogenized rocks corresponding to the equivalent zone farther west is present. South of here on Tsachanabis Farm (I8) a narrow zone of stage-2 schlieric biotite granite gneiss

is exposed. A very broad zone of stage-1 migmatites extends southwards to Kokerboomkloof Farm (J6).

It is readily apparent that the pattern of migmatization is markedly asymmetric. In the escarpment area there is no large stage-2 zone south of the central stage-3 zone as there is in the north. In the centre-west of the study area the position is reversed: stage-1 migmatites abut directly against the stage-3 Aus granite gneiss with no intervening stage-2 migmatites. This indicates that whereas the southern part of the Aus granite gneiss could have originated in situ, it is unlikely that this applies to the northern part. This suggests that the Aus granite gneiss has moved from its place of origin transgressing the stage 2 zone of migmatites that may have existed on its northern margin and now directly adjoins the metatectic migmatites of stage 1.

This pattern of migmatization, in which the central part of the study area is dominated by rocks of the highest migmatitic grade, is remarkably similar to that of the amphibolite grade metamorphism. Figures 52 and 55 imply that a thermal dome in the centre of the study area existed during amphibolite facies metamorphism and this may have been responsible for the observed pattern of migmatization.

Chapter 6

STRUCTURE

The structural history of the Aus area serves as a framework on which the concept of tectonic categories (described in Chapter 2) is based. Since the purpose of this section is to relate the structural evolution to the formation and metamorphism of the main rock units, the structural history is described qualitatively as was done by Appleyard (1974); there is little consideration of the geometry of the structures formed and no studies involving strain or stress analyses or quantitative fold classification. The intrusion of major rock types provides the basic framework for the structural history. Within this framework successive generations of folds are further distinguished by means of overprinting relations. Table 27 summarizes the structural history.

The successive episodes of deformation are referred to by the symbols D_1, D_2, etc. Measurable physical structures produced during these episodes of deformation are represented as follows: foliations and lineations are symbolized by s_1, s_2 and l_1, l_2, etc; the axes of successive generations of folds are symbolized by f_1, f_2, etc. (*after* Ramsay, 1967) and an $f2$ fold, for example, contains f_2 as its fold axis. Rock units affected by D_1 are 'pretectonic'; rocks intruded between D_1 and D_3 are loosely termed 'early syntectonic' and those produced between D_3 and D_4 are 'late syntectonic' (refer to Chapter 2 for a description of the tectonic categories).

6.1 PLANAR STRUCTURES

Following Turner and Weiss (1963, p.97) the term foliation in the present study refers to all types of mesoscopically recognizable s surfaces of metamorphic origin; foliation includes gneissic layering, preferred dimensional orientation of planar mineral grains, and surfaces of discontinuity and fissility.

TABLE 27

Synopsis of the structural history of the Aus area

ROCK UNIT, MIGMATIZATION	DEFORMATION PERIOD	MEGASCOPIC FEATURE	MINOR FOLD AXIS PREVALENCE INTERLIMB ANGLE AXIAL PLANE STRIKE	ASSOCIATED LINEATION	ASSOCIATED FOLIATION	METAMORPHIC GRADE OF ASSOCIATED FOLIATION
		NNW- and NNE-trending faults				
		folding of Nama in SE of area				
Nama G. d, q, pp, md		NNE-trending faults				
Tumuab g.					minor cataclasis near borders of igneous bodies	low
Klein Tiras g. Houmoed g. Tierkloof g.		NW-trending mylonite belts	f_6 0-100° variable strike	l_6 crenulation clast trains mineral elongation	s_6 axial-plane and mylonitic fabric	low
	$?D_4$		f_5 50-120° generally NW	l_5 crenulation common	s_4 and s_5 non-penetrative flex-slip surfaces or kink-bands; penetrative in completely retrogressed rocks	low-medium
			f_4 50-120° generally NE	l_4 crenulation common		low-medium
						GROUP 2
						GROUP 1
(minor mig.) ap,pp Tiras gneiss	D_3	f_3 open	f_3 0-120° common	l_3 mineral in Aus gg.	s_3 in granite gneisses and Tiras gneiss, also in broad zones of refoliation in older rocks	mainly high
(minor mig.) Pyramide gg. Anib gg. Biotite gg. Aus gg. Kubub gg. major migmatization						
Jakkalskop c. (with minor mig.)	D_2	f_2 tight to isoclinal	f_2 0-60° common	l_2 mineral common	s_2 axial plane fol. in places, no extensive regional refoliation	mainly high
Magnettafelberg s. (migmatization)	D_1		f_1 0-30° rare	l_1 mineral common	s_1 axial plane fol. common but not ubiquitous, regional foliation	mainly high
(migmatization) Tsirub g.						
Layered biotite g. Garub sequence					pre-D_1 foliation ?mylonitic	high

In the Aus area the foliation in layered rocks is predominantly parallel to the contacts between the constituent rock units; in foliated igneous rocks the foliation is commonly parallel to the contacts of the body. As shown below, the present study indicates that the dominant foliation in the pretectonic layered rocks was formed early in the structural history of the Aus area. Subsequent periods of deformation have deformed this foliation without producing extensive refoliation and have imprinted a fabric on newly-formed syntectonic igneous rocks.

In the present study the successive generations of foliation have been distinguished by two methods. Firstly by the relation of the foliation to characteristic intrusive rock units and secondly by overprinting criteria in areas of continuous outcrop. For instance, the foliation imprinted on biotite granite gneiss or pink aplite must be younger than the foliation defined by, for example, gneissic layering that is crosscut by these intruding rocks. Similarly a foliation is demonstrably younger if it is observed to crosscut,in the form of a zone of refoliation, another foliation developed in the same rock unit (e.g. Fig. 66c). All the descriptions that follow are taken from selected outcrops where these diagnostic criteria are present. In the absence of these criteria (viz. overprinting or relation to the syntectonic intrusions) the differentiation of the older fabrics (s_1-s_3) proved extremely difficult.

1. *Foliation* s_1

The oldest foliation is present in the pretectonic rock units, which constitute the oldest tectonic category. These rock units comprise the Garub sequence, layered biotite gneiss and Tsirub gneiss. The dominant foliation in these rocks is called s_1. This foliation is axial planar to most f_1 folds (Fig. 65). The metamorphic isograds described in Chapter 4 have been constructed largely on the basis of mineral parageneses defining this foliation; s_1 is therefore defined by the preferred orientation of high-grade mineral parageneses in most of the area. In addition s_1 has the form of gneissic layering parallel to the preferred mineral orientation and to the contacts between individual units of the sequence (e.g. marbles, calc-granofels, granofels, aluminous gneiss, biotite schist and iron formation of the Garub sequence and in layered biotite gneiss). The main foliation in the Tsirub gneiss is s_1. This foliation is parallel to the contact of Tsirub gneiss with the Garub sequence (Plates 13 and 14) and is present both in the inclusions of Garub rocks and in the surrounding Tsirub gneiss.

There is also evidence for the existence of a pre-s_1 foliation which has been folded around f_1. An outcrop southwest of Garub Station (GI) contains a foliation (Plate 47) of mylonitic appearance which may be parallel to the original bedding (Section 2.1.4.). This foliation is defined by the preferred orientation of hornblende grains and is parallel to the contacts of an interlayered sequence of amphibolite and quartz-feldspar rock (Plate 47). The metamorphic grade of the minerals defining this pre-s_1 foliation is amphibolite facies (indicated by 'hornblende + plagioclase' paragenesis and lack of epi-

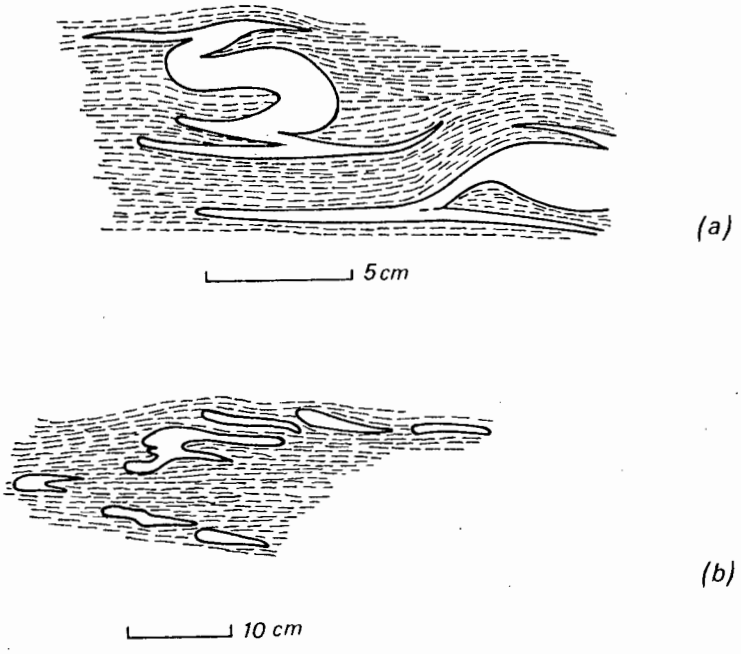

Figure 65. (a) complex f_1 fold forms (in pre-D_1 neosome) resulting from coalescence of hinge zones and attenuation of limbs during extreme flattening. s_1 is axial planar. Garub biotite schist (field sketch). 3 km SE of Arasab 43 farmstead (J6)
(b) transposition and disruption of pre-D_1 neosome during D_1. s_1 is axial planar to f_1 folds. Garub biotite schist (field sketch). Nama Escarpment 9 km N of Kokerboomkloof 65 farmstead (K7)

dote in the amphibolite). Dalziel et al. (1969) reported a similar mylonitic fabric, apparently produced during D_1, deformed by later deformation in rocks adjacent to the Grenville front, Canada.

2. *Foliation* s_2

The s_2 foliation was observed only in a minority of f_2 folds as an axial plane foliation. Plate 50 shows the appearance of s_2, which is defined by the preferred orientation of biotite grains parallel to the axial plane of the fold. Gneissic layering (s_1) has been folded during D_2 but is still preserved in the f_2 folds although the individual mineral grains defining the layering have been re-oriented to form s_2. The folded migmatite neosomes parallel to s_1 must have also recrystallized during D_2 because their constituent minerals show no signs of strain in thin section. Plate 51 illustrates more-strongly developed axial-plane foliation (s_2) in biotite-hornblende gneiss defined by the preferred

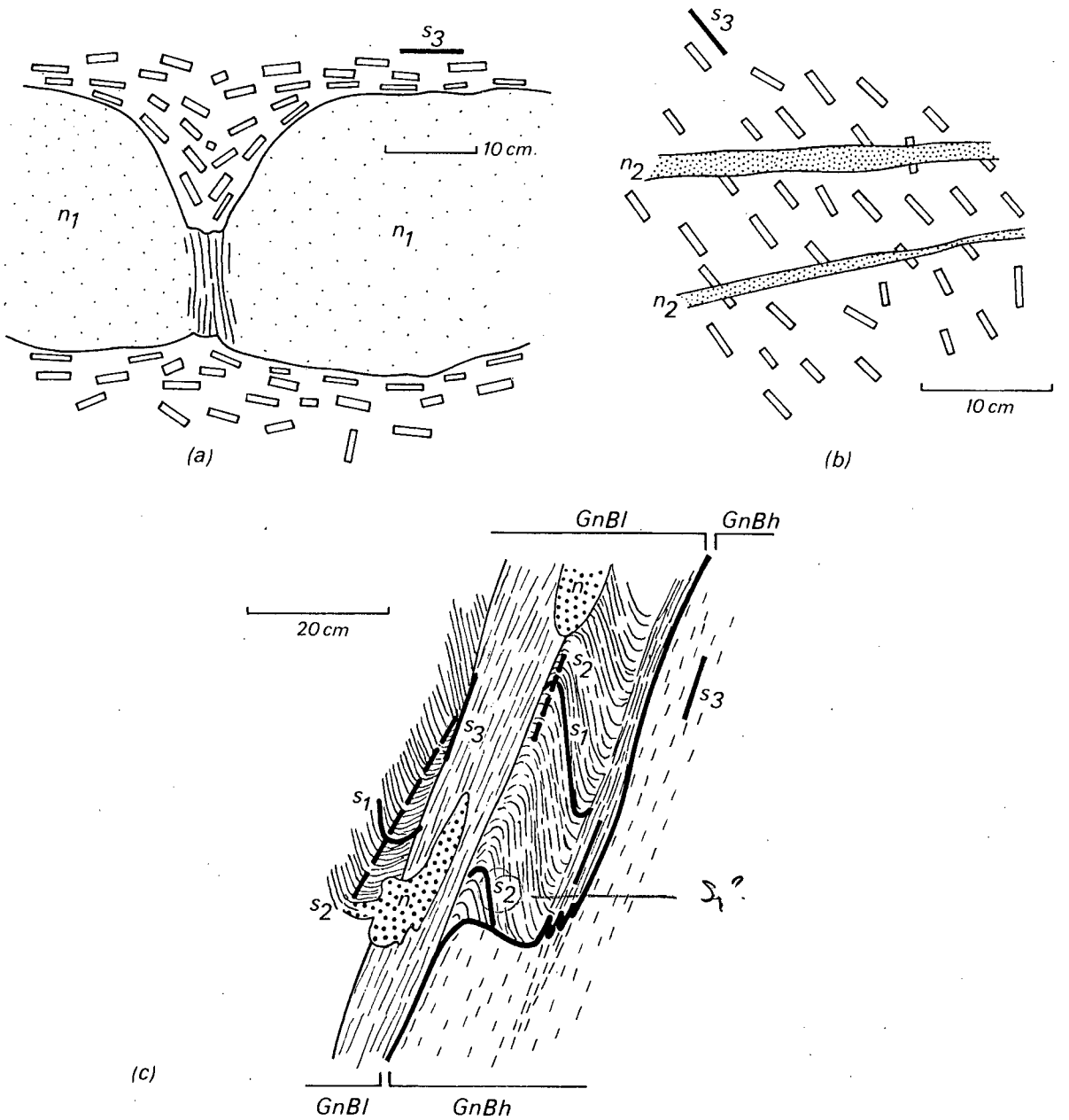

Figure 66. Examples of s_3:
(a) Pegmatoid neosome boudinaged during D_3 and surrounded by more-ductile gneiss (field sketch). 3 km SE of Harris 21 farmstead (J8)
(b) Post-D_3 migmatization. Mobilizate truncates s_3 defined by megacrysts in Aus granite gneiss (field sketch). 3 km SE of Harris 21 farmstead (J8)
(c) s_3 in biotite gneiss, *GnBl*, (parallel to s_3 in biotite granite gneiss, *GnBh*) cutting s_1 folded during D_2 (traced from a photograph). Aarkopf Hill (H5)

orientation of the dark minerals; s_1 is present in the form of gneissic layering.

Both s_1 and s_2 are high-grade fabrics and their differentiation is therefore extremely difficult in the absence of minor folds. An axial-plane foliation (s_2) is absent from the majority of f_2 folds, identified by other criteria (Section 6.3.2.). However, in the f_2 folds folded gneissic layering (s_1) is almost invariably present. This suggests that s_1 represents the main foliation in the pretectonic rocks and that no extensive refoliation took place during D_2.

3. *Foliation* s_3

The s_3 foliation is distinguished from older foliations by its development in the syntectonic intrusive rocks. All these rock units (viz. Jakkalskop charnockite and the Kubub, Aus, Anib and biotite granite gneisses) cross-cut s_1 and f_2 minor fold structures within inclusions of pretectonic rocks and are therefore post-D_2 in age. A foliation is not everywhere visible in the syntectonic rocks (see Chapter 3 for details) and is more common in the outer parts of the larger bodies. This foliation (s_3) is defined by the preferred orientation of biotite flakes and, in the Aus granite gneiss, by the common alignment of K-feldspar megacrysts.

D_3 was preceded and followed by migmatization on a limited scale. Figure 66a shows the effect of D_3 on a sheet of pegmatoid neosome which has cut Aus granite gneiss. The relatively competent neosome has been boudinaged, which resulted in necking and fracturing in the partition zone between boudins. More-ductile megacrystic granite gneiss has flowed into the gaps between the boudins during D_3 and the megacrysts have become strongly oriented along the margins of the pegmatoid boudins. Figure 66b shows post-D_3 neosomes cutting s_3 within the Aus granite gneiss. It must be emphasized, however, that the Aus granite gneiss is not commonly migmatized and field evidence indicates that the bulk of the regional migmatization occurred before the emplacement of this granite gneiss.

The s_3 foliation is also developed in the pretectonic rocks by refoliation during D_3. Figure 66c shows a case where this refoliation is demonstrably of the same age as s_3 in syntectonic biotite granite gneiss. Biotite granite gneiss (*GnBh*) has intruded layered biotite gneiss (*GnBl*) showing f_2 folds; both rock units have had s_3 imprinted on them. This foliation is penetratively developed in the lithologically homogeneous *GnBh* unit, but in the *GnBl* unit s_3 is strongly developed in discontinuous zones of refoliation subparallel to the contact; s_3 is continuous across the contact between the two rock units. The presence of unfoliated stichtolithic (Mehnert, 1968, p.11) neosome within the s_3 zones of refoliation suggests that a limited amount of melting in situ resulted from,but outlasted, D_3. Like D_1 and D_2, therefore, D_3 appears to have taken place under conditions of high-grade metamorphism. On Kahler Berg (G4) pretectonic Tsirub gneiss has been refoliated during D_3 so that the foliation within it is parallel to s_3 in the adjoining Aus granite gneiss (Fig. 67). At the same locality the older foliation (probably s_1) in the Tsirub

gneiss is preserved in xenoliths of this rock within the Aus granite gneiss and is crosscut by younger s_3 within the granite gneiss (Plate 20).

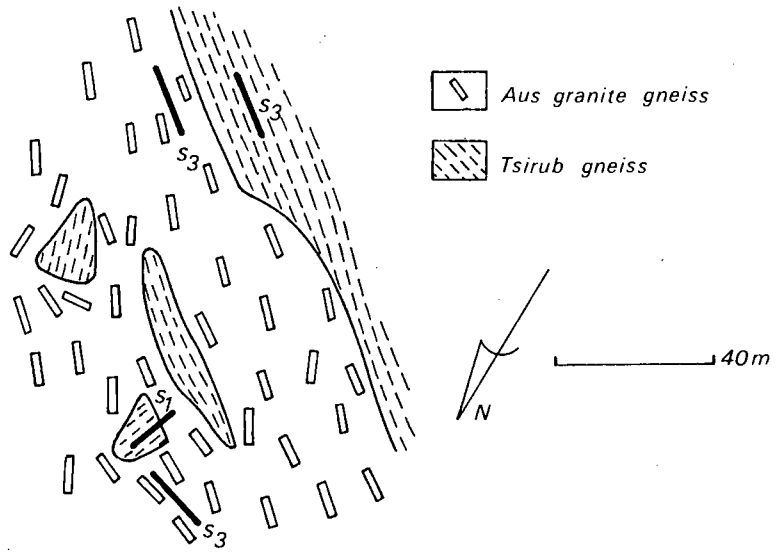

Figure 67. Refoliation of Tsirub gneiss during D_3 parallel to s_3 in Aus granite gneiss (field sketch). Kahler Berg (G5)

Figure 68a is a diagrammatic representation of a much larger zone of D_3 refoliation. Here s_1 (in the southeast) is deformed around f_3 which trends northeast. The f_3 folds become progressively tighter towards the northwest. The s_1 layering is destroyed and the rocks are converted to *B*-tectonites (Sander, 1930, p.58) which are devoid of layering but have a banded appearance in sections parallel to *b* because of the strongly developed rodding defining l_3, which is parallel to f_3 in the adjacent domain (Fig. 67b). Farther northwest the rocks have developed an $s-$ layering. The appearance of s_3 here differs from that of s_1 by being more fine-scale (mm instead of cm) and the constituent layers are more lithologically diverse.

At the above locality thin veins and sheets of pink aplite and pegmatite have been deformed during D_3 (the sheets have been folded around f_3 and contribute to the l_3 rodding) but some crosscut s_3 and l_3. This evidence suggests that the injection of the pink pegmatite-aplite suite began before D_3 and continued after this deformation had ended. Elsewhere the pink aplite is largely unfoliated but in places a weak foliation (s_3) is present.

4. *Post-*D_3 *foliations*

The post-D_3 foliations have only local development and, in contrast to the older foliations, they are all defined by mineral parageneses of low or

medium metamorphic grade.

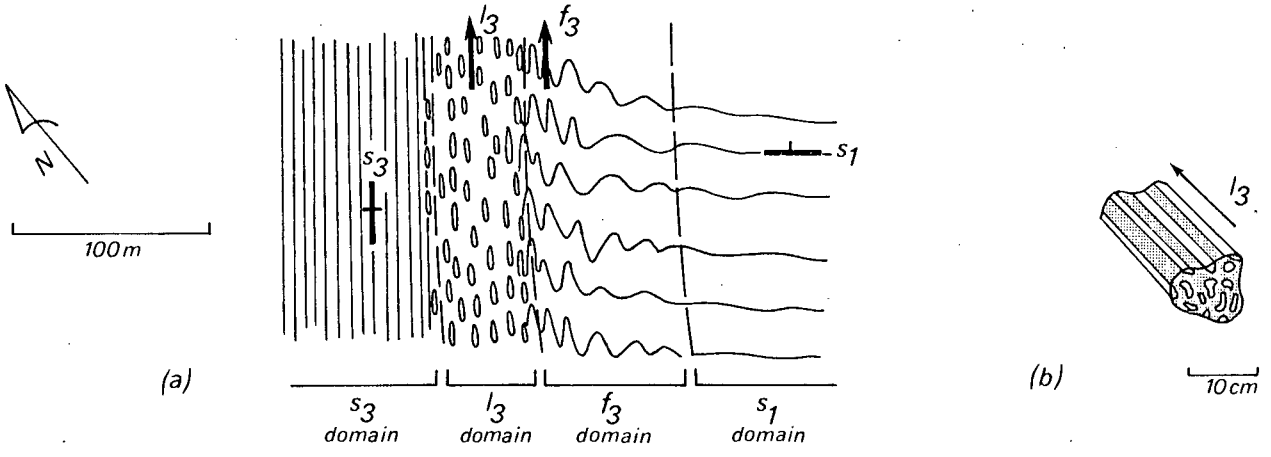

Figure 68. (a) Diagrammatic sketch of D_3 zone of refoliation (see text for explanation). 2 km SE of Keerbank 126 farmstead (J7)
(b) *B*-tectonite from the l_3 domain of the D_3 zone of refoliation (field sketch). Same locality as (a)

The s_4 and s_5 foliations are generally non-penetrative on the mesoscopic scale. They are present as discrete planes between surfaces of flexural slip in f_4 and f_5 folds (Plate 58, Fig. 72c). s_4 and s_5 are also developed within kink-bands correlated with f_4 and f_5; in this case the younger foliation is developed between the twin surfaces of discontinuity that represent the axial planes of paired kink folds (Fig. 72a). The foliation is defined by the preferred orientation of muscovite or chlorite flakes. In the central metamorphic zone these surfaces are retrogressed from high grade to medium grade ('muscovite + quartz', 'epidote + quartz') or low grade; in the south and northwest of the study area rocks are retrogressed from medium to low metamorphic grade ('chlorite + epidote + quartz').

The s_6 foliation is present in the Kuckaus and Excelsior mylonite belts. This foliation is defined by a mesoscopic and microscopic lithologic layering, flattening planes of megacrysts, and preferred orientation of muscovite-sericite and chlorite flakes in the mylonites. s_6 is also developed as an axial-plane foliation defined by chlorite flakes in f_1 folds in cataclastic biotite gneiss adjoining the Kuckaus mylonites. The mylonite belts are discussed in greater detail in Section 6.4.

6.2 LINEATIONS AND LINEAR STRUCTURES

Following Turner and Weiss (1963, p.101) the term lineation is applied to linear features that are penetrative on the scale of hand specimens or small outcrops; larger features are referred to as linear structures.

The oldest lineation in the Aus area is parallel to f_1 and hence is correlated with D_1. This lineation, l_1, is a penetrative mineral lineation defined by alignment of biotite and hornblende grains. Southeast of Garub Station (Plate 47) l_1 is defined by fine-scale crenulation of the pre-s_1 foliation, by mineral alignment of hornblende and by alignment of clast trains. However, since all f_1 folds identified elsewhere in the Aus area are exposed in only two dimensions, it was not possible to determine if the majority of l_1 are parallel to f_1.

The second generation of lineations, l_2, are well developed and are parallel to f_2 (Plate 52). These lineations are defined by the preferred orientation of prismatic and platy minerals such as biotite, hornblende, sillimanite and opaque minerals. Lineations shown on the geological map (Annexure 1) are correlated with D_1 and D_2. The l_2 lineation can only be confidently recognized in the hinge zones of f_2 folds; since both l_1 and l_2 are defined by the preferred orientation of minerals of high metamorphic grade, it is generally not possible to distinguish between these lineations in the absence of mesoscopic folds. In numerous cases l_1 was observed to be deformed around f_2 and to cross the f_2 fold hinges at an oblique angle. Where an axial-plane foliation is developed in f_2 folds, l_1 is destroyed by recrystallization.

Although they are rare, linear structures, too, were produced during D_2. These linear structures are visible in the hills south of Garub Station. Intersecting curved foliations outline irregular mullions in amphibolite. Parallel to the mullions is a mineral lineation defined by hornblende grains, which is parallel to f_2 in the same outcrop.

Lineations in the syntectonic granitoids are termed l_3. These structures are present mainly in the Aus granite gneiss and are defined by the preferred orientation of tabular megacrysts of K-feldspar and garnet trains. l_3 is also defined by mineral alignment of sillimanite and alignment of biotite aggregates in Kubub granite gneiss. The lineation is not strongly developed or common.

Lineations associated with f_4 and f_5 have been formed but are not common. The l_4 and l_5 lineations are formed by crenulation of a previously developed surface (usually s_1) in the hinge zones of f_4 and f_5 folds (Plate 54, Fig. 72c).

Lineations associated with the mylonitization episode (Table 27) have formed in the mylonites. The lineations are defined by clast trains and elongated rock and mineral fragments with s_6. More rarely l_6 is defined by fine striae on the contacts of quartz veins formed during mylonitization and emplaced parallel to the mylonite foliation, s_6.

6.3 FOLDS

1. *Description*

Folds of six generations have been observed in the Aus area. The three

Plate 47. f_1 elasticas deforming pre-D_1 foliation with l_1 parallel to f_1. The f_1 fold is isoclinally folded around f_2. Note extreme attenuation of f_1 fold limbs by deformation during D_2. Garub quartz-feldspar rock in marble. 9 km SW of Garub Station, Diamond Area (GI)

Plate 48. Open-to-isoclinal f_2 folds showing three f_1 fold closures (arrowed). Axial planes of f_2 folds have been deformed by gentle D_3 folding at base of outcrop. Same outcrop as in Plate 47

older generations (f_1, f_2 and f_3 folds) are referred to as group 1 folds, whereas the three younger generations (f_4, f_5 and f_6) constitute the group 2 folds. The group 1 folds are distinguished from the latter by the higher metamorphic grade of their associated foliations. This study is mainly concerned with the group 1 folds because of their association with high-grade metamorphism.

Group 1 Folds

Before outlining the properties of the group 1 folds in general, a specific locality will be described, where all three generations are visible in a single outcrop and can be differentiated by means of overprinting relations. Plate 47 illustrates an f_1 elasticas (*after* Ramsay, 1967, p.387) with a negative interlimb angle and rounded hinge zone. This fold deforms a pre-D_1 foliation and contains a penetrative lineation (l_1) parallel to f_1. The limbs of this fold have been greatly attenuated and the axial plane has been folded isoclinally by f_2 folds. The pre-D_1 foliation appears to have been accentuated in zones of high strain, as in the isoclinal f_2 folds. Plate 48 shows a broader view of the f_2 folds at the same outcrop in which three prominent f_1 fold closures are visible. The f_2 folds here have rounded hinges and isoclinal limbs; they deform the pre-D_1 foliation and l_1 (not visible in Plate 48). A few metres away these isoclinal f_2 folds have been deformed by tight-to-isoclinal (*after* Fleuty, 1964) f_3 folds (Plate 49). Here the deformation of the f_2 folds by coaxial f_3 folds has brought about interference patterns similar to Ramsay's (1967) Type 3. Neither f_2 or f_3 have a parallel lineation. At the above outcrop therefore an early s-surface has been preserved through, and intensified by, three successive periods of isoclinal folding. These relations are diagrammatically shown in Figure 69.

In general, however, the main foliation in the pretectonic rocks is s_1, rather than the pre-s_1 foliation described above, and is associated with f_1 folds. These folds are chiefly found in migmatized Garub biotite schist or aluminous gneiss. The f_1 folds are usually of complex shape and have the form of tightly adpressed multiple fold hinges with strongly attenuated fold limbs parallel to s_1, which is axial planar to the f_1 folds (Fig. 65).

As can be seen from Figure 65a the curvature (Ramsay 1967, p.350) of the folded layer depends partly upon its position in the fold: in the inner arc the hinge is sharp, whereas on the outer arc it is rounded. Figure 65b illustrates the other common appearance of the f_1 folds. The pre-D_1 neosome layer has been disrupted and transposed parallel to s_1. The fold illustrated contains isoclinal parasitic folds on the disrupted limbs. In many cases the process of transposition has advanced to such a degree that no fold closures are visible and all that remains of the former fold structure is a series of lenticular neosome streaks parallel to s_1.

In all f_1 folds observed the fold is defined by a migmatitic neosome; this suggests the existence of high-grade (upper amphibolite facies) metamorphism before D_1 or at an early stage of this period of deformation.

Plate 49. f_2 isoclinal folds deformed around tight-to-isoclinal coaxial f_3 folds. Granofels layers in marble. Same locality as Plate 47

Plate 50. Gneissic layering (s_1) folded tightly around f_2 with s_2 developed as an axial-plane foliation defined by alignment of biotite flakes. Garub biotite schist. 1 km SE of Klein Aus farmstead (G4)

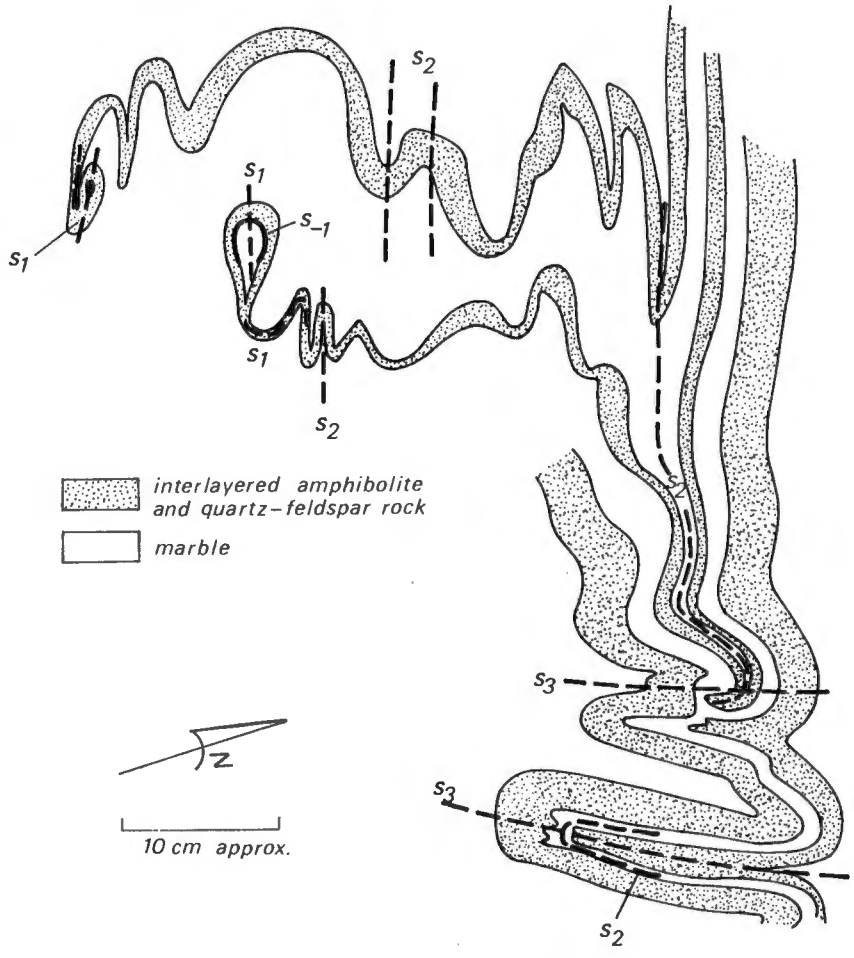

Figure 69. Diagrammatic sketch of relations between pre-D_1 foliation and f_1, f_2 and f_3 folds. s_1, s_2 and s_3 represent axial planes of these folds. 8 km SE of Garub Station, Diamond Area (G1)

The f_2 folds deform s_1 together with l_1 and f_1. The majority of minor folds observed in the Aus area belong to the f_2 generation. The style of these folds is variable. Plate 50 illustrates a tight f_2 fold in which the lower layers have rounded hinge zones, whereas the upper layers, in which an axial-plane foliation (s_2) is strongly developed, have more sharply curved hinge zones. These neosomes commonly have a 'pinch and swell structure'; the convex cuspate margins of these quartzofeldspathic layers suggests that they deformed competently with respect to their host rock and were thus solid bodies prior to deformation. Plate 52 and Figure 70a illustrate tight-to-isoclinal f_2 folds with hinge zones showing varying degrees of curvature. Figure 70c shows isoclinal f_2 folds in layered gneiss with complex interpenetrating forms. Figure 70d illustrates a parasitic fold of the intrafolial type; the fold deforms s_1 and is situated in the limb of a larger

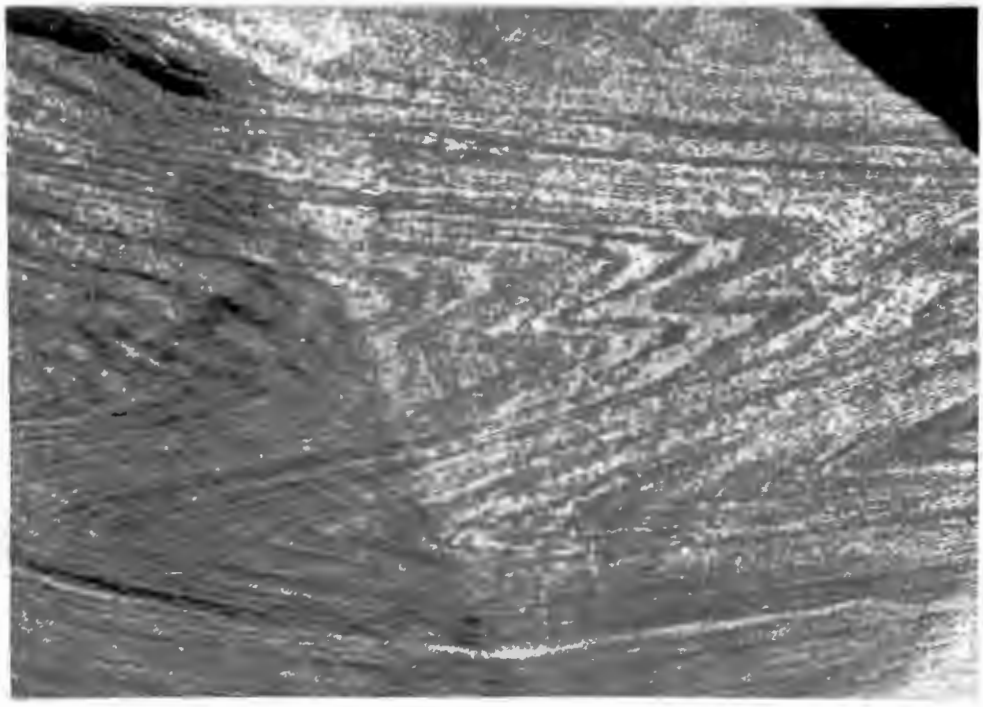

Plate 51. s_1 gneissic layering folded around f_2 defining tight folds with sharp hinges, approximating similar style. Axial-plane foliation (s_2) is defined by preferred orientation of dark minerals. Garub biotite-hornblende gneiss. Area shown is approximately 12x20 cm. 6 km WNW of Excelsior farmstead (B6)

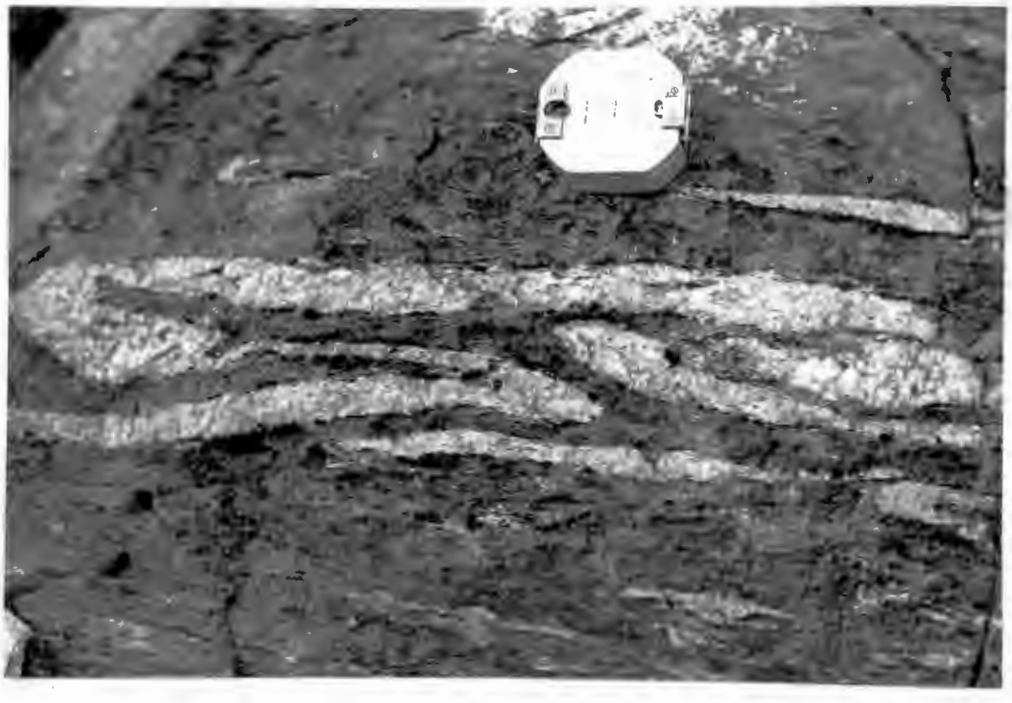

Plate 52. Migmatite neosomes defining isoclinal f_2 folds with rounded hinge zones in Garub aluminous gneiss. 1 km E of Zipfel, Kubub 15 (G4)

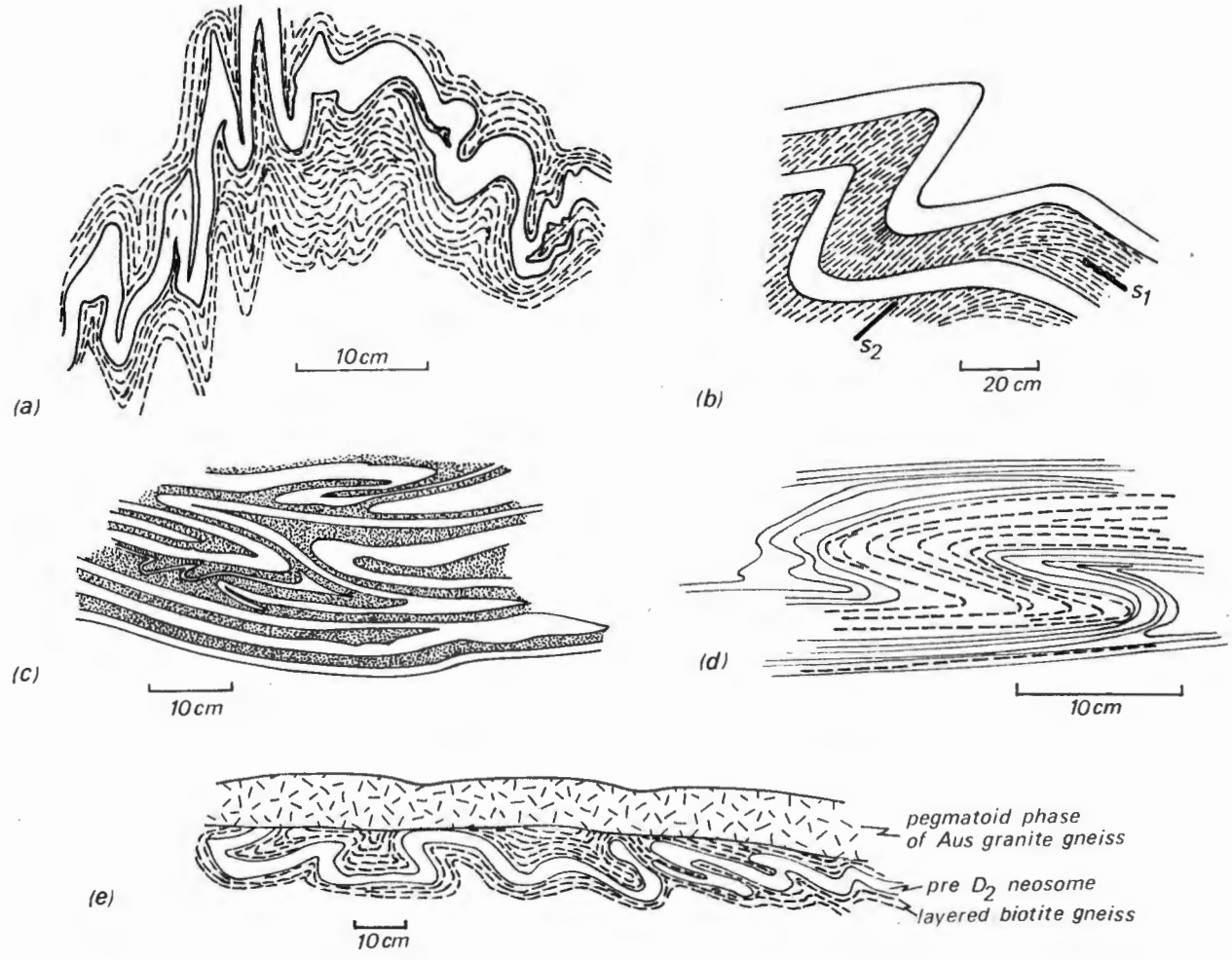

Figure 70. Examples of f_2 fold styles:

(a) f_2 fold train showing variation from open to isoclinal interlimb angles and both sharp and rounded hinge zones. Note lack of axial-plane foliation. Pre-D_2 neosome in Garub biotite schist (traced from a photograph). 1 km NE of Kububer Horn (H4)

(b) Axial-plane foliation (s_2) in f_2 fold showing rotation of s_1 in Garub biotite schist (field sketch). 1 km NE of Harris 21 farmstead (J8)

(c) Tight-to-isoclinal f_2 folds in mafic layered gneiss. Garub biotite schist (traced from a photograph). 6 km SE of Groot Löwenberg beacon (F5)

(d) Intrafolial f_2 fold deforming s_1 in mafic layered gneiss. Garub biotite schist (traced from a photograph). 6 km SW of Augustfelde 42 farmstead, 600 m NW of railway (G6)

(e) f_2 fold train, comprising open-to-isoclinal folds with variably oriented axial planes, deforming pre-D_2 neosome and s_1 in layered biotite gneiss cut by post-D_2 neosome (field sketch). 5 km S of Am Einschnitt beacon (F3)

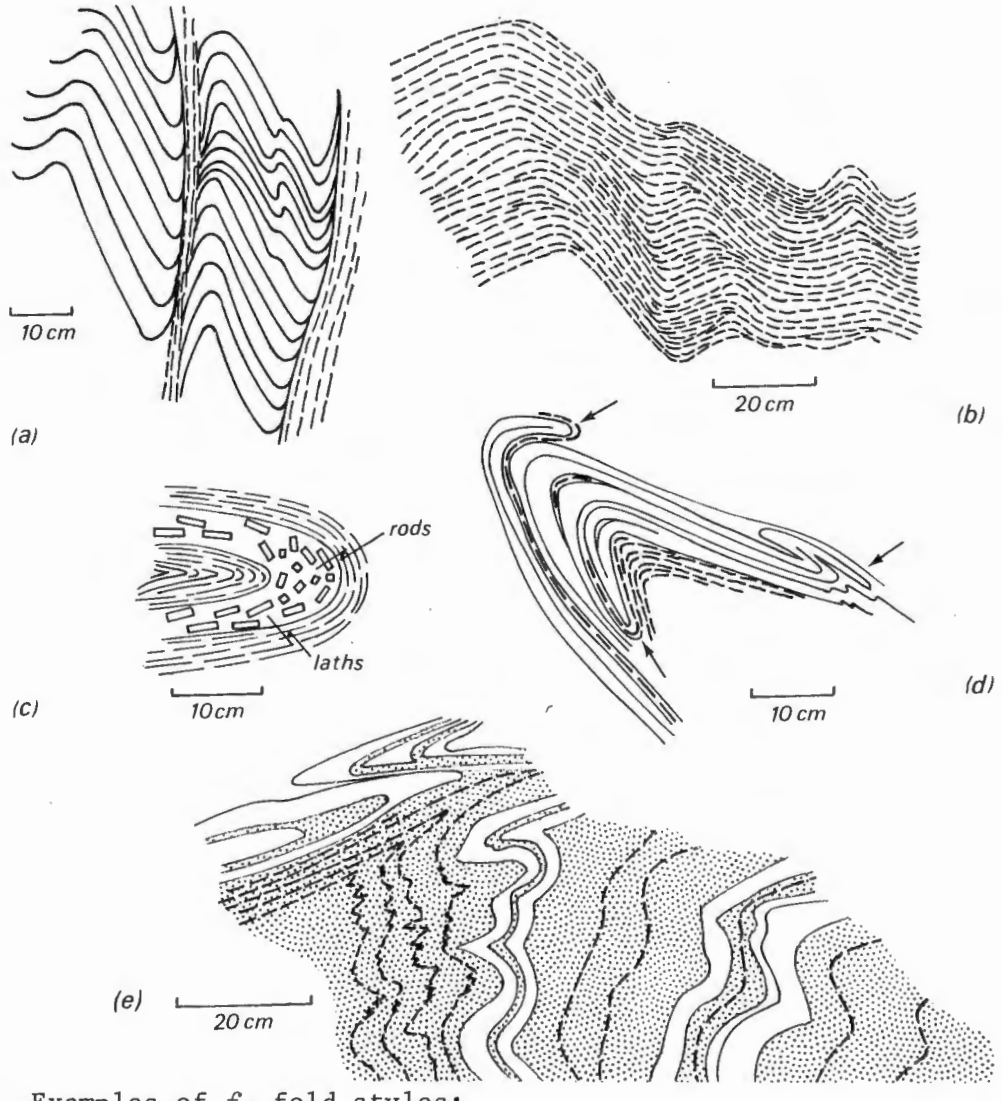

Figure 71. Examples of f_3 fold styles:

(a) s_1 tightly folded and largely transposed in zones of high strain parallel to f_3 fold axial planes. Garub biotite schist (traced from a photograph). Mittelkuppe Hills (H5)

(b) Open f_3 folds in Kubub granite gneiss (traced from a photograph). 2 km S of Aus Village (G4)

(c) Tight f_3 fold deforming f_1 in biotite schist and vein of Aus granite gneiss. Megacryst laths have apparently been rotated and deformed in the hinge zones to form rods parallel to f_3 (field sketch). 1 km NE of Harris 21 farmstead (J8)

(d) Tight f_3 fold deforming isoclinal f_2 folds (closures marked by arrows) which fold s_1. Layered biotite gneiss (traced from a photograph). Nama Escarpment 7 km SW of Precipice beacon (E8)

(e) Fold trains showing extreme variation in tightness from open (right) to near-isoclinal (left) in zone of higher strain. Migmatized Garub biotite schist (traced from a photograph) 3 km NW of Namies Hochberg (H3)

fold of the same generation. Figure 70e illustrates the extreme variability in style of a disharmonic f_2 fold train; in this case it is not known whether the folded neosome was formed during or prior to D_2.

The f_2 folds are not commonly associated with a new foliation and they deform s_1. In a number of cases, however, s_2 is developed as an axial-plane foliation in f_2 folds (Plate 50 and 51, Fig. 70b). Where s_2 is developed, the s_1 layering is preserved but the constituent mineral grains have recrystallized parallel to the axial planes of the f_2 folds.

A penetrative mineral lineation, l_2, is a conspicuous feature of many f_2 folds and is parallel to f_2 (Plate 53). As noted previously, however, the f_2 folds deform older l_1 structures, very similar in appearance to l_2.

The D_2 period of deformation was both preceded and followed by migmatization. Abundant quartzofeldspathic neosomes, which crosscut s_1, have been deformed around f_2. Younger neosomes crosscut the f_2 folds (Fig. 70e). In general the pre-D_2 neosomes are in the form of thin but extensive metatectic mobilizate, whereas the post-D_2 neosomes are in the form of larger, more continuous but widely dispersed, sheets which are metatectic or diatectic (see Chapter 6 for a discussion on migmatite types). Where developed, the s_2 axial plane foliation is defined by mineral parageneses of the same high metamorphic grade as those defining s_1.

The f_3 folds are distinguished from the f_2 folds by being present in the early-syntectonic granitoids; because the f_2 folds are older than the syntectonic granitoids, they are not developed within them. Because of their lithologic homogeneity, the Aus granite gneiss, biotite granite gneiss and Jakkalskop charnockite do not show prominent fold structures. Nevertheless the foliation within these bodies can be linked with f_3 folds developed in the adjoining country rocks. Thus Figure 71a shows s_1 in Garub biotite schist which has been tightly folded about f_3. Here s_1 has been rotated and largely transposed in zones of high strain to form a new foliation, s_3, which is parallel to the f_3 axial planes and to s_3 in the syntectonic Kubub granite gneiss (which thereby serves to date this deformational episode). Figure 71b illustrates the form of f_3 folds that are more open. In rare cases intrusive veins of these syntectonic granitoids are seen to have been folded around f_3. Figure 70c shows a folded vein of Aus granite gneiss; the long axes of the megacrysts have apparently taken up a position in the hinge parallel to f_3.

The f_3 folds can also be distinguished from the f_2 folds by overprinting relations. Such a case has already been described in the Garub marbles (Plate 49, Fig. 69). Another example is shown in Figure 71d in which f_2 isoclinal folds, deforming s_1, have been tightly folded during D_3; three f_2 fold closures are visible.

Unless such overprinting relations are present or unless the folds are seen to predate or postdate the syntectonic intrusive rocks, it is not possible to distinguish with confidence between folds of the D_2 and D_3 generations. For this reason specific examples described here have been identified only by the above criteria. Figures 70 and 71 demonstrate the great variability in style shown by the folds of both generations. Figure 71e shows a series of fold trains in which the tightness varies from open to isoclinal within a distance of 1 m. Joubert (1974a, p.21) reported a similar tightening

Plate 53. Tight f_2 fold showing well-developed l_2 mineral lineation parallel to f_2. Garub biotite schist. 3 km SW of Magnettafelberg, Diamond Area (D1)

Plate 54. Open f_4 flex-slip fold deforming older lineation (l_1 or l_2) and foliation (probably s_1). A crenulation lineation (l_4) is weakly developed in the hinge zone of the fold. Discontinuous planes of slip (s_4) are marked by thin layers of retrograde epidote-chlorite schist parallel to s_1. Garub biotite schist. 1 km SE of Magnettafelberg, Diamond Area (D2)

of his f_3 folds towards the core of mesoscopic shear zones. The fact that axial-plane foliations and mineral lineations parallel to b have been observed in f_2 folds but not in f_3 folds might serve to differentiate the f_2 folds where such features are present. Although the above generalizations on orientation and associated planar and linear structures serve as a guide to the differentiation between f_2 and f_3 folds, they are not diagnostic - as are the criteria listed at the start of this paragraph.

Where these foliations have been identified in key outcrops the metamorphic grade of the s_3 fabric is upper-amphibolite facies, like that of s_1 and s_2.

Group 2 Folds

The group 2 folds (f_4, f_5 and f_6) are distinguished from those of group 1 by the lower metamorphic grade of the foliation associated with them (see Section 6.1). The fold forms of f_4 and f_5 are of similar appearance and will accordingly be described together. Unlike the group 1 folds, which have an extremely variable orientation, the axial planes of the f_4 and f_5 folds have dips that are mainly subvertical. Minor folds of these generations are common around Magnettafelberg (D2) and on the farms Harris (J8) and Excelsior (C7). The morphology of these folds suggests a formation predominantly by flexural-slip. Discontinuous planes of slip (s_4) parallel to s_1 are marked by thin layers of retrograde epidote-chlorite schist within biotite schist. Plate 54 illustrates a common form of these folds: an open f_4 fold deforms an older lineation (l_1 or l_2) and foliation (probably s_1); a crenulation lineation (l_4) is weakly developed in the hinge zone of the fold. Plate 55 shows a much tighter f_4 fold with straight limbs and small-scale parasitic folds of chevron style in the core.

Kink-bands correlated with f_4 and f_5 are also present. Figure 72a illustrates a kink-band in biotite gneiss in which pairs of planar discontinuities offset an older foliation to produce small angular folds. Within and between the planes of discontinuity, biotite has been chloritized.

Figure 72b illustrates the change of style between folds of the same generation in contrasting lithologies. Metaquartzite has deformed by gentle buckling, whereas the less competent chlorite schist (retrograded cummingtonite schist) has been thrown into close chevron folds on either side of the competent layer. Figure 72c shows how the interlimb angle of individual folded layers varies according to their position within the fold. Where folds have maximum amplitude a crenulation lineation has formed.

Overprinting relations between the f_4 and f_5 folds have not been found; furthermore the fabrics associated with these folds are both retrogressive. It is therefore possible that these folds were produced during a single period of deformation and represent conjugate structures. It can be further speculated that these conjugate folds are related to the mylonite belts and that all the f_4, f_5 and f_6 folds were produced during the same deformational event, tentatively labelled D_4, characterized by retrogressive metamorphism (Table 27).

The f_6 folds associated with the mylonitization event are present in the cataclastic gneisses adjoining the mylonite south of Tsirub Letterkuppe (I1).

Plate 55. Tight, straight-limbed f_4 fold with small-scale chevron folding in core (bottom). 1 km SE of Magnettafelberg (D2)

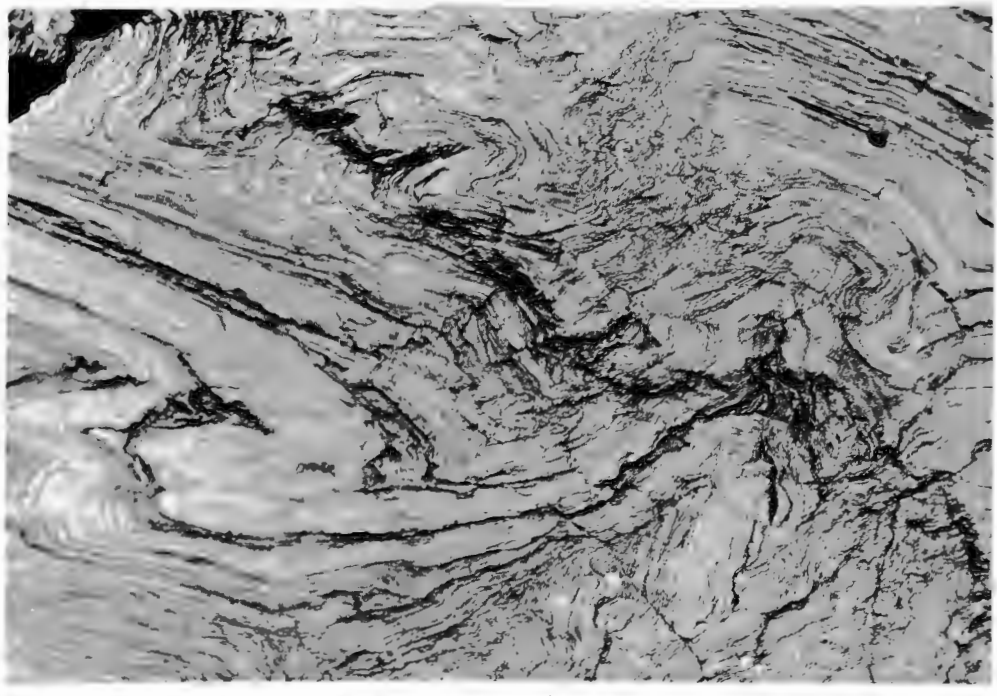

Plate 56. Polyclinal post-f_6 folds deforming the (s_6) mylonitic fabric. Folds are coaxial with vertically-plunging axes; unfolded mylonite at left (pin is 25 mm long). Excelsior mylonite belt. NW end of Tierkloof (A6)

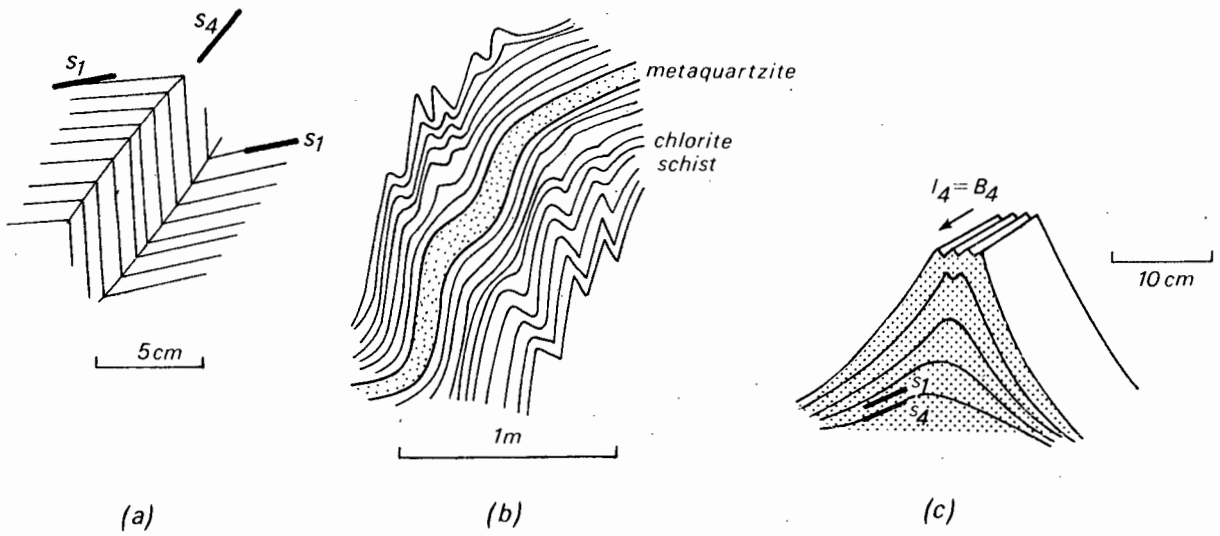

Figure 72. Examples of f_4 and f_5 folds:
(a) Kink-band showing relation of s_1 (medium grade) and s_4 (low grade). Layered biotite gneiss (field sketch) 1 km SW of Magnettafelberg (D1)
(b) Gentle f_4 buckle folds in metaquartzite passing into disharmonic tight chevron folds in chlorite schist. Garub sequence (field sketch). Excelsior 59, 2 km W of boundary with Neisip 34 (C7)
(c) f_4 fold showing variation in interlimb angle of individual folded layers depending on position in minor fold. s_4, which is non-penetrative and confined to planes of slip, is parallel to s_1, which is penetrative. Garub biotite-muscovite schist (field sketch). 1 km NE of Harris 21 farmstead (J8)

These folds are tight-to-isoclinal and are characterized by well-developed axial plane foliation (s_6) defined by the preferred orientation of chlorite and sericite. The form of these folds approximates that of the similar type.

Younger folds deform the s_6 mylonite fabric in Tierkloof (A6). Plate 56 shows polyclinal post-s_6 folds in mylonites of the Excelsior mylonite belt. The folds are coaxial with vertically plunging axes.

2. *Problems in the Correlation of Minor Structures*

Park (1969) and Williams (1970) have questioned the criteria commonly used in structural correlation of minor folds on a regional scale; Park (1969, p. 336) concluded that there are 'no reliable structural methods of correlating deformation phases across large tracts of country' in gneissic terrains. The structural history of these terrains cannot be reliably determined unless the structures of each generation can be differentiated with confidence. It is therefore important to examine the commonly-used criteria for the correlation of fold phases.

Correlation by Style

One feature of fold style employed in correlation of minor folds is that of the interlimb angle. Older folds are commonly described as being tight or isoclinal in contrast to younger folds, which are more open (e.g. Hopgood, 1973, p.46). Yet the interlimb angle of a fold may increase or decrease as a result of later folding. Ramsay (1967, p.511) described how minor folds of an older generation become more open than they were originally if they occupy the hinge zone of younger major folds, whereas older folds on the limbs of younger major folds become tightened (ibid., p.546); it was concluded that 'it is therefore not advisable in regions of superimposed folding to correlate minor folds of various generations by means of their tightness' (ibid).

Even in folds of the same generation that have not been refolded, the interlimb angle of minor folds varies according to their position in major folds of the same generation. Williams (1970, p.3287) reported that at Bermagui, New South Wales, minor folds in major hinge zones tend to be open structures whereas those in the limbs are commonly tight and almost isoclinal.

The interlimb angle in folds formed by buckling may also depend on the viscosity contrast and relative thickness of adjacent layers. Ramberg (1964) demonstrated experimentally that folds become progressively tighter, from open warps to tight ptygmatic-style folds, as the viscosity contrast increases. Williams (1970, p. 3287) reported that thinner beds are folded more tightly than thicker ones in natural folds.

The tightness of minor folds of the same generation is therefore influenced by layer thickness, viscosity contrast between adjacent layers, position on major folds of the same generation, and position on major folds of younger generations. An examination of natural fold profiles of both early and late generations indicates a wide variability in both interlimb angle and degree of curvature in folds of the same generation (Park, 1969; Williams, 1970; Olesen et al., 1973); there is every gradation from open rounded folds to tight angular folds in both early and late generations.

Together with the problem of variable style within a single fold generation there is the equivalent and compounding problem of similarity of style between folds of different generations. Coward (1973) has pointed out that rocks forming discrete competent bodies tend to act in a similar manner through succeeding deformation phases, providing metamorphic conditions are similar.

Correlation by Orientation

The correlation of minor folds on the basis of their common orientation with a particular episode of deformation assumes a coherent movement picture that operates simultaneously and consistently over large areas. This correlation further assumes that deformation in the crust operates spasmodically to produce well-defined deformational events (Park, 1969). It may well be the case that superposed deformation in gneissic terrains represents the result of continuous strain in a progressively changing stress field that is not everywhere similar. Furthermore, Ghosh (1966) and Ghosh and Ramberg (1968)

have demonstrated that if an element of simple shear is involved in folding, deformation results in the rotation of the strain ellipse axes thus producing folds of variable orientation during the same deformational event.

Because older minor folds may be deformed or reactivated after rotation by later deformation, their present orientation cannot be used as a basis for correlation. Even the axial planes of younger folds have been shown to vary widely in their orientation (e.g. Tobisch et al., 1970).

Correlation by Fabric

If the metamorphic grade of the fabric associated with different folds is the same, it is likely that the metamorphic conditions accompanying deformation were similar. An associated lineation or foliation can therefore be used to correlate minor folds on the basis of their *environment* of formation but not necessarily on their *time* of formation. Park (1969, p.333) has pointed out that it is extremely difficult to correlate high-grade fabrics of successive generations unless the foliation is obviously related to a particular fold generation. However, retrogression, as indicated by the formation of lower-grade minerals in the associated fabric, provides a useful criterion for distinguishing these folds from older folds associated with high-grade fabrics.

Foliations and folds in gneisses can also be correlated by means of overprinting criteria if outcrop areas can be surveyed continuously from end to end (Williams, 1970).

Fold Correlation in the Aus Area

From the above considerations therefore the correlation of folds by means of their associated fabric is more reliable than correlation by style or orientation. Minor folds in the Aus area are classified into two broad groups on the basis of the mineral grade of their associated planar and linear fabrics (described in Section 6.1). Group 1 folds are associated with predominantly high-grade fabrics; group 2 folds, which are younger, are associated with retrogressive fabrics containing chlorite, epidote or muscovite. In the outer parts of the study area, where muscovite is stable on a regional scale in the fabric of group 1 folds, group 2 folds can only be differentiated by means of overprinting relations with group 1 folds.

The folds constituting the two groups (f_1, f_2, f_3 and f_4, f_5, f_6) have been differentiated by means of the following criteria. The f_1 folds are axial planar to the dominant foliation (s_1) in the pretectonic layered rocks. The f_2 folds deform s_1 in the pretectonic rocks and also, in places, the f_1 fold axial planes. The f_3 folds are differentiated from the f_2 folds by their development in the syntectonic intrusive rocks (which postdate D_2); in the pretectonic rocks f_3 folds can only be differentiated by having axial planes parallel to s_3 in nearby syntectonic rocks or, in places, by their deformation of f_2 fold axial planes.

With respect to group 2 the f_4 and f_5 folds have been differentiated by the somewhat questionable criterion of orientation. The axial planes of both

fold generations have a subvertical dip, but one set of axial planes strikes approximately northeast whereas the other set strikes northwest. Minor folds of these generations are comparatively rare and the two generations have not been observed in the same outcrop. As stated above, they may represent conjugate fold sets. The f_6 folds have a cataclastic axial-plane foliation which is parallel to s_6 in the mylonites.

3. Problems in the Correlation of Major Structures

The outcrop pattern of basement rocks in the Aus area is characterized by widely scattered and isolated inselbergs. The outcrop areas are either separated by extensive sand-covered plains and dune fields or are covered by Nama sediments. Figure 73 illustrates the degree of exposure of pre-Nama rocks in the Aus area. Because of the acute lack of continuity between outcrop areas, the tracing and correlation of major structures across the study area proved extremely difficult. The potential variation in form and orientation of major folds within such an area is very large. For instance detailed mapping in an area of Moinian and Lewisian rocks in northern Scotland by Tobisch et al. (1970) has shown that the form and orientation of major structures varies considerably over comparatively small distances. Thus folds of the early Cannich generation form large crescent-shaped domes in one area and isoclinal major folds less than 10 km to the north of here; a few kilometres to the west folds of this generation are entirely lacking. Furthermore the axial planes of later generation folds vary by as much as 90° within a distance of 10 km (ibid.).

If the above variations are present in an area of 450 km^2 (ibid.), then the potential variations in a similar gneiss terrain of 10 000 km^2 (the Aus area) are very much greater. Such variations, combined with the widely dispersed outcrop pattern referred to above, render impossible the reliable correlation of major structures between isolated inselbergs. For these reasons no correlation of major fold structures has been attempted in the present study.

A trend-line map of foliations (Fig. 74) is presented for the central part of the Aus area, where outcrops are less scattered. This map shows the configuration of the major structures together with the axial traces of major folds identified in the field. The large synformal structure north of Aus Village (G4, F4) may represent part of a basin but the lack of outcrop at its eastern end prohibits any firm conclusion. The large antiformal structure north of Dicker Willem Mountain (E1) may also represent an incompletely-exposed interference structure. Since most of the foliations measured are from the pretectonic layered rocks, the trend-line map largely represents the strike of s_1; a minority of foliations are taken from syntectonic rocks and represent s_3.

Figure 75 is a trend-line map for l_1 and l_2 in the centre of the Aus area.

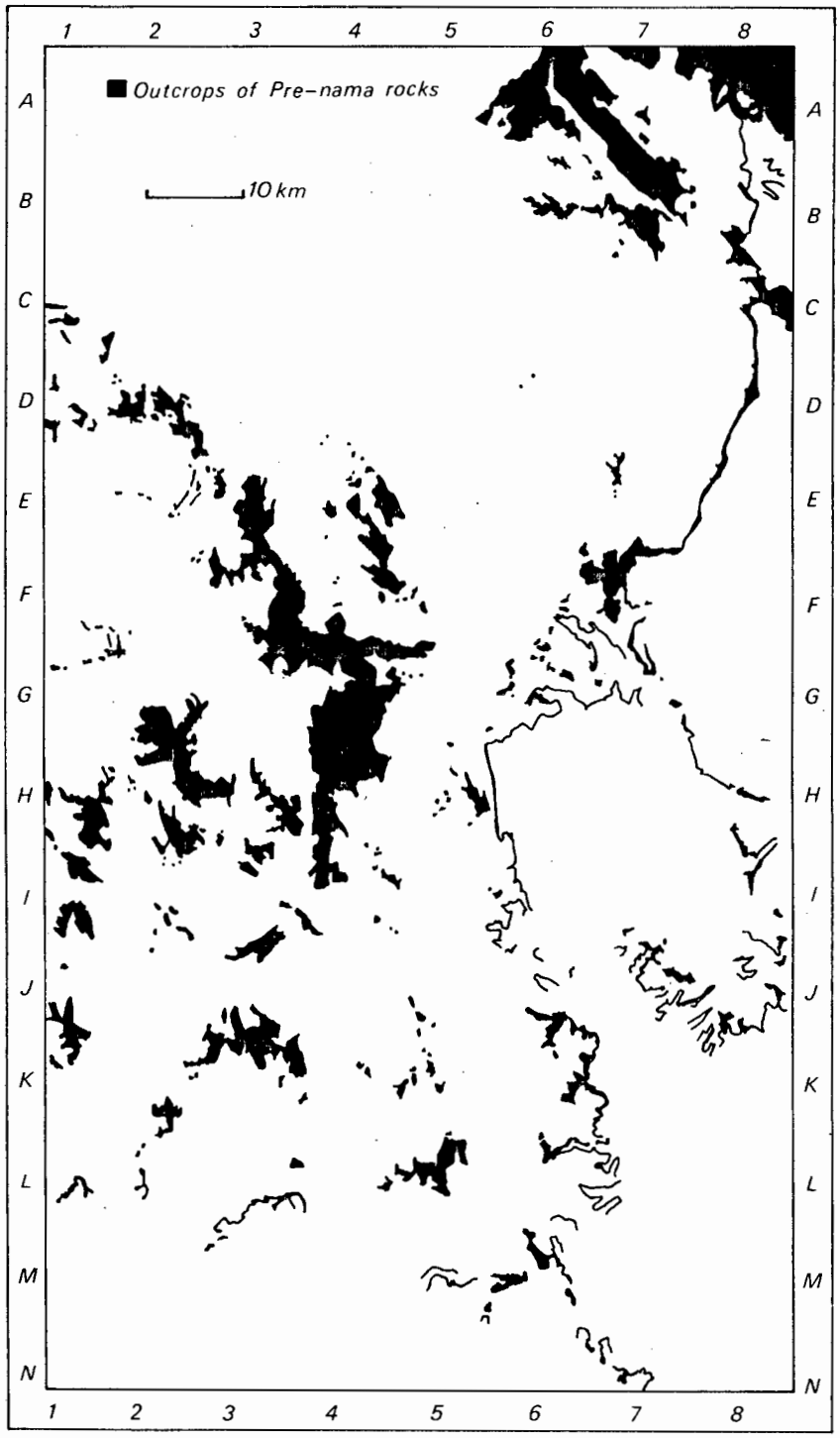

Figure 73. Sketch map showing outcrop areas (in black) of pre-Nama rocks in the Aus area

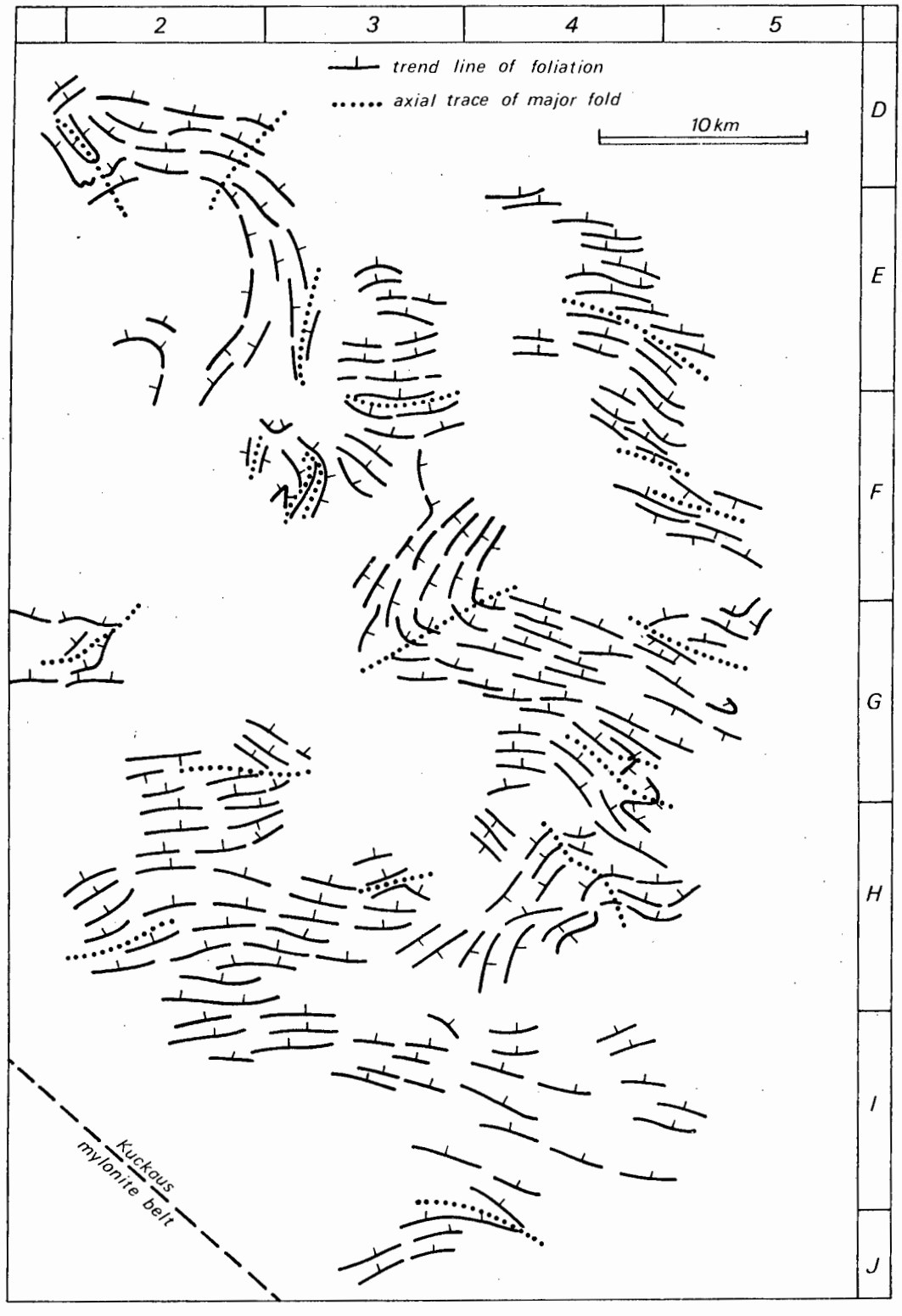

Figure 74. Trend-line map of foliations (mainly s_1) in the central part of the Aus area

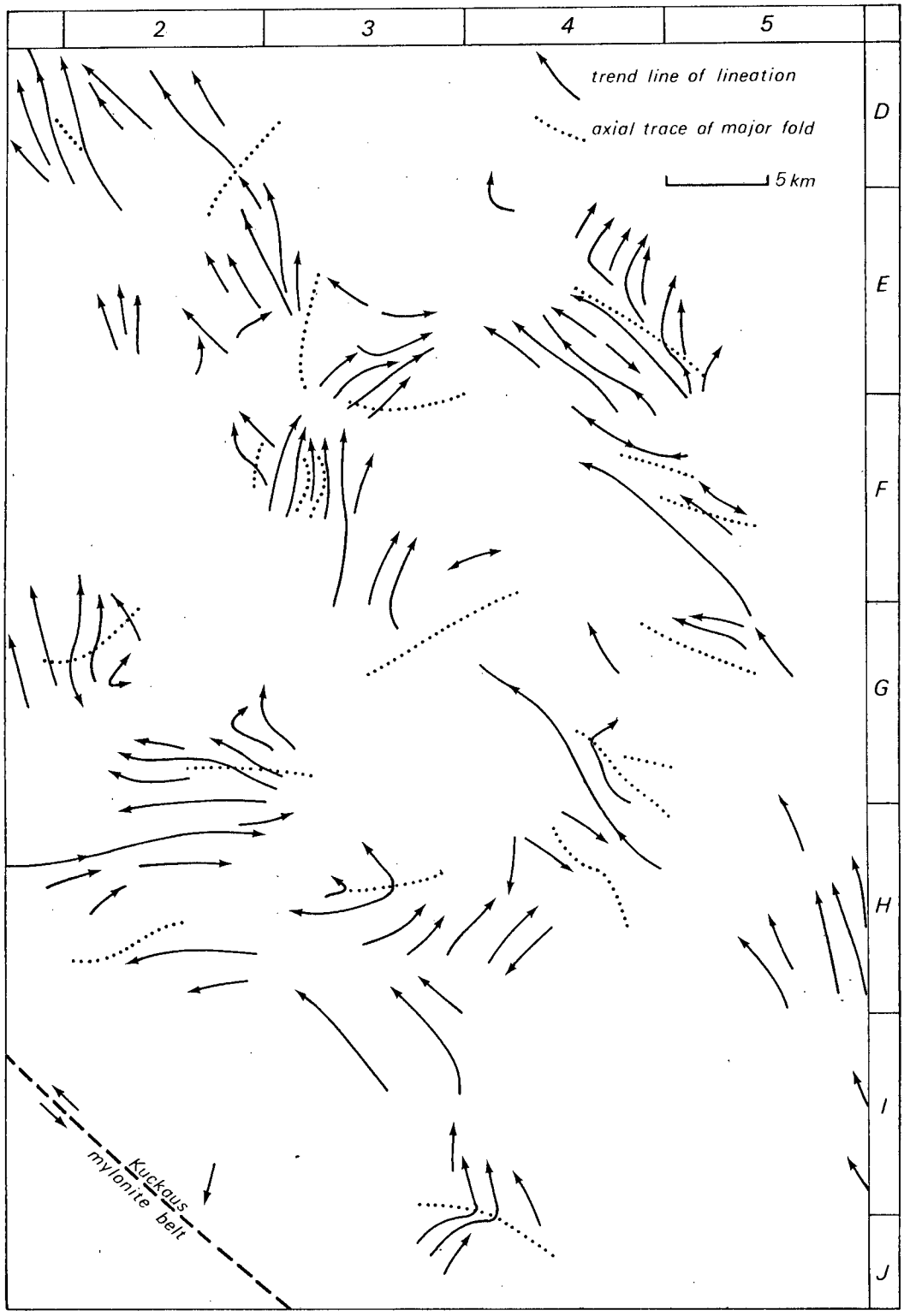

Figure 75. Trend-line map of lineations (l_1 and l_2) in the central part of the Aus area

6.4. SHEAR ZONES

Two large northwest-trending shear zones are present in the Aus area (Annexure 1, Figs. 25, 38, etc.). The mylonitic core of the northern zone was referred to as the 'Excelsior-Tierkloof mylonite zone' by von Brunn (1967, p. 110); in the present study it is named the *Excelsior mylonite belt* after the farm on which it is best developed. The southern shear zone is shown as a large 'fault' on the Official Geological Map of South West Africa (1963); this feature is named the *Kuckaus mylonite belt* after the mountains in which is is best exposed.

1. Excelsior Mylonite Belt

The Excelsior mylonite belt is exposed for a length of more than 30 km; it can be traced intermittently in a southeasterly direction for a further 10 km as a partially covered feature beneath sediments of the Nama Group (C8). In the northwest it passes beneath the sand cover of Springbokvlakte (A6) but is not visible in the Tumuab granite some 7 km on the northwestern side of the plain.

The zone of mylonites varies in width from 150 to 1000 m. At its northwestern end in Tierkloof (A6), where the zone attains maximum width, mylonite and cataclastic Tiras gneiss and Tierkloof lava are intercalated. A non-pervasive foliation dipping northwards at steep angles is present in the Tierkloof diorite up to 2 km from the mylonites; but nearer the mylonites the zones of sheared diorite become increasingly more extensive. Immediately adjacent to the mylonites the diorite is penetratively foliated. Phenocrysts of feldspar in the diorite are in random orientation within the zones of unsheared rock as close as 100 m from the mylonites. On shearing, the phenocrysts have been drawn out into oval crystals flattened in the plane of foliation and elongated to define a lineation (l_6) with a subhorizontal trend roughly parallel to the mylonites. With increasing strain the phenocrysts have been dispersed as trails of clasts appearing as ill-defined white streaks in schistose diorite. The preferred orientation of lenticular fragments in Tierkloof lava adjoining the mylonite zone also defines a lineation. The mylonite belt contains tectonic slices of lava intercalated with the mylonites, which are extremely fine-grained layered rocks characterized by dark-green (if derived from Tierkloof diorite) or pale-pink (if derived from Tiras gneiss) colour; mylonites derived from the Tiras gneiss are phyllonitic. The pink mylonites grade northwards into cataclastic Tiras gneiss in which s_6 is less pronounced and the grain size is coarser. At the southeastern end of the Excelsior belt on the farm Neisip (C8), the belt narrows to form two 10 m-wide mylonite zones separated by 50 m of cataclastic Tiras gneiss and veins of quartz breccia.

Along the belt the mylonitic fabric (s_6) defines a well-developed subvertical foliation parallel to the trend of the belt. The l_6 lineations, defined by striae, mullions and elongation of crystal and lithic fragments,

are developed within the foliation and plunge at variable angles (20-70°). The post-f_6 folds, which deform the s_6 mylonite fabric, are polyclinal but have coaxial, vertically-plunging fold axes (Plate 56).

North of the mylonite belt the Tiras gneiss has a penetrative cataclastic foliation (s_6) within 1-2 km of the mylonites; discontinuous zones of cataclastic rock can be found for at least 8 km north of the main mylonite belt and are parallel to it. Obliquely crossing this foliation are younger cataclastic foliations, commonly curved along strike, which are oblique to the trend of the belt.

South of the mylonite belt the zone of cataclastic rock varies between 1 and 2 km in width, but discontinuous narrow zones of cataclastic rock are present farther south. In the southeast part of Excelsior Farm (B7) minor f_2 or f_3 folds in the Garub rocks show progressive tightening as they are traced towards the belts. These folds are strongly asymmetric, with one set of limbs dipping northward at increasingly steep angles as they are traced northwards towards the belt; the other limbs are subvertical and greatly attenuated.

2. *Kuckaus Mylonite Belt*

This lineament can be traced for 80 km across the study area. In a northwesterly direction it can be traced in scattered outcrops for a further 65 km beyond the Aus area up to the Namib Sand Sea northeast of Lüderitz, but it was not found at the coast (Kröner and Jackson, 1974). In the southeastern part of the Aus area the mylonite belt passes beneath the Nama Group but its trace is visible by post-Nama faulting in the overlying sediments.

Discontinuous and parallel zones of mylonite, some 500-1000 m wide, are characteristic of the centre of the Kuckaus mylonite belt in the study area. Quartz veins have been emplaced into this zone (Plate 25) and the margins of these veins have steeply plunging striae which are parallel to l_6 defined by clast trains and mineral alignment in the mylonites. s_6 in the mylonites dips subvertically, as does the axial plane foliation of f_6 minor folds in the adjoining cataclastic gneiss. Deformation of the Tsirub gneiss, biotite gneiss and Anib granite gneiss within the mylonite belt has been described in Chapter 3.

Parallel mylonite belts of smaller size are present up to a distance of a few kilometres south of the main mylonite belt. On either side of this central zone of mylonites is a zone of rocks 1-2 km wide (Plate 25) which have been refoliated parallel to the mylonites and, although cataclastic, their pre-cataclastic lithology is still recognizable.

Northwestwards beyond the Aus area towards Lüderitz quartz and quartz-breccia veins with associated mylonites project through the sand cover at intervals in the form of en-echelon dislocation zones a few kilometres apart and mark the continuance of the shear zone.

3. *Discussion on the Kuckaus and Excelsior Mylonite Belts*

Both the Kuckaus and Excelsior mylonite belts have a northwestern trend and appear to be of the same age. The mylonitization is of pre-Nama age in both cases because the Nama sediments overlie the mylonites but are themselves not mylonitized. The mylonites of the Kuckaus belt are crosscut by pre-Nama north-northeast-trending dyke swarms (M6) which may be correlates of the pre-Nama Gannakouriep dyke suite (see Section 3,14) farther south. If these basic dykes and the Tumuab granite can be reliably dated,they will provide minimum ages for the Kuckaus and Excelsior mylonite belts respectively. The Tumuab granite has yielded an imprecise Rb/Sr whole-rock age of approximately 1250 Ma (von Brunn and Dodson, 1967). The Nama Group has been dislocated and downthrown on the northern side along northwest-trending faults overlying both mylonite belts, which indicates further movement along the lineaments in post-Nama times; fault scarps of recent age along the Kuckaus belt on Pockenbank Farm (M7) and farther north suggests that movement along the belt continues to the present day (Annexure 1).

Both the Kuckaus and Excelsior belts are parallel to a third mylonite belt of much smaller dimensions which is situated between them. Quartz-breccia veins and mylonite form a mylonite belt at least 14 km in length running through the Solo Hill (See Annexure 1, D2, C2) in the plain south of the Koichab River. This mylonite belt is likely to be a correlate of the larger belts to the north and south.

A correlation of the Excelsior mylonite belt with the Lord Hill mylonite belt, some 220 km to the southeast along strike, was suggested by Blignault et al. (1974). In the writer's view such a correlation is highly speculative and may not be correct; most localities of the Lord Hill mylonite belt visited by the writer consist of extrusive and intrusive rocks rather than mylonites and it is not certain how extensive is the mylonite zone.

The Kuckaus mylonite belt has been tentatively correlated (Jackson, 1974, p. 50; Blignault, 1974a, p. 44) with a similar structure to the southeast known as the Tantalite Valley Shear Zone (Blignault et al., 1974) or Pofadder Lineament (Joubert 1974a). The Kuckaus and Pofadder mylonite belts cannot be correlated with certainty because they are separated by 100 km of Nama sediments. However, both belts have similar strikes, average widths and age relations, and their correlation seems probable. Because of the extremely scattered outcrop pattern in the area in which the mylonite belt is situated, it is not possible to determine whether the large shearing-related interference structures described by Toogood (1976) for the Pofadder Lineament are present; but in outcrops adjoining the Kuckaus belt there is no indication of large-scale rotation of older structures. This may be because the lineament is exposed at a higher crustal level in the Aus area than farther southeast so that ductile deformation in the adjoining areas of the shear zone could not take place.

The possibility that these large mylonite belts separate crustal blocks of different tectonic levels has been suggested by Blignault (1974a), Blignault et al. (1974) and Toogood (1976). According to the model of Blignault a

central zone of high-grade metamorphites is separated by the northern (Lord Hill) and southern (Tantalite Valley) mylonite belts from adjoining areas of medium-grade metamorphites. Toogood (1976) has described a similar metamorphic transition from high grade north of the Pofadder Lineament to medium grade south of the lineament. Evidence for similar metamorphic discontinuities in the Aus area is slim but not necessarily contradictory. In general high-grade rocks are present north of the Kuckaus mylonite belt in the Aus area, whereas medium-grade rocks are present south of the belt. But the 'quartz + plagioclase + muscovite out' isograd crosses the mylonites obliquely and in the western fringe of the area high-grade rocks are present south of the belt as well as north of it (see Sections 4.2 and 4.5). With respect to the northern belt, there is insufficient evidence from the semi-pelitic rocks (because of their rarity) for a transition from high grade to medium grade on crossing the lineament northwards; there is no evidence of change of grade in any of the numerous metabasites examined (see Section 4.1). Furthermore medium-grade rocks are present in the northwest of the Aus area which, according to the model presented by Blignault (1974a), should be high grade. Thus although the mylonite belts undoubtedly represent surfaces of major discontinuity that may well separate different crustal domains, in the Aus area, at least, they do not appear to have greatly influenced the metamorphic zonation described in Section 4.5.

6.5 YOUNGER STRUCTURES

Sediments of the Nama Group are predominantly flat-lying in most of the study area. Only in those areas where the strata are not level has the strike and dip direction of bedding been shown on the geological map (Annexure 1). In all cases these irregularities were observed to be due to tilting or drag caused by faulting. In the southwest of the study area, however, the Nama Group has been folded into tight folds with subvertical axial planes striking northwest.

Basic dykes of pre-Nama age have been intruded along faults striking north-northeast. Extensive post-Nama faulting along directions of north-northwest and, less commonly, north-northeast has followed.

6.6 NOTE ON THE KOICHAB TROUGH

Beetz (1924) envisaged a large graben some 30 km wide, which he named the Koichab trough, lying between two horsts of uplifted basement forming the Aus mountains in the south and Tiras mountains in the north. The topographical depression marking the site of the trough is occupied by the Koichab dunes 'notorious among travellers for their impassibility' (ibid., p.27).

Beetz ascribed the formation of the graben to the lack of granite intrusions within it (ibid, p.25). Evidence for this depression being a structurally-induced trough was given as follows:

(i) preservation of Nama sediments at Dicker Willem Mountain, Koichab Pan, Tschaukaib Station, and Blue Mountain within the trough between the Nama Escarpment east of Aus and the Atlantic Coast

(ii) occurrence of alkaline rocks within the trough near the coast

(iii) zones of block faulting to the north and south of the trough

The evidence cited by Beetz (1924) can be disputed on the grounds that:

(i) the outcrops of calcareous rocks cited above are not correlates of the Nama Group; they are part of the Namaqua Metamorphic Complex or represent carbonatite of younger age (Jackson, 1974, p.53; Kröner and Jackson, 1974). The occurrence just north of Tschaukaib Station on Splitterkuppe is, however, an outlier of the Nama Group (G. Germs, pers. comm., 1972)

(ii) no alkaline rocks were found at Hottentot Bay at the westward extension of the presumed trough (Kröner and Jackson (1974). Conversely Marsh (1973) has described several large complexes of alkaline rocks (Lüderitz Alkaline Province) on the coast within the proposed 'Aus-Lüderitzbucht' horst

(iii) no evidence of block faulting of the type described by Beetz (1924) was found in the Aus area during the present survey

However, a number of features noted during the present mapping suggest that the Koichab trough, occupied by the Koichab dunes, between the Nama Escarpment and the Koichab Pan may well have a tectonic origin:

(i) the base of the Nama sequence on the escarpment at the mid-axis of the depression is situated 100-140 m below the equivalent points on the northern and southern margins on the farms Neisip and Kwessiepoort (Annexure 1). Downwarping of the crust has therefore taken place

(ii) additional subsidence in the centre of the depression has been caused by downfaulting of the entire central part of the Nama Escarpment along faults trending north-northeast (Annexure 1). West of these faults the base of the Nama has been downthrown approximately 450 m

(iii) the Excelsior and Solo mylonite belts have been mapped along the northern and southern margins of the trough and these dislocations may well have provided surfaces of movement for later subsidence of the trough; Recent fault scarps parallel to the related Kuckaus mylonite belt suggest that these major lineaments are still tectonically active

It would therefore appear that although the evidence cited by Beetz (1924) for the existence of the Koichab trough is ill-founded, this trough exists and is, at least in part, due to downwarping and downfaulting of the crust in this vicinity and cannot simply be ascribed to erosion by the Koichab River.

Chapter 7

SUMMARY ,CONCLUSIONS AND DISCUSSION

7.1 SUMMARY

The geological history of the Aus area is summarized in Table 28; further information on the structural history is given in Table 27. The geology is summarized in Figure 76, which shows the conjectural configuration of rock units under the extensive cover of sand between outcrop areas; the sketch map supersedes others for the same area given in Jackson (1974) and Blignault et al. (1974).

7.2. CONCLUSIONS

1.

Rocks of the basement complex around Aus (this report) and farther west to the coast (Jackson, 1974, p.53; Kröner and Jackson, 1974) are part of the Namaqua Metamorphic Complex and show many lithologic, structural and radiometric (Appendix 7) similarities with the basement rocks to the southeast in southern South West Africa (Blignault et al., 1974). Isolated exposures of medium-grade and high-grade metamorphites to the west, north and south of the Aus area that were originally of uncertain correlation (Greenman, 1966; von Brunn, 1967; McMillan, 1968) are also part of the Namaqua Metamorphic Complex. The northwestern extension of the Namaqua Mobile Belt is truncated by the Pan-African zone of refoliation along the Atlantic Coast (Kröner and Jackson, 1974). The southern margin of the NMC is represented by the Gaidab massif around Witputs which is separated from the Vioolsdrif complex by a shear zone (McMillan, 1968, p.165). The northernmost unit of the Namaqua Metamorphic Complex (the Houmoed granodiorite, this report) between Aus and

TABLE 28

Summary of the geological history of the Aus area

ROCK UNIT	DOMINANT MODE OF FORMATION	DEFORMATIONAL FEATURES			METAMORPHISM: Greenschist / Amphibolite / Granulite	MIGMATIZATION: Metatexis / Diatexis
Dicker Willem carbonatite *q*	intrusion					
		NNW- and NNE-trending faults				
		folding of Nama in SW of area				
Nama Group	sediment^{n}					
pp, ap, d, td, q	intrusion	NNE-trending faults				
Tumuab granite	intrusion			s_7		
Klein Tiras granite	intrusion					
Houmoed granodiorite	intrusion	f_6	l_6	s_6		
Tierkloof diorite	intrusion extrusion					
		f_5	l_5	s_5		
		f_4	l_4	s_4		
?*pd*						
		f_3	l_3	s_3		
Tiras gneiss	intrusion					
Pyramide granite gneiss	fusion intrusion					
Anib granite gneiss						
Biotite granite gneiss						
Aus granite gneiss						
Kubub granite gneiss						
Jakkalskop charnockite	intrusion				west / east	
		f_2	l_2	s_2		
Magnettafelberg serpentinite	intrusion					
		f_1	l_1	s_1		
Tsirub gneiss	intrusion					
				s		
Layered biotite gneiss Garub sequence	sediment^{n}, ?volcanism					

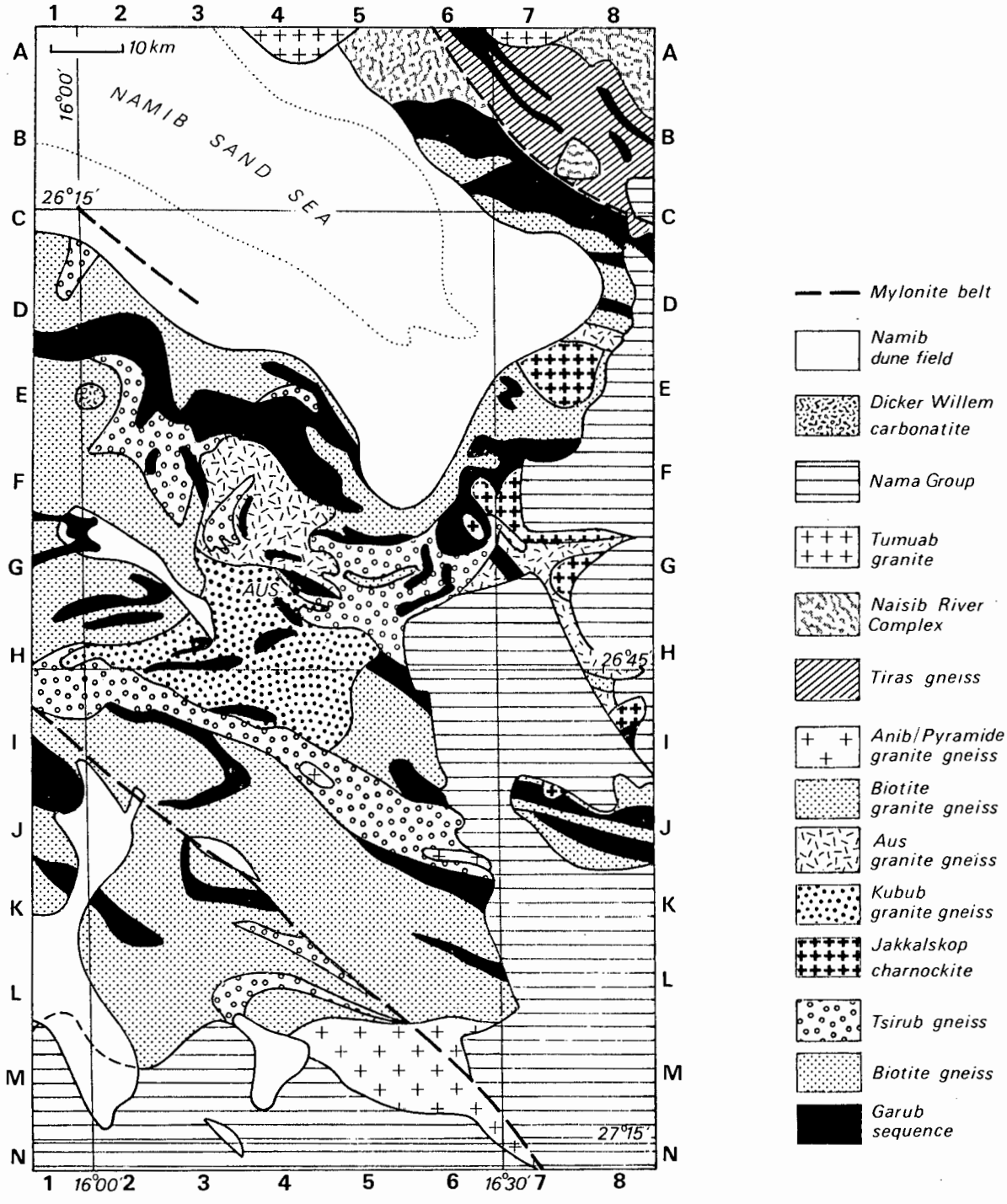

Figure 76. Conjectural geological sketch map of the Aus area

Helmeringhausen is overlain by the Nagatis Formation (von Brunn, 1967, p.7) which is the lowermost unit of the Sinclair Group (*after* Watters, 1974); isolated outcrops of amphibolite and quartzite reported farther north around Sinclair Mine (ibid., p.7) may represent relicts of the Namaqua Metamorphic Complex that are not covered by rocks of the Sinclair Group.

2.

The Garub sequence comprises the oldest rocks in the Aus area. This is a sequence of layered rocks of mainly semi-pelitic, pelitic, mafic, calcareous and quartzose composition. The sequence is extremely diverse and includes rocks of apparent sedimentary origin (metaquartzites, marbles, aluminous gneiss and iron formation) and of apparent igneous origin (most metabasites and magnesian rocks). The major metasedimentary rock types (viz., quartzose, calcareous and aluminous compositions) are concentrated in west-trending zones; gradations between these metasediments suggest original sedimentary lithofacies changes. The area of carbonate deposition broadens westwards from Aus; the marble bodies in the central Lüderitz District are the largest known from the entire Namaqua Metamorphic Complex.

Extensively developed layered biotite gneisses of psammitic composition may represent part of the same depositional sequence as the Garub rocks.

3.

The metamorphic grade of the mineral parageneses defining the various foliations suggests that deformation during the early structural history (deformation episodes D_1, D_2 and D_3) of the Aus area took place under conditions of medium-to-upper amphibolite facies metamorphism. In contrast granulite metamorphism appears to have been restricted both in time (following D_2) and place (to the east-centre of the area) and was most probably preceded, accompanied and followed by amphibolite metamorphism (Table 28). The present pattern of amphibolite facies isograds represents the outcome of this protracted and possibly continuous event of amphibolite metamorphism, which spanned the period from before D_1 to D_3. Later deformation was less intense and took place under retrogressive conditions.

Temperature estimates for amphibolite facies metamorphism range from 650°C on the border of the study area to 780-800°C in the centre. Medium-grade metamorphites are present in the south and northwest (zone I). Throughout the large central zone (zone III) the grade of metamorphism is the highest possible in the amphibolite facies. In zone III muscovite is not stable in any rocks; 'garnet + cordierite + sillimanite + K-feldspar' characterize the metapelites and 'hercynite + sillimanite + quartz' is present in places. Metabasites contain clinopyroxene, plagioclase with high anorthite contents (An_{55}-An_{95}) and brown hornblende with advanced edenitic and titanium substitution. Calcareous rocks contain the high-grade parageneses 'calcite + periclase' and

'diopside + forsterite + calcite'; wollastonite has formed by reaction of 'calcite + quartz' and 'grossularite + quartz'; anthophyllite, scapolite and vesuvianite are also stable.

The metamorphic zones constitute a low-pressure/high-temperature facies series that is essentially isobaric between pressure limits of 4,5 - 6 kb. High geothermal gradients of 30-50 ^{o}C/km were operative during amphibolite facies metamorphism.

4.

The distribution of granulite-grade metabasites of the Garub sequence (hypersthene-pyroclase granolites) defines two zones of granulite metamorphism, some 1350 km^2 in extent, east of Aus. Within the granulite zones are situated six bodies of charnockite which are mainly charno-enderbitic in composition and appear to be of intrusive origin. The petrology of the charnockites and surrounding granolites (which are also present as inclusions within the charnockites) suggests that the charnockites were intruded during the period of granulite metamorphism. Pressure estimates for this metamorphism are P_t = 5-7 kb, P_{H_2O} = 2 kb. The presence of carbonic fluid inclusions within the charnockite suggests that juvenile CO_2 may have been introduced during the intrusion of the charnockites. Dilution of the hydrous fluid phase in the country rocks by CO_2 may have been responsible for the development of granulite facies metamorphism.

Recent findings by a number of workers have shown that charnockites are present in at least 16 widely scattered localities elsewhere in the Namaqua Mobile Belt. At Aus, Klein Karas, Warmbad, Onseepkans, Kakamas, Marydale and O'Okiep granolites are associated with the charnockites. Available data on the modal composition of charnockites in southern South West Africa and the northern Cape indicate increasing amounts of SiO_2 and K_2O in a northeasterly direction away from the trend of the Pofadder Lineament (a major shear zone transecting southern South West Africa). These compositional trends may reflect a decrease in the prevailing pressures of the environment in which the charnockites formed.

5.

The amphibolite facies metamorphic zonation is paralleled by a migmatitic zonation. In the outer parts of the study area only metatectic migmatites are present on a regional scale. In the centre of the area (zone III), where temperatures during metamorphism were sufficient to melt dry biotite granite, diatectic neosomes are present in the migmatites. The large masses of syntectonic granite gneiss in the centre of the study area are believed to have formed by partial melting of semi-pelitic metamorphites during a hypothetical period of high heat flow that accompanied amphibolite facies metamorphism. At least four period of migmatization span the early deformational history

from before D_1 to after D_3 and suggest that conditions of high-grade metamorphism were present throughout this period.

7.3. DISCUSSION

1. Age of the Garub Sequence and Related Rocks

Rocks of supracrustal origin, possibly equivalent to the Garub sequence, have been reported from the Namaqua Metamorphic Complex by Benedict et al. (1964), von Backström (1964), Beukes (1973), Geringer (1973), Joubert (1971, 1974b), Vajner (1974), Blignault (1974), Kröner and Jackson (1974) and Toogood (1976).

Rocks of supracrustal origin in the Namaqua Metamorphic Complex include large proportions of metasediments. Semi-pelitic varieties are ubiquitous. South of the Orange River, metaquartzites are well developed (Joubert, in prep., Annexure 1), whereas north of the Pofadder Lineament (Joubert, 1974a) in south-eastern South West Africa quartzose rocks are markedly absent and 'pink gneiss', which is of psammitic composition, is the most abundant rock type of the sequence (Beukes, 1973; Toogood, 1976). Farther northwest around Klein Karas (Blignault, 1974a) and south of Aus (this report) metapelites are well developed. North of the metapelites around Aus a basin of calcareous and quartzose rocks broadens westwards. Calcareous rocks underlying metapelites are also present north of the Orange River in the northern Cape (Geringer, 1973) but the proportion of marble in this sequence is much lower than around Aus.

The vast majority of radiometric ages yielded by these paragneisses are of Kibaran age, i.e. approximately 1,1 Ga (Nicolaysen and Burger, 1965; Clifford, 1968; Burger and Coertze, 1973). There is no doubt that these ages reflect a particularly intense period of tectonism at this time and that the supracrustal sequences, such as the Bushmanland sequence, were deposited earlier than 1,1 Ga. In contrast to the Kibaride belt (Holmes, 1951), there are no geosynclinal sequences associated with the 1,1-Ga tectonic event in the Namaqua belt and the supracrustal remnants in the latter belt are older than this tectonism (Clifford, 1972; Kröner, 1976a).

Paragneisses of the Namaqua Metamorphic Complex have traditionally been correlated with the Kheis sequence (e.g. Gevers et al., 1937; Coetzee, 1941; de Jager and von Backström, 1961; von Backström, 1964, 1967; Martin, 1965; Truswell, 1970; Clifford, 1972). Leube (*in* Martin, 1965) and Vajner (1974, p.18) report that the 2,0 Ga-old (U/Pb, Burger and Coertze, 1973) Draghoender granite intrudes the Kheis rocks. The antiquity of the Kheis sequence is, however, disputed by Cornell (1975) who obtained a whole-rock Rb/Sr age of 1,9 Ga from greenschist facies Marydale lavas of the Kheis sequence farther south; he considered this age to represent the time of their extrusion. Correlation of the northern parts of the Kheis sequence with the 2,0-1,8 Ga-old Matsap sequence (Crampton, 1974) has also been proposed (e.g. Beukes, 1973, p.183) although this is disputed by Vajner (1974).

However, lithologic similarities between the Namaqua paragneisses and the Kheis sequence become less apparent as more areas of the Namaqua belt are mapped in detail and recent workers have been reluctant to correlate the two sequences. Thus Beukes (1973, p.ix) and Geringer (1973, p.65) suggested that the Namaqua paragneisses north of the Orange River may be eugeosynclinal correlates of the 2,0 Ga-old Transvaal sequence on the basis of certain lithologic similarities. But there appears to be little evidence for the Namaqua paragneisses representing a 'normal geosynclinal succession' as asserted by Beukes, or for the extensive volcanism that typically accompanies the formation of eugeosynclinal sequences.

Both Bertrand (1976) and Kröner (1976b) suggest the possibility of a correlation between the paragneisses in Bushmanland (Joubert, 1974b) and the 1,9 Ga-old Haib volcanics of the Orange River Group (Blignault, 1974b). According to Bertrand (1976) the predominantly volcanic Haib sequence near Goodhouse, metamorphosed to medium grade, appears to grade eastwards into the Bushmanland sequence; in the Namaqua Metamorphic Complex east of Goodhouse metaquartzites and sillimanite schists are interlayered with metamorphic derivatives of the lavas.

The Garub sequence in the central Lüderitz District may be of equivalent age. Dr. A.J. Burger has obtained a minimum age of ∿1755 Ma (zircon Pb^{207}/Pb^{206}) from folded migmatite near Lüderitz at the northwestern end of the Namaqua belt (Kröner, 1975, p.56). Farther north along the coast at Hottentot Bay similar rocks intrude metaquartzites of the Aurus sequence, a correlate of the Garub sequence to the east (Kröner and Jackson, 1974).

At the moment, therefore, the age of the Namaqua paragneisses is open to speculation. Since the various sequences are separated by distances of many hundreds of kilometres, it would be an unfounded assumption to assume that they are all coeval and such generalizations should be avoided.

A closely related problem concerns the basement on which the Namaqua paragneisses were deposited. It is indisputable that these sequences were deposited onto some sort of basement, yet in almost all areas that have been recently mapped the paragneiss sequences are the oldest rocks there on the basis of intrusive contacts with other units (e.g. Joubert, 1972, 1974b; Geringer, 1973; Beukes, 1973; Vajner, 1974; Toogood, 1975; Jackson, 1975). The original basement on which these sequences were deposited must have undergone remobilization on a vast scale; remobilized rocks have then intruded the cover rocks, perhaps by a similar mechanism to that proposed by Eskola (1949) for mantled gneiss domes.

The nature of this original basement is conjectural, but the biotite gneisses probably represent the most likely rock types. The Grenville Supergroup, Canada, was deposited on an older basement consisting mainly of biotite gneisses (Wynne-Edwards, 1969). Similar biotite gneisses in the Namaqua Metamorphic Complex, variously known as grey gneiss, mixed gneiss or other 'sack names', include rocks of varying origin and tectonic category; but some of them may also represent basements on which the Namaqua supracrustal rocks were deposited. According to J. Moore (pers. comm., 1976) biotite gneiss around Namiesberg, near Pofadder, contains the imprint of at least one de-

formational event predating the deposition of the Bushmanland sequence; f_1 folds deform bedding in the cover sequence but they deform a pre-f_1 foliation in the biotite gneisses. Biotite gneiss in the Pella area also apparently contains structures predating the Bushmanland sequence (H. Voets, pers. comm., 1975). If such biotite gneisses are in fact remnants of the basement on which the Bushmanland sequence was deposited, they have escaped the extensive remobilization typical of the basement in other parts of the belt and may provide significant clues as to the early history of the Namaqua Mobile Belt.

Possible indications of the age of this 'basement' are given by recent mapping in the contact zone of the Namaqua Metamorphic Complex and the Vioolsdrif complex (which includes the Orange River Group and the Vioolsdrif granitoids). According to Bertrand (1976) layered biotite gneiss and associated amphibolite and sillimanite-cordierite gneiss are crosscut by granodiorites of the Vioolsdrif suite (dated at 1,9 Ga) near Henkries. Similarly Kröner (pers. comm., 1976) reports that Vioolsdrif granite intrudes previously tectonized layered biotite gneiss on the farm Witputs 258 in the Warmbad District.

It would therefore appear that biotite gneisses had already been deformed and metamorphosed to amphibolite facies before intrusion of the 1,9 Ga-old Vioolsdrif suite. It is possible that the former rocks represented a basement on which were deposited the supracrustal Orange River Group and rocks of the Namaqua Metamorphic Complex such as the Bushmanland sequence.

2. *The Age of the Namaqua Charnockites*

Saggerson and Owen (1969, p.342) noted that most African charnockites yield radiometric ages greater than 2,5 Ga. Clifford (1974, p.1) concluded that two distinct ages of granulite metamorphism, at 1,2 Ga and 3,0 Ga, could be recognized. Granolite-charnockite suites are present in structural domains ranging from 300-3000 Ma old, but the granulite facies rocks yielding radiometric ages other than those of the two main events mentioned above merely reflect the overprinting of younger lower-grade metamorphism (ibid.).

All geochronological data presently available indicates that the charnockites and granolites of the Namaqua-Natal belt were formed during the younger granulite metamorphic episode referred to above. Thus Nicolaysen and Burger (1965) obtained a Rb/Sr age of 1,1 Ga on biotite from biotite gneiss around the charnockite near Kakamas, northern Cape. According to von Backström (1964), the charnockite postdates the regional metamorphism. The granolites around Nababeep, Namaqualand, yield a whole-rock Rb/Sr age of 1,2 Ga which, according to Clifford et al. (1975a), reflects the period of granulite metamorphism. Charnockites intruded into the granolites yield a zircon age of 1070 Ma (ibid.). Cornell (1975) has dated granulite facies metabasites of the Kheis sequence south of Marydale, northern Cape, at 1,4 Ga by Rb/Sr; he considers this age to represent the granulite-facies 'Sonqua' metamorphic event which was followed by the retrogressive 'Namaqua' event at 1,1-0,8 Ga. In Natal, at the eastern end of the Namaqua-Natal Mobile Belt, charnockites have been intruded into hypersthene granolites (Gevers and Dunne, 1942; McIver, 1966); one of the younger

charnockites in this group has been dated by Rb/Sr at 1,0 Ga by Nicolaysen and Burger (1965).

All presently-known charnockites in the Namaqua Metamorphic Complex postdate the Namaqua paragneisses. If the paragneisses are approximately 1,9 Ga old, as suggested in the previous section, then Kröner's (1976a, p.148) proposal of a late-Archaean age for the Namaqua charnockites is not tenable.

In each of the cases cited above, the Namaqua charnockites have been emplaced into granulite-facies country rocks, suggesting that the onset of granulite metamorphism preceded their emplacement. The data of Clifford et al. (1975a) indicate that the time interval between granulite metamorphism and charnockite intrusion in the Namaqua belt may have been relatively short. It is noteworthy that charnockites also intrude much older granolites in the Pongola Supergroup (2,9 Ga), Swaziland, (Saggerson, 1973, p.223), in the Limpopo belt (∿3,0 Ga), Rhodesia, (Robertson, 1973), and in the Ancient Gneiss Complex (>3,4 Ga), Swaziland, (Hepworth, 1971, *in* Clifford, 1974).

In contrast, however, there are indications that the formation of the Namaqua granolites accompanied the emplacement of the charnockites in southeastern South West Africa. According to Toogood (1976), foliated granolites on the margins of the charnockite bodies grade into coeval charnockitic rocks with magmatic textures. Around Aus the charnockites have been intruded into previously metamorphosed and deformed rocks, but none of the granolites found within the charnockite contain a pre-charnockite fabric. It is not clear whether granulite metamorphism accompanied or predated the intrusion of the charnockites.

The relation between the charnockites and the syntectonic granite gneisses also varies from place to place in the Namaqua Mobile Belt. Around Springbok augen gneisses (Nababeep-Brandberg gneisses) predate the charnockite (Clifford et al., (1975a) and the same relation appears to be true around Aus. However, around Onseepkans other augen gneisses (Beenbreek granite) postdate the charnockites (Toogood, 1976). Around Springbok most syntectonic granitoids (e.g. Rietberg and Concordia granites) predate the charnockites (Clifford et al., 1975a), whereas most or all of the syntectonic granitoids postdate them around Aus (this report) and Onseepkans (Toogood, 1976). There thus exist alternative possibilities: either the generation and emplacement of syntectonic granitoids took place at different times in different parts of the belt; or the Namaqua granitoids are all of Kibaran age and the O'Okiep charnockites were emplaced much later than those of South West Africa.

3. *Amphibolite Facies Metamorphism and the Syntectonic Granite Gneisses*

The present study has shown that the granulite metamorphism represents the culmination of prograde regional metamorphism in the Aus area; similar conclusions were reached by Joubert (1971) and Clifford (1974) in Namaqualand. Amphibolite facies metamorphism at Aus is known to have outlasted the granulite metamorphism because migmatite neosomes produced during amphibolite facies metamorphism crosscut the charnockites and granolites. Amphibolite metamorphism

appears to have preceded, accompanied and followed in time the granulite metamorphism, which was restricted to only a part of the Aus area. It seems probable that the present metamorphic grade of mobile belt rocks represents the outcome of a continuous response to the high-temperature conditions present in the katazone rather than the imprint of well-defined metamorphic events. Saggerson and Turner (1976) suggested that the post-Bulawayan and post-Shamvaian metamorphic episodes in the Rhodesian craton and Limpopo belt may represent one prolonged metamorphic event. Wynne-Edwards (1969, p.180) concluded that the Grenville sequence, Canada, remained in high-grade metamorphic conditions of the katazone for some 500 Ma; age measurements by van Breeman and Dodson (1969) indicate a similar period of metamorphism for the Messina sequence in the Limpopo belt (Bahnemann, 1972).

The amphibolite-facies metamorphic zonation and metamorphic facies series suggests that a thermal dome was centred around the locality of Aus and that the regional geothermal gradient during metamorphism was particularly high there (Section 4.5). Differences in metamorphic grade between the central zone and outer metamorphic zones of the study area are ascribed mainly to this temperature gradient. Saggerson and Turner (1976, p.44) suggested that a thermal anticline existed over the Limpopo belt in Shamvaian times (2,7-2,9 Ga) and that upward displacement of isotherms may have taken place under a thick sedimentary pile as described by Richardson (1970). Comparison of the amphibolite-facies zonation at Aus with the granulite-facies zone suggests that the area of maximum metamorphism moved westwards from the Jakkalskop area during granulite metamorphism to the area around Aus Village during later amphibolite metamorphism.

It appears to be no coincidence that the maximum development of syntectonic granitoids (Aus granite gneiss, Kubub granite gneiss) also occurred around Aus, where the thermal dome was centred (Fig. 76). Saggerson and Turner (1976, p.47) suggested that the generation of the Rhodesian granitoids was also a function of the regional geothermal control; the granitoids are postulated to have formed by partial melting as a response to high geothermal gradients. Bahnemann (1973) suggested a similar origin for the Singelele granite gneiss in the Limpopo belt by fusion of a tonalitic basement, typified by the Bulai gneiss.

The potassium-rich nature of the Aus and Kubub granite gneisses can be ascribed to the high-grade environment of their formation. Saggerson and Turner (1976, p.48) have described the common association of potassium-rich syntectonic granitoids with high-grade metamorphites, granodiorites with low/medium-grade metamorphites, and sodium-rich tonalites with low-grade metamorphites. A zone of lenticular bodies of syntectonic potassic porphyritic granite more than 100 km in length is present at the interface between the granulite-facies Limpopo belt and the amphibolite-facies margin of the Rhodesian craton (Robertson, 1973). This occurrence leads to comparison with the syntectonic megacrystic granites, which are also potassium-rich, in the Namaqua belt around Aus (Aus granite gneiss) and Klein Karas (Grabwasser granite gneiss *after* Genis *in* Blignault, 1975). Near Aus and Klein Karas (Fig. 1c) these extensive granite gneisses are closely associated with and intrude charnockites and granolites (this report) and may have been produced

during the same prolonged period of metamorphism as the granulite-facies rocks (cf. Robertson, 1973, and Bahnemann, 1973, in the Limpopo belt). An origin for these potassium-rich granites by crustal fusion and limited upward migration under high geothermal gradients appears more likely than the upward streaming of volatiles from the mantle and large-scale metasomatism invoked by Anhaeusser et al. (1968, p.22).

The tectonic setting and field relations of the potassium-rich granite gneisses in the Namaqua belt around Aus resemble those of the chelogenic (Sutton, 1963) or shield-forming granites of the early Precambrian. They contrast strongly with the granitoids of the Naisib River Complex north of Aus; the latter are sharply crosscutting, largely unfoliated and apparently unrelated to the regional metamorphism, resembling the anorogenic late-formed plutons of cratonic areas (Hunter, 1973).

REFERENCES CITED

AL KHATIB, R. and TOURET, J. (1973) Fluides carboniques dans les roches du faciès granulite. Utilisation semi-quantitative de la surplatine à écrasement. *Soc. Géol. France Bull.*, 7, 15, 3/4, 321-325.

ALTHAUS, E. (1967) The triple point andalusite - sillimanite - kyanite. *Contrib. Mineral Petrol.*, 16, 29-44.

——— (1968) Der Einfluss des Wassers auf metamorphe Mineralreaktionen. *Neues Jahrb. Mineral. Monatsh.*, 9, 289-306.

——— (1969) Das System Al_2O_3 -SiO_2- H_2O. Experimentelle Untersuchungen und Folgerungen für die Petrogenese der metamorphen Gesteine. Teil II,III. *Neues Jahrb. Mineral. Abhandl.*, 111, 2, 111-161.

——— NITSCH, K.H., KAROTKE, E. and WINKLER, H.G.F. (1970) An experimental re-examination of the upper stability limit of muscovite plus quartz. *Neues Jahrb. Mineral. Monatsh.*, 1970, 325-336.

ANASTASIOU, P. and SEIFERT, F. (1972) Solid soluability of Al_2O_3 in enstatite at high temperatures and 1-5 kb water pressure. *Contrib. Mineral. Petrol.* 34, 272-287.

ANHAEUSSER, C.R., MASON, R., VILJOEN, M.J. and VILJOEN, R.P. (1968) A re-appraisal of some aspects of Precambrian shield geology. *Econ. Geol. Res. Unit, Univ. Witwatersrand, Inf. Circ.* 49, 30p.

APPLEYARD, E.C. (1974) Basement/cover relationships within the Grenville Province in eastern Ontario. *Can. J. Earth Sci.*, 11, 369-379.

BAGNOLD, R.A. (1941) *The Physics of Blown Sand and Desert Dunes.* Methuen, London, 265p.

BAHNEMANN, K.P. (1972) *A Review of the Structure, the Stratigraphy and the Metamorphism of the Basement-rocks in the Messina District, N. Transvaal.* Unpubl. D.Sc. thesis, Univ. Pretoria.

——— (1973) The origin of the Singelele granite-gneiss near Messina, northern Transvaal *in* Lister, L.A. (Ed.), Symposium on granites, gneisses and related rocks, 235-244. *Geol. Soc. S. Africa Spec. Publ.*, 3, 509p.

BANNO, S. (1958) Glaucophane schists and associated rocks in the Omi district, Niigata Prefecture, Japan. *Japan. J. Geol. Geogr.*, 29, 29-44.

——— (1964) Petrologic studies on Sanbagawa crystalline schists in the Bessi-Ino district, central Sikoku, Japan. *Tokyo Univ. Fac. Sci. J. Sect.* II, 15, 203-319.

——— TATSUMI, T., OGURA, Y. and KATSURA, T. (1963) Petrographic studies on rocks from the area around Lutzow-Holmbukta. *Antarctic Geol., SCAR Proc.* 1963, 405-414.

BARD, J.P. (1969) *Le Metamorphisme Regional Progressif des Sierras d'Aracena en Andalousie Occidentale (Espagne).* Univ. Montpellier, unpublished.

——— (1970) Composition of hornblendes formed during the Hercynian progressive metamorphism of the Aracena metamorphic belt (SW Spain). *Contrib. Mineral. Petrol.*, 28, 117-134.

BATHURST, R.G.C. (1971) *Carbonate Sediments and Their Diagenesis*. Elsevier, Amsterdam, 320p.

BEETZ, W. (1924) On a great trough-valley in the Namib. *Geol. Soc. S. Africa Trans.*, 27, 1-33.

BENEDICT, P.C., WIID, D. de N., CORNELISSEN, A.K. and STAFF (1964) Progress report on the geology of the O'okiep Copper District *in* Haughton, S.H. (Ed.), *The geology of some ore deposits in southern Africa, Vol. 2*, 239-302. Geol. Soc. S. Africa, Johannesburg, 739p.

BERTHELSEN, A. (1960) Structural studies in the Precambrian of West Greenland. Geology of Tovquasap Nuna. *Medd. Gronland*, 123, 1-226.

BERTRAND, J.M.L. (1976) Granitoids and deformation sequence in the Goodhouse-Henkries area. A new interpretation of the relationship between rocks in the Vioolsdrif-Goodhouse area and the Namaqualand and Bushmanland gneisses. *Precambrian Res. Unit, Univ. Cape Town, Ann. Rept.* 13, (in press).

BEUKES, G.J. (1973) *N' Geologiese Ondersoek van die Gebied Suid van Warmbad, Suidwes-Afrika, met Spesiale Verwysing na die Metamorf-Magmatiese Assosiasies van die Voorkambriese Gesteentes*. Unpubl. D.Sc. thesis, Univ. Orange Free State, 333p.

BHATTACHARYYA, C. (1972) Granitization in relation to evolution of the charnockite series from the Eastern Ghat hills, Strikakulam district, Andra Pradesh, India. *Neues Jahrb. Mineral. Monatsh.*, 1972, 220-240.

BILLINGS, M.P. and WHITE, W.S. (1950) Metamorphosed mafic dikes of the Woodsville quadrangle, Vermont and New Hampshire. *Am. Mineral.*, 35, 629-643.

BINNS, R.A. (1964) Zones of progressive regional metamorphism in the Willyama Complex, Broken Hill District, New South Wales. *Geol. Soc. Australia Jour.*, 11, 283-330.

——— (1965) The mineralogy of metamorphosed basic rocks from the Willyama Complex, Broken Hill District, New South Wales, Part I. Hornblendes. *Mineral Mag.*, 35, 306-326.

——— (1969) Ferromagnesian minerals in high-grade metamorphic rocks. *Geol. Soc. Austr. Spec. Paper*, 2, 323-332.

BLIGNAULT, H.J. (1972) Geotectonic implications of a structural-metamorphic investigation in the Ai-Ais/Klein Karas area. *Precambrian Res. Unit, Univ. Cape Town, Ann. Rept.* 7-9, 20-25.

——— (1974a) The tectonic zonation of part of the Namaqua Province in the lower Fish River/Narubis cross-section. *Precambrian Res. Unit, Univ. Cape Town, Ann. Rept.* 10-11, 43-45.

——— (1974b) Aspects of the Richtersveld Province *in* Kröner, A. (Ed.), Contributions to the Precambrian geology of southern Africa, 49-56. *Precambrian Res. Unit, Univ. Cape Town, Bull* 15, 213p.

——— (1975) Towards a stratigraphic nomenclature for the Namaqua Metamorphic Complex and associated rocks. *Precambrian Res. Unit, Univ. Cape Town, Ann. Rept.* 12, 41-42.

——— (1976) The tectonic evolution of the Richtersveld and Namaqua provinces in the Ai-Ais and Haib River areas, South West Africa. *Precambrian Res. Unit, Univ. Cape Town, Bull.* (in prep.).

———JACKSON, M.P.A., BEUKES, G.J. and TOOGOOD, D.J. (1974) The Namaqua Tectonic Province in South West Africa *in* Kröner, A. (Ed.), Contributions to the Precambrian geology of southern Africa. *Precambrian Res. Unit., Univ. Cape Town, Bull.* 15, 29-47.

BOETTCHER, A.L. (1970) The system CaO - Al_2O_3 - SiO_2 - H_2O at high pressures and temperatures. *J. Petrol.*, 11, 337-379.

BORG, J.Y. (1963) On conventional calculations of amphibole formulae from chemical analyses with inaccurate H_2O (+) and F determinations. *Mineral Mag.*, 36, 280, 583-590.

BOWEN, N.L. (1922) The reaction principle in petrogenesis. *Jour. Geol.*, 30, 177-198.

BOYD, F.R. (1959) Hydrothermal investigations of amphiboles *in* Abelson, P.H. (Ed.), *Researches in Geochemistry.* John Wiley, New York, 377-396.

——— FINGER, L.W. and CHAYES, F. (1968) Computer reduction of electron-probe data. *Carnegie Inst. Washington, Yearbook* 67, 210-215.

BRAUN, E. and MÜLLER, G. (1975) Zur chemischen Variabilität regionalmetamorph gebildeter Plagioklase, Epidote und Granate. *Contrib. Mineral. Petrol.*, 52, 193-211.

BREED, C.S., FRYBERGER, S.G., McCAULEY, C. and LENNARTZ, F. (in press) A study of global sand seas. *Geol. Surv. United States Prof. Paper.*

BUDDINGTON, A.F. (1963) Isograds and the role of H_2O in metamorphic facies of orthogneisses of the northwest Adirondack area, New York. *Geol. Soc. Am. Bull.*, 74, 1155-1181.

BURGER, A.J. and COERTZE, F.J. (1973) Radiometric age measurements on rocks from Southern Africa to the end of 1971. *Geol. Surv. S. Africa Bull.*, 58, 46p.

CARMICHAEL, D.M. (1969) On the mechanism of prograde metamorphic reactions in quartz-bearing pelitic rocks. *Contrib. Mineral. Petrol.*, 20, 244-267.

CLIFFORD, T.N. (1968) Radiometric dating and the pre-Silurian geology of Africa *in* Hamilton, E.I. and Farquhar, R.M. (Eds.), *Radiometric Dating for Geologists*, 299-416. Interscience Publs., London.

——— (1970) The structural framework of Africa *in* Clifford, T.N. and Gass, I. G. (Eds.), *African Magmatism and Tectonics*, 1-26, Oliver & Boyd, Edinburgh.

——— (1972) The evolution of the African crust. *Maroc Service Géol. Notes et Mém.*, 236, 29-39.

——— (1974) Review of African granulites and related rocks. *Geol. Soc. Am. Spec. Paper*, 156, 49p.

——GRONOW, J., REX, D.C. and BURGER, A.J. (1975a) Geochronological and petrogenetic studies of high-grade metamorphic rocks and intrusives in Namaqualand, South Africa. *J. Petrol.*, 16, 1, 154-188.

——McIVER, J.R. and STUMPFL, E.F. (1975b) A sapphirine-cordierite-bronzite-phlogopite paragenesis from Namaqualand, South Africa. *Mineral. Mag.*, 40, 347-356.

COETZEE, C.B. (1941) The petrology of the Goodhouse-Pella area, Namaqualand, South Africa. *Geol. Soc. S. Africa Trans.*, 44, 167-206.

COOKE, R.U. and WARREN, A. (1973) *Geomorphology in Deserts*. B.T. Batsford, London, 374p.

COOPER, A.F. (1972) Progressive metamorphism of metabasic rocks from the Haast Schist Group of southern New Zealand. *J. Petrol.*, 13, 457-492.

COORAY, P.G. (1962) Charnockites and their associated gneisses in the Pre-Cambrian of Ceylon. *Geol. Soc. Lond. Quart. J.*, 118, 239-273.

——(1969) Charnockites as metamorphic rocks. *Am. J. Sci.*, 267, 969-982.

CORNELL, D. (1975) *Petrology of the Marydale Metabasites*. Unpubl. Ph.D. thesis, Univ. Cambridge, 216p.

COWARD, M.P. (1973) Heterogeneous deformation in the development of the Laxfordian complex of South Uist, Outer Hebrides. *Geol. Soc. London J.*, 129, 139-160.

CRAMPTON, D. (1974) A note on the age of the Matsap Formation of the northern Cape Province. *Geol. Soc. S. Africa Trans.*, 77, 1, 71-72.

CURRIE, K.L. (1971) The reaction '3 cordierite = 2 garnet + 4 sillimanite + 5 quartz' as a geological thermometer in the Opinicon Lake region, Ontario. *Contrib. Mineral. Petrol.*, 33, 215-226.

DALZIEL, J.W.D., BROWN, J.M. and WARREN, T.E. (1969) The structural and metamorphic history of the rocks adjacent to the Grenville front near Sudbury, Ontario, and Mount Wright, Quebec. *Geol. Assoc. Canada Spec. Paper* 3, 207-224.

DAVIDSON, L.R. (1968) Variation in ferrous iron-magnesium distribution coefficients of metamorphic pyroxenes from Quairading, Western Australia. *Contrib. Mineral. Petrol.*, 19, 239-259.

DAVIS, J.C. (1973) *Statistics and Data Analysis in Geology*. John Wiley, New York, 550p.

DEER, W.A., HOWIE, R.A. and ZUSSMAN, J. (1966) *An Introduction to the Rock-forming Minerals*. Longman, London, 528p.

DE JAGER, D.H. and VON BACKSTRÖM, J.W. (1961) The sillimanite deposits in Namaqualand near Pofadder. *Geol. Surv. S. Africa Bull.*, 33.

DE VILLIERS, J. and SÖHNGE, P.G. (1959) The geology of the Richtersveld. *Geol. Surv. S. Africa Mem.*, 48.

DE WAARD, D. (1964) Mineral assemblages and metamorphic sub-facies in the granulite facies terrane of the Little Moose Mountain syncline, south-central Adirondack highlands. *Koninkl. Ned. Akad. Wetenschap. Proc. Ser. B.*, 67, 344-362.

——(1965a) The occurrence of garnet in the granulite-facies terrane of the Adirondack Highlands. *J. Petrol.*, 6, 1, 165-191.

——(1965b) A proposed subdivision of the granulite facies. *Am.J. Sci.*, 263, 455-461.

——(1973) Classification and nomenclature of felsic and mafic rocks of high grade regional-metamorphic terrains. *Neues Jahrb. Mineral. Monatsh.*, 1973, 9, 381-392.

DIETRICH, R.V. (1960) Banded gneisses. *J. Petrol.*, 1, 99-120.

—— and MEHNERT, K.R. (1960) Proposal for the nomenclature of migmatites and associated rocks. *Intern. Geol. Congr. 21st, Copenhagen 1960, Rept. Session, Norden, Suppl. Vol. Sect.*, 1-21, 56-67.

DOSTAL, J. (1975) The origin of garnet-cordierite-sillimanite bearing rocks from Chandros Township, Ontario. *Contrib. Mineral. Petrol.*, 49, 163-175.

DU TOIT, M.C. (1965) *A Geological Investigation and Correlation of Rocks belonging to the Koras Formation in the Gordonia and Kenhardt Districts, Northern Cape Province.* Unpubl. M.Sc. thesis, Univ. Orange Free State, 110p.

ENGEL, A.E.J. and ENGEL, C.G. (1962a) Progressive metamorphism of amphibolite northwest Adirondack Mountains, New York *in* Engel, A.E.J. et al. (Eds.), *Petrologic Studies* (*Buddington Vol.*) Geol. Soc. Am., 37-82.

—— (1962b) Hornblendes formed during progressive metamorphism of amphibolites, northwest Adirondack Mountains, New York. *Geol. Soc. Am. Bull.* 73, 1499-1514.

ERNST, W.G. (1968) *Amphiboles: Crystal Chemistry, Phase Relations and Occurrence.* Springer-Verlag, New York, 115p.

ESKOLA, P. (1914) On the petrology of the Orijärvi region in southwestern Finland. *Comm. Geol. Finlande Bull.*, 40.

—— (1939) Die metamorphen Gesteine *in* Barth, T.F.W., Correns, C.W. and Eskola, P., *Die Entstehung der Gesteine*, 263-407. Julius Springer, Berlin.

——(1949) The problem of mantled gneiss domes. *Geol. Soc. Lond. Quart. J.*, 104, 461-476.

——(1961) Granitentstehung bei Orogenese und Epirogenese. *Geol. Rundschau*, 50, 105-123.

ERNST, W.G. (1965) Mineral parageneses in Franciscan metamorphic rocks, Panoche Pass, California. *Geol. Soc. Am. Bull.*, 76, 879-914.

FABRIÈS, J. (1968) Nature des hornblendes et types de métamorphisme. *Internat. Mineral. Assoc., 5th General Meeting 1966, Papers and Proc.*, Mineral. Soc. London, 204-211.

FLEUTY, M.J. (1964) The description of folds. *Geol. Assoc. Proc.*, 75, 461-492.

FYFE, W.S. (1962) On the relative stability of talc, anthophyllite and enstatite. *Am. J. Sci.*, 260, 460-466.

——— (1971) Some thoughts on granitic magmas *in* Newall, G. and Rast, N., *Mechanism of Igneous Intrusion.* Geol. J. Spec. Issue 2, Gallery Press, Liverpool, 201-216.

——— (1973) Granites past and present *in* Lister, L.A. (Ed.), Symposium on granites, gneisses and related rocks, 13-16. *Geol. Soc. S. Africa Spec. Publ.*, 3, 509p.

——— TURNER, F.J. and VERHOOGAN, J. (1958) Metamorphic reactions and metamorphic facies. *Geol. Soc. Am. Mem.*, 73, 259p.

GARY, M., McAFEE, R.M., and WOLF, C.L. (Eds.) (1972) *Glossary of Geology.* Am. Geol. Inst., Washington, 805p.

GEMUTS, I. (1965) Regional metamorphism in the Lamboo complex, East Kimberley area. *Geol. Surv. W. Austr. Ann. Rept 1964*, 36-41.

GERINGER, G.J. (1973) *Die Geologie van die Argeiense Gesteentes en Jongere Formasies in die Gebied Wes van Upington met Spesiale Verwysing na die Verskillende Granietvoorkomste.* Unpubl. D.Sc. thesis, Univ. Orange Free State, 203p.

GERMS, G.J.B. (1972) The stratigraphy and palaeontology of the lower Nama Group, South West Africa. *Precambrian Res. Unit, Univ. Cape Town, Bull.* 12, 250p.

GEVERS, T.W. and DUNNE, J.C. (1942) Charnockitic rocks near Port Edward in Alfred County, Natal. *Geol. Soc. S. Africa Trans.*, 45, 183-213.

——— PARTRIDGE, F.C. and JOUBERT, G.K. (1937) The pegmatite area south of the Orange River in Namaqualand. *Geol. Surv. S. Africa Mem.*, 31.

GHOSH, S.K. (1966) Experimental tests of buckling folds in relation to strain ellipsoid in simple shear deformations. *Tectonophysics*, 3, 3, 169-185.

——— and RAMBERG, H. (1968) Buckling experiments on intersecting fold patterns. *Tectonophysics*, 5, 2, 89-105.

GOLDSMITH, R. (1959) Granofels, a new metamorphic rock name. *J. Geol.*, 67, 109-110.

GORDON, T.M. and GREENWOOD, H.J. (1971) The stability of grossularite in H_2O - CO_2 mixtures. *Am. Mineral.*, 56, 1674-1688.

GRAPES, R.H. (1975) Actinolite-hornblende pairs in metamorphosed gabbros, Hidaka Mountains, Hokkaido. *Contrib. Mineral. Petrol.*, 49, 125-140.

GREEN, D.H. and RINGWOOD, A.E. (1967) An experimental investigation of the gabbro to eclogite transformation and its petrological applications. *Geochim. Cosmochim. Acta*, 31, 767-833.

GREENMAN, L. (1966) *The Geology of Area 2515C Lüderitz, South West Africa.* Unpubl. M.Sc. thesis, Univ. Cape Town, 105p.

GREENWOOD, H.J. (1963) The synthesis and stability of anthophyllite. *J. Petrol.*, 4, 317-351.

———(1967) Wollastonite: stability in H_2O - CO_2 mixtures and occurrence in a contact-metamorphic aureole near Salmo, British Columbia, Canada. *Am. Mineral*, 52, 1669-1680.

GROVES, A.W. (1935) The charnockite series of Uganda, British East Africa. *Geol. Soc. Lond. Quart. J.*, 91, 150-207.

GRUBENMANN, U. (1904) *Die Kristallinen Schiefer.* Gebrüder Borntraeger, Berlin, 2 vol.

GUENTHER, W.C. (1965) *Concepts of Statistical Inference.* McGraw-Hill, New York, 353p.

HARKER, R.I. and TUTTLE, O.F. (1955) Studies in the System CaO - MgO - CO_2, Part I. *Am. J. Sci.*, 253, 209-244.

———(1956) Experimental data on the P_{CO_2}- T curve for the reaction: calcite + quartz ⇄ wollastonite + carbon dioxide. *Am. J. Sci.*, 254, 239-256.

HARRIS, N.B.W. (1974) Some migmatite types and their origins, from the Barousse Massif, central Pyrenees. *Geol. Mag.*, 111, 4, 319-328.

HAUGHTON, S.H. (1969) *Geological History of Southern Africa.* Geol. Soc. S. Africa, Cape and Transvaal Printers, Cape Town, 535p.

HEDBERG, H.D. (1970) Preliminary report on lithostratigraphic units. *Internat. Subcomm. Stratigr. Classif. Rept.* 3, Montreal, 30p.

HENSEN, B.J. and GREEN, D.H. (1971) Experimental study of the stability of cordierite and garnet in pelitic compositions at high pressures and temperatures, I. Compositions with excess alumino-silicate. *Contrib. Mineral. Petrol.*, 33, 309-330.

———(1972) Experimental study of the stability of cordierite and garnet in pelitic compositions at high pressures and temperatures, II. Compositions without excess alumino-silicate. *Contrib. Mineral. Petrol.*, 35, 331-354.

———(1973) Experimental study of the stability of cordierite and garnet in pelitic compositions at high pressures and temperatures, III. Synthesis of experimental data and geological applications. *Contrib. Mineral. Petrol.*, 38, 151-166.

HEWINS, R.H. (1975) Pyroxene geothermometry of some granulite facies rocks. *Contrib. Mineral. Petrol.*, 50, 205-209.

HIRSCHBERG, A. and WINKLER, H.G.F. (1968) Stabilitätsbeziehungen zwischen Chlorit, Cordierit und Almandin bei der Metamorphose. *Contrib. Mineral. Petrol.*, 18, 17-42.

HOLDAWAY, M.J. (1972) Thermal stability of Al-Fe epidote as a function of fO_2 and Fe content. *Contrib. Mineral. Petrol.*, 37, 307-340.

HOLMES, A. (1951) The sequence of Pre-Cambrian orogenic belts in south and central Africa. *Intern. Geol. Congr. 18, London 1948*, 14, 254-269.

HOPGOOD, A.M. (1973) The significance of deformational sequence in discriminating between Precambrian terrains *in* Lister, L.A. (Ed.), Symposium on granites, gneisses and related rocks, 45-51. *Geol. Soc. S. Africa Spec. Publ.*, 3, 509p.

HOWIE, R.A. (1955) The geochemistry of the charnockite series of Madras, India. *Royal Soc. Edinburgh Trans.*, 62, 725-768.

HUNTER, D.R. (1973) The granitic rocks of the Precambrian in Swaziland *in* Lister, L.A. (Ed.), Symposium on granites, gneisses and related rocks, 131-147. *Geol. Soc. S. Africa Spec. Publ.*, 3, 509p.

HUTCHEON, I., FROESE, E. and GORDON, T.M. (1974) The assemblage quartz-sillimanite-garnet-cordierite as an indicator of metamorphic conditions in the Daly Bay Complex N.W.T. *Contrib. Mineral. Petrol.*, 44, 29-34.

HYNDMAN, D.W. (1972) *Petrology of Igneous and Metamorphic Rocks.* McGraw-Hill, New York, 533p.

IRVING, A.J. and GREEN, D.H. (1970) Experimental duplication of mineral assemblages in basic inclusions of the Delegate breccia pipes. *Phys. Earth Planet. Interiors*, 3, 385-389.

JACKSON, M.P.A. (1974) Migmatization and metamorphism in a terrain of high-grade gneisses, Lüderitz District, South West Africa. *Precambrian Res. Unit, Univ. Cape Town, Ann. Rept.* 10-11, 46-52.

——(1975) Field relations between key lithological units of the Namaqua Metamorphic Complex and the Naisib River Complex in the eastern Lüderitz District. *Precambrian Res. Unit, Univ. Cape Town, Ann. Rept.* 12, 33-40.

JAMES, H.L. (1955) Zones of regional metamorphism in the Precambrian of northern Michigan. *Geol. Soc. Am. Bull.*, 66, 1455-1488.

JOHANNES, W. (1969) An experimental investigation of the system $MgO-SiO_2-H_2O-CO_2$. *Am. J. Sci.*, 267, 1083-1104.

——and METZ, P. (1968) Experimentelle bistimmugen von gleichgewichtsbeziehungen im system $MgO-CO_2-H_2O$. *Neues Jahrb. Mineral. Monatsch.*, 1968, 15-26.

JOLY, F. (1972) Geomorphological mapping in arid regions *in* Demek, J. (Ed.), *Manual of Detailed Geomorphological Mapping*, 185-191. Internat. Geogr. Union Comm. Geomorph. Surv. Mapping, Academia, Prague.

JOUBERT, P. (1971) The regional tectonism of the gneisses of part of Namaqualand. *Precambrian Res. Unit, Univ. Cape Town, Bull.* 10, 220p.

——(1972) Geological survey of part of Namaqualand and Bushmanland. *Precambrian Res. Unit, Univ. Cape Town, Ann. Rept.* 7-9, 4-11.

——(1974a) Wrench-fault tectonics in the Namaqualand Metamorphic Complex *in* Kröner, A. (Ed.), Contributions to the Precambrian Geology of southern Africa. *Precambrian Res. Unit, Univ. Cape Town, Bull.* 15, 17-27.

——(1974b) The gneisses of Namaqualand and their deformation. *Geol. Soc. S. Africa Trans.*, 77, 3, 339-345.

——(in prep.) The Namaqualand Metamorphic Complex around Pofadder, northern Cape. *Precambrian Res. Unit, Univ. Cape Town, Bull.*

KAISER, E. (1926) *Die Diamantenwüste Südwestafrikas. Mit Beltragen von W. Beetz, J. Böhm, R. Martin, R. Rauff, M. Storz, E. Stromer, W. Weissermel, und K. Willman. 2 vol.* Dietrich Reimer, Berlin.

KATADA, M. (1965) Petrography of Ryoke metamorphic rocks in northern Kiso district, central Japan. *J. Japan. Assoc. Mineral. Petrol. Econ. Geol.*, 53, 77-90, 155-164, 187-204.

KATZ, M.B. (1970) Banded gneisses: thickness distribution of layers and their lithologic transitions. *Lithos*, 3, 1-13.

KATZ, M.B. (1972) The nomenclature of granulite facies rocks. *Neues Jahrb. Mineral. Monatsh.*, 1972, 4, 152-159.

KERRICK, D.M. (1970) Contact metamorphism in some areas of the Sierra Nevada, California. *Geol. Soc. Am. Bull.*, 81, 2913-2938.

KRÖNER, A. (1974) The Gariep Group, Part I. Late-Precambrian formations in the western Richtersveld, northern Cape Province. *Precambrian Res. Unit, Univ. Cape Town, Bull. 13*, 115p.

——— (1975) Geochronology. *Precambrian Res. Unit, Univ. Cape Town, Ann. Rept.* 12, 56-58.

——— (1976a) Proterozoic crustal evolution in parts of Southern Africa and evidence for extensive sialic crust since the end of the Archaean. *Royal Soc. London Phil. Trans. Ser. A* (in press).

——— (1976b) The Namaqua Mobile Belt within the framework of Precambrian crustal evolution in southern Africa. *Geol. Soc. S. Africa Spec. Publ*, 4, (in press).

——— and BLIGNAULT, H.J. (1976) Towards a definition of some tectonic and igneous provinces in western South Africa and southern South West Africa. *Geol. Soc. S. Africa Trans.* (in press).

——— and JACKSON, M.P.A. (1974) Geological reconnaissance of the coast between Lüderitz and Marble Point, South West Africa *in* Kröner, A. (Ed.), Contributions to the Precambrian geology of southern Africa. *Precambrian Res. Unit, Univ. Cape Town, Bull.* 15, 79-97.

KUSHIRO, I. and YODER, H.S., Jr. (1966) Anorthite-forsterite and anorthite-enstatite reactions and their bearing on the basalt-eclogite transformation. *J. Petrol.*, 7, 337-362.

LAL, R.K. and MOORHOUSE, W.W. (1969) Cordierite-gedrite rocks and associated gneisses of Fishtail Lake, Harcourt Township, Ontario. *Can. J. Earth Sci.*, 6, 145.

LAMBERT, I.B. and HEIER, K.S. (1968) Geochemical investigations of deep-seated rocks in the Australian Shield. *Lithos*, 1, 30-53.

——— ROBERTSON, J.K. and WYLLIE, P.J. (1969) Melting reactions in the system $KAlSi_3O_8$-SiO_2-H_2O to 18,5 kilobars. *Am. J. Sci.*, 267, 609-626.

LEAKE, B.E. (1965) The relationship between composition of calciferous amphibole and grade of metamorphism *in* Pitcher, W.S. and Flinn, G.W. (Eds.), *Controls of Metamorphism.* Oliver and Boyd, Edinburgh, 299-317.

——— (1968) A catalog of analysed calciferous and subcalciferous amphiboles together with their nomenclature and associated minerals. *Geol. Soc. Am. Spec. Paper*, 98, 210p.

LEE, D.E., COLEMAN, R.G. and ERD, R.C. (1963) Garnet types from the Cazadero area, California. *J. Petrol.*, 4, 460-492.

LIOU, J.G. (1973) Synthesis and stability relations of epidote, $Ca_2Al_2FeSi_3O_{12}(OH)$. *J. Petrol.*, 14, 381-414.

LOGAN, R.F. (1960) The central Namib Desert, South West Africa. *Nat. Acad. Sci.— Nat. Res. Council Publ.*, 758, Washington D.C.

LUNDGREN, L.W. (1966) Muscovite reactions and partial melting in south-eastern Connecticut. *J. Petrol.*, 7, 421-453.

McIVER, J.R. (1966) Orthopyroxene-bearing granitic rocks from southern Natal. *Geol. Soc. S. Africa Trans.*, 69, 99-117.

McKEE, E.D. and BREED, C.S. (1974) An investigation of major sand seas in desert areas throughout the world *in Third Earth Resources Technology Satellite - 1 Symposium*, Washington D.C., 1973, NASA SP-1351, 665-679.

McMILLAN, M.D. (1968) The geology of the Witputs-Sendelingsdrif area. *Precambrian Res. Unit, Univ. Cape Town, Bull.* 4, 177p.

MARSH, J.S. (1973) *Alkaline Igneous Rocks of the Coastal Belt South of Lüderitz, South West Africa: a Petrological Study*. Unpubl. Ph.D. thesis, Univ. Cape Town.

MARTIN, H. (1965) *The Precambrian Geology of South West Africa and Namaqualand.* Precambrian Res. Unit, Univ. Cape Town, 159p.

MASON, B. (1962) Metamorphism in the southern Alps of New Zealand. *Am. Museum. Nat. Hist. Bull.*, 123, 211-248.

MEHNERT, K.R. (1963) Petrographie und Abfolge der Granitisation im Schwarzwald, Part 4. *Neues Jahrb. Mineral.*, 99, 161-199.

——— (1968) *Migmatites and the Origin of Granitic Rocks.* Elsevier, Amsterdam, 405p.

——— (Compiler) (1972) Granulites: results of a discussion, II. *Neues Jahrb. Mineral. Monatsh.*, 1972, 4, 139-150.

METZ, P. (1967) Die obere Stabilitätsgrenze von Tremolit bei der Metamorphose von kieseligen Karbonaten. *Contrib. Mineral. Petrol.*, 15, 3, 272-280.

——— (1970) Experimentelle Untersuchung der Metamorphose von kieselig dolomitischen Sedimenten, II. Die Bildungsbedingungen des Diopsids. *Contrib. Mineral. Petrol.*, 28, 221-250.

——— (1973) Isobaric T-X_{CO_2} diagram at P_f = 5 kb for reactions in siliceous dolomites *in* Winkler, H.G.F. (1974) *Petrogenesis of Metamorphic Rocks, 3rd Ed.*, p.120. Springer-Verlag, New York.

——— and TROMMSDORFF, V. (1968) On phase equilibria in metamorphosed siliceous dolomites. *Contrib. Mineral. Petrol.*, 18, 305-309.

MISCH, P.H. (1964) Stable association wollastonite-anorthite, and other calc-silicate assemblages in amphibolite-facies crystalline schists of Nanga Parbat, northwest Himalayas. *Beitr. Mineral. Petrogr.*, 10, 315-356.

MIYASHIRO, A. (1958) Regional metamorphism of the Gosaisyo-Takanuki district in the central Abukuma Plateau. *Tokyo Univ. Fac. Sci. J. Sect. 2*, 11, 219-272.

—— (1973) *Metamorphism and Metamorphic Belts*. George, Allen & Unwin, London, 492p.

MOORE, J.M. (1975) Preliminary report on the geology of the Namiesberg range near Pofadder, northern Cape. *Precambrian Res. Unit, Univ. Cape Town, Ann. Rept.* 12, 43-45.

MUKHERJEE, A. and REGE, S.M. (1972) Stability of wollastonite in the granulite facies: some evidences from E. Ghats, India. *Neues Jahrb. Mineral. Abhandl.*, 118, 1, 22-43.

NASH, C.R. (1971) Metamorphic petrology of the SJ Area, Swakopmund District, South West Africa. *Precambrian Res. Unit, Univ. Cape Town, Bull.* 9, 77p.

NEWTON, R.C. (1966) Some calc-silicate equilibrium relations. *Am. J. Sci.*, 264, 204-222.

NICOLAYSEN, L.O. and BURGER, A.J. (1965) Note on an extensive zone of 1000 million-year old metamorphic and igneous rocks in Southern Africa. *Sci. Terre*, 10, 497-516.

NITSCH, K.-H. and WINKLER, H.G.F. (1965) Bildungsbedingungen von Epidot und Orthozoisit. *Beitr. Mineral. Petrol.*, 11, 470-486.

NOCKOLDS, S.R. (1954) Average chemical compositions of some igneous rocks. *Geol. Soc. Am. Bull.*, 65, 1007-1032.

O'HARA, M.J. (1961) Zones of ultrabasic and basic gneiss masses in the early Lewisian metamorphic complex at Scourie, Sutherland. *J. Petrol.*, 2, 248-276.

OLESEN, N.Ø., HANSEN, E.S., KRISTENSEN, L.H. and THYRSTED, T. (1973) A preliminary account on the geology of the Selbu-Tydal area, the Trondheim Region, Central Norwegian Caledonides. *Leidse Geol. Mededel.*, 49, 2, 259-277.

PARK, R.G. (1969) Structural correlation in metamorphic belts. *Tectonophysics*, 7, 4, 323-338.

PHILPOTTS, A.R. (1966) Origin of the anorthosite-mangerite rocks in Southern Quebec. *J. Petrol.*, 7, 1-64.

PICHAMUTHU, C.S. (1953) *The Charnockite Problem*. Mysore Geologists' Association, Bangalore, 178p.

POLDERVAART, A. (1966) Archaean charnockitic adamellite phacoliths in the Keimoes-Kakamas region, Cape Province, South Africa. *Geol. Soc. S. Africa Trans.*, 69, 139-154.

—— and VON BACKSTRÖM, J.W. (1949) A study of an area at Kakamas (Cape Province) *Geol. Soc. S. Africa Trans.*, 52, 433-495.

PRETORIUS, D.A. (1964) Towards a regional synthesis of the results of research work. *Econ. Geol. Res. Unit, Univ. Witwatersrand, Ann. Rept.* 6, 25-27.

RAASE, P. (1974) Al and Ti contents of hornblende, indicators of pressure and temperature of regional metamorphism. *Contrib. Mineral. Petrol.*, 45, 231-236.

RAMASWAMY, A. and MURTY, M.S. (1973) The charnockite series of Amaravathi, Gunther District, Andhra Pradesh, South India. *Geol. Mag.*, 110, 2, 171-184.

RAMBERG, H. (1964) Selective buckling of composite layers with contrasted rheological properties. A theory for simultaneous formation of several orders of folds. *Tectonophysics*, 1, 307-341.

RAMSAY, J.G. (1967) *Folding and Fracturing of Rocks*. McGraw-Hill, New York, 568p.

RANGE, P. (1910) Sketch of the geology of German Namaqualand. *Geol. Soc. S. Africa Trans.*, 13, 1-9.

RAVOIR, E. and HINRICHSEN, Th. (1975) Upper stability of synthetic anthophyllite mixed crystals. *Neues Jahrb. Mineral. Monatsh.*, 4, 162-166.

READ, H.H. (1951) Metamorphism and granitization. Alex du Toit Memorial Lecture 2. *Geol. Soc. S. Africa Trans. Annex.*, 54, 1-27.

REID, D.L. (1974) Preliminary report on petrologic studies of volcanic and intrusive rocks in the Vioolsdrif region, lower Orange River *in* Kröner, A. (Ed.), Contributions to the Precambrian geology of southern Africa, 57-68. *Precambrian Res. Unit, Univ. Cape Town, Bull.* 15, 213p.

REINHARDT, E.W. (1968) Phase relations in cordierite-bearing gneisses from the Gananoque area, Ontario. *Can. J. Earth Sci.*, 5, 455-482.

——and SKIPPEN, G.B. (1970) *Geol. Surv. Can. Rept. Activities Paper 70-1 Pt. B.* 48-54.

RICHARDSON, S.W. (1968) Staurolite stability in a part of the system Fe-Al-Si-O-H. *J. Petrol.*, 9, 3, 467-488.

——(1970) The relation between a petrogenetic grid, facies series, and the geothermal gradient in metamorphism. *Fortschr. Mineral.*, 47, 65-76.

——BELL, P.M. and GILBERT, M.C. (1968) Kyanite-sillimanite and equilibrium between 700° and 1500°C. *Am. J. Sci.*, 266, 513-541.

——GILBERT, M.C. and BELL, P.M. (1969) Experimental determination of kyanite-andalusite and andalusite-sillimanite equilibria; the aluminium silicate triple point. *Am. J. Sci.*, 267, 259-272.

ROBERTSON, I.D.M. (1973) Potash granites of the southern edge of the Rhodesian craton and the northern granulite zone of the Limpopo Mobile Belt *in* Lister, L.A. (Ed.), Symposium on granites, gneisses and related rocks, 265-276. *Geol. Soc. S. Africa Spec. Publ.*, 3, 509p.

ROGERS, J. (1976) Sediments on the continental margin off the Orange River and the Namib Desert. *Joint Geol. Surv./Univ. Cape Town. Mar. Geol. Prog. Bull.* (in prep).

ROYAL NAVY AND SOUTH AFRICAN AIR FORCE METEOROLOGICAL SERVICES (1944) *Weather on the Coasts of Southern Africa.* Vol. II, Part I. The west coast of Africa from River Congo to Olifants River, 61p.

SAGGERSON, E.P. (1973) Metamorphic facies series in Africa: a contrast *in* Lister, L.A. (Ed.), Symposium on granites, gneisses and related rocks, 227-234. *Geol. Soc. S. Africa Spec. Publ.*, 3, 509p.

—— and OWEN, L.M. (1969) Metamorphism as a guide to the depth of the top of the upper mantle in Southern Africa *in* Upper Mantle Symp. *Geol. Soc. S. Africa Spec. Publ.*, 2, 335-349.

—— and TURNER, L.M. (1976) A review of the distribution of metamorphism in the ancient Rhodesian craton. *Precambrian Res.*, 3, 1-53.

SANDER, B. (1930) *Gefügekunde der Gesteine*. Springer, Vienna, 352p.

SAXENA, S.K. (1969) Distribution of elements in coexisting minerals and the problem of chemical disequilibrium in metamorphosed basic rocks. *Contrib. Mineral. Petrol.*, 20, 177-197.

SCHRIJVER, K. (1973) Correlated changes in mineral assemblages and in rock habit and fabric across an orthopyroxene isograd, Grenville Province, Quebec. *Am. J. Sci.*, 273, 171.

SCHULTZ, R. (1975) First progress report on a project entitled 'The origin and mode of emplacement of hypersthene-bearing granitoids and associated rocks in parts of the Upington geotraverse'. *Precambrian Res. Unit, Univ. Cape Town, Ann. Rept.* 12, 20-22.

SEN, S.K. and RAY, S. (1971a) Breakdown reactions for natural hornblendes in granulite facies. *Neues Jahrb. Mineral. Abhandl.*, 114, 3, 301-319.

—— (1972b) Hornblende-pyroxene granulites versus pyroxene granulites: a study from the type charnockite area. *Neues Jahrb. Mineral. Abhandl.*, 115, 291-314.

SHARMA, R.S. (1969) On banded gneisses and migmatites from Lavertezzo and Rozzera (Valle Verzasca, Canton Ticino). *Schweiz. Mineral. Petrogr. Mitt.*, 49, 199-276.

SHIDO, F. (1958) Plutonic and metamorphic rocks of the Nakoso and Iritono districts in the central abukuma Plateau. *Tokyo Univ. Fac. Sci. J., Sect. 2*, 11, 131-217.

SIMONEN, A. (1960) Plutonic rocks of the Svecofennides in Finland. *Comm. Géol. Finlande Bull.*, 189, 1-101.

SPRY, A. (1969) *Metamorphic Textures.* Pergamon Press, London, 350p.

SOUTH AFRICAN COMMITTEE FOR STRATIGRAPHY (1971) South African code of stratigraphic terminology and nomenclature. *Geol. Soc. S. Africa Trans.*, 74, 3, 111-131.

STEUHL, H.H. (1962) Die experimentelle Metamorphose und Anatexis eines Parabiotitgneises aus dem Schwarzwald. *Chem. Erde*, 21, 413-449.

STEYN, P. (1975) Note on compositional variation of biotite in basic rocks of the O'okiep copper district. Abstract Vol. *Geol. Soc. S. Africa Congr. 16*, Stellenbosch, 1975, 131.

STONE, R.O. (1967) A desert glossary. *Earth-Science Reviews*, 3, 211-268.

STORRE, B. and KAROTKE, E. (1971) An experimental determination of the upper stability limit of 'muscovite + quartz' in the range 7 - 20 kb water pressure. *Neues Jahrb. Mineral. Monatsh.*, 1971, 237.

——— (1972) Experimental data on melting reactions of muscovite + quartz in the system K_2O-Al_2O_3-SiO_2-H_2O to 20 kb water pressure. *Contrib. Mineral. Petrol.*, 36, 4, 343-345.

——— and NITSCH, K.-H. (1973) The upper stability of margarite in the presence of quartz. *Naturwissenschaften*, 60, 3, 152.

STRECKEISEN, A. (1967) Classification and nomenclature of igneous rocks. *Neues Jahrb. Mineral. Abhandl.*, 107, 144-240.

STRÖMGÅRD, K.-E. (1973) Stress distribution during formation of boudinage and pressure shadows. *Tectonophysics*, 16, 3/4, 215.

STUMPFL, E.F. and VAN ZYL, D. (1975) Variations in silicate, oxide and sulphide mineralogy in the O'okiep copper district. Abstract Vol. *Geol. Soc. S. Africa Congr. 16*, Stellenbosch 1975, 136-138.

SUBRAMANIAN, A.P. (1956) Petrology of the anorthosite-gabbro mass at Kadavur, Madras, India. *Geol. Mag.*, 93, 287-300.

SUTTON, J. (1963) Long-term cycles in the evolution of continents. *Nature*, 189, 4882.

TERRY, R.D. and CHILINGAR, G.V. (1955) Charts for estimating percentage composition of rocks and sediments. *J. Sed. Petrol.*, 25, 229-234.

TILLEY, C.E. (1927) Vesuvianite and grossular as products of regional metamorphism. *Geol. Mag.*, 64, 372-376.

TOBI, A.C. (1971) The nomenclature of the charnockitic rock suite. *Neues Jahrb. Mineral. Monatsh.*, 1971, 5, 193-205.

——— (1972) The nomenclature of the charnockitic rock suite: reply to a discussion. *Neues Jahrb. Mineral. Monatsh.*, 1972, 2, 78-79.

TOBISCH, O.T., FLEUTY, M.J., MERH, S.S., MUKHOPADHYAY, D. and RAMSAY, J.G. (1970) Deformational and metamorphic history of Moinian and Lewisian rocks between Strathconan and Glen Afric. *Scott. J. Geol.*, 6, 3, 243-265.

TOOGOOD, D.J. (1974) Preliminary report on the geology of the Onseepkans area, south-eastern South West Africa. *Precambrian Res. Unit, Univ. Cape Town, Ann. Rept.* 10-11, 31-37.

——— (1975) Tectonic interpretation of the Namaqua mobile belt in south-eastern South West Africa. *Precambrian Res. Unit, Univ. Cape Town, Ann. Rept.* 12, 27-32.

——— (1976) The structural and metamorphic evolution of a gneiss terrain in the Namaqua belt near Onseepkans, South West Africa. *Precambrian Res. Unit, Univ. Cape Town, Bull.* (*in press*).

TORSKE, T. (1972) The nomenclature of the charnockitic rock suite: a discussion. *Neues Jahrb. Mineral. Monatsh.*, 1972, 2, 74-77.

TOURET, J. (1971) Le faciés granulite en Norvège méridionale, I: Les associations minéralogiques. *Lithos*, 4-3, 239-249. II: Les inclusions fluides. *Lithos*, 4-4, 423-436.

(1972) Le faciès granulite en Norvège méridionale et les inclusions fluide: paragneiss et quartzites. *Sci. Terre Nancy*, 17, 1/2, 179-193.

——— (1974) Fluid inclusions in high-grade metamorphic rocks *in Volatiles in Metamorphism*. NATO Advanced Study Instit., Nancy 1974.

TROMMSDORFF, V. (1966) Progressive Metamorphose Kieseliger Karbonatgesteine in den Zentralalpen Zwischen Bernina und Simplon. *Schweiz. Mineral. Petrogr. Mitt*, 46, 431-460.

———(1968) Mineralreaktionen mit Wollastonit und Vesuvian in einem Kalksilikatfels der alpinen Disthenzone (Claro, Tessin). *Schweiz. Mineral. Petrogr. Mitt.*, 48, 655-666, 828-829.

TRUSWELL, J.F. (1970) *An Introduction to the Historical Geology of South Africa*. Purnell, Cape Town, 167p.

TURNER, F.J. (1968) *Metamorphic Petrology*. McGraw-Hill, New York, 403p.

——— and WEISS, L.E. (1963) *Structural Analysis of Metamorphic Tectonites*. McGraw-Hill, New York, 545p.

VAJNER, V. (1974) The tectonic development of the Namaqua Mobile Belt and its foreland in parts of the Northern Cape. *Precambrian Res. Unit, Univ. Cape Town, Bull* 14, 201p.

——— (1975) Preliminary report on the geology and structure of parts of the Namaqua foreland in the Upington area. *Precambrian Res. Unit, Univ. Cape Town, Ann. Rept.* 12, 11-19.

VAN BREEMAN, O. and DODSON, M.H. (1969) Metamorphic chronology of the Limpopo Belt, southern Africa. *Geol. Soc. Am. Bull.*, 83, 2005-2018.

VAN ZYL, D. (1975) A petrological approach towards the ore-bearing potentialities of the O'okiep basic intrusives in Namaqualand. Abstract Vol. *Geol. Soc. S. Africa Congr. 16*, Stellenbosch 1975, 160-163.

VERWOERD, W.J. (1966) South African carbonatites and their probable mode of origin. *Univ. Stellenbosch Ann.*, 41, A2, 115-233.

VON BACKSTRÖM, J.W. (1964) The geology of an area around Keimoes, Cape Province, with special reference to phacoliths of charnockitic adamellite-porphyry. *Surv. S. Africa Mem.*, 53, 218p.

———1967) The Geology and mineral deposits of the Riemvasmaak area, northwest Cape Province. *Geol. Surv. S. Africa Ann.*, 6, 43-51.

VON BRUNN, V. (1967) *Acid and Basic Igneous Rock Associations West of Helmeringhausen, South West Africa.* Unpubl. Ph.D. thesis, Univ. Cape Town, 170p.

——— and DODSON, M.H. (1967) Post-Kheis/pre-Nama igneous rocks from the Helmeringhausen area, South West Africa. *Precambrian Res. Unit, Univ. Cape Town, Ann. Rept.* 5, 40-44.

VON PLATEN, H. and HÖLLER, N. (1966) Experimentelle Anatexis des Stainzer Plattengneises von der Koralpe, Steiermark, bei 2, 4, 7 und 10 kb H_2O-Druk. *Neues Jahrb. Mineral. Abhandl.*, 106, 106-130.

WATTERS, B.R. (1974) Stratigraphy, igneous petrology and evolution of the Sinclair Group in southern South West Africa. *Precambrian Res. Unit, Univ. Cape Town, Bull.* 16, 235p.

WENK, E. (1962) Plagioklas als Indexmineral in den Zentralalpen. *Schweiz. Mineral. Petrog. Mitt.*, 42, 139-152.

——— and KELLER, F. (1969) Isograde in Amphibolitserien der Zentralalpen. *Schweiz. Mineral. Petrogr. Mitt.*, 49, 157-198.

WILLIAMS, P.F. (1970) A criticism of the use of style in the study of deformed rocks. *Geol. Soc. Am. Bull*, 81, 215-228.

WILSON, A.E. (1959) The charnockitic rocks of Australia. *Geol. Rundsch.*, 47, 491-510.

WINKLER, H.G.F. (1967) *Petrogenesis of Metamorphic Rocks, 2nd ed.* Springer-Verlag, New York, 237p.

———(1970) Abolition of metamorphic facies, introduction of the four divisions of metamorphic stage, and of a classification based on isograds in common rocks. *Neues Jahrb. Mineral. Monatsh.*, 5, 189,248.

———(1974) *Petrogenesis of Metamorphic Rocks, 3rd ed.* Springer-Verlag, New York, 320p.

——— and SEN, S.K. (1973) Nomenclature of granulites and other high grade metamorphic rocks. *Neues Jahrb. Mineral Monatsh.*, 1973, 9, 393-402.

——— and VON PLATEN, H. (1961) Experimentelle Gesteinsmetamorphose, Part III. *Geochim. Cosmochim. Acta*, 24, 48-69, 250-259.

WISEMAN, J.D.H. (1934) The central and south-west Highland epidiorites: a study in progressive metamorphism. *Geol. Soc. Lond., Quart. J.*, 90, 354-417.

WOLF, K.H., EASTON, A.J. and WARNE, S. (1967) Techniques of examining and analysing carbonate skeletons, minerals and rocks *in* Chilingar, G.V., Bissell, H.J. and Fairbridge, R.W. (Eds.), *Carbonate Rocks, Physical and Chemical Aspects.* Elsevier, Amsterdam, 253-341.

WYLLIE, P.J., COX, K.G. and BIGGAR, G.M. (1962) The habit of apatite in synthetic systems and igneous rocks. *J. Petrol.*, 3, 238-243.

WYNNE-EDWARDS, H.R. (1969) Tectonic overprinting in the Grenville Province, southwestern Quebec. *Geol. Assoc. Canada Special Pap.*, 5, 163-182.

——— (1972) The Grenville Province *in* Price, R.A. and Douglas, R.J.W. (Eds), *Variations in Tectonic Styles in Canada.* Geol. Assoc. Canada Spec. Paper, 11, 264-334.

——— and HAY, P.W. (1963) Coexisting cordierite and garnet in regionally metamorphosed rocks from the Westport area, Ontario. *Can. Mineral.*, 7, 453-478.

——— LAURIN, A.F., SHARMA, K.N.M., NANDI, A., KEHLENBECK, M.M. and FRANCONI, A. (1970) Computerized geological mapping in the Grenville Province, Quebec. *Can. J. Earth Sci.*, 7, 6, 1357-1373.

YODER, H.S. Jr. (1955) Role of water in metamorphism. *Geol. Soc. Am. Spec. Paper*, 62, 505-524.

ZECK, H.P. (1972) A contribution to the granulite discussion. *Neues Jahrb. Mineral. Monatsh*, 1972, 4, 163-166.

ZEN, E-An, (1971) Comments on the thermodynamic constants and hydrothermal stability relations of anthophyllite. *Am. J. Sci.*, 270, 136-150.

APPENDIX 1 OUTCROP SCHEDULE

Explanatory Notes

1. This outcrop schedule is based on that devised by Wynne-Edwards et al. (1970); it has been expanded to include more information and some terms have been changed.

2. When filling out the schedule applicable features are ringed. 'Boxes' contain information such as numerical values, 2-letter colour symbols, 4-letter rock-type symbols, and map symbols.

3. All percentages are estimated by visual comparison with abundance charts prepared by Terry and Chilingar (1955) and reproduced as *Data Sheet 6* by *Geotimes*, available from the American Geological Institute, Washington.

4. Colours were recorded in the form of the following symbols, prefixed by *l* (light), *m* (medium) or *d* (dark shades):

wt white	*bt* buff/tan	*pk* pink
gy grey	*yw* yellow	*gr* green
bk black	*og* orange	*bg* blue-grey
br brown	*rd* red	*mv* mauve
		mp maroon/purple

5. Minerals were recorded according to the abbreviations given in the preliminary pages of this study. Rock-type symbols were adapted from those of Wynne-Edwards et al. (1970). Map symbols follow those shown on the geological map (Annexure 1).

6. Migmatite styles are based on Mehnert (1968).

7. Additional information on the foliation type (i.e. whether defined by gneissosity, schistosity, layering, axial-plane foliation, flattening planes, etc.) are recorded in the margin of the page together with further structural and lithologic properties and their relations in the form of sketches if required.

APPENDIX 1 OUTCROP SCHEDULE FOR AUS PROJECT

LITHOLOGY | thin section? | No.

Date | Area | Airphoto | Photo | Sheet

SPECIMEN: *Type* *No.* MJ
rock/orientated/ *Quantity*
economic/museum/

ROCK VARIABILITY: migmatitic/ homogeneous/banded/

CONTACT: *character*: sharp/ gradational/intercalated/
width: [ ] m.

FOLIATED TEXTURE; weak/slatey schistose/gneissose/mylonitic/ layering/ribbon qtz/

MINERAL DISTRIBUTION: scattered/ homogeneous/banded | <3mm> | blob

NON-FOLIATED: *Equigranular*: mosaic/cataclastic/
Inequigranular: crush-breccia/ porphyroblastic/poikiloblastic/ coronitic/

COLOUR: (fresh) GRAIN SIZE (mm)

		<1	1-5	5-10	10>
megacryst					
rock	%				

WEATHERING: *colour*
style: spheroidal/slab-like/ laminated/

MIGMATITIC: breccia/shear-net raft/veined/stromatic/boudin/ ptygmatic/augen/fleck/ schlieren/nebulitic/

<30	30-60	>60	COLOUR INDEX
<10	10-30	30-60	60> NEOSOME %

VISIBLE MINERALOGY:

					name
					%

ROCK NAME: *Major* *Minor*

MAP SYMBOL

STRUCTURE

PLANAR SURFACES:
1 Bedding
2 Foliation
3 Joint
4 Fault

s	s	s	*order*
			type
			strike
			dip

PLANAR TRACE: *Trend*: [ ]
dyke/qtz-vein /minor shear zone

LINEATIONS:

l	*l*	*l*	*order*
			type
			plunge
			trend

1 s-intersections
2 mineral segregations
3 mineral
4 mullions/rods
5 boudins
6 clast trains
7 micro-fold axes

MINOR FOLDS: *Profile*:
parallel/similar/ rounded/angular harmonic/disharmonic chevron/box/kink band/

Wavelength: | >0,1 | >1 | 1-10> | metres
Symmetry: | M | S | Z |
Closure: | 0 | 0-30 | 30-70 | 70>
's' *Deformation*: crenulation/ attenuation/boudin/transposition/

plunge	*trend*			*dip*	*strike*
		f	*fold*	*f*	
		f	*axes*	*f*	
		f		*f*	

fold axial plane

FAULTS & SHEAR ZONES: *Width* [ ] m *Throw* [ ] m
Deformation: brecciation/mylonitization/drag/slickenside/ striae/parallel to foliation/transgressive/

AGE RELATIONS	
Older deformation	
Deformation	
Younger Deformation	

APPENDIX 2

```
C -----------------------------------------------------------------
C
C    G  R  A  B
C         A PROGRAM TO PREPARE ASSOCIATION FREQUENCY AND ASSOCIATION
C         PROBABILITY MATRICES FROM A SAMPLE OF ROCK TYPE ASSOCIATIONS
C         DRAWN FROM A NUMBER OF OBSERVATION STATIONS
C
C         WRITTEN BY C.J. HARTNADY, PRECAMBRIAN RESEARCH UNIT, UCT.
C          MARCH  1975.     REVISED MARCH  1976.
C
C -----------------------------------------------------------------
      DIMENSION NARRAY(28,28), NCODE(14), NTRACE(28), NRTOTL(28),
     1          PARRAY(28,28)
C
C -----------------------------------------------------------------
C         SPECIFY INPUT/OUTPUT FORMATS AND UNITS
C -----------------------------------------------------------------
C
      DATA ICDR, LPRT /8,5/
 1000 FORMAT (14I1)
 2000 FORMAT (1H1)
 2001 FORMAT (1HO,2814)
 2002 FORMAT (1HO,2914)
 2003 FORMAT (1HO,28F4,2)
C
C -----------------------------------------------------------------
C         INITIALIZE ARRAYS AND VECTORS
C -----------------------------------------------------------------
C
      DO 100 I=1,28
      NRTOTL (I)=0
      DO 100 J=1,28
      PARRAY (I,J)=0
  100 NARRAY (I,J)=0
C
C -----------------------------------------------------------------
C         READ DATA CARDS AND PREPARE INITIAL 28X28 COUNT MATRIX.
C
C         EACH DATA CARD REPRESENTS ONE OBSERVATION STATION AND
C         HAS DATA PUNCHED IN 14 COLUMNS, EACH COLUMN REPRESENTING
C         A PARTICULAR ROCK TYPE.  THE DATA CODE IS:
C         0   -    ROCK TYPE NOT PRESENT IN ASSOCIATION
C         1   -    ROCK TYPE PRESENT AS MINOR COMPONENT OF ASSOCIATION
C         2   -    ROCK TYPE PRESENT AS MAJOR COMPONENT OF ASSOCIATION
C         EACH DATA CARD IS READ INTO AN INTEGER VECTOR, NCODE.
C         NCODE IS THEN SCANNED FOR NON-ZERO COMPONENTS (PRIMARY SCAN).
C         EACH TIME A NON-ZERO COMPONENT IS ENCOUNTERED, A SECONDARY
C         SCAN IS BEGUN.  EVERY TIME A NON-ZERO COMPONENT IS ENCOUNT-
C         ERED IN THE SECONDARY SCAN, A UNIT VALUE IS COUNTED INTO AN
C         APPROPRIATE PLACE IN A 28X28 MATRIX.  IN THIS WAY A MATRIX
```

```
C        IS PREPARED WHICH SHOWS THE NUMBER OF TIMES A ROCK TYPE WAS
C        FOUND IN ASSOCIATION (MAJOR OR MINOR) WITH ANY OTHER ROCK
C        TYPE, INCLUDING ITSELF.
C ---------------------------------------------------------------------
C
  110 READ (ICDR, 1000, END=999) NCODE
      DO 104 I=1,14
      IF (NCODE (I).EQ.0) GO TO 104
      IF (NCODE (I).EQ.1) GO TO 102
      DO 101 J=1,14
      IF (NCODE (J).EQ.1) NARRAY(I,J+14) = NARRAY(I,J+14)+1
      IF (NCODE (J).EQ.2) NARRAY(I,J) = NARRAY(I,J)+1
  101 CONTINUE
      GO TO 104
  102 DO 103 J=1,14
      IF (NCODE (J).EQ.1) NARRAY (I+14, J+14) = NARRAY(I+14, J+14)+1
      IF (NCODE (J).EQ.2) NARRAY(I+14, J) = NARRAY(I+14, J)+1
  103 CONTINUE
  104 CONTINUE
      GO TO 110
C
C ---------------------------------------------------------------------
C        WRITE THE INITIAL COUNT MATRIX ON A NEW PAGE
C ---------------------------------------------------------------------
C
  999 WRITE (LPRT, 2000)
      WRITE (LPRT, 2001) ((NARRAY(I,J), J=1,28), I=1,28)
C
C ---------------------------------------------------------------------
C        PREPARE A VECTOR, NTRACE, CONTAINING THE TRACE (LEADING
C        DIAGONAL) OF THE ABOVE MATRIX.  EACH COMPONENT OF NTRACE
C        REPRESENTS THE TOTAL NUMBER OF TIMES THE CORRESPONDING
C        MAJOR OR MINOR ASSOCIATED ROCK TYPE WAS OBSERVED TO BE
C        PRESENT.  THE ASSOCIATION FREQUENCY MATRIX - REPRESENTING THE
C        NUMBER OF TIMES A PARTICULAR ROCK TYPE WAS FOUND IN
C        ASSOCIATION WITH ANY OTHER ROCK TYPE - IS OBTAINED SIMPLY
C        BY CANCELLING THE LEADING DIAGONAL OF THE INITIAL COUNT
C        MATRIX.  IN THE COURSE OF THIS, A VECTOR, NRTOTL, OF AFM
C        ROW TOTALS IS PREPARED
C ---------------------------------------------------------------------
C
      DO 105 I=1,28
      DO 105 J=1,28
      IF (I.EQ.J) NTRACE(I)=NARRAY(I,J)
      IF (I.EQ.J) NARRAY(I,J)=0
      NRTOTL(I)=NRTOTL(I) + NARRAY(I,J)
  105 CONTINUE
C
C ---------------------------------------------------------------------
C        WRITE THE VECTOR NTRACE ON A NEW PAGE
C ---------------------------------------------------------------------
```

```
C
      WRITE (LPRT,2000)
      WRITE (LPRT,2001) NTRACE
C
C ---------------------------------------------------------------------
C        WRITE THE AFM ON A NEW PAGE WITH AN END COLUMN OF ROW TOTALS
C ---------------------------------------------------------------------
C
      WRITE (LPRT,2000)
      WRITE (LPRT,2002) ((NARRAY(I,J),J=1,28),NRTOTL(I),I=1,28)
C
C ---------------------------------------------------------------------
C        PREPARE THE ASSOCIATION PROBABILITY MATRIX BY DIVIDING
C        EACH ROW OF THE AFM BY THE CORRESPONDING NRTOTL COMPONENT
C ---------------------------------------------------------------------
C
      DO 106 I=1,28
      DO 106 J=1,28
      IF (NRTOTL(I).EQ.0) GO TO 106
      RTOTAL=FLOAT(NRTOTL(I))
      PARRAY(I,J)=FLOAT(NARRAY(I,J))
      PARRAY(I,J)=PARRAY(I,J)/RTOTAL
  106 CONTINUE
C
C ---------------------------------------------------------------------
C        WRITE THE ASSOCIATION PROBABILITY MATRIX ON A NEW PAGE
C ---------------------------------------------------------------------
      WRITE (LPRT,2000)
      WRITE (LPRT,2003) ((PARRAY(I,J),J=1,28),I=1,28)
C
C ---------------------------------------------------------------------
C        END PROGRAM
C ---------------------------------------------------------------------
C
      STOP
      END
```

APPENDIX 3 DETERMINATIVE MINERALOGY

Dolomite was differentiated from calcite by staining thin sections with a molar solution of $Cu(NO_3)_2$ for 4-10 hours followed by brief immersion in concentrated NH_4OH solution (Wolf et al., 1967).

The Z absorption colour of hornblende and biotite was determined in tungsten light with a 'daylight' blue filter. In order to make the colour determinations as objective as possible, the entire sequence of specimens (90 hornblende— and 110 biotite-bearing rocks) was examined in one session, with the thin sections being taken in random order. This examination was then carried out again and the results of the second run were compared against those of the first; observations that differed in the first two runs were examined a third time.

Anorthite percentages of plagioclase were determined by electron microprobe analysis (Appendices 4 and 5).

Modal analyses in this study have been estimated by means of visual comparison with abundance charts prepared by Terry and Chilingar (1955) for this purpose. The absolute error varies from 1% (abundance of component 5% or 95%) to about 5% (abundance of component 25-75%). The speed of this method enabled numerous modal analyses to be carried out.

APPENDIX 4 MICROPROBE ANALYTICAL METHODS

Hornblende, plagioclase, clinopyroxene, orthopyroxene and cummingtonite from Garub metabasites were analysed on a Cambridge Microscan 5 electron probe micro-analyser in the Department of Geochemistry, University of Cape Town, using natural and synthetic mineral standards. The data were computer-processed by the ABFAN programme (Boyd et al., 1968). Cation proportions for the various minerals were calculated on the basis of the following numbers of oxygen anions: hornblende; 23 (O); cummingtonite, 23 (O); pyroxenes, 6 (O); plagioclase, 8 (O). All analyses were carried out by the writer, unless marked (†); the latter, by R.S. Rickard. Additional information regarding details of techniques and standards used may be obtained from the author.

APPENDIX 5 TABLES OF ANALYSES

Structural formulae of hornblendes analysed are given in Tables A5-1 to A5-3. Chemical analyses of all minerals are given in Tables A5-4 to A5-6.

TABLE A5-1

Structural formulae of hornblendes in Garub epidote amphibolites, showing cations per 23 oxygen anions (averages of 3-5 grains per specimen)

SPECIMEN		MJ 960	MJ 969	MJ1020	MJ1054	MJ1061	MJ 397
	Si	6,443	6,943	6,448	6,901	6,949	6,700
	Al	1,557	1,057	1,552	1,099	1,051	1,300
	$\Sigma(Z^{IV})$	8,000	8,000	8,000	8,000	8,000	8,000
M_1-M_3 sites	Al	0,963	0,411	0,848	0,391	0,440	0,440
	Ti	0,051	0,047	0,049	0,061	0,048	0,070
	Mn†	0,040	0,040	0,040	0,040	0,040	0,040
	Fe	1,628	1,764	1,793	1,762	1,778	1,986
	Mg	2,318	2,738	2,270	2,746	2,694	2,464
	$\Sigma(Y^{VI})$	5,000	5,000	5,000	5,000	5,000	5,000
M_4 site	Mg	0,335	0,140	0,312	0,146	0,210	0,253
	Ca	1,665	1,860	1,688	1,854	1,790	1,747
	$\Sigma(X^{VIII-VI})$	2,000	2,000	2,000	2,000	2,000	2,000
A site	Ca	0,090	0,135	0,084	0,109	0,112	0,150
	Na	0,356	0,241	0,481	0,297	0,263	0,328
	K	0,036	0,121	0,040	0,153	0,115	0,169
	$\Sigma(W^{XII-X})$	0,482	0,497	0,605	0,559	0,490	0,647

Structural formulae *after* Ernst (1968)

†Mn estimated from average value of hornblendes in Binns (1965) and Bard (1970)

TABLE A5-2

Structural formulae of hornblendes in Garub amphibolites, showing cations per 23 oxygen anions (averages of 3-5 grains per specimen)

SPECIMEN		MJ 49	MJ835	MJ747	MJ102	MJ712	MJ196	MJ 84	MJ 56	MJ 28	MJ296	MJ183
	Si	6,754	6,264	6,459	6,577	6,743	6,922	7,223	6,834	6,675	6,539	6,738
	Al	1,246	1,736	1,541	1,423	1,257	1,078	0,777	1,166	1,325	1,461	1,262
$\Sigma(Z^{IV})$		8,000	8,000	8,000	8,000	8,000	8,000	8,000	8,000	8,000	8,000	8,000
M_1-M_3 sites	Al	0,356	0,646	0,520	0,375	0,470	0,531	0,310	0,357	0,325	0,642	0,656
	Ti	0,141	0,116	0,170	0,147	0,117	0,091	0,068	0,154	0,185	0,098	0,075
	Mn†	0,040	0,040	0,040	0,040	0,040	0,040	0,040	0,040	0,040	0,040	0,040
	Fe	2,230	2,961	2,715	2,560	2,288	2,422	1,478	2,085	2,202	2,470	1,408
	Mg	2,233	1,237	1,555	1,878	2,085	1,916	3,104	2,364	2,248	1,750	2,821
$\Sigma(Y^{VI})$		5,000	5,000	5,000	5,000	5,000	5,000	5,000	5,000	5,000	5,000	5,000
M_4 site	Mg	0,251	0,213	0,191	0,230	0,326	0,104	0,184	0,251	0,196	0,380	0,386
	Ca	1,749	1,787	1,809	1,770	1,674	1,896	1,816	1,749	1,804	1,620	1,614
$\Sigma(X^{VIII-VI})$		2,000	2,000	2,000	2,000	2,000	2,000	2,000	2,000	2,000	2,000	2,000
A site	Ca	0,036	0,127	0,095	0,136	0,085	0,033	0,036	0,016	0,065	0,113	0,031
	Na	0,448	0,375	0,392	0,378	0,384	0,276	0,250	0,443	0,365	0,375	0,425
	K	0,169	0,307	0,177	0,185	0,075	0,103	0,084	0,110	0,201	0,102	0,048
$\Sigma(W^{XII-X})$		0,653	0,809	0,664	0,699	0,544	0,412	0,370	0,569	0,631	0,590	0,504

Structural formulae *after* Ernst (1968)

†Mn estimated from average value of hornblendes in Binns (1965) and Bard (1970)

TABLE A5-3

Structural formulae of hornblendes in Garub diopside amphibolites (left) and hypersthene granolites (right), showing cations per 23 oxygen anions (averages of 3-5 grains per specimen)

SPECIMEN		MJ 13	MJ546	MJ 92	MJ 32	MJ266	MJ345	MJ740	MJ377	MJ437
	Si	6,252	6,361	7,106	6,923	6,334	6,701	6,868	6,540	6,199
	Al	1,748	1,639	0,894	1,077	1,666	1,299	1,132	1,460	1,801
$\Sigma(Z^{IV})$		8,000	8,000	8,000	8,000	8,000	8,000	8,000	8,000	8,000
M_1-M_3 sites	Al	0,560	0,614	0,333	0,291	0,437	0,470	0,278	0,465	0,778
	Ti	0,232	0,108	0,083	0,103	0,249	1,140	0,168	0,158	0,104
	Mn†	0,040	0,040	0,040	0,040	0,040	0,040	0,040	0,040	0,040
	Fe	1,937	2,359	1,541	1,537	1,571	1,590	1,765	1,580	1,093
	Mg	2,231	1,879	3,003	3,029	2,703	2,760	2,749	2,757	2,985
$\Sigma(Y^{VI})$		5,000	5,000	5,000	5,000	5,000	5,000	5,000	5,000	5,000
M_4 site	Mg	0,125	0,158	0,191	0,049	0,131	0,135	0,218	0,136	0,262
	Ca	1,864	1,842	1,809	1,848	1,869	1,865	1,782	1,864	1,738
	Na	0,011	-	-	0,103	-	-	-	-	-
$\Sigma(X^{VIII-VI})$		2,000	2,000	2,000	2,000	2,000	2,000	2,000	2,000	2,000
A site	Ca	-	0,116	0,038	-	0,039	0,026	0,031	0,087	0,131
	Na	0,527	0,439	0,300	0,333	0,507	0,385	0,371	0,326	0,646
	K	0,290	0,221	0,099	0,135	0,240	0,191	0,165	0,258	0,075
$\Sigma(W^{XII-X})$		0,817	0,776	0,437	0,468	0,786	0,602	0,567	0,671	0,852

Structural formulae *after* Ernst (1968)

†Mn estimated from average value of hornblendes in Binns (1965) and Bard (1970)

TABLE A5-4

Microprobe analyses of hornblendes in Garub amphibolites and granolites

Specimen	MJ 13			MJ 28				
Grain	1	2	3	1†	2†	3†	4†	5†
SiO_2	41,64	41,67	41,81	44,99	45,13	44,92	44,77	44,18
Al_2O_3	12,97	13,05	13,16	9,15	9,37	9,52	9,49	9,53
FeO,Fe_2O_3	15,30	15,51	15,56	17,74	17,56	17,66	17,77	17,61
MgO	10,59	10,53	10,50	11,16	11,04	10,95	10,92	10,96
TiO_2	2,09	1,92	2,15	1,68	1,67	1,65	1,60	1,65
CaO	11,65	11,52	11,65	11,57	11,81	11,71	11,79	11,65
Na_2O	1,80	1,87	1,87	1,26	1,26	1,31	1,28	1,21
K_2O	1,52	1,46	1,56	1,02	1,05	1,09	1,09	1,04
Total	97,56	97,53	98,25	98,57	98,89	98,80	98,71	97,83
Si	6,254	6,261	6,242	6,700	6,695	6,676	6,668	6,638
Al	2,296	2,312	2,315	1,607	1,639	1,668	1,665	1,688
Fe	1,921	1,949	1,942	2,209	2,179	2,195	2,214	2,213
Mg	2,371	2,360	2,336	2,477	2,442	2,425	2,424	2,454
Ti	0,236	0,217	0,242	0,188	0,186	0,184	0,179	0,186
Ca	1,875	1,854	1,864	1,846	1,877	1,865	1,882	1,876
Na	0,525	0,546	0,542	0,365	0,363	0,376	0,369	0,352
K	0,292	0,280	0,297	0,193	0,199	0,207	0,207	0,200

Specimen	MJ 32			MJ 49			MJ 56	
Grain	1	2	3	1	2	3	1	2
SiO_2	47,01	47,21	47,61	44,99	44,98	44,91	46,27	46,34
Al_2O_3	8,92	8,53	8,03	9,03	8,92	9,18	8,71	8,66
FeO,Fe_2O_3	12,51	12,59	12,55	17,92	17,81	17,51	16,97	16,79
MgO	13,87	14,02	14,41	11,13	11,18	10,97	11,92	11,82
TiO_2	0,95	0,97	0,87	1,20	1,25	1,29	1,40	1,45
CaO	11,82	11,76	11,74	11,14	10,99	11,14	11,12	11,26
Na_2O	1,57	1,55	1,49	1,54	1,49	1,59	1,55	1,51
K_2O	0,74	0,72	0,71	0,89	0,88	0,89	0,59	0,58
Total	97,38	97,36	97,41	97,85	97,50	97,46	98,53	98,41
Si	6,886	6,917	6,967	6,748	6,763	6,751	6,831	6,844
Al	1,541	1,474	1,385	1,598	1,581	1,626	1,516	1,508
Fe	1,533	1,543	1,536	2,248	2,240	2,201	2,096	2,073
Mg	3,028	3,063	3,144	2,489	2,506	2,458	2,622	2,603
Ti	0,105	0,107	0,096	0,136	0,142	0,145	0,156	0,162
Ca	1,855	1,847	1,841	1,791	1,771	1,793	1,758	1,781
Na	0,445	0,442	0,422	0,447	0,435	0,463	0,444	0,432
K	0,138	0,135	0,133	0,170	0,168	0,170	0,111	0,109

TABLE A5-4 (Continued)

Microprobe analyses of hornblendes in Garub amphibolites and granolites

Specimen	MJ 56	MJ 84			MJ 92			MJ 102
Grain	3	1	2	3	1	2	3	1†
SiO_2	46,16	49,87	48,73	48,99	49,48	48,87	49,33	43,51
Al_2O_3	8,86	5,82	6,88	6,15	7,06	7,60	6,99	10,12
FeO,Fe_2O_3	16,86	11,93	12,43	11,75	12,76	12,71	12,82	20,20
MgO	11,88	15,31	14,62	15,15	14,90	14,61	15,02	9,53
TiO_2	1,29	0,59	0,72	0,55	0,85	0,62	0,82	1,33
CaO	11,08	11,73	11,75	11,86	11,92	11,98	11,92	11,89
Na_2O	1,58	0,83	0,97	0,83	1,08	1,06	1,08	1,30
K_2O	0,59	0,40	0,51	0,45	0,56	0,56	0,51	1,00
Total	98,30	96,48	96,61	95,73	98,61	98,00	98,49	98,88
Si	6,827	7,290	7,151	7,228	7,123	7,081	7,113	6,556
Al	1,545	1,003	1,190	1,069	1,197	1,298	1,187	1,798
Fe	2,086	1,458	1,525	1,450	1,536	1,540	1,546	2,545
Mg	2,619	3,336	3,197	3,332	3,197	3,155	3,229	2,141
Ti	0,143	0,064	0,079	0,061	0,092	0,067	0,089	0,151
Ca	1,756	1,837	1,846	1,874	1,839	1,860	1,842	1,918
Na	0,452	0,235	0,276	0,238	0,301	0,299	0,301	0,380
K	0,111	0,074	0,095	0,084	0,102	0,103	0,093	0,193

Specimen	MJ102				MJ183			MJ196
Grain	2†	3†	4†	5†	1	2	3	1
SiO_2	43,78	43,67	43,85	43,81	46,24	46,66	46,73	47,44
Al_2O_3	10,21	10,22	10,08	10,05	10,91	11,36	11,44	8,61
FeO,Fe_2O_3	20,16	20,44	20,46	20,48	10,92	11,95	12,03	19,79
MgO	9,42	9,37	9,37	9,32	14,76	14,84	15,01	9,28
TiO_2	1,30	1,26	1.28	1,31	0,77	0,64	0,67	0,79
CaO	11,80	11,81	11,85	11,80	10,62	10,34	10,84	12,07
Na_2O	1,29	1,29	1,27	1,33	1,51	1,54	1,51	0,85
K_2O	0,95	0,97	0,97	0,93	0,28	0,24	0,25	0,49
Total	98,92	99,02	99,13	99,03	95,99	97,55	98,48	99,32
Si	6,583	6,569	6,589	6,590	6,771	6,742	6,702	7,005
Al	1,810	1,812	1,786	1,781	1,883	1,935	1,934	1,500
Fe	2,535	2,572	2,570	2,576	1,337	1,444	1,444	2,444
Mg	2,112	2,101	2,098	2,090	3,221	3,194	3,206	2,043
Ti	0,147	0,143	0,145	0,148	0,085	0,069	0,072	0,088
Ca	1,901	1,904	1,908	1,901	1,666	1,601	1,667	1,910
Na	0,375	0,376	0,371	0,389	0,427	0,430	0,419	0,244
K	0,183	0,185	0,185	0,178	0,052	0,045	0,047	0,092

TABLE A5-4 (continued)

Microprobe analyses of hornblendes in Garub amphibolites and granolites

Specimen	MJ196			MJ266				MJ296
Grain	2	3	4	1†	2†	3†	4†	1
SiO_2	44,69	47,13	46,87	42,25	43,36	43,90	44,30	43,71
Al_2O_3	10,82	7,93	9,32	12,15	12,26	12,39	12,16	11,79
FeO,Fe_2O_3	19,73	18,91	19,44	13,23	13,27	12,56	12,44	19,58
MgO	8,27	9,96	8,93	16,60	12,84	13,18	13,57	9,57
TiO	1,05	0,63	0,79	2,28	2,28	2,34	2,14	0,84
CaO	12,09	12,91	12,05	12,12	12,18	12,21	12,20	10,63
Na_2O	1,14	0,82	1,02	1,68	1,86	1,86	1,78	1,26
K_2O	0,70	0,43	0,54	1,28	1,32	1,34	1,20	0,58
Total	98,50	98,00	98,96	97,59	99,38	99,78	99,79	97,96
Si	6,699	7,039	6,945	6,282	6,322	6,345	6,388	6,564
Al	1,913	1,396	1,628	2,128	2,106	2,111	2,066	2,088
Fe	2,473	2,362	2,409	1,646	1,618	1,519	1,500	2,459
Mg	1,848	2,217	1,973	2,792	2,790	2,839	2,916	2,143
Ti	0,119	0,070	0,088	0,255	0,250	0,254	0,232	0,095
Ca	1,942	1,950	1,913	1,931	1,903	1,892	1,886	1,711
Na	0,331	0,237	0,293	0,484	0,526	0,522	0,497	0,368
K	0,135	0,082	0,102	0,244	0,246	0,246	0,222	0,110

Specimen	MJ296		MJ345			MJ377		
Grain	2	3	1	2	3	1	2	3
SiO_2	43,56	43,66	44,96	46,83	44,88	44,32	44,34	44,06
Al_2O_3	12,23	11,70	10,35	9,69	10,55	11,09	10,99	11,07
FeO,Fe_2O_3	19,88	19,69	13,12	12,56	13,07	13,08	12,88	12,37
MgO	9,46	9,58	13,03	13,59	12,99	13,12	13,07	13,20
TiO	0,90	0,87	1,22	0,95	1,63	1,53	1,44	1,29
CaO	11,14	10,63	12,02	12,00	11,95	12,31	12,33	12,30
Na_2O	1,38	1,24	1,30	1,34	1,41	1,15	1,10	1,16
K_2O	0.47	0,55	0,99	1,00	1,06	1,36	1,41	1,34
Total	99,02	97,92	96,98	97,96	97,55	97,96	97,55	96,79
Si	6,489	6,563	6,662	6,826	6,616	6,525	6,549	6,546
Al	2,147	2,074	1,807	1,666	1,833	1,924	1,914	1,938
Fe	1,477	2,475	1,627	1,531	1,612	1,611	1,591	1,537
Mg	2,100	2,146	2,878	2,954	2,854	2,877	2,879	2,924
Ti	0,101	0,098	0,136	0,104	0,181	0,170	0,159	0,144
Ca	1,777	1,712	1,909	1,875	1,888	1,944	1,952	1,958
Na	0,398	0,360	0,375	0,377	0,404	0,329	0,314	0,335
K	0,89	0,106	0,187	1,186	0,199	0,255	0,265	0,253

TABLE A5-4 (continued)

Microprobe analyses of hornblendes in Garub amphibolites and granolites

Specimen	MJ397			MJ437			MJ546	
Grain	1	2	3	1	2	3	1	2
SiO_2	45,53	44,45	45,23	43,11	43,12	43,12	42,60	42,42
Al_2O_3	9,52	10,53	9,74	15,22	15,39	15,06	12,76	12,79
FeO,Fe_2O_3	15,61	16,45	15,88	8,94	9,16	9,18	18,99	18,74
MgO	12,53	11,89	12,37	15,19	15,13	15,14	9,18	9,10
TiO	0,58	0,68	0,63	0,99	0,98	0,90	1,05	0,96
CaO	11,99	11,84	11,92	12,27	11,97	12,17	12,16	12,26
Na_2O	1,03	1,22	1,16	2,32	2,29	2,34	1,54	1,51
K_2O	0,82	1,00	0,87	0,40	0,41	0,41	1,16	1,19
Total	97,63	98,05	97,78	98,45	98,44	97,72	99,44	98,97
Si	6,762	6,616	6,721	6,182	6,182	6,232	6,356	6,356
Al	1,667	1,848	1,705	2,572	2,601	2,566	2,244	2,259
Fe	1,939	2,047	1,973	1,072	1,098	1,109	2,369	2,348
Mg	2,774	2,639	2,739	3,246	3,233	3,262	2,041	2,033
Ti	0,065	0,076	0,070	0,107	0,105	0,099	0,118	0,108
Ca	1,908	1,887	1,897	1,885	1,839	1,884	1,944	1,969
Na	0,298	0,352	0,334	0,646	0,636	0,656	0,446	0,440
K	0,155	0,189	0,164	0,073	0,075	0,076	0,220	0,228

Specimen	MJ546	MJ712			MJ740			
Grain	3	1	2	3	1†	2†	3†	4†
SiO_2	42,62	45,67	46,08	45,70	47,33	46,91	47,56	47,58
Al_2O_3	12,79	10,22	9,60	10,05	8,22	8,34	8,11	8,00
FeO,Fe_2O_3	18,86	18,78	18,60	18,40	14,66	14,64	14,51	14,59
MgO	9,14	10,79	11,17	11,02	13,55	13,68	13,72	13,84
TiO	0,87	1,10	1,00	1,07	1,55	1,61	1,51	1,50
CaO	12,24	11,21	11,27	10,99	11,72	11,68	11,50	11,63
Na_2O	1,49	1,34	1,22	1,48	1,34	1,33	1,26	1,31
K_2O	1,13	0,42	0,36	0,41	0,89	0,90	0,84	0,92
Total	99,13	99,53	99,31	99,11	99,26	99,09	99,01	99,35
Si	6,372	6,715	6,779	6,735	6,872	6,828	6,906	6,896
Al	2,254	1,771	1,664	1,746	1,407	1,432	1,388	1,367
Fe	2,359	2,309	2,288	2,268	1,780	1,821	1,763	1,768
Mg	2,036	2,364	2,449	2,421	2,932	2,969	2,969	2,989
Ti	0,098	0,122	0,111	0,119	0,169	0,176	0,165	0,163
Ca	1,960	1,766	1,777	1,735	1,823	1,821	1,789	1,768
Na	0,431	0,382	0,349	0,422	0,378	0,375	0,354	0,369
K	0,216	0,079	0,068	0,077	0,165	0,168	0,156	0,169

TABLE A5-4 (continued)

Microprobe analyses of hornblendes in Garub amphibolites and granolites

Specimen	MJ740	MJ747			MJ835			MJ960
Grain	5	1	2	3	1	2	3	1
SiO_2	46,93	41,48	41,49	41,39	40,83	40,14	40,32	43,53
Al_2O_3	8,47	11,80	11,49	10,38	12,63	13,02	13,48	14,73
FeO,Fe_2O_3	14,22	20,90	20,99	20,63	22,79	22,94	22,83	13,46
MgO	13,71	7,45	7,54	7,57	6,98	5.33	6.56	12,05
TiO	1,51	1,51	1,44	1,41	1,01	0,90	1,09	0,50
CaO	11,71	11,40	11,39	11,42	11,59	11,44	11,56	10,98
Na_2O	1,34	1,32	1,35	1,23	1,22	1,23	1,30	1,27
K_2O	0,90	0,95	0,91	0,82	1,47	1,59	1,60	0,19
Total	98,80	96,80	96,59	94,85	98,53	96,58	98,74	96,71
Si	6,838	6,413	6,433	6,532	6,281	6,313	6,197	6,411
Al	1,455	2,151	2,100	1,931	2,290	2,414	2,442	2,556
Fe	1,733	2,702	2,721	2,723	2,931	3,017	2,934	1,658
Mg	2,977	1,716	1,743	1,780	1,600	1,248	1,503	2,644
Ti	0,166	0,175	0,168	0,167	0,117	0,106	0,126	0,055
Ca	1,733	1,889	1,892	1,931	1,911	1,927	1,904	1,732
Na	0,378	0,394	0,405	0,377	0,365	0,375	0,386	0,364
K	0,168	0,188	0,179	0,165	0,289	0,319	0,314	0,036

Specimen	MJ960		MJ969				MJ1020	
Grain	2	3	1†	2†	3†	4†	1†	2†
SiO_2	43,77	43,74	46,52	47,48	48,26	46,35	44,27	44,02
Al_2O_3	14,21	14,57	8,79	8,48	7,75	8,79	14,00	13,95
FeO,Fe_2O_3	12,80	13,32	13,79	14,79	13,82	14,89	14,67	14,71
MgO	12,08	12,09	12,85	13,04	13,86	12,69	11,94	11,75
TiO	0,45	0,43	0,47	0,42	0,37	0,45	0,43	0,47
CaO	11,20	11,13	12,60	12,77	12,69	12,52	11,27	11,33
Na_2O	1,28	1,18	0,83	0,86	0,80	0,89	1,79	1,63
K_2O	0,19	0,18	0,67	0,67	0,52	0,70	0,21	0,22
Total	95,98	96,64	96,51	98,50	98,06	97,27	98,57	98,07
Si	6,478	6,439	6,916	6,941	7,039	6,877	6,446	6,446
Al	2,478	2,528	1,541	1,462	1,332	1,537	2,402	2,407
Fe	1,585	1,640	1,715	1,808	1,686	1,847	1,787	1,801
Mg	2,664	2,652	2,848	2,842	3,014	2,807	2,593	2,564
Ti	0,050	0,048	0,052	0,046	0,040	0,050	0,047	0,051
Ca	1,776	1,756	2,007	2,000	1,983	1,991	1,758	1,778
Na	0,368	0,336	0,239	0,244	0,226	0,256	0,505	0,462
K	0,037	0,034	0,128	0,126	0,096	0,132	0,038	0,041

TABLE A5-4 (cont.). *Microprobe analyses of hornblendes*

Specimen	MJ1020		MJ1054				MJ1061		
Grain	3†	4†	1	2	3	4	1	2	3
SiO_2	43,87	44,64	48,59	46,98	46,76	47,34	46,38	48,81	46,76
Al_2O_3	13,84	14,06	7,57	9,21	9,28	8,68	8,81	8,14	8,89
FeO,Fe_2O_3	14,67	14,72	13,55	14,92	14,78	14,66	14,88	13,61	14,95
MgO	11,90	11,89	13,91	13,03	13,08	13,30	13,41	13,40	13,00
TiO	0,45	0,43	0,47	0,58	0,58	0,58	0,43	0,43	0,45
CaO	11,32	11,41	12,72	12,50	12,51	12,63	12,05	12,18	12,05
Na_2O	1,78	1,60	0,84	1,09	1,19	1,09	0,99	0,81	0,97
K_2O	0,21	0,23	0,65	0,93	0,93	0,79	0,70	0,49	0,64
Total	98,03	98,98	98,30	99,23	99,12	99,08	97,65	97,87	97.71
Si	6,431	6,468	7,064	6,836	6,815	6,888	6,849	7,097	6,891
Al	2,390	2,400	1,298	1,579	1,595	1,489	1,534	1,396	1,545
Fe	1,799	1,784	1,648	1,816	1,801	1,783	1,837	1,655	1,843
Mg	2,603	2,569	3,015	2,827	2,841	2,885	2,953	2,904	2,856
Ti	0,049	0,047	0,051	0,064	0,064	0,064	0,048	0,047	0,050
Ca	1,779	1,771	1,982	1,949	1,954	1,968	1,907	1,897	1,903
Na	0,506	0,449	0,236	0,309	0,336	0,308	0,282	0,229	0,278
K	0,038	0,042	0,121	0,172	0,172	0,147	0,132	0,092	0,120

TABLE A5-5. *Microprobe analyses of cummingtonite (Cm), clinopyroxene (Cp) and orthopyroxene (Op) in amphibolites (left) and hypersthene granolites (right)*

Specimen	MJ960	MJ1319		MJ345		MJ377	
Grain	1(Cm)	1(Cp)	2(Cp)	1(Cp)	2(Cp)	1(Op)	2(Op)
SiO_2	52,42	52,00	52,26	49,75	48,21	52,20	51,58
Al_2O_3	0,53	0,80	0,65	1,41	1,44	1,30	1,47
FeO,Fe_2O_3	20,07	9,27	9,42	7,43	8,52	23,14	19,07
MgO	19,66	11,31	11,39	14,24	12,21	21,21	21,41
TiO	0,00	0,08	0,05	0,17	0,19	0,06	0,07
CaO	0,80	24,16	24,24	23,45	21,90	0,63	0,58
Na_2O	0,07	0,26	0,19	0,40	0,41	0,06	0,06
K_2O	0,01	0,00	0,00	0,00	0,00	0,00	0,00
Total	93,56	97,88	98,21	96,84	92,89	98,59	94,23
Si	7,890	1,996	2,000	1,923	1,949	1,976	2,005
Al	0,095	0,036	0,029	0,064	0,069	0,058	0,067
Fe	2,526	0,298	0,302	0,240	0,288	0,733	0,620
Mg	4,410	0,647	0,650	0,821	0,736	1,197	1,240
Ti	0,000	0,002	0,001	0,005	0,006	0,002	0,002
Ca	0,129	0,994	0,994	0,971	0,948	0,025	0,024
Na	0,021	0,019	0,014	0,030	0,032	0,004	0,004
K	0,002	0,000	0,000	0,000	0,000	0,000	0,000

TABLE A5-6

Microprobe analyses of plagioclases in Garub amphibolites and granolites

Specimen	MJ 13			MJ 28			MJ 32	
Grain	1	2	3	1†	2†	3†	1	2
SiO_2	47,51	44,69	47,46	55,53	55,90	55,64	48,88	51,12
Al_2O_3	35,10	34,97	33,95	28,70	29,18	29,10	30,76	30,55
FeO,Fe_2O_3	0,13	0,12	0,04	0,08	0,10	0,10	0,05	0,04
MgO	0,03	0,03	0,03	0,05	0,00	0,03	0,03	0,02
TiO_2	0,00	0,00	0,00	0,02	0,00	0,03	0,00	0,00
CaO	16,62	16,18	15,44	10,61	11,07	11,04	13,92	13,15
Na_2O	2,18	2,53	2,68	5,56	5,43	5,37	4,33	4,64
K_2O	0,00	0,04	0,04	0,26	0,15	0,20	0,11	0,14
Total	101,56	98,56	99,65	100,81	101,84	101,51	98,08	99,64
Si	2,146	2,089	2,180	2,484	2,475	2,472	2,281	2,337
Al	1,868	1,926	1,838	1,512	1,523	1,524	1,692	1,646
Fe	0,005	0,005	0,002	0,003	0,004	0,004	0,002	0,001
Mg	0,002	0,002	0,002	0,003	0,000	0,002	0,002	0,001
Ti	0,000	0,000	0,000	0,001	0,000	0,001	0,000	0,000
Ca	0,804	0,810	0,760	0,508	0,525	0,526	0,696	0,644
Na	0,191	0,229	0,239	0,482	0,466	0,462	0,392	0,411
K	0,000	0,002	0,002	0,015	0,008	0,011	0,007	0,008

Specimen	MJ 32	MJ 49			MJ 56			MJ 84
Grain	3	1	2	3	1	2	3	1
SiO_2	50,81	51,76	52,07	52,11	54,75	53,13	53,09	52,32
Al_2O_3	30,30	30,44	30,18	30,16	31,06	31,61	31,27	29,23
FeO,Fe_2O_3	0,07	0,08	0,09	0,04	0,09	0,08	0,10	0,07
MgO	0,03	0,02	0,02	0,00	0,02	0,02	0,03	0,03
TiO_2	0,00	0,00	0,00	0,00	0,00	0,00	0,00	0,00
CaO	13,36	13,27	13,09	12,92	13,06	13,89	13,48	11,41
Na_2O	4,50	4,01	4,13	4,13	4,61	4,36	4,58	5,29
K_2O	0,07	0,09	0,10	0,06	0,14	0,11	0,15	0,20
Total	99,14	99,67	99,68	99,43	103,73	103,20	102,71	98,54
Si	2,336	2,358	2,371	2,376	2,393	2,343	2,352	2,407
Al	1,642	1,635	1,620	1,621	1,600	1,643	1,633	1,585
Fe	0,003	0,003	0,003	0,001	0,003	0,003	0,004	0,003
Mg	0,002	0,001	0,001	0,000	0,001	0,001	0,002	0,002
Ti	0,000	0,000	0,000	0,000	0,000	0,000	0,000	0,000
Ca	0,658	0,648	0,639	0,631	0,612	0,656	0,640	0,563
Na	0,401	0,354	0,365	0,365	0,391	0,373	0,393	0,472
K	0,004	0,005	0,006	0,004	0,008	0,006	0,008	0,012

TABLE A5-6 (continued)

Microprobe analyses of plagioclases in Garub amphibolites and granolites

Specimen	MJ 84		MJ 92			MJ102		
Grain	2	3	1	2	3	1†	2†	3†
SiO_2	49,74	51,96	46,58	46,40	46,55	44,85	44,47	46,30
Al_2O_3	31,09	31,05	35,50	35,65	35,49	35,27	34,72	35,55
FeO, Fe_2O_3	0,08	0,05	0,05	0,10	0,10	0,13	0,26	0,20
MgO	0,02	0,00	0,03	0,02	0,03	0,02	0,02	0,02
TiO_2	0,00	0,00	0,00	0,00	0,00	0,03	0,00	0,00
CaO	13,64	13,24	18,37	18,39	18,25	18,40	18,33	18,46
Na_2O	4,26	4,29	1,54	1,47	1,41	1,04	1,08	1,30
K_2O	0,13	0,14	0,02	0,02	0,02	0,04	0,02	0,05
Total	98,96	100,72	102,10	102,06	101,87	99,77	98,91	101,87
Si	2,296	2,345	2,103	2,096	2,105	2,074	2,077	2,096
Al	1,691	1,652	1,889	1,898	1,891	1,922	1,911	1,897
Fe	0,003	0,002	0,002	0,004	0,004	0,005	0,010	0,007
Mg	0,001	0,000	0,002	0,001	0,002	0,001	0,001	0,001
Ti	0,000	0,000	0,000	0,000	0,000	0,001	0,000	0,000
Ca	0,674	0,640	0,888	0,890	0,884	0,912	0,917	0,895
Na	0,381	0,375	0,135	0,129	0,124	0,093	0,098	0,114
K	0,008	0,008	0,001	0,001	0,001	0,002	0,001	0,003

Specimen	MJ102			MJ183			MJ266	
Grain	4†	5†	6	1	2	3	1†	2†
SiO_2	46,11	45,78	42,68	47,23	47,11	46,80	49,10	48,86
Al_2O_3	35,47	35,79	34,82	34,22	34,33	34,72	33,51	33,44
FeO, Fe_2O_3	0,23	0,20	0,18	0,03	0,04	0,03	0,05	0,10
MgO	0,03	0,03	0,00	0,03	0,03	0,05	–	–
TiO_2	0,00	0,02	0,03	0,00	0,00	0,00	–	–
CaO	18,29	18,70	18,76	17,49	17,61	18,00	16,46	16,28
Na_2O	1,23	1,05	0,87	1,77	1,77	1,62	2,60	2,48
K_2O	0,05	0,02	0,04	0,02	0,00	0,02	0,04	0,06
Total	101,41	101,58	97,39	100,79	100,89	101,24	101,76	101,24
Si	2,096	2,080	2,031	2,153	2,147	2,128	2,211	2,211
Al	1,900	1,916	1,953	1,838	1,844	1,861	1,778	1,783
Fe	0,009	0,007	0,007	0,001	0,001	0,001	0,002	0,004
Mg	0,002	0,002	0,000	0,002	0,002	0,003	–	–
Ti	0,000	0,001	0,001	0,000	0,000	0,000	–	–
Ca	0,891	0,910	0,957	0,854	0,859	0,877	0,794	0,789
Na	0,108	0,092	0,080	0,156	0,156	0,143	0,227	0,218
K	0,003	0,001	0,002	0,001	0,000	0,001	0,002	0,004

TABLE A5-6 (continued)

Microprobe analyses of plagioclases in Garub amphibolites and granolites

Specimen	MJ266	MJ345	MJ377			MJ437	MJ712	
Grain	3	1	1	2	3	1	1	2
SiO_2	48,95	49,70	46,13	46,13	45,65	44,47	55,13	55,91
Al_2O_3	33,46	33,62	35,30	35,27	35,49	37,27	28,01	28,09
FeO,Fe_2O_3	0,07	0,07	0,25	0,14	0,18	0,03	0,10	0,12
MgO	-	0,03	0,05	0,05	0,05	0,03	0,00	0,02
TiO	-	0,00	0,00	0,00	0,00	0,00	0,00	0,00
CaO	16,46	15,10	19,25	19,07	19,11	19,52	9,67	9,77
Na_2O	2,58	3,04	1,23	1,25	1,19	0,41	6,32	6,14
K_2O	0,05	0,10	0,02	0,04	0,04	0,00	0,07	0,05
Total	101,56	101,66	102,22	101,95	101,70	101,72	99,30	100,09
Si	2,209	2,232	2,088	2,091	2,076	2,019	2,510	2,512
Al	1,780	1,779	1,883	1,885	1,902	1,995	1,497	1,488
Fe	0,002	0,002	0,009	0,005	0,007	0,001	0,004	0,004
Mg	-	0,002	0,003	0,003	0,003	0,002	0,000	0,001
Ti	-	0,000	0,000	0,000	0,000	0,000	0,000	0,000
Ca	0,796	0,727	0,933	0,926	0,931	0,949	0,470	0,470
Na	0,226	0,265	0,108	0,110	0,105	0,036	0,555	0,535
K	0,003	0,006	0,001	0,002	0,002	0,000	0,004	0,003

Specimen	MJ712	MJ740					MJ747	
Grain	3	1†	2†	3†	4†	5†	1	2
SiO_2	55,71	48,38	47,59	48,22	49,25	48,35	53,20	54,90
Al_2O_3	28,21	34,42	34,76	34,59	33,69	34,19	28,27	27,64
FeO,Fe_2O_3	0,07	0,05	0,16	0,07	0,07	0,10	0,07	0,04
MgO	0,03	0,02	0,03	0,00	0,02	0,00	0,03	0,03
TiO	0,02	0,00	0,03	0,02	0,03	0,00	0,00	0,00
CaO	9,70	16,60	17,03	16,58	16,20	16,84	10,09	9,40
Na_2O	6,31	2,47	2,05	2,31	2,55	2,18	5,95	6,28
K_2O	0,06	0,09	0,06	0,10	0,09	0,09	0,11	0,14
Total	100,10	102,01	101,72	101,88	101,89	101,74	97,71	98,42
Si	2,505	2,175	2,149	2,170	2,213	2,180	2,458	2,510
Al	1,494	1,824	1,850	1,835	1,784	1,817	1,539	1,489
Fe	0,002	0,002	0,006	0,002	0,002	0,004	0,003	0,002
Mg	0,002	0,001	0,002	0,000	0,001	0,000	0,002	0,002
Ti	0,001	0,000	0,001	0,001	0,001	0,000	0,000	0,000
Ca	0,467	0,800	0,825	0,800	0,780	0,813	0,500	0,460
Na	0,550	0,215	0,180	0,202	0,222	0,190	0,533	0,556
K	0,004	0,005	0,004	0,006	0,005	0,005	0,007	0,008

TABLE A5-6 (continued)

Microprobe analyses of plagioclases in Garub amphibolites and granolites

Specimen	MJ747	MJ835			MJ960			MJ969
Grain	3	1	2	3	1	2	3	1†
SiO_2	52,68	50,54	48,63	48,38	45,86	45,84	45,42	53,33
Al_2O_3	28,13	32,60	34,60	34,42	34,89	34,71	34,80	30,25
FeO,Fe_2O_3	0,07	0,12	0,17	0,21	0,00	0,01	0,04	0,03
MgO	0,03	0,02	0,03	0,00	0,00	0,00	0,03	-
TiO	0,00	0,00	0,00	0,00	0,00	0,00	0,00	-
CaO	9,90	14,39	16,68	16,59	17,32	17.06	16,99	12,50
Na_2O	6,37	3,96	2,08	2,10	1,90	1,92	1,96	4,63
K_2O	0,12	0,07	0,04	0,09	0,00	0,00	0,00	0,06
Total	97,31	101,70	102,22	101,79	99,96	99,55	99,24	100,79
Si	2,450	2,270	2,179	2,179	2,111	2,118	2,106	2,396
Al	1,541	1,725	1,827	1,827	1,893	1,890	1,901	1,602
Fe	0,003	0,004	0,006	0,008	0,000	0,001	0,002	0,001
Mg	0,002	0,001	0,002	0,000	0,000	0,000	0,002	-
Ti	0,000	0,000	0,000	0,000	0,000	0,000	0,000	-
Ca	0,493	0,693	0,801	0,801	0,854	0,844	0,844	0,602
Na	0,574	0,345	0,180	0,184	0,170	0,172	0,176	0,403
K	0,007	0,004	0,002	0,005	0,000	0,000	0,000	0,004

Specimen	MJ969		MJ1020					MJ1054
Grain	2†	3†	1†	2†	3†	4†	5	1
SiO_2	56,17	55,37	49,58	50,74	51,95	47,63	51,86	55,78
Al_2O_3	28,84	29,10	31,45	32,09	30,43	31,26	31,44	27,97
FeO,Fe_2O_3	0,03	0,03	0,00	0,00	0,07	0,04	0,00	0,07
MgO	-	-	0,02	0,03	0,00	0,00	0,02	0,06
TiO	-	-	0,03	0,00	0,00	0,00	0,00	0,00
CaO	10,84	11,32	13,98	14,41	12,34	14,22	13,66	9,19
Na_2O	5,70	5,38	3,80	3,79	4,73	3,82	3,86	6,59
K_2O	0,07	0,06	0,07	0,04	0,05	0,05	0,05	0,17
Total	101,66	101,26	98,93	101,10	99,55	97,02	100,89	99,82
Si	2,489	2,466	2,286	2,288	2,367	2,248	2,334	2,514
Al	1,506	1,528	1,709	1,706	1,634	1,739	1,668	1,486
Fe	0,001	0,001	0,000	0,000	0,002	0,002	0,000	0,002
Mg	-	-	0,001	0,002	0,000	0,000	0,001	0,004
Ti	-	-	0,001	0,000	0,000	0,000	0,000	0,000
Ca	0,515	0,540	0,690	0,696	0,602	0,719	0,659	0,444
Na	0,490	0,465	0,340	0,332	0,417	0,350	0,337	0,575
K	0,004	0,004	0,004	0,002	0,003	0,003	0,003	0,010

TABLE A5-6 (continued)

Microprobe analyses of plagioclases in Garub amphibolites and granolites

Specimen	MJ1054		MJ1061			MJ1319		
Grain	2	3	1	2	3	1	2	3
SiO_2	55,80	56,01	58,83	59,03	59,12	50,02	48,90	51,27
Al_2O_3	28,06	27,40	27,74	27,52	27,15	31,35	32,14	31,08
FeO,Fe_2O_3	0,07	0,12	0,07	0,07	0,07	0,08	0,00	0,03
MgO	0,02	0,03	0,00	0,02	0,00	0,02	0,03	0,05
TiO	0,00	0,00	0,00	0,00	0,00	0,00	0,00	0,00
CaO	8,53	8,96	8,16	8,02	7,58	14,21	14,92	13,84
Na_2O	6,54	6,49	7,21	7,28	7,33	3,87	3,44	4,10
K_2O	0,17	0,11	0,12	0,15	0,20	0,09	0,02	0,11
Total	99,19	99,12	102,13	102,08	101,45	99,62	99,45	100,48
Si	2,524	2,538	2,578	2,587	2,604	2,292	2,248	2,325
Al	1,496	1,463	1,433	1,421	1,409	1,693	1,741	1,661
Fe	0,002	0,004	0,002	0,002	0,002	0,003	0,000	0,001
Mg	0,001	0,002	0,000	0,001	0,000	0,001	0,002	0,003
Ti	0,000	0,000	0,000	0,000	0,000	0,000	0,000	0,000
Ca	0,413	0,435	0,383	0,377	0,358	0,697	0,735	0,672
Na	0,573	0,570	0,612	0,618	0,626	0,344	0,306	0,360
K	0,010	0,006	0,007	0,008	0,011	0,005	0,001	0,006

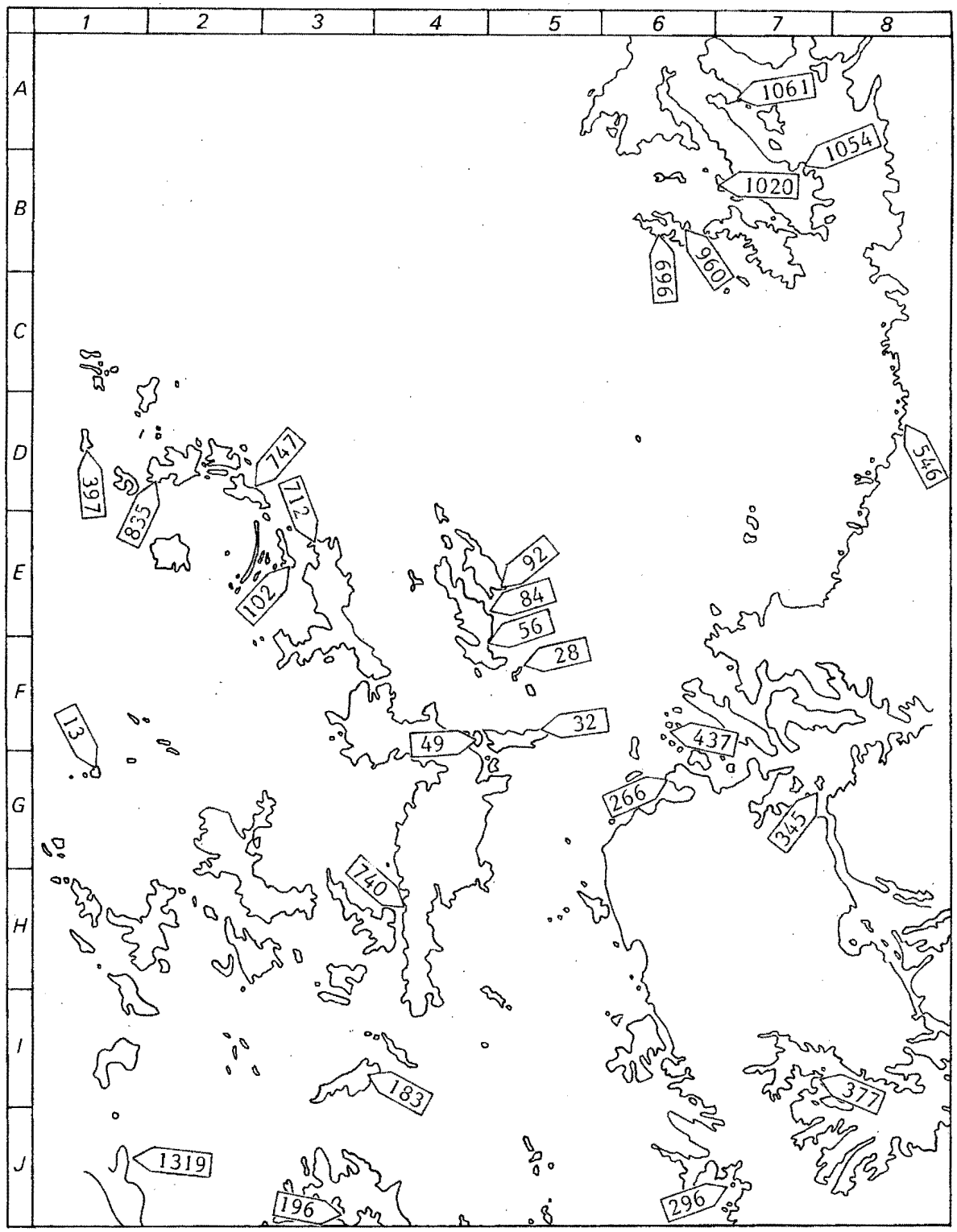

Appendix 6. Locality map for Garub metabasite specimens analysed by electron microprobe

TABLE A7-1

Specimens collected from the Aus area for age dating

PRU Specimen	Collector's No.	Locality			Rock unit	Rock type
		latitude	longitude	farm		
	MJ 843	26°34'S	15°59'E	Garub St.	Garub sequence	biotite schist
114	MJ1312b	26°35'S	16°19'E	Aus	Tsirub gneiss	tonalitic biotite-garnet augen gneiss
115	MJ1342	26°07'S	16°25'E	Excelsior	Tierkloof diorite	hornblende-biotite-quartz-monzodiorite
113	MJ3051	26°05'S	16°42'E	Houmoed	Houmoed granodiorite	hornblende-biotite granodiorite

TABLE A7-2

Analytical data for U-Pb (zircon) age determinations

Specimen	Conc. (p.p.m.)		Isotopic ratios			Calculated ages (Ma)				
	U	Pb	Pb^{206}/Pb^{204}	Pb^{207}/Pb^{204}	Pb^{208}/Pb^{204}	Pb^{207}/Pb^{206}	Pb^{207}/U^{235}	Pb^{206}/U^{238}	N^{207}/N^{235}	N^{206}/N^{238}
MJ 843	–	–	–	–	–	1116	–	–	–	–
MJ1312b	371	63,9	202,5	164,8	420,5	1052	960	920	1,5749	0,1537
MJ1342	836	80,9	154,0	25,85	64,77	1080	508	392	0,6506	0,06265
MJ3051	325	61,04	191,72	28,71	61,54	1078	894	822	1,3825	0,1345

APPENDIX 7 GEOCHRONOLOGIC RESULTS

Dr. A.J. Burger, National Physical Research Laboratory of the South African Council for Scientific and Industrial Research, has determined minimum U-Pb ages by single zircons in rocks from the Aus area. The results, all of which are preliminary, are given in Table A7-2.

APPENDIX 8 CLIMATE AND GEOMORPHOLOGY

1. *Climate*

Climatically and geomorphologically the Aus area falls within the Namib Desert. The eastern half of the study area is classified as 'arid' and the western half, as 'extremely arid' (Meigs, 1953 *in* Cooke and Warren, 1973). Rainfall around Aus is extremely sparse and irregular with no marked seasonal variation. The mean annual rainfall at Aus Village is less than 100 mm (Table A8-1). The rainfall decreases to the south, west and north of Aus (except in the Tiras Mountains in the extreme northwest, which are comparatively well-watered). Lüderitz, due west of Aus on the coast, receives a mean annual rainfall of only 18 mm a year (Table A8-1). The study area therefore receives between 20 and 100 mm of rain a year. Very rarely the coastal fog penetrates into the Aus area as far as 120 km inland up the Koichab River (D5) or on the plains around Dicker Willem Mountain (E2).

TABLE A8-1

Annual rainfalls of Aus and Lüderitz, recorded over 36 years (mm)

	LÜDERITZ	AUS
mean	18	96
maximum	33	279
minimum	5	23

Data from Royal Navy and South African Air Force Meteorological Services (1944)

The Namib is classified as a hot (mean annual temperature >18°C) low-latitude (15-35° lat.) desert (Stone, 1967). However, the generally high relief in the neighbourhood of Aus (1000-1500 m) results in relatively cool temperatures there. Daily readings of maximum and minimum shade temperatures taken by the writer during 1972 and 1973 are shown in Table A8-2. In winter minimum temperatures are low; sub-zero temperatures were recorded on six days during 1972 and snow had fallen twice around Aus in the previous decade (1963-1973). Combined with moderate maximum temperatures these low minimum temperatures result in very high diurnal variations of up to 32,5°C during winter. The absolute maximum temperature recorded during winter in 1973 was 40,5°C. No data are available for temperatures in the low-lying parts of the study area or for summer temperatures, which are likely to be higher.

The southern Namib Desert is characterized by three régimes of surface winds (Breed et al., in prep.). The coastal régime is unidirectional and is dominated by the extremely powerful onshore wind from the south and southwest;

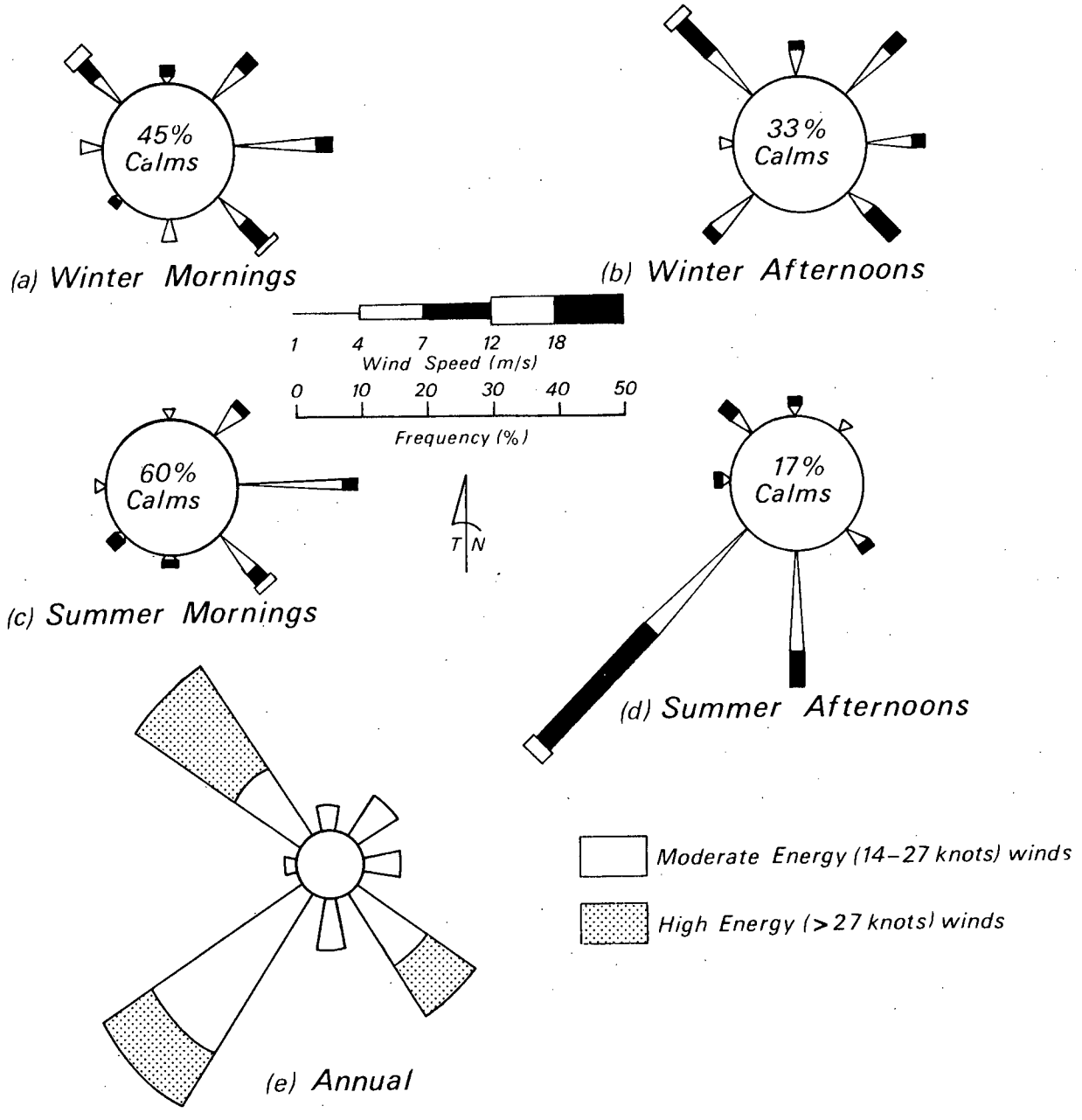

Figure A8-1. Wind roses for Aus Village. Data sources: (a-d) Royal Navy and South African Air Force (1944); (e) Breed et al. (in prep.).

this wind is strongest during the summer because of the influence of the South Atlantic high (ibid.). The central régime is bimodal because of the combined influence of the onshore wind (which gradually diminishes in force inland) and the northeasterly 'Berg' wind. The interior of the Namib has a multidirectional wind régime of lower energy.

TABLE A8-2

Maximum and minimum temperatures recorded during 1972 and 1973 around Aus

WINTER (June 22 - Sept.23)				EARLY SPRING (Sept.23 - Nov.20)			
		TEMP. (°C)	DATE			TEMP. (°C)	DATE
mean minimum		6,0	-	mean minimum		14,0	-
absolute minimum		-2,5	3/8/72	absolute minimum		1,5	27/9/73
mean maximum		27,0	-	mean maximum		31,0	-
absolute maximum		40,5	10/9/73	absolute maximum		38,0	4/10/73
diurnal variation	greatest	32,5	4/8/72	diurnal variation	greatest	20,5	29/10/73
	mean	20,5			mean	16,0	-
	smallest	7,5	10/8/73		smallest	14,0	5/11/72
mean		16,5		mean		22,5	

The surface winds of the Namib interior are markedly seasonal (Fig. A8-1). The winter climate at Aus is dominated by the intermittent but powerful 'Berg' wind which blows most strongly from the southeast and seems, in part, to be caused by northeasterly anticyclonic circulation in the interior of the subcontinent (ibid.). The 'Berg' wind is bitterly cold around Aus, but it warms adiabatically farther westward and gives rise to hot, dry conditions at the coast. Surface winds consistently blow from the northwest on winter afternoons (unless the 'Berg' wind is blowing), starting as a light breeze around noon and increasing in intensity during the afternoon. In spring and summer the powerful southwest wind predominates. This trimodal wind régime is reflected in the annual wind rose for Aus (Fig. A8-1).

2. *Geomorphology*

The Aus area comprises three principal geomorphological domains. Domain A is represented by the Nama Plateau, which lies on the eastern fringe of the study area; southeast of Aus Village this feature is shown on topographical maps as the Huib-Hoch Plateau. The plateau is bounded in the west by a precipitous north-trending escarpment, which varies between 250 and 350 m in height. The altitude of the Nama Escarpment varies from 1250 m in the south at Anusi Farm (M6) to 1805 m at Aar beacon (H6) east of Aus Village; farther north the escarpment descends to an altitude of 1655 m in the centre of the Koichab trough (D8) and rises to 1815 m at Geimasis (A8) in the extreme north.

Domain B, the 'Plain Namib' of King (1963), occupies most of the study area and comprises rolling plains and steep-sided inselbergs concentrated in the centre of the area around Aus Village and in the northeast. The Tiras Mountains (B7), with an altitude of 1867 m, form the highest point in the study area; elsewhere the elevation of domain B varies from 1700 m (Kububer Höhe, H4) and 1731 m (Groot Löwenberg, F4) above mean sea level in the mountains around Aus to 712 m near Garub Station (F1) and 674 m southwest of Tsaus Mountain (N2) above m.s.l.; almost all the study area has an altitude of more than 1000 m.

Domain C is represented by dune fields in the low-lying western areas and by the Namib Sand Sea, which extends 300-400 km northwards from the Koichab River to the Kuiseb River.

Domain A: the Nama Plateau

Domain A is characterized by advanced pediplanation, probably during King's (1963) 'African cycle'. The interior of the Nama Plateau has been dissected by rivers draining southeast and forming part of the Orange River catchment area. This drainage regime, in the form of the Nastom and Tsagaanibis Rivers (I8, J8), extends into the southeast parts of the study area. The precipitous Nama Escarpment epitomizes the contrast between steep and gentle slopes characteristic of landforms in arid climates (Joly, 1972, p.188). This feature results partly from faulting, which trends north-northeast (E8), north-northwest (I6) and northwest (M6,M7) and partly from erosion by west-draining ephemeral streams such as the Naisib (B8), Horab (G6), Assab (J6) and Arasab (K6) Rivers. The pediment along the base of the escarpment has a very gentle slope and varies from 1 to 13 km in width. It consists of coarse boulder-strewn colluvium and is dissected by a close network of shallow rill channels.

Domain B: the Plain Namib

Domain B lies to the west of the Nama Escarpment. Within this domain there are two systems of ephemeral streams. The northern half of the study area is dominated by the Koichab River and its tributaries which drain the mountainland north of Aus Village and the northern part of the escarpment. The Koichab flows westwards along the southern margin of the Namib Sand Sea to within 60 km of the coast, at which point it is impounded by the dunes within a large basin known as the Koichab Pan. The Naisib River drains the northeast part of the study area. South of Aus Village is a very poorly integrated network of streams. These dry washes arise in pediments of the inselbergs or the escarpment; they all terminate on reaching the aeolian sand sheet or one of the dune fields. Claypans are situated at the ends of some of these streams at the margins of the dunes (e.g. B6, N3). After one of the rare periods of rain many of these pans contain temporary sheets of water derived by surface runoff. Periods of stream flow are short but the stream load is high, giving rise to shifting ill-defined shallow channels rather than single stream courses.

Surface deposits in domain B comprise three categories: aeolian sand, colluvium-alluvium and calcrete (Annexure 1). Aeolian sand covers most of the area and is fine, well sorted and deep red in colour. The thickness of this mantle on the plains is considerable: a borehole penetrated 600 m without striking bedrock. Colluvium and alluvium form broad pediments on the downslope side of the inselbergs. No alluvial fans or cones have been formed and the pediments gradually become narrower as they extend farther into the aeolian sand sheet. Exposures of calcrete are largely restricted to the Diamond Area in the plain between the Garub Hills (G1) and Magnettafelberg (D2). The inselbergs upslope from these calcrete-covered areas contain large exposures of Garub marble; the distribution of marble may have been the most important factor controlling the formation of calcrete (see Annexure 1). Beds of calcrete, covered by younger deposits and therefore not shown on the geological map, are exposed by stream erosion and roadmaking in the plains between Am Einschnitt and Groot Löwenberg. Calcified root tubules below the calcrete horizon west of the Garub pump-station suggest that this extremely arid area supported stable vegetation at one stage of its geological history.

Projecting through the surface deposits are rock outliers in the form of inselbergs. In this area the rainfall is too low to produce the 'badlands' terrain characterized by dense systems of deep gullies and integrated stream systems (Joly, 1972, p.186). Granite and gneiss form large exfoliated domes characterized by 'onion-skin' weathering, whereas resistent marble, carbonatite and metaquartzite weather into irregular shapes. Desert varnish is characteristic of charnockite and diorite/granodiorite. Because of the extensive surface deposits, hammadas are not present in the study area but are common farther southwest near the coast. Wind abrasion of outcrops within the saltation zone (Bagnold, 1941) is common in the west of the study area and wind-facetted pebbles are present in the southwest. Although surface processes are predominantly depositional, the effects of deflation are visible in places, most markedly in the bed of the Koichab River where the root systems of acacia trees have been exposed by wind erosion to a depth of more than 2 m.

3. Domain C: the Dune Namib

Approximately 1300 km^2 of the Namib Sand Sea fall within the study area (see Fig. 68). Aeolian deposits in the sand sea become increasingly more red eastwards from the coast: the sand is almost white at the coast, yellow at Koichab Pan and deep red north of Aus. This type of colour change was believed by Logan (1960) to reflect the increasingly greater ages of sand in the interior of the sand sea; McKee and Breed (1974) believe this colour change to be a function of the length of time that the sand is exposed to a subaerial environment. The major dune structures of the Namib Sand Sea constitute three principal domains (Breed et al., in prep.):

(i) transverse and barchanoid dunes at the coast, controlled by a highly energetic, unidirectional southwest wind

(ii) mainly linear dunes in a central zone formed by bidirectional winds from the southwest and northeast

(iii) highly complex and diverse dunes in the interior zone of the sand sea formed under the influence of multidirectional winds of varying strengths.

The Namib Sand Sea near Aus belongs to the third category above. The southern margin of the sand sea is marked by an escarpment of aeolian sand along the northern bank of the Koichab River. This escarpment is formed by a chain of star dunes, some of which exceed 200 m in height. These dunes consist of a central peak from which radiate three sharp-crested buttresses trending north, south and east. Breed et al. (in prep.) suggested that the trimodal wind régime around Aus may have been responsible for the formation of the star dunes. The southeastern margin of the sand sea, around Inselkuppe (D5), is marked by a series of longitudinal dunes with well-defined interdune troughs. The eastern boundary of the sand sea is represented by arcuate, discontinuous and poorly-defined transverse dunes (Annexure 1). Within the sand sea is an extensive massif of dunes with poorly-defined shape and form separated by large blowout basins. Active dune formation and migration is taking place at a relatively slow rate within this area. While the 'Berg' wind is blowing, the air above the sand sea contains a pall of red dust. Smoking crests (Cooke and Warren, 1973) observed by the writer confirm that aeolian transport is active both in a northwest and southeast direction; inverted dune crests confirm the interaction of these two winds. At the eastern edge of the dune field the dunes have been fixed by vegetation.

Other dune fields farther south are of much smaller size and appear to be partially fixed by vegetation. Longitudinal dunes between Garub Station and Heinrichsfelde Farm (G2, G3) contain two slip faces and appear to have formed under the influence of the southeast and northwest winds. A prominent falling dune of domelike form has formed in the lee of Sesselberg (G2). In the southeast of the study area a reticular dune pattern has formed by interaction of transverse and longitudinal dunes; the arcuate form of these dunes suggest deflection of the winds by the Agub and Numitsoab inselbergs.

ACKNOWLEDGEMENT

I am indebted to John Rogers, UCT/Geological Survey Marine Geoscience Unit, for providing published and pre-published material on the climate and dune formations of the Namib Desert.